

Anita da Silva Lourenço

## DEVELOPMENT OF NOVEL FLOCCULANTS TO TREAT OILY WATERS USING HEALTH-FRIENDLY PROCESSES

PhD Thesis in Chemical Engineering, supervised by Professor Doctor Maria da Graça Bontempo Vaz Rasteiro and Doctor David Hunkeler and submitted to the Department of Chemical Engineering, Faculty of Sciences and Technology of the University of Coimbra

January 2018



UNIVERSIDADE DE COIMBRA

Anita da Silva Lourenço

# Development of novel flocculants to treat oily waters using health-friendly processes

Doctoral Thesis in the scientific area of Chemical Engineering, submitted to the Department of Chemical Engineering,  
Faculty of Science and Technology, University of Coimbra

**Supervisor(s):**

Professor Doctor Maria da Graça Bontempo Vaz Rasteiro

Doctor David Hunkeler

**Host institutions:**

CIEPQPF — Research Centre on Chemical Processes and Forest Products, Department of Chemical Engineering, University of  
Coimbra, Portugal

Aqua+Tech Specialities SA, Switzerland

**Financing:**

Marie Curie Initial Training Networks (ITN) — European Industrial Doctorate (EID)

Grant agreement FP7-PEOPLE-2013-ITN-604825

January 2018



UNIVERSIDADE DE COIMBRA



*You must do the things you think you cannot do.*

**Eleanor Roosevelt**



*To my parents,  
Aurora and Pedro*



---

## ACKNOWLEDGEMENTS

First and foremost I offer my sincerest gratitude to both my supervisors, Prof. Dr. Graça Rasteiro and Dr. David Hunkeler, for welcoming me as their student, for the constant and unconditional guidance and for all the precious help in the development and the writing of this thesis. Thank you both, it was a great pleasure to work with you.

I would like to acknowledge to the ECOFLOC Project members; Mr. Julien Arnold, Dr. Olivier Cayre and Dr. José Gamelas, for all the knowledge, precious suggestions and wise advices during these 3 years.

My sincere thank you:

To the University of Coimbra and Research Centre on Chemical Processes and Forest Products people for all the help and support during my time there, especially to Eng. Maria João Bastos, Prof. Dr. Fernando Garcia, Prof. Dr. Hermínio Sousa, Dr. Mara Braga, D. Dulce Pancas, Sr. José Santos, Sr. Manuel, D. Fernanda Ferreira, D. Mafalda Fernandes, Dr. Adamo Caetano e Dr. Luís Santos.

To the helpful and supportive team in Aqua+Tech, Mrs. Sylvie Dilonardo, Mrs. Sabine Lamassiaude, Mr. Nestor Benito, Dr. Jane Royston, Dr. Peter Urben and Thomas Uldry.

To University of Leeds members (especially to Andy Leeson) for receiving me over four weeks and introducing me to new and so interesting techniques.



To Adventech Group (Dr. Rui Martins, Dr. Nuno Amaral, Dr. Paulo Nunes and Dr. Sérgio Silva), Lactogal Produtos Alimentares S.A. (Eng. Rita Costa) and Firmenich (Geneva) for readily provide me samples so many times.

To Prof. Dr. Marco Reis for introducing me to the world of statistic models, and for all the patience for my doubts.

To Dr. Pedro Cruz and Prof. José Gaspar Martinho for the technical analysis.

To the international entities that tested my polymers, Monash University, Zeus and Fontis.

To Croda, ExxonMobil and Hopax, which supplied me so appreciated samples.

To my office colleagues and friends, Deividson and Mónica, for all the work breaks and coffees.

To Kinga Grenda, my PhD partner and English teacher, for your support and friendship over the last three years, a big thank you.

To all my loyal and dear friends who have always been there, a very special thank you. You know who you are.

To Marie Curie Actions for the funding, through the grant agreement FP7-PEOPLE-2013-ITN-604825.

Last, but definitely not least, my deepest thank you to my parents, Aurora and Pedro, for always believe in me, help me and look after me. There is no words to express how grateful I am for having you in my life.

My special thank you as well to my sister, Carolina, my grandparents, Celeste and Manuel, and remaining family, my godmother, Miguel, Lino, Gina, Rosário, Tó, Rita, João, Luís, Francisca and Lara. You are the best.

Finally, to the best boyfriend in the world, António, for the unconditional support and patience, and for always put a smile on my face. Also, of course, for all the hours waiting in the airport and for presenting me to the navigation pane.

For all of you, my most sincere and heartfelt thank you.

---

## ABSTRACT

Oily wastewater, which constitute a large part of industrial wastewaters, can contain emulsified oil and surfactants, a wide variety of hydrocarbons and related contaminants, inorganic salts and organic matter. Conventional treatment techniques include dissolved air flotation, gravity separation, chemical breaking of emulsions, coagulation and flocculation. However, these techniques have several drawbacks, such as complex operational procedures, low efficiency in the case of small-diameter oil droplets and a large amount of sludge produced, which, in itself, represents an environmental and economic problem. Flocculation of oily wastewaters employ often polymers designed for other applications and used at dosages tenfold higher than for those used in sludge dewatering. Hence, it is not surprising that companies with such oily wastes, including dairies, food-processing or edible oil producers, are often reluctant to try to recover assets from their water resource while they are still recoverable (i.e. in the plant).

The main purpose of this work is twofold: the development of novel flocculants to treat oily wastewaters, especially from food industry, and to use more health-friendly formulations in their synthesis. In this way, it is possible to produce a specific product to treat a defined wastewater, avoiding the problems of having to overdose polymers designed for other types of waters. Besides this, it is also possible to do this development using processes that are safer for health, replacing the hazardous compounds used in their synthesis, especially the aromatic compounds.

The first step to synthesize the target products was the development of health-friendly formulations for inverse-emulsion polymerization of well-known polyelectrolytes (copolymers of acrylamide and 2-(acryloyloxy) ethyltrimethyl ammonium chloride), replacing the traditional

organic phase and optimizing the surfactant formulations. The procedures established proved to be able to polymerize the expected flocculants and the characterization techniques showed that the products synthesized had the suitable characteristics for the final applications, not much different from the characteristics of the polymers produced in the traditional media.

The second stage was the synthesis of cationic and anionic polyelectrolytes based on acrylamide monomer and using cationic, anionic and neutral hydrophobic monomers different from the well-known copolymer combination, selected by their reactivity with acrylamide, affinity for oily mixtures and price. The monomers [3-(methacryloylamino)propyl] trimethylammonium chloride (MAPTAC), acrylamido-2-methyl-1-propanesulfonic acid (Na-AMPS), ethyl acrylate (EA), lauryl methacrylate (LMA) and stearyl methacrylate (SMA) were chosen to develop the copolymers Poly(AAm-MAPTAC) and Poly(AAm-Na-AMPS), and the terpolymers Poly(AAm-MAPTAC-SMA), Poly(AAm-Na-AMPS-EA), Poly(AAm-Na-AMPS-LMA) and Poly(AAm-Na-AMPS-SMA). Polymers with several charge densities were produced by inverse-emulsion polymerization, using the previously mentioned health-friendly formulations as the synthesis media. The polyelectrolytes were synthesized as co- or terpolymers, including or not the introduction of a hydrophobic monomer. Three different hydrophobic monomers were tested, varying in the length of the hydrophobic chain. The obtained polymers were extensively characterized, studying their composition and final morphology. It was shown that the selected monomers combination was able to be polymerized using the selected method, leading to stable products, and that the composition of the final polymers has an important influence on its final characteristics, which proved to be suitable for the final application.

The performance tests of the developed polyelectrolytes, applied as flocculants, were carried out using industrial effluents from olive oil mill, dairy and potato crisps manufacturing industries. The base performance indicators used were the reduction of turbidity, chemical oxygen demand (COD) and total solids, for each dosage and pH tested. In general, the developed flocculants revealed very good performance in the reduction of turbidity, showing reductions above 90% for the tested wastewaters, without needing further addition of any aids other than the variation of the pH. Cationic polyelectrolytes, based on acrylamide and MAPTAC monomers, performed better for olive oil mill effluent treatment, while anionic polyelectrolytes, based on acrylamide and Na-AMPS monomers, showed better results in the treatment of dairy and potato crisps manufacturing effluents. The introduction of hydrophobicity proved to be beneficial for the treatment efficiency, although an optimum content could be defined for each case. A comparison with reference copolymers also based

on acrylamide monomer, usually used in these treatments, namely flocculants of similar charge and charge density supplied by Aqua+Tech Specialities SA., showed that polymers developed in this study exhibited higher efficiencies at lower dosages, suggesting a positive effect of the introduction of suitable hydrophobicity in flocculant structure.

Finally, an evaluation of the flocculation process was performed using the effluent from potato crisps manufacturing industry, revealing that laser diffraction spectroscopy (LDS) is a suitable technique for the flocculation monitoring in real effluents. It was possible to prove that this technique can be used to supply information about the flocculation kinetics, supplying, simultaneously, information on the evolution of flocs structure with time. Thus, it will be possible, in the future, to use this technique as a pre-screening methodology to select a range of best flocculants for a specific application, which will avoid making an intensive use of expensive pilot trials, which can be minimized.

Using data obtained from the LDS monitoring, a statistical model was developed as well, in order to identify the most important flocculant parameters influencing the flocs size and structure. The results obtained suggested that hydrodynamic diameter, charged fraction and concentration are the parameters having stronger influence in the characteristics of flocs obtained using copolymers, while charged fraction, concentration and hydrophobic content have a stronger effect on the characteristics of the flocs produced using terpolymers. These predictive models, are also capable of future industrial use for the selection of flocculants for specific/target applications.

As results of the studies conducted, a wide range of flocculants was prepared, apparently with suitable characteristics for application in the treatment of oily wastewaters from organic nature. The developed flocculants and application procedures on oily wastewaters treatment show to be very promising, suggesting to be worthy of pursuing in research with the view to achieve a possible future practice at an industrial scale. The same applies to the monitoring methodology developed, which was applied for the first time in this work, to follow the flocculation process in a real effluent.

This work is inserted in a European Project of European Industrial Doctorates (FP7 Marie Curie-EID), involving the collaboration of a company with large experience in polyelectrolytes production, especially tuned polymers, which is also partner of the Project.



---

## RESUMO

As águas residuais oleosas, que constituem uma grande parte das águas residuais industriais, podem conter óleo e surfactantes, uma grande variedade de hidrocarbonetos e contaminantes relacionados, sais inorgânicos e matéria orgânica. As técnicas convencionais de tratamento incluem flutuação por ar dissolvido, separação por gravidade, quebra química de emulsões, coagulação e floculação. No entanto, estas técnicas têm várias desvantagens, como procedimentos operacionais complexos, baixa eficiência no caso de gotas de óleo de pequeno diâmetro e uma grande quantidade de lama produzida, o que, por si só, representa um problema ambiental e económico. A floculação de águas residuais oleosas aplica muitas vezes polímeros projetados para outras aplicações, que são utilizados em doses dez vezes superiores às utilizadas na desidratação de lamas. Assim, não é surpreendente que as empresas com resíduos oleosos, incluindo indústrias de laticínios, produtores de alimentos ou de óleos alimentares, geralmente se mostrem relutantes em recuperar ativos de seus efluentes enquanto ainda são recuperáveis (isto é, na planta).

O objetivo principal deste trabalho é duplo e inclui o desenvolvimento de novos floculantes para tratar as águas residuais oleosas, especialmente da indústria alimentar, e o uso de formulações mais favoráveis à saúde na sua síntese. Desta forma, é possível produzir um produto específico para o tratamento de águas residuais definidas, evitando problemas como a sobredosagem de polímeros destinados a outros tipos de águas. Além disso, também é possível fazer esse desenvolvimento usando processos menos prejudiciais para a saúde, substituindo os compostos perigosos utilizados na síntese, especialmente os compostos aromáticos.

O primeiro passo para sintetizar os produtos em questão foi o desenvolvimento de formulações favoráveis à saúde, para a polimerização em emulsão-inversa de polieletrólitos largamente usados como floculantes (copolímeros de acrilamida e acrilato de 2-(dimetilamino)etil quaternizado), substituindo a fase orgânica tradicional e o surfactante na formulação de síntese. O procedimento estabelecido demonstrou a capacidade de polimerizar os floculantes previstos, e as técnicas de caracterização mostraram que os produtos sintetizados possuíam as características adequadas para a aplicação final, e não muito diferentes das características dos polímeros produzidos com as formulações tradicionais.

A segunda fase incluiu a síntese de polieletrólitos catiônicos e aniônicos usando acrilamida (AAm) e monómeros catiônicos, aniônicos e hidrofóbicos, diferentes da combinação de copolímeros já usada, selecionados pela sua reatividade com a acrilamida, afinidade para misturas oleosas e custo. Os monómeros cloreto de 3-trimetilamoniopropil-metacrilamida (MAPTAC), ácido acrilamido-2-metil-1-propanosulfônico (Na-AMPS), acrilato de etilo (EA), metacrilato de dodecil (LMA) e metacrilato de octadecil (SMA) foram escolhidos para desenvolver os copolímeros Poli(AAm-MAPTAC) e Poli(AAm-Na-AMPS) e os terpolímeros Poli(AAm-MAPTAC-SMA), Poli(AAm-Na-AMPS-EA), Poli(AAm-Na-AMPS-LMA) e Poli(AAm-Na-AMPS-SMA). Os polímeros foram produzidos com várias densidades de carga por polimerização por emulsão-inversa, utilizando as formulações favoráveis à saúde mencionadas anteriormente como meio de síntese. Os polieletrólitos foram sintetizados como co- ou terpolímeros, incluindo ou não a introdução de um monômero hidrofóbico. Foram testados três monómeros hidrofóbicos diferentes, variando no comprimento da cadeia hidrofóbica. Os polímeros obtidos foram caracterizados, analisando sua composição e morfologia final. Mostrou-se que as combinações de monómeros selecionados foram possíveis de ser polimerizadas usando o método selecionado, originando produtos estáveis, e que a composição final dos polímeros tem uma relevante influência nas suas características, que provaram ser adequadas para a aplicação final.

Os testes de desempenho dos polieletrólitos desenvolvidos, aplicados como floculantes, foram realizados em efluentes industriais de natureza orgânica das indústrias de fabricação de azeite, laticínios e produção de batatas fritas. Os indicadores de desempenho utilizados foram a redução da turbidez, da carência química de oxigênio (CQO) e de sólidos totais, para as várias dosagens e pHs testados. Em geral, os floculantes desenvolvidos revelaram um desempenho favorável na redução da turbidez, apresentando reduções acima de 90% para as águas residuais testadas, sem necessidade de adição adicional de outros auxiliares, além da alteração do pH. Os polieletrólitos catiônicos, constituídos por monómeros de acrilamida e

MAPTAC, mostraram melhores resultados no tratamento do efluente de lagar de azeite, enquanto os polieletrólitos aniônicos, constituídos por monómeros de acrilamida e Na-AMPS, apresentaram melhores resultados no tratamento de efluentes da indústria de laticínios da produção de batatas fritas. A introdução da hidrofobicidade provou ser benéfica na eficiência do tratamento, embora possa ser definida uma quantidade ótima para cada caso. Uma comparação com os copolímeros de referência, também construídos por acrilamida e geralmente utilizados nestes tratamentos, nomeadamente floculantes de carga e densidade de carga semelhantes, fornecidos pela Aqua+Tech Specialties SA, mostraram que os polímeros desenvolvidos neste estudo apresentaram melhores eficiências com o uso de doses inferiores, sugerindo como efeito positivo a introdução da hidrofobicidade adequada na estrutura do floculante.

Finalmente, uma monitorização do processo de floculação foi realizada, utilizando o efluente da indústria de produção de batatas fritas, revelando que a espectroscopia de difração laser (LDS) é uma técnica adequada para o acompanhamento da floculação em efluentes reais. Foi possível provar que esta técnica pode ser usada para fornecer informações sobre a cinética de floculação, fornecendo, simultaneamente, informações sobre a evolução da estrutura dos flocos com o tempo. Assim, no futuro, será possível usar esta técnica como uma metodologia de pré-seleção de uma gama de melhores floculantes para uma aplicação específica, o que reduzirá o uso intensivo de ensaios piloto dispendiosos, que poderão assim ser minimizados.

Com base nos dados obtidos a partir da monitorização por LDS, um modelo estatístico foi desenvolvido para identificar as características dos floculantes com mais influência no tamanho e estrutura dos flocos obtidos. Os resultados alcançados sugerem que o diâmetro hidrodinâmico, a fração carregada e a concentração de floculante são os parâmetros que têm maior influência nas características dos flocos obtidos usando copolímeros, enquanto a fração carregada, a concentração e o conteúdo hidrofóbico têm um efeito mais evidente nas características dos flocos produzidos usando terpolímeros. Estes modelos preditivos, também poderão ser usados industrialmente no futuro para a seleção de floculantes para aplicações específicas.

Como resultado dos estudos realizados, uma ampla gama de floculantes foi produzida, aparentemente com características adequadas para aplicação no tratamento de águas residuais oleosas de natureza orgânica. Os floculantes desenvolvidos e os procedimentos de aplicação no tratamento de águas residuais oleosas mostram ser muito promissores, sugerindo que a sua pesquisa deve prosseguir com o objetivo de alcançar futuramente uma possível prática em



escala industrial. O mesmo se aplica à metodologia de monitorização desenvolvida, que foi aplicada em efluentes reais pela primeira vez neste trabalho, para acompanhar o processo de floculação.

Este trabalho está inserido num Projeto Europeu de Doutoramentos Industriais Europeus (FP7 Marie Curie-EID), envolvendo a colaboração de uma empresa com grande experiência em produção de polielectrólitos, sendo também parceira do Projeto.

---

# LIST OF CONTENTS

<b>Acknowledgements</b> .....	i
<b>Abstract</b> .....	iii
<b>Resumo</b> .....	vii
<b>Nomenclature</b> .....	xxv
<b>Chapter 1</b>	
<b>Introduction</b> .....	1
1. Project Motivation.....	3
2. Objectives .....	5
3. Thesis Outline .....	7
<b>Chapter 2</b>	
<b>State of the art</b> .....	9
1. Oily wastewaters .....	11
1.1. Organic oily wastewater treatments.....	12
2. Polyelectrolytes .....	19
2.1. Synthesis of polyelectrolytes .....	19
2.2. Applications of polyelectrolytes .....	21
3. Flocculation	
3.1. Flocculation mechanisms.....	25
3.2. Flocculants in wastewater treatment .....	28
3.2.1. Cationic polyelectrolytes .....	28
3.2.2. Anionic polyelectrolytes.....	31

3.2.3.	Hydrophobically modified polyelectrolytes.....	32
3.3.	Flocculation of industrial oily effluents.....	35
3.3.1.	Olive oil mill effluent.....	36
3.3.2.	Dairy effluent.....	39
3.3.3.	Effluent from the manufacturing of fried snacks.....	44
4.	Relevance for the present work .....	47

### **Chapter 3**

	<b>Health-friendly synthesis formulations .....</b>	<b>49</b>
1.	Introduction.....	51
2.	Polyelectrolyte synthesis.....	55
2.1.	Materials.....	55
2.2.	Experimental description .....	56
2.2.1.	Inverse-emulsion polymerization.....	56
2.2.2.	Isolation of polyelectrolytes.....	57
2.2.3.	Characterization techniques.....	57
2.3.	Results and discussion.....	61
3.	Preliminary evaluation of performance .....	67
3.1.	Experimental description .....	67
3.2.	Results and discussion.....	67
4.	Conclusions.....	69

### **Chapter 4**

	<b>Synthesis of novel polyelectrolytes.....</b>	<b>71</b>
1.	Introduction.....	73
2.	Cationic polyelectrolytes .....	75
2.1.	Experimental.....	75
2.1.1.	Materials.....	75
2.1.2.	Inverse-emulsion polymerization.....	75
2.1.3.	Isolation of polymers.....	77
2.1.4.	Characterization techniques.....	77
2.2.	Results and discussion.....	78
3.	Anionic polyelectrolytes.....	83
3.1.	Experimental.....	83
3.1.1.	Materials.....	83
3.1.2.	Inverse-emulsion polymerization.....	83

3.1.3.	Isolation of polymers.....	85
3.1.4.	Characterization techniques .....	85
3.2.	Results and discussion .....	87
4.	Conclusions .....	95
<b>Chapter 5</b>		
	<b>Application of the novel polyelectrolytes in industrial effluents.....</b>	<b>97</b>
1.	Introduction .....	99
2.	Olive oil mill industry effluent.....	101
2.1.	Procedure to evaluate flocculation performance.....	101
2.2.	Initial wastewater characterization.....	101
2.3.	Results and discussion .....	103
3.	Dairy industry effluent.....	115
3.1.	Procedure to evaluate flocculation performance.....	115
3.2.	Initial wastewater characterization.....	115
3.3.	Results and discussion .....	116
4.	Potato crisps manufacturing industry effluent .....	127
4.1.	Procedure to evaluate flocculation performance.....	127
4.2.	Initial wastewater characterization.....	127
4.3.	Results and discussion .....	128
5.	Conclusions .....	139
<b>Chapter 6</b>		
	<b>Flocculation process analysis.....</b>	<b>141</b>
1.	Introduction .....	143
2.	Flocculation process monitored by LDS .....	147
2.1.	Experimental.....	147
2.1.1.	Materials .....	147
2.1.2.	Flocculation tests .....	147
2.2.	Results and discussion .....	149
3.	Experimental design methodology .....	161
3.1.	Methods.....	161
3.2.	Results and discussion .....	161
3.2.1.	Case 1: charged fraction, hydrodynamic diameter and concentration as predictor variables and SE as response variable, using OLS regression for copolymers.....	163

3.2.2.	Case 2: charged fraction, hydrodynamic diameter and concentration as predictor variables and d0.5 as response variable, using OLS regression for copolymers .....	167
3.2.3.	Case 3: hydrophobic content, number of carbons in hydrophobic chain, charged fraction, hydrodynamic diameter and concentration as predictor variables and SE as response variable, using OLS regression for terpolymers.....	169
3.2.4.	Case 4: hydrophobic content, number of carbons in hydrophobic chain, charged fraction, hydrodynamic diameter and concentration as predictor variables and d0.5 as response variable, using OLS regression for terpolymers.....	173
3.2.5.	Case 5: hydrophobic content, number of carbons in hydrophobic chain, charged fraction, hydrodynamic diameter and concentration as predictor variables and SE as response variable, using OLS regression for co- and terpolymers .....	175
3.2.6.	Case 6: hydrophobic content, number of carbons in hydrophobic chain, charged fraction, hydrodynamic diameter and concentration as predictor variables and SE as response variable, using PLS regression for co- and terpolymers .....	177
3.2.7.	Case 7: hydrophobic content, number of carbons in hydrophobic chain, charged fraction, hydrodynamic diameter and concentration as predictor variables and d0.5 as response variable, using OLS regression for co- and terpolymers .....	181
3.2.8.	Case 8: hydrophobic content, number of carbons in hydrophobic chain, charged fraction, hydrodynamic diameter and concentration as predictor variables and d0.5 as response variable, using PLS regression for co- and terpolymers .....	182
4.	Conclusions.....	187
<b>Chapter 7</b>		
	<b>Final remarks</b> .....	189
1.	Final Conclusions.....	191
2.	Recommendations for future work.....	195
	<b>References</b> .....	197
	<b>Appendix</b> .....	223
	Appendix A .....	225
	Appendix B .....	243
	Appendix C .....	289
	Appendix D.....	305

---

## LIST OF TABLES

<b>Table 2.1</b> Specifications of liquid wastewater to be disposed in public systems, in Portugal. Adapted from Decreto-Lei n° 236/98 of 01-08-1998.....	17
<b>Table 2.2</b> Oily wastewaters treatment by combined technologies reported in the literature. ..	18
<b>Table 2.3</b> Summary of linear cationic polyelectrolytes used as flocculants in previous studies, including structure, monomers and testing medium. ....	30
<b>Table 2.4</b> Summary of linear anionic polyelectrolytes used as flocculants in previous studies, including structure, monomers, and testing medium. ....	32
<b>Table 2.5</b> Summary of hydrophobically modified polyelectrolytes used as flocculants in previous studies, including structure, monomers, and testing medium.....	34
<b>Table 2.6</b> Removal efficiencies of olive mill wastewater treatment using coagulation-flocculation processes.....	38
<b>Table 2.7</b> Removal efficiencies of dairy wastewater treatment using coagulation-flocculation processes. ....	43
<b>Table 3.1</b> Trade name and chemical composition of the health-friendly organic phases used.	53
<b>Table 3.2</b> Comparison between traditional and alternative health-friendly oils used in inverse-emulsion polymerizations. ....	55
<b>Table 3.3</b> Monomers ratios in the feed mixture and organic phases used for the copolymers production. 40 series for 40 wt% of AETAC, 60 series for 60 wt% of AETAC and 80 series for 80 wt% of AETAC. ....	57

<b>Table 3.4</b> Charged fractions calculated from the initial mass balance and estimated by titration for Poly(AAm-AETAC) copolymers. ....	61
<b>Table 3.5</b> Zeta potential measured by ELS, hydrodynamic diameter measured by DLS, Intrinsic viscosity in 0.05M NaCl calculated according with Huggins equation and weight-average molecular weight measured by SLS.....	65
<b>Table 3.6</b> Absorbance reduction for effluents from dairy and potato crisps manufacturing industries.....	68
<b>Table 4.1</b> Summary of the cationic polyelectrolytes developed. Initial composition at the beginning of the polymerization and organic phase used in the health-friendly formulation are described. Copolymers Poly(AAm-MAPTAC): 25MC, 25MP, 60MC and 60MP. Terpolymers Poly(AAm-MAPTAC-SMA): 25M1SC, 25M2SC, 60M1SC and 60M2SC. ....	77
<b>Table 4.2</b> Charged fractions for the cationic polyelectrolytes, calculated from the initial mass balance and estimated by titration. Poly(AAm-MAPTAC): 25MC, 25MP, 60MC and 60MP. Poly(AAm-MAPTAC-SMA): 25M1SC, 25M2SC, 60M1SC and 60M2SC. ....	79
<b>Table 4.3</b> Polyelectrolytes characterization: zeta potential, hydrodynamic diameter and weight-average molecular weight. Poly(AAm-MAPTAC): 25MC, 25MP, 60MC and 60MP. Poly(AAm-MAPTAC-SMA): 25M1SC, 25M2SC, 60M1SC and 60M2SC. ....	81
<b>Table 4.4</b> Summary of the anionic polyelectrolytes developed. Initial composition at the beginning of the polymerization and organic phase used in the health-friendly formulation are described. Copolymers Poly(AAm-Na-AMPS): 50AC, 80AC, 50AP and 80AP. Terpolymers Poly(AAm-Na-AMPS-EA): 50A1EC, 50A3EC, 80A1EC and 80A3EC. Terpolymers Poly(AAm-Na-AMPS-LMA): 50A1LC, 50A3LC, 80A1LC and 80A3LC. Terpolymers Poly(AAm-Na-AMPS-SMA): 50A1SC, 50A3SC, 80A1SC and 80A3SC.....	85
<b>Table 4.5</b> Charged fractions for anionic polyelectrolytes, calculated from the initial mass balance and estimated by elemental analysis. Poly(AAm-Na-AMPS): 50AC, 80AC, 50AP and 80AP. Poly(AAm-Na-AMPS-EA): 50A1EC, 50A3EC, 80A1EC and 80A3EC. Poly(AAm-Na-AMPS-LMA): 50A1LC, 50A3LC, 80A1LC and 80A3LC. Poly(AAm-Na-AMPS-SMA): 50A1SC, 50A3SC, 80A1SC and 80A3SC.....	88
<b>Table 4.6</b> Polyelectrolytes characterization: zeta potential, hydrodynamic diameter and weight-average molecular weight. Poly(AAm-Na-AMPS): 50AC, 80AC, 50AP and 80AP. Poly(AAm-Na-AMPS-EA): 50A1EC, 50A3EC, 80A1EC and 80A3EC. Poly(AAm-Na-AMPS-LMA): 50A1LC, 50A3LC, 80A1LC and 80A3LC. Poly(AAm-Na-AMPS-SMA): 50A1SC, 50A3SC, 80A1SC and 80A3SC.....	92
<b>Table 5.1</b> Characteristics of the industrial olive oil mill effluent sample. ....	102

<b>Table 5.2</b> Characteristics of dairy effluent sample tested before any treatment.....	115
<b>Table 5.3</b> Characteristics of the industrial potato crisps manufacturing effluent tested before any treatment. ....	127
<b>Table 6.1</b> Summary of the experimental value of SE after 6 minutes of flocculation for each cationic polyelectrolyte applied and maximum floc size for each concentration tested.....	157
<b>Table 6.2</b> Summary of the experimental value of SE after 6 minutes of flocculation for each anionic polyelectrolyte and maximum floc size for each concentration tested. ....	158
<b>Table 6.3</b> Summary of the experimental values used for the experimental design methodology.....	162
<b>Table 6.4</b> Effect summary table for case 1. ....	163
<b>Table 6.5</b> Summary of fit report for case 1.....	164
<b>Table 6.6</b> Analysis of variance report for case 1. ....	165
<b>Table 6.7</b> Parameter estimates report for case 1.....	165
<b>Table 6.8</b> Effect summary table for case 2. ....	167
<b>Table 6.9</b> Summary of fit report for case 2.....	167
<b>Table 6.10</b> Analysis of variance for case 2. ....	168
<b>Table 6.11</b> Parameter estimates for case 2.....	168
<b>Table 6.12</b> Effect summary for case 3. ....	170
<b>Table 6.13</b> Summary of fit for case 3.....	170
<b>Table 6.14</b> Analysis of variance for case 3. ....	170
<b>Table 6.15</b> Parameter estimates for case 3. ....	171
<b>Table 6.16</b> Effect summary for case 4. ....	173
<b>Table 6.17</b> Summary of fit for case 4.....	173
<b>Table 6.18</b> Analysis of variance for case 4. ....	173
<b>Table 6.19</b> Parameter estimates for case 4. ....	174
<b>Table 6.20</b> Parameter estimates for case 5.....	176
<b>Table 6.21</b> Model comparison summary for case 6. ....	178
<b>Table 6.22</b> Parameter estimates for case 7.....	181
<b>Table 6.23</b> Model comparison summary for case 8.....	183





---

## LIST OF FIGURES

<b>Figure 2.1</b> Schematic view of a charge neutralisation mechanism.....	26
<b>Figure 2.2</b> Polymer bridging between particles.....	27
<b>Figure 2.3</b> Charge neutralization flocculation by patch mechanism. Arrows show attraction of opposite charged zones.....	28
<b>Figure 3.1</b> Representation of the synthesis reaction for Poly(AAm-AETAC), using as monomers acrylamide and AETAC.....	56
<b>Figure 3.2</b> A typical representation of a Debye plot <sup>218</sup> . .....	59
<b>Figure 3.3</b> <sup>13</sup> C NMR spectra for the Poly(AAm-AETAC) copolymer 80_Marcol82.....	62
<b>Figure 3.4</b> ATR-FTIR spectra for Poly(AAm-AETAC) copolymers developed in the same health-friendly formulation (Carnation as organic phase), 40_Carnation, 60_Carnation and 80_Carnation. ....	63
<b>Figure 3.5</b> ATR-FTIR spectra of Poly(AAm-AETAC) copolymers obtained, with similar charge density and employing different health-friendly formulations, 60_Puresyn4, 60_Carnation and 60_Marcol82. ....	63
<b>Figure 4.1</b> Representation of the synthesis reaction for Poly(AAm-MAPTAC), using monomers of acrylamide and MAPTAC.....	76
<b>Figure 4.2</b> Representation of the synthesis reaction for Poly(AAm-MAPTAC-SMA), using monomers of acrylamide, MAPTAC and SMA. ....	76

<b>Figure 4.3</b> ATR-FTIR spectra for the cationic polyelectrolytes prepared. Copolymers Poly(AAm-MAPTAC): 25MC, 25MP, 60MC and 60MP. Terpolymers Poly(AAm-MAPTAC-SMA): 25M1SC, 25M2SC, 60M1SC and 60M2SC. ....	80
<b>Figure 4.4</b> Schematic molecular structure of the final polymers obtained: Poly(AAm-Na-AMPS) (a), Poly(AAm-Na-AMPS-EA) (b), Poly(AAm-Na-AMPS-LMA) (c) and Poly(AAm-Na-AMPS-SMA) (d). ....	84
<b>Figure 4.5</b> ATR-FTIR spectra examples for some of the anionic polyelectrolytes prepared. Poly(AAm-Na-AMPS): 50AC and 80AC. Poly(AAm-Na-AMPS-EA): 80A1EC and 80A3EC. Poly(AAm-Na-AMPS-LMA): 80A1LC and 80A3LC. Poly(AAm-Na-AMPS-SMA): 50A3SC and 80A3SC.....	90
<b>Figure 4.6</b> <sup>1</sup> H NMR spectra for some of the polyelectrolytes prepared. Poly(AAm-Na-AMPS): 80AC. Poly(AAm-Na-AMPS-EA): 80A1EC and 80A3EC. Poly(AAm-Na-AMPS-LMA): 80A1LC and 80A3LC.....	91
<b>Figure 5.1</b> Zeta potential distribution for the olive oil mill effluent at pH 3, 5 and 10.....	103
<b>Figure 5.2</b> Turbidity reduction curves for the industrial olive oil mill effluent treated by cationic copolymers Poly(AAm-MAPTAC): 25MC, 25MP, 60MC and 60MP, at three different pHs. ....	105
<b>Figure 5.3</b> Turbidity reduction curves for the industrial olive oil mill effluent treated by cationic terpolymers Poly(AAm-MAPTAC-SMA): 25M1SC, 25M2SC, 60M1SC and 60M2SC, at three different pHs.....	106
<b>Figure 5.4</b> Turbidity reduction curves for the industrial olive oil mill effluent treated by reference polymer, AplineFloc DHMW, at various pHs. ....	107
<b>Figure 5.5</b> COD and total solids removal after the treatment of the industrial olive oil mill effluent with 60MC, 60MP, 60M1SC and 60M2SC flocculants, in optimized conditions of pH (pH 3) and concentration (103 mg/L for 60MC and 60MP, and 78 mg/L for 60M1SC and 60M2SC).....	107
<b>Figure 5.6</b> Initial olive oil mill effluent (a) and effluent after treatment with flocculants 60MC (b), 60MP (c), 60M1SC (d), and 60M2SC (e), in optimized conditions of pH (pH 3) and concentration (103 mg/L for 60MC and 60MP, and 78 mg/L for 60M1SC and 60M2SC). .	108
<b>Figure 5.7</b> Turbidity reduction curves for the industrial olive oil mill effluent treated by the anionic copolymers Poly(AAm-Na-AMPS): 50AC, 80AC, 50AP and 80AP, at three different pHs. ....	109

<b>Figure 5.8</b> Turbidity reduction curves for the industrial olive oil mill effluent treated by anionic terpolymers Poly(AAm-Na-AMPS-EA): 50A1EC, 50A3EC, 80A1EC and 80A3EC, at three different pHs. ....	110
<b>Figure 5.9</b> Turbidity reduction curves for the industrial olive oil mill effluent treated by anionic terpolymers Poly(AAm-Na-AMPS-LMA): 50A1LC, 50A3LC, 80A1LC and 80A3LC, at three different pHs. ....	111
<b>Figure 5.10</b> Turbidity reduction curves for the industrial olive oil mill effluent treated by anionic terpolymers Poly(AAm-Na-AMPS-SMA): 50A1SC, 50A3SC, 80A1SC and 80A3SC, at three different pHs. ....	111
<b>Figure 5.11</b> Turbidity reduction curves for the industrial olive oil mill effluent treated by reference anionic polymer, AplineFloc Z1, at various pHs. ....	112
<b>Figure 5.12</b> COD and total solids removal after the treatment of the industrial olive oil mill effluent with 80AC, 80AP, 80A1EC, 80A3EC, 80A1SC and 80A3SC flocculants, in optimized conditions of pH (pH 3) and concentration (78 mg/L for 80AC, 80A1EC and 80A3EC, and 53 mg/L for 80AP, 80A1SC and 80A3SC). ....	113
<b>Figure 5.13</b> Zeta potential distribution for the dairy industry effluent at pH 3, 5 and 10. ....	116
<b>Figure 5.14</b> Turbidity reduction curves for the industrial dairy effluent treated by cationic copolymers Poly(AAm-MAPTAC): 25MC, 25MP, 60MC and 60MP, at three different pHs. ....	117
<b>Figure 5.15</b> Turbidity reduction curves for the industrial dairy effluent treated by cationic terpolymers Poly(AAm-MAPTAC-SMA): 25M1SC, 25M2SC, 60M1SC and 60M2SC, at three different pHs. ....	118
<b>Figure 5.16</b> Turbidity reduction curves for the industrial dairy effluent treated by a reference cationic polymer, AplineFloc DHMW, at various pHs. ....	119
<b>Figure 5.17</b> Turbidity removal curves for dairy industry effluent treated by anionic copolymers Poly(AAm-Na-AMPS): 50AC, 80AC, 50AP and 80AP, at various pH. ....	121
<b>Figure 5.18</b> Turbidity removal curves for dairy industry effluent treated by anionic terpolymers Poly(AAm-Na-AMPS-EA): 50A1EC, 50A3EC, 80A1EC and 80A3EC, at various pH. ....	122
<b>Figure 5.19</b> Turbidity removal curves for dairy industry effluent treated by anionic terpolymers Poly(AAm-Na-AMPS-LMA): 50A1LC, 50A3LC, 80A1LC and 80A3LC, at various pH. ....	122
<b>Figure 5.20</b> Turbidity removal curves for dairy industry effluent treated by anionic terpolymers Poly(AAm-Na-AMPS-SMA): 50A1SC, 50A3SC, 80A1SC and 80A3SC, at various pH. ....	123

<b>Figure 5.21</b> Turbidity removal curves for dairy industry effluent treated by anionic reference polymer, AlpineFloc Z1, at various pH. ....	124
<b>Figure 5.22</b> COD and total solids removal for treatment of dairy industry effluent with 50AC, 80AC, 80A1EC, 80A3EC, 80A1SC, 80A3SC and AlpineFloc Z1, in optimized conditions of pH (pH 5) and concentration (78 mg/L for 50AC, 53 mg/L for 80AC, 80A1EC, 80A3EC, 80A1SC and 80A3SC, and 27 mg/L for AlpineFloc Z1).....	124
<b>Figure 5.23</b> Initial dairy effluent (a) and effluent after treatment with flocculants 80AC (b), 80A3EC (c) and 80A3SC (d), in optimized conditions of pH (pH 5) and concentration (53 mg/L for 80AC, 80A3EC and 80A3SC). ....	125
<b>Figure 5.24</b> Zeta potential distribution for potato crisps manufacturing effluent at pH 3, 6 and 10.....	128
<b>Figure 5.25</b> Turbidity reduction curves for the industrial potato crisps manufacturing effluent treated by cationic copolymers Poly(AAm-MAPTAC): 25MC, 25MP, 60MC and 60MP, at three different pHs.....	129
<b>Figure 5.26</b> Turbidity reduction curves for the industrial potato crisps manufacturing effluent treated by cationic terpolymers Poly(AAm-MAPTAC-SMA): 25M1SC, 25M2SC, 60M1SC and 60M2SC, at three different pHs. ....	130
<b>Figure 5.27</b> Turbidity reduction curves for the industrial potato crisps manufacturing effluent treated by reference cationic polymer, AplineFloc DHMW, at various pHs. ....	131
<b>Figure 5.28</b> COD and total solids removal after the treatment of the industrial potato crisps manufacturing effluent with cationic flocculants 60MC, 60MP and AlpineFloc DHMW, in optimized conditions of pH (pH 6) and concentration (27 mg/L for 60MC and 53 mg/L for 60MP and AlpineFloc DHMW).....	131
<b>Figure 5.29</b> Initial potato crisps manufacturing effluent (a) and effluent after treatment with flocculants 60MC (b) and 60MP (c), in optimized conditions of pH (pH 6) and concentration (27 mg/L for 60MC and 53 mg/L for 60MP). ....	132
<b>Figure 5.30</b> Turbidity removal curves for potato crisps manufacturing industry effluent treated by anionic copolymers Poly(AAm-Na-AMPS): 50AC, 80AC, 50AP and 80AP, at various pH. ....	134
<b>Figure 5.31</b> Turbidity removal curves for potato crisps manufacturing industry effluent treated by anionic terpolymers Poly(AAm-Na-AMPS-EA): 50A1EC, 50A3EC, 80A1EC and 80A3EC, at various pH. ....	134

<b>Figure 5.32</b> Turbidity removal curves for potato crisps manufacturing industry effluent treated by anionic terpolymers Poly(AAm-Na-AMPS-LMA): 50A1LC, 50A3LC, 80A1LC and 80A3LC, at various pH. ....	135
<b>Figure 5.33</b> Turbidity removal curves for potato crisps manufacturing industry effluent treated by anionic terpolymers Poly(AAm-Na-AMPS-SMA): 50A1SC, 50A3SC, 80A1SC and 80A3SC, at various pH.....	135
<b>Figure 5.34</b> Turbidity removal curves of potato crisps manufacturing industry effluent treated by reference anionic polymer, AlpineFloc Z1, at various pH. ....	136
<b>Figure 5.35</b> COD and total solids removal for the treatment of potato crisps manufacturing industry effluent with anionic flocculants 50AC, 50AP, 50A1EC, 50A3EC, 50A1LC, 50A3LC and AlpineFloc Z1, in optimized conditions of pH (pH 6) and concentration (13 mg/L for 50A1EC, 27 mg/L for 50AC, 50AP, 50A3EC and 50A3LC, 53 mg/L for 50A1LC and 104 mg/L for AlpineFloc Z1). ....	137
<b>Figure 5.36</b> Initial potato crisps manufacturing effluent (a) and effluent after treatment with anionic flocculants 50AC (b), 50AP (c) 50A3EC (d) and 50A3LC (e), in optimized conditions of pH (pH 6) and concentration (27 mg/L for 50AC, 50AP, 50A3EC and 50A3LC). ....	137
<b>Figure 6.1</b> Representation of the flocs size distribution for a stirring speed test, using 13 mg/L of the polyelectrolyte 60MC. ....	148
<b>Figure 6.2</b> Example of the plot of scattering intensity versus $q$ , with identification of the first and second regions. ....	149
<b>Figure 6.3</b> Particle size distribution of the initial effluent, pH 6 adjusted effluent and floc size distribution at the end of the flocculation with terpolymer 80A3EC, for the optimum dosage concentration (13 mg/L). ....	150
<b>Figure 6.4</b> Evolution of average particle size ( $d_{50}$ ) over time obtained via LDS for three different flocculant dosages for copolymers 60MC and 60MP. ....	151
<b>Figure 6.5</b> Evolution of average particle size ( $d_{50}$ ) over time obtained via LDS for three different flocculant dosages for copolymers 50AC, 80AC, 50AP and 80AP. ....	152
<b>Figure 6.6</b> Evolution of average particle size ( $d_{50}$ ) over time obtained via LDS for three different flocculant dosages for terpolymers 50A1EC, 50A3EC, 80A1EC and 80A3EC.....	152
<b>Figure 6.7</b> Evolution of average particle size ( $d_{50}$ ) over time obtained via LDS for three different flocculant dosages for terpolymers 50A1LC, 50A3LC, 80A1LC and 80A3LC. ....	153
<b>Figure 6.8</b> Evolution of floc structure (SE) for the cationic copolymers 60MC and 60MP, at different concentrations. ....	154

<b>Figure 6.9</b> Evolution of floc structure (SE) for the anionic copolymers 50AC, 80AC, 50AP and 80AP, at different concentrations. ....	155
<b>Figure 6.10</b> Evolution of floc structure (SE) for the anionic terpolymers 50A1EC, 50A3EC, 80A1EC and 80A3EC, at different concentrations.....	155
<b>Figure 6.11</b> Evolution of floc structure (SE) for the anionic terpolymers 50A1LC, 50A3LC, 80A1LC and 80A3LC, at different concentrations. ....	156
<b>Figure 6.12</b> Floc size after 6 min, for the higher concentration tested (13 mg/L), as function of hydrophobic content quantified by the ratio (mol%) of monomer 3 in the polyelectrolyte composition.....	159
<b>Figure 6.13</b> SE after 6 min, for the higher concentration tested (13 mg/L), as function of hydrophobic content quantified by the ratio (mol%) of monomer 3 in the polyelectrolyte composition.....	160
<b>Figure 6.14</b> Prediction profiler plots for case 1. ....	166
<b>Figure 6.15</b> Actual versus predicted plot for case 1. ....	167
<b>Figure 6.16</b> Prediction profiler for case 2. ....	169
<b>Figure 6.17</b> Actual versus predicted plot for case 2. ....	169
<b>Figure 6.18</b> Prediction profiler for case 3. ....	172
<b>Figure 6.19</b> Actual versus predicted plot for case 3. ....	172
<b>Figure 6.20</b> Prediction profiler for case 4. ....	175
<b>Figure 6.21</b> Actual versus predicted plot for case 4. ....	175
<b>Figure 6.22</b> Prediction profiler for no hydrophobic content for case 5. ....	176
<b>Figure 6.23</b> Prediction profiler for maximum hydrophobic content (3 mol%) for case 5. ...	177
<b>Figure 6.24</b> Variable importance plot for case 6. ....	179
<b>Figure 6.25</b> Prediction profiler for no hydrophobic content for case 6. ....	180
<b>Figure 6.26</b> Prediction profiler for maximum hydrophobic content (3 mol%), for case 6. ..	180
<b>Figure 6.27</b> Prediction profiler for no hydrophobic content for case 7. ....	181
<b>Figure 6.28</b> Prediction profiler for maximum hydrophobic content (3 mol%), for case 7. ..	182
<b>Figure 6.29</b> Variable importance plot for case 8. ....	183
<b>Figure 6.30</b> Prediction profiler for no hydrophobic content for case 8. ....	184
<b>Figure 6.31</b> Prediction profiler for maximum hydrophobic content (3 mol%), for case 8....	185

---

# NOMENCLATURE

---

---

## A

AA	Acrylic acid
AAm	Acrylamide
AETAC	[2-(Acryloyloxy)ethyl]trimethyl ammonium chloride
AMHP	Acryloylamino-2-hydroxypropyl trimethylammonium chloride
ATR	Attenuated total reflection
ATRP	Atom transfer radical polymerization

---

## B

BA	Butylacrylate
BOD	Biochemical oxygen demand

---

## C

$^{13}\text{C}$ NMR	Carbon-13 nuclear magnetic resonance
COD	Chemical oxygen demand

---

## D

DADMAC	Diallyldimethylammonium chloride
DAF	Dissolved air flotation
$d_f$	Fractal dimension
DLS	Dynamic light scattering
DMA	Dimethylacrylamide
DMAEMA	Dimethylaminoethyl methacrylate



DMAPA	Dimethylaminopropylamine
DMC	Methacryloxyethyl trimethylammonium chloride
DPA	Decyloxypropylamine
DTPA	Diethylenetriaminepentaacetic acid
<hr/>	
<b>E</b>	
EA	Ehtyl acrylate
EDTA	Ethylendiamine tetraacetic acid
ELS	Electrophoretic light scattering
<hr/>	
<b>F</b>	
FBRM	Focused beam reflectance microscopy
FRP	Free radical polymerization
FTIR	Fourier-transform infrared spectroscopy
<hr/>	
<b>H</b>	
<sup>1</sup> H NMR	Proton nuclear magnetic resonance
HLB	Hydrophilic-lipophilic balance
HPA	Hexyloxypropylamine
<hr/>	
<b>I</b>	
IAF	Induced air flotation
INCI	International nomenclature of cosmetic ingredients
IV	intrinsic viscosity
<hr/>	
<b>L</b>	
LMA	Lauryl methacrylate
LS	Light scattering
<hr/>	
<b>M</b>	
MA	Methyl acrylate
MAPMS	Methacryloxypropyl trimethoxysilane
MAPTAC	[3-(Methacryloylamino)propyl] trimethylammonium chloride
MBS	Metabisulfite
MF	Microfiltration
MMA	Methyl methacrylate
MPDSA	[3-(Methacryloylamino)propyl] dimethyl(3-sulfopropyl) ammonium hydroxide
MW	Molecular weight

---

<b>N</b>	
Na-AMPS	2-Acrylamido-2-methyl-1-propanesulfonic acid sodium salt solution
Na-SS	Sodium 4-styrene sulfonate
NVP	Vinyl pyrrolidone

---

<b>O</b>	
OME	Olive oil mill effluents

---

<b>P</b>	
PAA	Polyacrylamide
PAC	Polyaluminum chloride
PDADMAC	Poly-N,N-diallyl-N,N-dimethylammonium
PDI	Polydispersity index
PFS	Polyferric sulfate
PPVS	Potassium polyvinyl sulfate

---

<b>R</b>	
RAFT	Reversible addition fragmentation transfer
RI	Refractive index
RO	Reverse osmosis

---

<b>S</b>	
SAS	Sodium allylsulfonate
SE	Scattering exponent
SEC	Size exclusion chromatography
SLS	Static light scattering
SMA	Stearyl methacrylate
SS	Suspended solids

---

<b>T</b>	
TBHP	Tert-butyl hydroperoxide
TP	Total phosphorus
TS	Total solids
TSS	Total suspended solids

---

<b>U</b>	
UF	Ultrafiltration
UV	Ultraviolet
UVI	Ultraviolet irradiation

---

**V**

VA	Vinyl acetate
VTMS	Vinyltrimethoxysilane

---

# CHAPTER 1

## Introduction



## 1. PROJECT MOTIVATION

Water purification is one of the most inevitable problems affecting people throughout the world. Industrial wastewaters, as well as recirculating process water, are the most problematic and challenging, and have become a concern as scarcity and costs of water both become more pronounced. The development and implementation of solutions to enhance water treatment is crucial.

Several traditional and advanced technologies have been applied in wastewater treatment, including coagulation, flocculation, flotation, adsorption, membrane filtration, biological or electrolytic methods. Flocculation is an extensively used technique in separation processes applied in many industrial wastewaters treatment, both on its own or complementing other treatments. This process is able to remove suspended and dissolved impurities, using a simply, versatile and low energy technology.

Although the progress in treatment methodologies, flocculation still remains a vital process for treating industrial wastewater, since, for instance, if used as a pre-treatment it can reduce the costs and increase the efficiency of the following treatment stages. Hence, the development of suitable flocculation products to optimize the process performance is very important. Moreover, the concern with environmental issues is increasing, shifting the research toward to the use of eco-friendly alternatives to the products frequently used in numerous industries. Finally, due to the extensive variety of wastewaters produced, the selection and tuning of the ideal solution and treatment conditions is still a time-consuming mission, based in screening of several potential options.

To improve the flocculant's performance, specific customized products for a target application should be developed. Additionally, to meet the actual environmental requirements, these must be developed using eco-friendly approaches. A deep analysis of their performance in real wastewaters must also be performed, in order to establish a correspondence between flocs quality, and thus ability to be removed, and flocculant characteristics.

This project results from a collaboration between the Department of Chemical Engineering of the University of Coimbra and the company Aqua+Tech Specialities SA. This company develops and markets water soluble polymers for application in water treatment, cosmetics, and other industries such as paper, tissue or mining. The main goals of the project include the synthesis of novel, more environmentally-friendly flocculants, based on new monomers combinations, and optimization of their performance, through the identification of the ideal

process parameters. Also, the most appropriate flocculant for each process wastewater must be identified using an advanced screening process, in which the floc properties resulting from the application of a product (flocculant or mixture of additives) with specific characteristics, can be easily evaluated, minimizing, in this way, expensive pilot trials. Target industries for the testing can include sugar, textile, food processing, pharmaceutical, oil, among others.

## 2. OBJECTIVES

Oily wastewaters present one of the main challenges not only in petroleum, petrochemical and steel industries but also in food, cosmetics and pharmaceutical production. Several complementary techniques, e.g. coagulation/flocculation, floatation, centrifugation and filtration, have been developed to remove pollutants from oily waters. However the coagulation/flocculation method is one of the most widely used for its capability of destabilizing and aggregating colloids. Flocculation is a crucial process in industrial wastewater treatment and can be used in combination with other more advanced techniques. Organic polymeric flocculants are extensively used currently due to their remarkable ability to flocculate efficiently at low dosage, producing large aggregates, in contrast to what happens when using traditional inorganic coagulants. Some traditional water treatment flocculants are now applied in oily waters, however, as they were designed for aqueous systems without oil, the dosages required are high and the efficiency relatively low. The improvement of methods to break oil-in-water emulsions would have a notable utility and environmental benefits. The cost allied to treatment operations would be more economical if the level of residual oil in treated wastewaters or the speed of the oil removal process could be improved. These enhancements would provide an economic and environmental benefits.

Some of the flocculants mentioned previously have been conventionally synthesized using aliphatic mineral oils, thus presenting a mild health concern as they are irritants. Consequently, it might be useful to develop treatment methodologies that combine all the environmental concerns, being health-friendly, efficient and cost-effective.

This 3-years thesis is designed, specifically, to produce novel cationic and anionic flocculants to treat oily wastewaters, mostly organic in nature, using more health-friendly formulations in their synthesis. The study aims to overcome the disadvantages of using traditional water treatment chemicals in oily waters, tuning the flocculants to the target application, and reducing simultaneously the amount of additives and the dosages, providing a more economical process. The development of these products will be based in the inverse-emulsion polymerization technique. The final products obtained will be tested in real industrial oily effluents, from three different activities. Besides this, the development of a new screening methodology to pre-select the best flocculant for a specific application, based on laser diffraction spectroscopy (LDS) will be performed. This methodology will also supply information of the flocs morphology (size and structure) which will highlight the underlying flocculation mechanisms. Moreover, and based on the data obtained, predictive models to



select the best flocculant for each type of wastewater will be developed. All this will allow the detailed analysis of the obtained aggregates using the different flocculation products and find the combination of characteristics that result in specific floc properties.

### 3. THESIS OUTLINE

In addition to the present Chapter 1, which includes as well an introduction to the project motivation and the study objectives, this thesis is divided in six more chapters. In Chapter 2, a state of the art on oily wastewaters, origins and treatment procedures, polyelectrolytes and flocculation process is presented.

Since one of the objectives of this work was to develop health-friendly formulations to synthesize the novel flocculants, it was first necessary to evaluate the viability of possible health-friendly media to synthesize polymers using inverse-emulsion polymerization. This was accessed through the polymerization of a well-known polymer (copolymer of acrylamide and 2-(acryloyloxy) ethyltrimethyl ammonium chloride), and evaluation of its performance, which is described in Chapter 3. This preliminary study allowed to choose three new health-friendly media which were then used in further synthesis.

The first step regarding the development of novel flocculants was to evaluate potential monomers suitable to produce innovative flocculants to treat oily wastewaters. From this list, the selected monomers need to be economically viable and able to be polymerized together to produce high-molecular weight cationic and anionic polyelectrolytes. The previous selected monomers were then polymerized in the selected health-friendly formulations, and the resulting copolymers and terpolymers were characterized in terms of composition, hydrodynamic diameter, charge and molecular weight, which is presented in Chapter 4.

Chapter 5 describes the application of the developed flocculants in the treatment of industrial oily effluents, namely from olive oil mill, dairy and potato crisps manufacturing industries. The main performance indicator used was reduction of turbidity, though chemical oxygen demand and total solids reduction were also assessed.

In Chapter 6, an analysis of the flocculation process is presented. Monitoring of flocculation is performed using laser diffraction spectroscopy, and results regarding floc size and structure, and flocculation kinetics are shown. Moreover, statistical models are developed in order to find the combination of flocculant characteristics that can be used to better predict the properties of the obtained flocs.

Finally, Chapter 7 includes the main conclusions from this work, along with recommendations for future work.

*List of publications resulting from this work (available in Appendix D):*

Paper 1: Lourenço, A.; Arnold, J.; Gamelas, J. A. F.; Rasteiro, M. G. A more eco-friendly synthesis of flocculants to treat wastewaters using health-friendly solvents. *Colloids Polym. Sci.* **2017**, 295 (11), 2123–2131.

Paper 2: Lourenço, A.; Arnold, J.; Gamelas, J. A. F.; Cayre, O. J.; Rasteiro, M. G. Pre-treatment of industrial olive oil mill effluent using low dosage health-friendly cationic polyelectrolytes. *J. Environ. Chem. Eng.* **2017**, 5, 6053–6060.

Paper 3: Lourenço, A.; Arnold, J.; Cayre, O. J.; Rasteiro, M. G. Flocculation treatment of an industrial effluent: performance assessment by Laser Diffraction Spectroscopy. *Reply to reviews submitted to Ind. Eng. Chem. Res.* **2017**.

Paper 4: Lourenço, A.; Arnold, J.; Gamelas, J. A. F.; Cayre, O. J.; Rasteiro, M. G. Health-friendly anionic polyelectrolytes for application as flocculants in industrial oily effluents. *In preparation*.

Paper 5: Lourenço, A.; Arnold, J.; Gamelas, J. A. F.; Cayre, O. J.; Rasteiro, M. G. Statistical modelling of the complex interaction of relevant flocculant's properties on the floc size and structure. *In preparation*.

*List of communications resulting from this work:*

- Lourenço, A.; Arnold, J.; Rasteiro, M. G. Development of flocculants using healthy-friendly processes. *2nd EuCheMS Congress on Green and Sustainable Chemistry* (Lisbon, Portugal)

- Lourenço, A.; Arnold, J.; Rasteiro, M. G. Improvement of flocculants to treat oily waters using health-friendly processes. *11th International Symposium on Polyelectrolytes* (Moscow, Russia)

- Lourenço, A.; Arnold, J.; Hunkeler, D.; Rasteiro, M. G. A health-friendly approach by replacing traditional oils in the synthesis of polyelectrolyte flocculants for effluents treatment. *Marie Skłodowska-Curie actions ESOF satellite event – Researcher and Society* (Manchester, UK)

- Lourenço, A.; Arnold, J.; Cayre, O. J.; Rasteiro, M. G. Treatment of oily industrial effluents using health-friendly synthesized cationic flocculants. *10th World Congress of Chemical Engineering* (Barcelona, Spain)

---

# CHAPTER 2

## State of the art



## 1. OILY WASTEWATERS

Oily wastewaters present one of the main challenges regarding disposal, not only in petroleum, petrochemical and steel industries, but also in food, cosmetics and pharmaceutical production. Oil contaminated effluents have been documented as one of the most concerned pollution sources<sup>1</sup>. They are considered as hazardous industrial wastewaters due to the presence of toxic substances such as phenols, petroleum hydrocarbons and polyaromatic hydrocarbons, which are inhibitory to plant and animal growth and also are carcinogenic and mutagenic to humans<sup>2</sup>. Also, the low biodegradability of such substances impact the biosphere, since the oil in water fields, even in very low concentration, will decrease the penetration of light and the oxygen transfer, affecting aquatic life<sup>3</sup>. The composition of oily wastewaters is different depending on which industrial field it came from, however, independently of the source, a significant part of oil is present in emulsified form, which typically leads to a difficult separation from the water phase. There are, in general, two great classes of oily waters: those from biological/organic sources (e.g. animal fats, vegetable oils), which mostly result from food processing and are mainly composed of triglycerides; and those with a mineral origin (e.g. hydrocarbon solvents, gasoline, lube oils, paraffins), which typically result from crude manufacturing processes, and consist in a mixture of hydrocarbons with different chemical configurations<sup>4</sup>.

The dispersion and stability of oil in aqueous medium have impact in the separation methods needed for the treatment. The type of oil-water mixture is usually classified in four categories, according to the physical form: free oil, dispersed oil, emulsified oil or dissolved oil<sup>5</sup>. Free oil typically occurs when an oil-water mixture has droplets greater than or equal to 150  $\mu\text{m}$  in size and the oil rises quickly to the water surface, under quiescent conditions, due to the imbalance of forces. A dispersed oil is characterized by the presence of a droplet size range between 20 and 150  $\mu\text{m}$ , and it is an array of fine droplets stabilized by their electrical charges and other particle forces, without the presence of surfactants. An emulsified oil mixture has droplet sizes smaller than 20  $\mu\text{m}$  and it has a similar distribution as dispersed oil, but its stability is enhanced due to the chemical action of surface active substances. Finally, an oil-water mixture, where the oil is truly chemically dissolved or dispersed in extremely fine droplets that are not visible to the naked eye, is classified as dissolved oil and the oil droplets size is normally less than 5  $\mu\text{m}$ <sup>6</sup>. The latter is, in many countries, not regulated for discharge.

Oils and greases in wastewaters need to be removed before water is reused in closed-loop processes, or discharged into sewer systems or surface waters. Excessive discharges of oil and grease to sewerage systems can lead to problems such as blockage of sewers and interference

with biological treatment processes. Thus, oily wastewaters should not be discharged directly to the environment, though they are in many countries including those which supply foodstuffs to Europe. There are in literature several technologies for their treatment<sup>4</sup>, though the broad diversity of chemical and physical characteristics create a challenge in their management<sup>7</sup>.

### **1.1. Organic oily wastewater treatments**

As previously referred, the presence of oily wastes in wastewater can occur in many forms. Of the four forms, the treatment to separate either dissolved or emulsified oil is in general more complex and expensive. Usually, the addition of chemicals like detergents or other solubilizing agents is used in industry to induce the oil to stay in the emulsified form, requiring, thereafter, the need of harsh processes, during the treatment, to break the emulsion before the oil can be successfully removed. Moreover, many of the industrial organic oily effluents also contain high solids content, which need to be separated to clarify the system.

#### *Conventional methods*

Removal of oil and grease from wastewater resulting of oil processing industries can be performed by the use of widely established techniques. The removal of oil and grease depends on the condition of the oil-water mixture, so the type of process must be carefully selected. The treatment of oily wastewaters comprises a primary or gravity treatment step, followed by a secondary process, and, when needed, a tertiary step for enhancement of quality parameters<sup>4</sup>.

The primary treatment is used to remove free oils, including tramp oils, from the emulsion or suspension. Common techniques include gravity methods, with quiescent flow conditions for the free oil to move to surface, or centrifugal separation. This is only really possible for oil levels higher than 1000 mg/L. In cases of high solids content in the wastewater, sedimentation promoted by stagnant conditions is used to settle those solid impurities<sup>6</sup>. The secondary treatment is aimed to reduce the organic load that remains after the primary treatment, break emulsions and remove dispersed oil that does not separate spontaneously under the action of gravity. Generally, breaking of emulsions can be stimulated by several chemical, electrical and physical methods. Chemical approaches are the most usual and destabilize the oil droplets by the addition of ingredients such as aluminum or iron salts. The more recent electrical processes work by the coagulation promoted by consumable electrodes, which release metallic

coagulants to the wastewater<sup>8</sup>. Lastly, physical methods, such as heating, centrifugation, filtration or dissolved air flotation, promote coalescence through change of physical properties of the droplets or by application of forces<sup>6</sup>. When further effluent refinement is need, a tertiary treatment is applied, involving a more selective technology. Tertiary treatment includes physicochemical processes to reduce the levels of dissolved organic and inorganic compounds. Nanofiltration, reverse osmosis and activated carbon adsorption are the main treatments used<sup>9</sup>.

### *Primary treatment*

Primary treatment takes advantage of gravity and density difference to separate the oil in free form, solids and unstable colloidal particles from the aqueous matrix. Gravity separators consist in tanks or channels where the horizontal flow is low and does not affect oil rise or solids deposition, allowing quiescence of the wastewater<sup>10</sup>. Viscosity and density difference are the factors with main influence in the oil rise velocity. Since the higher the viscosity of the fluid the lower the rising rate, decrease the viscosity by increasing the temperature can enhance phase separation. Another alternative is the change of the separator design in order to have larger surface areas, which will decrease the surface-loading rate and improve the separation. At the end of the quiescence time, the oil and sludge are removed from the top and bottom of the separator, respectively. The less dense part is gathered through an oil-skimming device, at the surface, while the sediment is removed manually or using a scraper and a sludge pump, from the bottom<sup>6</sup>.

### *Secondary treatment*

The secondary treatment is the step that requires more attention, since it aims to remove the remaining oil dispersed in very small droplets, stabilised by surface active agents or particle forces.

When water contains more than about 5% oil it no longer behaves like an aqueous, Newtonian, fluid but rather like a non-Newtonian fluid. The main difference is the propagation of charge. Water has a high dielectric constant whereas oil has a much lower one. Therefore, charge mechanisms in water prevail and we can clean the water, for example, with chemical approaches. In hydrocarbon dominated systems we must first coalesce the droplets to reduce the total surface area. Therefore, oily waters treatment requires, in addition



to the presence of electrostatic forces, the manipulation of the surface (interfacial chemistry). Several different chemical methods can be used to break the emulsion in oily wastewaters and the degree of oil removal is dependent on the physical nature of the oil and its droplet size<sup>11,12</sup>. This breakage can be achieved using pH changes, coagulants, polymers or surface destabilization by adsorbing molecules at the oil-water interface. Oil droplets in an aqueous medium usually carry a surface charge, and as two droplets approach each other, electrostatic repulsion prevents them from forming larger aggregates. Using chemical additives destabilizes the dispersed phase by reducing the charge on the surface of oil droplets, leading to emulsion break and promoting droplet coalescence. In real organic oily wastewaters, dispersed phase includes not only the oily material but also solid particles, thus dispersed phase aggregation can be accomplished by two mechanisms: coagulation and flocculation, which in most cases are complementary. These processes use inorganic salts and organic polymers, known as coagulants and flocculants, respectively. The most used coagulants in oily wastewater treatment include iron and aluminum salts, which are cheap and easily available<sup>13-16</sup>. Also, for this purpose, calcium salts, as calcium chloride or lime, and polyaluminum chloride (PAC) have been used<sup>17-19</sup>. Nevertheless, chemical methods with inorganic salts has as disadvantage the large amount of hazardous sludge produced, which usually involves a costly treatment<sup>20</sup>. Thus, organic and biodegradable products have been tested to replace inorganic salts. Polyelectrolytes and organic polymers are often used for direct flocculation of the oil droplets. They either change the surface charge of the oil droplets or form aggregates of the solid particles by bridging mechanisms, which are then easier to separate from the aqueous medium<sup>21</sup>. In all cases, chemical treatment promotes coalescence of oil droplets and aggregation of solids, which can then be removed by several techniques. The most common natural organic coagulant used in oily wastewater treatment is chitosan. It is a natural polymer and it is believed to work based on adsorption and coagulation<sup>20,22</sup>.

Separation of aggregated particles from the aqueous system can be achieved using physical methods, such as sedimentation or flotation, being dissolved air flotation (DAF) the most used<sup>16,23</sup>. DAF uses compressed air that is dissolved in the liquid, under pressure, and comes out from the solution as very fine gas bubbles when the pressure is reduced. The gas bubbles rise to the surface carrying attached oil and suspended solids. The feed stream, often treated with flocculating agents, enters the inlet mixing chamber as does the recycle stream, which is supersaturated with air. The stream then enters the flotation zone, where the oil/solids/bubble assemblies migrate to the surface and are mechanically skimmed. Coagulants and flocculants stimulate the aggregation of oil droplets and also enhance the

adhesion of oil to the air bubbles, facilitating the flotation of oily material<sup>15</sup>. With similar characteristics, induced air flotation (IAF) techniques produce larger bubbles and higher turbulence. IAF is a process on which a mixture of air is forced through nozzles providing the shearing action necessary to create millions of bubbles, which are then dispersed throughout the flotation chamber. Oil and suspended solids in the air bubbles are carried to the surface of the water forming a foam and a skimmer paddle sweeps the oil and solids into an overflow compartment<sup>24</sup>. The major differences between DAF and IAF are the bubble size and mixing conditions. In DAF, the bubbles are about 50–60  $\mu\text{m}$  in diameter, while in IAF bubbles are bigger (around an order of magnitude larger). Recently, other flotation techniques have been presented and tested for wastewater treatment. Foam separation is based in spontaneous formation of air bubbles in the present of a foaming agent, which improves the interaction between flocs and bubbles, bringing to the surface oily matter and suspended solids<sup>17</sup>.

On the other hand, electrical techniques are based in electrochemistry and increase the coagulation and flocculation efficiencies. Electrocoagulation involves generation of coagulants *in situ*, through consumable electrodes, while in electroflotation, gas bubbles are generated by the electrolysis of water, simulating an air flotation process<sup>12</sup>. The most important advantage of the electrical methods is that usually they are combined in a treatment process, leading to high efficiency increases. Moreover, the use of electroflotation reduces the amount of hazardous sludge produced, since the electrodes are insoluble<sup>25,26</sup>.

Application of physical separation methods, such as heating, coalescence or filtration, can be an alternative when gravity separation, chemical and electrochemical methods lead to insufficient results<sup>27</sup>. Centrifugation is also a possible technique to separate the aggregated part from aqueous medium and can be applied directly to oil-in-water emulsions. However, this method needs the addition of coagulants or demulsifiers in order to remove the smallest oil droplets and reduce chemical oxygen demand (COD) levels. Membrane technology is used in oily wastewater and it has a high oil removal efficacy, low energy cost and compact design compared with other treatment methods<sup>28</sup>. This technology has several advantages including stable effluent quality and small area requirement. The chemical nature of the membrane may have a big effect on the filtration performance, as well as the affinity of the membrane material to the oil and water. Membranes can vary from superhydrophobic to superhydrophilic, and from superoleophilic to superoleophobic. One more significant characteristic is the membrane pore size, which defines the process as microfiltration (MF), ultrafiltration (UF) or reverse osmosis (RO). MF membranes give higher permeate fluxes but have a higher risk of oil permeation. Since MF has larger pores, it is often used as pre-

treatment in a two-step membrane treatment<sup>29,30</sup>. UF membranes, which have tighter pores, have been selected in most applications to ensure steady permeate quality, and have been used as secondary or tertiary treatment. However, high operating pressures and specific cleaning and regeneration methods are necessary to guarantee a smoothly running of UF<sup>29</sup>. Membrane filtration is most successful in separating emulsified and dissolved oil, as all the other kinds of oily wastes can be removed readily by the mechanical separations previously described. The major drawback in membrane processes is the decline in permeate flux with time, mainly because of concentration, polarization and membrane fouling – due to surfactant or oil adsorption on the pore walls – gel layer formation or pore blocking by oil droplets. Furthermore, the porosity of the membrane limits its flow rate to a certain volume per day<sup>31</sup>. This can be minimized through suitable pre-treatments, in order to remove a considerable part of oil and suspended solids, and careful choice of membrane parameters and operating conditions<sup>15</sup>.

#### *Biological treatment*

Biological reactors are a cheap and easily accessible technology in wastewater treatment. The biological treatment uses the microbial metabolism to convert organic pollutants in to harmless stable substances. Oils from biological sources are commonly easier to biodegrade, and are mostly constituted by soluble substances and very finely divided droplets<sup>18</sup>. Presently, this process involves equipment comprising more actual technology and is used usually in activated sludge and biological filter techniques. In the biological filter technique the microorganisms are attached to the filter when the wastewater goes through the filter surface from top to down. During the adsorption of organic pollutants, the simultaneous decomposition takes place by microorganisms. Several microorganisms have shown able to degrade oil wastewater, such as bacteria and yeasts<sup>32-34</sup>. Drawbacks related with biological treatment processes include the volume of sludge produced, the fact that wastewaters flow is often low, the relatively large plants required and the consequent large investment costs.

#### *Tertiary treatment*

Tertiary treatment is normally used when an effluent with great quality is desired, for instance for water reuse. NF and RO membranes can provide a very high quality permeate, however they are expensive methods to operate<sup>35</sup>. Furthermore, RO allow the separation of salts,

frequently found in oily effluents from petroleum and food industries. Advanced oxidation processes are also alternatives for tertiary treatment, due to their ability to eliminate dissolved organic matter, reducing COD content<sup>36</sup>. Adsorption processes by porous materials, such as activated carbon, is as well an alternative to remove the remaining low molecular weight dissolved organic contaminants, colour related compounds. Phenols are particularly susceptible to irreversible adsorption onto some activated carbons<sup>37</sup>. Many materials may be used for the manufacture of activated carbon, such as petroleum coke, sawdust, lignite, coal, peat, wood, charcoal, nutshell and fruit pits. At an industrial level, pollutants are removed from wastewater by using the columns and contractors filled with the required adsorbent<sup>38</sup>. Advantages of activated carbon include simple application and the possibility of regeneration and reuse. Examples of membranes used in oily wastewaters include ceramic, carbon or porous glass membranes<sup>39-41</sup>.

#### *Combined Technologies*

Many of the above-mentioned treatment methods effectively reduce the amount of oil present in wastewaters, but in most cases a combination of two or more separation processes (integrated or hybrid process) is required to reach the most severe discharge standards. In Table 2.1 it is possible to see the standard limits of some parameters for liquid wastewaters to be disposed in public systems, in Portugal. The treatment processes used to clean wastewaters to be discharged must ensure that the final effluent follows these specifications.

Table 2.1 Specifications of liquid wastewater to be disposed in public systems, in Portugal. Adapted from Decreto-Lei n° 236/98 of 01-08-1998.

<b>Parameters</b>	<b>Standard limit</b>
Temperature (°C)	Increase of 3°C
pH	6.9-9.0
BOD (mg/L)	40
COD (mg/L)	150
TS (mg/L)	60
Aluminum (mg/L)	10
Total Iron (mg/L)	2.0
Oils and greases (mg/L)	15
Phenols (mg/L)	0.5

Integrated processes may reduce total production cost, energy consumption, and capital cost, and give better oil separation efficiency. The selection of a suitable integrated or hybrid process depends on the characteristics of the oily effluent to be treated, and some of the most commonly used are described briefly in the literature (Table 2.2).

Table 2.2 Oily wastewaters treatment by combined technologies reported in the literature.

Methods	Source of oily wastewater	Reference
Physicochemical and biological treatment	Vegetable oil refinery	Pandey <i>et al.</i> <sup>42</sup>
Filtration, demulsification/centrifugation, UF and peat bed filtration	Cutting oil residue from metalworking	Benito <i>et al.</i> <sup>43</sup>
Different types of membranes	Synthetic bilge water	Peng and Tremblay <sup>29</sup>
Advanced oxidation processes and biological filtration supported on granular activated carbon	Petroleum wastewater	Souza <i>et al.</i> <sup>44</sup>
Sedimentation, centrifugation, filtration and sorption on activated clay	Olive mill effluent	Al-Malah <i>et al.</i> <sup>45</sup>
Coagulation, sedimentation and sorption	Palm oil mill effluent	Ahmad <i>et al.</i> <sup>46</sup>
DAF and active sludge reactor and clarifier	Refinery wastewater	Otadi <i>et al.</i> <sup>47</sup>
DAF, acidification and coagulation	Biodiesel wastewater	Rattanapan <i>et al.</i> <sup>48</sup>
Acidification, electrocoagulation and biomethanization	Biodiesel wastewater	Siles <i>et al.</i> <sup>49</sup>
Membrane bioreactors, electrocoagulation and electroflotation	Simulated restaurant wastewater	Yang <i>et al.</i> <sup>50</sup>
Electroflotation and flocculation	Synthetic oil-in-water emulsion	Mostefa and Tir <sup>51</sup>
UF and RO	Refinery wastewater	Salahi <i>et al.</i> <sup>51</sup>
Flocculation and MF	Refinery wastewater	Zhong <i>et al.</i> <sup>52</sup>
Membrane bioreactor and UF	Synthetic wastewater containing fuel oil and lubricating oils	Scholz and Fuchs <sup>53</sup>
Coagulation and MF	Synthetic oily wastewater	Abbasi <i>et al.</i> <sup>54</sup>

Abbreviations: UF, Ultrafiltration; DAF, Dissolved air flotation; RO, Reverse osmosis; MF, Microfiltration.

## 2. POLYELECTROLYTES

Polyelectrolytes are water-soluble macromolecules from natural or synthetic sources, containing ionic charges along the polymer chain. According with their charges in side-chain groups or on the backbone, they can be classified into anionic (negative charge), cationic (positive charge) and amphoteric (both negative and positive charges)<sup>55</sup>. Chemical structure, charge density and molecular weight are the most important characteristics of polyelectrolytes. Depending on the type and distribution of charge, and low, medium or high molecular weight, they can be used for many applications in industry, namely in effluents treatment.

### 2.1. Synthesis of polyelectrolytes

Free radical polymerization (FRP) is the most widely method used in industry to obtain macromolecules. The FRP mechanism is based on highly reactive radicals that have the strong ability to add to double bonds, starting with decomposition of an initiator, which creates radicals. Then, in the presence of unsaturated bonds in the monomers, new radicals in the monomer units are generated and so on, leading to the polymer chain growing. FRP is a versatile polymerization technique, which can be applied in homogenous or heterogeneous processes, and in many reactor configurations, either continuous, batch or semi-batch<sup>56</sup>. Atom transfer radical polymerization (ATRP) and reversible addition fragmentation transfer (RAFT) have also been successfully applied in the synthesis of tailor-made polyelectrolytes with adjusted structure and molecular properties. In ATRP, the radicals are generated through a reversible redox process catalysed by a transition metal complex<sup>57</sup>. RAFT makes use of a chain transfer agent in the form of a dithio compound, which will react with the initiator after decomposition, to give transferred chains, assuring control over the generated polymer molecular weight and polydispersity<sup>58</sup>. From the generated free radicals, polymer chains grow by the addition of the intermediate radicals to monomers and terminate, as in a conventional FRP. Ultraviolet irradiation (UVI) polymerization is an easy operation process and environmental friendly, which allows the achievement of products with high molecular weight consuming low amounts of initiator and requiring short reaction times<sup>59</sup>. The previous types of polymerizations can be applied in several polymerization methodologies, such as solution polymerization, precipitation polymerization, suspension/emulsion polymerization or inverse-suspension/emulsion polymerization. Suspension or emulsion processes differ on the size of the polymer particles produced. Fluids containing droplets or particles smaller than about 1

$\mu\text{m}$  are known as emulsions (latex or colloids), and those containing particles larger than about  $1\ \mu\text{m}$  as suspensions<sup>60</sup>.

### *Solution polymerization*

Solution polymerization is carried out in solvents like water, formamide, formic acid, acetic acid or dimethylsulfoxide, which dissolve monomers and polymers. The kinetics of polymerization and properties of the final polymer are affected by the solvent, temperature, pH, presence of complexing agents, surfactants or chain transfer agents<sup>61</sup>. Very low chain transfer to the solvent and hindering the termination reaction, through protection of the propagating polymer radical, are the main advantages of the polymerization in aqueous media. Moreover, establishment of hydrogen bonds between monomers and water can increase the monomers reactivity<sup>62</sup>. On the other hand, solution polymerization has limitations in monomer conversion due to the high viscosity of the final polymer solution<sup>61</sup>. This techniques is used to produce polymers including vinyl acetate, acrylonitrile or esters of acrylic acid<sup>63,64</sup>.

### *Precipitation polymerization*

In precipitation polymerization, the reactions occur in a medium which dissolves the monomers, but not the polymer. The system starts in homogeneous conditions and then, as the polymerization continues, the precipitation of the polymer happens and the reaction becomes heterogeneous. In these conditions, the mixture never reaches high viscosities and the polymer isolation and purification is simplified. The typical solvents for this polymerization technique include acetone, tetrahydrofuran, acetonitrile, dioxane, ethanol and tertbutanol. Organic-aqueous systems are also used to facilitate the monomers dissolution<sup>65</sup>. Precipitation polymerization has the advantage of the absence of any stabilizer in the process, providing a quite simple, straightforward and highly efficient procedure for the preparation of uniform and clean polymer particles. On the other hand, with increasing solid loading of the reaction, collision between the particles might increase, causing coagulation. This coagulation during the polymerization affects the stability and leads to particles with larger size distribution and irregular morphologies. Also, separation of the product from the solvent can be difficult and expensive. Acrylonitrile in water is an example of a polymer synthesized using this technique<sup>66</sup>.

*Inverse-suspension/emulsion polymerization*

Nowadays, most of the commercial polyelectrolytes are synthesized by polymerization in inverse-emulsion. This process involves the dispersion of aqueous monomers solution in a continuous oil phase (water-in-oil). The process advantages include possibility of obtaining polymers with very high molecular weight, due to the high monomer concentration in the aqueous droplets distributed in the organic phase; high polymer content in the final product as result of good heat transfer in the reactor and low viscosity of the final dispersion; and simple post-treatment process due to easy handling of inverse latexes. Kinetics of the polymerization are affected by the nature and amount of stabilizer, stirring rate, organic solvent and temperature<sup>67</sup>. The main drawbacks include solids level of about 30-50%, transport costs that may be higher than for dried powders and it is also a hard and expensive method if a solid polymer product is required. The organic phases used include aromatic, aliphatic or halogenated hydrocarbons. The main examples of polymers produced by water-in-oil polymerization include polyacrylamide and water soluble acrylates<sup>68,69</sup>.

**2.2. Applications of polyelectrolytes**

Polyelectrolytes have many applications, mostly related to modifying flow conditions, inducing agglomeration or improving the stability of aqueous colloids and gels. Since they are water-soluble, they also have been used in biochemical and medical applications such as implant coatings and controlled drug release systems, besides environmental applications<sup>61,65</sup>.

Synthetic polyelectrolytes such as polyacrylamide and its copolymers have attracted much attention as flocculants for wastewater treatment. Polyelectrolytes with high molecular weight and medium to high charge densities have been applied as flocculants in direct flocculation or combined with inorganic coagulants like aluminum, ferric chloride or ferric sulphate. Polyelectrolytes with a large number of charges along the polymer chain can interact with charged particles of wastewater and destabilize the aqueous dispersion by charge neutralization, leading to the particles sedimentation and, thus, clarifying the system. The aforementioned feature also allows to promote the polyelectrolytes application in sludge dewatering<sup>70</sup>. The sludges are colloids which include two-phase systems and may be found in municipal wastes, pulp, paper and other industrial wastes. Mechanical assistance, such as mixing, centrifuging, vacuum or pressure, increase the drainage rate and the amount of water released from the sludge, and the dewatering performance is dependent of both the chemical treatment and the mechanical equipment. Furthermore, in mineral processing, the suspended



finer particles, from crushing and grinding, which must be separated from the liquid part, where the mineral of interest is in solution. This process can be facilitated using polyelectrolytes as flocculants to promote the thickening and concentration increase of foam flotation and clarification steps<sup>71</sup>.

Water-soluble polyelectrolytes are also used in many oilfield operations, including drilling, water flooding, and chemical flooding. Those polyelectrolytes include polyacrylamide, polyethylenimine, styrene and acrylic acid, among others<sup>72</sup>. To enhance oil recovery, the polymer acts as a viscosity modifier, increasing the viscosity of the aqueous phase. Thus, water-soluble polymers can be added to the flooding water to improve the water/oil mobility ratio, a key parameter in determining the efficiency in the process, since water's viscosity generally is much lower than the viscosity of the oil<sup>65</sup>.

Polyelectrolytes are one of the most important additives used in drilling fluids<sup>73</sup>. To prevent wellbore instability and dispersion of drilled cutting, polymeric additives are used in ecological-friendly water-based drilling fluids. Polyelectrolytes have high affinity for clay, and polymer adsorption is able to reduce the water content. Also, inhibitive properties of polyelectrolytes, related with the polymer structure, reduce the dispersion and disintegration of clay cuttings<sup>74</sup>. Possible polymeric additives can include copolymers of different kinds of monomers, such as acrylamide, acrylic acid and sodium 4-styrenesulfonate<sup>75</sup>.

Enhancement of soil stabilization to better control erosion, using synthetic and water-soluble polymers is, as well, an application of polyelectrolytes like copolymers of acrylic acid and acrylamide or poly-N,N-diallyl-N,N-dimethylammonium chloride (PDADMAC)<sup>76</sup>. Charged polyelectrolyte chains adsorb, through hydrogen bonding interaction between silanol and aluminum hydroxyl OH groups, at the soil particles surface and larger particles are formed by bridging mechanism. This allows holding smaller soil particles together, making the soil more resistant to the erosion forces and shear<sup>61</sup>.

Dispersing agents enhance the dispersion process and guarantee a fine particle size in the matrix. Polymeric dispersants containing ionic functional groups provide electrostatic and steric stabilization of particles and have good performance in keeping a uniform distribution of solid particles in the liquid phase, for instance in mineral ores, inorganic pigments in ceramics, and materials for the construction industry. They have been used in a wide variety of industries, including mining, ceramics, paint, ink, coating and construction<sup>77</sup>.

The rheological behaviour of polyelectrolytes also allows that they are applied in conditioners, cosmetics and shampoos<sup>78</sup>. Formulations for personal care products contain polymeric foam stabilizers and diamines for improvement of mildness and skin feel. Cationic polyelectrolytes, like PDADMAC, are used in conditioners and foam stabilizers, while anionic ones, like polysulfonic acid, are often used in hair-fixative polymers and gels<sup>65,79</sup>.

Retention agents are used in the papermaking industry and added in the paper machine to improve retention of fine particles and fillers during the formation of paper, and also of other papermaking chemicals, such as sizing and cationic starches. Cationic polyelectrolytes have been selected as retention aids, also referred as flocculants<sup>80</sup>. The improved retention of papermaking additives improves the operational efficiency of the paper machine, reduces the solids and organic loading in the process water loop, lowering the overall chemical costs. Usual polyelectrolytes used as retention aids include polyacrylamides, polyethyleneoxide and polyethyleneimine<sup>81,82</sup>. Polyelectrolytes also have potential application in papermaking as strength additives. The use of the synthetic polyelectrolytes such as poly(allylamine hydrochloride) or polyacrylic acid, combined with a natural polyelectrolyte, proved to increase considerably the paper properties<sup>83</sup>.

Sodium carboxymethyl cellulose is an example of a semi-synthetic polyelectrolyte with many applications in the food industry<sup>84</sup>. The edible sodium carboxymethyl cellulose can act as an emulsifying stabilizer in the drinks containing fat and protein, and can play a role in the gelling processes in the production of jelly, panna cotta, jam, among other foods<sup>85</sup>.



### 3. FLOCCULATION

Organic polyelectrolytes are extensively used, currently, as flocculants due to their ability to aggregate/flocculate efficiently at low dosage. Flocculation is the most extensively used separation process to remove suspended and dissolved solids, colloids and organic substances in industrial wastewater<sup>21</sup>. Generally, flocs formation involves several steps occurring sequentially, such as dispersion of the flocculant in the solution, diffusion near and to the solid-liquid interface, adsorption of the flocculant to the surface of the particles, collision of particles containing adsorbed agent with other particles, adsorption of the flocculant on the free surface of those neighbor particles in order to form aggregates and to enable growth of the microflocs to larger and stronger flocs by consecutive collisions and adsorption, or, alternatively, establishment of bonds between flocculant chains absorbed in different particles<sup>86</sup>.

To optimize the flocculation performance there are several parameters that need to be controlled during the process. The ideal amount of flocculant usually depends on the content of suspended solids and colloids in the wastewater and on the characteristics of the polymer, and the treatment success usually increases with the increase of flocculant input. However, the treatment efficiency can achieve a maximum and decrease if the input dosage is too high<sup>87</sup>. An important mechanical factor in the flocculation process is the stirring, which helps the contact between the flocculant and the suspended colloids in the system, allowing the formation of flocs, however can also lead to flocs breakage if excessive. There are two stages in the mixing process in a typical flocculation process, corresponding to a rapid and a slow stirring stage. The fast stirring is used to give a good dispersion of the flocculant after addition and to destabilize the colloidal system, while slow stirring is used to promote the flocs growth and limit the breakup of aggregates<sup>88</sup>.

#### 3.1. Flocculation mechanisms

Destabilization of colloids and suspensions by polymers can be associated to different flocculation mechanisms such as charge neutralization, polymer bridging and electrostatic patches interactions. These mechanisms are strongly related with the way adsorption of flocculants on particle surfaces occurs, which depends on the affinity between the polymer and the particle surface<sup>21</sup>.

### Charge neutralization

Charge neutralization is assumed as the main mechanism when the flocculant and the particle have opposite charge. The flocculation process can occur due to decrease of electrical repulsion force between colloidal particles, resulting from the reduction of surface charge (zeta potential), which facilitates initial aggregation of colloidal and fine suspended materials, as the result of Van der Waals forces of attraction (Figure 2.1). It has been reported that optimal flocculation occurs using polyelectrolytes dosages that are just the necessary amount to completely neutralize the particle charge, leading to a zeta potential close to zero. When this occurs, the particles start to agglomerate by the influence of the Van der Waals' forces and the suspension is destabilized<sup>89</sup>. When the amount of polymer used is too high, a charge reversal can happen and the particles will disperse again<sup>87</sup>. The flocs formed by charge neutralization can be loosely packed and fragile, which will lead to a slow settling<sup>90</sup>.

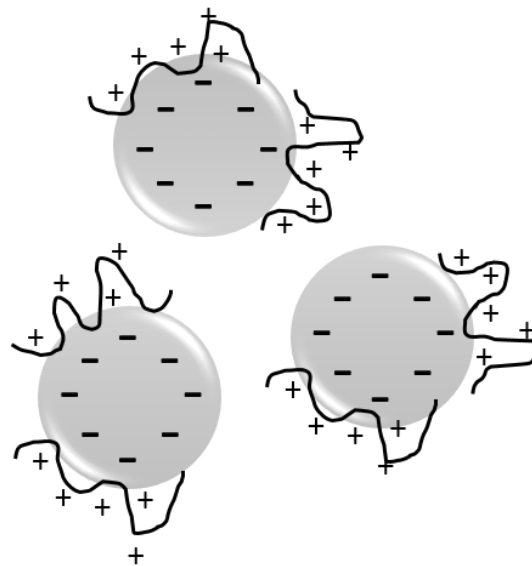


Figure 2.1 Schematic view of a charge neutralisation mechanism.

### Polymer bridging

Polymer bridging occurs when polymers with high molecular weight and low charge density are used. The long polymer chains adsorb on the particle surface and long loops extend in solution overpassing the electrical double layer<sup>91</sup>. The interaction of these polymer segments with other particles, with a charge opposite to that of the polymer, becomes possible and,

when occurring, leads to a ‘bridge’ between particles (Figure 2.2)<sup>24</sup>. It is well documented that polymer bridging can give much larger and stronger flocs when compared with other mechanisms. The polymer chains need to be long enough to extend from one particle to another, in order to perform an effective connection and, for this reason, a polymer with high molecular weight is preferred. If the amount of polymer is excessive, the particle surface will be over coated, which can lead to the situation where there is no available sites to ‘bridge’ with other particles and, in this way, the particles tend to repel. In contrast with this, if the adsorbed amount is too low it may not be enough to form bridging contact between particles. Again, this means that an optimal amount of polymer is needed and too high levels can result in restabilization of the colloidal particles<sup>87</sup>.

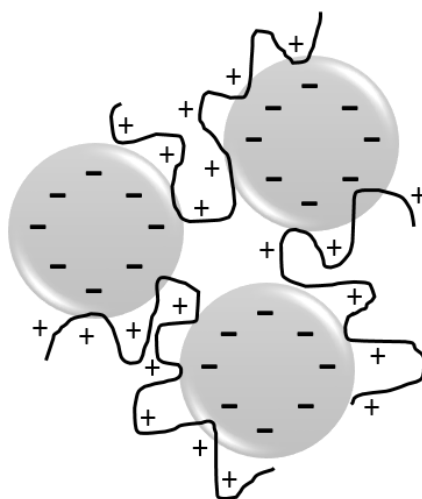


Figure 2.2 Polymer bridging between particles.

#### *Electrostatic patch*

Bridging capability is reduced when polyelectrolytes with low molecular weight and high charge density adsorb on the surface of oppositely charged particles, allowing the ‘electrostatic patch’ mechanism to occur (Figure 2.3). When a highly charged polymer with small chains adsorbs on a weakly oppositely charged surface it is physically impossible for the particle surface to be neutralized by the polyelectrolyte and achieve an overall neutrality. So, there is formation of charged ‘patches’ in the same surface where there are uncoated regions<sup>24</sup>. The consequence of this is the electrostatic attraction between patches and regions with opposite charge of different particles not covered by the polymer, leading to particle attachment and consequent flocculation. Flocs formed based on this mechanism are stronger than flocs

formed by simple charge neutralization in the presence of metal salts<sup>24</sup>. For an efficient electrostatic patch flocculation, the polymer charge density needs to be significantly high. If the charge density is too low, the bridging mechanism becomes more likely<sup>92</sup>.

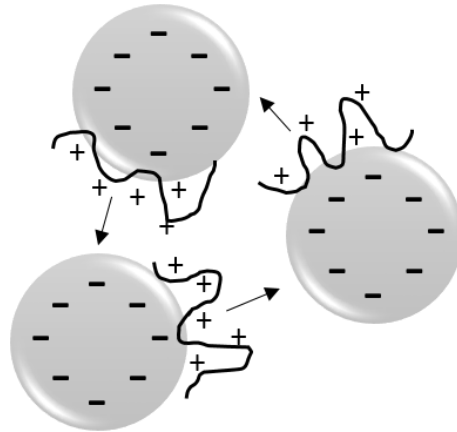


Figure 2.3 Charge neutralization flocculation by patch mechanism. Arrows show attraction of opposite charged zones.

## 3.2. Flocculants in wastewater treatment

A large diversity of wastewaters are produced in industries and domestic environments. These wastewaters contain high quantities of dispersed solids, organic and inorganic particles, metal ions and other impurities. Flocculation is frequently used to promote the solid-liquid separation of wastewater suspensions in many industrial processes, at least as a wastewater pre-treatment process. Synthetic polyelectrolytes have been commonly used, in the last years, as flocculants to enhance the flocculation process efficiency, and the results are promising<sup>93</sup>. Characteristics like molecular weight, structure (linear or branched), charge density, charge type and composition have a strong influence on the flocculation process<sup>94</sup>. Cationic and anionic polyelectrolytes are the mainly used flocculants in industrial wastewaters flocculation processes.

### 3.2.1. Cationic polyelectrolytes

Water-soluble cationic polyelectrolytes present usually one of the three following functional groups: ammonium, sulfonium and phosphonium quaternaries. Quaternary ammonium is the

most frequently reported cationic structure. The positive fragment in the polymers can strongly interact with negatively charged particles present in wastewaters from several industries, such as textile, paper production, oily water clarification, paint manufacturing, dairy and food processing, among others.

The majority of the commercial available linear cationic flocculants are based on copolymerization of acrylamide and methacryloyloxyethyl trimethylammomium chloride or acryloyloxyethyl trimethylammomium<sup>95</sup>. Okada *et al.*<sup>96</sup> presented the radiation-induced copolymerization of the methyl chloride salt of dimethylaminoethyl methacrylate quaternized methyl chloride with acrylamide to prepare a cationic polymer flocculant, which was tested in sludge from sugar manufacturing. Wang *et al.*<sup>97,98</sup> developed a water-soluble cationic flocculant, copolymer of acrylamide and acryloylamino-2-hydroxypropyl trimethylammonium chloride, through the dispersion polymerization method in aqueous ammonium sulphate solution, and tested it in 0.25 wt% kaolin suspensions. A cationic terpolymer was prepared from dimethylaminoethyl methacrylate, vinyl pyrrolidone and vinyl acetate using the solution polymerization technique, by Nasr *et al.*<sup>99</sup>. The terpolymer solution was used as flocculant in a river Nile sample clarification. Razali *et al.*<sup>100</sup> reported self-synthesized poly(diallyldimethylammonium chloride) flocculants used in the treatment of pulp and paper mill wastewater. In Lu *et al.*<sup>101</sup>, copolymers of methyl acrylate and the cationic monomer 2-acryloyloxyethyl trimethylammonium chloride were synthesized via emulsion polymerization, and used as sludge dewatering aid in wastewater treatment. Abdiyev *et al.*<sup>102</sup> investigated radical copolymerization of diallyldimethylammonium chloride with dimethylacrylamide, and the flocculating ability was studied for bentonite suspensions and animal manure slurries. Palomino *et al.*<sup>103</sup> synthesized a copolymer of acrylamide with dimethylaminoethyl acrylate quaternized methyl chloride by inverse-emulsion polymerization and used it to induce flocculation of monodisperse latex suspensions. Summarized literature in this area is presented in Table 2.3.



Table 2.3 Summary of linear cationic polyelectrolytes used as flocculants in previous studies, including structure, monomers and testing medium.

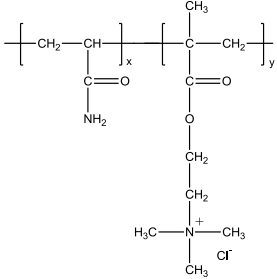
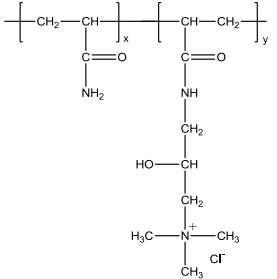
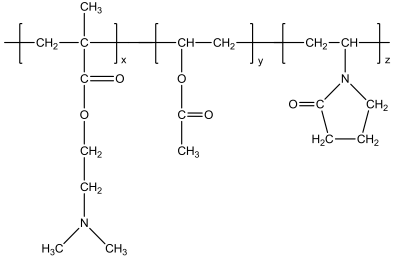
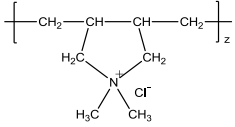
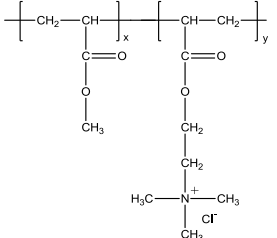
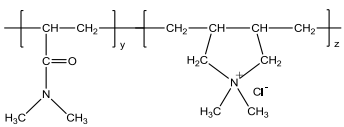
Polyelectrolyte structure	Comonomers <sup>a</sup>	Testing medium	Reference
	AAm and DMAEM	Sludge from sugar manufacturing	Okada <i>et al.</i> <sup>96</sup>
	AAm and AMHP	Kaolin suspension	Wang <i>et al.</i> <sup>97,98</sup>
	DMAEMA, NVP and VA	River water	Nasr <i>et al.</i> <sup>99</sup>
	DADMAC	Pulp and paper mill wastewater	Razali <i>et al.</i> <sup>100</sup>
	MA and AETAC	Waste sludge	Lu <i>et al.</i> <sup>101</sup>
	DADMAC and DMA	Bentonite suspensions and animal manure slurries	Abdiyev <i>et al.</i> <sup>102</sup>

Table 2.3 (Contd.)

Polyelectrolyte structure	Comonomers <sup>a</sup>	Testing medium	Reference
	AAM and AETAC	Latex suspensions	Palomino <i>et al.</i> <sup>105</sup>

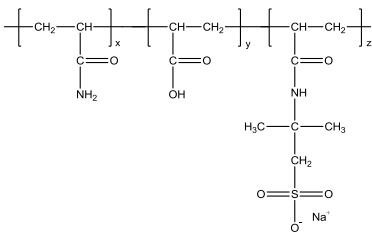
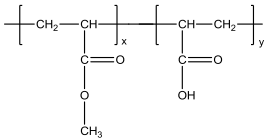
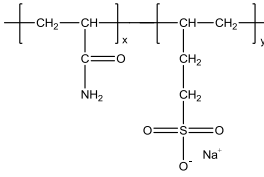
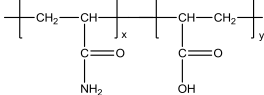
<sup>a</sup>Abbreviations: AAm, acrylamide; DMAEM, dimethylaminoethyl methacrylate; AMHP, acryloylamino-2-hydroxypropyl trimethylammonium chloride; DADMAC, diallyldimethylammonium chloride; DMAEMA, dimethylaminoethyl methacrylate; NVP, vinyl pyrrolidone; VA, vinyl acetate; AETAC, 2-acryloyloxyethyl trimethylammonium chloride; MA, methyl acrylate; DMA, dimethylacrylamide.

### 3.2.2. Anionic polyelectrolytes

Anionic polyelectrolytes can be used in the treatment of municipal wastewaters and effluents from industries such as mineral processing, tanning, sugar processing, paper production, metal working and gravel washing, among others<sup>93</sup>. Most of the commercial linear anionic flocculants present carboxylate and sulfonate ions in their structure as functional groups, and are often copolymers of acrylamide.

Acrylamide copolymerized with acrylic acid and acrylamido-2-methyl-1-propanesulfonic acid sodium salt, through ultraviolet irradiation polymerization, and its application in flocculation of simulated wastewaters and dewatering of waste sludge was reported by Ma *et al.*<sup>104,105</sup> and Zheng *et al.*<sup>106,107</sup>. Lu *et al.*<sup>108</sup> developed a polymeric anionic flocculant of methyl acrylate and acrylic acid by emulsion polymerization and tested it in the reduction of turbidity of clay suspension. Feng *et al.*<sup>109</sup> synthesized an acrylamide and sodium allylsulfonate copolymer, using ultraviolet-initiated template polymerization, and the flocculation performance was evaluated in a simulated mining wastewater, with high turbidity. Jha *et al.*<sup>110</sup> studied the flocculation efficiency of a copolymer of acrylamide and acrylic acid, prepared in aqueous medium, in a tannery waste. As alternatives, anionically modified polysaccharides as flocculation agents have also been recently reported in literature<sup>111–114</sup>, however the control of the properties in these natural-based polyelectrolytes is much more complicated. A summary of the literature in this domain is presented in Table 2.4.

Table 2.4 Summary of linear anionic polyelectrolytes used as flocculants in previous studies, including structure, monomers, and testing medium.

Polyelectrolyte structure	Comonomers <sup>a</sup>	Testing medium	Reference
	AAm, AA and Na-AMPS	Simulated wastewaters and waste sludge	Ma <i>et al.</i> <sup>104,105</sup> and Zheng <i>et al.</i> <sup>106,107</sup>
	MA and AA	Clay suspension	Lu <i>et al.</i> <sup>108</sup>
	AAm and SAS	Simulated mining wastewater	Feng <i>et al.</i> <sup>109</sup>
	AAm and AA	Tannery waste	Jha <i>et al.</i> <sup>110</sup>

<sup>a</sup>Abbreviations: AA, acrylic acid; Na-AMPS, acrylamido-2-methyl-1-propanesulfonic acid sodium salt; MA, methyl acrylate; AAm, acrylamide; SAS, sodium allylsulfonate.

### 3.2.3. Hydrophobically modified polyelectrolytes

Recently, hydrophobic modification of polymers have been extensively investigated for application in solid-liquid separation, due to their capacity of enhance polymer performance<sup>115</sup>. Hydrophobically modified polymers can be obtained by chemical grafting or copolymerization procedures, through the introduction of a relatively low amount of hydrophobic monomer into the polymer structure<sup>116</sup>. The synergetic effects between the charge functionality and the hydrophobic group have shown a remarkable performance in wastewater treatment<sup>115,117</sup>.

Several well-known polyelectrolytes have been hydrophobically modified, including polyacrylamide or PDADMAC, and the final polymer characteristics have promoted the performance in wastewater treatment. Zhao *et al.*<sup>118</sup> copolymerized the hydrophobic monomer VTMS with DADMAC to produce a hydrophobically modified cationic polyelectrolyte and apply it in treating negatively charged kaolinite, dye liquor and oily wastewater. Dragan *et al.*<sup>119</sup> synthesised hydrophobic cationic polyelectrolytes and investigated the flocculating efficiency

on montmorillonite suspension in water. Cationic polyelectrolytes with quaternary ammonium salt groups in the backbone and hydrophobic side chains were produced using epichlorohydrin, dimethylamine, 1,3-dimethyltrimethylenediamine and two primary amines with nonpolar chains (hexyloxypropylamine and decyloxypropylamine). Ren *et al.*<sup>117</sup> studied the copolymerization of acrylamide with 3-acrylamido-2-hydroxypropyltrialkylammonium chloride, in which alkyls were ethyl, butyl and octyl, respectively. The developed hydrophobic cationic polyelectrolytes were tested in flocculation of kaolin suspensions. Later, Lee *et al.*<sup>120</sup> produced homologous series of the previous ones, using larger hydrophobic chain lengths and tested them also in kaolin suspensions. A series of hydrophobically modified cationic polyacrylamides were synthesised, by means of trihexylamine, trioctylamine and tridodecylamine. Shang *et al.*<sup>121</sup> synthesized a hydrophobically modified and cationic flocculant of acrylamide, methacryloxyethyl trimethylammonium chloride and methacryloxypropyl trimethoxysilane by inverse emulsion polymerization, and studied the flocculation performance on reactive brilliant red X-3B dye solution and 0.10 wt% kaolin suspension. Yang *et al.*<sup>122</sup> produced a hydrophobic cationic polyacrylamide, with dimethyldiallylammonium chloride and butylacrylate, by the micellar free radical copolymerization technique, and the oil removal efficiency in oily wastewater was verified. Shang *et al.*<sup>123</sup> synthesized acrylamide with diallyldimethylammonium chloride and vinyltrimethoxysilane by inverse free-radical emulsion polymerization technique, and applied it as flocculant in dye molecules removal. Zheng *et al.*<sup>124,125</sup> developed a new composite flocculant through the copolymerization of acrylamide, acryloyloxyethyltrimethylammonium chloride, and butylacrylate, under ultraviolet radiation, and its performance in a textile sewage sludge and activated sludge dewatering was evaluated. Later, Lü *et al.*<sup>126</sup> successfully produced a hydrophobically modified cationic flocculant, via dispersion copolymerization of acrylamide, 2-methylacryloyloxyethyl trimethylammonium chloride and methyl methacrylate, in aqueous ammonium sulphate solution. Its flocculation performance was assessed in the treatment of an oily wastewater. A summary of hydrophobically modified polyelectrolytes used as flocculants in literature is presented in Table 2.5

Table 2.5 Summary of hydrophobically modified polyelectrolytes used as flocculants in previous studies, including structure, monomers, and testing medium.

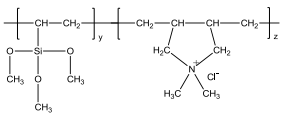
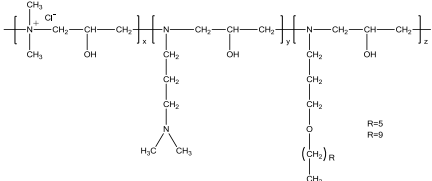
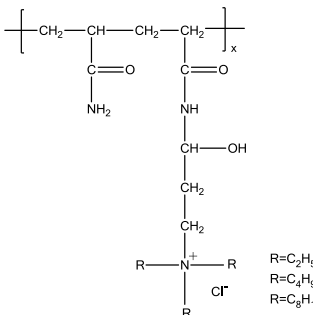
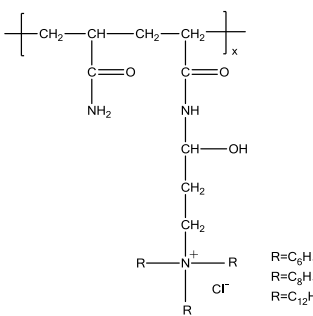
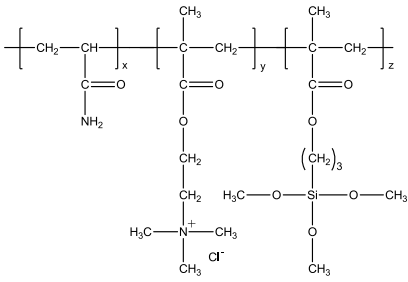
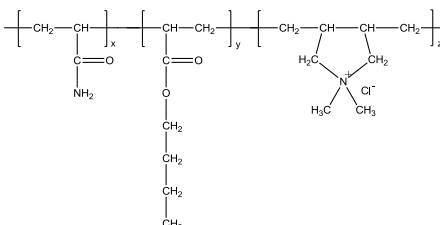
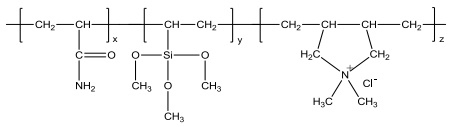
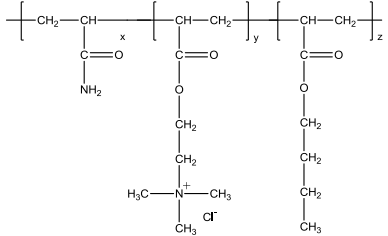
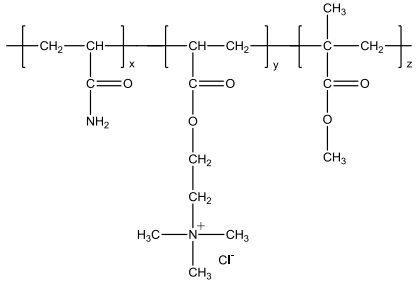
Polyelectrolyte structure	Comonomers <sup>a</sup>	Testing medium	Reference
	DADMAC and VTMS	Kaolinite suspensions, dye liquor, and oily wastewater	Zhao <i>et al.</i> <sup>118</sup>
	Epichlorohydrin, dimethylamine, DMAPA, HPA and DPA	Montmorillonite suspension	Dragan <i>et al.</i> <sup>119</sup>
	AAm, epichlorohydrin, triethylamine, tributylamine and trioctylamine	Kaolin suspension	Ren <i>et al.</i> <sup>117</sup>
	AAm, epichlorohydrin, trihexylamine, trioctylamine and tridodecylamine	Kaolin suspension	Lee <i>et al.</i> <sup>120</sup>
	AAm, DMC and MAPMS	Dye solution and kaolin suspension	Shang <i>et al.</i> <sup>121</sup>
	AAm, DADMAC and BA	Oily wastewater	Yang <i>et al.</i> <sup>122</sup>

Table 2.5 (Contd.)

Polyelectrolyte structure	Comonomers <sup>a</sup>	Testing medium	Reference
	AAm, DADMAC and VTMS	Dye solutions	Shang <i>et al.</i> <sup>123</sup>
	AAm, AETAC and BA	Textile and activated sludge	Zheng <i>et al.</i> <sup>124,125</sup>
	AAm, DMC and MMA	Oily wastewater	Lü <i>et al.</i> <sup>126</sup>

<sup>a</sup>Abbreviations: AAm, acrylamide; DMC, methacryloxyethyl trimethylammonium chloride; MAPMS, methacryloxypropyl trimethoxysilane; DADMAC, diallyldimethylammonium chloride; BA, butylacrylate; VTMS, vinyltrimethoxysilane; AETAC, 2-acryloyloxyethyl trimethylammonium chloride; DMC, 2-methylacryloyloxyethyl trimethylammonium chloride; MMA, methyl methacrylate; DMAPA, dimethylamino propylamine; HPA, hexyloxypropylamine and DPA, decyloxypropylamine

### 3.3. Flocculation of industrial oily effluents

Oily wastewaters are generated in many industrial processes, where three main activities, as described below, generate the oily effluents sources. From the petroleum industry originate, via crude oil extraction and oil refineries, salty wastewaters which contain very high concentrations of hydrocarbons as well as ammonia, sulphides, chlorides and phenol<sup>127</sup>. The manufacturing of metal pieces in metalworking industries produce wastewaters containing oil-in-water emulsions resulting from the use of cutting, cooling and lubricating fluids. During cleaning operations, the diluted metalworking fluids originate effluents with several grams of oil per liter<sup>128,129</sup>. Food processing industries, including production and transformation of both animal and vegetable products, also produce large volumes of oily wastewaters. Meat processing, dairy industries, refining of vegetable oils from sunflower, cotton-seed, soybean or rapeseed, palm and olive oil mill facilities, are some examples of food-related activities that result in oily effluents<sup>42,130,131</sup>.

Among the extensive list of industrial oily effluents, the present work will focus only on three of them: olive oil mill effluent, dairy effluent and potato crisps manufacturing effluent, considering their importance in Portugal.

### 3.3.1. Olive oil mill effluent

Olive oil mill effluents (OME) have increased significantly in the last years as a result of the rapidly increasing demand for olive oil, and the existing oil extraction techniques that involve high amounts of water<sup>132</sup>. The composition of the produced wastewater changes with climate, cultivation conditions and milling processes<sup>133</sup>. Typically, OME presents a high concentration of solids resulting from washing actions, show intense dark color, acid pH and strong odor. These effluents, when disposed to the environment, lead to severe problems including coloration and pollution of waters, changes in soil quality and phytotoxicity, plants growth inhibition and odor nuisance<sup>134</sup>.

OME must be treated before disposal and several treatment technologies and integrated processes have been developed to shape a suitable and effective method to deal with the produced wastewater<sup>135</sup>. Direct discharge on fields decreases the amount of dissolved oxygen, harming aquatic fauna<sup>136</sup>. Open evaporating ponds or lagooning leads to insect reproduction and increase the risk of surface and groundwater contamination<sup>137</sup>. Biological methods include microbiological treatment, co-composting, aerobic and anaerobic digestion. However, the OME have high concentration of fats, lipids and phenols that can compromise the growth of microorganisms and, consequently, the OME degradability<sup>138</sup>. Advanced oxidation processes, consisting in Fenton and Fenton-like oxidation and ozonation, can also be applied<sup>139,140</sup>. Physico-chemical treatment methods such as ultrafiltration, reverse osmosis, sedimentation, centrifugation, coagulation-flocculation and electro-coagulation are actually predominant<sup>141-143</sup>. Nevertheless, most of these treatment processes on their own are not cost effective and reported results present significant drawbacks, indicating that combined technologies are needed in order to reduce the overall portion of organic load, and thus reducing the operating costs. These hybrid systems can include ozonation and aerobic biological treatment, coagulation-flocculation combined with anaerobic biological process, electron-Fenton and anaerobic digestion or chemical oxidative procedure in combination with aerobic biological treatment<sup>144,145</sup>.

Coagulation-flocculation processes have proved to be very useful as a pre-treatment stage in the OME processing methodologies<sup>146,147</sup>, involving low associated costs and carbon dioxide

emissions<sup>148</sup>. The addition of organic and inorganic compounds stimulates the destabilization of colloidal materials and promotes the agglomeration of small particles in large flocs able to settle. Coagulants, such as aluminum, ferric sulfate, starch, chitosan and lime, and cationic or anionic flocculants, like PDADMAC, poly(allylamine) or poly(allylamine) hydrochloride, have been tested<sup>142,149,150</sup>. Experiments showed considerable reduction of solids, color and COD in the pre-treated effluent. However, it is usually needed a combination of both (inorganic and organic additives) or, when in single use, a very high concentration of polymer, which generates large amounts of sludge<sup>151</sup>.

The minimization of sludge production is important considering the costs related with subsequent sludge treatment and disposal<sup>152</sup>. Ginos *et al.*<sup>142</sup> tested inorganic materials such as lime, iron, magnesium and aluminum, four cationic and two anionic commercial polyelectrolytes either alone or in various combinations. Combining lime or ferrous sulphate (in the range of several g/L) with cationic polyelectrolytes (in the range of 200–300 mg/L) led to total modest suspended solids (TSS), COD and total phosphorous (TP) removals between about 18-95%, 10-40% and 30-80%, respectively, depending on the materials and the effluent used. Rizzo *et al.*<sup>153</sup> studied the pre-treatment of OME by coagulation using chitosan and found that the optimum coagulant concentration was 400 mg/L. The efficiency of the chitosan coagulation was found to be for TSS about 81% and turbidity about 94%. Meysami and Kasaeian<sup>154</sup> used aluminum as the main coagulant and chitosan as a coagulating aid which was effective in reducing the primary turbidity of the emulsions (90%), at concentrations of 15 and 25 mg/L, respectively. In Sarika *et al.*<sup>155</sup>, four cationic and two anionic polyelectrolytes were tested in direct flocculation and showed to be capable to remove nearly completely TSS and reduce considerably COD (55%) with a minimum dosage of about 2500-3000 mg/L, is the best cases. Michael *et al.*<sup>131</sup> investigated coagulation/flocculation as pre-treatment in the application of a solar-driven advanced oxidation process (solar Fenton), using ferrous sulfate (6670 mg/L) as the coagulant, and an anionic polyelectrolyte (287 mg/L) as flocculant, leading to approximately 44% of COD removal and TSS were removed by 94%. Iakovides *et al.*<sup>150</sup> presented experiments of coagulation/flocculation with electrolytes salts [ferric chloride, calcium hydroxide, calcium oxide, calcium chloride) and polyelectrolytes [poly(allylamine), poly(allylamine) hydrochloride, PDADMAC, and Floccan 23-20 (a commercially available anionic polyacrylamide)] separately or in combination. The best results were obtained with a combination of calcium hydroxide at 20000 mg/L and 1250 mg/L of PDADMAC, where reductions of 43% in total solids (TS), 27% in TSS, 56% in COD, and 76% in phenols were achieved. Azbar *et al.*<sup>156</sup> evaluated the feasibility of using chemical pretreatment to improve the



anaerobic biological degradation of industrial effluents. Aluminum sulfate was the best chemical agent in terms of removing color (65%), and as the concentration of aluminum salt increased from 500 to 6000 mg/L, the removal in COD also increased (21%, 32% and 47%, respectively). In the work of Kestioğlu *et al.*<sup>134</sup>, addition of ferric chloride to olive mill effluent resulted in a 95% COD, 90% total phenol and 99% suspended solids (SS) removals at a dosage of 3000 mg/L. Two inorganic materials, polyaluminum chloride and aluminum sulfate, and two organic polyelectrolytes, anionic polyacrylamides, were used in a study by Pelendridou *et al.*<sup>148</sup>. The best results were achieved, using polyaluminum chloride as coagulant, and the maximum removal efficiencies of all parameters tested corresponded to a concentration of 4000 mg/L and a flocculant dosage of 10 mg/L (36%, 37% and 92% for COD, TS and TSS, respectively). In Yazdanbakhsh *et al.*<sup>157</sup>, the performance of aluminum, ferric chloride and polyaluminum chloride was studied as coagulants in olive oil mill wastewater treatment. Ferric chloride showed the best results in comparison with the others, removing 91.2% of COD, 98.9% of total suspended solids and 99.2% of turbidity at pH 6 and with 3000 mg/L coagulant dosage. A summary of the main literature in this subject is presented in Table 2.6.

Table 2.6 Removal efficiencies of olive mill wastewater treatment using coagulation-flocculation processes.

Initial parameters	Coagulant/Flocculant	Removals (%)			Reference
		Turbidity	COD	TS	
COD=61-29 g/L TSS=37-53 g/L	Lime or ferrous sulfate (5000-50000 mg/L) and cationic or anionic commercial polyelectrolytes (200–300 mg/L)		10-40		Ginos <i>et al.</i> <sup>142</sup>
COD=61-29 g/L TSS=37-53 g/L	Lime or ferrous sulfate (5000-50000 mg/L) and cationic or anionic commercial polyelectrolytes (200–300 mg/L)		10-40		Ginos <i>et al.</i> <sup>142</sup>
COD=53 g/L TSS=7 g/L Turbidity=10000 NTU	Chitosan (400 mg/L)	94			Rizzo <i>et al.</i> <sup>153</sup>

Table 2.6 (Contd.)

Initial parameters	Coagulant/Flocculant	Removals (%)			Reference
		Turbidity	COD	TS	
Turbidity=250 NTU	Aluminum (15 mg/L) and chitosan (25 mg/L)	90			Meyssami and Kasaeian <sup>154</sup>
COD=5-89 g/L TSS=0.5-101 g/L	Four cationic and two anionic commercial polyelectrolytes (2500-3000 mg/L)		55		Sarika <i>et al.</i> <sup>155</sup>
COD=14 g/L TSS=50 g/L TS=20 g/L	FeSO <sub>4</sub> (6670 mg/L) and anionic commercial polyelectrolyte (287 mg/L)		44		Michael <i>et al.</i> <sup>131</sup>
COD=40-82 g/L TSS=11-15 g/L TS=29-56 g/L	Ca(OH) <sub>2</sub> (20000 mg/L) and PDADMAC (1250 mg/L)		56	43	Iakovides <i>et al.</i> <sup>150</sup>
COD=98 g/L	Al <sub>2</sub> SO <sub>4</sub> (6000 mg/L)		47		Azbar <i>et al.</i> <sup>156</sup>
COD=186 g/L TSS=65 g/L	FeCl <sub>3</sub> (3000 mg/L)		95		Kestioğlu <i>et al.</i> <sup>134</sup>
COD=22-88 g/L TSS=15-39 g/L TS=32-93 g/L	PAC (4000 mg/L)		36	37	Pelendridou <i>et al.</i> <sup>148</sup>
COD=59 g/L TSS=28 g/L Turbidity=25250 NTU	Ferric chloride (3000 mg/L)	99	91		Yazdanbakhsh <i>et al.</i> <sup>157</sup>

Abbreviations: COD, chemical oxygen demand; TSS, total suspended solids; TS, total solids; FeSO<sub>4</sub>, ferrous sulfate; FeCl<sub>3</sub>, ferric chloride; Ca(OH)<sub>2</sub>, calcium hydroxide; PDADMAC, poly(diallyldimethyl ammonium chloride); Al<sub>2</sub>SO<sub>4</sub>, aluminum sulfate; PAC, polyaluminum chloride.

### 3.3.2. Dairy effluent

The dairy industry is considered as one of the most polluting food industries, due to the high demand for milk and derived products, the large water consumption in cleaning and washing operations and the characteristics of the resulting effluent<sup>158</sup>. Presence of fats, nutrients, lactose, detergents and sanitizing agents can cause serious environmental problems, by affecting the aquatic life and leading to eutrophication of receiving waters<sup>158</sup>. Since the dairy industry produces several different products, such as milk, cheese, butter, yogurt or ice-cream,

the raw effluent can vary broadly in quantity and composition<sup>159,160</sup>. Furthermore, wide ranges of variations in pH, concentration of solids, COD and biochemical oxygen demand (BOD) have been reported in literature<sup>161</sup>. The aforementioned aspects contribute to the complexity of the treatment of this wastewater and the necessity for studies using modern and innovative treatment techniques, considering the environmental sustainability.

In the countries where dairy effluents are treated, biological methods are typically applied to treat them, considering the presence of a high load of organic matter, but often combined with physico-chemical treatment processes, required to remove suspended, colloidal, and dissolved constituents. Activated sludge process, aerated lagoons, biological filters, sequencing batch reactor, anaerobic sludge blanket reactor or anaerobic filters, in combination with coagulation/flocculation with various inorganic or organic polymers, or membrane processes, like nanofiltration or reverse osmosis or adsorption are some examples of treatments adopted in this industrial sector<sup>162</sup>. Anaerobic treatment seems to be the most widely process used for treatment dairy wastewaters, nevertheless not all compounds of dairy effluent are biodegradable, protein and fats are not easily degraded due to the presence of long-chain fatty acids, which are inhibitory to methanogenic bacteria<sup>163,164</sup>. In this way, additional treatment is necessary. Aerobic treatment methods require high amounts of energy, so physico-chemical treatment processes are frequently applied as primary procedure purification of dairy effluents treatment.

Adsorption is an attractive method for removing organic content. Activated carbon, coal fly ash, rice husk ash, straw dust, saw dust, coconut coir and bagasse fly ash are some examples of adsorbents used<sup>165</sup>. Using electrocoagulation, the waste matter is removed from wastewater by electrostatic attraction followed by coagulation, with no chemical reagents added, which results in a sludge with no additional pollutants<sup>166</sup>. Thus it has been attracting interest, due to its flexibility and environmental capability. The membrane-treatment processes include microfiltration, ultrafiltration, nanofiltration, reverse osmosis, dialysis and electrodialysis. The several membrane techniques have advantages and disadvantages: microfiltration and ultrafiltration have lower energy costs than nanofiltration or reverse osmosis due to high flux of permeate at low transmembrane pressure<sup>167</sup>, however microfiltration and ultrafiltration show low reduction of COD values<sup>168,169</sup>. Moreover, an additional problem in using membrane filtration by itself is the obstruction of the membranes due to the accumulation of proteinous material on the surface<sup>170</sup>.

Coagulation and flocculation processes are of greatest importance and widely used in dairy effluents treatments, due to its simplicity and effectiveness<sup>171</sup>. Addition of coagulants and flocculants can also improve filtration performance, by reducing the organic matter and the amount of suspended and colloidal particles, responsible for the turbidity of the effluent<sup>172,173</sup>. This treatment method can be applied in previously anaerobically treated dairy wastewater or in raw dairy effluent<sup>174</sup>. In the literature the ability of conventional salts and polymeric coagulants for the treatment of different kinds of dairy wastewater has been studied. Metal salts are effective coagulants through hydrolysis of monomeric and polymeric species that will neutralize the surface of the colloids and soluble particles. However, wastewater from the dairy industry treated with conventional coagulation requires large amounts of reactive inorganic chemicals and generates large volumes of non-biodegradable sludge. Moreover, coagulants from natural sources may not be appropriate, or more difficult to tune, for treatment of industrial dairy wastewaters due to their low availability in large-scale and the wide range of wastewater characteristics. On the other hand, polymer flocculants, especially ionic polymers, destabilize colloids through surface neutralization and particle bridging, leading to flocs growing, improving the efficiency of settling and filtration. However, only few studies are reported in the literature for the flocculation of dairy wastewater.

Rusten *et al.*<sup>175</sup> tested four different combinations of coagulants. Using ferric chloride sulfate showed the best results, removing 2-3% more COD than sulfuric acid combined with carboxy methyl cellulose, and 4-6% more COD than lactic acid combined with carboxy methyl cellulose. Selmer-Olsen *et al.*<sup>176</sup> applied different types of chitosan as coagulant and achieved nearly 60% removal of COD and 90% removal of particles, for dosages of 5-15 mg/L at pH 4.5-5. Hamdani *et al.*<sup>177</sup> treated dairy effluent with iron chloride, aluminum sulfate and calcium hydroxide, removing 40% of organic matter and nitrogen content, and reducing the suspended matter in 94% and total phosphorus in 89% with calcium hydroxide. Sarkar *et al.*<sup>178</sup> applied coagulation by chitosan, followed by adsorption with powdered activated carbon, in treating dairy wastewater before a membrane separation method. At pH 4.0 the reductions were 48% in total dissolved solids and 57% in COD at 10-50 mg/L chitosan.

Kushwaha *et al.*<sup>165</sup> reported the treatment of simulated dairy wastewater with inorganic coagulants such as poly aluminum chloride, ferrous sulfate and aluminum potassium sulfate. Optimum pH was found to be 8.0 and 300, 800 and 500 mg/L for poly aluminum chloride, ferrous sulfate and aluminum potassium sulfate, respectively, resulted in 69.2, 66.5 and 63.8% COD removal efficiency. Tchamango *et al.*<sup>179</sup> compared electrocoagulation with chemical coagulation with aluminum sulfate. Both gave similar removal rates for nitrogen and turbidity,

however the removals of phosphorus and COD are slightly higher by chemical coagulation. The turbidity was practically eliminated, while phosphorus, nitrogen, and COD were reduced up to 94, 81 and 63% respectively, at concentrations above 950 mg/L. Rivas *et al.*<sup>180</sup> treated cheese wastewater by means of a coagulation-flocculation process with three different coagulants, ferrous sulfate, aluminum sulfate, and ferric chloride. The optimum conditions for ferrous sulfate were obtained using 250 mg/L at pH 8.5 and 50% of COD was removed. Aluminum sulfate achieved slightly lower reductions of COD, while the amount needed was significantly higher (1000 mg/L). With ferric chloride, similar results to those obtained with ferrous sulfate were verified, 250 mg/L was enough to eliminate COD in the range of 40-60%, depending on operating conditions.

Formentini-Schmitt *et al.*<sup>174</sup> investigated the pretreatment of dairy industry wastewater by coagulation/flocculation/sedimentation using *Moringa oleifera* as coagulant. The efficiency of the pretreatment step with a coagulant concentration of 1500 mg/L was of 97.6% for turbidity reduction and 39.4% for COD removal. Prakash *et al.*<sup>181</sup> studied the effectiveness of coagulation and Fenton's oxidation in a simulated dairy wastewater. Individually, coagulation resulted in 67% COD removal, with a dosage of ferrous sulfate of 800 mg/L at pH 6.0. Loei *et al.*<sup>182</sup> investigated the effect of the coagulation process on the treatment of simulated dairy wastewater. Different types of inorganic and polymeric coagulants were tested, such as aluminum and ferrous sulfate, polyacrylamide and polyferric sulfate. The optimum conditions for aluminum and polyferric sulfate were 1000 mg/L and pH 5.0, reaching a COD removal efficiency of 68% and 62%, respectively. Addition of 20 mg/L of polyferric sulfate or polyacrylamide in combination with aluminum sulfate can increase the COD removal efficiency by 83% and 86%, respectively, requiring only 100 mg/L of aluminum sulfate. Aysegul Tanik *et al.*<sup>183</sup> investigated ferric chloride, ferrous sulfate and aluminum as coagulants for the treatment of dairy wastewater originating from a dairy products plant. Optimum coagulant dosage was determined as 200 mg/L for all the coagulants with the optimum pH values between 4-4.5 for ferric chloride and ferrous sulfate, and 5-6 for aluminum. The maximum overall COD removal efficiencies were 72, 59 and 54% for ferric chloride, ferrous sulfate and aluminum, respectively. Most of the flocculation processes in dairy effluents use inorganic or natural-based products. However, considering the results described above, there is still a need for flocculants with distinct characteristics, tuned for this specific process, which are immediately soluble in aqueous systems, highly efficient in little quantities and that generate large and strong flocs, leading to a good settling performance and providing,

thereafter, smaller sludge volumes. A summary of the present literature state, on the use of coagulation/flocculation in this type of effluent, is presented in Table 2.7.

Table 2.7 Removal efficiencies of dairy wastewater treatment using coagulation-flocculation processes.

Initial parameters	Coagulant/Flocculant	Removals (%)			Reference
		Turbidity	COD	TS	
COD=1.2-2.7 g/L TSS=0.3-0.5 g/L Turbidity=360-910 NTU	Chitosan (5-15 mg/L)		57	90	Selmer-Olsen <i>et al.</i> <sup>176</sup>
COD=1.5-3 g/L TSS=0.3-0.6 g/L Turbidity=15-30 NTU	Chitosan (10-50 mg/L)		57		Sarkar <i>et al.</i> <sup>178</sup>
COD=3.9 g/L TS=3.1 g/L Turbidity=1744 NTU	PAC (300 mg/L) FeSO <sub>4</sub> (800 mg/L) KAl(SO <sub>4</sub> ) <sub>2</sub> ·12H <sub>2</sub> O (500 mg/L)		69 67 64		Kushwaha <i>et al.</i> <sup>165</sup>
N/A	Aluminum sulfate (950 mg/L)		63		Tchamango <i>et al.</i> <sup>179</sup>
COD=9-26 g/L TS=7-8 g/L Turbidity= 1331-2004 NTU	FeSO <sub>4</sub> (250 mg/L) FeCl <sub>3</sub> (250 mg/L)		50 40-60		Rivas <i>et al.</i> <sup>180</sup>
COD=3.2 g/L Turbidity=897 NTU	<i>Moringa oleifera</i> (1500 mg/L)	98	39		Formentini-Schmitt <i>et al.</i> <sup>174</sup>
COD=3.6 g/L TS=2.7 g/L Turbidity= 1410 NTU	Ferrous sulfate (800 mg/L)		67		Prakash <i>et al.</i> <sup>181</sup>
COD=3.2 g/L Turbidity=97 NTU	Aluminum sulfate (100 mg/L) and PFS or PAA (20mg/L)		86		Loloei <i>et al.</i> <sup>182</sup>

Abbreviations: COD, chemical oxygen demand; TSS, total suspended solids; TS, total solids; FeSO<sub>4</sub>, ferrous sulfate; KAl(SO<sub>4</sub>)<sub>2</sub>·12H<sub>2</sub>O, aluminum potassium sulphate; FeCl<sub>3</sub>, ferric chloride; PAA, polyacrylamide; PFS, polyferric sulphate.

### 3.3.3. Effluent from the manufacturing of fried snacks

Huge amounts of effluent with high organic load are generated in potato crisps and other fried snacks manufacturing industries during the several processes of washing, peeling, slicing and blanching, requiring an efficient treatment before discharging. These effluents present usually high levels of fats and oil, solids, COD and BOD. Conventional biological treatment methods are widely applicable, due to the readily biodegradable nature of the organic content, combining different aerobic and anaerobic processes<sup>184,185</sup>. However, the long retention times and large tanks required, and the sensitivity of the microorganisms used are still significant drawbacks of these techniques<sup>186</sup>. On the other hand, despite the use of highly reactive oxidizing agents in advanced oxidation processes (such as fenton reaction, ultra-violet (UV) photolysis, ozonation and electrochemical oxidation)<sup>187</sup>, the economic and operational benefits are worthy enough for their application. Ozonation is a promising technique since ozone is a powerful oxidizing agent, efficiently used to reduce organic matter<sup>188</sup>, with single-step degradation, easy operation, smaller reactor volumes and no sludge formation<sup>189</sup>. Despite the advantages, high production costs and reasonably low solubility in water make ozonation economically unattractive. More recently, due to the environmental compatibility, easy operation and low amounts of resulting sludge, electrocoagulation has been applied effectively. To the best of our knowledge, potato crisps manufacturing effluent treatment using a direct flocculation process was not reported in literature so far.

Lin *et al.*<sup>190</sup> evaluated the performance of an aerated lagoon, succeeding anaerobic lagoon-filter units, in treating unsettled potato-processing wastewater. In the end, 68% of COD removal was the highest result obtained. Thermophilic aerobic digestion was tested in the treatment of potato-processing wastewater by Malladi and Ingham<sup>191</sup>, reaching a decrease in BOD and total suspended solids of the supernatant of 98% and 75%, respectively. Hadjivassilis *et al.*<sup>184</sup> designed and installed a small industrial effluent treatment plant for the treatment of wastewater from a potato chips and snacks factory. The apparatus included a simple up-flow anaerobic reactor with internal settling and gas collection units, with a subsequent aerobic treatment based on the activated sludge process with diffused air system. The treatment process efficiencies were 99.2% for COD removal and 99.5% for BOD removal. The feasibility of the up-flow anaerobic sludge bed process for the treatment of raw potato-maize wastewater of a chip-processing industry was demonstrated by Kalyuzhnyi *et al.*<sup>192</sup>. Treatment efficiency around 63% for COD removal was obtained. El-Gohary *et al.*<sup>193</sup> tested the performance of laboratory-scale aerobic and anaerobic systems in treating food-processing wastewater from a potato-chips factory. The results obtained showed that it is possible to

reduce BOD and COD, respectively, by 92.4% and 91.5% using an up-flow anaerobic sludge blanket reactor, while for an activated sludge system the results were about 86% and 84%, respectively.

Sayed *et al.*<sup>194</sup> presented a study to assess the feasibility of using a pilot scale aerobic side stream membrane bioreactor for treatment of potato-processing wastewater. The tested system was able to give a COD removal efficiency of 98.2 %. The treatment of wastewater from potato chips manufacturing by electrocoagulation was investigated by Kobya *et al.*<sup>186</sup> Aluminum and iron electrodes were used, and aluminum electrodes presented the higher removal rate of COD, turbidity and suspended solids. The removal efficiencies of COD and turbidity were 60% and 98%, respectively. The effect of three different types of glycerol on the performance of up-flow anaerobic sludge blanket reactors treating potato processing wastewater was studied by Ma *et al.*<sup>195</sup> High COD removals were obtained, around 85%. Kupusović *et al.*<sup>196</sup> tested a two-stage aerobic treatment consisting of conventional active sludge treatment followed by membrane bio reactor, to treat high strength wastewater from the potato chip industry. The overall pollutant removal efficiencies were about 97.1% for COD, 99.5% for BOD, 94.7% for total nitrogen and 72.9% total phosphorous.

A study was conducted by Haydar *et al.*<sup>197</sup> to assess the performance of anaerobic-aerobic treatment system in a local potato processing industry. The wastewater treatment plant consisted of primary treatment, up-flow anaerobic sludge blanket, activated sludge process and secondary clarifier. The removal efficiency in activated sludge system for TSS, BOD and COD was around 70%, 57% and 48%, respectively, while the removal efficiency of combined anaerobic-aerobic system was found to be 93%, 90% and 80%, respectively. An evaluation of a laboratory-scale aerobic method for the treatment of potato-processing wastewater was investigated by Manhokwe *et al.*<sup>198</sup> Composite samples were exposed to active sludge treatment in a continuously stirred tank reactor. Average COD reduction of 86% was obtained with a total solids reduction of 57%. Arslan *et al.*<sup>199</sup> studied the application of ozone/ultra-violet/hydrogen peroxide advanced oxidation process to treat potato chips manufacturing wastewater. The efficiency of the system was evaluated considering total organic carbon removal, which reached an efficiency higher than 80%. Considering that all the processes referred above are cost intensive processes, it may be interesting to combine these processes with a pre-treatment by coagulation/flocculation to decrease the level of the usual control parameters in the effluent (COD, TSS or turbidity). In this way the more expensive processes only have to deal with less contaminated effluents, thus reducing their costs (investment and operation).





#### 4. RELEVANCE FOR THE PRESENT WORK

The research on water treatment methodologies has been progressively growing and, currently, flocculation and polyelectrolytes play an important role on the techniques applied in industrial effluents treatment.

The literature review exposed that treatment of oily effluents is frequently based on coagulation/flocculation methods, with great impact in the environment, due to the materials used in their production and the sludge produced during the treatment process. Moreover, the dosages applied in the procedures are much above of what should be desirable.

For the specific industrial oily wastewaters reviewed, large improvements could be achieved in order to lower the dosages of the products applied and to optimize the performances achieved. In general, direct flocculation is a simple technique, easy to apply and with lower associated costs. Additionally, using this method, the sludge is generated in considerably lower volumes and it is, as well, less toxic, since organic polymers are used.

Overall, the production of novel flocculants specifically designed to treat oily effluents through direct flocculation with low dosages presents high potential to be explored, specially aiming their application in oily effluents from organic nature.

Furthermore, flocculation can be combined with subsequent treatment processes, with the objective to reduce the costs, mainly operation costs, of the so called more advanced technical processes that allow the achievement of a final effluent obeying regulatory directives.



---

CHAPTER **3**

**Health-friendly synthesis**  
**formulations**



## 1. INTRODUCTION

The inverse-emulsion polymerization method has been conventionally employing aliphatic mineral oils as continuous phase. Examples of hydrocarbon fluids applied for many years, in this type of synthesis, include mixtures of normal paraffins, iso-paraffins, cyclo-paraffins and aromatics<sup>95,200,201</sup>. These oils allow high chemical and oxidative stability, as well as inertness to provide high performance during the inverse polymerization processes<sup>95,202</sup>. They also have a similar molar volume to typical fatty acid ester surfactants, enabling the formation of a relatively condensed interface and stable droplets. However, the presence of aromatic compounds does not meet health or environmental regulations, exhibiting human and aquatic toxicity levels, and potentiating their classification under the reference GSH08 “Health hazard” as irritants in contact with skin<sup>203</sup>. Even if at residual levels as low as 0.01 wt%, they may not be toxic, they can present long-term health effects.

Vegetable or plant oils represent a promising renewable route to develop sustainable products. Their ready availability, inherent biodegradability, low toxicity and the relatively low cost, make plant oils an industrially attractive material. Such natural and inexpensive alternative to existing methods have been investigated by Abramson *et al.*<sup>204</sup> for the preparation of magnetic iron oxide/silica nanocomposite particles. The use of water-in-oil emulsions based on vegetable oils instead of usual solvents led to microsized or nanosized magnetic silica spheres exhibiting similar characteristics to those of classical procedures. Unfortunately, to perform an emulsion polymerization using a vegetable oil as continuous phase has not, so far, proved successful for the production of high molecular weight products. The main constituents of plant oils are triglycerides, products of the esterification of glycerol with fatty acids. The double bonds and ester groups present in these triglycerides are reactive sites and may act as radical scavengers or increase the tendency for the oil to polymerize itself<sup>205,206</sup>. Alternatively, the organic phase used in inverse-emulsion polymerization should have no free hydroxyl groups. The high density is also an important parameter of the oil, reducing the driving force that promotes sedimentation of the emulsion.

Carmichael *et al.*<sup>207</sup> patented the development of inverse-emulsion polymerization for personal care products, using as continuous oil phase ester oils based on alkoxyated alcohol. Villarroya *et al.*<sup>208</sup> reported an enzymatic emulsion polymerization of water-soluble acrylamide in a water-in-carbon dioxide emulsion. More precisely, the continuous phase used was supercritical carbon dioxide, which is an inexpensive, non-flammable, non-toxic and environmentally inert solvent. However, the majority of the polymers are insoluble in supercritical carbon dioxide,

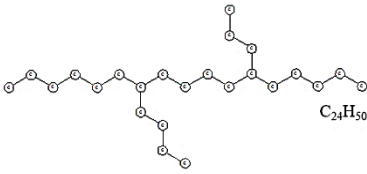
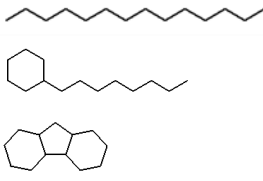
and this methodology requires specific and expensive equipment. Chang *et al.*<sup>209</sup> patented an environmentally friendly oil phase system for water-in-oil emulsion polymerization, in which the oil phase system used was a mixture of soy lecithin and a hydrocarbon solvent, a fatty ester. Quinn *et al.*<sup>210</sup> developed a water-in-d-limonene emulsion with bimetallic particles in the emulsion droplets, where d-limonene is a terpenic bio-solvent that fulfils the requirements to be considered a green solvent. Later, Pérez-Mosqueda *et al.*<sup>211</sup> examined the influence of using a natural gum (rosin gum) and d-limonene in oil-in-water emulsions, leading to very stable systems.

There is still a need for an alternative continuous phase that allows to obtain products with comparable properties of the ones produced in traditional formulations, in order not to compromise their final application. Alternative continuous phases may include white mineral oils or hydrogenated polyalphaolefins. These are inert water insoluble organic liquids, with high density, so that the driving force that promotes sedimentation and/or creaming of the inverse-emulsions is reduced. White mineral oils are highly refined mineral oils, products of distillation and processing by several methods of crude petroleum oils. The various fractions produced from crude oil distillation result in products with different molecular weight, viscosity and boiling range. These fractions can suffer further refinement by solvent extraction in order to remove the toxic polycyclic aromatics and the heavy metals. These alternative oils are listed in the International Nomenclature for Cosmetics Ingredients (I.N.C.I.) under the designation “Paraffinum Liquidum” and comply with many pharmacopoeia and FDA regulations<sup>212</sup>. They are non-irritating, with high boiling point, high stability and high purity, free of harmful ingredients, color, odor and taste. These oils differ by their chemical composition and viscosity, and they are of high-interest to industry, due to their physical properties, minimal environmental impact and the level of purity which is required for use in personal care, food and pharmaceuticals<sup>213,214</sup>.

Considering the objectives of this thesis, in the present chapter, a well-known copolymer of acrylamide and 2-(acryloyloxy) ethyltrimethyl ammonium chloride, Poly(AAm-AETAC), used in water treatment, with high molecular weight, was synthesized by inverse-emulsion polymerization<sup>200</sup> using three different health-friendly formulations, which replaced the organic phase and surfactants of traditional formulations by using health-friendly oils, according to the INCI, as organic phase: two white mineral oils, an iso-paraffin (Carnation) and a mixture of liquid saturated paraffinic hydrocarbons (Marcol82), and an hydrogenated polydecene (Puresyn4). Chemical compositions of the oils are present in Table 3.1. Different monomers ratios were tested in order to evaluate if it is possible the control of charge density

in the synthesized polymers using this new formulations. To evaluate the preliminary performance of flocculants developed with the novel health-friendly formulations, they were applied for treatment of oily wastewaters from two different industries, namely dairy and potato crisps manufacturing.

Table 3.1 Trade name and chemical composition of the health-friendly organic phases used.

Trade name	Chemical composition	Chemical composition structures
Carnation	Iso-paraffin	
Marcol82	Mixture of liquid saturated paraffinic hydrocarbons	
Puresyn4	Hydrogenated polydecene	$\text{CH}_3(\text{CH}_2)_7\underset{\text{CH}_3}{\text{CH}}\text{CH}_2\underset{(\text{C}_{10}\text{H}_{21})_x}{\text{CH}}(\text{CH}_2)_7\text{CH}_3$ <p>where <math>x = 1</math> to <math>4</math></p>





## 2. POLYELECTROLYTES SYNTHESIS

### 2.1. Materials

Acrylamide (AAm) solution, at 50 wt%, was purchased from Kemira (Botlek, Netherlands). The monomer 2-(acryloyloxy)ethyltrimethyl ammonium chloride (AETAC), at 80 wt%, was purchased from BASF (Bradford, UK) and used as received. Tert-butyl hydroperoxide (TBHP) was purchased from Acros Organics (Geel, Belgium). Sodium metabisulfite (MBS) was purchased from Brenntag (Esseco, Italy). Diethylenetriaminepentaacetic acid pentasodium salt solution (Pentasodium DTPA) was purchased from Keininghaus Chemie (Essen, Germany). Adipic acid was purchased from Merck (Hohenbrunn, Germany). The surfactants Sorbitan isostearate (Crill 6) and Synperonic LF/30 were purchased from Croda (Goole, England). PEG-7 hydrogenated castor oil (Cremophor WO7) was purchased from BASF (Ludwigshafen, Germany). The hydrogenated polydecene (Puresyn4) and the mixture of liquid saturated paraffinic hydrocarbons (Marcol82) were supplied by ExxonMobil (Switzerland). The iso-paraffin (Carnation) was purchased from Sonneborn (Amsterdam, Netherlands). Deuterium oxide, potassium polyvinyl sulphate (PPVS) and methylene blue were supplied by Sigma-Aldrich (St. Louis, USA). Sodium Chloride (NaCl), hexane, acetone and isopropanol were purchased from VWR (Leuven, Belgium). Ferric chloride was supplied by Brenntag Química (Sevilla, Spain).

Table 3.2 compares the characteristics of an example of a traditional oil applied<sup>103</sup>, Exxsol D100, with the health-friendly oils under the commercial names Carnation, Puresyn4, and Marcol82.

Table 3.2 Comparison between traditional and alternative health-friendly oils used in inverse-emulsion polymerizations.

	<b>Aromatic content (wt%)</b>	<b>Density (g/ml)</b>	<b>Viscosity (mm<sup>2</sup>/s at 40°C)</b>	<b>Flash point (°C)</b>
Exxsol D100	<0.5	0.819	3.1	103
Carnation	0	0.829-0.859	18.3	186
Puresyn4	0	0.820	18.0	221
Marcol82	0	0.842-0.855	14.5-17.5	182

## 2.2. Experimental description

### 2.2.1. Inverse-emulsion polymerization

Inverse-emulsion polymerizations were carried out in a 500 mL glass reactor. Prior to reaction, the aqueous phase was prepared with deionized water, acrylamide, AETAC and 0.625 wt % of adipic acid for hydrolytic stability of the polymers. The copper was chelated with 334 ppm of pentasodium DTPA and the viscosity was controlled by adding lactic acid in the suitable amount. The total monomer level of the initial emulsion was 40 wt %. Sorbitan isostearate and PEG-7 hydrogenated castor oil were the surfactants blended to obtain a hydrophilic–lipophilic balance (HLB) between 4.5 and 5.5 depending on the organic phase. Carnation, Puresyn4 and Marcol82 were used as organic phases. The aqueous phase was added to the organic phase under mechanical stirring at 700 rpm for 30 min using an homogenizer, and the viscosity was measured. The monomers emulsion was then degassed with nitrogen for 60 min under mechanical stirring (700 rpm). Polymerizations were initiated by injecting 100 ppm of TBHP aqueous solution to the reactor and then a solution of 1.0 wt% sodium MBS. TBHP and sodium MBS were used as the initiator redox couple. The peak temperature was between 60 and 65 °C, being the exact maximum of the exotherm dependent on the monomers ratio. Additional quantities of TBHP and sodium MBS were added to scavenge residual monomer. After the batch had cooled down to 32 °C, 2.20 wt% of wetting agent (Synperonic LF/30) was added to allow a rapid inversion of the polymer when added to water. For each organic phase, three different monomers ratios were used (see Table 3.3). A schematic representation of the synthesis reaction of the copolymer Poly(AAm-AETAC) is shown in Figure 3.1.

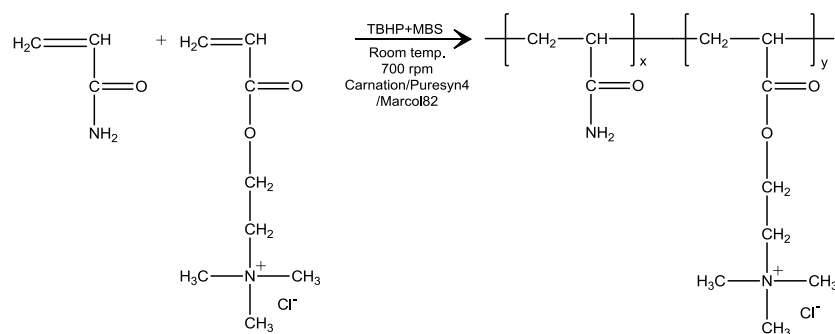


Figure 3.1 Representation of the synthesis reaction for Poly(AAm-AETAC), using as monomers acrylamide and AETAC.

Table 3.3 Monomers ratios in the feed mixture and organic phases used for the copolymers production. 40 series for 40 wt% of AETAC, 60 series for 60 wt% of AETAC and 80 series for 80 wt% of AETAC.

Polymer designation	AAm ratio		AETAC ratio		Organic phase
	(wt%)	(mol%)	(wt%)	(mol%)	
40_Puresyn4	60	80	40	20	Puresyn4
40_Carnation	60	80	40	20	Carnation
40_Marcol82	60	80	40	20	Marcol82
60_Puresyn4	40	65	60	35	Puresyn4
60_Carnation	40	65	60	35	Carnation
60_Marcol82	40	65	60	35	Marcol82
80_Puresyn4	20	41	80	59	Puresyn4
80_Carnation	20	41	80	59	Carnation
80_Marcol82	20	41	80	59	Marcol82

### 2.2.2. Isolation of polyelectrolytes

All polymers were isolated by dilution of 3 g of emulsion in 9 mL of hexane and following addition to a mixture of 240 mL of acetone and 18 mL of isopropanol under stirring. After 15 min, the precipitate was filtered under vacuum, washed with fresh acetone and dried in an oven at 60 °C overnight. The samples were stored in a desiccator.

### 2.2.3. Characterization techniques

The fourier-transform infrared (FTIR) spectra were recorded on a Bruker Tensor 27 spectrometer, equipped with an attenuated total reflection (ATR) MKII Golden Gate accessory with a diamond crystal 45° top plate. The spectra were collected in the 500-4000  $\text{cm}^{-1}$  range with a resolution of 4  $\text{cm}^{-1}$  and a number of scans of 128. For the measurements, polymers in the powder state were used.

Charge density was determined by the colloid titration method with PPVS using methylene blue as indicator, as described in the literature previously<sup>215</sup>. At least three measurements for each sample were performed.

The carbon nuclear magnetic resonance (<sup>13</sup>C NMR) spectra were recorded on a Bruker Avance III 400 MHz NMR spectrometer. Samples were dissolved at room temperature in deuterium oxide at about 5% (w/v) concentration and put inside 5 mm NMR tubes. <sup>13</sup>C NMR

spectra were acquired at 25 °C using a spectral width of 220 ppm, relaxation delay 2 s, acquisition time 1.37 s, 90° pulse, and 20 000 scans. Signals were referenced to 3-(trimethylsilyl)propionate-d<sub>4</sub>.

The intrinsic viscosity (IV) of the isolated and redissolved copolymers was determined in 0.05 M NaCl aqueous solution at 20 ± 0.1°C by dilution viscometry, using an automatic capillary viscometer Viscologic T11 (Sematech, France), with a capillary of 0.58 mm. At least two measurements were conducted for each test. The extrapolation to zero concentration was performed according to Huggins equation (3-1)<sup>216</sup>.

$$\frac{\eta_{sp}}{c} = [\eta] + k_H[\eta]^2 \quad (3-1)$$

where  $\eta_{sp}$  is the specific viscosity of a polymer in solution, which is the ratio of the polymer viscosity to that of the solvent,  $c$  is the concentration of the polymer in solution,  $[\eta]$  is the intrinsic viscosity and  $k_H$  is the Huggins coefficient

Hydrodynamic diameter, molecular weight and zeta potential of isolated and redissolved polymers were determined by dynamic light scattering (DLS), static light scattering (SLS) and electrophoretic light scattering (ELS), respectively, in a Malvern Zetasizer Nano ZS, model ZEN3600 (Malvern Instruments Ltd, UK).

Particles in solution are constantly interacting with the solvent molecules, which leads to Brownian motion<sup>217</sup>. The velocity of this movement is dependent on the particle size and on the viscosity of the medium. DLS uses a laser beam that interacts with the particles and gives rise to light scattering. The scattered light presents a fluctuation of intensity which is dependent on the particles movement. The frequency of that fluctuation can be related to the size of particles. Smaller particles move quicker, so the intensity fluctuation rate is higher. This oscillation in scattering intensity is then converted into the particle hydrodynamic diameter after being processed in a digital correlator in the equipment. The correlogram is then treated with the adequate model, dependent on the particle characteristics, to extract information about the particle size distribution<sup>217</sup>. For hydrodynamic diameter, stock solutions of 0.1 g/L of each polymer were prepared in ultrapure water and stirred overnight, using polymers in powder state. All samples were sonicated during 2 min and passed through 1-µm syringe filters prior to analysis. The measurement temperature was set to 25 °C, backscatter detection

(173° angle) was used and CONTIN model was used to treat the correlogram, with at least three measurements for each sample performed.

When using SLS, the equipment measures the intensity of the scattered light for several concentrations of each polymer sample and compares this with the scattering resulting from the standard used. The intensity of the scattered light is represented against the polymer concentration giving the so called Debye plot.

If the Rayleigh equation (3-2) is used to correlate the intensity of light scattered by a particle in solution with the solution concentration<sup>217</sup>:

$$\frac{KC}{R_\theta} = \left( \frac{1}{MW} + 2A_2C \right) P_\theta \quad (3-2)$$

where  $R_\theta$  is the Rayleigh ratio (ratio of scattered light to incident light on the sample),  $C$  is the concentration,  $MW$  is the weight-average molecular weight,  $A_2$  is the 2<sup>nd</sup> virial coefficient describing the molecule-solvent interaction strength,  $P_\theta$  is a correction shape factor and  $K$  is an optical constant, which is dependent on the laser wavelength and on the influence of concentration on the refractive index of the solution. This equation can as well be plotted in the Debye plot (Figure 3.2).

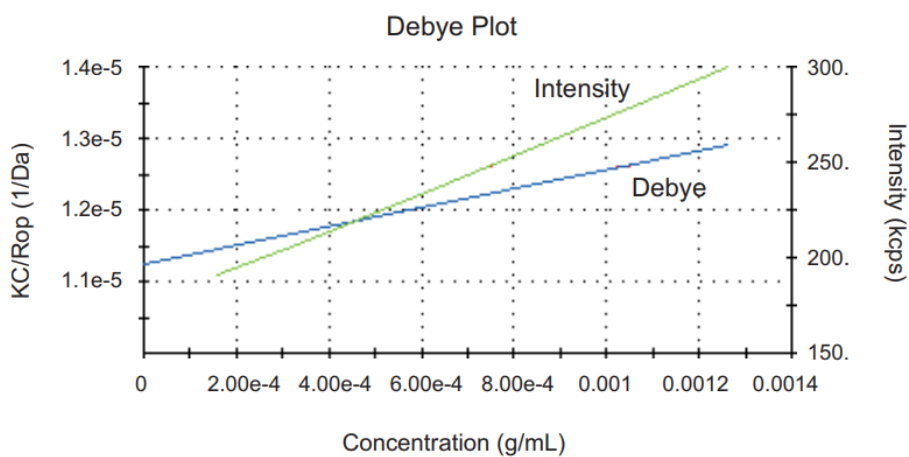


Figure 3.2 A typical representation of a Debye plot<sup>217</sup>.

In this case, the weight-average molecular weight (MW) of the polymer is determined from the interception point on the X axis of the Debye plot, which provides the value of  $1/\text{MW}$ , according to equation (3-2)(see in Figure 3.2 an example of a typical Debye plot).

Molecular weight measurements of polymers were performed using stock solutions (0.1 g/L) of each polymer prepared in NaCl 0.05 M and stirred overnight. The samples for analysis were then obtained by diluting the stock solutions to concentrations from 0.09-0.06 g/L. All samples were sonicated during 2 min and passed through 0.45- $\mu\text{m}$  syringe filters prior to analysis. Toluene was used as standard. Previously, the refractive index (RI) of each solution was determined, in the refractometer Atago RX-5000D. The measurements were performed at 25 °C and the calibration of the equipment was completed using the solvent used, in this case NaCl 0.05 M. After this, each solution of the different concentrations was analysed and the RI acquired. By plotting RI versus concentration we could obtain  $dn/dc$ , through the extraction of the slope of the best fit, which was then supplied to the SLS software. The complete data is available in Appendix A, Figure A.11 to A.13.

In ELS measurements, an electric field is applied to the sample and the charged particles are attracted and migrate to the electrode of opposite charge. The speed of this migration is related to the electrophoretic mobility and it depends on the strength of the electric field applied, dielectric constant, viscosity of the medium and the zeta potential of the particles. To determine the zeta potential, the Henry equation (3-3) is applied<sup>217</sup>:

$$U_E = \frac{2\mathcal{E}z\zeta f(ka)}{3\mu} \quad (3-3)$$

where  $U_E$  is the electrophoretic mobility,  $\mathcal{E}$  is the dielectric constant,  $\zeta$  is the zeta potential,  $f(ka)$  is the Henry's function and  $\mu$  is the medium viscosity. When this measurement is performed in aqueous media,  $f(ka)$  is 1.5, referred to as the Smoluchowski approximation.

For zeta potential measurements, 1 mL of each stock solution (0.2 g/L) in ultrapure water was carefully injected with a syringe into a folded capillary cell (ref. DTS1070), closed by cell stoppers. At least three measurements were conducted for each sample.

### 2.3. Results and discussion

Based on previous literature referring copolymers of acrylamide and AETAC<sup>200</sup>, series of this copolymer with various charge densities were developed using the health-friendly new formulations in the inverse-emulsion polymerization. After a complete purification of the copolymers they were characterized for their chemical compositions (Table 3.4). In general, all produced polymers present lower charged fraction than the expected estimated from the ratios of monomers at the start of the reaction. These differences suggest a possible incomplete polymerization, due to, for example, the presence of oxygen molecules in the synthesis, that react with the radicals, interfering with the polymerization. For the same charged fractions, there is no large variance between different oils used in the health-friendly formulation.

Table 3.4 Charged fractions calculated from the initial mass balance and estimated by titration for Poly(AAm-AETAC) copolymers.

<b>Polymer designation</b>	<b>Charged fraction from the initial mass balance (wt%)</b>	<b>Charged fraction estimated by titration (wt%)</b>
40_Puresyn4	40	37 ± 4
40_Carnation	40	37 ± 7
40_Marcol82	40	35 ± 7
60_Puresyn4	60	50 ± 1
60_Carnation	60	55 ± 7
60_Marcol82	60	55 ± 7
80_Puresyn4	80	68 ± 9
80_Carnation	80	68 ± 8
80_Marcol82	80	69 ± 10

<sup>13</sup>C NMR spectroscopy (example for 80\_Marcol82 in Figure 3.3) evidenced the presence of the two different monomers. The <sup>13</sup>C NMR spectra were dominated by a very intense signal at 54 ppm due to the resonance of the three methyl carbons of the AETAC unit; signals due to the carbons from the amide functions of AAm and ester functions of AETAC, were also observed (marked with asterisk in Figure 3.3). The complete data for other polyelectrolytes is available in Appendix A, Figure A.1 to A.4.



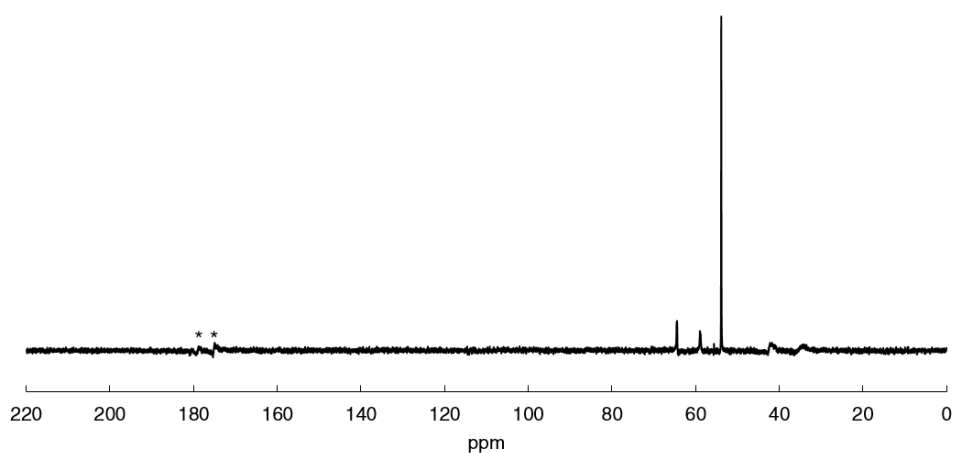


Figure 3.3  $^{13}\text{C}$  NMR spectra for the Poly(AAm-AETAC) copolymer 80\_Marcol82.

ATR-FTIR spectroscopy provided a good insight into the main structural features of the poly(AAm-AETAC) copolymers obtained using the health-friendly formulations. Bands due to both constituents of the copolymer were clearly distinguished in the spectra. The spectra (Figure 3.4 and Figure 3.5) showed the characteristic bands of AAm monomers at ca.  $3345\text{ cm}^{-1}$  and  $3185\text{ cm}^{-1}$ , due to the asymmetric and symmetric  $\text{NH}_2$  stretching<sup>218</sup>. A band at  $1655\text{ cm}^{-1}$  due to the  $\text{C}=\text{O}$  stretching (amide 1) of AAm was also observed, which was accompanied by the amide 2 band at  $1615\text{ cm}^{-1}$ , which reduced in relative intensity when a lower amount of AAm was used in the synthesis (see Figure 3.4). Besides, AETAC characteristic bands<sup>219</sup> were also observed:  $1730\text{ cm}^{-1}$  from the  $\text{C}=\text{O}$  stretching in ester bond,  $1478\text{ cm}^{-1}$  (asymmetric bending of  $\text{CH}_3$  groups),  $1163\text{ cm}^{-1}$  ( $\text{C}-\text{O}$  stretching in ester bond) and  $952\text{ cm}^{-1}$  (asymmetric stretching of  $\text{C}-\text{N}$  bonds). The relative intensity of the bands from AETAC increased with the increase of the amount of AETAC (vs. AAm) used in the synthesis (see Figure 3.4). Interestingly, for the same monomers' ratio, similar infrared spectra were obtained regardless of the oil used in the copolymerization reaction (see Figure 3.5 for 60 series), which indicates that the composition of the final products did not differ much with the organic phase used if the reaction conditions were kept similar.

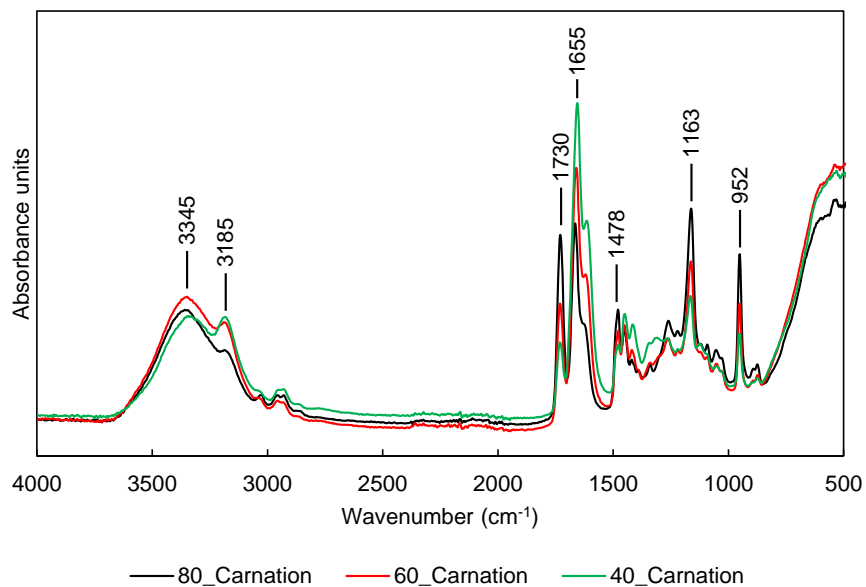


Figure 3.4 ATR-FTIR spectra for Poly(AAm-AETAC) copolymers developed in the same health-friendly formulation (Carnation as organic phase), 40\_Carnation, 60\_Carnation and 80\_Carnation.

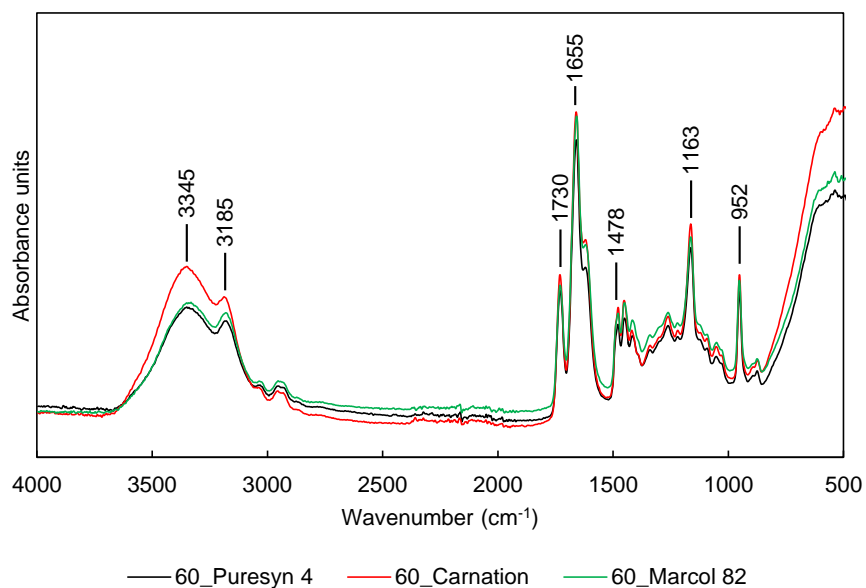


Figure 3.5 ATR-FTIR spectra of Poly(AAm-AETAC) copolymers obtained, with similar charge density and employing different health-friendly formulations, 60\_Puresyn4, 60\_Carnation and 60\_Marcol82.

Table 3.5 summarizes the results of the characterization of the final polyelectrolytes (zeta potential hydrodynamic diameter, intrinsic viscosity, polydispersity index (PDI) and weight-

average molecular weight). Detailed data and plots are available in Appendix A, Figure A.5 to A.19.

Zeta potential revealed consistent results, considering the three different charge density ranges of the polymers estimated from titration method, which is the key parameter affecting this value (see Table 3.4). The polymers with lower charge density have lower values of zeta potential while the polymers with higher charge density have higher values of zeta potential. The values are also similar between polymers with the same charge density produced using different oils, more significant with the increase of the charged fraction.

The particle size of the copolymers was determined by DLS and the results are also presented in Table 3.5. In water solution the smaller particles have a mean diameter 40 nm and the larger particles 77 nm. For same charge density, Puresyn4 leads always to higher hydrodynamic diameter while Marcol82 resulted always in lower values. This can be attributed to a tendency for polymer aggregation when using Puresyn4 as organic phase, as confirmed by the PDI values in Table 3.5, and by the complete size distribution in Appendix A (Figure A.8 to A.10). On the other hand, Marcol82, as a mixture of hydrocarbons, presents higher variability in their chemical composition, thus this variability may affect the polymerization yield, as well as the final size of the polymer<sup>220</sup>.

All the values of weight-average molecular weight and intrinsic viscosity (IV) possess similar order of magnitude, meaning that the different oils used in the synthesis process do not have a considerable influence in the final length of the polymer chain. The same trends were observed for IV as for the hydrodynamic diameter of the polymers, higher values were obtained for the polyelectrolytes developed using Puresyn4, while lower values were obtained for the polyelectrolytes obtained using Marcol82. Regarding molecular weight, the same trend for the influence of the synthesis medium, which has just been described for hydrodynamic diameter and IV, can be observed for the higher and lower charge densities (40 and 80 series), however for median charge density (60 series) this was not observed. Since the values of molecular weight are not exactly the same, associations are difficult to be verified, however, comparing 40\_Marcol82 with 80\_Carnation and 80\_Marcol82, which present similar molecular weight, the IV values are higher in the last two cases, where the charge density is also higher. The same can be verified for 60\_Puresyn4 and 80\_Puresyn4, presenting also similar molecular weight.

In general, the values for IV of the developed polymers are slightly lower than reported in literature for similar copolymers, analyzed in similar conditions<sup>95,103,221</sup>. However, the IV values

still represent polymers of high molecular weight, which is the main objective, as is possible to observe in Table 3.5.

Table 3.5 Zeta potential measured by ELS, hydrodynamic diameter measured by DLS, Intrinsic viscosity in 0.05M NaCl calculated according with Huggins equation and weight-average molecular weight measured by SLS.

<b>Polymer designation</b>	<b>Zeta potential (mV)</b>	<b>Hydrodynamic diameter (nm)</b>	<b>Intrinsic viscosity (mL/g)</b>	<b>Polydispersity index</b>	<b>Weight-average molecular weight (10<sup>6</sup> Da)</b>
40_Puresyn4	26 ± 4	73 ± 5	1 546	0.47	0.36 ± 0.002
40_Carnation	17 ± 3	45 ± 3	1 207	0.19	0.30 ± 0.07
40_Marcol82	19 ± 4	44 ± 1	1 123	0.15	0.27 ± 0.001
60_Puresyn4	47 ± 4	70 ± 2	1 550	0.45	0.51 ± 0.03
60_Carnation	47 ± 4	41 ± 2	1 460	0.14	0.49 ± 0.08
60_Marcol82	32 ± 3	40 ± 4	1 434	0.22	0.64 ± 0.1
80_Puresyn4	84 ± 5	75 ± 3	1 638	0.45	0.56 ± 0.05
80_Carnation	87 ± 4	63 ± 5	1 353	0.42	0.22 ± 0.04
80_Marcol82	87 ± 6	44 ± 1	1 214	0.45	0.22 ± 0.01

In Palomino *et al.*<sup>103</sup>, a polymer similar to 80 series developed in the present study, though produced in traditional medium, is characterized (AlpineFloc BHMW, 80 wt% charge). Values of zeta potential for the polymers here developed using health-friendly formulations are slightly higher, while values for hydrodynamic diameter and molecular weight are lower. In theory, higher values of zeta potential should lead to higher hydrodynamic diameter, however the corresponding molecular weight is also lower, which corroborates the lower hydrodynamic diameter.



### 3. PRELIMINARY EVALUATION OF PERFORMANCE

#### 3.1. Experimental description

For each polymer, 200-mL of stock solution of 0.4 wt% concentration were prepared under magnetic stirring and keeping the mixing for sixty minutes. Polymers in inverse-emulsion state were used. Polymer solution samples of 1 mL were added to 200-mL samples of pre-agitated wastewater with a successive increase of concentration from 27 mg/L until a maximum of 108 mg/L. In each addition, the suspension-polymer mixture was manually agitated for 10 seconds. For the dairy industry effluent the tests were conducted at pH 5 and with addition of 5 drops of ferric chloride 1.0% solution before the flocculant addition, since it is a common coagulant for treatment of this type of effluent and which proved to help in the flocculation process. For the potato crisps manufacturing effluent the tests were performed at pH 11.6 without the addition of any aid, since different coagulants were tested and no improvement in the flocs formation was observed. The conditions chosen were based on a pre-screening for all pH range and using combinations with common aids (ferric chloride and polyaluminum chloride). The size of the flocculated particles was visually assessed and the absorbance of the treated supernatant water was measured for the polymer concentration that showed better results, after 30 min of settling, using a UV/Vis spectrophotometer (Beckman, DU 650).

Oily wastewaters tested include an effluent obtained from dairy industry (Lactogal, Portugal) and an effluent from potato crisps manufacturing industry (supplied by Adventech Group, Portugal).

#### 3.2. Results and discussion

Two oily wastewaters from industry were used to evaluate the developed flocculants performance. Table 3.6 summarizes the results obtained, for each polymer, for the best conditions (pH and presence or not of aid) and with the optimized concentration of flocculant, from which no more absorbance reduction was observed. The flocculation performance is described by the absorbance reduction of the supernatant waters. Considering the effluent from dairy industry, the cationic flocculant 80\_Carnation provided the best results, for the mentioned conditions, giving the highest absorbance reduction. This is the polymer which combines higher zeta potential with a high hydrodynamic diameter. Using other polymers with lower cationic charges produced in Carnation as organic phase, 60\_Carnation and 40\_Carnation, the reduction of absorbance was not significant and the floc

formation was not visible. The same happened when the synthesis was conducted in Puresyn4 or Marcol82, with the cationic flocculants 80\_Puresyn4 or 80\_Marcol82, presenting reasonable reduction, but lower than for 80\_Carnation. The lower reduction is obtained for the case of 80\_Marcol82, however this is also the polymer with lowest hydrodynamic diameter in the 80 series, even if charge density is similar to the other two polymers of the 80 series. Thus, a higher charge density and a higher hydrodynamic diameter are necessary for the polymer to be effective for this effluent treatment, probably combining the patching and bridging mechanisms.

Table 3.6 Absorbance reduction for effluents from dairy and potato crisps manufacturing industries.

Polymer designation	Dairy industry effluent (pH 5 and addition of 5 drops of ferric chloride)		Potato crisps manufacturing industry effluent (pH 11.6 and no coagulant)	
	Absorbance reduction (%)	Dosage (mg/L)	Absorbance reduction (%)	Dosage (mg/L)
40_Puresyn4	9	80	67	108
40_Carnation	8	80	72	108
40_Marcol82	21	80	70	108
60_Puresyn4	28	80	75	108
60_Carnation	7	80	74	108
60_Marcol82	17	80	73	108
80_Puresyn4	61	80	74	108
80_Carnation	74	80	76	108
80_Marcol82	37	80	75	108

Regarding the effluent from potato crisps manufacturing industry, the cationic flocculant 80\_Carnation provided again the best results, giving an absorbance reduction of 76%, even if the flocculants 40\_Carnation and 60\_Carnation showed similar results. Furthermore, for this effluent, all the polymers developed presented high absorbance reduction, with the exception of 40\_Puresyn4, that showed a slightly lower absorbance reduction. Apparently, for this effluent the synthesis medium does not seem to have a strong effect on the flocculant performance.

#### 4. CONCLUSIONS

The tested health-friendly formulations showed to be able to be used in inverse-emulsion polymerization of documented cationic polyelectrolytes applied in industrial wastewater treatment. Characterization of the polymers revealed suitable characteristics for the developed polymers, which confirm good copolymerization performance, adequate molecular weight and tunable charge density, though slightly distinct when comparing with similar polymers developed in traditional medium. These characteristics were confirmed by several characterization techniques. Despite some differences in the characteristics of the polymers developed with the new formulations when compared with the traditional ones, evaluation of performance using the developed polymers suggests an effective flocculation ability in two oily wastewaters from different industries. The best results were accomplished with polymers with the highest charge density and using Carnation oil as organic phase.

Finally, based on the obtained results, Puresyn4 and Carnation were the organic phases chosen for the health-friendly formulations to be used to proceed for the further development of novel polyelectrolytes for application in oily wastewater treatment, since they are more viable from the economic point of view and no superior performance was observed with Marcol82.





---

CHAPTER 4

**Synthesis of novel polyelectrolytes**



## 1. INTRODUCTION

The efficiency of flocculation using organic polyelectrolytes is much higher than with inorganic coagulants. Even in low dosages, polyelectrolytes can effectively promote floc growing and improve separation effect<sup>222</sup>.

This chapter describes the development of novel cationic and anionic polyelectrolytes designed to the application as flocculants to treat oily effluents, using health-friendly formulations, described in the previous chapter, in their synthesis. Inverse-emulsion polymerization was applied, using different non-irritating continuous phases with high boiling point, high purity and high stability. In particular, Poly(acrylamide-co-[3-(methacryloylamino)propyl] trimethylammonium chloride) (Poly(AAm-MAPTAC)) and Poly(acrylamide-co-acrylamido-2-methyl-1-propanesulfonic acid) (Poly(AAm-Na-AMPS)) were synthesized, in different polymer compositions.

In addition to the aforementioned copolymers, polyelectrolytes comprising also a hydrophobic monomer were also developed. These hydrophobic monomers were chosen based on the different number of methylene groups in the aliphatic chains, in order to evaluate the influence of the hydrophobic chain length in the performance of the flocculants. For example, in Lee *et al.*<sup>120</sup> the influence of hydrophobic chain length with six, eight and twelve methylene groups in flocculation performance was evaluated. In the present work it is studied the effect of hydrophobic chain lengths up to eighteen methylene groups. In the case of the cationic polyelectrolyte, stearyl methacrylate (SMA) was used to synthesize the terpolymer Poly(AAm-MAPTAC-SMA), while for anionic polyelectrolyte, the hydrophobic monomers ethyl acrylate (EA), lauryl methacrylate (LMA) and SMA were used to produce the terpolymers Poly(AAm-Na-AMPS-EA), Poly(AAm-Na-AMPS-LMA) and Poly(AAm-Na-AMPS-SMA), respectively.

Carnation and Puresyn4 were chosen as organic phases in the inverse-emulsion polymerization of these polyelectrolytes. The selection was related with the results observed in the previous chapter and also with economic issues. Since Carnation and Puresyn4 led to very similar copolymer characteristics, as it will be presented, subsequent hydrophobic modification was conducted only using the oil Carnation. The polyelectrolytes obtained were characterized in terms of final composition, hydrodynamic diameter, zeta potential and molecular weight. Their flocculation performance was evaluated in the following chapter, in industrial oily effluents from olive oil mill, dairy and potato crisps manufacturing industries without presence of any aid.



## 2. CATIONIC POLYELECTROLYTES

### 2.1. Experimental

#### 2.1.1. Materials

Acrylamide solution, at 50 wt%, was purchased from Kemira (Botlek, Netherlands). The monomer [3- (Methacryloylamino) propyl] trimethyl ammonium chloride (MAPTAC) was purchased from Qingdao Finechem Chemical Co. (Qingdao, China) and used as received. Stearyl methacrylate was purchased from BASF (Ludwigshafen, Germany). TBHP was purchased from Acros Organics (Geel, Belgium). MBS was purchased from Brenntag (Esseco, Italy). Diethylenetriaminepentaacetic acid pentasodium salt solution (Pentasodium DTPA) was purchased from Keininghaus Chemie (Essen, Germany). Adipic acid was purchased from Merck (Hohenbrunn, Germany). The surfactants Sorbitan isostearate (Crill 6) and Synperonic LF/30 were purchased from Croda (Goole, England). PEG-7 hydrogenated castor oil (Cremophor WO7) was purchased from BASF (Ludwigshafen, Germany). The oil Puresyn4, a hydrogenated polydecene, was supplied by ExxonMobil (Switzerland). Carnation, an iso-paraffin, was purchased from Sonneborn (Amsterdam, Netherlands). PPVS and methylene blue were supplied by Sigma-Aldrich (St. Louis, USA).

#### 2.1.2. Inverse-emulsion polymerization

Inverse-emulsion polymerization was carried out in a 500 mL glass reactor. Prior to reaction, the aqueous phase was prepared with deionized water, acrylamide, MAPTAC and 0.625 wt% of adipic acid for hydrolytic stability of the polymers. The copper was chelated with 334 ppm of Pentasodium DTPA. The total monomer level of the initial emulsion was 34 wt%. Sorbitan isostearate and PEG-7 hydrogenated castor oil were the surfactants blended to obtain a HLB between 5.0 and 5.3, according with the monomers ratios. Carnation, an iso-paraffin, and Puresyn4, an hydrogenated polydecene, were used as organic phases. The aqueous phase was slowly added to the organic phase under mechanical stirring for 30 min. In the case of the hydrophobically modified terpolymers (Poly(AAm-MAPTAC-SMA)), the desired amount of hydrophobic monomer SMA, was added at this point to the emulsion. The monomers emulsion was then degassed with nitrogen for 60 min under mechanical stirring (700 rpm), at room temperature. Polymerizations were initiated by injecting 100 ppm of TBHP aqueous solution to the reactor and then a solution of sodium MBS 1.0 wt%. TBHP and sodium MBS were used as the initiator redox couple. The peak temperature was between 45 and 52 °C,

being the exact maximum temperature of the exotherm dependent on comonomer composition. After the completion of reaction, additional quantities of TBHP and sodium MBS were added to scavenge residual monomer. After the batch had cooled down to 32 °C, 2.20 wt% wetting agent (Synperonic LF/30) was added to allow a rapid inversion of the flocculant when added to water. A schematic representation of the synthesis reaction of the cationic co- and terpolymers (Poly(AAm-MAPTAC) and Poly(AAm-MAPTAC-SMA)) is shown in Figure 4.1 and Figure 4.2.

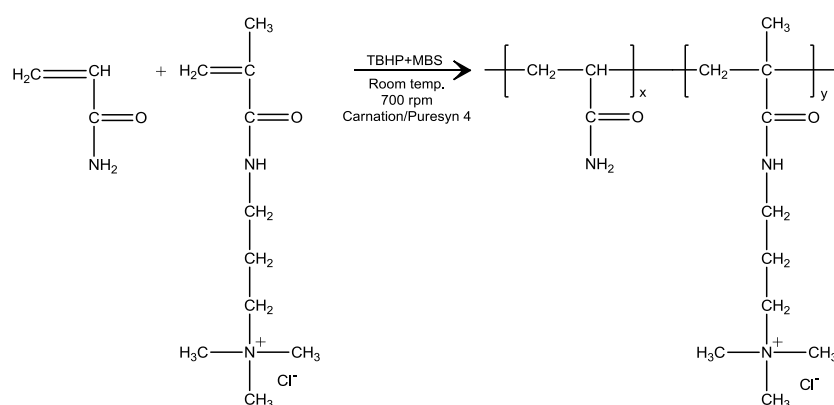


Figure 4.1 Representation of the synthesis reaction for Poly(AAm-MAPTAC), using monomers of acrylamide and MAPTAC.

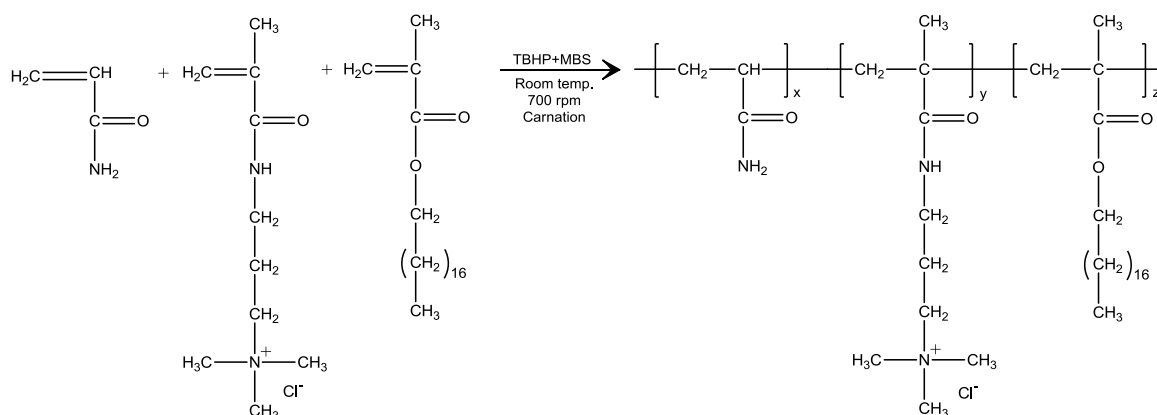


Figure 4.2 Representation of the synthesis reaction for Poly(AAm-MAPTAC-SMA), using monomers of acrylamide, MAPTAC and SMA.

Table 4.1 summarizes the composition of the developed polyelectrolytes. Lower cationic fraction is named as the 25 series, while higher cationic fraction is named as the 60 series. MC

and MP series in the list correspond to the use of Carnation or Puresyn4, respectively, as health-friendly organic phases.

Table 4.1 Summary of the cationic polyelectrolytes developed. Initial composition at the beginning of the polymerization and organic phase used in the health-friendly formulation are described. Copolymers Poly(AAm-MAPTAC): 25MC, 25MP, 60MC and 60MP. Terpolymers Poly(AAm-MAPTAC-SMA): 25M1SC, 25M2SC, 60M1SC and 60M2SC.

Polymer designation	AAm ratio		MAPTAC ratio		SMA ratio		Organic phase
	(wt%)	(mol%)	(wt%)	(mol%)	(wt%)	(mol%)	
25MC	75.0	90.0	25.0	10.0			Carnation
60MC	40.0	67.0	60.0	33.0			Carnation
25MP	75.0	90.0	25.0	10.0			Puresyn4
60MP	40.0	67.0	60.0	33.0			Puresyn4
25M1SC	73.0	90.0	23.0	9.0	4.0	1.0	Carnation
25M2SC	71.0	89.0	21.0	9.0	8.0	2.0	Carnation
60M1SC	38.5	67.0	58.5	32.0	3.0	1.0	Carnation
60M2SC	37.0	66.0	57.0	32.0	6.0	2.0	Carnation

### 2.1.3. Isolation of polymers

For detailed information regarding isolation of polymers see Section 2.2.2. of Chapter 3.

### 2.1.4. Characterization techniques

Charge density was determined by the colloid titration method with PPVS using methylene blue as indicator, as described in the literature previously<sup>215</sup>. At least three measurements for each sample were performed.

FTIR spectra were recorded on a Bruker Tensor 27 spectrometer, equipped with an attenuated total reflection (ATR) MKII Golden Gate accessory with a diamond crystal 45° top plate. The spectra were collected in the 500-4000 cm<sup>-1</sup> range with a resolution of 4 cm<sup>-1</sup> and a number of scans of 128. For the measurements, polymers in the powder state were used.

Hydrodynamic diameter, molecular weight and zeta potential of isolated and redissolved polymers were determined by DLS, SLS and ELS, respectively, in a Malvern Zetasizer Nano ZS, model ZEN3600 (Malvern Instruments Ltd, UK). For detailed information regarding



these techniques, samples preparation and measurement settings see Section 2.2.3. of Chapter 3.

For the hydrodynamic diameter, stock solutions of 0.1 g/L for copolymers Poly(AAm-MAPTAC) and 0.05 g/L for terpolymers Poly(AAm-MAPTAC-SMA) were prepared in ultrapure water and stirred overnight, using polymers in powder state.

Weight- average molecular weight measurements of polymers were performed using stock solutions (0.5 g/L) of each polymer prepared in NaCl 0.1 M and stirred overnight. The samples for analysis were then obtained by diluting the stock solutions at several concentrations from 0.5-0.02 g/L. All samples were sonicated during 2 min and passed through 0.45  $\mu\text{m}$  syringe filters prior to analysis. The measurements were performed at 25 °C and the calibration of the equipment was completed using the solvent used, in this case NaCl 0.1 M. The complete data is available in Appendix B, Figure B.9 to B.20.

For zeta potential measurements, 1 mL of each stock solution (0.1 g/L) in ultrapure water was used. At least three measurements were conducted for each sample.

## 2.2. Results and discussion

After purification of the polymers, their compositions were assessed (Table 4.2). The amount of charged groups and the corresponding real charge density for all synthesized polymers was evaluated by titration<sup>215</sup>. For copolymers, it was observed that the amount of charged groups was slightly lower in the final polymer than the initial monomer ratios of the formulation, which can be due to both a difference in monomer reactivity ratios and/or a non-complete polymerization of the feed monomers. In the case of the terpolymers, it is clear that the charged fraction increased as compared to the corresponding polyelectrolytes that do not contain any hydrophobic monomer, suggesting a non-complete reaction of the acrylamide monomer, possibly due to the presence of some impurity in the hydrophobic monomer SMA, which is acting as transfer agent and absorbing the radicals during the polymerization process.

Table 4.2 Charged fractions for the cationic polyelectrolytes, calculated from the initial mass balance and estimated by titration. Poly(AAm-MAPTAC): 25MC, 25MP, 60MC and 60MP. Poly(AAm-MAPTAC-SMA): 25M1SC, 25M2SC, 60M1SC and 60M2SC.

Polymer designation	Charged fraction from the initial mass balance (wt%)	Charged fraction estimated by titration (wt%)
25MC	25.0	23 ± 0.8
60MC	60.0	42 ± 2.2
25MP	25.0	23 ± 0.7
60MP	60.0	43 ± 0.2
25M1SC	23.0	29 ± 0.1
25M2SC	21.0	28 ± 0.1
60M1SC	58.5	47 ± 0.2
60M2SC	57.0	46 ± 0.2

ATR-FTIR spectroscopy was used to characterize the copolymers for their main structural features (25MC, 60MC, 25MP and 60MP). The spectra of the copolymers (Figure 4.3) showed bands at ca. 3330  $\text{cm}^{-1}$  and 3190  $\text{cm}^{-1}$ , attributed to the N-H stretching vibrations in the monomers. The characteristic amide I band (C=O stretching in the amide groups) of the monomers appeared as a very strong band with maximum at 1651-1660  $\text{cm}^{-1}$ . The frequency of this absorption maximum changed slightly between copolymers depending on the relative content of each monomer, i.e., acrylamide (primary amide) and MAPTAC (secondary amide) in the polyelectrolyte, whose amide functions absorb at a slightly different frequency. Bands showing clearly the presence of MAPTAC were observed at 1532  $\text{cm}^{-1}$  (amide II of secondary amide), 1479  $\text{cm}^{-1}$  (asymmetric bending of CH<sub>3</sub> groups), 967  $\text{cm}^{-1}$  and 915  $\text{cm}^{-1}$  (asymmetric stretching of C4-N bonds), with an increased intensity for the polyelectrolytes with a higher content of MAPTAC (60 series).

It is noteworthy that FTIR spectroscopy confirmed the aforementioned results of the monomer composition in the copolymers, determined by colloidal titration (Table 4.2), as demonstrated by the similar spectra obtained for copolymers 25MC and 25MP and 60MC and 60MP (of comparable monomer composition) and terpolymers 25M1SC and 25M2SC, and terpolymers 60M1SC and 60M2SC. Results also confirmed the reduced influence of the oil used as medium in the polymerization reactions (similar FTIR spectra were obtained for the copolymers 25MC and 25MP, and for the 60MC and 60MP, produced using different health-friendly formulations).

The presence of the hydrophobic monomer SMA used in the preparation of terpolymers Poly(AAm-MAPTAC-SMA) was revealed by the appearance of two sharp bands in the region of the C-H stretching, at 2922 and 2852  $\text{cm}^{-1}$ , which are better resolved in the spectra of polyelectrolytes 60M1SC and 60M2SC. These bands are due to the asymmetric and symmetric stretching of the  $\text{CH}_2$  groups of the hydrophobic chain, respectively. Additionally, for the terpolymers 60M1SC and 60M2SC, a band of small intensity at 1729  $\text{cm}^{-1}$  was visible in the FTIR spectra, due to the C=O stretching in the ester bonds of the SMA monomer.

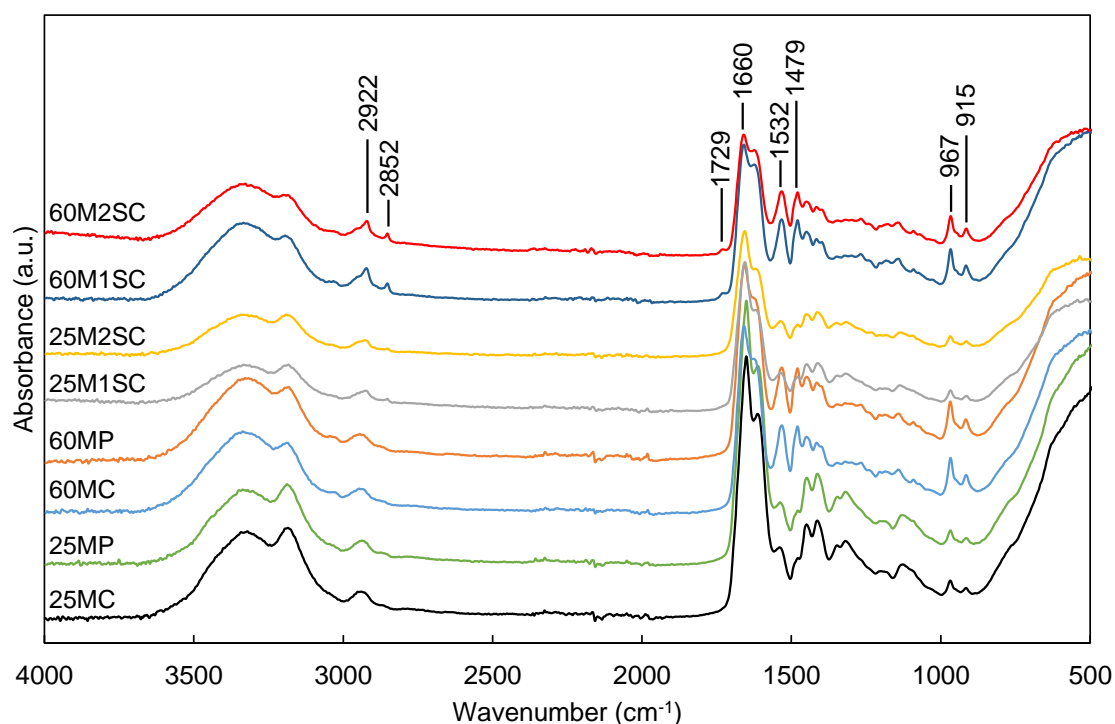


Figure 4.3 ATR-FTIR spectra for the cationic polyelectrolytes prepared. Copolymers Poly(AAm-MAPTAC): 25MC, 25MP, 60MC and 60MP. Terpolymers Poly(AAm-MAPTAC-SMA): 25M1SC, 25M2SC, 60M1SC and 60M2SC.

A summary of the polyelectrolytes characterization, including zeta potential, hydrodynamic diameter, polydispersity index and weight-average molecular weight is given in Table 4.3. The complete data is available in Appendix B, Figure B.1 to B.20.

The zeta potential values for the different polymers are consistent with the charge density of the polyelectrolytes evaluated by titration (Table 4.2). Charged groups are the crucial parameter affecting this value. Comparing the copolymers produced in the two different formulations, it is possible to observe that polyelectrolytes synthesized using Puresyn4 oil

present higher zeta potential values, and also higher charged fraction, when compared with polyelectrolytes synthesized using Carnation oil. Furthermore, comparing co- and terpolymers developed using the same oil in the formulation (Carnation), when hydrophobic content is present the zeta potential increases, as well as the charged fraction in the final polymer is also higher as seen in Table 4.2 (compare 25MC with 25M1SC and 25M2SC, and 60MC with 60M1SC and 60M2SC).

Table 4.3 Polyelectrolytes characterization: zeta potential, hydrodynamic diameter and weight-average molecular weight. Poly(AAm-MAPTAC): 25MC, 25MP, 60MC and 60MP. Poly(AAm-MAPTAC-SMA): 25M1SC, 25M2SC, 60M1SC and 60M2SC.

Polymer designation	Zeta Potential (mV)	Hydrodynamic diameter (nm)	Polydispersity index	Weight-average molecular weight ( $10^6$ Da)
25MC	$44 \pm 2$	$70 \pm 2$	0.68	$0.5 \pm 0.02$
60MC	$75 \pm 1$	$234 \pm 9$	0.62	$2.9 \pm 0.7$
25MP	$51 \pm 2$	$66 \pm 1$	0.64	$0.4 \pm 0.04$
60MP	$79 \pm 2$	$287 \pm 13$	0.51	$3.1 \pm 0.03$
25M1SC	$61 \pm 1$	$101 \pm 5$	0.91	$1.1 \pm 0.03$
25M2SC	$62 \pm 1$	$138 \pm 1$	0.61	$1.1 \pm 0.2$
60M1SC	$97 \pm 1$	$138 \pm 9$	0.63	$1.0 \pm 0.09$
60M2SC	$89 \pm 1$	$159 \pm 7$	0.44	$1.3 \pm 0.01$

The hydrodynamic diameter supplies information about the polymer conformation in solution. There is a good correlation between hydrodynamic diameter and polymer molecular weight for polymers with identical cationic fraction. Also, when charge density increases for similar molecular weight, the hydrodynamic diameter increases, as expected, since repulsion between charges makes the polymer less coiled (compare 25M1SC and 60M1SC, and 25M2SC and 60M2SC). Since the hydrodynamic diameters were measured in water solutions, the hydrophobicity present in the polyelectrolytes can affect their conformation in water, leading to similar diameters even when charge density increases (compare 25M2SC and 60M1SC). That is, a higher hydrophobic content results, usually, in a less coiled polymer. Regarding the hydrodynamic diameters distribution, this appears to be significantly broad, considering the PDI values in Table 4.3, as can also be verified by the plots presented in Appendix B, Figure B.5 to B.8. In copolymers, for both MC and MP series, increase of cationic fraction also increases the molecular weight, suggesting that the cationic monomer (MAPTAC) has higher

reactivity than acrylamide. However, the introduction of the hydrophobic monomer affects this reactivity, since terpolymers have very similar molecular weight values, independently of the cationic fraction.

It is worth noting that molecular weight measured by SLS may not represent the exact real values of the absolute molecular weight, due to all the interferences (dust contaminations or polymer aggregation) that can affect the measurements, even if very good correlation coefficients were always obtained in the Debye plots, as can be seen in Appendix B, Figure B.13 to B.20. However, the trends detected seem to be correct, considering the very good correlation between the hydrodynamic diameters and the molecular weights measured. On the other hand, the molecular weight values obtained are in accordance with the molecular weight ranges presented in the literature for copolymers comprising the same monomers, acrylamide and MAPTAC which are, in some cases lower and in other cases higher, depending on the polymerization method used<sup>223,224</sup>.

### 3. ANIONIC POLYELECTROLYTES

#### 3.1. Experimental

##### 3.1.1. Materials

The monomer Acrylamido-2-methyl-1-propanesulfonic acid sodium salt solution (Na-AMPS), at 50 wt%, was purchased from Lubrizol (Bradford, UK) and used as received. Ethyl acrylate (EA) and lauryl methacrylate (LMA) were purchased from Evonik (Darmstadt, Germany). Sodium chloride and sodium dihydrogen phosphate were supplied by PanReac (Barcelona, Spain). Sodium azide was purchased from Sigma (St. Louis, USA). For details of remaining materials, see Section 2.1.1. of the present Chapter.

##### 3.1.2. Inverse-emulsion polymerization

As described previously for the cationic polyelectrolytes, inverse-emulsion polymerization was carried out in a 500 mL glass reactor. Prior to reaction, the aqueous phase was prepared with deionized water, acrylamide, Na-AMPS and, again, with 0.625 wt% of adipic acid for hydrolytic stability of the polymers. The copper was chelated in the same way as for the cationic polyelectrolytes. The total monomer level of the initial emulsion was 34 wt%. Sorbitan isostearate and PEG-7 hydrogenated castor oil were, as well, the surfactants blended to obtain a HLB between 4.75 and 5.75, according with the monomers composition and organic phase used. Carnation and Puresyn4 were used as organic phases. The aqueous phase was slowly added to the organic phase under mechanical stirring for 30 min. In the case of the combination with hydrophobic monomers, the desired amount of hydrophobic monomer (EA, LMA or SMA) was added at this point to the emulsion. The monomers emulsion was then degassed with nitrogen for 60 min under mechanical stirring (700 rpm), at room temperature. Polymerizations were initiated, in the same way as for the cationic polyelectrolytes, by injecting 100 ppm of TBHP aqueous solution to the reactor and then a solution of sodium MBS 1.0 wt%. TBHP and sodium MBS were used as the initiator redox couple. The peak temperature was between 41 and 57 °C, being the exact maximum temperature of the exotherm, dependent on comonomers composition. After finishing the reaction, additional quantities of TBHP and sodium MBS were added to scavenge residual monomer. After the batch had cooled down to 32 °C, 2.20 wt% wetting agent (Synperonic LF/30) was also added to allow a rapid inversion of the flocculant when added to water. Schematic representation of the several final polymer structures Poly(AAm-Na-AMPS),

Poly(AAm-Na-AMPS-EA), Poly(AAm-Na-AMPS-LMA) and Poly(AAm-Na-AMPS-SMA) are shown in Figure 4.4.

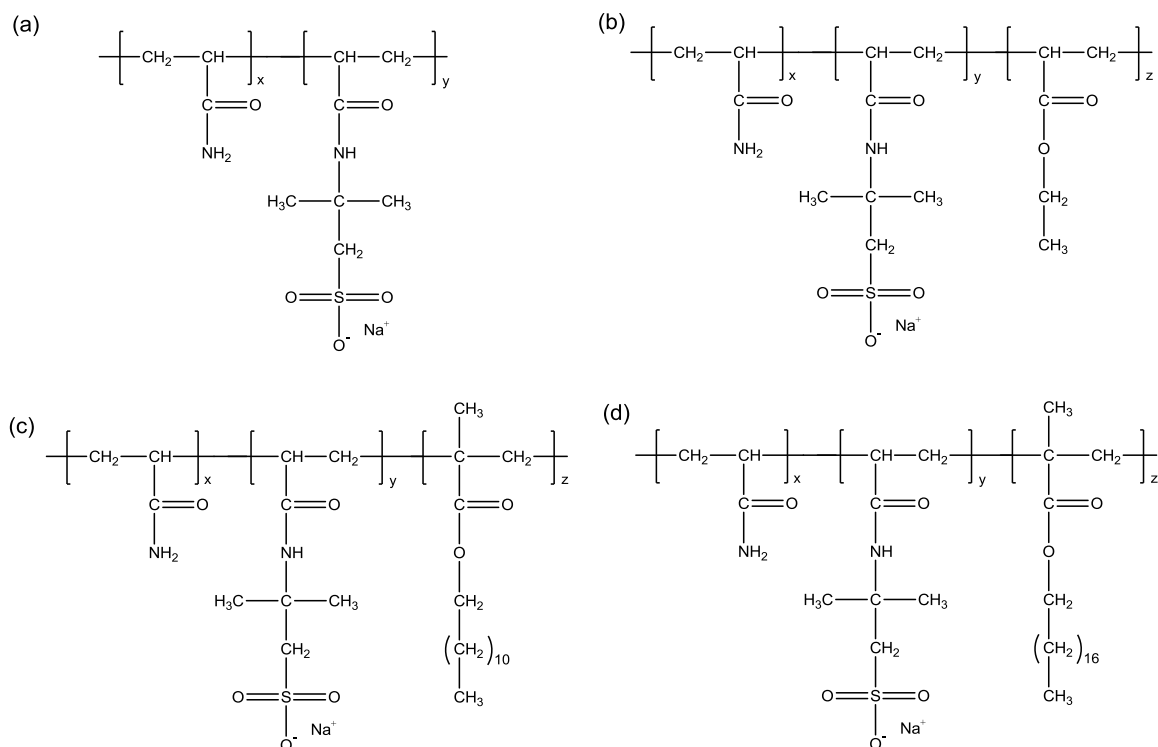


Figure 4.4 Schematic molecular structure of the final polymers obtained: Poly(AAm-Na-AMPS) (a), Poly(AAm-Na-AMPS-EA) (b), Poly(AAm-Na-AMPS-LMA) (c) and Poly(AAm-Na-AMPS-SMA) (d).

Table 4.4 summarizes the composition of the developed polyelectrolytes. Lower anionic fraction is represented as the 50 series, while higher anionic fraction is represented as the 80 series. MC and MP series in the list correspond to the use of Carnation and Puresyn4, respectively, as the health-friendly synthesis organic phase. For the terpolymers, only Carnation was used as organic phase, as discussed previously for the cationic polyelectrolytes (see Section 1 of the present chapter)

Table 4.4 Summary of the anionic polyelectrolytes developed. Initial composition at the beginning of the polymerization and organic phase used in the health-friendly formulation are described. Copolymers Poly(AAm-Na-AMPS): 50AC, 80AC, 50AP and 80AP. Terpolymers Poly(AAm-Na-AMPS-EA): 50A1EC, 50A3EC, 80A1EC and 80A3EC. Terpolymers Poly(AAm-Na-AMPS-LMA): 50A1LC, 50A3LC, 80A1LC and 80A3LC. Terpolymers Poly(AAm-Na-AMPS-SMA): 50A1SC, 50A3SC, 80A1SC and 80A3SC.

<b>Polymer designation</b>	<b>AAm ratio</b>		<b>Na-AMPS ratio</b>		<b>Hydrophobic monomer</b>	<b>Ratio (wt<sup>0</sup>%)</b>	<b>Ratio (mol<sup>0</sup>%)</b>	<b>Organic phase</b>
	<b>(wt<sup>0</sup>%)</b>	<b>(mol<sup>0</sup>%)</b>	<b>(wt<sup>0</sup>%)</b>	<b>(mol<sup>0</sup>%)</b>				
50AC	50.0	74.0	50.0	26.0	-	-	-	Carnation
80AC	20.0	42.0	80.0	58.0	-	-	-	Carnation
50AP	50.0	74.0	50.0	26.0	-	-	-	Puresyn4
80AP	20.0	42.0	80.0	58.0	-	-	-	Puresyn4
50A1EC	49.4	74.0	49.4	25.0	EA	1.2	1.0	Carnation
50A3EC	48.5	72.0	48.5	25.0	EA	3.0	3.0	Carnation
80A1EC	19.7	42.0	79.7	57.0	EA	0.6	1.0	Carnation
80A3EC	19.0	40.0	79.0	57.0	EA	2.0	3.0	Carnation
50A1LC	48.5	74.0	48.5	25.0	LMA	3.0	1.0	Carnation
50A3LC	47.0	73.0	47.0	25.0	LMA	6.0	3.0	Carnation
80A1LC	19.0	41.0	79.0	58.0	LMA	2.0	1.0	Carnation
80A3LC	17.5	39.0	77.5	58.0	LMA	5.0	3.0	Carnation
50A1SC	48.0	74.0	48.0	25.0	SMA	4.0	1.0	Carnation
50A3SC	46.0	72.0	46.0	25.0	SMA	8.0	3.0	Carnation
80A1SC	19.0	41.0	79.0	58.0	SMA	2.0	1.0	Carnation
80A3SC	17.0	38.0	77.0	59.0	SMA	6.0	3.0	Carnation

### 3.1.3. Isolation of polymers

For detailed information regarding isolation of polymers see Section 2.2.2. of Chapter 3.

### 3.1.4. Characterization techniques

Charge density was determined by elemental analysis using an element analyzer EA 1108 CHNS-O (Fisons) and 2,5-Bis(5-tert-butyl-benzoxazol-2-yl) thiophene as standard. C, H and N elemental analyses were performed and the N element was used in the calculation of the charged fraction. At least three measurements for each sample were performed.

The FTIR spectra were recorded, as before, on a Bruker Tensor 27 spectrometer, equipped with an attenuated total reflection (ATR) MKII Golden Gate accessory with a diamond crystal



45° top plate. The spectra were collected in the 500-4000  $\text{cm}^{-1}$  range with a resolution of 4  $\text{cm}^{-1}$  and a number of scans of 128. For the measurements, polymers in the powder state were used.

The  $^1\text{H}$  NMR spectra were recorded on a Bruker Avance III 400 MHz NMR spectrometer. Samples were dissolved at room temperature in deuterium oxide at about 5% (w/v) concentration and placed inside 5 mm NMR tubes.  $^1\text{H}$  NMR spectra were acquired at 25 °C and signals were referenced to sodium 3-(trimethylsilyl)propionate- $\text{d}_4$ .

Hydrodynamic diameter, molecular weight and zeta potential of isolated and redissolved polymers were determined by DLS, SLS and ELS, respectively, in a Malvern Zetasizer Nano ZS, ZEN3600 model (Malvern Instruments Ltd, UK), as described previously for the cationic polyelectrolytes. For detailed information regarding these techniques, samples preparation and measurement settings see section 2.2.3. of Chapter 3.

For the hydrodynamic diameter, stock solutions of 0.05 g/L for copolymers and 0.03 g/L for terpolymers were prepared in ultrapure water and stirred overnight.

Weight-average molecular weight measurements of polymers were performed using stock solutions (0.5 g/L) of each polymer prepared in NaCl 0.5 M and stirred overnight. The samples for analysis were then obtained by diluting the stock solutions at several concentrations from 0.02-0.5 g/L. All samples were sonicated during 2 min and passed through 0.45  $\mu\text{m}$  syringe filters prior to analysis. The complete data is available in Appendix B, Figure B.37 to B.60. From the SLS measurements the Debye plot was produced which provided information about the molecular weight average of the polymers, as has been described in more detail in Section 2.1.4. of the present Chapter.

For zeta potential measurements 1 mL of each stock solution (0.1 g/L) in ultrapure water was used. At least three measurements were conducted for each sample.

Weight-average molecular weight was also estimated by size exclusion chromatography (SEC), for three of the anionic polyelectrolytes developed, in order to confirm the values obtained by SLS. SEC uses a special type of chromatographic columns in which it is assumed that there are no enthalpy interactions between the sample and the stationary phase. Molecules are separated considering their hydrodynamic volume. Large molecules are eluted first, while small molecules will enter the pores of the stationary phase and take longer to elute. For quantitative measurements, at least one concentration detector must to be used, such as ultra-violet (UV), refractive index or light scattering detector (LS). Multi-angle LS is the most common LS

detector for the analysis of molecular weight distributions<sup>225</sup>. The chromatography equipment was a Shimadzu Prominence consisting of a LC-20AD peristaltic pump, a DGU-20A3R degassing unit and a Rheodyne 7725i injector (injection volume of 20  $\mu$ l). Three detectors in series were used: a Shimadzu Prominence RF-20A fluorimetric detector, a multi-angle static light-scattering Wyatt MiniDawn Treos detector and a Shimadzu RID-10A Refractive Index detector (internal temperature 40 °C). Data acquisition and analysis were performed with the Astra 5.3.2.1 software from Wyatt. The chromatography columns were two Waters Ultrahydrogel Linear WAT011545 analytical columns, of 300 mm length and 7.8 mm internal diameter, connected in series. The columns were in a Shimadzu Prominence CTO-20AC column oven ( $T = 35$  °C). The eluent was an aqueous solution of sodium chloride 1 mol/L, sodium dihydrogen phosphate 0.15 mol/L, sodium azide 4.6 mmol/L, pH 4.5, at a flow of 0.8 mL/min, 35 °C<sup>226</sup>. Polymer solutions with concentrations of 0.002 mg/L were prepared using the described eluent and used for the analysis.

### 3.2. Results and discussion

Charge density of polyelectrolytes was assessed by elemental analysis, using the N element ratio as reference for the functional anionic group quantification (Table 4.5). Results confirm the viability of using health-friendly formulations to produce the desired polyelectrolytes, as reported already above. Generally, all polyelectrolytes present lower charge fraction than the theoretical value estimated from the ratios of monomers at the start of the reaction. These discrepancies are typically justified by the different reactivity ratios of the monomers in the copolymerization, or by a possible incomplete polymerization, due to the presence of oxygen molecules in the synthesis, that react with the radicals, interfering with the polymerization. The same was already verified previously for the cationic polyelectrolytes.

Table 4.5 Charged fractions for anionic polyelectrolytes, calculated from the initial mass balance and estimated by elemental analysis. Poly(AAm-Na-AMPS): 50AC, 80AC, 50AP and 80AP. Poly(AAm-Na-AMPS-EA): 50A1EC, 50A3EC, 80A1EC and 80A3EC. Poly(AAm-Na-AMPS-LMA): 50A1LC, 50A3LC, 80A1LC and 80A3LC. Poly(AAm-Na-AMPS-SMA): 50A1SC, 50A3SC, 80A1SC and 80A3SC.

<b>Polymer designation</b>	<b>Charged fraction from the initial mass balance (wt%)</b>	<b>Charged fraction estimated from elemental analysis (wt%)</b>
50AC	50.0	42 ± 0.2
80AC	80.0	63 ± 0.5
50AP	50.0	42 ± 2.3
80AP	80.0	68 ± 2.1
50A1EC	49.4	40 ± 0.4
50A3EC	48.5	40 ± 1.2
80A1EC	79.7	62 ± 1.7
80A3EC	79.0	62 ± 1.5
50A1LC	48.5	41 ± 0.2
50A3LC	47.0	39 ± 4.6
80A1LC	79.0	57 ± 3.3
80A3LC	77.5	63 ± 0.3
50A1SC	48.0	41 ± 2.1
50A3SC	46.0	41 ± 1.5
80A1SC	79.0	58 ± 0.6
80A3SC	77.0	57 ± 0.3

For polyelectrolytes in the same series, with and without the presence of hydrophobic content, it is possible to observe a lower anionic fraction for the hydrophobically modified samples (terpolymers), when compared with the equivalent non-modified (e.g. compare 50AC with 50A1EC, 50A3EC, 50A1LC, 50A3LC, 50A1SC and 50A3SC), indicative of a lower reactivity of the monomers, contrary to what happen with the cationic polyelectrolytes. Two different organic phases were tested for the synthesis of the non-hydrophobically modified polymers Poly(AAm-Na-AMPS), however since both formulations lead to similar compositions, and Carnation oil is economically more accessible, this oil was chosen for the following synthesis with the hydrophobic modification.

The developed polyelectrolytes were characterized by ATR-FTIR spectroscopy. The spectra of the polymers (Figure 4.5) showed bands at ca. 3330  $\text{cm}^{-1}$  and 3200  $\text{cm}^{-1}$ , attributed to the N-H stretching vibrations in the monomers. The characteristic amide I band (C=O stretching in the amide groups) of the acrylamide and Na-AMPS monomers appeared at 1656-1660  $\text{cm}^{-1}$ . A

shoulder at ca.  $1620\text{ cm}^{-1}$  due to the amide II band of acrylamide was also observed in the spectra of the polymers with a higher content of acrylamide (50 series). Bands showing the presence of Na-AMPS were observed at  $154\text{ cm}^{-1}$  (amide II),  $1184\text{ cm}^{-1}$  (asymmetric stretching of  $\text{S}(=\text{O})_2$ ),  $1042\text{ cm}^{-1}$  (symmetric stretching of  $\text{S}(=\text{O})_2$ ), and  $625\text{ cm}^{-1}$  (S-O stretching), with an increased intensity for the polymers with a higher content of Na-AMPS (80 series). FTIR spectra of copolymers 50AC and 50AP were similar to each other, as well as spectra of copolymers 80AC and 80AP, confirming the reduced influence of the oil used as a solvent in the copolymerization reactions.

The incorporation of a low content of a ter-monomer was revealed by FTIR only in a few cases. For the terpolymers with added ethyl acrylate, the spectra were close to those of the 50AC and 80AC samples. Thus, it was not possible the detection of the hydrophobic component. As for the terpolymers prepared with the addition of lauryl methacrylate, in spite of the fact that this hydrophobic monomer possesses a structure with a larger number of methylene ( $-\text{CH}_2-$ ) groups in the aliphatic chain (Figure 4.4), it could also not be identified unambiguously by ATR-FTIR spectroscopy, being the spectra of 50A1LC and 50A3LC similar to that of 50AC and the spectra of 80A1LC and 80A3LC similar to that of 80AC. In both cases, probably, the hydrophobic monomers are present in amounts below the sensitivity of the FTIR equipment or their bands are masked by the bands from the major constituents of the copolymers, precluding their detection by FTIR spectroscopy. On the other hand, the spectra of the polyelectrolytes 50A3SC and 80A3SC prepared with 3 mol% of added stearyl methacrylate were different from the spectra of the copolymers 50AC and 80AC, respectively. In particular, changes were noted in the region of  $2800\text{-}3000\text{ cm}^{-1}$ , by the appearance of two new bands at  $2923$  and  $2853\text{ cm}^{-1}$ , which can be assigned to the asymmetric and symmetric stretching, respectively, of the  $\text{CH}_2$  groups of the incorporated hydrophobic chain. A shoulder was also observed at ca.  $1730\text{ cm}^{-1}$ , due to the C=O stretching in the ester bonds of the hydrophobic monomer. For the terpolymers 50A1SC and 80A1SC prepared with 1 mol% of added stearyl methacrylate these differences were less distinguishable and the spectra were closer to those of the copolymers without added stearyl methacrylate (50AC and 80AC).

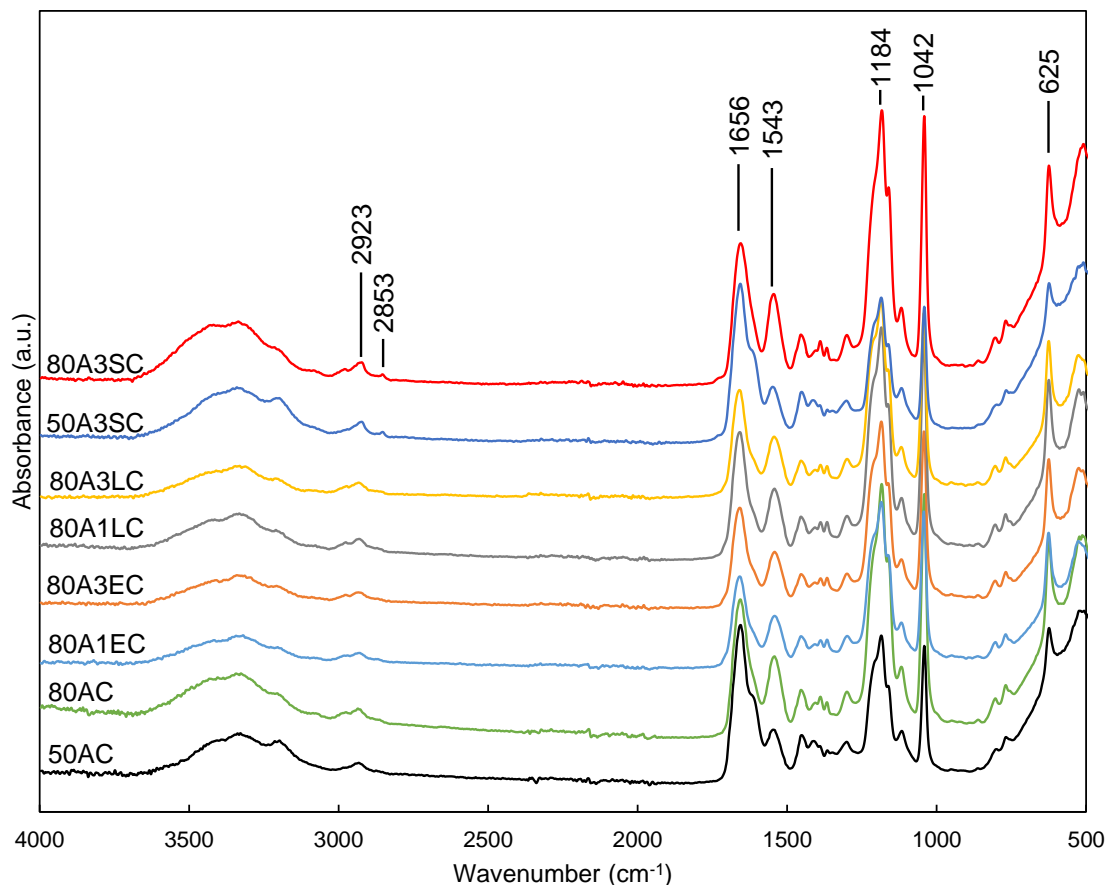


Figure 4.5 ATR-FTIR spectra examples for some of the anionic polyelectrolytes prepared. Poly(AAm-Na-AMPS): 50AC and 80AC. Poly(AAm-Na-AMPS-EA): 80A1EC and 80A3EC. Poly(AAm-Na-AMPS-LMA): 80A1LC and 80A3LC. Poly(AAm-Na-AMPS-SMA): 50A3SC and 80A3SC.

$^1\text{H}$  NMR spectroscopy was then used to obtain an additional insight on the presence of the hydrophobic components in the terpolymers. Spectra for the copolymer 80AC and related terpolymers with EA and LMA were registered (Figure 4.6). The spectrum of 80AC showed signals at 3.33, 2.15, 2.03 and 1.43 ppm, which can be assigned to methylene ( $-\text{CH}_2-$ ) protons next to the sulfonic acid groups of the Na-AMPS monomer, CH and  $\text{CH}_2$  protons in the linear chain of the copolymer and methyl ( $\text{CH}_3$ ) protons from the Na-AMPS monomer. For the terpolymers 80A1EC, 80A3EC, 80A1LC and 80A3LC, where different amounts of EA and LMA, respectively, was added in the synthesis, new signals arose in the  $^1\text{H}$ -NMR spectra, including a very small intensity signal at 3.94 ppm and a signal at 1.10 ppm, whose intensities were higher for 80A3EC and 80A3LC. These can be attributed to methylene protons in the  $\text{O}-\text{CH}_2-\text{C}$  and  $\text{C}-\text{CH}_2-\text{C}$  linkages, respectively, of the EA and LMA chain. The intensity of the signal at 2.15 ppm also increased greatly for these four terpolymers samples, in comparison to

80AC. Thus, although not observable by FTIR spectroscopy, the presence of the EA and LMA monomers in the terpolymers could be detected by  $^1\text{H-NMR}$ .

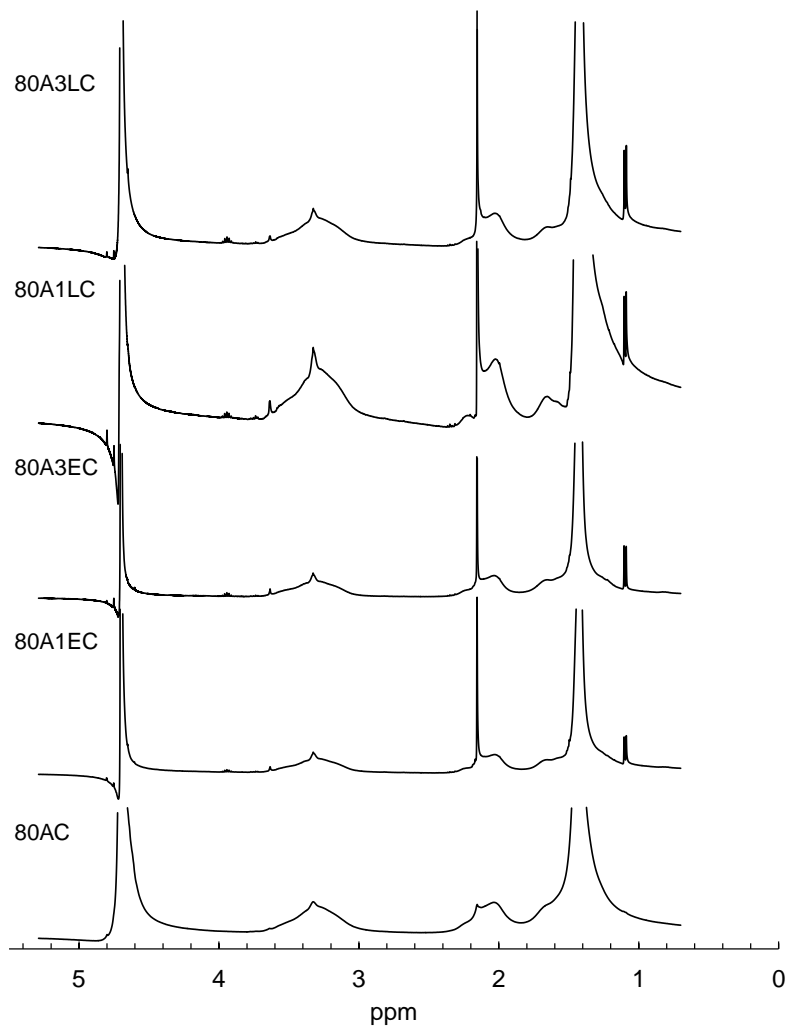


Figure 4.6  $^1\text{H NMR}$  spectra for some of the polyelectrolytes prepared. Poly(AAm-Na-AMPS): 80AC. Poly(AAm-Na-AMPS-EA): 80A1EC and 80A3EC. Poly(AAm-Na-AMPS-LMA): 80A1LC and 80A3LC.

Results for zeta potential, hydrodynamic diameter, polydispersity index and weight-average molecular weight of polyelectrolytes are presented in Table 4.6. The complete data is available in Appendix B, Figure B.22 to B.63.

Table 4.6 Polyelectrolytes characterization: zeta potential, hydrodynamic diameter and weight-average molecular weight. Poly(AAm-Na-AMPS): 50AC, 80AC, 50AP and 80AP. Poly(AAm-Na-AMPS-EA): 50A1EC, 50A3EC, 80A1EC and 80A3EC. Poly(AAm-Na-AMPS-LMA): 50A1LC, 50A3LC, 80A1LC and 80A3LC. Poly(AAm-Na-AMPS-SMA): 50A1SC, 50A3SC, 80A1SC and 80A3SC.

Polymer designation	Zeta		Polydispersity index	Weight-average molecular weight ( $10^6$ Da)	
	Potential (mV)	Hydrodynamic diameter (nm)		By SLS	By SEC
50AC	$-71 \pm 2$	$67 \pm 2$	0.43	$0.9 \pm 0.07$	$7.6 \pm 0.7$
80AC	$-80 \pm 1$	$72 \pm 1$	0.47	$1.0 \pm 0.08$	$8.2 \pm 1.1$
50AP	$-72 \pm 1$	$265 \pm 37$	0.61	$2.5 \pm 0.09$	
80AP	$-85 \pm 1$	$147 \pm 4$	1.00	$1.3 \pm 0.2$	$8.7 \pm 0.4$
50A1EC	$-65 \pm 2$	$70 \pm 1$	0.35	$0.6 \pm 0.02$	
50A3EC	$-58 \pm 1$	$282 \pm 32$	0.63	$3.5 \pm 0.07$	
80A1EC	$-79 \pm 1$	$143 \pm 10$	1.00	$1.5 \pm 0.2$	
80A3EC	$-79 \pm 2$	$206 \pm 22$	0.62	$2.4 \pm 0.08$	
50A1LC	$-66 \pm 1$	$129 \pm 10$	0.94	$1.4 \pm 0.007$	
50A3LC	$-64 \pm 1$	$209 \pm 28$	0.46	$2.5 \pm 0.3$	
80A1LC	$-75 \pm 1$	$174 \pm 28$	0.67	$2.2 \pm 0.2$	
80A3LC	$-78 \pm 1$	$124 \pm 13$	0.87	$0.8 \pm 0.03$	
50A1SC	$-69 \pm 1$	$219 \pm 19$	0.35	$2.4 \pm 0.1$	
50A3SC	$-72 \pm 1$	$180 \pm 14$	0.48	$1.3 \pm 0.1$	
80A1SC	$-84 \pm 1$	$132 \pm 7$	0.83	$1.1 \pm 0.007$	
80A3SC	$-84 \pm 1$	$81 \pm 18$	0.56	$0.7 \pm 0.2$	

As expected, zeta potential values are in accordance with charge density (Table 4.5), determined by elemental analysis. Polymers of the 50 series have lower charge density and lower zeta potential than polymer of the 80 series. Similarly to charge density tendency, comparing polyelectrolytes of the same series, with and without presence of hydrophobic content, it is possible to observe a decrease in zeta potential in the hydrophobically modified polymers, with exception for three samples synthesized in the presence of the hydrophobic monomer SMA (50A3SC, 80A1SC and 80A3SC). This fact was already previously verified in the cationic polyelectrolytes hydrophobically modified using the same monomer, suggesting that this may be related with this specific hydrophobic monomer (see section 2.2. of the present Chapter). Considering that the mentioned hydrophobic monomer comprises the largest hydrophobic chain length (eighteen methylene groups), this may lower the monomer solubility in the reaction medium, leading to a higher possibility for the charged monomer,

highly soluble in the medium, to react, thus increasing the charged fraction in the final polymer.

In the remaining terpolymers, the decrease of zeta potential when compared with the relative copolymers can be due to the steric hindrance promoted by the aliphatic chain of the hydrophobic monomer, which can affect the anionic monomer addition to the chain.

For the same molecular weight and hydrophobicity, hydrodynamic diameter in water should increase consistently with zeta potential, since the repulsion in the molecule charged site increases. However, for these specific polymers, the molecular weight range is wide, since the size of the polymer is influenced by many factors in the polymerization process, preventing the correct confrontation between hydrodynamic diameter and zeta potential results. In a singular case of polymers 50AC, 80AC and 80AP, which have similar molecular weight, the tendency is verified and the hydrodynamic diameter increases with the increase of zeta potential. On the other hand, there is a notorious correlation between hydrodynamic diameter and molecular weight, for polyelectrolytes with similar charge density, where both values (hydrodynamic diameter and molecular weight) increase in parallel. Moreover, for similar molecular weights, the introduction of hydrophobic monomer leads to higher hydrodynamic diameter (compare 50AC with 50A1EC, 50A1LC and 50A3SC, and also 80AC with 80A1EC, 80A3LC, 80A1SC and 80A3SC), probably due to the less coiled conformation in solution, resulting from the presence of the hydrophobic molecule. Regarding hydrodynamic diameters distributions, PDI values suggest that they are considerably wide, as can also be confirmed by the plots presented in Appendix B, Figure B.29 to B.36.

The introduction of hydrophobic molecules seems to have also some influence in the molecular weight of the polymer, especially for higher hydrophobic content. For polyelectrolytes with 3 mol% of hydrophobic monomer, using hydrophobic monomers with higher number of methylene groups in the aliphatic chain, results in a decrease of final molecular weight (compare 50A3EC, 50A3LC and 50A3SC, and 80A3EC, 80A3LC and 80A3SC), possibly due to the steric hindrance in the polymer chain. Additionally, in general, increasing the hydrophobic content leads to a decrease of final molecular weight for terpolymers with larger hydrophobic chain length (compare 80A1LC with 80A3LC, 50A2SC and 50A3SC, and 80A1SC and 80A3SC), suggesting that when the hydrophobicity of the molecule is higher, this hinders the polymerization process, due to the difficulty in originating a free radical by the hydrophobic monomer, consequently inducing the finalization of polymer chains, which reduces the final molecular weight obtained. When the chain length is shorter,



the impact in the final polymer characteristics is less. Both these observations were previously mentioned by Lee *et al.*<sup>120</sup>, in a study regarding hydrophobically modified cationic polyacrylamides for application in flocculation.

Additionally, and since the molecular weight determination of charged molecules is very much dependent on the technique used<sup>227,228</sup>, it was decided to use as well SEC to determine the molecular weight of some of the copolymers, in order to obtain a confirmation of the trends observed. The complete data is available in Appendix B, Figure B.63. It must be noted that SEC was not available in our laboratorial premises at the University of Coimbra. As can be observed, the values acquired by SEC are higher than the ones obtained by SLS, even if of the same order of magnitude and, additionally, they show the same tendency, as mentioned already for SLS. Moreover, the values of molecular weight obtained for the copolymers 50AC, 80AC, 50AP and 80AP were compared with similar copolymers of acrylamide and Na-AMPS presented in literature<sup>226</sup>. It is possible to see that the values referred in the work of Lounis *et al.*<sup>226</sup> show slightly lower molecular weight, in one order of magnitude, than the ones presented in the present work, possibly due to differences in the polymerization method. On the other hand, in Qi *et al.*<sup>229</sup> the values of molecular weight for similar copolymer, however with lower proportion of Na-AMPS, are in the same order of magnitude, with values between the ones obtained by SLS and SEC in the present study. Furthermore, since molecular weight is a significant factor for this study application, it is possible to confirm that the values obtained are in agreement with the expected for this type of application<sup>21</sup>.

## 4. CONCLUSIONS

The health-friendly formulations used in the development of the flocculation agents, presented in this chapter, led to cationic and anionic polyelectrolytes with suitable characteristics for the final application. It was possible to produce co- and terpolymers with various chemical charge densities. Moreover, the characterization of the polyelectrolytes proved the success of the hydrophobic content integration, in several levels, without affecting factors like zeta potential or molecular weight. In both cases (anionic and cationic polyelectrolytes) charged fraction and zeta potential present very good correlation, as well as hydrodynamic diameter and molecular weight. In the case of cationic polyelectrolytes the increase of cationic fraction increase the molecular weight, however the introduction of a hydrophobic monomer increases zeta potential, but leads to very similar hydrodynamic diameters and molecular weights for the different terpolymers. Considering anionic polyelectrolytes, the addition of hydrophobic content conduct to lower anionic fractions and, consequently, lower zeta potential values, for most of the cases. The increase of hydrophobic content leads to lower molecular weight values in the terpolymers with long hydrophobic chain lengths and, for the polyelectrolytes with higher hydrophobic content, the larger chain length leads to lower the molecular weight obtained and, accordingly, hydrodynamic diameter also decreases. In the following chapter, their application as flocculants in oily wastewaters will be analysed.



---

CHAPTER **5**

**Application of the novel  
polyelectrolytes in industrial effluents**



## 1. INTRODUCTION

The addition of organic and inorganic compounds stimulate the destabilization of colloidal mixtures and promote the agglomeration of sub-millimetre particles into flocs that are able to settle over a period of seconds to hours. Experiments have shown considerable reduction in turbidity, suspended solids, colour and chemical oxygen demand. However, usually a combination of both inorganic and organic additives is required. Alternatively, when a flocculant is applied alone a high concentration may be necessary. The total dose of minerals, coagulants and flocculants contributes to sludge generation. This presents important costs as well as environmental impacts. Therefore, the minimization of sludge production is important considering the costs related with consequent sludge treatment and disposal. Thus, there is a need for flocculants with distinct characteristics, immediately soluble in aqueous systems, highly efficient in little quantities and that generate large and strong flocs, leading to good settling performance and, thus, minimizing the amount of sludge produced. Ideally a flocculant will also permit a reduction in the inorganic coagulant dosage and not require adsorbents or pH adjustment as well.

In this chapter, cationic and anionic polyelectrolytes (presented and characterized in Chapter 4) were applied as low dosage flocculation agents in the treatment of several oily wastewaters, namely from olive oil mill, dairy and potato crisps manufacturing industries. Their performance was studied in terms of turbidity reduction, and chemical oxygen demand and total solids removal at several concentrations and pHs. Moreover, the influence of the hydrophobic content in the polymers, as well as the optimum conditions of concentration and pH were assessed.



## 2. OLIVE OIL MILL INDUSTRY EFFLUENT

### 2.1. Procedure to evaluate flocculation performance

For each polymer developed, a 200-mL stock solution at a 0.4 wt% concentration was prepared with distilled water using magnetic stirring for sixty minutes. Polymers in inverse-emulsion state were used. A volume of 75-mL of pre-agitated wastewater (industrial effluent) was adjusted to three different pHs using hydrochloric acid (HCl) or sodium hydroxide (NaOH) aqueous solutions, with a pH meter SCAN3BW (Scansci). Specifically, 3 mL of HCl 1 mol/L were added for pH 3, and 0.2 mL and 5.5 mL of NaOH 1 mol/L were added for pH 5 and 10, respectively. Polymer solution samples with different volumes were added to the wastewater sample, with a successive increase of flocculant concentration from 13 mg/L until a maximum of 180 mg/L. In each addition, the suspension-polymer mixture was manually agitated for 10 seconds, allowed to settle for 2 min and the turbidity of the supernatant assessed with at least three repetitions, using a Photometer MD600 (Lovibond, UK). The variance in the measurements of turbidity was always below 1.0 %. Solids content and chemical oxygen demand of the treated supernatant water were measured for selected polymers. For COD test, 2 mL of sample was added to a COD Kit (Lovibond) and allowed to remain at 150 °C for 2 h in a thermoreactor (VELP Scientifica). After reaching the room temperature, the COD value was measured in a Photometer MD600 (Lovibond). For total solids content, 10 mL of each sample was dried overnight at 105 °C and the value was accessed gravimetrically. All the measurements were performed at least in duplicate.

Commercially available polymer flocculants provided by Aqua+Tech Specialities SA were also evaluated, as references, in the same conditions described previously. These are the polymers under the commercial name AlpineFloc DHMW and Z1, high molecular weight cationic and anionic polyelectrolytes with 60 wt% and 50 wt% charged fraction, respectively.

The zeta potential of the effluent was measured by electrophoretic light scattering, in a Malvern Zetasizer Nano ZS, model ZEN3600 (Malvern Instruments Ltd, UK).

### 2.2. Initial wastewater characterization

The olive oil mill effluent sample used in this study (supplied by Adventech Group, Portugal) was characterized in terms of pH, COD, total solids and turbidity, and the obtained results are



summarized in Table 5.1. All the flocculation tests were performed using this wastewater sample.

Table 5.1 Characteristics of the industrial olive oil mill effluent sample.

Parameter	Values
pH	4.7
COD (gO <sub>2</sub> /L)	11.8
Total solids (g/L)	5.99
Turbidity (NTU)	3440

The stability of the effluents is determined mainly by the charge of the particles surface, which is significantly affected by the pH of the aqueous medium.

The zeta potential of the effluent after adjustment for the three pH values used in the performance tests was measured, and the obtained zeta potential distributions are presented in Figure 5.1. For pH 5 and 10, the effluent particles have a surface mainly negatively charged, with a median zeta potential of the -57 mV and -62 mV, respectively, while for pH 3 the particles show both positive and negative charges in their surface, presenting a median zeta potential of -2 mV, indicative of an essentially electroneutral heterogeneous effluent. This presence of both charges promotes a visible destabilization of the effluent, although not enough to form flocs or settle. Moreover, at pH 10, which is the more similar with the initial pH of the effluent, the particles charge is totally negative, explaining the stability of the initial effluent, due to the repulsion effect.

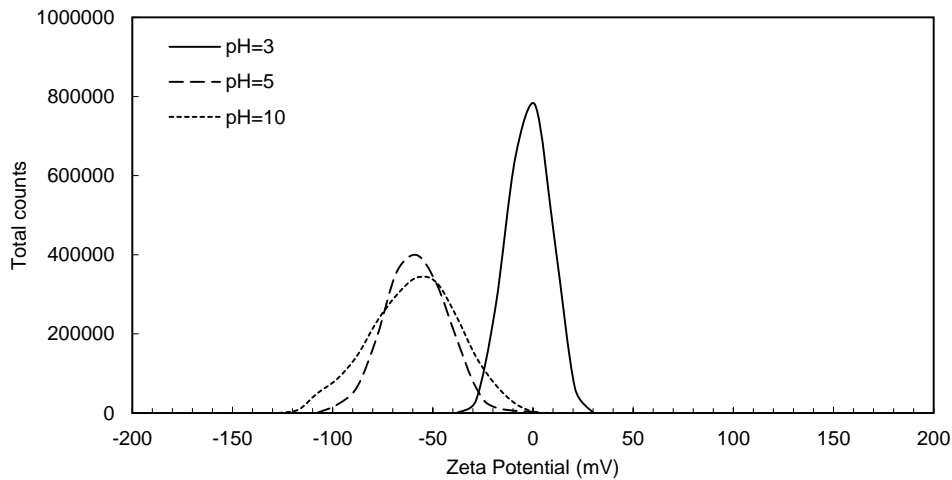


Figure 5.1 Zeta potential distribution for the olive oil mill effluent at pH 3, 5 and 10.

### 2.3. Results and discussion

Cationic flocculants have inherent positively charged groups, which are active in neutralization of negative charges on suspended colloidal particles and oil droplets during the flocculation process of oily wastewater<sup>103</sup>. Also, long polymer chains with medium charge density can promote the bridging effect between the particles, due to the polymer adsorption on the particle surface in a way that is extended and can interact with other particles<sup>21,87,94</sup>.

The influence of pH and dosage of each flocculant was evaluated. Herein, the supernatant water turbidity was used to evaluate the treatment efficiency. Figure 5.2 and Figure 5.3 show the cationic polyelectrolytes performance in olive oil mill effluent treatment at different pHs and concentrations, from 0-180 mg/L, for the different co- and terpolymers produced. As can be seen, with increasing dosage, gradual increase was observed in the reduction of turbidity, until reaches a maximum. Acidic conditions always appear to lead to higher removal efficiencies in this case. Furthermore, the addition of flocculant did not change the effluent pH, based on the measurements conducted after the flocculant addition. The adjustment of the effluent to pH 3 decreased, by itself, the turbidity in about 20%, leading also to a visual destabilization of the effluent, possibly explained by the reduction of particles repulsion due to the change in their surfaces, which have, at this pH, both positive and negative charges, as verified by the zeta potential assessment (see Figure 5.1). Moreover, a distribution from -39.4 to 31.9 mV in zeta potential, suggests the adequacy of using cationic flocculants. Thus, at pH 3, the turbidity reduction was at the highest level for all the polymers tested. Regarding copolymers (see Figure 5.2), the turbidity reduction was above 90% for dosages above 80

mg/L for the polyelectrolytes with the highest charge density (60 series). In the case of the polymer 60MC, higher turbidity reduction is achieved even for a much lower dosage (27 mg/L). When the cationic fraction is lower (25 series), the concentration of polymer required to achieve the same turbidity reduction is higher. This may be attributed to the fact that lower cationic charge density is less effective in neutralizing the negative charge on the oil droplets, and also to the lower molecular weight of polyelectrolytes of 25 series, compared with the polyelectrolytes of 60 series (see Table 4.3 in Section 2.2. of Chapter 4). When these four flocculants were used for different pHs (5 and 10), the wastewater needed much higher concentrations of polymer to reduce turbidity, without achieving the same maximum reduction of the testing at pH 3, even for the higher concentrations. Moreover, adjusting pH to basic conditions increased the turbidity of the initial wastewater by itself (thus the negative reduction values), severely reducing the flocculant efficiency.

Considering the terpolymers, when the hydrophobic monomer is introduced in the polymer chain, higher turbidity reductions were achieved with the lower polymer dosages tested, for polyelectrolytes with both lower and higher cationic fraction (see Figure 5.3). In addition, significant turbidity reductions were obtained for dosages as low as 13 mg/L. The better performance was obtained again for the higher charge densities. When the amount of the hydrophobic monomer increased from 1 to 3 mol%, the performance of the polymer did not improve significantly. The best results were achieved with terpolymers 60M1SC and 60M2SC, similar in both cases, where it was possible to reduce 89% of turbidity using only a concentration of flocculant of 53 mg/L. For terpolymers with lower cationic fraction (25 series), the performance for the optimal pH was considerably improved, when compared with the corresponding copolymers, particularly for the lower dosages tested. On the other hand, in testing at pH 5 it was observed that in this case it is possible to achieve similar maximum turbidity reductions to the ones obtained at pH 3, however with higher dosages of flocculant, which represents an improvement when compared with the corresponding copolymers. On the contrary, using the terpolymers at pH 10 led to slightly worse results than for the corresponding copolymers, especially when compared with the copolymers synthesized using Carnation as organic phase.

The use of either an iso-paraffin, Carnation, or a hydrogenated polydecene, Puresyn4, in the synthesis process did not affect significantly the performance of the polyelectrolytes (compare MC and MP series of polymers), which is consistent with the similarity of the characterization parameters (zeta potential, hydrodynamic diameter and molecular weight) for these two types

of polyelectrolytes for similar cationic fraction (see table Table 4.3 in Section 2.2. of Chapter 4).

Considering that molecular weight of the higher charge density hydrophobically modified polymers (60M1SC and 60M2SC) is lower (see Table 4.3 in Section 2.2. of Chapter 4), improvement of performance must be justified by the affinity between the hydrophobic part of the polymer and the oil droplets in the effluent. Previously Lü *et al.*<sup>126</sup> and Bratskaya *et al.*<sup>115</sup> demonstrated that oil removal efficiency was significantly enhanced using hydrophobically modified cationic flocculants, due to the affinity between hydrophobic regions of the polyelectrolyte and the oily particles of the effluent.

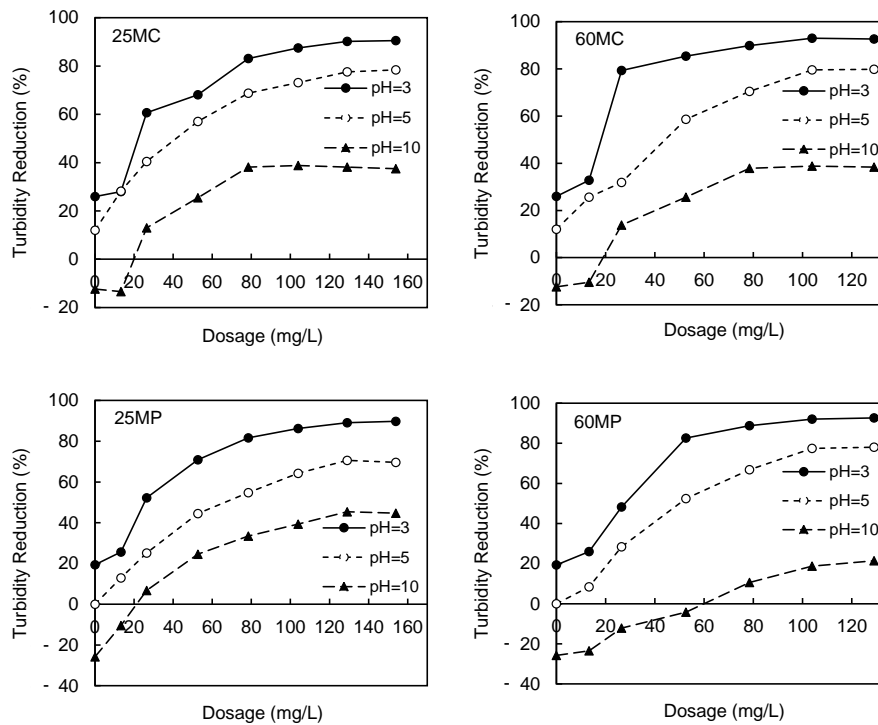


Figure 5.2 Turbidity reduction curves for the industrial olive oil mill effluent treated by cationic copolymers Poly(AAm-MAPTAC): 25MC, 25MP, 60MC and 60MP, at three different pHs.

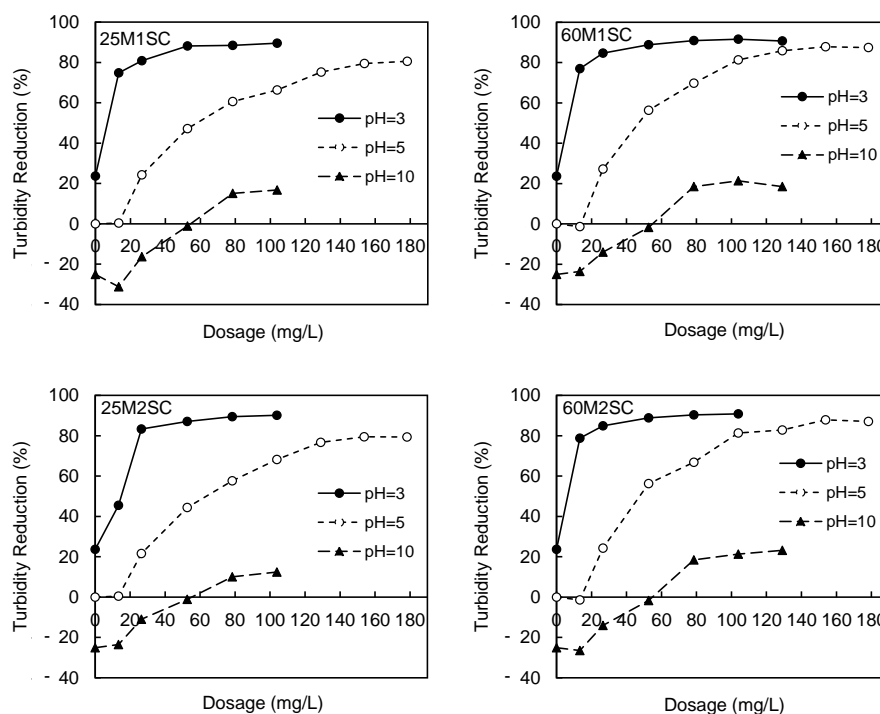


Figure 5.3 Turbidity reduction curves for the industrial olive oil mill effluent treated by cationic terpolymers Poly(AAm-MAPTAC-SMA): 25M1SC, 25M2SC, 60M1SC and 60M2SC, at three different pHs.

The performance of the cationic polyelectrolytes developed in the treatment of the olive oil mill effluent was compared with the reference polymer commercially available (Figure 5.4), AlpineFloc DHMW, which has a similar charge density to the 60 series. Looking at the results for pH 3, which provided the highest turbidity removal efficiency, the reference polymer showed a similar behaviour as the newly developed copolymers with analogous cationic fraction (60MC and 60MP) for the highest dosage tested. Nevertheless, 60MC and 60MP achieved higher turbidity reduction values than AlpineFloc DHMW when comparing the lower dosages tested. On the other hand, comparing the performance of the hydrophobically modified polyelectrolytes developed (60M1SC and 60M2SC) with this reference commercial polymer, the former show much higher removal efficiency. This evidence proves once again that addition of a hydrophobic monomer to the copolymers considerably improves the flocculation performance of polyelectrolytes in the treatment of industrial olive oil mill effluents.

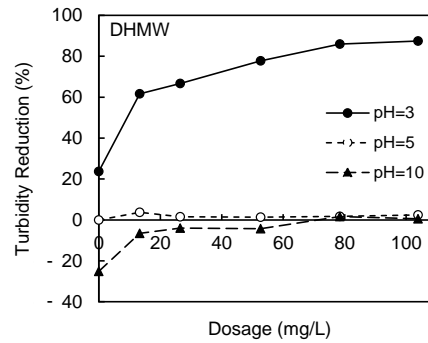


Figure 5.4 Turbidity reduction curves for the industrial olive oil mill effluent treated by reference polymer, AplineFloc DHMW, at various pHs.

The total solids and COD removal efficiencies were measured for the terpolymers that presented higher turbidity reduction, and corresponding copolymer, in the optimized conditions of pH and concentration, in order to confirm that pre-treatment was also efficient regarding these two parameters (Figure 5.5). For both parameters, the removal for the different polymers tested was very similar with a slightly better performance of the polyelectrolyte 60M1SC. Comparing these results with previous publications<sup>150</sup>, the level of purification is similar, however much lower dosage was needed to reach the same effect.

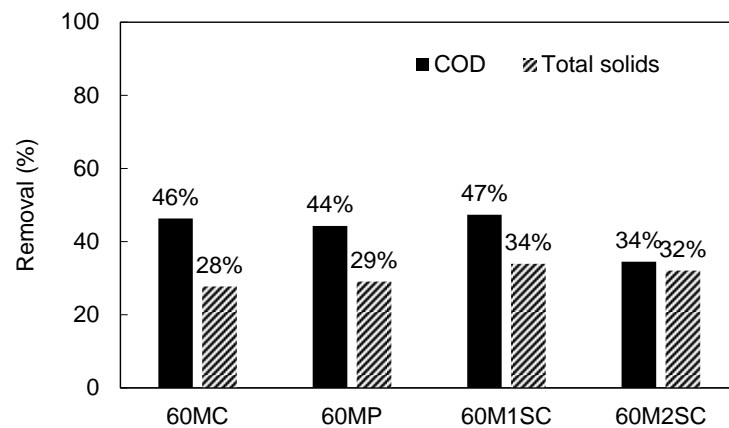


Figure 5.5 COD and total solids removal after the treatment of the industrial olive oil mill effluent with 60MC, 60MP, 60M1SC and 60M2SC flocculants, in optimized conditions of pH (pH 3) and concentration (103 mg/L for 60MC and 60MP, and 78 mg/L for 60M1SC and 60M2SC).

The photographs displayed in Figure 5.6 show the flocs after addition of the suitable dosage of 60MC (b), 60MP (c), 60M1SC (d) and 60M2SC (e) to the initial effluent sample (a), at pH 3.

Flocs resulting from the flocculation with the developed polyelectrolytes had very fast growing and settling performance, presenting a high resistance to breaking actions (transition of the flocs and supernatant between two recipients by pouring the mixture) and strong and compact structure after formation, suggesting a low water content in the flocculated fraction.

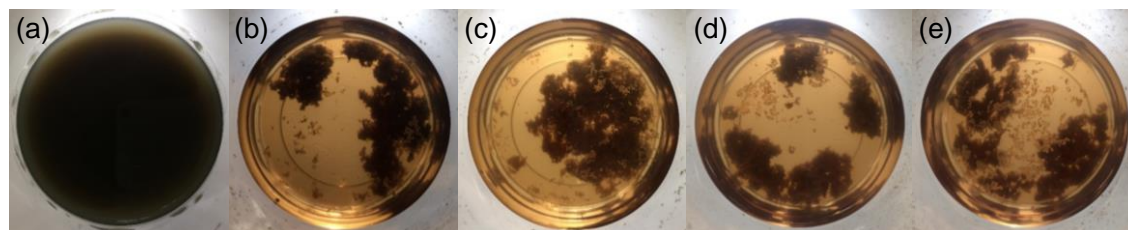


Figure 5.6 Initial olive oil mill effluent (a) and effluent after treatment with flocculants 60MC (b), 60MP (c), 60M1SC (d), and 60M2SC (e), in optimized conditions of pH (pH 3) and concentration (103 mg/L for 60MC and 60MP, and 78 mg/L for 60M1SC and 60M2SC).

Anionic flocculants hold negative charges in their molecules, which can establish strong ionic interactions with cations available on the suspended particles of the effluents. Considering that in acidic conditions the effluent possesses both positive and negative particles (see Figure 5.1), the developed anionic polyelectrolytes were also tested in turbidity reduction of the olive oil mill effluent for three different pHs (3, 5 and 10) and with concentrations of polymer from 0-104 mg/L (Figure 5.7 to Figure 5.10). As mentioned before for the cationic polyelectrolytes, also with the anionic polyelectrolytes, the best results were obtained when the pH was adjusted to 3. Using pH 5 and 10 proved not to be appropriate for the mentioned effluent, for all the anionic polyelectrolytes tested, since in first case there was no turbidity reduction with the addition of the flocculants and in the second case was verified an increase in the turbidity of the effluent. For the copolymers Poly(AAm-Na-AMPS), developed using two different health-friendly formulations, it is possible to observe that using different organic phases (MC and MP series) does not show significant influence in the polyelectrolytes performance (see Figure 5.7). When comparing polymers with different charge densities (50 and 80 series), superior maximum turbidity reductions are obtained when using the flocculant with higher anionic fraction (80 series), where also better results were achieved with lower concentrations. Specifically, using the copolymer 80AC, 79% turbidity was reduced using a dosage of 27 mg/L.

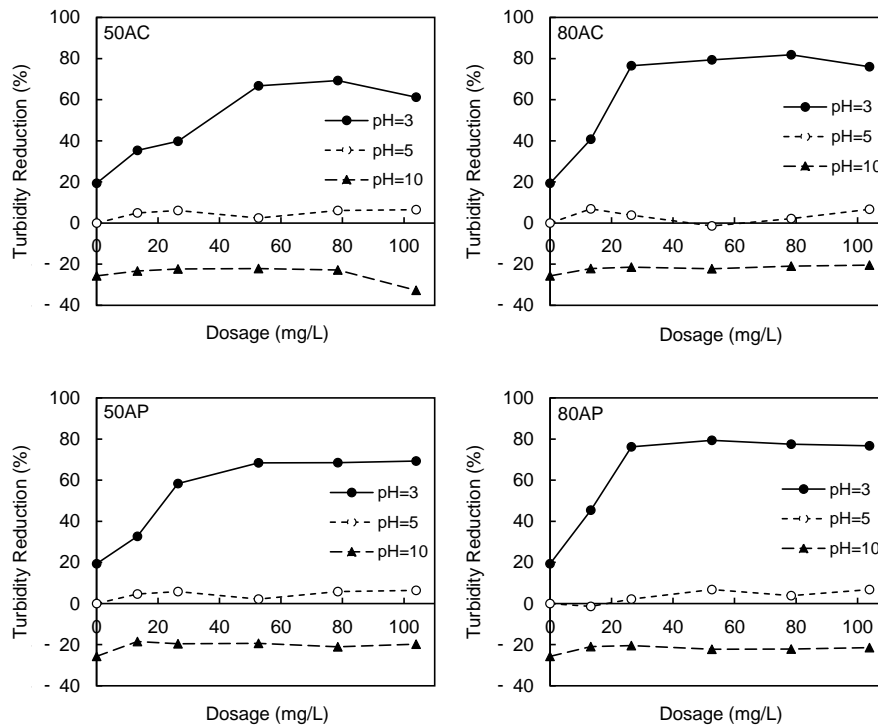


Figure 5.7 Turbidity reduction curves for the industrial olive oil mill effluent treated by the anionic copolymers Poly(AAm-Na-AMPS): 50AC, 80AC, 50AP and 80AP, at three different pHs.

Regarding the hydrophobically modified terpolymers, Poly(AAm-Na-AMPS-EA), Poly(AAm-Na-AMPS-LMA) and Poly(AAm-Na-AMPS-SMA), for some specific polyelectrolytes it was verified an improvement of performance, when comparing with the corresponding copolymers (Figure 5.8 to Figure 5.10). Considering the terpolymers Poly(AAm-Na-AMPS-EA) in Figure 5.8, for polyelectrolytes with lower charge density (50 series) there was a lower performance than with corresponding copolymers, and for polyelectrolytes with higher charge density (80 series) a similar effectiveness compared to the corresponding copolymers was observed. On the other hand, for Poly(AAm-Na-AMPS-LMA) in Figure 5.9, an improvement of performance was verified applying lower dosages, for both the 50 and 80 series. In all the four flocculants it was achieved a turbidity reduction of 72-80% with only 13 mg/L of polymer concentration. However, the maximum turbidity reduction achieved was only slightly higher than with the corresponding copolymers. Finally, in case of Poly(AAm-Na-AMPS-SMA) in Figure 5.10, the results were very similar to the ones for Poly(AAm-Na-AMPS-LMA). Therefore, the results obtained suggest a positive effect of the hydrophobic modification, however dependent on the number of methylene groups in the hydrophobic aliphatic chain (see Figure 4.4 in Section 3.1.2. of Chapter 4). A hydrophobic chain larger than 2 methylene groups (EA monomer) is needed to produce a significant effect, though a chain



larger than 12 methylene groups (LMA monomer) is no longer necessary, since Poly(AAm-Na-AMPS-SMA) and Poly(AAm-Na-AMPS-LMA) show comparable efficiencies. Ren *et al.*<sup>117</sup> already discussed in the literature that larger chain length than two methylene groups, in hydrophobically modified flocculants, has a positive effect in flocculation.

Regarding the amount of the hydrophobic monomer, the use of the highest fraction (3 mol%) showed not to improve significantly the flocculation performance. Similar behaviour was already reported by Lee *et al.*<sup>120</sup>

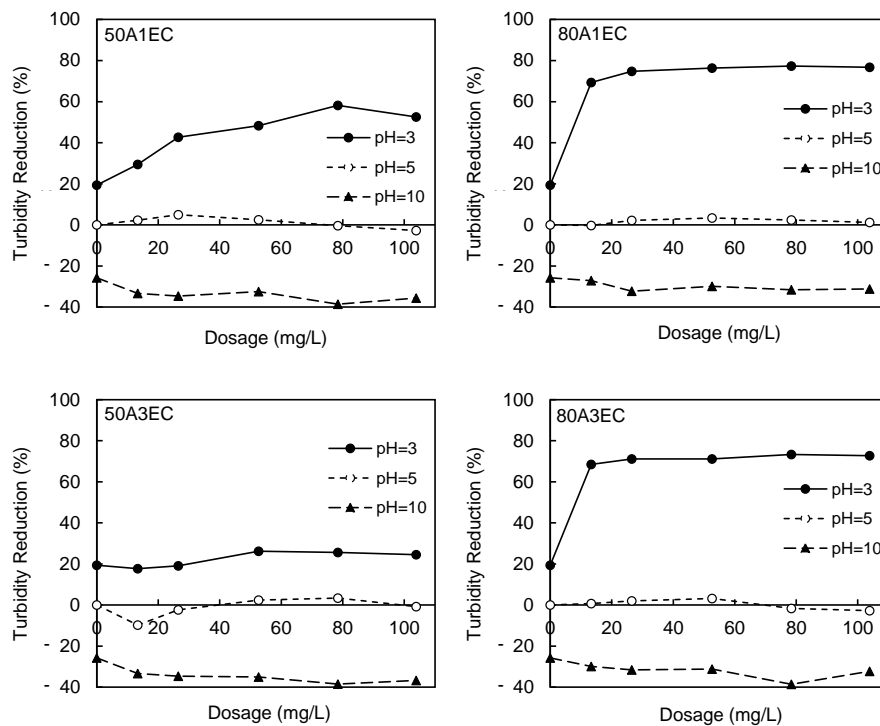


Figure 5.8 Turbidity reduction curves for the industrial olive oil mill effluent treated by anionic terpolymers Poly(AAm-Na-AMPS-EA): 50A1EC, 50A3EC, 80A1EC and 80A3EC, at three different pHs.

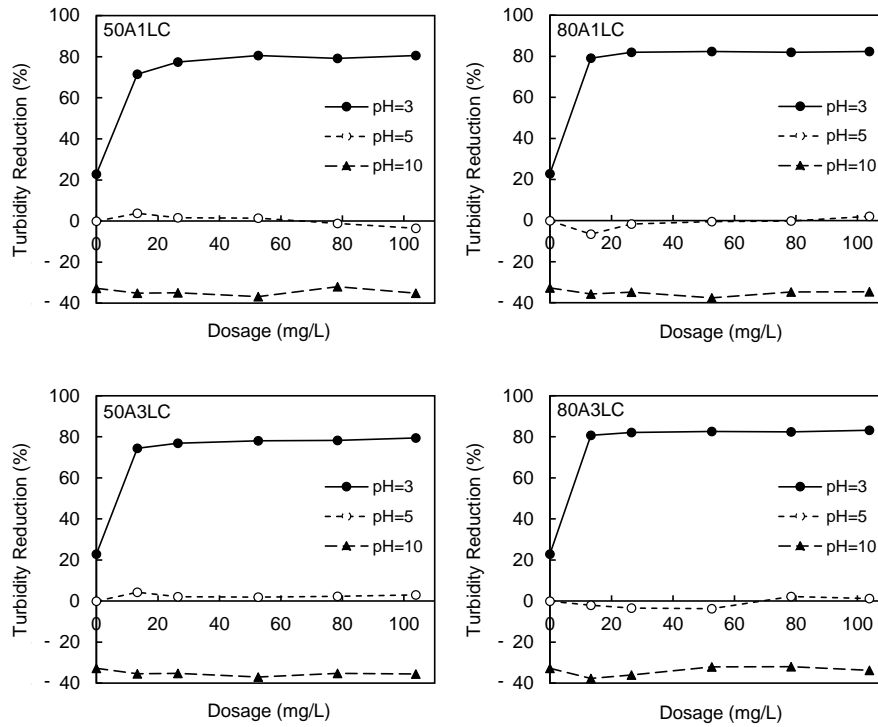


Figure 5.9 Turbidity reduction curves for the industrial olive oil mill effluent treated by anionic terpolymers Poly(AAm-Na-AMPS-LMA): 50A1LC, 50A3LC, 80A1LC and 80A3LC, at three different pHs.

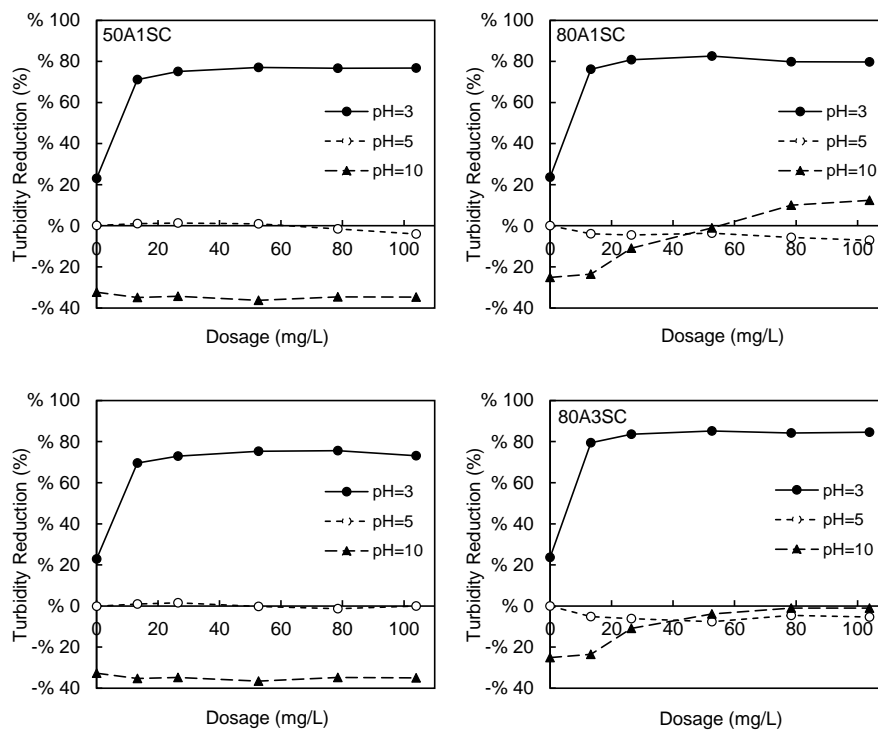


Figure 5.10 Turbidity reduction curves for the industrial olive oil mill effluent treated by anionic terpolymers Poly(AAm-Na-AMPS-SMA): 50A1SC, 50A3SC, 80A1SC and 80A3SC, at three different pHs.

The performance of the developed anionic polyelectrolytes was also compared with an anionic reference polymer commercially available, AlpineFloc Z1, which has comparable charge density with the 50 series presented previously (Figure 5.11). For the optimum pH (pH 3), the reference polymer proved to be more efficient in reduction of turbidity than polyelectrolytes 50AC and 50AP. When compared with the hydrophobically modified 50 series, the results were very similar regarding the maximum reduction of turbidity. However, comparing the reduction for the lowest dosage tested (13 mg/L), 50A1LC, 50A3LC, 50A1SC and 50A3SC presented better performance than the reference AlpineFloc Z1, with a turbidity reduction above 70% for the developed polymers. The other pHs tested showed similar behaviour to the one observed for the novel developed anionic polyelectrolytes.

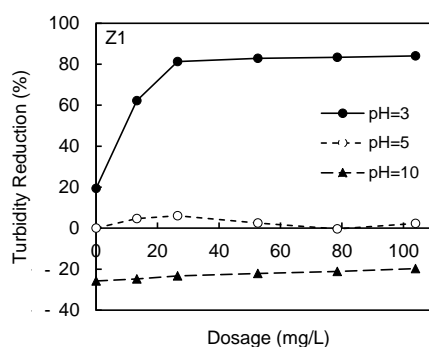


Figure 5.11 Turbidity reduction curves for the industrial olive oil mill effluent treated by reference anionic polymer, AlpineFloc Z1, at various pHs.

In the case of anionic flocculants, COD and total solids removal efficiency were also evaluated for the terpolymers that showed higher turbidity reductions and corresponding copolymers, in the optimum conditions of pH and dosage (Figure 5.12). Regarding COD, copolymer 80AC performed the best, with 44% removal, even if the terpolymers 80A1EC, 80A3EC, 80A1SC and 80A3SC exhibited not so different COD removal efficiencies. In the case of total solids the highest removal was 30%, obtained with the terpolymer 80A1SC.

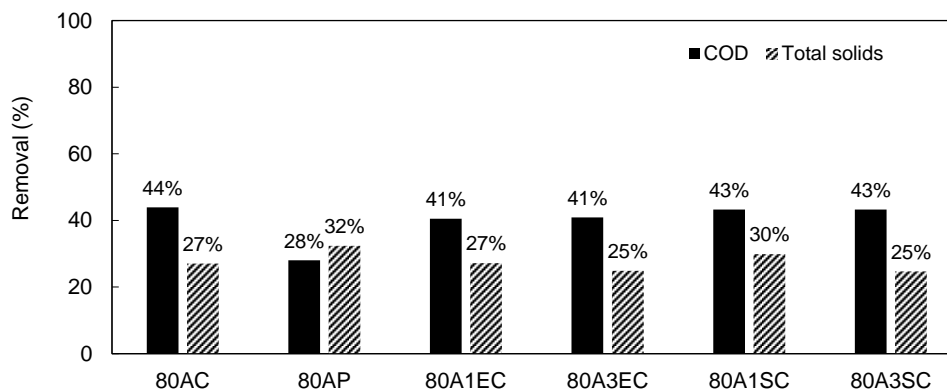


Figure 5.12 COD and total solids removal after the treatment of the industrial olive oil mill effluent with 80AC, 80AP, 80A1EC, 80A3EC, 80A1SC and 80A3SC flocculants, in optimized conditions of pH (pH 3) and concentration (78 mg/L for 80AC, 80A1EC and 80A3EC, and 53 mg/L for 80AP, 80A1SC and 80A3SC).

Analysing the overall results of the developed anionic polyelectrolytes, terpolymer 80A1SC proved to be the one with better performance, achieving 87% turbidity reduction with 53 mg/L of concentration, and removing COD and total solids in 43% and 30%, respectively. Furthermore, this polyelectrolyte also reduces 82% turbidity with 27 mg/L of concentration.

In general, the results presented for cationic and anionic polyelectrolytes applied as flocculants in the treatment of the olive oil mill effluent suggest that both cationic and anionic polyelectrolytes behave well, in adequate conditions (pH 3), in low dosages and without needing the addition of aids (such as coagulants, salts or inorganic products). Nevertheless, cationic polyelectrolytes with higher charged fraction (60 series) seem to present superior performance, since they present greater flexibility to pH changes and slightly higher turbidity reductions, namely in lower concentrations. Moreover, the hydrophobic modifications appear to be beneficial for the flocculation performance, especially using hydrophobic aliphatic chains larger than two methylene groups, in suitable proportion. These polyelectrolytes also revealed better performance than the reference polymer tested. It is worth noting that the use of a lower hydrophobic content flocculant reduces the costs associated to the process, since the hydrophobic monomers are relatively costly.



### 3. DAIRY INDUSTRY EFFLUENT

#### 3.1. Procedure to evaluate flocculation performance

For detailed description of flocculation performance procedure, see Section 2.1 of the present Chapter.

#### 3.2. Initial wastewater characterization

The characteristics of the dairy effluent sample used in the flocculation tests are summarized in Table 5.2. The sample was supplied by the company Lactogal Produtos Alimentares S.A. (Portugal). All the flocculation tests were performed using this wastewater sample.

Table 5.2 Characteristics of dairy effluent sample tested before any treatment.

Parameter	Values
pH	11.7
COD (gO <sub>2</sub> /L)	3.3
Total solids (g/L)	6.2
Turbidity (NTU)	680

The zeta potential distribution for the initial effluent, after adjustment for the three pH values used, was determined and is presented in Figure 5.13. Zeta potential values obtained are relative to the surface charge of the impurities particles present in the effluent, which can vary according with the pH of the medium. Regarding the acidic conditions tested, for pH 3, a distribution from -40 to 15 mV was observed, with a median value of -13 mV, while for pH 5 a distribution from -25 mV to 10 mV was acquired, with a median value of -7 mV. At pH 10, the closest to the initial effluent pH, a mainly negative distribution was detected, with a median value of -19 mV, ranging from -35 to -4 mV, proving the stability of the effluent, induced by the repulsion of charges.

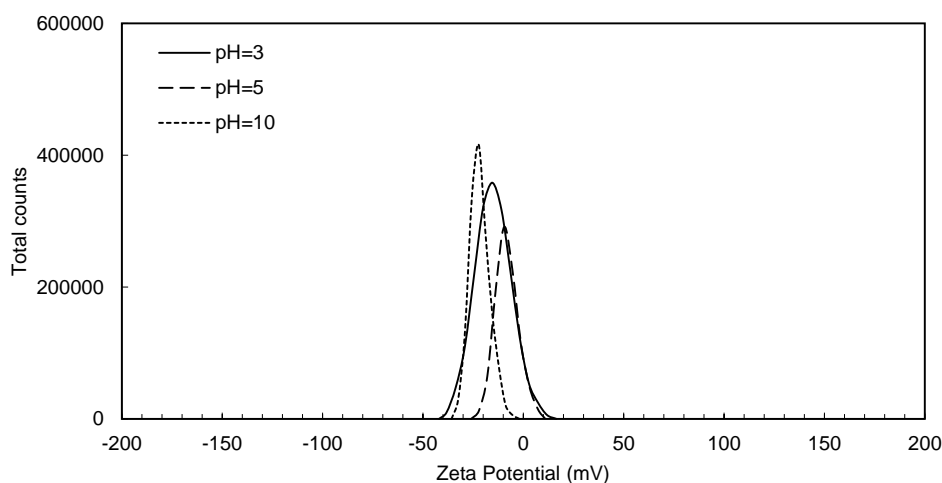


Figure 5.13 Zeta potential distribution for the dairy industry effluent at pH 3, 5 and 10.

### 3.3. Results and discussion

Cationic polyelectrolytes were applied as flocculants in the treatment of the real effluent from dairy industry. Considering the zeta potential distribution for the pH values tested (see Figure 5.13), it was indicated that positively charged polyelectrolytes would promote flocculation, since particles in the effluent presented mostly negatively charged surfaces. Performance tests were conducted using several polymer concentrations, from 0-104 mg/L for three different pHs, 3, 5 and 10 (Figure 5.14 and Figure 5.15). The best results were obtained adjusting the pH to 5, which, by itself, provided a slight destabilization of the effluent, though not reducing turbidity noticeably. Modifying the pH of the effluent to other values (3 or 10) decreased the turbidity around 20%, however addition of flocculant did not produce any further turbidity reduction. In general, flocculants with higher cationic fraction (60 series) presented better results in turbidity reduction. In this case, hydrophobic modification improved the performance (60M1SC and 60M2SC), however in the case of higher hydrophobic content (60M2SC) this improvement was verified using lower dosages of flocculant and not so much in the maximum turbidity reduction, which was lower than using the polyelectrolytes with less hydrophobic content (60M1SC), and even lower than the corresponding copolymer 60MC. The terpolymer 60M1SC was the best flocculant, achieving 84% of turbidity reduction with a polymer concentration of 53 mg/L. On the other hand, polyelectrolytes with lower cationic fraction (25 series) revealed very poor performance, with a maximum turbidity reduction reached of 39% with 25MC, suggesting that the amount of positive charges was not enough to induce flocculation efficiently. Indeed, the addition of hydrophobicity proved to be inefficient

in this charge density level, even reducing the effectiveness in the case of (25M1SC), with lower content of hydrophobic monomer. Furthermore, comparing the polymers produced with different synthesis formulations (MC and MP series), a higher turbidity reductions were achieved using Carnation as organic phase in the health-friendly formulation (MC series).

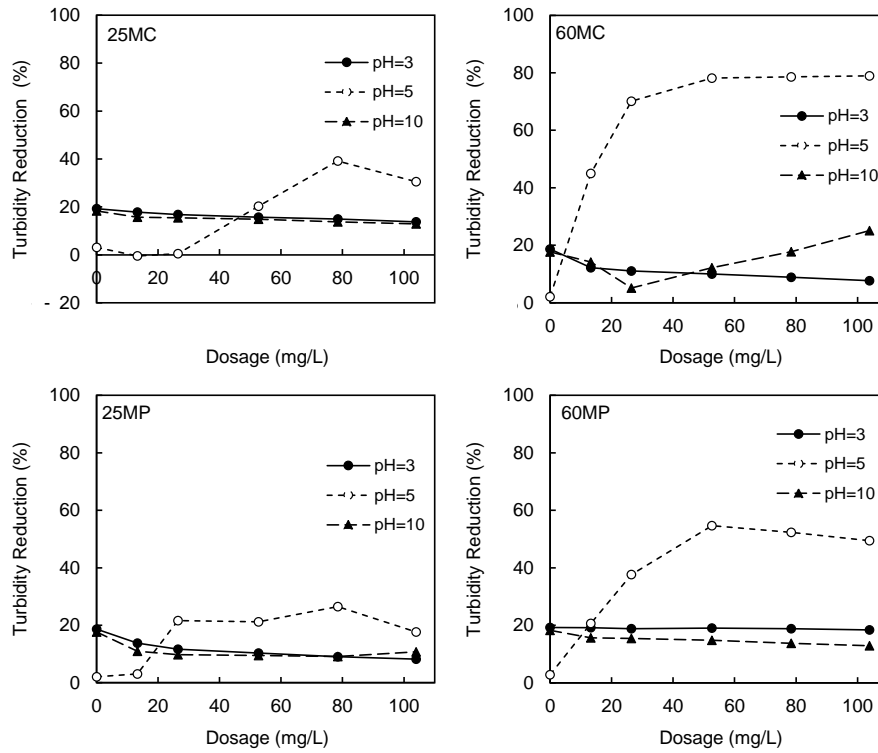


Figure 5.14 Turbidity reduction curves for the industrial dairy effluent treated by cationic copolymers Poly(AAm-MAPTAC): 25MC, 25MP, 60MC and 60MP, at three different pHs.



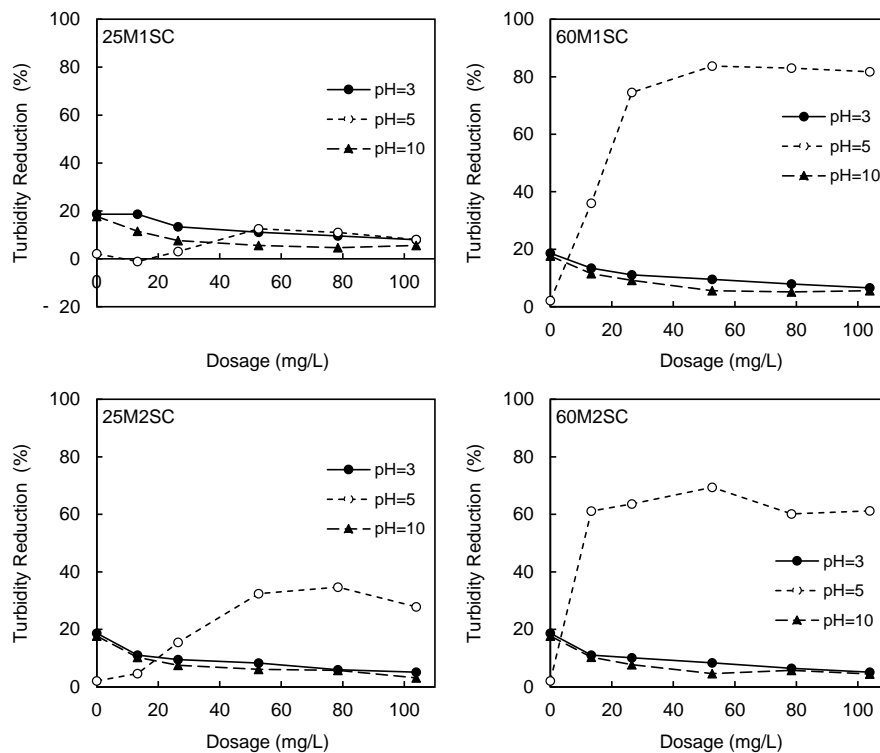


Figure 5.15 Turbidity reduction curves for the industrial dairy effluent treated by cationic terpolymers Poly(AAm-MAPTAC-SMA): 25M1SC, 25M2SC, 60M1SC and 60M2SC, at three different pHs.

The cationic flocculants developed were compared with the commercial reference AlpineFloc DHMW, which has a comparable cationic fraction with the 60 series polyelectrolytes (Figure 5.16). The obtained performance was very similar to the polyelectrolyte 60MC, reaching similar turbidity reductions, around 80%, for pH 5. However, comparing with the hydrophobically modified terpolymers, a better performance was obtained using the 60M1SC flocculant, illustrating once again the importance of hydrophobicity in the polymers used to treat oily effluents<sup>115,126</sup>.

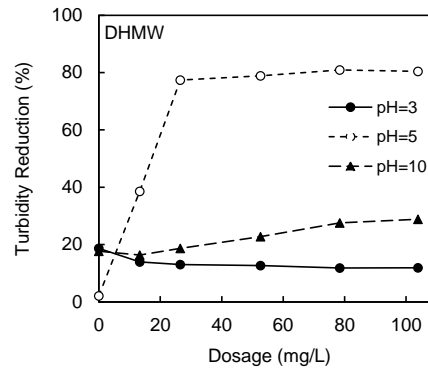


Figure 5.16 Turbidity reduction curves for the industrial dairy effluent treated by a reference cationic polymer, AplineFloc DHMW, at various pHs.

The newly developed anionic polyelectrolytes were also tested in the dairy effluent sample presented in Table 5.2. The zeta potential of the dairy effluent at pH 5, value that promoted destabilization of the effluent, ranged from -25 mV to 10 mV (see Figure 5.13), suggesting a possible effectiveness of using anionic flocculants for its treatment, since the interaction between negative flocculant chains and positive effluent particles should be enough to induce the flocculation process. The high molecular weight of these flocculants (see Table 4.6 in Section 3.2. of Chapter 4) may also promote an efficient aggregation of dispersed particles to form large aggregates which will settle and clarify the wastewater<sup>230</sup>.

Figure 5.17 to Figure 5.20 shows the turbidity removal curves for pH 3, 5 and 10, and for flocculant concentrations from 0-104 mg/L. In general, for all the polymers, at pH 3 and 5, there is an increase of turbidity reduction with increasing dosage. The best results were obtained for pH 5, as for the cationic polyelectrolytes, since, as mentioned previously, it is for this pH that the effluent particles are more destabilized. Polyelectrolytes of the 80 series lead to better results than the 50 series, suggesting that higher charge density is more favorable to induce flocculation, as was to be expected.

In most of the 80 series polyelectrolytes it was possible to achieve turbidity reductions around 90% with less than 40 mg/L of flocculant, only with the exception of hydrophobically modified polymers using the LMA monomer. Indeed, for both the 50 and 80 series, the terpolymers with LMA presence were the only polymers where the hydrophobic modification did not improve the flocculation performance, actually reducing it when compared with the corresponding copolymers. This suggests that the number of methylene groups in the aliphatic chain of the hydrophobic monomer is not suitable for interactions with the oily fraction of the dairy effluent. Lee *et al.*<sup>120</sup> evaluated in a previous study, the effect of the hydrophobic chain

length in the flocculation process, and the polymer comprising a dodecyl group (12 methylene groups, similar to LMA) also presented inferior performance, requiring a higher dosage, when compared with the other hydrophobically modified polymers, comprising shorter chain lengths. The authors suggested a relation with molecular weight, which is lower for polyelectrolytes with larger hydrophobic chain lengths. In the case of the polyelectrolytes developed in the present work, in general, the ones comprising LMA also present lower molecular weight values when compared with the ones comprising EA (shorter hydrophobic chain length than LMA), which can explain the worse performance of the terpolymers containing LMA (see Table 4.6 in Section 3.2. of Chapter 4). However, when comparing with the polyelectrolytes comprising SMA (larger hydrophobic chain length than LMA), these ones show better performance and present lower molecular weight values. Still, as referred in Chapter 4, the polyelectrolytes comprising SMA exhibit higher zeta potential values (see Table 4.6 in Section 3.2. of Chapter 4), which can possibly explain their superior performance.

For the 50 series, the presence of hydrophobicity improves the performance in flocculation in most of the cases (as mentioned previously with exception for polyelectrolyte 50A1LC), considering the maximum reduction of turbidity. For 80 series, increasing the amount of the hydrophobic monomer did not show significant effect in improving the turbidity reduction, with exception for the terpolymer 80A3SC, where the efficacy with the lower dosage (13 mg/L) increased and lead to a turbidity reduction of about 88%. In addition, analysis of Poly(AAm-Na-AMPS) copolymers suggests that charge density has more influence in the flocculation performance than molecular weight, for this specific effluent, since the copolymer 50AP presents a much higher molecular weight than 80AC and 80AP (see Table 4.6 in Section 3.2 of Chapter 4), but 80AC and 80AP show better performances. Thus, when introducing the hydrophobic monomer, performance of the 50 series is improved, in relation with the corresponding copolymer, however still not better than the 80 series copolymers, since the charge density is not high enough. Finally, the higher reductions of turbidity were achieved with flocculants 80AC (93% turbidity reduction), 80A1EC (90%), 80A3EC (90%), 80A1SC (91%) and 80A3SC (95%), always for pH 5 and dosage of 53 mg/L.

Observing the zeta potential distribution plot (Figure 5.13) and comparing it with the turbidity reduction results, it is possible to see that for the pHs that show zeta potential distribution in both negative and positive regions (3 and 5), anionic flocculants promote reasonable or very good flocculation. However, at pH 10, which leads to a zeta potential distribution only in the negative region, very poor performances were observed. This suggests that anionic flocculants are suitable for this specific effluent.

Comparing the turbidity reduction results with reported literature reveal that much lower polymer concentration is needed, when using the novel developed polyelectrolytes, to achieve the same efficiencies<sup>174,179</sup>. The majority of the literature is based on inorganic coagulants, however the use of organic flocculants requires lower amount of treatment agent, which generates less volume of sludge and ready for disposal after simple treatment, reducing the overall treatment cost. These benefits are even more notorious for the novel polyelectrolytes obtained in the present work, as was also noted previously.

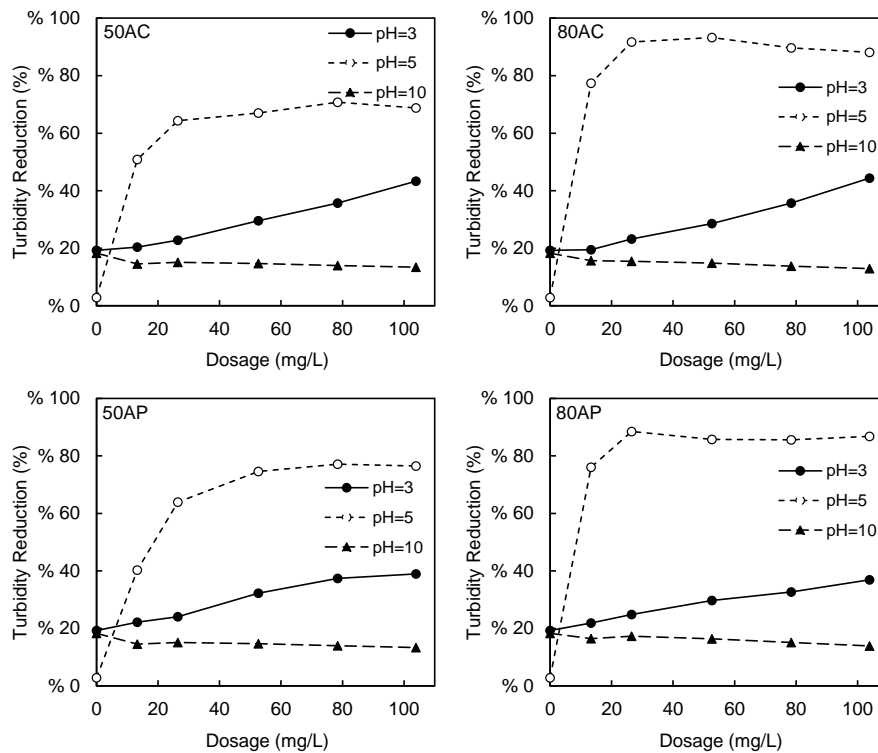


Figure 5.17 Turbidity removal curves for dairy industry effluent treated by anionic copolymers Poly(AAm-Na-AMPS): 50AC, 80AC, 50AP and 80AP, at various pH.

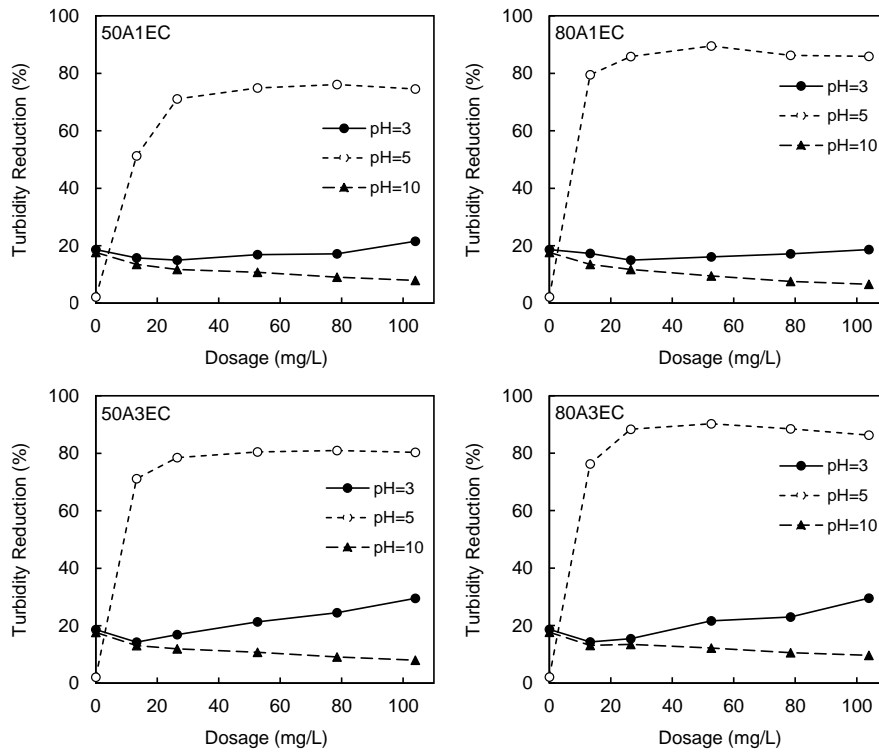


Figure 5.18 Turbidity removal curves for dairy industry effluent treated by anionic terpolymers Poly(AAm-Na-AMPS-EA): 50A1EC, 50A3EC, 80A1EC and 80A3EC, at various pH.

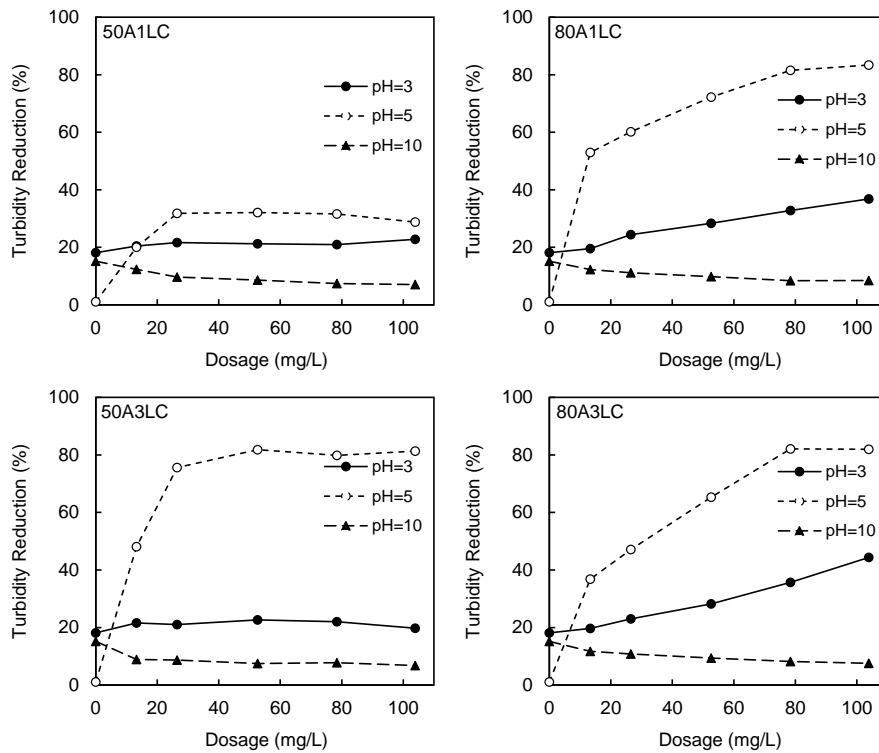


Figure 5.19 Turbidity removal curves for dairy industry effluent treated by anionic terpolymers Poly(AAm-Na-AMPS-LMA): 50A1LC, 50A3LC, 80A1LC and 80A3LC, at various pH.

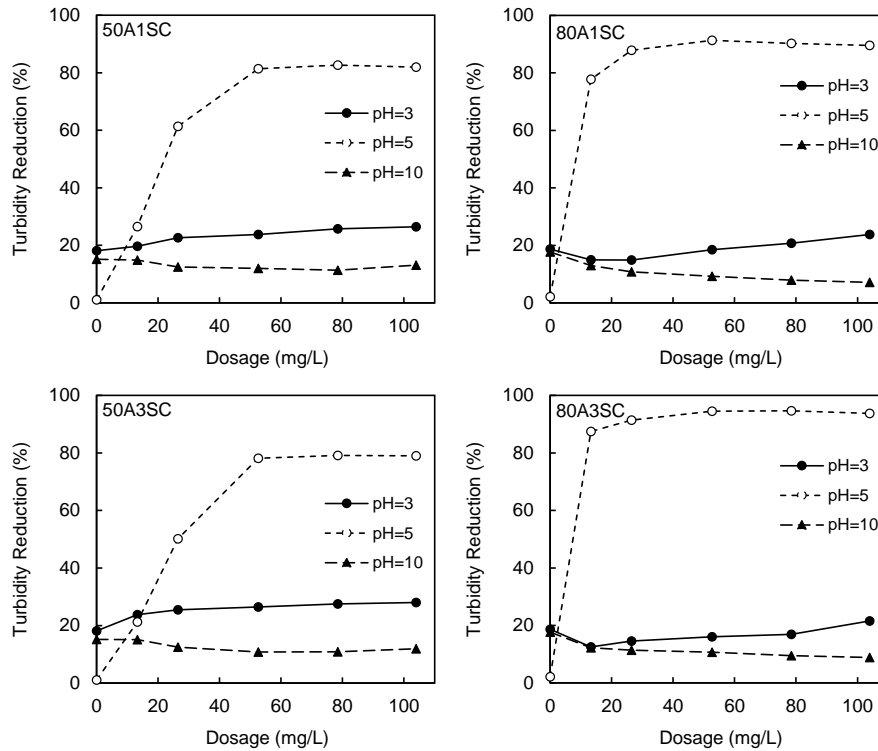


Figure 5.20 Turbidity removal curves for dairy industry effluent treated by anionic terpolymers Poly(AAm-Na-AMPS-SMA): 50A1SC, 50A3SC, 80A1SC and 80A3SC, at various pH.

An anionic polymer reference, AlpineFloc Z1, which has similar charge density to 50 series, was also evaluated (Figure 5.21). At pH 3 and 10 the performance was worse than for all 50 series polymers (Figure 5.17 to Figure 5.20). At optimum pH of 5, with AlpineFloc Z1 it was possible to achieve 80% turbidity reduction with 27 mg/L, slightly higher than with the developed polyelectrolytes with similar charge density, where the maximum of 83% was achieved only for 78 mg/L of 50A1SC. However, the higher turbidity reductions for this effluent were achieved with polyelectrolytes with higher charged fraction (80 series polyelectrolytes).

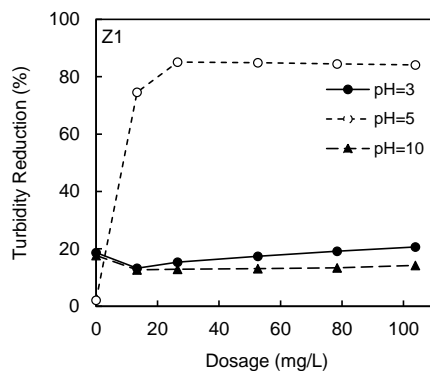


Figure 5.21 Turbidity removal curves for dairy industry effluent treated by anionic reference polymer, AlpineFloc Z1, at various pH.

For the terpolymers that presented best performance in turbidity reduction, as well as the reference polymer and corresponding copolymer, COD and total solids removals efficiency was tested for optimum conditions of pH and dosage (Figure 5.22). The COD removal was obtained in the range of 40-45%, considerably close to the values reported in literature for similar processes<sup>165,175,179,180</sup>, while total solids removals was in the range of 55-57% removal. Considering overall results, flocculant 80A3SC seems to be the polyelectrolyte that performs the best in treatment of dairy industry effluent (higher turbidity reduction with a low dosage, and high COD and total solids removals).

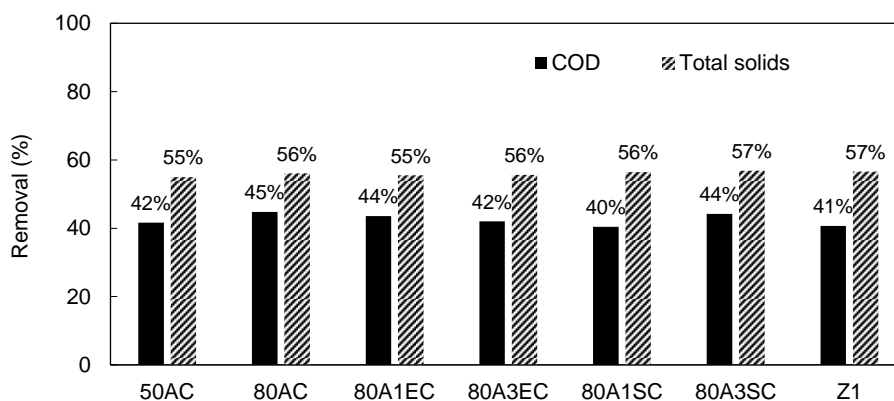


Figure 5.22 COD and total solids removal for treatment of dairy industry effluent with 50AC, 80AC, 80A1EC, 80A3EC, 80A1SC, 80A3SC and AlpineFloc Z1, in optimized conditions of pH (pH 5) and concentration (78 mg/L for 50AC, 53 mg/L for 80AC, 80A1EC, 80A3EC, 80A1SC and 80A3SC, and 27 mg/L for AlpineFloc Z1).

When the flocculation tests were performed, the first indication of flocculation was the visual observations. As soon as the lowest dosage was added, flocs formation was immediately observed. Figure 5.23 shows photographs of the dairy effluent before (a) and after the treatment with flocculants 80AC (b), 80A3EC (c) and 80A3SC (d) in the optimum conditions. It is possible to see a clear reduction of turbidity, as well as strong and compact flocs aggregation, which settled quickly when the mixing was stopped.

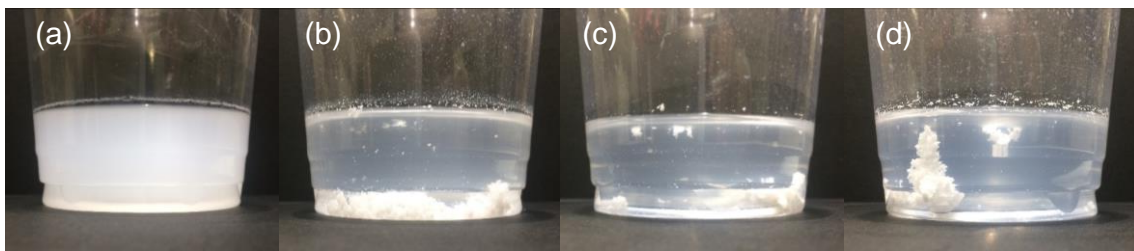


Figure 5.23 Initial dairy effluent (a) and effluent after treatment with flocculants 80AC (b), 80A3EC (c) and 80A3SC (d), in optimized conditions of pH (pH 5) and concentration (53 mg/L for 80AC, 80A3EC and 80A3SC).

Therefore, results obtained for cationic and anionic flocculants applied in the flocculation of dairy effluent indicate that anionic polyelectrolytes with higher charged fraction (80 series) have superior performance in the treatment process, leading to the higher maximum turbidity reductions (above 90%), using concentrations of approximately 53 mg/L. Moreover, the better conditions of treatment suggest an ideal adjustment of the pH of the effluent to a value of 5. The hydrophobic modification improved flocculation performance, especially when using the monomer with larger hydrophobic aliphatic chain (SMA), however not that significantly, since the corresponding copolymer (80AC) already presented very good turbidity reductions. It is worth noting that some anionic flocculants reached turbidity reductions above 90% with concentrations around 27 mg/L and without addition of any aids. These polyelectrolytes revealed as well superior performance than the reference polymer tested.





## 4. POTATO CRISPS MANUFACTURING INDUSTRY EFFLUENT

### 4.1. Procedure to evaluate flocculation performance

For detailed description of flocculation performance procedure, see Section 2.1 of the present Chapter.

### 4.2. Initial wastewater characterization

The characteristics of the industrial potato crisps manufacturing effluent sample used in the flocculation tests (supplied by Aventech Group, Portugal) are summarized in Table 5.3. The effluent presents high turbidity, COD and solids content, what makes it a challenging effluent for treatment. All the flocculation tests were performed using this wastewater sample.

Table 5.3 Characteristics of the industrial potato crisps manufacturing effluent tested before any treatment.

Parameter	Values
pH	12.8
COD (gO <sub>2</sub> /L)	21.6
Total solids (g/L)	9.7
Turbidity (NTU)	3050

Zeta potential distribution for the initial effluent after adjustment for the three pH values used was determined and is presented in Figure 5.24. For all pHs, the effluent always presents negatively and positively charged particles, even if for pH 10 the effluent presents a higher proportion of particles with negatively charged surfaces, which may justify the stability of the initial effluent sample. The median values of zeta potential were 6 mV, -5 mV and -14 mV, for pH 3, 6 and 10, respectively. In general, the zeta potential values obtained in different pHs for this effluent are lower than the values obtained for the effluents from olive oil mill or dairy industries.

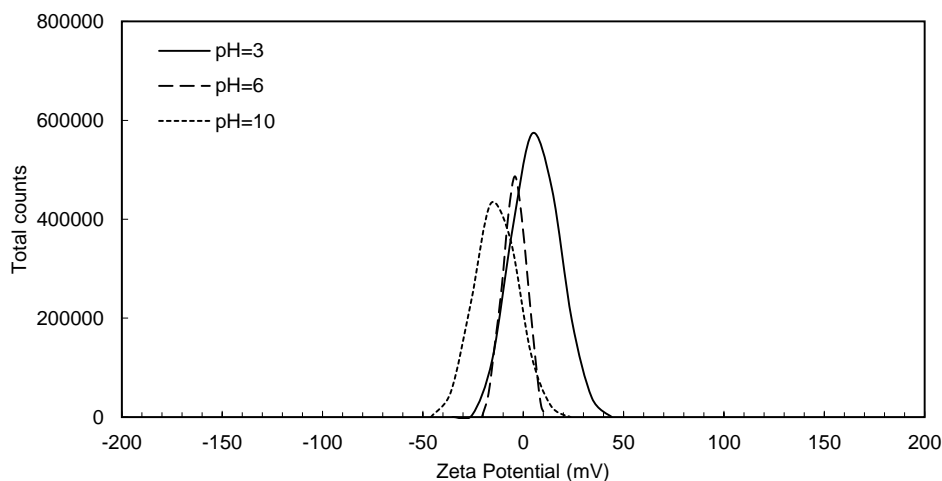


Figure 5.24 Zeta potential distribution for potato crisps manufacturing effluent at pH 3, 6 and 10.

### 4.3. Results and discussion

Industrial potato crisps manufacturing effluent was also used to test the developed cationic polyelectrolytes as flocculation agents. Modifying the effluent pH to a value of 6 promoted a higher destabilization of the effluent (median zeta potential of -5 mV), which only by itself reduced turbidity around 35%. At this pH there is heterogeneity in the surface charge of the effluent particles (Figure 5.24), however a large part still possess negatively charge surface, suggesting a possible good performance of cationic polyelectrolytes in promoting flocculation. Performance tests were conducted for three different pHs (3, 6 and 10), for flocculant dosages varying from 0-104 mg/L. Using pHs of 3 and 10, very minimal water clarification was observed, even after addition of flocculant dosages above 100 mg/L. Using the optimum pH, the highest extent turbidity reduction were achieved using higher cationic fraction polymers (60 series). Specifically, the copolymer 60MC conducted to 98% of turbidity reduction at a concentration of 27 mg/L. Hydrophobic modification did not show an improvement of performance, possibly due to the already very high efficiency of the copolymers (see Figure 5.26). Moreover, lower and higher hydrophobic content did not present significant differences in turbidity reduction.

Lower cationic fraction polyelectrolytes (25 series) proved not be as efficient as the higher cationic fraction ones (60 series), proving that higher amount of positive charges in the polymer chain can promote more interaction with the impurity particles of the effluent. Still, it was possible to reduce turbidity in 98% with a higher dosage of 78 mg/L using the flocculant 25MC. Again, adding a hydrophobic monomer did not improve the removal efficiency.

Regarding the different formulations used in the polyelectrolytes synthesis (see Figure 5.25), polymers developed using Carnation as organic phase (MC series) proved to be more efficient than polymers developed using Puresyn4 (MP series), not only in terms of maximum turbidity reduction achieved, but also concerning the dosage needed to reach the same efficiency.

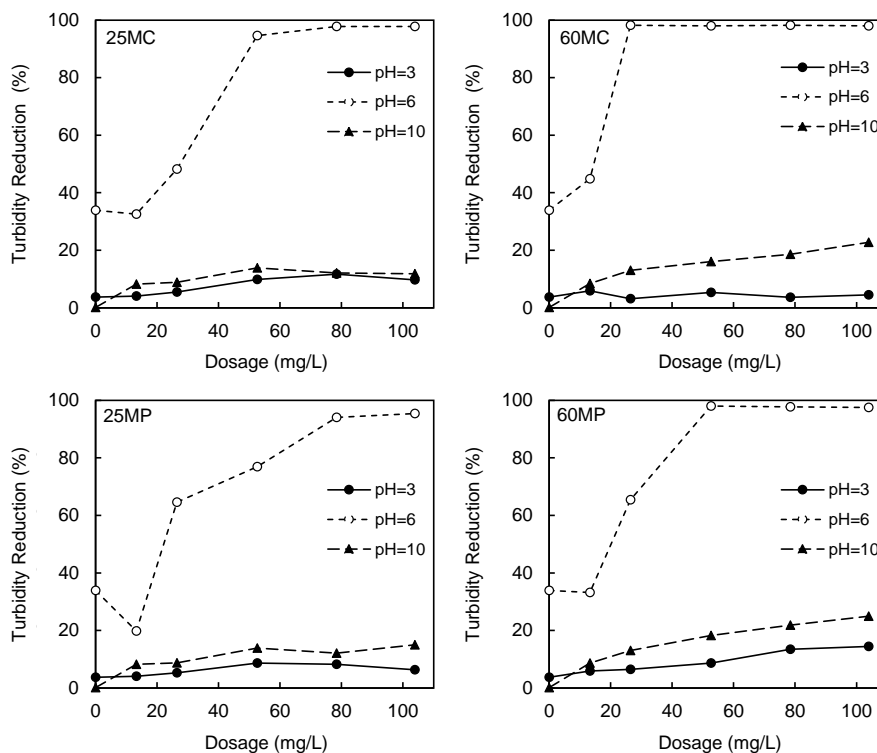


Figure 5.25 Turbidity reduction curves for the industrial potato crisps manufacturing effluent treated by cationic copolymers Poly(AAm-MAPTAC): 25MC, 25MP, 60MC and 60MP, at three different pHs.

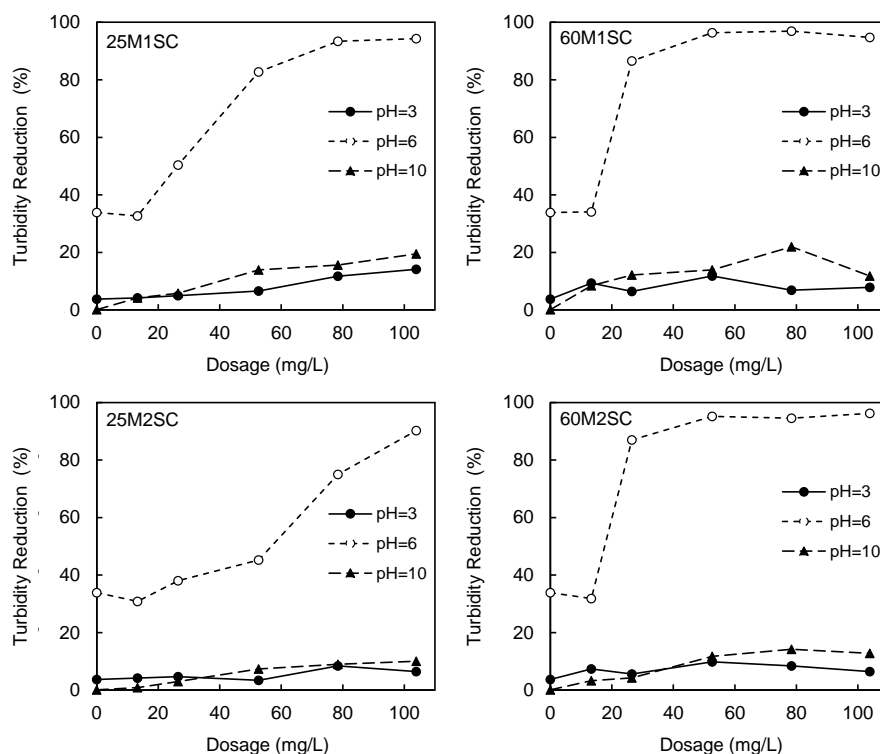


Figure 5.26 Turbidity reduction curves for the industrial potato crisps manufacturing effluent treated by cationic terpolymers Poly(AAm-MAPTAC-SMA): 25M1SC, 25M2SC, 60M1SC and 60M2SC, at three different pHs.

Comparing the performance of the developed polyelectrolytes with the cationic commercially available reference, AlpineFloc DHMW, a similar behaviour was observed for the ideal pH (see Figure 5.27). With this polymer it was possible to achieve a maximum turbidity reduction of 97% using a concentration of 53 mg/L, however a slightly higher maximum turbidity reduction was obtained for the developed copolymer 60MC, at lower concentration. Still, for other pHs tested, 3 and 10, a superior efficiency was obtained for the reference polymer, indicating that this polymer in this specific effluent is less subjective to the pH changes.

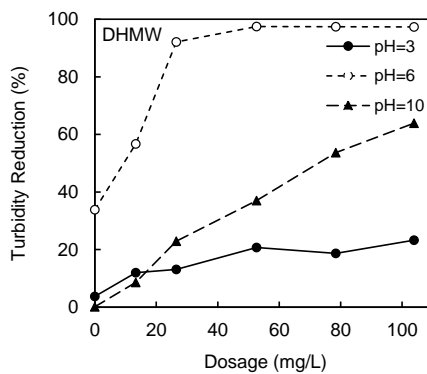


Figure 5.27 Turbidity reduction curves for the industrial potato crisps manufacturing effluent treated by reference cationic polymer, AlpineFloc DHMW, at various pHs.

The evaluation of the polyelectrolytes' efficiency in wastewater treatment was also accessed for other parameters, such as the COD and total solids removals. This was carried for the flocculants that showed best performance in turbidity reduction, namely copolymers 60MC and 60MP, as well as the commercial reference AlpineFloc BHMW (Figure 5.28). Both copolymers 60MC and 60MP performed very well in COD removal, at approximately 90%, showing a similar efficiency to the one obtained with the reference AlpineFloc DHMW. Regarding total solids, copolymer 60MC performed slightly better, reaching 53% removal.

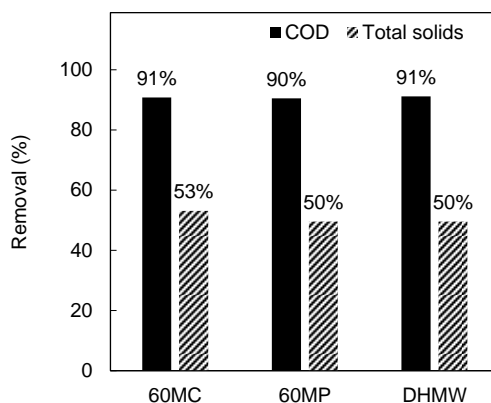


Figure 5.28 COD and total solids removal after the treatment of the industrial potato crisps manufacturing effluent with cationic flocculants 60MC, 60MP and AlpineFloc DHMW, in optimized conditions of pH (pH 6) and concentration (27 mg/L for 60MC and 53 mg/L for 60MP and AlpineFloc DHMW).

Figure 5.29 present photographs of flocs formed for the potato crisps manufacturing effluent, using as flocculants 60MC (b) and 60MP (c), in comparison with the initial sample (a). Flocs produced with 60MP look slightly smaller than flocs formed with 60MC, however the

turbidity removal is similar and very high (above 97%) in both cases, as previously presented. Flocc structure suggests strong and heavy floccs that settle fast (in few seconds).

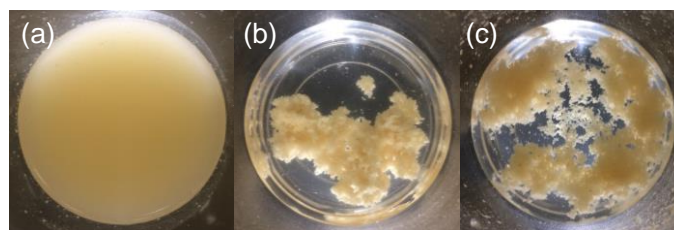


Figure 5.29 Initial potato crisps manufacturing effluent (a) and effluent after treatment with flocculants 60MC (b) and 60MP (c), in optimized conditions of pH (pH 6) and concentration (27 mg/L for 60MC and 53 mg/L for 60MP).

As mentioned in Section 4.2. of the present Chapter, the effluent presents a broad zeta potential distribution, in both positive and negative regions, at optimum pH of treatment, suggesting the suitability of using also anionic polymers on its treatment. Results for the turbidity removal with developed anionic flocculants at pH 3, 6 and 10 are presented in Figure 5.30 to Figure 5.33. For this effluent, anionic copolymers show already very high turbidity reduction, with values above 97% at concentrations below 60 mg/L for the optimum pH (pH 6) and for both anionic fractions (50 and 80 series). With these results, evaluation of the hydrophobic effect of terpolymers may be difficult. However, looking at performances of hydrophobically modified terpolymers, there is a reduction of efficacy with the increase of the number of methylene groups in the aliphatic chain, more visible in the 50 series. Flocculants with presence of the SMA monomer (higher number of methylene groups) results in less turbidity reductions, indicating that hydrophobicity is not beneficial for this specific effluent. Moreover, this decrease of performance is more notorious when the content of this hydrophobic monomer increases.

Considering that introduction of hydrophobicity was beneficial in the flocculation of the other two effluents tested, these observations suggest that the hydrophobicity benefit may be dependent on the triglyceride composition in the wastewater. The effluent from potato crisps manufacturing industry likely has a much higher content in polyunsaturated fats, resulting from the crisps frying process, than olive oil or dairy effluents, indicating that introduction of hydrophobicity is more beneficial when there is higher content of monounsaturated or saturated fats, triglycerides expected to be present in higher content in olive oil and dairy wastewaters.

In summary, best performances were achieved with flocculants 50AC (97% turbidity reduction at 27mg/L dosage), 50AP (97% at 27 mg/L), 50A1EC (97% at 13 mg/L), 50A3EC (97% at 27 mg/L), 50A1LC (98% at 53 mg/L) and 50A3LC (98% at 27 mg/L). In general, polymers with a higher molecular weight and medium charge density, which favors the bridging mechanism. Flocculation using polyelectrolytes with high molecular weight and medium charge density promotes the bridging effect, since the polymer chain adsorbs on the effluent particles surface and extends enough to interact with several particles. In addition, it is worth to note that the 50 series polyelectrolytes may have lower production costs, when compared with the 80 series, since the charged fraction is lower. In the case of this specific effluent, there is no previous flocculation results reported in literature for comparison. However, the obtained results in this study are quite promising, encouraging the use of this treatment process in the referred effluent.

In general, and looking at the turbidity reduction efficiencies, this effluent does not seem to need very sophisticated polymer structures to induce flocculation. This indicates that the effluent may not have a very stable composition, and it can be destabilized easily with the addition of a charged polyelectrolyte.

At pH 3 there is also significant turbidity removals for most of the polymers studied, since zeta potential distribution indicate a large amount of positively charged particles, however not as efficient as at pH 6 due to the initial destabilization of the effluent particles observed at this specific pH. On the other hand, at pH 10 substantial reductions are only observed with the 80 series flocculants. At this pH the range of zeta potential is even larger, -58 to 28 mV, suggesting that it is necessary higher charge density to induce flocculation. Furthermore, for the copolymers Poly(AAm-Na-AMPS), a similar behavior was observed for polyelectrolytes developed with Carnation (an iso-paraffin) or Puresyn4 (an hydrogenated polydecene), suggesting that the oil in the synthesis formulation does not affect the flocculation performance, and thus Carnation is a better choice since it is more economic.



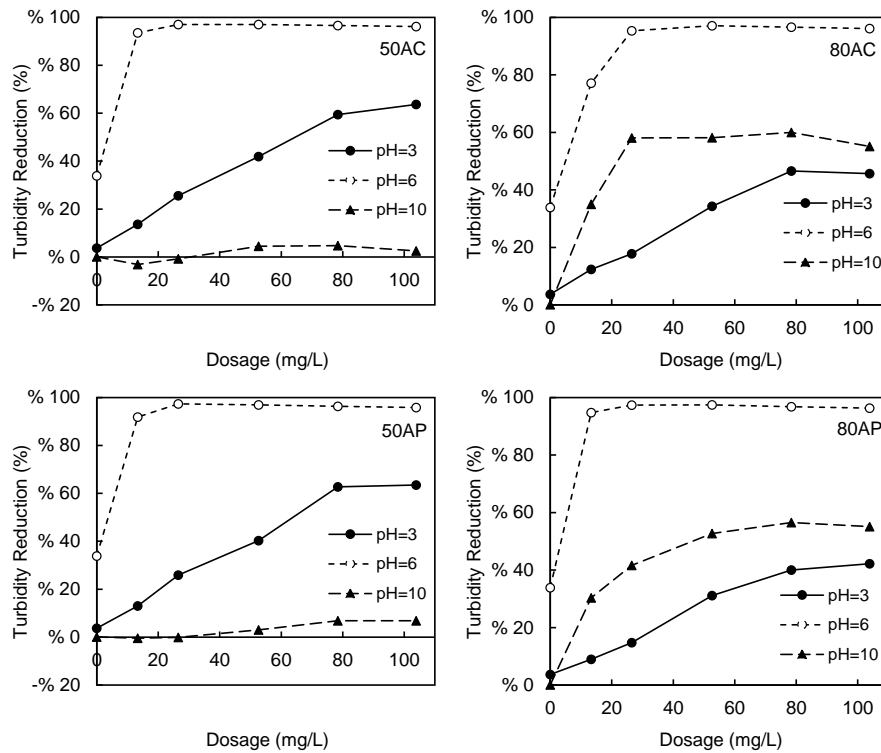


Figure 5.30 Turbidity removal curves for potato crisps manufacturing industry effluent treated by anionic copolymers Poly(AAm-Na-AMPS): 50AC, 80AC, 50AP and 80AP, at various pH.

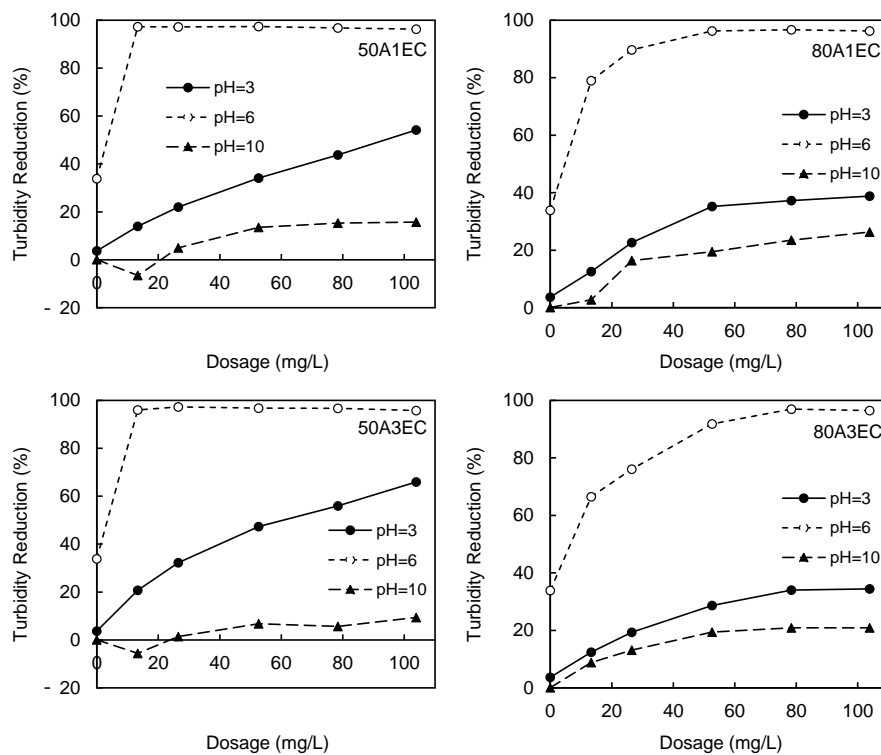


Figure 5.31 Turbidity removal curves for potato crisps manufacturing industry effluent treated by anionic terpolymers Poly(AAm-Na-AMPS-EA): 50A1EC, 50A3EC, 80A1EC and 80A3EC, at various pH.

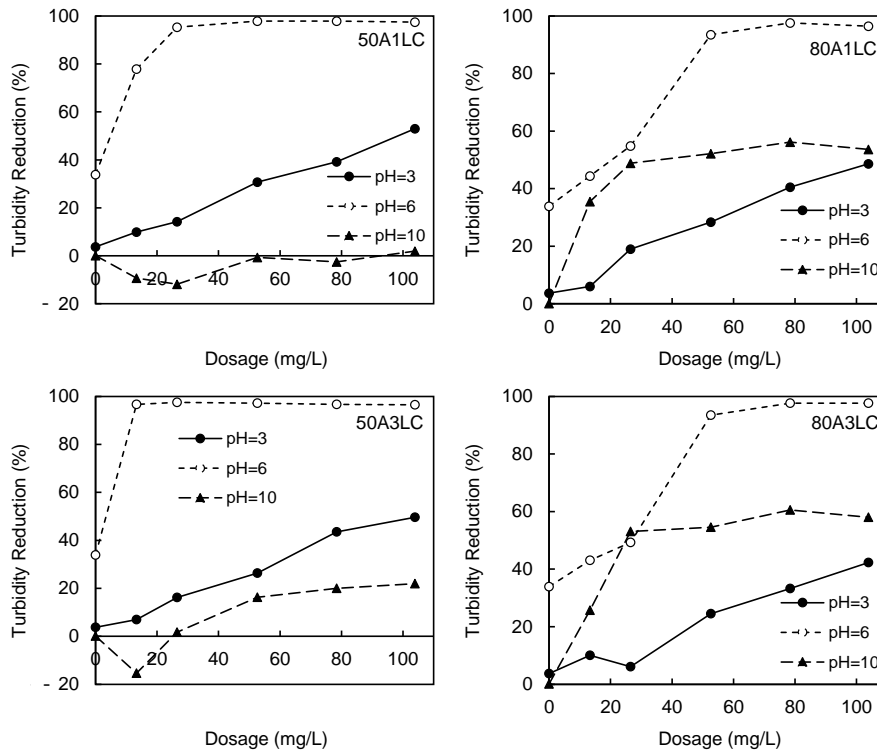


Figure 5.32 Turbidity removal curves for potato crisps manufacturing industry effluent treated by anionic terpolymers Poly(AAm-Na-AMPS-LMA): 50A1LC, 50A3LC, 80A1LC and 80A3LC, at various pH.

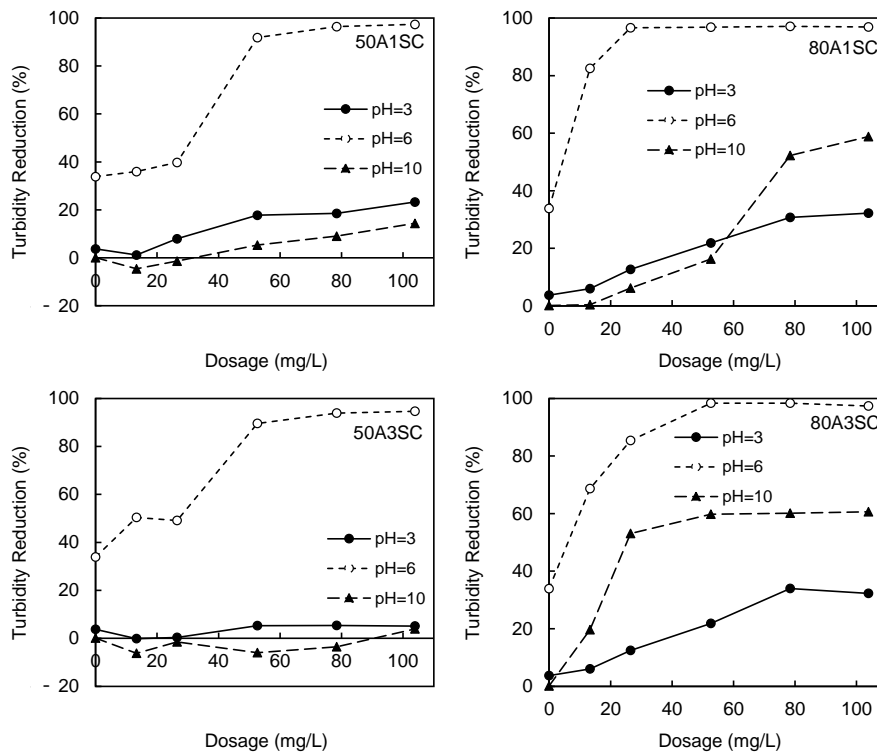


Figure 5.33 Turbidity removal curves for potato crisps manufacturing industry effluent treated by anionic terpolymers Poly(AAm-Na-AMPS-SMA): 50A1SC, 50A3SC, 80A1SC and 80A3SC, at various pH.

A reference anionic polymer AlpineFloc Z1, which has similar charge density to the 50 series of polymers developed, was also tested in this effluent (Figure 5.34). The turbidity reduction profile obtained was noticeably different from the profiles for the developed flocculants (Figure 5.30 to Figure 5.33). Looking at low dosages of polymer, AlpineFloc Z1 presented better results at pH 10 than at pH 5, optimum pH for the novel developed polyelectrolytes. Still, the removal was much lower than the maximum removal achieved with the developed polyelectrolytes at low dosages, around 80% for 27 mg/L. However, at higher dosages, pH 6 allows to reach higher turbidity reduction, 97% at 104 mg/L concentration. Nevertheless, the performance was inferior to the one of the developed polyelectrolytes, where it was possible to reach 98% turbidity reduction with 27 mg/L of 50A3LC.

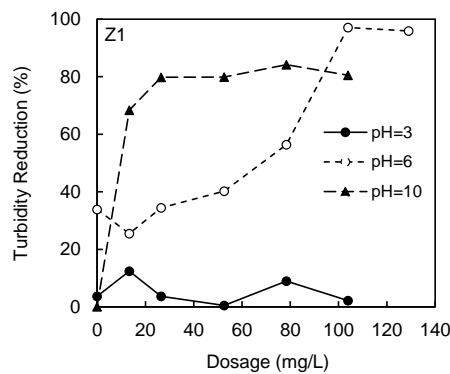


Figure 5.34 Turbidity removal curves of potato crisps manufacturing industry effluent treated by reference anionic polymer, AlpineFloc Z1, at various pH.

For terpolymers that presented best performance in turbidity reduction, and corresponding copolymers, COD and total solids removals efficiency were tested (Figure 5.35). COD was initially considerably high in this effluent, and the removal efficiency was always above 90%, for all the conditions shown in Figure 5.35. Total solids removal was around 50-55%. Both COD and total solids removals, using the developed polyelectrolytes, was similar to the values obtained with the reference polymers, even if the last one required a higher dosage.

In general, for this specific effluent it was possible to reduce the COD value in much higher extent than for the other two effluents tested, however this effluent also presented an initial value of COD much higher than the other ones.

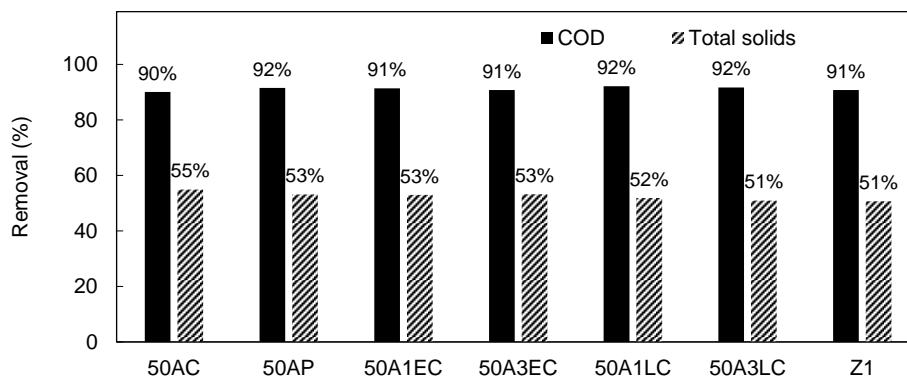


Figure 5.35 COD and total solids removal for the treatment of potato crisps manufacturing industry effluent with anionic flocculants 50AC, 50AP, 50A1EC, 50A3EC, 50A1LC, 50A3LC and AlpineFloc Z1, in optimized conditions of pH (pH 6) and concentration (13 mg/L for 50A1EC, 27 mg/L for 50AC, 50AP, 50A3EC and 50A3LC, 53 mg/L for 50A1LC and 104 mg/L for AlpineFloc Z1).

Analysing Figure 5.36, it is possible to visualize the flocs appearance after the treatment of the potato crisps manufacturing effluent (a) with the flocculants 50AC (b), 50AP (c), 50A3EC (d) and 50A3LC (e). A clear separation of the solid and liquid phases is noticeable, along with strong and large flocs.

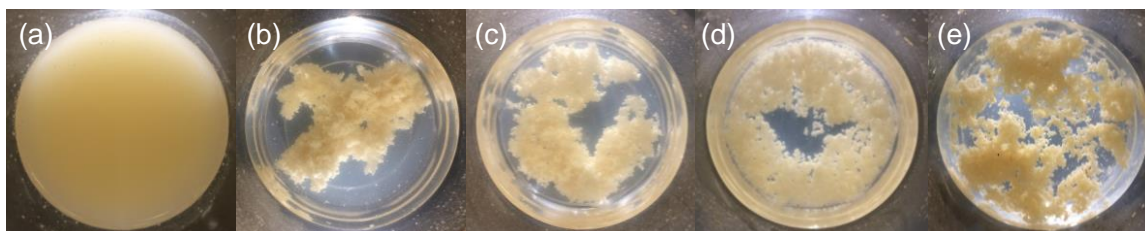


Figure 5.36 Initial potato crisps manufacturing effluent (a) and effluent after treatment with anionic flocculants 50AC (b), 50AP (c) 50A3EC (d) and 50A3LC (e), in optimized conditions of pH (pH 6) and concentration (27 mg/L for 50AC, 50AP, 50A3EC and 50A3LC).

The results achieved for cationic and anionic polyelectrolytes, applied in the treatment of potato crisps manufacturing effluent by flocculation, show turbidity reduction, reaching 98% reduction with dosages as low as 27 mg/L. In fact, anionic copolymers with lower charged fraction (50 series) have shown even superior performance in the treatment process, leading to turbidity reductions above 95% using concentrations of 13 mg/L. Considering these data, higher charged fraction would not be necessary, nor would the addition of coagulants. The hydrophobically modified polyelectrolytes using the monomer with shorter hydrophobic aliphatic chain (EA) also presented very promising results, however considering the success of

the copolymers (50AC and 80AC), this modification may not be necessary, since it would correspond to an increase of cost. These polyelectrolytes also revealed considerably higher performance than the reference polymer presented. Lastly, the suitable conditions of treatment suggest an ideal pH of 6 for both cationic and anionic flocculants.

## 5. CONCLUSIONS

Flocculation is one of the most widely used solid-liquid separation method for removal of suspended and dissolved particles, colloids and organic matter from industrial effluents, due to its high efficiency with low dosage and easy handling.

The polymers developed shown to be suitable for the flocculation of olive oil mill, dairy and potato chips manufacturing effluents. For all cases it was possible to achieve turbidity reductions above 90% with polymer dosages below 60 mg/L. Moreover, COD and total solids removals also showed good results, between 45-92% and 37-56%, respectively, for the best conditions. Hydrophobic-modification presented benefits in the treatment efficacy, although using lower hydrophobic content (1 mol%) proved to be more favourable. Specifically, cationic flocculants with higher cationic fraction (60 series with around 41-47 wt% charged fraction) demonstrated higher suitability for olive oil mill effluent, while anionic flocculants, with higher anionic fraction (80 series with around 57-68 wt% charged fraction) and lower anionic fraction (50 series with around 39-42 wt% charged fraction), performed better for dairy and potato crisps manufacturing effluent, respectively.

In general, polyelectrolytes produced using the oil Carnation as organic phase led to superior performances in the turbidity reduction. Although the molecular weight and zeta potential of the polyelectrolytes developed using Puresyn4 are higher, their performance is slightly inferior in most of the cases. There are few possible explanations for this evidence, including the inverting surfactant used that may be slightly less efficient in the inverse-emulsions containing Puresyn4, or the lower density and larger hydrocarbon chains of the oil Puresyn4, when compared with Carnation oil, that affect its solubility, though it was not yet possible to prove any of these hypothesis, which will require additional studies in the future.

A bridging mechanism was the predominant effect in the flocculation process, mainly due to the high molecular weight of the flocculants. However, in some cases where the effluent is mainly positive or negatively charged, a combination of the mechanisms of charge neutralization and bridging can occur. In general, it could be qualitatively seen that the flocs obtained were large and compact, enabling fast settling (within seconds). This must lead to compact sludge easier to handle in further processing.

It is possible to conclude that the polyelectrolytes developed for direct flocculation of oily wastewaters proved to be a highly effective treatment solution for the harsh effluents targeted, and also a possible more economical solution, when compared with alternative/standard

coagulation-flocculation procedures which use larger amounts of flocculant and thus generate high volumes of sludge, expensive to treat. Moreover, in relation with the performances of coagulation/flocculation processes presented in literature, considerably lower dosages have to be applied using the presented flocculants.

In the next chapter the flocculation process, including flocculation kinetics, for the potato crisps manufacturing effluent, will be analysed in detail to better understand the mechanisms involved.

---

CHAPTER **6**

**Flocculation process analysis**





## 1. INTRODUCTION

In order to investigate how flocs characteristics evolve during the formation process, as well as the flocculation kinetics, the floc characteristics can be monitored *in-situ* using a laser diffraction particle size analyser system (LDS). Normally, when there are no particles in solution, the light beam moves through the sample without changing its direction, however, when there is a particle in the way, the light beam is reflected and/or scattered in general. The scattering angle, the angle between the incident and scattered lights, is inversely correlated with the particles size, while the number of particles in each size class determines the intensity of the scattered light. The information collected regarding the different scattering angles and the intensity, results in the scattering matrix, from which the particle size and size distribution can be collected using the adequate model<sup>231</sup>. Light scattering analysis can be static or dynamic, though static light scattering is more suitable for the analysis of large particles. Breakage of flocs must be taken in consideration when studying flocculation kinetics, as well as the fact that the size distribution is often broader than detected by other techniques<sup>232</sup>.

It is well reported in the literature that LDS is useful to follow flocculation processes, even if most studies refer to model systems<sup>233</sup>. Rasteiro *et al.*<sup>232,233</sup> presented the application of LDS to monitor flocculation in papermaking and to evaluate the flocculation mechanisms in flocculation studies of precipitated calcium carbonate. Using LDS it is possible to perform an evaluation of the flocculants performance, providing information on floc size distribution, average size and aggregate structure described by the fractal dimension ( $d_f$ ) and scattering exponent (SE), in a continuous approach<sup>234</sup>. The fractal dimension provides information regarding the primary particles that fill the space in the nominal volume of an aggregate, being a useful parameter to characterize the density of the flocs<sup>235</sup>. However, for secondary aggregates, the fractal theory cannot be applied and the scattering exponent is used to obtain information regarding the flocs structure, providing information for the larger length scales of the large flocs<sup>234</sup>. Moreover, flocculation can be conducted in controlled hydrodynamic conditions that can easily be reproduced in industrial flocculation processes<sup>236</sup>.

Besides LDS, other techniques can be used to give information about aggregates size and structure, and their evolution with time. Alternative techniques include image analysis and focused beam reflectance microscopy (FBRM)<sup>231</sup>.

Chakraborti *et al.*<sup>237</sup> described a nonintrusive photographic system coupled with digital image processing for *in-situ* monitoring of aggregates formed by the addition of aluminum sulphate to lake water and to a montmorillonite clay suspension. Wågberg *et al.*<sup>238</sup> investigated the use

of image analysis as a very efficient technique to study the flocculation of cellulosic fibres. Image analysis is probably the most direct measuring technique used, and refers to a process which includes image capture and processing in three main steps. Sample preparation and image acquisition is the first stage, including a carefully sample preparation and the capture of images using a digital camera coupled to a microscope. The image acquisition system can be optical, fluorescence, confocal laser scanning or electron microscopy<sup>239–241</sup>. The second step includes the image processing, which includes a set of operations to improve the quality of the images, remove the background light differences and reduce the noise. Then, a labelled or binary image is obtained, through a segmentation process of the image. The further processing includes shape and size operations<sup>242</sup>. Finally, the last step is where the morphological parameters are analysed. Determination of size, shape, composition and structure is then accessed. Size and structure parameters are obtained by automatically counting of pixels belonging to each object, while the shape is referred to morphological parameters that describe the object including its circularity, elongation, roundness, compactness or eccentricity<sup>242</sup>. This technique allows to exclude impurities from the analysis in a high level, since the examination is performed for each particle, giving also information about the variability in the structure. However, this methodology works better in large and high contrast particles<sup>243</sup>. Also, the statistical representativeness must always be considered, and, to guarantee this, the technique is usually very time consuming.

FBRM was developed in the early 1990s and is a promising technique for real-time monitoring of critical performance features in large scale processes, and has been widely used in flocculation research. De Clercq *et al.*<sup>244</sup> introduced the FBRM technique for monitoring wastewater treatment systems and compared the performance with other techniques. This work also proved the capability to evaluate the performance of settling tanks. Blanco *et al.*<sup>24</sup> presented a study on monitoring flocculation processes in papermaking and floc properties analysis using FBRM. Thapa *et al.*<sup>245</sup> demonstrated that FBRM could be used to screen the changes in particle population during flocculation of anaerobic digestion with cationic polyelectrolytes. FBRM is a technique based on light scattering and no sampling procedure is needed. The highly focused beam laser is projected into the suspension and moves around at a high speed. When the beam crosses a particles or aggregate, the backward scattering light will be collected by an optical photodiode detector<sup>246</sup>. The particle reflection has a time duration, which is multiplied by the scan speed of the beam, calculating a distance known as the chord length of a particle. In the case of flocculation studies, the large particles are the ones of interest and the mean square weighted chord length distribution must be used<sup>24</sup>. The key

advantages of FBRM over the other techniques are the ability to handle concentrated suspensions and its *in-situ* detection of particle size. However, FBRM is also affected by several factors, including the shape of the particles and the solids concentrations, while the presence of the probe can affect as well the flow conditions<sup>247</sup>. Moreover, FBRM fails to detect the small particles in the system, having difficulty in following the initial flocculation stages<sup>236</sup>.

In this chapter, the flocculation process followed continuously by LDS is described for the first time for a real industrial effluent. Potato crisps manufacturing industry effluent was treated with two cationic polyelectrolytes and twelve anionic polyelectrolytes, being four copolymers and eight hydrophobically modified terpolymers, already presented and characterized in previous chapters. Results regarding size, structure and strength of the flocs were obtained and analysed, and the prevailing flocculation mechanisms are discussed in the light of these results. The effect of the incorporation of hydrophobicity at different contents onto the efficiency of the flocculation process was also studied. Statistical models that allow to correlate flocs size and structure, described by the scattering exponent, with the flocculants characteristics and concentration are also presented. The main objective of this chapter is to identify the most important characteristics of flocculants and find the combination of factors that may be used to better predict the properties of the flocs obtained.



## 2. FLOCCULATION PROCESS MONITORED BY LDS

### 2.1. Experimental

#### 2.1.1. Materials

The flocculation tests were carried out on real oily effluent from potato crisps manufacturing industry, supplied by Adventech Group (Portugal). Health-friendly synthesized cationic and anionic polyelectrolytes, the co- and terpolymers Poly(AAm-MAPTAC), Poly(AAm-Na-AMPS), Poly(AAm-Na-AMPS-EA) and Poly(AAm-Na-AMPS-LMA), fully described, characterized and tested as flocculants in previous chapters, were used for the flocculation experiments. Flocculant solutions were prepared with distilled water at 0.4 wt%. In order to guarantee the effectiveness of the flocculants, the diluted solutions must be prepared every day.

#### 2.1.2. Flocculation tests

LDS was used to monitor the flocculation process in slight turbulent conditions and supplies information about the flocculation kinetics and, simultaneously, on the evolution with time of the floc structure according to previous studies<sup>233,236</sup>. The tests were conducted in a Malvern Masterziser 2000 (Malvern Instruments). Effluent sample of 200-mL was added to 600 mL of distilled water in the equipment beaker, and the pH was maintained at a value of 6 using hydrochloric acid. Dilution was required to ensure an acceptable level of obscuration, which was initially below 80%, to guarantee that during the flocculation process obscuration value was always above 5%, as suggested by Rasteiro *et al.*<sup>233</sup>. The measurements of the initial effluent were carried out at a stirring speed of 2000 rpm. The flocculant was added after the first particle size acquisition of initial effluent at pH 6, as to obtain overall concentrations of the flocculant in the system of 3.3, 6.5 and 13 mg/L, according with the turbidity tests presented previously. Considering that, in most of the turbidity tests performed, the lowest concentration used (13 mg/L) conducted to very high turbidity reductions, thus only this concentration and lower concentrations than this one were selected for these experiments, in order to see considerable differences in floc sizes, and try to understand the presence of different and eventually complementary flocculation mechanisms. Moreover, economic consideration led also to the selection of concentration of 13 mg/L as the basis concentration for the LDS tests. The predetermined amount of flocculant solution was added at once to the effluent. After that, during the entire flocculation process, the flocculation vessel was stirred

mechanically using the sample unit of the Malvern Mastersizer 2000 at a stirring speed of 300 rpm to avoid floc breakage but still guaranteeing that floc sedimentation was not occurring. Different stirring speeds were tested for this step, from 200 to 900 rpm, however 300 rpm was found to be the optimized speed allowing the largest floc size, while ensuring that flocs were successfully circulating in the system (see Figure 6.1). For 200 rpm the flocs were settling in the vessel and could not be pumped homogeneously to the measuring cell. The size of the flocs was measured every 36 sec for a period of 6.6 min. The reported values of the median particle size ( $d(0.5)$ ) represent an average of at least three measurements, provided by the equipment. Error bars are not shown to avoid confused graphs.

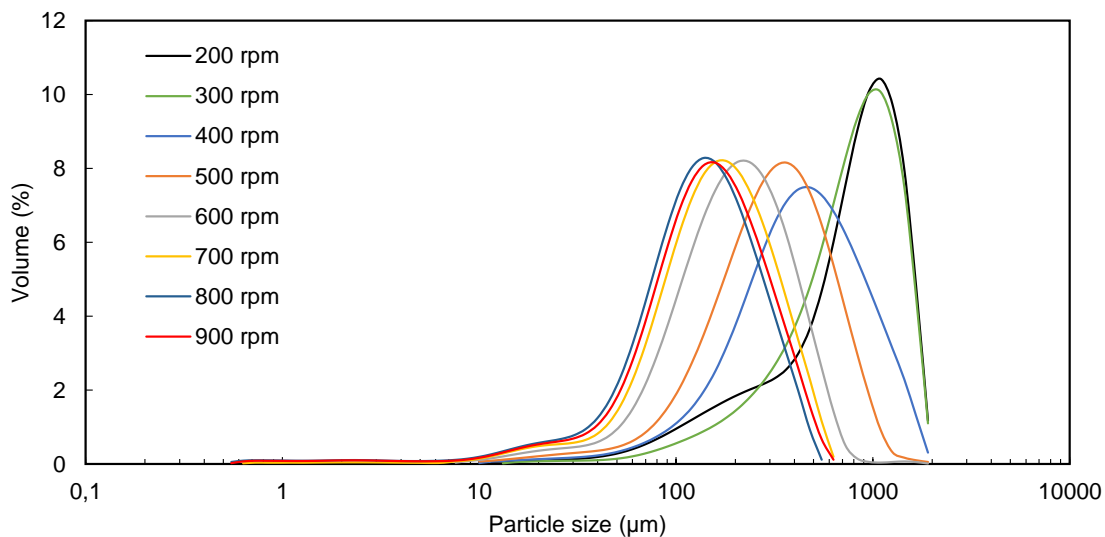


Figure 6.1 Representation of the flocs size distribution for the stirring speed test, using 13 mg/L of the polyelectrolyte 60MC.

Moreover, the scattering exponent of the flocs was calculated at the end of the flocculation process, from the scattering matrix obtained by LDS. This scattering exponent provides information about floc structure and is determined from the scattering pattern, corresponding to scattering at large length scales, considering that we are dealing with large and quite open aggregates<sup>94</sup>. From the scattering matrix obtained by LDS, it is possible to plot, in logarithmic scale, the scattering intensity versus  $q$ , and the slope of the first region of the plot is related to the SE (see Figure 6.2). The complete data is available in Appendix C, Figure C.1 to C.14. The  $q$  value is defined by the following equation (6-1):

$$q = \frac{4\pi n_0}{\lambda_0} \sin(\theta/2) \quad (6-1)$$

where  $n_0$  is the refractive index of the dispersion medium,  $\theta$  is the scattering angle and  $\lambda_0$  is the incident light wavelength. The scattering matrix is exported through the Malvern software to an excel spreadsheet and the data is then processed, offline, for each acquisition, in order to obtain the scattering exponents.

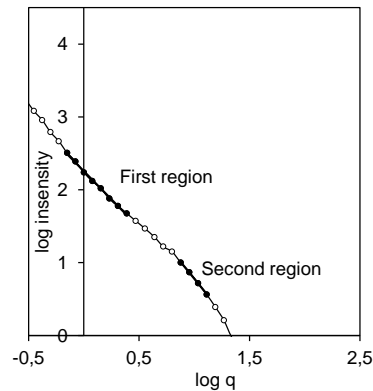


Figure 6.2 Example of the plot of scattering intensity versus  $q$ , with identification of the first and second regions.

## 2.2. Results and discussion

The chosen polyelectrolytes have different characteristics, as proved in previous chapters, which will allow to observe differences in the flocculation process.

An example of the particle size distribution of the initial effluent, the effluent with pH 6 adjusted and the effluent at the end of the flocculation process are shown in Figure 6.3, for treatment with the terpolymer 80A3EC. The particle size distribution evolves from a bimodal to monomodal distribution, being displaced, with time, towards higher particle sizes, as expected. The median size of the particles in the initial effluent, measured by laser diffraction spectroscopy, was 39  $\mu\text{m}$ , while after the pH adjustment it was 22  $\mu\text{m}$  due to the effluent destabilization. Addition of flocculant increased drastically the median size of the particles. Specifically, adding a dosage of 80A3EC around 13 mg/L, increased the median particle size to a value of 514  $\mu\text{m}$ .



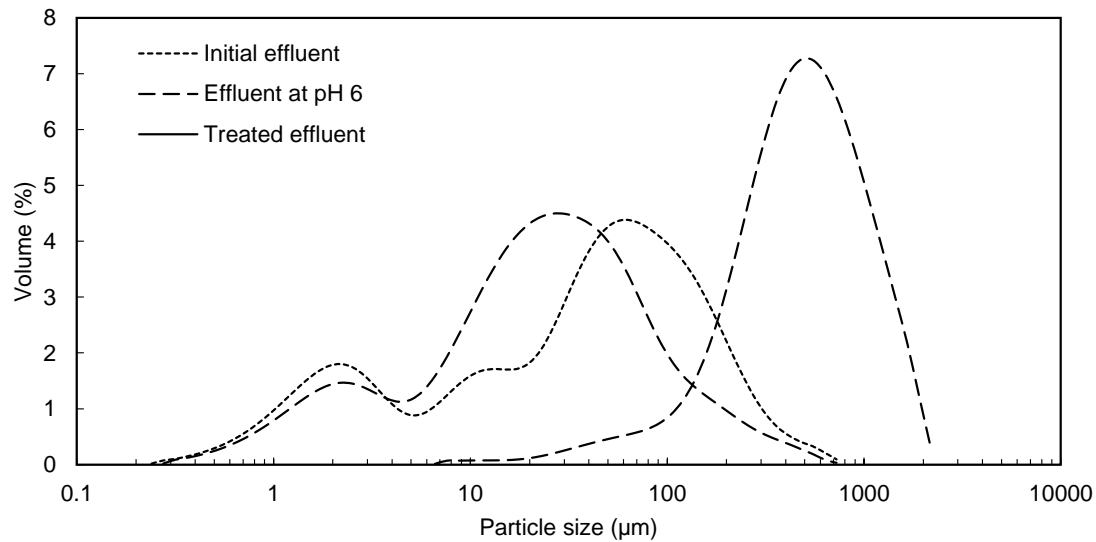


Figure 6.3 Particle size distribution of the initial effluent, pH 6 adjusted effluent and floc size distribution at the end of the flocculation with terpolymer 80A3EC, for the optimum dosage concentration (13 mg/L).

As referred, industrial effluent flocculation was monitored by measuring the aggregate size over time using the LDS technique. Figure 6.4 to Figure 6.7 provide representation of the evolution of average particle size over time, obtained by laser diffraction spectroscopy for the cationic (60MC and 60MP) and anionic (50AC, 80AC, 50AP, 80AP, 50A1EC, 50A3EC, 80A1EC, 80A3EC, 50A1LC, 50A3LC, 80A1LC and 80A3LC) polyelectrolytes tested, for three different polymer concentrations (3.3, 6.5 and 13 mg/L). The trend in these curves is, in general, similar for all the cases tested. The average floc sizes reach their maximum within 2 min after flocculant addition and then stabilize, without any apparent aggregate reformation<sup>234</sup>. Considering the instability of the flocs size over the time of flocculation, for some of the systems tested it is possible to conclude that flocs are considerably large and sensitive to the turbulent environment. Flocs break due to some turbulence but re-aggregate easily, without apparent re-conformation. When equilibrium between breakage and re-aggregation is reached, the floc size stabilizes. The dosage of the polymers tested the let to higher flocs size was always 13 mg/L, the highest concentration used in this study. Using lower concentration always resulted in smaller floc sizes. Additionally, the health-friendly formulation used to synthesize the polyelectrolytes seems not to have influence in the flocs produced (compare 60MC and 60MP, 50AC and 50AP, and 80AC and 80AP).

Use of cationic flocculants lead to significantly larger flocs, likely due to the higher amount of negatively charged effluent particles present at pH 6 (see Figure 5.24 in Section 4.2. of Chapter 5). Moreover, for these cationic flocculants the influence of concentration is more

pronounced, since low dosages will only be able to bridge few particles as the polymers charges are easily used up, bridging must be the main flocculation mechanism for these polymers. Apparently, from Figure 6.4, it is obvious that the synthesis medium (Carnation or Puresyn4), has no influence on the kinetic curves and flocs size obtained, in the case of the cationic polymers, as was expected also due to the similar molecular weight and zeta potential of these polyelectrolytes (see Table 4.3 in Section 2.2. of Chapter 4).

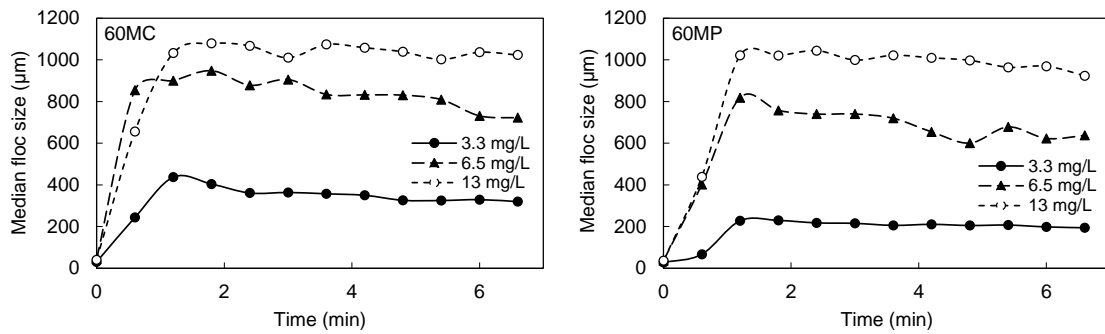


Figure 6.4 Evolution of average particle size ( $d_{50}$ ) over time obtained via LDS for three different flocculant dosages for copolymers 60MC and 60MP.

Regarding the kinetics of the flocculation process induced by the anionic polyelectrolytes (Figure 6.5 to Figure 6.7), lower median flocs size range was obtained, when compared with the flocs obtained using the cationic polyelectrolytes (Figure 6.4). Looking closer into the kinetic plots for the 13 mg/L concentration, it can, in general, be observed a floc size decrease after reaching a maximum size. This can be a consequence of the breakage of flocs by the hydrodynamic forces resulting from mixing, since the particles do appear to re-flocculate following breakage without significant restructuring, which would lead to a much more accentuated decrease of size<sup>236</sup>. However, for lower concentrations of polymer, this behavior is less pronounced and the floc sizes are smaller and more stable over time, confirming, as expected, that larger flocs are more sensitive to hydrodynamic forces.

In most of the cases, the floc size obtained using 3.3 and 6.5 mg/L of flocculant are similar, although always smaller than with 13 mg/L, as mentioned previously. Comparing co- and terpolymers tested, it can be stated that terpolymers seem to form more sensitive flocs, due to the higher instability of the flocs size over time curves (see Figure 6.6 and Figure 6.7), when compared with the corresponding copolymers 50Ac and 80AC (see Figure 6.5).

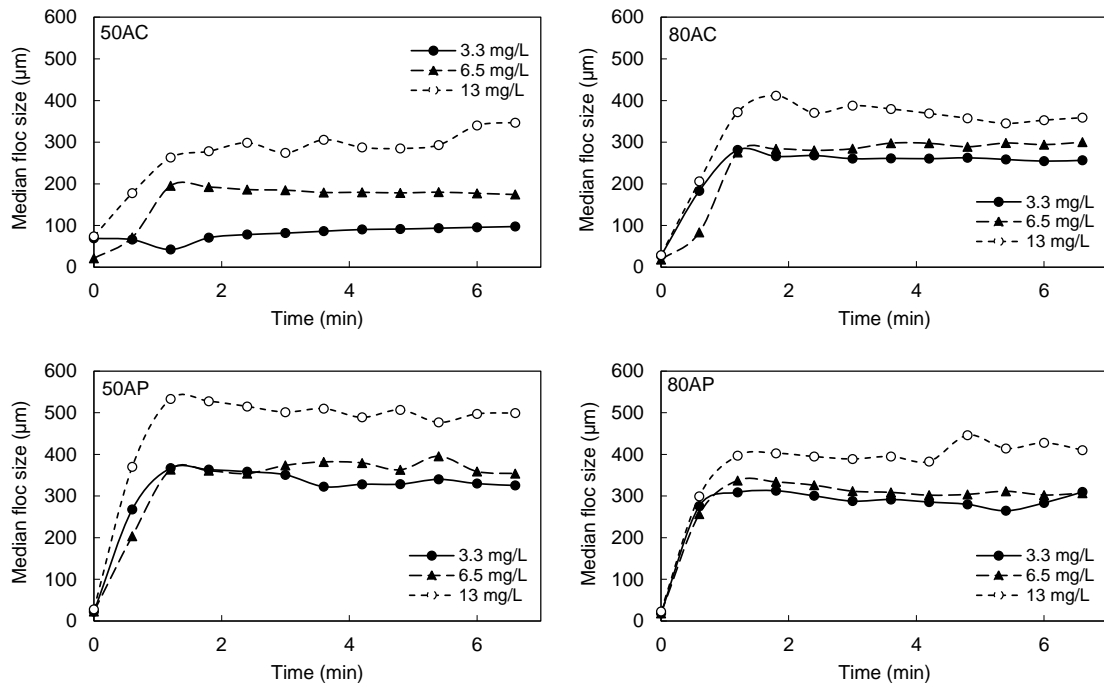


Figure 6.5 Evolution of average particle size ( $d_{50}$ ) over time obtained via LDS for three different flocculant dosages for copolymers 50AC, 80AC, 50AP and 80AP.

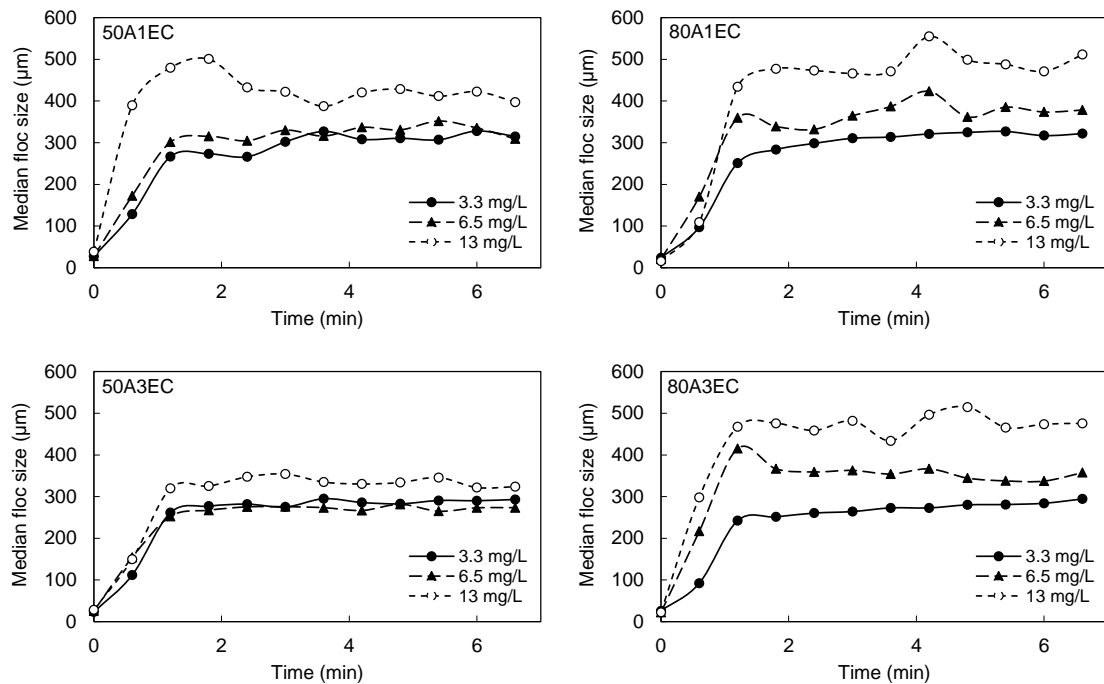


Figure 6.6 Evolution of average particle size ( $d_{50}$ ) over time obtained via LDS for three different flocculant dosages for terpolymers 50A1EC, 50A3EC, 80A1EC and 80A3EC.

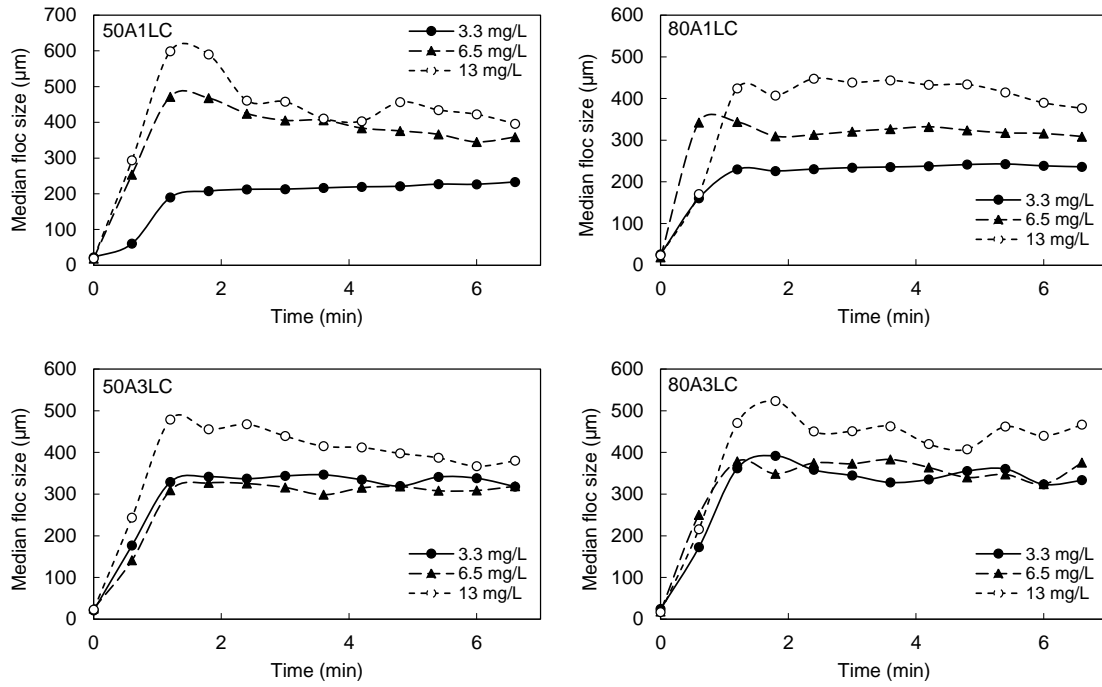


Figure 6.7 Evolution of average particle size ( $d_{50}$ ) over time obtained via LDS for three different flocculant dosages for terpolymers 50A1LC, 50A3LC, 80A1LC and 80A3LC.

The SE profiles, calculated from the scattering matrix obtained by LDS, were plotted (Figure 6.8 to Figure 6.11). For all the cases, the scattering exponent increases rapidly at the beginning of the flocculation process, when a rapid growth of the floc size occurs. Higher SE values mean more compact flocs. As the flocs grow, more particles are integrated within the flocs and the SE value increases correspondingly, until it eventually stabilizes within a few minutes. Although it was not possible to obtain a value of SE for the initial effluent due to the very small size of the particles, a continuous increase of SE is still verified, revealing an increase of flocs compactness during flocculation. In general, and comparing with literature<sup>201,236</sup>, where systems of calcium carbonate were used, values of SE for this specific effluent flocculation are lower, as a consequence of more porous flocs obtained. These results regarding floc structure suggest that the aggregation process takes place mainly by the bridging mechanism, supported by the fast flocculation rate, large flocs obtained and by the open floc structure. For both anionic and cationic flocculants, a higher polymer concentration leads to more porous flocs. Comparing all the polymers, the more porous flocs achieved are the ones obtained with the cationic flocculants 60MC and 60MP, which agrees with the much large size of these flocs (see Figure 6.4), specially for the highest concentration, as already referred previously. This agrees with what has already been referred in literature, larger stabilized flocs, for the same particles, being more porous<sup>234</sup>. It is also obvious that higher charge densities leads to more compact

flocs, with higher SE (compare the 60 series with the 80 series in Figure 6.9 to Figure 6.11). This is the result of a less extended conformation of the polymer chain on the particles surface, when charge density increases<sup>87</sup>. Additionally, the presence of the hydrophobic monomer within the polymer flocculant results in slightly more compact flocs, when compared with the relative copolymers, for the same concentration, more notorious in the case of the terpolymer 80A3EC, even if these flocs are larger than with the corresponding copolymer 80AC (Figure 6.5). This must be a result of a higher affinity of the hydrophobic modified polymer to the effluent particles, especially when the EA monomer is used, as already referred in Chapter 5. It is also interesting that for the hydrophobically modified polymers of the 50 series, polymer concentration seems to have little influence on the flocs structure. Apparently, the influence of the presence of hydrophobicity surpasses all the other influences (charge density and polymer concentration) becoming the main factor conditioning the flocs structure. When charged fraction is higher (80 series), this is no longer true, and there is a cumulative influence of charge density and hydrophobicity, and thus concentration plays again a stronger role in the flocs structure.

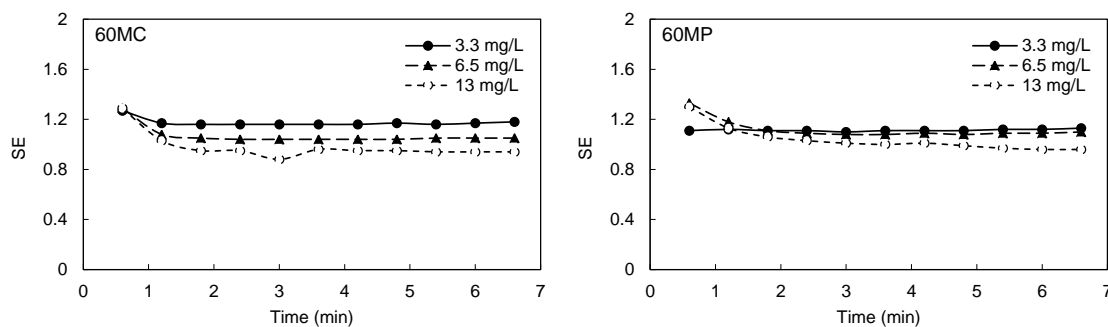


Figure 6.8 Evolution of floc structure (SE) for the cationic copolymers 60MC and 60MP, at different concentrations.

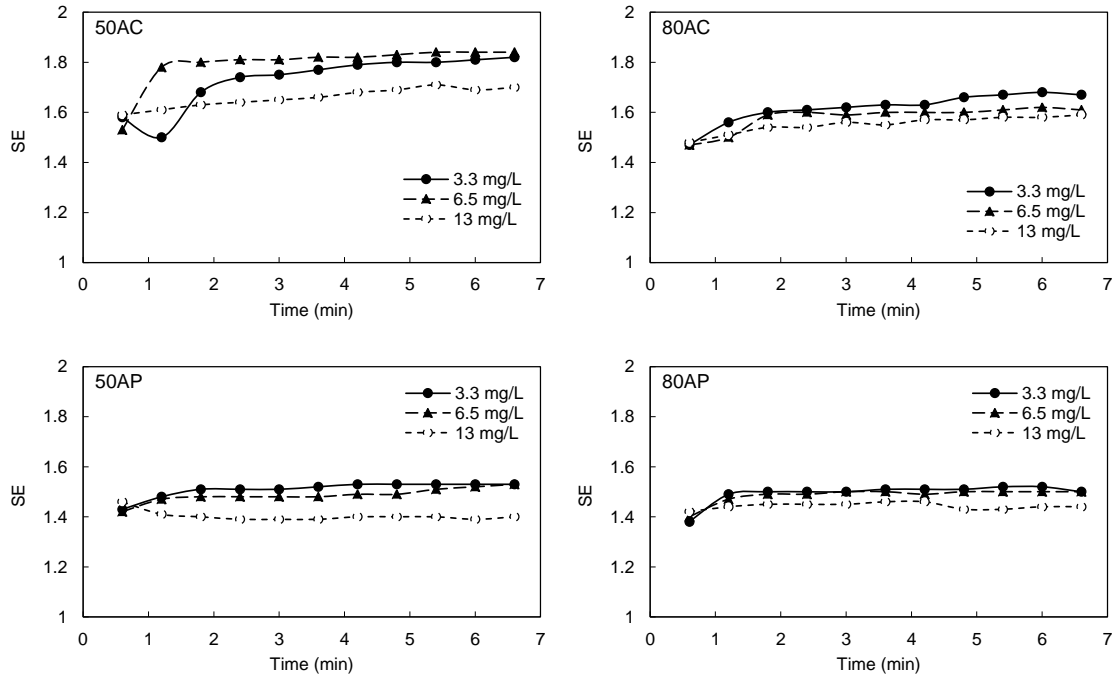


Figure 6.9 Evolution of floc structure (SE) for the anionic copolymers 50AC, 80AC, 50AP and 80AP, at different concentrations.

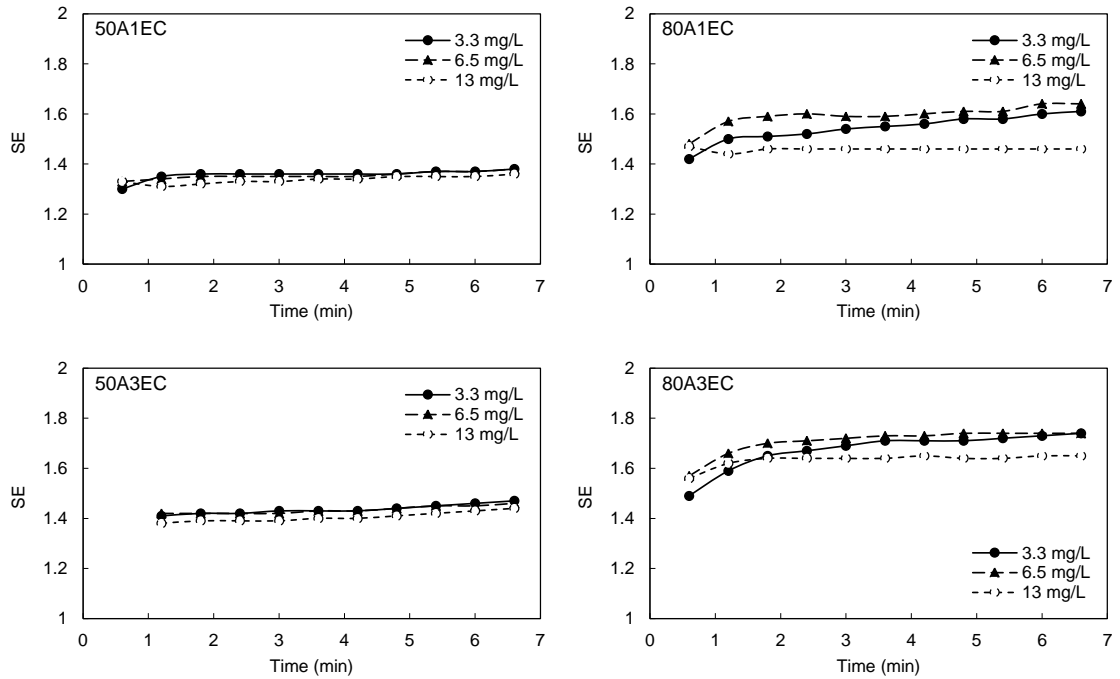


Figure 6.10 Evolution of floc structure (SE) for the anionic terpolymers 50A1EC, 50A3EC, 80A1EC and 80A3EC, at different concentrations.

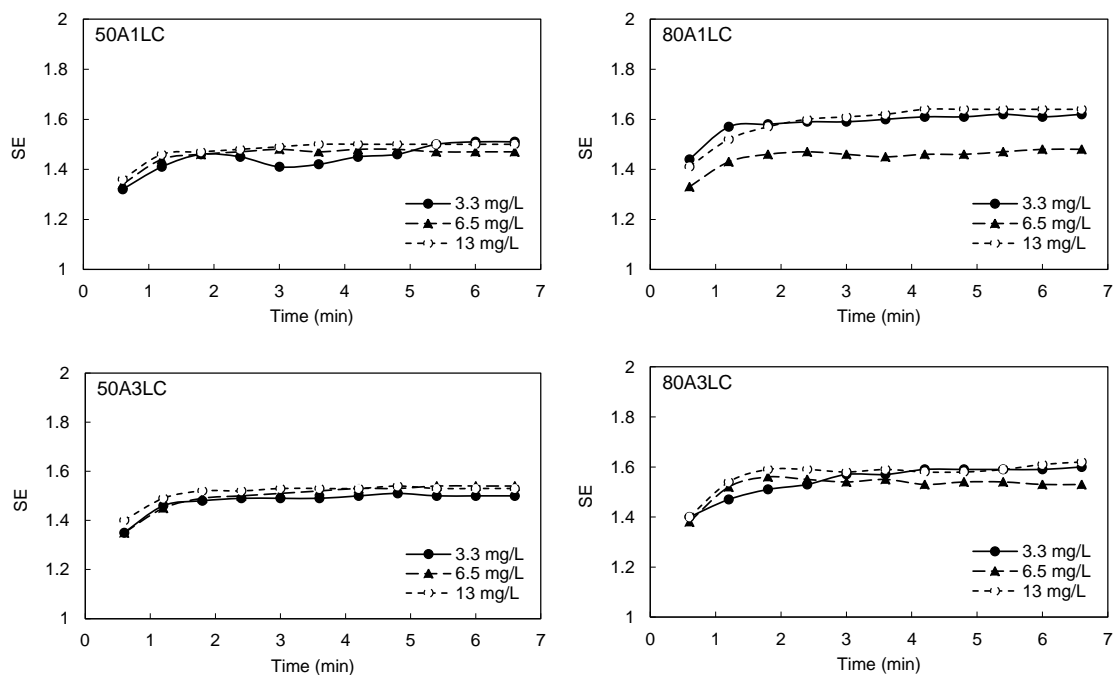


Figure 6.11 Evolution of floc structure (SE) for the anionic terpolymers 50A1LC, 50A3LC, 80A1LC and 80A3LC, at different concentrations.

In general, introducing hydrophobic content in the chain lead to larger and more compact flocs, suggesting an additional interaction promoted by the affinity between the oily effluent and the hydrophobic part of the polyelectrolytes. Moreover, comparing polyelectrolytes in 50 and 80 series with similar hydrophobic content, it is possible to see higher SE values for the 80 series, which means more compact flocs, compatible with the larger number of negative charges in the polymer chain (compare, for instance, 50A3EC and 80A3EC in Figure 6.10). Additionally, flocs obtained with P series polymers (50AP and 80AP) are larger and more porous, in agreement with the higher molecular weight of these polymers.

The SE value after 6 min of flocculation, for each concentration and polymer, was extracted, and are summarized in Table 6.1 and Table 6.2, for cationic and anionic polyelectrolytes tested, respectively, alongside with particle sizes recorded also 6 min after addition of the corresponding flocculant. The 6 min were chosen in order to guarantee that floc size and SE values had already reached a stable value in the curves over time.

Concerning the median floc size values (after 6 min) in Table 6.1 and Table 6.2, for each polymer tested, an increase was observed with the increase of the flocculant concentration, which was expected since more polymer in solution allows to create larger flocs by aggregating more particles, as long as the concentration lies below the optimum concentration. Also,

comparing polyelectrolytes with the same characteristics of hydrophobicity, it is visible a tendency where larger flocs are obtained using flocculants with higher charge density for the lower concentrations (e.g. compare 50AC with 80AC or 50A1EC and 80A1EC). The exception is when comparing 50AP and 80AP, possible due to the much higher molecular weight of 50AP. In fact, even if higher charge density usually leads to less extended conformation of the polymer chain on the particle surface, which could result in smaller flocs, higher charge density polymers also have the ability to aggregate more particles, which can result in larger aggregates, unless the polymer concentration approaches the optimum concentration. Moreover, higher charge density leads, in general, to more compact flocs, for similar polymers, in spite of the larger flocs obtained in this case, confirming the less extended conformation of the higher charged polymers (compare, for instance, 50AC with 80AC or 50A3EC with 80A3EC).

The flocculation kinetics are largely dependent on the flocculant characteristics and on the flocculation mechanism involved<sup>233</sup>. Bridging is likely the main flocculation mechanism, since the polymers charge density varies between 25 and 58 mol% and, for lower charges, more extended conformation of the polymer chain is obtained on the effluent particle surface, due to the lower number of sites available in the polymer for adsorption, leading to large and more open flocs. This is more evident by the analysis of the 50 series of anionic polyelectrolytes. The lowest values of SE (very open flocs), correspond to the larger flocs (see Table 6.2).

Table 6.1 Summary of the experimental value of SE after 6 minutes of flocculation for each cationic polyelectrolyte applied and maximum floc size for each concentration tested.

<b>Polymer designation</b>	<b>Concentration (mg/L)</b>	<b>SE after 6 min</b>	<b>Floc size after 6min (<math>\mu\text{m}</math>)</b>
60MC	3.3	1.17	329
	6.5	1.05	731
	13	0.94	1037
60MP	3.3	1.12	198
	6.5	1.09	623
	13	0.96	969



Table 6.2 Summary of the experimental value of SE after 6 minutes of flocculation for each anionic polyelectrolyte and maximum floc size for each concentration tested.

<b>Polymer designation</b>	<b>Concentration (mg/L)</b>	<b>SE after 6 min</b>	<b>Floc size after 6min (<math>\mu\text{m}</math>)</b>
50AC	3.3	1.81	95
	6.5	1.84	177
	13	1.69	340
80AC	3.3	1.68	254
	6.5	1.62	294
	13	1.58	352
50AP	3.3	1.53	330
	6.5	1.52	359
	13	1.39	497
80AP	3.3	1.52	283
	6.5	1.50	302
	13	1.44	428
50A1EC	3.3	1.37	328
	6.5	1.37	335
	13	1.35	423
50A3EC	3.3	1.46	290
	6.5	1.45	273
	13	1.43	322
80A1EC	3.3	1.60	317
	6.5	1.64	374
	13	1.46	471
80A3EC	3.3	1.73	284
	6.5	1.74	337
	13	1.65	474
50A1LC	3.3	1.51	227
	6.5	1.47	345
	13	1.5	422
50A3LC	3.3	1.5	338
	6.5	1.54	309
	13	1.53	367
80A1LC	3.3	1.61	238
	6.5	1.48	316
	13	1.64	390
80A3LC	3.3	1.59	323
	6.5	1.53	324
	13	1.61	440

In Figure 6.12, median floc size is plotted as a function of hydrophobic content of the polymer flocculant (for polyelectrolytes synthesized using the same organic phase (Carnation)), which is indicated by the molar ratio of hydrophobic monomer in the polyelectrolyte composition. Each polymer series contains a different ratio of hydrophobic monomer within the polymer composition (0%, 1% and 3% as indicated previously in Table 4.4 in Section 3.1.2 of Chapter 4). The hydrophobic content considered is related with the amount of hydrophobic monomer introduced in the feed mixture for polymerization, since the final amount was only qualitatively and not quantitatively assessed. For each polymer series, there is an increase of the maximum floc size with the addition of the lower amount of hydrophobic content (1 mol%) to the initially fully hydrophilic composition, which then stabilizes or decreases when the hydrophobic content is increased to higher concentrations (3 mol%). This suggests that the presence of hydrophobicity is favourable for the flocculation process, though there is an optimum content that improves the floc size and, above that value, the presence of a higher degree of hydrophobicity can be detrimental, in spite of the higher molecular weights obtained. This behaviour was also verified by Lee *et al.*<sup>120</sup>, and can be attributed, for instance, to a more difficult dissolution of the polymer. The improvement of flocculation performance in the presence of hydrophobically modified polyelectrolytes was already discussed in the literature<sup>115,126</sup>. The affinity between the hydrophobic part of the polymer and the oil droplets in the effluent appears to significantly enhance the treatment efficiency, as observed in the present study.

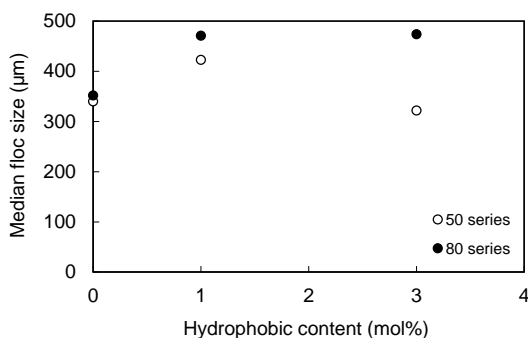


Figure 6.12 Floc size after 6 min, for the higher concentration tested (13 mg/L), as function of hydrophobic content quantified by the ratio (mol%) of monomer 3 in the polyelectrolyte composition.

In the same way, in Figure 6.13, SE after 6 min is plotted as a function of hydrophobic content of the polymer flocculant. It is possible to observe that the polyelectrolytes with higher charged fraction (80 series) and introduction of hydrophobic monomer lead to more

compact flocs, presenting higher SE values. This can be explained by the higher number of charges available to interact with the impurity particles in the oily effluent, as well as by the presence of hydrophobicity, which also increases that interaction. Moreover, comparing this plot with the plot in Figure 6.12, a clear decrease in SE values with the increase of median floc can be observed. This tendency indicates that larger flocs are more open, while smaller flocs are more compact, as previously mentioned.

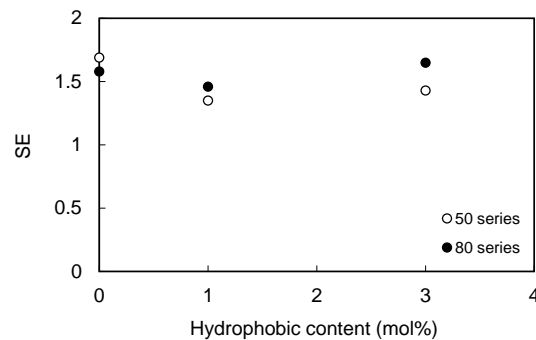


Figure 6.13 SE after 6 min, for the higher concentration tested (13 mg/L), as function of hydrophobic content quantified by the ratio (mol%) of monomer 3 in the polyelectrolyte composition.

In summary, it is possible to state that the LDS technique allows to differentiate the performance of the different polyelectrolytes in the flocculation of the selected effluent, be it at the level of the flocs size, flocs structure or flocculation kinetics. Therefore, this make LDS a very useful tool to pre-screen polymers for a specific application, in relation with effluents treatment processes, taking in to consideration the final target: to obtain large flocs or rather to obtain more compact flocs, or still to reach very fast flocculation kinetics, as a function of the final process envisaged (filtration, sedimentation, etc.).

### 3. EXPERIMENTAL DESIGN METHODOLOGY

#### 3.1. Methods

Ordinary least squares (OLS) regression is a method used in the analysis of linear and non-linear relations between a response variable and one or more predictor variables. OLS regression will compute the values of the model parameters that provide the best fit of the observations, in the least squares sense<sup>248</sup>. Partial least squares (PLS) regression is a statistical technique that correlates response and predictor variables through a linear multivariate model. PLS is able to deal with highly collinear predictor variables, as well as with noisy or incomplete data from both variables. PLS finds the combination of predictors, latent variables, which present maximum covariance with the response<sup>249</sup>. JMP was the program used for both regressions<sup>250</sup>.

#### 3.2. Results and discussion

In the present study, five predictor variables were considered: charged fraction, hydrophobic content, number of methylene groups in the hydrophobic aliphatic chain (Nr of carbons in hydrophobic chain), hydrodynamic diameter (Rh) and concentration. Molecular weight was not considered, since there is a linear correlation between the molecular weight values and the hydrodynamic diameter values (see Appendix C, Figure C.15), thus there is no need to overload the model input, as suggested by good practices. The response variables are the scattering exponent (SE) and median floc size after 6 min of flocculation (d0.5). A combination of variables was applied in each case studied. OLS methodology was the first approach used for all the models. However in cases where the OLS estimation face collinearity problems, PLS regression was used to stabilise the estimates.

Table 6.3 summarizes the experimental values used. The main goal of this study is to identify the most important variables and evaluate how they influence the final characteristics of the produced flocs. Only anionic flocculants were considered, since a little number of data was obtained for cationic flocculants in the flocculation process monitoring (see Section 2.2. of the present Chapter). The hydrophobic content considered (1 or 3 mol%) was related with the amount of hydrophobic monomer introduced in the feed mixture for polymerization, as referred previously. Different cases studies were analysed considering different sets of polymers, to better evaluate the effect of different parameters such as charge density,

hydrophobicity, among others. In the last case studies (cases 5-8) all polymers considered were applied to the model simultaneously.

Table 6.3 Summary of the experimental values used for the experimental design methodology.

Polymer designation	Hydrophobic content (%mol)	Nr of carbons in hydrophobic chain	Charged fraction (%wt)	Rh (nm)	Concentration (mg/L)	SE	d0.5
50AC	0		41.5	67	3.3	1.81	95
50AC	0		41.5	67	6.5	1.84	177
50AC	0		41.5	67	13	1.69	340
80AC	0		62.9	72	3.3	1.68	254
80AC	0		62.9	72	6.5	1.62	294
80AC	0		62.9	72	13	1.58	352
50AP	0		41.9	265	3.3	1.53	330
50AP	0		41.9	265	6.5	1.52	359
50AP	0		41.9	265	13	1.39	497
80AP	0		68.1	147	3.3	1.52	283
80AP	0		68.1	147	6.5	1.5	302
80AP	0		68.1	147	13	1.44	428
50A1EC	1	2	39.5	70	3.3	1.37	328
50A1EC	1	2	39.5	70	6.5	1.37	335
50A1EC	1	2	39.5	70	13	1.35	423
50A3EC	3	2	39.7	282	3.3	1.46	290
50A3EC	3	2	39.7	282	6.5	1.45	273
50A3EC	3	2	39.7	282	13	1.43	322
80A1EC	1	2	62.2	143	3.3	1.6	317
80A1EC	1	2	62.2	143	6.5	1.64	374
80A1EC	1	2	62.2	143	13	1.46	471
80A3EC	3	2	61.6	206	3.3	1.73	284
80A3EC	3	2	61.6	206	6.5	1.74	337
80A3EC	3	2	61.6	206	13	1.65	474
50A1LC	1	12	41	129	3.3	1.51	227
50A1LC	1	12	41	129	6.5	1.47	345
50A1LC	1	12	41	129	13	1.5	422

Table 6.3 (Contd.)

Polymer designa-tion	Hydrophobic content (%mol)	Nr of carbons in hydrophobic chain	Charged fraction (%wt)	Rh (nm)	Concentration (mg/L)	SE	d0.5
50A3LC	3	12	39	209	3.3	1.5	338
50A3LC	3	12	39	209	6.5	1.54	309
50A3LC	3	12	39	209	13	1.53	367
80A1LC	1	12	57	174	3.3	1.61	238
80A1LC	1	12	57	174	6.5	1.48	316
80A1LC	1	12	57	174	13	1.64	390
80A3LC	3	12	63	124	3.3	1.59	323
80A3LC	3	12	63	124	6.5	1.53	324
80A3LC	3	12	63	124	13	1.61	440

### 3.2.1. Case 1: charged fraction, hydrodynamic diameter and concentration as predictor variables and SE as response variable, using OLS regression for copolymers

Table 6.4 presents the summary of the effects. The *p-value* reflects the significance of the effect. The lower the *p-value*, the more significant the effect is. A *p-value* below 0.01 (the significant level) is considered to be significant. *LogWorth* is defined as  $-\log_{10}(p\text{-value})$ . This transformation adjusts *p-values* to provide an appropriate scale. A value that exceeds 2 is considered to be highly significant (it corresponds to a  $p\text{-value} < 0.01$ ). The bar graph shows the *LogWorth* values and has a blue reference line at 2. Hydrodynamic diameter is the most important factor in this case, followed by charged fraction and concentration.

Table 6.4 Effect summary table for case 1.

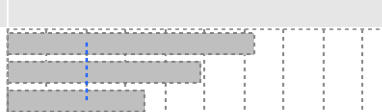
Source	LogWorth		PValue
Rh (nm)	6,257		0,00000
Charged fraction (%wt)	4,918		0,00001
Concentration (mg/L)	3,484		0,00033

Table 6.5 shows the summary of fit report. *RSquare* estimates the proportion of variation in the dependent variable that is explained by the estimated regression model. An *RSquare* closer to 1 indicates a better fit to the data. An *RSquare* near 0 indicates that the model is not capable

to explain the variation of the response. For this specific case, *RSquare* is about 0.97, suggesting a good fitting ability. *RSquare Adj* is the *RSquare* adjusted for the number of parameters in the model. *Root Mean Square Error* estimates the standard deviation of the random error. This quantity is the square root of the *Mean Square for Error*, available in the analysis of variance report (Table 6.6). *Mean of response* shows the overall mean of the response values and *Observations* gives the number of observations used in the model.

Table 6.5 Summary of fit report for case 1.

RSquare	0,971505
RSquare Adj	0,960819
Root Mean Square Error	0,0276
Mean of Response	1,593333
Observations (or Sum Wgts)	12

Table 6.6 is the analysis of variance report. *Source* lists the three sources of variation: *Model*, *Error*, and *C. Total* (corrected total). *DF* gives the associated degrees of freedom for each source of variation. In *C. Total*, *DF* is always the number of observations less one. Then, the *DF* value in *C. Total* is partitioned into degrees of freedom for the *Model* and *Error*. The *Model* degrees of freedom is the number of parameters (other than the intercept) used to fit the model, and *The Error* degrees is the difference between the *DF* in *C. Total* and the *DF* in *Model*. *Sum of Squares* gives the associated sum of squares for each source of variation. The *Sum of Squares* in *C. Total* is the sum of the squared differences between the response values and the sample mean. It represents the total variation in the response values that are expected to be explained. The *Sum of Squares* in *Error* is the sum of the squared differences between the fitted values and the actual values. It represents the variability that remains unexplained by the fitted model. The *Sum of Squares* in *Model* is the difference between *Sum of Squares* in *C. Total* and *Sum of Squares* in *Error*. It represents the variability explained by the model. *Mean Square* is the sum of squares divided by its corresponding *DF*. *F Ratio* shows the model mean square divided by the error mean square. The *F Ratio* is the model mean square divided by the error mean square, and represents the test statistic used to decide whether the model as a whole has statistically significant predictive capability. *Prob>F* gives the *p-value* for the test, which indicates a statistically significant model, since the value is below 0.01.

Table 6.6 Analysis of variance report for case 1.

Source	DF	Sum of Squares	Mean Square	F Ratio
Model	3	0,20777252	0,069258	90,9168
Error	8	0,00609414	0,000762	<b>Prob &gt; F</b>
C. Total	11	0,21386667		<,0001 *

The parameter estimates report shows the estimates of the model parameters (Table 6.7). *Estimate* gives the parameter estimates for each term. These are the estimates of the model coefficients. *Std Error* represents the standard deviation of the estimated coefficients. *t Ratio* tests whether the true value of the parameter is zero. It corresponds to the *Estimate* value divided by the *Std Error*, which tells us how large the coefficient is relative to its estimation uncertainty. If the uncertainty is large, then its *t Ratio* will be smaller. *Prob> |t|* lists the *p-value* for the test where the true parameter value is zero, against the two-sided alternative that it is not. *VIF* presents the variance inflation factor for each term in the model. High *VIFs* indicate a collinearity issue among the terms in the model. This value should be inferior to 5. The *VIFs* values obtained in this case indicate no collinearity issues, suggesting that the regression method used is suitable for describing the experimental data.

Table 6.7 Parameter estimates report for case 1.

Term	Estimate	Std Error	t Ratio	Prob> t	VIF
Intercept	2,24141	0,046593	48,11	<,0001 *	.
Charged fraction (%wt)	-0,006589	0,000691	-9,54	<,0001 *	1,0904748
Rh (nm)	-0,001489	0,000104	-14,32	<,0001 *	1,0904748
Concentration (mg/L)	-0,011819	0,001974	-5,99	0,0003 *	1

The prediction profiler plots give information about the model tendency (Figure 6.14). It is possible to see how the response varies when changing settings of individual factors, set desirability goals for the responses, find optimal settings for factors assess the importance of factors relative to model predictions in a way that is independent of the model and simulate response distribution based on specified distributions for both predictors and responses. The purpose of the desirability function methodology is to find operating conditions that ensure compliance with the criteria of all the involved responses and, at the same time, to provide the best value of compromise in the desirable joint response.



Considering the influence of each parameter in the structure of the flocs, SE values decrease with the increase of the hydrodynamic diameter and concentration. This result can be explained since when there is higher amount of polymer and the polymer chains are longer, there is more space between bridged particles, conducting to more open flocs (lower SE). On the other hand, the influence of charged fraction on SE values is opposite of what was to be expected. It was expected that higher charge density conducted to more compact flocs (higher SE), due to the higher number of regions able to adsorb the effluent particles. However, since hydrodynamic diameter increases with charge density, this can contradict the expected effect of charge density on flocs compactness.

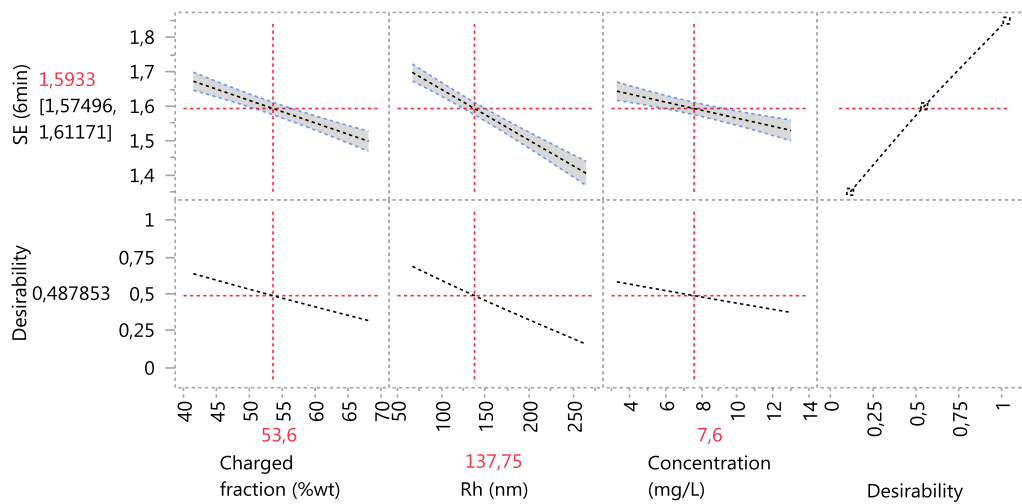


Figure 6.14 Prediction profiler plots for case 1.

Figure 6.15 shows an actual by predicted plot, which plots the observed values of response against the predicted values of response. This plot is the leverage plot for the whole model. It is possible to infer if the model is significant, if the confidence curves cross the horizontal line at the mean of the response. The line solid red is the fit and the confidence bands are shown as dashed red curves. It is possible to verify that all the observations lay within the prediction intervals, confirming the stability and accuracy of the model developed for SE for the copolymers.

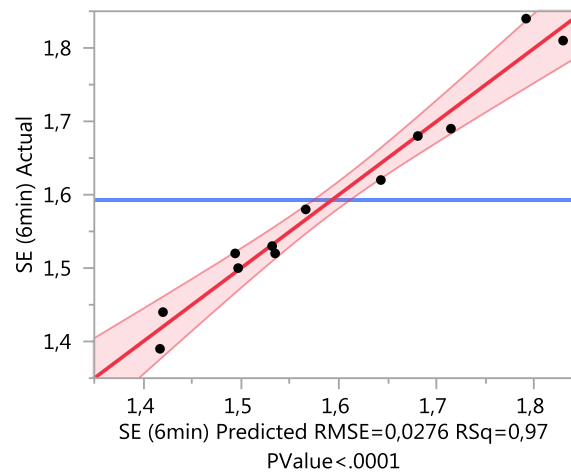


Figure 6.15 Actual versus predicted plot for case 1.

### 3.2.2. Case 2: charged fraction, hydrodynamic diameter and concentration as predictor variables and $d_{0.5}$ as response variable, using OLS regression for copolymers

For this case, considering the effect summary table (Table 6.8), the variables with the highest positive contribution to flocs size are concentration and hydrodynamic diameter but the influence of charged fraction must not be neglected.

Table 6.8 Effect summary table for case 2.

Source	LogWorth		PValue
Concentration (mg/L)	3,848		0,00014
Rh (nm)	3,733		0,00018
Charged fraction (%wt)	1,788		0,01631

Table 6.9 shows the summary of the fit report for this case. *RSquare* is about 0.92, indicating also a good fitting ability.

Table 6.9 Summary of fit report for case 2.

RSquare	0,918178
RSquare Adj	0,887495
Root Mean Square Error	35,38909
Mean of Response	309,25
Observations (or Sum Wgts)	12

Table 6.10 is the analysis of variance report and the  $Prob>F$  value is below 0.01, which suggests a statistically significant model.

Table 6.10 Analysis of variance for case 2.

Source	DF	Sum of Squares	Mean Square	F Ratio
Model	3	112431,15	37477,0	29,9245
Error	8	10019,10	1252,4	<b>Prob &gt; F</b>
C. Total	11	122450,25		0,0001 *

The parameter estimates report (Table 6.11) shows the  $VIF$ s values obtained for this case, which are always below 5, indicating no collinearity issues and suggesting that the regression method used is suitable for this model.

Table 6.11 Parameter estimates for case 2.

Term	Estimate	Std Error	t Ratio	Prob> t	VIF
Intercept	-84,59951	59,7414	-1,42	0,1945	.
Charged fraction (%wt)	2,6843108	0,885906	3,03	0,0163 *	1,0904748
Rh (nm)	0,8689676	0,133334	6,52	0,0002 *	1,0904748
Concentration (mg/L)	17,14081	2,531411	6,77	0,0001 *	1

Figure 6.16 shows the prediction profiler for the present case, comprising the influence of each parameter in the size of the flocs. Specifically, the median floc size increase with the increase of the charged fraction, hydrodynamic diameter and concentration, resulting from the superior number of attachment regions in the polymer chain to adsorb particles, leading to larger flocs. This agrees with the increase of SE with charged fraction, discussed in the previous case, since larger flocs usually correspond to more porous flocs<sup>234</sup>.

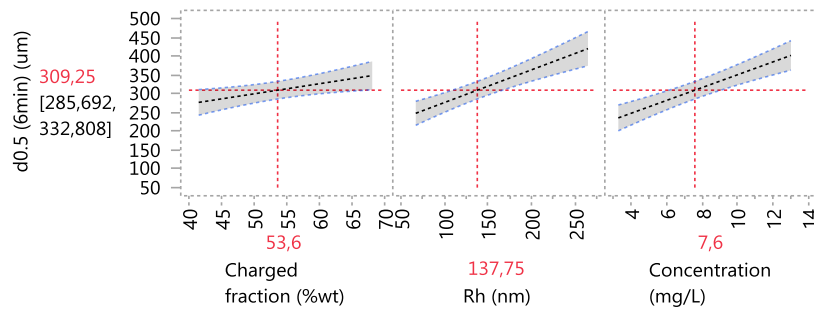


Figure 6.16 Prediction profiler for case 2.

Figure 6.17 plots the actual response against the predicted response for this case. The plot indicates that the model describes the observations quite well. Furthermore, most of the observations are inside or very close to the confidence levels.

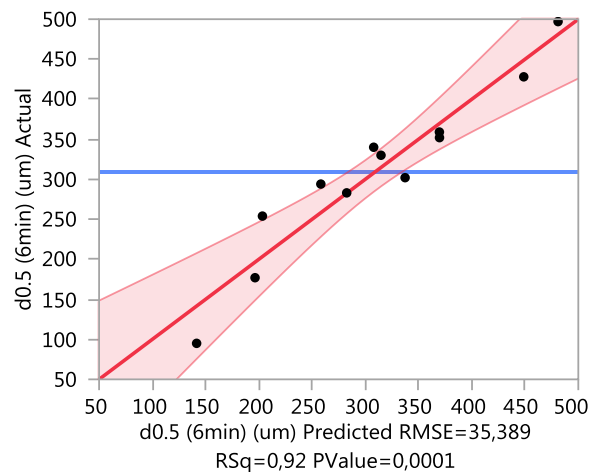


Figure 6.17 Actual versus predicted plot for case 2.

### 3.2.3. Case 3: hydrophobic content, number of carbons in hydrophobic chain, charged fraction, hydrodynamic diameter and concentration as predictor variables and SE as response variable, using OLS regression for terpolymers

For this case, according with the effect summary table (Table 6.12), obviously charged fraction is the factor having higher contribution to the response, followed by hydrodynamic diameter, number of methylene groups in the hydrophobic chain, and the interaction between charged fraction and hydrodynamic diameter, and between number of methylene groups in the hydrophobic aliphatic chain and charged fraction. Still, as in the previous cases, the two main

parameters influencing the response are charge fraction and hydrodynamic diameter. For this specific case, charged fraction seems to have more influence than hydrodynamic diameter, in contrast with the last two cases (for copolymers), perhaps due to the more evident superior performance of the 50 series, when compared with the 80 series, for the terpolymers tested for this effluent (see Figure 5.31 and Figure 5.32 in Section 4.3. of Chapter 5).

Table 6.12 Effect summary for case 3.

Source	LogWorth		PValue
Charged fraction (%wt)	6,105		0,00000
Rh (nm)	2,663		0,00217
Nr of carbons in hydrophobic chain	1,468		0,03404
Charged fraction (%wt)*Rh (nm)	1,406		0,03928
Nr of carbons in hydrophobic chain*Charged fraction (%wt)	1,316		0,04827

For this specific case, the summary of fit report (Table 6.13) presents a *RSquare* of about 0.81, indicating also good fitting ability.

Table 6.13 Summary of fit for case 3.

RSquare	0,809255
RSquare Adj	0,756271
Root Mean Square Error	0,052705
Mean of Response	1,531667
Observations (or Sum Wgts)	24

Table 6.14 is the analysis of variance report and the *Prob>F* value is below 0.01, which confirms a statistically significant model.

Table 6.14 Analysis of variance for case 3.

Source	DF	Sum of Squares	Mean Square	F Ratio
Model	5	0,21213279	0,042427	15,2734
Error	18	0,05000054	0,002778	<b>Prob &gt; F</b>
C. Total	23	0,26213333		<,0001 *

The parameter estimates report is present in Table 6.15.  $VIF_s$  values obtained in this case are also below 5, indicating no collinearity issues and leading to the conclusion that the model is suitable for this case.

Table 6.15 Parameter estimates for case 3.

Term	Estimate	Std Error	t Ratio	Prob> t	VIF
Intercept	0,9382344	0,08559	10,96	<,0001 *	.
Nr of carbons in hydrophobic chain	0,0052985	0,00231	2,29	0,0340 *	1,1523451
Charged fraction (%wt)	0,0077009	0,001046	7,36	<,0001 *	1,0859821
Rh (nm)	0,0010305	0,000288	3,57	0,0022 *	2,6801474
(Nr of carbons in hydrophobic chain-7)*(Charged fraction (%wt)-50,375)	-0,000462	0,000218	-2,12	0,0483 *	1,1776512
(Charged fraction (%wt)-50,375)*(Rh (nm)-167,125)	5,8761e-5	2,644e-5	2,22	0,0393 *	2,6367067

Figure 6.18 displays the prediction profiler for the current case, showing an increase in SE values with the increase of the charged fraction, hydrodynamic diameter and number of methylene groups in hydrophobic chain. Considering the influence of hydrophobic chain and charged fraction, this indicates that more regions in the polymer chain are able to interact with the effluent particles increasing the compactness of the flocs (higher SE values). On the other hand, and as mentioned in a previous case, the SE values were expected to decrease for higher hydrodynamic diameters, due to the larger space between particles, which should lead to more open flocs. This was not verified in this case, suggesting that the influence of hydrophobic content overlays the influence of hydrodynamic diameter, since the present case just considers terpolymers. In fact, higher hydrodynamic content can lead to higher hydrodynamic diameters (for similar molecular weights) but, on the other hand increases as well the interaction with the oily effluent particles, which may justify the tendencies detected for the SE parameter.

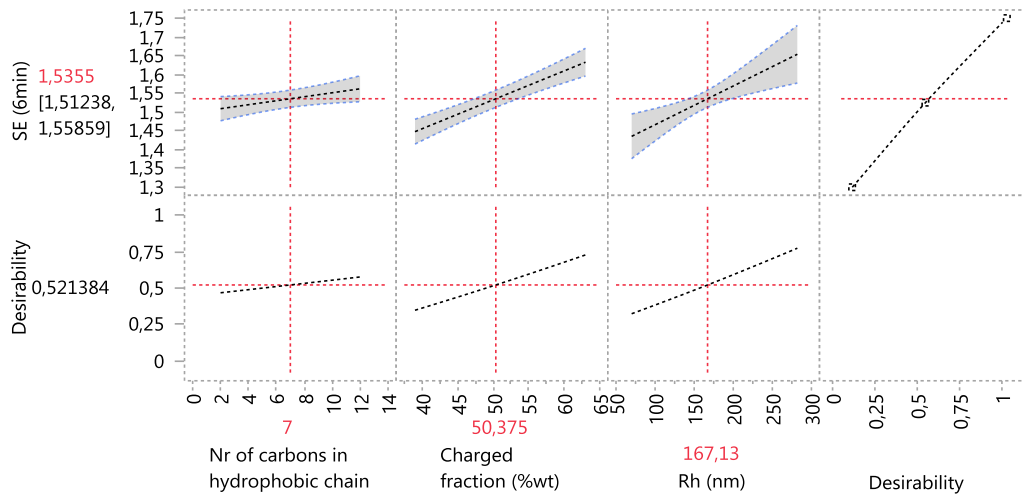


Figure 6.18 Prediction profiler for case 3.

Figure 6.19 plots the actual response against the predicted response for this case. The plot indicates that the model describes quite well for most of the observations. However, a few observations have a larger distance to the fitting, find some of them lay out of the confidence levels.

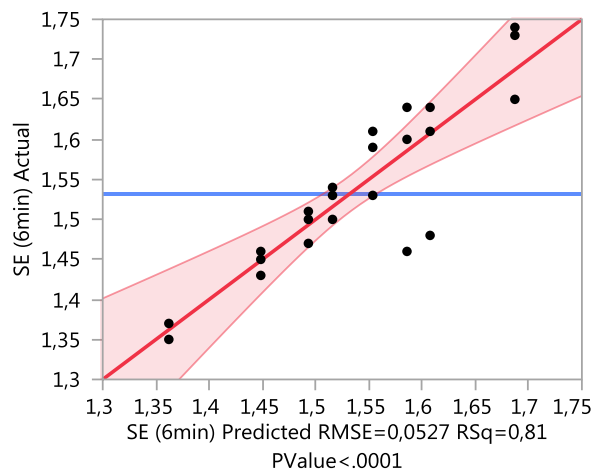


Figure 6.19 Actual versus predicted plot for case 3.

### 3.2.4. Case 4: hydrophobic content, number of carbons in hydrophobic chain, charged fraction, hydrodynamic diameter and concentration as predictor variables and d0.5 as response variable, using OLS regression for terpolymers

For this case, according with the effect summary table (Table 6.16), obviously concentration is the most important factor, however the parameters hydrodynamic diameter, charged fraction and interaction between charged fraction and concentration cannot be neglected.

Table 6.16 Effect summary for case 4.

Source	LogWorth		PValue
Concentration (mg/L)	6,264		0,00000
Rh (nm)	1,430		0,03718
Charged fraction (%wt)*Concentration (mg/L)	1,244		0,05703
Charged fraction (%wt)	1,153		0,07033 ^

For this case, in the summary of fit report (Table 6.17), *RSquare* is about 0.78, indicating a significant fitting capability.

Table 6.17 Summary of fit for case 4.

RSquare	0,782735
RSquare Adj	0,736995
Root Mean Square Error	33,65943
Mean of Response	344,4583
Observations (or Sum Wgts)	24

Table 6.18 is the analysis of variance report and the *Prob>F* value is below 0.01, which indicates a statistically significant model.

Table 6.18 Analysis of variance for case 4.

Source	DF	Sum of Squares	Mean Square	F Ratio
Model	4	77551,765	19387,9	17,1127
Error	19	21526,193	1133,0	<b>Prob &gt; F</b>
C. Total	23	99077,958		<,0001 *



The parameter estimates report (Table 6.19) shows *VIFs* values obtained in this case, which are below 5 indicating no collinearity issues and suggesting that the regression method used is suitable for this model.

Table 6.19 Parameter estimates for case 4.

Term	Estimate	Std Error	t Ratio	Prob> t	VIF
Intercept	229,02485	42,21761	5,42	<,0001 *	.
Charged fraction (%wt)	1,2386714	0,645975	1,92	0,0703	1,0150161
Rh (nm)	-0,253982	0,113346	-2,24	0,0372 *	1,0150161
Concentration (mg/L)	12,563447	1,702492	7,38	<,0001 *	1
(Charged fraction (%wt)-50,375)*(Concentration (mg/L)-7,6)	0,3219009	0,158878	2,03	0,0570	1

Prediction profiler for the current case is shown in Figure 6.20. An increase in median flocs size is verified with the increase of charged fraction and concentration, which agrees with the larger number of attachment regions in the polymer chain to adsorb particles when the both parameters increase, and thus larger flocs were expected. In contrast, the influence of hydrodynamic diameter is the opposite of what was foreseen, since larger flocs were expected when the hydrodynamic diameter is also higher. Once again, this suggests an influence of the hydrophobic content. First, the previous cases showed that SE increased with the increase of the hydrodynamic diameter of the polymer, most probably due to the effect of hydrophobicity, as explained, thus, more compact flocs should correspond to smaller flocs if the other conditions are kept constant, and therefore the tendency detected in Figure 6.20. Additionally, it was shown in Section 2.2. of the present Chapter that there may be an optimum content of hydrophobic monomer that maximize flocculation efficiency, thus larger hydrophobic diameter coming from a higher hydrophobic content may not always lead to larger flocs. As verified in Table 6.16, concentration is the variable with highest contribution to the flocs size, and in the prediction profiler plot, concentration is also the variable that induces stronger variances in the floc size, compared with charged fraction and hydrodynamic diameter, which induce much smaller variations.

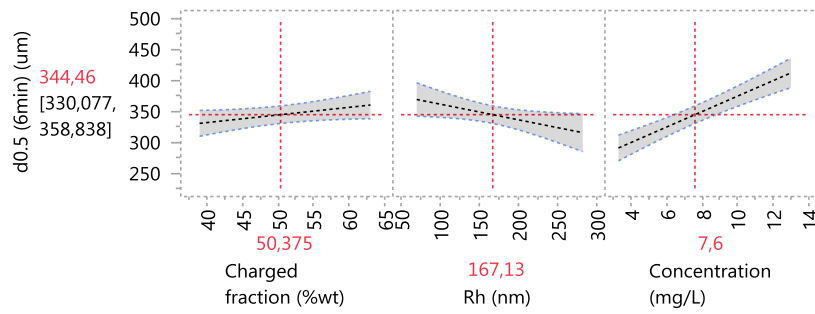


Figure 6.20 Prediction profiler for case 4.

Figure 6.21 shows the actual response against the predicted response for this case. The model describes the observations quite well for most of the observations. However, a higher number of points lay out of confidence levels. It must be stressed that the models considering terpolymers have higher number of observations, making more difficult to have a single model fitting all the points.

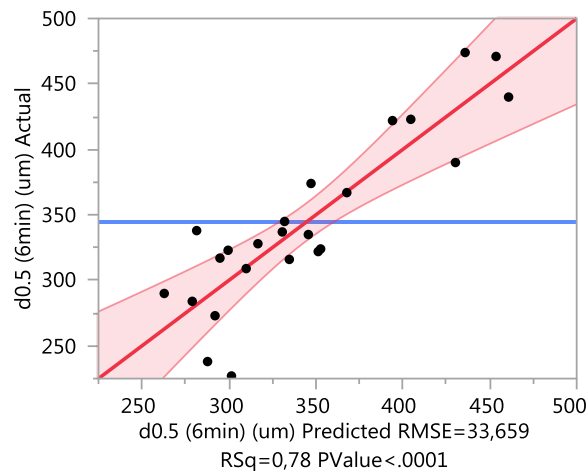


Figure 6.21 Actual versus predicted plot for case 4.

### 3.2.5. Case 5: hydrophobic content, number of carbons in hydrophobic chain, charged fraction, hydrodynamic diameter and concentration as predictor variables and SE as response variable, using OLS regression for co- and terpolymers

It was also decided to investigate the possibility of producing a common model to fit simultaneously all the polymers considered. The cases reported next (case 5 to case 8) correspond to that study. The parameter estimates report (Table 6.20) shows  $VIF_s$  values

obtained in this case, which are above 5, indicating collinearity issues. This model has in consideration a higher number of observations (36) than the previous ones (12 and 24) with more diverse characteristics, thus a more robust methodology must be used to stabilize de estimation.

Table 6.20 Parameter estimates for case 5.

Term	Estimate	Std Error	t Ratio	Prob> t	VIF
Intercept	2,1864793	0,070417	31,05	<,0001 *	.
Hydrophobic content (%mol)	-0,938562	0,079579	-11,79	<,0001 *	179,90641
Nr of carbons in hydrophobic chain	-0,012264	0,012312	-1,00	0,3291	76,288219
Charged fraction (%wt)	-0,005753	0,001054	-5,46	<,0001 *	2,5806974
Rh (nm)	-0,001424	0,000165	-8,63	<,0001 *	2,3944195
Concentration (mg/L)	-0,0111014	0,002453	-4,49	0,0002 *	1,7903226
Hydrophobic content (%mol)*Nr of carbons in hydrophobic chain	0,0082558	0,001704	4,85	<,0001 *	8,4598432
Hydrophobic content (%mol)*Charged fraction (%wt)	0,0108915	0,000898	12,13	<,0001 *	65,654722
Hydrophobic content (%mol)*Rh (nm)	0,001644	0,000185	8,88	<,0001 *	50,198705
Nr of carbons in hydrophobic chain*Charged fraction (%wt)	-0,000447	0,000169	-2,64	0,0143 *	38,657513
Nr of carbons in hydrophobic chain*Rh (nm)	0,0001605	4,826e-5	3,32	0,0028 *	32,078748
Nr of carbons in hydrophobic chain*Concentration (mg/L)	0,0011816	0,000349	3,38	0,0025 *	5,3367819

Still, the influence of polymer characteristics in the SE values was evaluated using the current regression method (Figure 6.22), in order to be compared with the alternative one. Thus, it was observed that when there is no hydrophobic content, that is regarding copolymers only, the same behaviour of Case 1 was observed (Figure 6.14). SE values decrease with the increase of the hydrodynamic diameter and concentration, since high amount of polymer and longer polymer chains lead to more space between bridged particles, conducting to more open flocs (lower SE). Also, the influence of charged fraction is the same as detected in case 1.

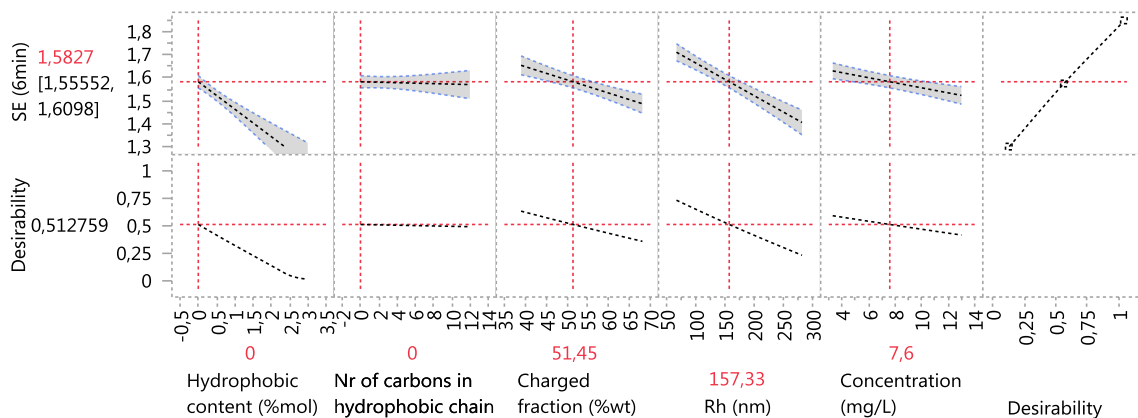


Figure 6.22 Prediction profiler for no hydrophobic content for case 5.

When the hydrophobic content is maximum (Figure 6.23), which is terpolymers with 3 mol% of hydrophobic content, the same behaviour of Case 3 was observed (Figure 6.18). SE values increase with the increase of the charged fraction, hydrodynamic diameter and number of methylene groups in hydrophobic chain. Considering the influence of hydrophobic chain and charged fraction, this is due to the increased regions in the polymer chain able to interact with effluent particles, that also increase the compactness of the flocs (higher SE values). The tendency for SE to decrease with higher hydrodynamic diameters was already discussed in case 3, suggesting a strong influence of the hydrophobic content. Concentration demonstrates to have very little influence on the response, which is in accordance with the Case 3, where the regression method excluded this parameter. Also, all the other factors seem to have a stronger influence than presented in Case 3, for these specific terpolymers.

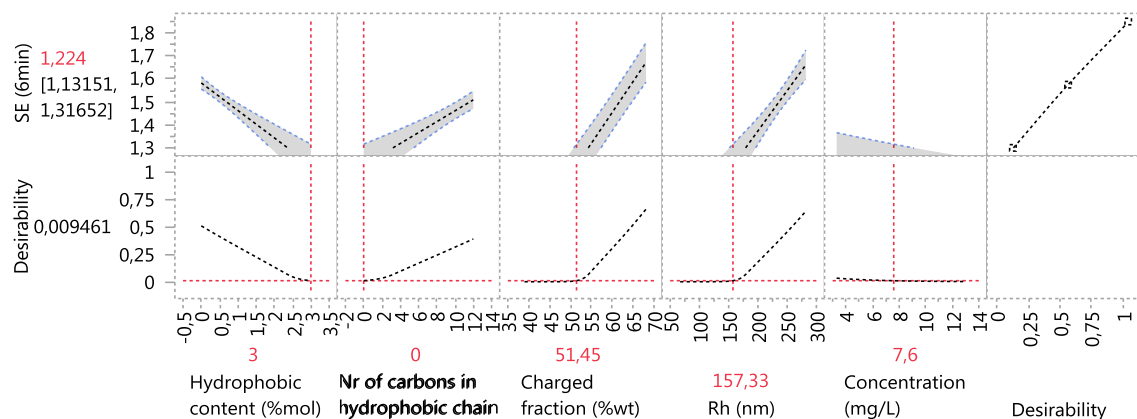


Figure 6.23 Prediction profiler for maximum hydrophobic content (3 mol%) for case 5.

### 3.2.6. Case 6: hydrophobic content, number of carbons in hydrophobic chain, charged fraction, hydrodynamic diameter and concentration as predictor variables and SE as response variable, using PLS regression for co- and terpolymers

The model comparison summary shows a summary of the results obtained for the fitted model (Table 6.21). *Method* shows the type of model fitting algorithm specified in the model launch control panel. In this case the method selected was NIPALS, nonlinear iterative partial least squares. *Method* shows the analysis method specified in the model launch control panel. *Number of rows* shows the number of observations used in the training set. *Number of factors* shows the number of extracted factors or latent variables. In this case the optimal model has eight factors. If the method selected eight factors, it means that improvement was not

achieved with a higher number of factors. This value is related with the minimum Root Mean PRESS statistic, obtained with different numbers of factors. Root Mean PRESS for a specific number of factors is the square root of the average of the PRESS values (prediction sum squares) across all responses. *Percent Variation Explained for Cumulative X* shows the percent of variation in predictor variables that is explained by the model. *Percent Variation Explained for Cumulative Y* shows the percent of variation in response variables that is explained by the model. With the selected factors, the model explains 90% of the response. *Number of VIP > 0.8* shows the number of model effects with *VIP* (variable importance in projection) values greater than 0.8. The *VIP* score is a measure of a variable's importance relative to modelling response variables. In this case, seven variables have *VIP* value above 0.8.

Table 6.21 Model comparison summary for case 6.

Method	Number of rows	Number of factors	Percent Variation Explained for Cumulative X	Percent Variation Explained for Cumulative Y	Number of VIP > 0.8
NIPALS	36	8	73,677277	90,559136	7

The variable importance plot represents the *VIP* values for each predictor variable (Figure 6.24). If a variable has a small coefficient and a small *VIP*, then it is a candidate for deletion from the model. A value of 0.8 is generally considered to be a significant *VIP* and a blue line is drawn on the plot at 0.8. As mentioned before, seven variables have *VIP* values above 0.8. In this case, hydrodynamic diameter, hydrophobic content interacted with charged fraction and number of methylene groups in aliphatic chain interacted with hydrodynamic diameter, seems to be the variables that have greater influence in the response, even if hydrophobic content and charged fraction also have a quite high influence in the model.

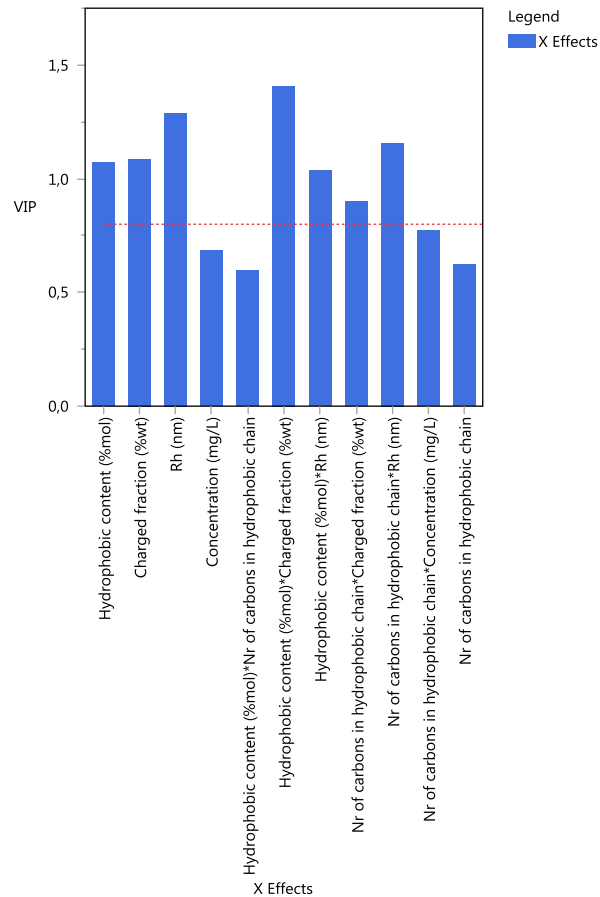


Figure 6.24 Variable importance plot for case 6.

Again, the influence of polymer characteristics in the SE values was evaluated using the current regression method (Figure 6.25). It was observed that when there is no hydrophobic content (copolymers only), the same behaviour of Cases 1 (Figure 6.14) and 5 (Figure 6.22) was observed. SE values decrease with the increase of the hydrodynamic diameter and concentration, since when there is high amount of polymer and the polymer chains are longer, there is more space between bridged particles, conducting to more open flocs (lower SE). Understandably, there is no influence of the number of methylene groups on the response SE.

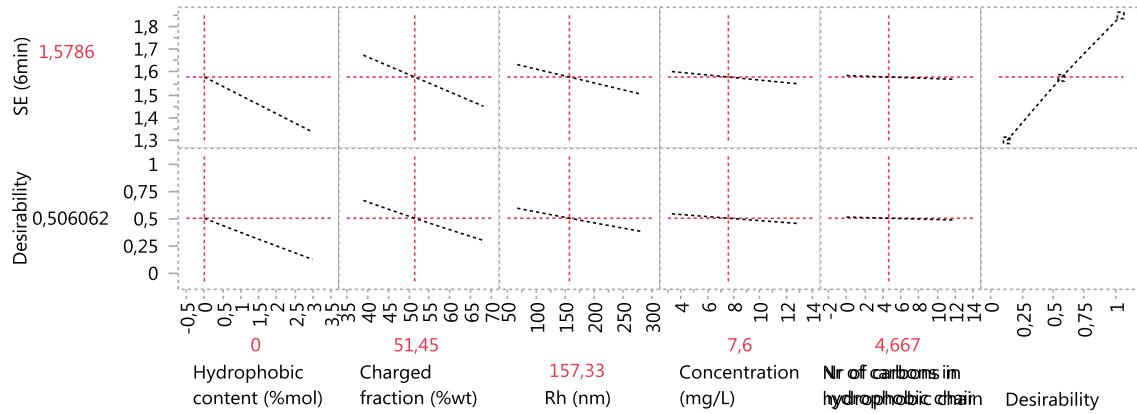


Figure 6.25 Prediction profiler for no hydrophobic content for case 6.

When the hydrophobic content is at a maximum (terpolymers with 3 mol% of hydrophobic content) (Figure 6.26) the same behaviour of Case 3 (Figure 6.18) and 5 (Figure 6.23) was observed. SE values increase with the increase of the charged fraction, hydrodynamic diameter and number of methylene groups in hydrophobic chain. The influence of hydrophobic chain and charged fraction it is due to the increased regions in the polymer chain able to interact with the oily effluent particles, which increase the compactness of the flocs (higher SE values).

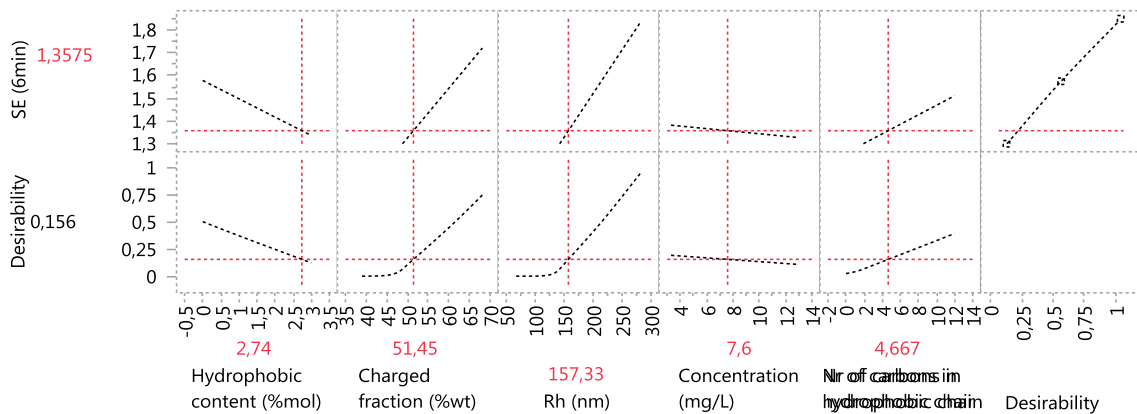


Figure 6.26 Prediction profiler for maximum hydrophobic content (3 mol%), for case 6.

### 3.2.7. Case 7: hydrophobic content, number of carbons in hydrophobic chain, charged fraction, hydrodynamic diameter and concentration as predictor variables and d0.5 as response variable, using OLS regression for co- and terpolymers

The parameter estimates report (Table 6.22) shows *VIFs* values obtained in this case, which are also above 5, indicating collinearity issues and suggesting that a more robust regression method should be used to stabilize de estimation.

Table 6.22 Parameter estimates for case 7.

Term	Estimate	Std Error	t Ratio	Prob> t	VIF
Intercept	-95,66413	50,88818	-1,88	0,0718	.
Hydrophobic content (%mol)	307,96768	57,64038	5,34	<,0001 *	177,87263
Nr of carbons in hydrophobic chain	8,6111817	6,293099	1,37	0,1834	37,558494
Charged fraction (%wt)	2,8635408	0,752168	3,81	0,0008 *	2,476758
Rh (nm)	0,8822614	0,119783	7,37	<,0001 *	2,3762336
Concentration (mg/L)	17,227648	1,95522	8,81	<,0001 *	2,1428571
Hydrophobic content (%mol)*Nr of carbons in hydrophobic chain	-3,241097	1,137315	-2,85	0,0086 *	7,1030239
Hydrophobic content (%mol)*Charged fraction (%wt)	-1,784574	0,650991	-2,74	0,0111 *	65,007226
Hydrophobic content (%mol)*Rh (nm)	-0,874979	0,120871	-7,24	<,0001 *	40,304911
Hydrophobic content (%mol)*Concentration (mg/L)	-2,35381	1,070918	-2,20	0,0374 *	5,6893164
Nr of carbons in hydrophobic chain*Charged fraction (%wt)	-0,204317	0,121907	-1,68	0,1062	37,829777

Still, the influence of polymer characteristics in the median flocs size was evaluated using the current regression method (Figure 6.27), in order to compare the results with the alternative one. Thus, it was observed that when there is no hydrophobic content, that is regarding copolymers only, the same behaviour of Case 2 was observed (Figure 6.16). The median flocs size increase with the increase of the charged fraction, hydrodynamic diameter and concentration, due to a superior number of attachment regions in the polymer chain to adsorb particles, that leads to larger flocs. Obviously, there is no influence of the number of methylene groups.

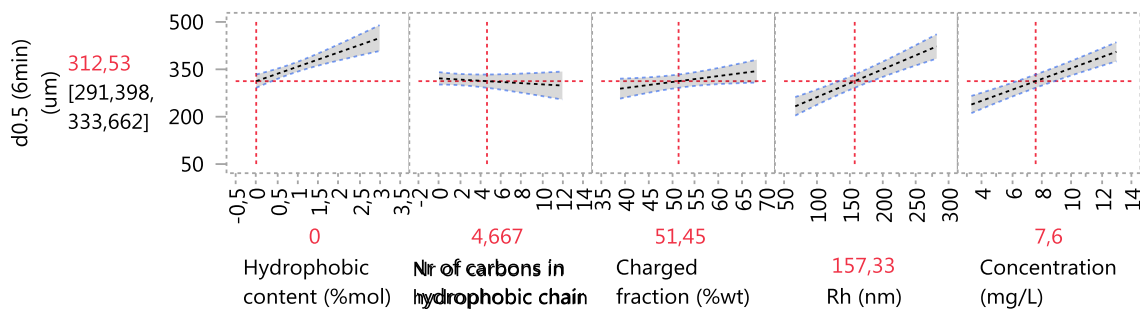


Figure 6.27 Prediction profiler for no hydrophobic content for case 7.



When the hydrophobic content is maximum, meaning terpolymers with 3 mol% of hydrophobic content (Figure 6.28), similar behaviours to Case 4 (Figure 6.20) were observed. An increase in median flocs size is verified with the increase of concentration, due to the superior number of attachment regions in polymer chain to adsorb particles, as concentration increases. The influence of hydrodynamic diameter is the same as obtained in case 4, and was already discussed there. Regarding the charged fraction, the influence is the opposite of what was obtained in case 4, the same happening for the case of the hydrophobic content (Figure 6.27). Once more, this suggests an influence of the hydrophobic content on the flocs morphology. The influence of the number of methylene groups was not considered having large influence in Case 4, however it seems to be significant when polymers with higher hydrophobic content (3 mol%) are considered. Thus, larger number of methylene groups led to smaller flocs, suggesting that there is an ideal length of hydrophobic chain that is beneficial to obtain large flocs and high flocculation efficiency.

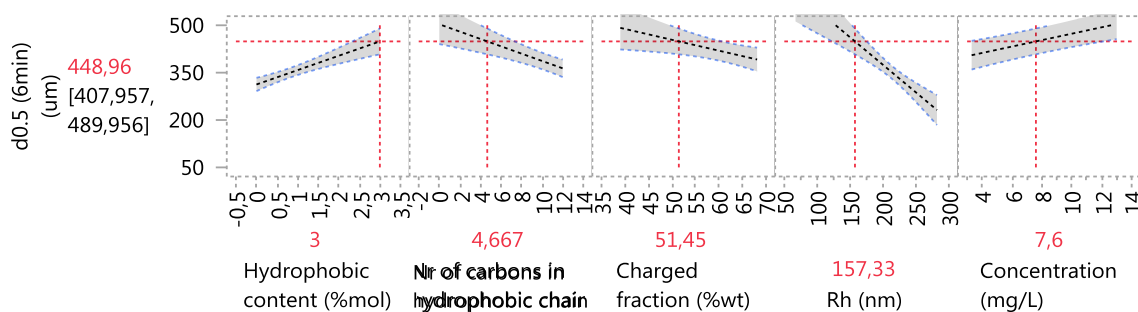


Figure 6.28 Prediction profiler for maximum hydrophobic content (3 mol%), for case 7.

### 3.2.8. Case 8: hydrophobic content, number of carbons in hydrophobic chain, charged fraction, hydrodynamic diameter and concentration as predictor variables and d0.5 as response variable, using PLS regression for co- and terpolymers

The model comparison summary is shown in Table 6.23. *Number of factors* in the present case is 7, however the *Number of VIP > 0.8* is only 2, representing the number of parameters that show a *VIP value* higher than 0.8.

Table 6.23 Model comparison summary for case 8.

Method	Number of rows	Number of factors	Percent Variation Explained for Cumulative X	Percent Variation Explained for Cumulative Y	Number of VIP > 0.8
NIPALS	36	7	73,311882	88,698431	2

Variable importance plot for case 8 is present in Figure 6.29. Concentration and hydrophobic content interacted with hydrodynamic diameter appear to be the variables that have larger influence in the flocs size, even if the hydrodynamic diameter also has a significant influence in the response. Hydrophobic content interacted with the number of carbons, hydrophobic content interacted with concentration and number of carbons interacted with charged fraction have the shortest bars, indicating that they are not much correlated to flocs size.

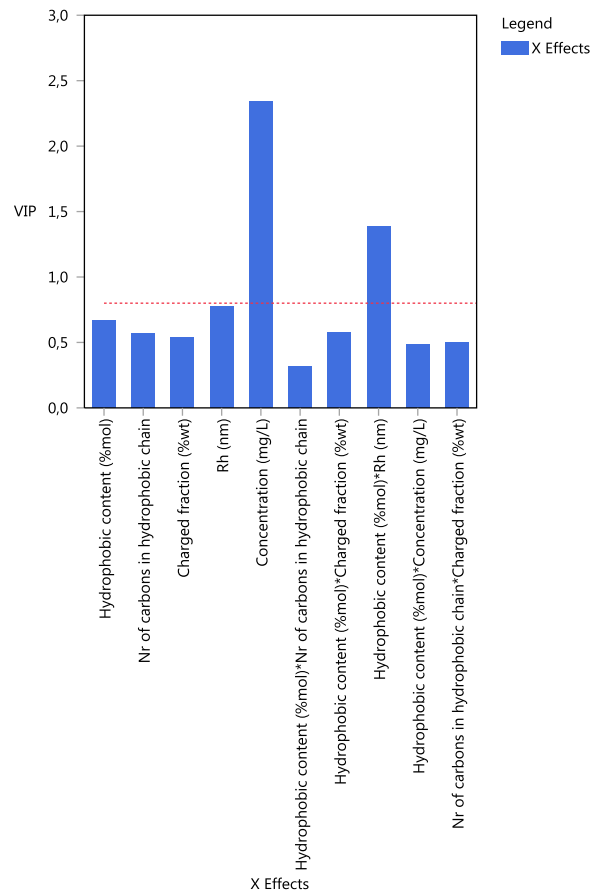


Figure 6.29 Variable importance plot for case 8.

The influence of polymer characteristics in the median flocs size was evaluated using the PLS regression method (Figure 6.30). It was detected that when there is no hydrophobic content

(copolymers only), the same behaviour of Cases 2 (Figure 6.16) and 7 (Figure 6.27) was observed. The median flocs size increase with the increase of the charged fraction, hydrodynamic diameter and concentration, due to a superior number of attachment regions in polymer chain to adsorb particles, that leads to larger flocs. Obviously, there is no influence of the number of methylene groups.

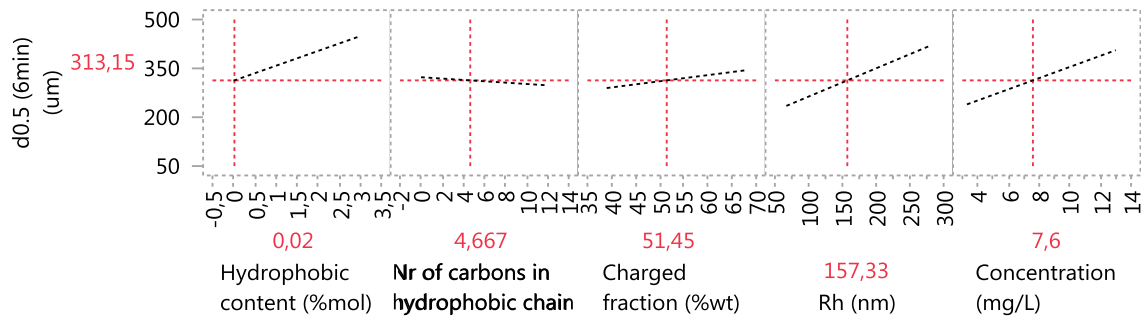


Figure 6.30 Prediction profiler for no hydrophobic content for case 8.

When the hydrophobic content is maximum (terpolymers with 3 mol% of hydrophobic content) (Figure 6.31), similar tendencies to Case 7 were observed (Figure 6.28). An increase in median flocs size is verified with the increase of concentration. Oppositely, the influence of charged fraction and hydrodynamic diameter is the opposite of what was to be expected, since larger flocs were expected when the hydrodynamic diameter and charged fraction are also higher. Once again, this suggests an influence of the hydrophobic content, as was already discussed previously. The influence of the number of methylene groups seems to be stronger when polymer comprises higher hydrophobic content. Thus, larger number of methylene groups led to smaller flocs, suggesting that there is an ideal length of hydrophobic chain that is beneficial to obtain large flocs and high flocculation efficiency.

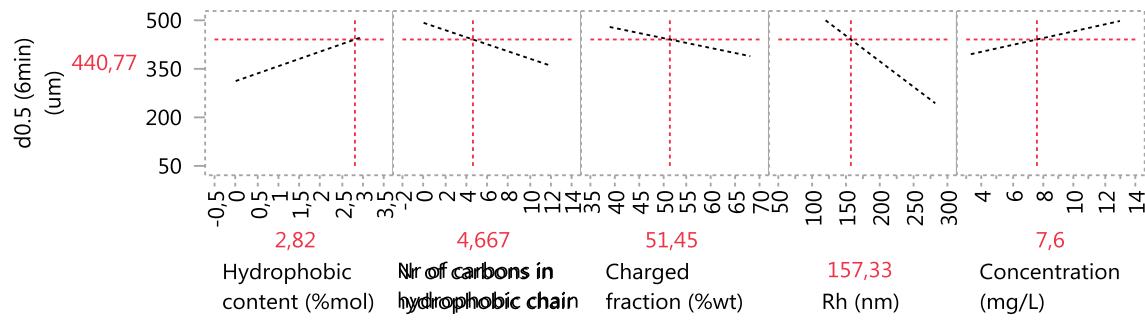


Figure 6.31 Prediction profiler for maximum hydrophobic content (3 mol%), for case 8.

The two methodologies developed (OLS and PLS) led to similar conclusions, however it is not possible to have one single model describing all the co- and terpolymers considered in this study. Separate models including, independently, polyelectrolytes with and without hydrophobicity must be used to have a consistent model describing the different parameters influence on the flocs size and structure. This is predominantly due to the interactions established between oily particles in the effluent and hydrophobic flocculants, which affect the polyelectrolytes performance.

Comparing the influence of the several flocculant parameters on the flocs size and structure, the influence of some variables in the responses, namely charged fraction and hydrodynamic diameter, are different for both sets of polymers, due to the influence of the hydrophobicity, as referred previously, which justifies the fact that it is not possible to have one single predictive model for both co- and terpolymers.



## 4. CONCLUSIONS

The results obtained in this study confirm the feasibility of using the LDS technique to access and understand the flocculation progression in a real industrial oily effluent, and to determine some important floc characteristics in a mild turbulent environment.

Cationic and anionic polyelectrolytes, varying in charge density, molar mass and hydrophobicity were tested in terms of performance in flocculation, revealing to be very promising for the application. The experimental technique used, which was tested for the first time in a real industrial effluent, allowed extracting information on the influence of the polyelectrolytes characteristics on the flocculation process. This can be extremely important in the future, when dealing with the selection/optimization of the right flocculant to treat a specific effluent, as well as the tuning of the operational conditions, minimizing expensive pilot trials. As expected, results show that high molecular weight polyelectrolytes with medium to high charge density induce flocculation by bridging mechanism. Results also demonstrate the influence of increasing flocculant concentration: floc size increases and more porous aggregates are obtained. The experimental design allowed to conclude that polyelectrolytes characteristics proved to be critical for the floc size and structure obtained. Hydrodynamic diameter, charged fraction and concentration are the parameters with greatest influence in the size and structure of flocs obtained with the copolymers, while charged fraction, concentration and hydrophobic content proved to have more effect in the characteristics of the flocs produced using ter-polymers. The effect of the hydrophobic content suggests that the presence of hydrophobicity is favourable for the flocculation process, however there is an optimum hydrophobic content that improves the floc size and above that value the effect is no longer beneficial.

Finally, the analysis conducted showed that it is not possible to have a single model describing all the polyelectrolytes considered in this study. Distinct models comprising independently co- and terpolymers must be employed, in order to have consistent models analysing the polymers' parameters impact on the flocs size and structure. This result is mostly due to the distinct interaction between the effluent oily particles and the hydrophobic flocculants, which affects the polyelectrolytes performance.



---

CHAPTER **7**

**Final remarks**





## 1. FINAL CONCLUSIONS

The present work demonstrated the possibility to develop novel flocculants to treat oily wastewaters from food industries, using health-friendly formulations in their synthesis. It was possible to produce specific products to treat defined wastewaters, through direct flocculation, and using low dosages of flocculant. Besides this, it was also possible to apply in the polymerization process formulations, specifically synthesis media, which are safer for health, replacing the oils traditionally employed in their synthesis.

The development of the health-friendly formulations for the production of well-known polyelectrolytes through inverse-emulsion polymerization was performed using three different health-friendly oils as organic phase. These organic phases proved to be able to polymerize established monomers used in water treatment. The characterization showed that the polymers obtained possessed the suitable characteristics for the final application. High molecular weight was obtained. Preliminary evaluation of performance showed potential application as flocculants in wastewater treatment.

Two health-friendly formulations selected based on this preliminary study were adopted for the manufacturing of cationic and anionic polyelectrolytes, by inverse-emulsion polymerization, based on acrylamide monomer and anionic, cationic and hydrophobic monomers. The flocculants produced and studied can be divided in two categories: copolymers, comprising acrylamide and a cationic or anionic monomer, and terpolymers, including, in addition to acrylamide and the charged monomer, a hydrophobic monomer. Three different hydrophobic monomers were tested, with different hydrophobic chain lengths. The obtained polymers were fully characterized, in terms composition, zeta potential, hydrodynamic diameter and molecular weight. It was proved that the monomers combinations were able to be produce stable polymers by inverse-emulsion polymerization, with different charge densities, as desired. The composition of the polyelectrolytes also demonstrated that the hydrophobic modification was successfully performed, not affecting to a great extent the final characteristics of the polymer regarding molecular weight and charge density. High molecular weight was obtained for all the polyelectrolytes, showing good correlation with the hydrodynamic diameter.

Industrial effluents from olive oil mill, dairy and potato crisps manufacturing industries were used to carry out the performance evaluation of the developed polyelectrolytes as flocculants. In most cases a good flocculation could be observed at dosages below 20 mg/L. The main performance indicator tested was reduction of turbidity, although COD and total solids

reduction have also been assessed. It was demonstrated that the polymers synthesized herein performed very well in the reduction of the turbidity in low dosages and with no addition of other additives. Cationic polyelectrolytes with the higher charged fraction tested, higher molecular weight and presence of hydrophobicity showed the best results in the flocculation of olive oil mill effluent, presenting superior reductions of turbidity. In the optimal case it was possible to achieve reductions of 89% in turbidity, 47% in COD and 34% in total solids, using a concentration of 78 mg/L of the polyelectrolyte 60M1SC, at pH 3. On the other hand, anionic polyelectrolytes showed better results in the treatment of dairy and potato crisps manufacturing effluents. For the dairy industry effluent, specifically anionic polyelectrolytes with higher charged fraction, medium molecular weight and highest hydrophobic content of the monomer SMA performed better, and the best result was obtained using the polyelectrolyte 80A3SC, conducting to reductions of 95% in turbidity, 44% in COD and 57% in total solids, at a concentration of 53 mg/L and pH 5. In the potato crisps manufacturing effluent, the application of the polyelectrolyte 50AC, with the lower charged fraction tested, high molecular weight and no hydrophobicity, presented a reduction of 97% in turbidity, 90% in COD and 55% in total solids, using a pH of 6 and a concentration of 27 mg/L, even if this polyelectrolyte must have a higher cost, due to the incorporation of the larger content of hydrophobic monomer. The choice of the best polyelectrolyte is based on a compromise between results achieved (turbidity, COD and total solids reductions), concentration needed and the possible cost associated (dependent on the monomers' price).

Additionally, must be also mentioned that for many cases, using concentrations below 20 mg/L lead also to very good performances, for instance in case of the application of anionic flocculants in the potato crisps manufacturing effluent. Moreover, worth also noting that hydrophobic modification proved to have significant potential in the improvement of the treatment efficiency of oily wastewaters at low dosages, since the addition of hydrophobic monomer considerably improved the turbidity reduction in several polyelectrolytes, even if the results obtained showed that in most cases an optimum amount of the hydrophobic monomer incorporated in the polymer chain can be defined.

Laser diffraction spectroscopy was successfully applied in the study of the flocculation process, using the effluent from potato crisps manufacturing industry, proving the possibility of applying this methodology to the monitoring of the flocculation kinetics of real industrial effluents. With this methodology for continuous monitoring of the flocculation process in real effluent, it is possible to obtain simultaneously information about the kinetics in floc size evolution, and also about the evolution of floc structure with time, based on the calculation of

the scattering exponent for each time, through the adequate treatment of the scattering matrix supplied by LDS. This is an important output, since by using the developed methodology it will be possible to perform a pre-screening of polymers to be used in the flocculation treatment of a specific effluent, minimizing, in this way, pilot trials. Moreover, LDS allows to understand the underlying flocculation mechanisms behind the action of each polymer, and the influence that they have on the morphology of the flocs obtained. The overall study of the flocculation process revealed that flocculant characteristics are important parameters to consider when a specific size and structure of flocs are required in the further treatment process.

The statistical model developed to correlate flocculant parameters with the produced flocs size and structure, revealed to explain quite well the experimental observations. The results presented propose that hydrodynamic diameter, charged fraction and concentration are the parameters having stronger influence on the characteristics of flocs obtained using copolymers, while charged fraction, concentration and hydrophobic content show more effect on the characteristics of the flocs produced using terpolymers. Furthermore, it was possible to conclude that is not possible to have a single model describing all the polyelectrolytes tested in this study, models comprising separately co- and terpolymers must be applied in order to accurately evaluate the influence of each parameter on the characteristics of the flocs obtained. This fact is mainly justified by the influence of the hydrophobicity of the polyelectrolytes on the flocculation process, due to the interaction between the oily particles of the effluent and the hydrophobic part of the flocculants. Nevertheless, these models allow to better select in the future, the ideal flocculants that must be used to obtain targeted floc characteristics and flocculation efficiencies.

From the above results, it can be concluded that the procedures established for the development and application of flocculants for oily wastewaters treatment show great potential to be applied at the industrial scale. Additionally, the use of lower dosages of flocculant and without needing the addition of further additives can reduce substantially the overall cost of the treatment process.

Finally, the studies presented in this dissertation can be a good incentive to the use of direct flocculation processes induced by the present polyelectrolytes as pre-treatment method, in the considered oily effluents management. This pre-treatment can be applied prior to the use of a more advanced and expensive technology, in order to perform a reduction in the main

effluent control parameters (turbidity, COD, among other), enabling a higher efficacy of the subsequent methods, and, perhaps, a reduction in the total operation costs.

## 2. RECOMMENDATIONS FOR FUTURE WORK

The work developed during these three years and the results obtained suggest that some further studies are still required in order to complete the information achieved so far, and allow the production at industrial scale of some of the studied products. Therefore, the recommendations for future work are:

- Study the possibility of the introduction of branching to the already developed polyelectrolytes, with the objective of increasing their molecular weight and, consequently, their efficiency in flocculation.
- Perform toxicity tests on the used health-friendly oils, as well as on the final polyelectrolyte in the usual commercial form of inverse-emulsion.
- Explore the possible development and application of different co-polymers based on the following cationic, anionic or amphoteric monomers: (vinylbenzyl) trimethylammonium chloride (cationic), sodium 4-vinylbenzenesulfonate (anionic) and [3-(methacryloylamino)propyl] dimethyl (3-sulfo)propyl ammonium hydroxide (amphoteric), which were also in the preliminary list of possible monomers to polymerize with acrylamide.
- Test different effluents such as: restaurant wastewaters, fish processing cheese manufacturing or oil industry effluents.
- Evaluate the flocculation performance of the developed flocculants that did not present good results in dual systems, for instance combined with natural-based coagulants or flocculants.
- Monitor the settling performance of the flocculation process using suitable equipment (e.g. Turbiscan), acquiring information that could be useful to complete the map of flocs.
- Define the target market and perform studies on economic viability for the developed products in large-scale production, including raw materials, equipment and production costs, with the goal of choosing which ones are worth to follow to the upscaling process.
- Perform scaling-up studies, in order to evaluate the viability to produce the developed products in pilot-scale, as well as defining the optimum conditions of production.
- Use the LDS monitoring technique with other effluents, to establish the possibility of using this methodology, at the industrial level, for the pre-screening of flocculants to treat in industrial wastewaters.

- Consider the possibility of using hybrid processes, combining flocculation using the developed polyelectrolytes tuned to treat oily effluents, with advanced treatment processes (filtration, biological treatment or sedimentation), that allow higher COD reduction and meeting the regulations.

---

# REFERENCES





- (1) Rhee, C. H.; Martyn, P. C.; Kremer, J. G. Removal of oil and grease in oil processing wastewater. *Sanit. Dist. Los Angeles County, USA* **1989**.
- (2) Mater, L.; Sperb, R. M.; Madureira, L. A. S.; Rosin, A. P.; Correa, A. X. R.; Radetski, C. M. Proposal of a sequential treatment methodology for the safe reuse of oil sludge-contaminated soil. *J. Hazard. Mater.* **2006**, *136* (3), 967–971.
- (3) Wahi, R.; Chuah, L. A.; Choong, T. S. Y.; Ngaini, Z.; Nourouzi, M. M. Oil removal from aqueous state by natural fibrous sorbent: An overview. *Sep. Purif. Technol.* **2013**, *113*, 51–63.
- (4) Pintor, A. M. A.; Vilar, V. J. P.; Botelho, C. M. S.; Boaventura, R. A. R. Oil and grease removal from wastewaters: Sorption treatment as an alternative to state-of-the-art technologies. A critical review. *Chem. Eng. J.* **2016**, *297*, 229–255.
- (5) Cheryan, M.; Rajagopalan, N. Membrane processing of oily streams. Wastewater treatment and waste reduction. *J. Memb. Sci.* **1998**, *151* (1), 13–28.
- (6) Coca-Prados, J.; Gutiérrez-Cervelló, G. *Water purification and management*; Springer: Dordrecht, Netherlands, 2010.
- (7) Jamaly, S.; Giwa, A.; Hasan, S. W. Recent improvements in oily wastewater treatment: Progress, challenges, and future opportunities. *J. Environ. Sci.* **2015**, *37*, 15–30.
- (8) Eyvaz, M. Treatment of brewery wastewater with electrocoagulation: improving the process performance by using alternating pulse current. *Int. J. Electrochem. Sci.* **2016**, *11*, 4988–5008.
- (9) Diya'uddeen, B. H.; Daud, W. M. A. W.; Abdul Aziz, A. R. Treatment technologies for petroleum refinery effluents: A review. *Process Saf. Environ. Prot.* **2011**, *89* (2), 95–105.
- (10) Brunsmann, J. J.; Cornelissen, J.; Eilers, H. Improved oil separation in gravity separators. *J. (Water Pollut. Control Fed.* **1962**, *34*, 44–55.
- (11) Safa, M.; Alemzadeh, I.; Vossoughi, M. Oily wastewater treatment using membrane bioreactor. *Int. J. Glob. Warm.* **2014**, *6* (2–3), 295–302.
- (12) Yang, C.-L. Electrochemical coagulation for oily water demulsification. *Sep. Purif. Technol.* **2007**, *54* (3), 388–395.
- (13) Santo, C. E.; Vilar, V. J. P.; Botelho, C. M. S.; Bhatnagar, A.; Kumar, E.; Boaventura, R. A. R. Optimization of coagulation–flocculation and flotation parameters for the

- treatment of a petroleum refinery effluent from a Portuguese plant. *Chem. Eng. J.* **2011**, *183*, 117–123.
- (14) Cañizares, P.; Martínez, F.; Jiménez, C.; Sáez, C.; Rodrigo, M. A. Coagulation and electrocoagulation of oil-in-water emulsions. *J. Hazard. Mater.* **2008**, *151* (1), 44–51.
- (15) Ahmad, A. L.; Ismail, S.; Ibrahim, N.; Bhatia, S. Removal of suspended solids and residual oil from palm oil mill effluent. *J. Chem. Technol. Biotechnol.* **2003**, *78* (9), 971–978.
- (16) Zouboulis, A. I.; Avranas, A. Treatment of oil-in-water emulsions by coagulation and dissolved-air flotation. *Colloids Surfaces A Physicochem. Eng. Asp.* **2000**, *172*, 153–161.
- (17) Suzuki, Y.; Maruyama, T. Removal of emulsified oil from water by coagulation and foam separation. *Sep. Sci. Technol.* **2005**, *40* (16), 3407–3418.
- (18) Chipasa, K. B. Limits of physicochemical treatment of wastewater in the vegetable oil refining industry. *Polish J. Environ. Stud.* **2001**, *10* (3), 141–147.
- (19) Benito, J. M.; Cambiella, A.; Lobo, A.; Gutiérrez, G.; Coca, J.; Pazos, C. Formulation, characterization and treatment of metalworking oil-in-water emulsions. *Clean Technol. Environ. Policy* **2010**, *12* (1), 31–41.
- (20) Ahmad, A. L.; Sumathi, S.; Hameed, B. H. Coagulation of residue oil and suspended solid in palm oil mill effluent by chitosan, alum and PAC. *Chem. Eng. J.* **2006**, *118*, 99–105.
- (21) Lee, C. S.; Robinson, J.; Chong, M. F. A review on application of flocculants in wastewater treatment. *Process Saf. Environ. Prot.* **2014**, *92* (6), 489–508.
- (22) Chi, F. H.; Cheng, W. P. Use of chitosan as coagulant to treat wastewater from milk processing plant. *J. Polym. Environ.* **2006**, *14* (4), 411–417.
- (23) Karhu, M.; Leiviskä, T.; Tanskanen, J. Enhanced DAF in breaking up oil-in-water emulsions. *Sep. Purif. Technol.* **2014**, *122*, 231–241.
- (24) Blanco, A.; Fuente, E.; Negro, C.; Tijero, J. Flocculation monitoring: focused beam reflectance measurement as a measurement tool. *Can. J. Chem. Eng.* **2008**, *80* (4), 1–7.
- (25) Hosny, A. Y. Separating oil from oil-water emulsions by electroflotation technique. *Sep. Technol.* **1996**, *6*, 9–17.
- (26) Mansour, L. Ben; Chalbi, S. Removal of oil from oil/water emulsions using

- electroflotation process. *J. Appl. Electrochem.* **2006**, *36* (5), 577–581.
- (27) Zhou, Y.-B.; Tang, X.-Y.; Hu, X.-M.; Fritschi, S.; Lu, J. Emulsified oily wastewater treatment using a hybrid-modified resin and activated carbon system. *Sep. Purif. Technol.* **2008**, *63*, 400–406.
- (28) Decloux, M.; Lameloise, M.-L.; Brocard, A.; Bisson, E.; Parmentier, M.; Spiraers, A. Treatment of acidic wastewater arising from the refining of vegetable oil by crossflow microfiltration at very low transmembrane pressure. *Process Biochem.* **2007**, *42* (4), 693–699.
- (29) Peng, H.; Tremblay, A. Y. Membrane regeneration and filtration modeling in treating oily wastewaters. *J. Memb. Sci.* **2008**, *324*, 59–66.
- (30) Rezaei, S.; Abadi, H.; Sebzari, M. R.; Hemati, M.; Rekabdar, F.; Mohammadi, T. Ceramic membrane performance in microfiltration of oily wastewater. *Desalination* **2011**, *265*, 222–228.
- (31) Barhate, R. S.; Ramakrishna, S. Nanofibrous filtering media: Filtration problems and solutions from tiny materials. *J. Memb. Sci.* **2007**, *296*, 1–8.
- (32) Ergüder, T. ; Güven, E.; Demirer, G. . Anaerobic treatment of olive mill wastes in batch reactors. *Process Biochem.* **2000**, *36* (3), 243–248.
- (33) Ammar, E.; Nasri, M.; Medhioub, K. Isolation of phenol degrading Enterobacteria from the wastewater of olive oil extraction process. *World J. Microbiol. Biotechnol.* **2005**, *21* (3), 253–259.
- (34) Dhouib, A.; Ellouz, M.; Aloui, F.; Sayadi, S. Effect of bioaugmentation of activated sludge with white-rot fungi on olive mill wastewater detoxification. *Lett. Appl. Microbiol.* **2006**, *42* (4), 405–411.
- (35) Mondal, S.; Wickramasinghe, S. R. Produced water treatment by nanofiltration and reverse osmosis membranes. *J. Memb. Sci.* **2008**, *322*, 162–170.
- (36) Oller, I.; Malato, S.; Sánchez-Pérez, J. A. Combination of advanced oxidation processes and biological treatments for wastewater decontamination—A review. *Sci. Total Environ.* **2011**, *409*, 4141–4166.
- (37) Cooney, D. O.; Xi, Z. Activated carbon catalyzes reactions of phenolics during liquid-phase adsorption. *AIChE J.* **1994**, *40* (2), 361–364.

- (38) Temmink, H.; Grolle, K. Tertiary activated carbon treatment of paper and board industry wastewater. *2005*, *96* (15), 1683–1689.
- (39) Hua, F. L.; Tsang, Y. F.; Wang, Y. J.; Chan, S. Y.; Chua, H.; Sin, S. N. Performance study of ceramic microfiltration membrane for oily wastewater treatment. *Chem. Eng. J.* **2007**, *128* (2–3), 169–175.
- (40) Song, C.; Wang, T.; Pan, Y.; Qiu, J. Preparation of coal-based microfiltration carbon membrane and application in oily wastewater treatment. *Sep. Purif. Technol.* **2006**, *51* (1), 80–84.
- (41) Sun, D.; Duan, X.; Li, W.; Zhou, D. Demulsification of water-in-oil emulsion by using porous glass membrane. *J. Memb. Sci.* **1998**, *146* (1), 65–72.
- (42) Pandey, R. A.; Sanyal, P. B.; Chattopadhyay, N.; Kaul, S. N. Treatment and reuse of wastes of a vegetable oil refinery. *Resour. Conserv. Recycl.* **2003**, *37* (2), 101–117.
- (43) Benito, J. M.; Ríos, G.; Ortea, E.; Fernández, E.; Cambiella, A.; Pazos, C.; Coca, J. Design and construction of a modular pilot plant for the treatment of oil-containing wastewaters. *Desalination* **2002**, *147* (1–3), 5–10.
- (44) Souza, B. M.; Cerqueira, A. C.; Sant’Anna, G. L.; Dezotti, M. Oil-refinery wastewater treatment aiming reuse by advanced oxidation processes (AOPs) combined with biological activated carbon (BAC). *Ozone Sci. Eng.* **2011**, *33* (5), 403–409.
- (45) Al-Malah, K.; Azzam, M. O. J.; Abu-Lail, N. I. Olive mills effluent (OME) wastewater post-treatment using activated clay. *Sep. Purif. Technol.* **2000**, *20*, 225–234.
- (46) Ahmad, A. L.; Bhatia, S.; Ibrahim, N.; Sumathi, S. Adsorption of residual oil from palm oil mill effluent using rubber powder. *Brazilian J. Chem. Eng.* **2005**, *22* (3), 371–379.
- (47) Otadi, N.; Hassani, A. H.; Javid, A. H.; Khiabani, F. F. Oily compounds removal in wastewater treatment system of pars oil refinery to improve its efficiency in a lab scale pilot. *J. Water Chem. Technol.* **2010**, *32* (6), 370–377.
- (48) Rattanapan, C.; Sawain, A.; Suksaroj, T.; Suksaroj, C. Enhanced efficiency of dissolved air flotation for biodiesel wastewater treatment by acidification and coagulation processes. *Desalination* **2011**, *280*, 370–377.
- (49) Siles, J. A.; Gutiérrez, M. C.; Martín, M. A.; Martín, A. Physical-chemical and biomethanization treatments of wastewater from biodiesel manufacturing. *Bioresour.*

- Technol.* **2011**, *102*, 6348–6351.
- (50) Yang, B.; Chen, G.; Chen, G. Submerged membrane bioreactor in treatment of simulated restaurant wastewater. *Sep. Purif. Technol.* **2012**, *88*, 184–190.
- (51) Mostefa, N. M.; Tir, M. Coupling flocculation with electroflotation for waste oil/water emulsion treatment. Optimization of the operating conditions. *Desalination* **2004**, *161*, 115–121.
- (52) Zhong, J.; Sun, X.; Wang, C. Treatment of oily wastewater produced from refinery processes using flocculation and ceramic membrane filtration. *Sep. Purif. Technol.* **2003**, *32* (1–3), 93–98.
- (53) Scholz, W. Treatment of oil contaminated wastewater in a membrane bioreactor. *Water Res.* **2000**, *34* (14), 3621–3629.
- (54) Abbasi, M.; Sebzari, M. R.; Mohammadi, T. Effect of metallic coagulant agents on oily wastewater treatment performance using mullite ceramic MF membranes. *Sep. Sci. Technol.* **2012**, *47* (16), 2290–2298.
- (55) Koetz, J.; Kosmella, S. *Polyelectrolytes and nanoparticles*; New York: Springer: Berlin, Heidelberg, 2007.
- (56) Serra, C. Free Radical Polymerization. In *Micro Process Engineering: A Comprehensive Handbook*; Wiley-VCH Verlag GmbH & Co. KGaA: Weinheim, Germany, 2013; pp 197–212.
- (57) Matyjaszewski, K.; Xia, J. Atom transfer radical polymerization. *Chem. Rev.* **2001**, *101* (9), 2921–2990.
- (58) Uzulina, I.; Kanagasabapathy, S.; Claverie, J. Reversible addition fragmentation transfer (RAFT) polymerization in emulsion. *Macromol. Symp.* **2000**, *150* (1), 33–38.
- (59) Decker, C. The use of UV irradiation in polymerization. *Polym. Int.* **1998**, *45* (2), 133–141.
- (60) Vivaldo-Lima, E.; Wood, P. E.; Hamielec, A. E.; Penlidis, A. An updated review on suspension polymerization. *Ind. Eng. Chem. Res.* **1997**, *36*, 939–965.
- (61) Rabiee, A.; Ershad-Langroudi, A.; Zeynali, M. E. A survey on cationic polyelectrolytes and their applications: acrylamide derivatives. *Rev. Chem. Eng.* **2015**, *31* (3), 239–261.

- (62) Gromov, V. F.; Bune, E. V; Teleshov, E. N. Characteristic features of the radical polymerisation of water-soluble monomers. *Russ. Chem. Rev.* **1994**, *63* (6), 507–517.
- (63) Bajaj, P.; Sen, K.; Bahrami, S. H. Solution polymerization of acrylonitrile with vinyl acids in dimethylformamide. *J. Appl. Polym. Sci.* **1996**, *59* (10), 1539–1550.
- (64) Priest, W. J. Partice growth in the aqueous polymerization of vinyl acetate. *J. Phys. Chem.* **1952**, *56* (9), 1077–1082.
- (65) Rabiee, A. Acrylamide-based anionic polyelectrolytes and their applications: A survey. *J. Vinyl Addit. Technol.* **2010**, *16* (2), 111–119.
- (66) Bamford, C. H.; Jenkins, A. D. Studies in polymerization. VI. Acrylonitrile: The behaviour of free radicals in heterogeneous systems. *Proc. R. Soc. A Math. Phys. Eng. Sci.* **1953**, *216* (1127), 515–539.
- (67) Liu, L.; Yang, W. Photoinitiated, inverse emulsion polymerization of acrylamide: Some mechanistic and kinetic aspects. *J. Polym. Sci. Part A Polym. Chem.* **2004**, *42* (4), 846–852.
- (68) Peng, X.; Peng, X. Water-soluble copolymers. II. Inverse emulsion terpolymerization of acrylamide, sodium acrylate, and acryloyloxyethyl trimethylammonium chloride. *J. Appl. Polym. Sci.* **2006**, *101* (3), 1381–1385.
- (69) Hernández-Barajas, J.; Hunkeler, D. J. Inverse-emulsion polymerization of acrylamide using block copolymeric surfactants: mechanism, kinetics and modelling. *Polymer (Guildf)*. **1997**, *38* (2), 437–447.
- (70) Rembaum, A.; Sélégny, E. *Polyelectrolytes and their Applications*; Springer: Dordrecht, Netherlands, 1975.
- (71) Leimbach, J.; Rupprecht, H. Adsorption of ionic surfactants on polar surfaces with a low content of chemically adsorbed alkyl chains. *Colloid Polym. Sci.* **1993**, *271* (3), 307–309.
- (72) Raffa, P.; Broekhuis, A. A.; Picchioni, F. Polymeric surfactants for enhanced oil recovery: A review. *J. Pet. Sci. Eng.* **2016**, *145*, 723–733.
- (73) Clark, R. K.; Scheuerman, R. F.; Rath, H.; Van Laar, H. G. Polyacrylamide/potassium-chloride mud for drilling water-sensitive shales. *J. Pet. Technol.* **1976**, *28* (6), 719–727.
- (74) Souza, C. E. C.; Fonseca, M. V.; Sá, C. H.; Nascimento, R. S. V. Inhibitive properties of cationic polymers in a borehole environment. *J. Appl. Polym. Sci.* **2006**, *102* (3), 2158–

- 2163.
- (75) Wan, T.; Yao, J.; Zishun, S.; Li, W.; Juan, W. Solution and drilling fluid properties of water soluble AM-AA-SSS copolymers by inverse microemulsion. *J. Pet. Sci. Eng.* **2011**, *78*, 334–337.
- (76) Zezin, A. B.; Mikheikin, S. V.; Rogacheva, V. B.; Zansokhova, M. F.; Sybachin, A. V.; Yaroslavov, A. A. Polymeric stabilizers for protection of soil and ground against wind and water erosion. *Adv. Colloid Interface Sci.* **2015**, *226*, 17–23.
- (77) Crees, O. L.; Senogles, E.; Whayman, E. The flocculation of cane sugar muds with acrylamide–sodium acrylate copolymers. *J. Appl. Polym. Sci.* **1991**, *42* (3), 837–844.
- (78) Pojják, K.; Bertalanits, E.; Mészáros, R. Effect of salt on the equilibrium and nonequilibrium features of polyelectrolyte/surfactant association. *Langmuir* **2011**, *27* (15), 9139–9147.
- (79) Llamas, S.; Guzmán, E.; Baghdadli, N.; Ortega, F.; Cazeneuve, C.; Rubio, R. G.; Luengo, G. S. Adsorption of poly(diallyldimethylammonium chloride)—sodium methyl-cocoyl-aurate complexes onto solid surfaces. *Colloids Surfaces A Physicochem. Eng. Asp.* **2016**, *505*, 150–157.
- (80) Antunes, E.; Garcia, F. A. P.; Ferreira, P.; Blanco, A.; Negro, C.; Graça Rasteiro, M. Use of new branched cationic polyacrylamides to improve retention and drainage in papermaking. *Ind. Eng. Chem. Res.* **2008**, *47* (23), 9370–9375.
- (81) Porubská, J.; Alince, B.; Van De Ven, T. G. M. Homo- and heteroflocculation of papermaking fines and fillers. *Colloids Surfaces A Physicochem. Eng. Asp.* **2002**, *210*, 223–230.
- (82) Xiao, H.; Pelton, R.; Hamielec, A. Retention mechanisms for two-component systems based on phenolic resins and PEO or new PEO-copolymer retention aids. *J. pulp Pap. Sci.* **1996**, *22* (12), J475–J485.
- (83) Mocchiutti, P.; Galván, M. V.; Peresin, M. S.; Schnell, C. N.; Zanuttini, M. A. Complexes of xylan and synthetic polyelectrolytes. Characterization and adsorption onto high quality unbleached fibres. *Carbohydr. Polym.* **2015**, *116*, 131–139.
- (84) Saha, D.; Bhattacharya, S. Hydrocolloids as thickening and gelling agents in food: a critical review. *J. Food Sci. Technol.* **2010**, *47* (6), 587–597.



- (85) Diftis, N.; Kiosseoglou, V. Improvement of emulsifying properties of soybean protein isolate by conjugation with carboxymethyl cellulose. *Food Chem.* **2003**, *81* (1), 1–6.
- (86) Bolto, B.; Gregory, J. Organic polyelectrolytes in water treatment. *Water Res.* **2007**, *41* (11), 2301–2324.
- (87) Biggs, S.; Habgood, M.; Jameson, G. J.; Yan, Y. Aggregate structures formed via a bridging flocculation mechanism. *Chem. Eng. J.* **2000**, *80* (1), 13–22.
- (88) Thomas, D. N.; Judd, S. J.; Fawcett, N. Flocculation modelling: a review. *Water Res.* **1999**, *33* (7), 1579–1592.
- (89) Kleimann, J.; Gehin-Delval, C.; Auweter, H.; Borkovec, M. Super-stoichiometric charge neutralization in particle-polyelectrolyte systems. *Langmuir* **2005**, *21* (8), 3688–3698.
- (90) Ahmad, A.; Wong, S.; Teng, T.; Zuhairi, A. Improvement of alum and PACl coagulation by polyacrylamides (PAMs) for the treatment of pulp and paper mill wastewater. *Chem. Eng. J.* **2008**, *137* (3), 510–517.
- (91) Caskey, J. A.; Primus, R. J. The effect of anionic polyacrylamide molecular conformation and configuration on flocculation effectiveness. *Environ. Prog.* **1986**, *5* (2), 98–103.
- (92) Eriksson, L.; Alm, B.; Stenius, P. Formation and structure of polystyrene latex aggregates obtained by flocculation with cationic polyelectrolytes. *Colloids Surfaces A Physicochem. Eng. Asp.* **1993**, *70* (1), 47–60.
- (93) Dao, V. H.; Cameron, N. R.; Saito, K. Synthesis, properties and performance of organic polymers employed in flocculation applications. *Polym. Chem.* **2016**, *7* (1), 11–25.
- (94) Pinheiro, I.; Ferreira, P. J.; Garcia, F. A.; Reis, M. S.; Pereira, A. C.; Wandrey, C.; Ahmadloo, H.; Amaral, J. L.; Hunkeler, D.; Rasteiro, M. G. An experimental design methodology to evaluate the importance of different parameters on flocculation by polyelectrolytes. *Powder Technol.* **2013**, *238*, 2–13.
- (95) Hernandez-Barajas, J.; Wandrey, C.; Hunkeler, D. Polymer flocculants with improved dewatering characteristics. U.S. Pat. 6,294,622 B1, 2003.
- (96) Okada, T.; Ishigaki, I.; Suwa, T.; Machi, S. Synthesis of cationic flocculant by radiation-induced copolymerization of methyl chloride salt of N,N-dimethylaminoethyl methacrylate with acrylamide in aqueous solution. *J. Appl. Polym. Sci.* **1979**, *24* (7), 1713–

- 1721.
- (97) Wang, L.-J.; Wang, J.-P.; Zhang, S.-J.; Chen, Y.-Z.; Yuan, S.-J.; Sheng, G.-P.; Yu, H.-Q. A water-soluble cationic flocculant synthesized by dispersion polymerization in aqueous salts solution. *Sep. Purif. Technol.* **2009**, *67* (3), 331–335.
- (98) Wang, L.-J.; Wang, J.-P.; Yuan, S.-J.; Zhang, S.-J.; Tang, Y.; Yu, H.-Q. Gamma radiation-induced dispersion polymerization in aqueous salts solution for manufacturing a cationic flocculant. *Chem. Eng. J.* **2009**, *149* (1), 118–122.
- (99) Nasr, H. E.; Farag, A. A.; Sayyah, S. M.; Samaha, S. H. Flocculation behavior of terpolymer prepared from dimethyl aminoethyl methacrylate, vinyl pyrrolidone, and vinyl acetate using solution polymerization technique. *J. Dispers. Sci. Technol.* **2010**, *31* (4), 427–437.
- (100) Razali, M. A. A.; Ahmad, Z.; Ahmad, M. S. B.; Ariffin, A. Treatment of pulp and paper mill wastewater with various molecular weight of polyDADMAC induced flocculation. *Chem. Eng. J.* **2011**, *166* (2), 529–535.
- (101) Lu, L.; Pan, Z.; Hao, N.; Peng, W. A novel acrylamide-free flocculant and its application for sludge dewatering. *Water Res.* **2014**, *57*, 304–312.
- (102) Abdiev, K. Z.; Toktarbay, Z.; Zhenissova, A. Z.; Zhursumbaeva, M. B.; Kainazarova, R. N.; Nuraje, N. The new effective flocculants – Copolymers of N,N-dimethyl-N,N-diallyl-ammonium chloride and N,N-dimethylacrylamide. *Colloids Surfaces A Physicochem. Eng. Asp.* **2015**, *480*, 228–235.
- (103) Palomino, D.; Hunkeler, D.; Stoll, S. Comparison of two cationic polymeric flocculant architectures on the destabilization of negatively charged latex suspensions. *Polymer (Guildf)*. **2011**, *52* (4), 1019–1026.
- (104) Ma, J. Y.; Zheng, H. L.; Tang, X. M.; Chen, W.; Xue, W. W.; Liao, Y.; Guan, Q. Q.; Liao, Y. Research on flocculation behavior in diethyl phthalate removal from water by using anionic flocculants P(AM-AA-AMPS). *Appl. Mech. Mater.* **2013**, *361*, 726–729.
- (105) Ma, J.; Zheng, H.; Tan, M.; Liu, L.; Chen, W.; Guan, Q.; Zheng, X. Synthesis, characterization, and flocculation performance of anionic polyacrylamide P (AM-AA-AMPS). *J. Appl. Polym. Sci.* **2013**, *129* (4), 1984–1991.
- (106) Zheng, H.; Ma, J.; Zhai, J.; Zhu, C.; Tang, X.; Liao, Y.; Qian, L.; Sun, Y. Optimization

- of flocculation process by response surface methodology for diethyl phthalate removal using anionic polyacrylamide. *Desalin. Water Treat.* **2014**, *52* (28–30), 5390–5400.
- (107) Zheng, H.; Ma, J.; Zhu, C.; Zhang, Z.; Liu, L.; Sun, Y.; Tang, X. Synthesis of anion polyacrylamide under UV initiation and its application in removing dioctyl phthalate from water through flocculation process. *Sep. Purif. Technol.* **2014**, *123*, 35–44.
- (108) Lu, L.; Pan, Z.; Hao, N.; Peng, W. A novel acrylamide-free flocculant and its application for sludge dewatering. *Water Res.* **2014**, *57*, 304–312.
- (109) Feng, L.; Zheng, H.; Gao, B.; Zhang, S.; Zhao, C.; Zhou, Y.; Xu, B. Fabricating an anionic polyacrylamide (APAM) with an anionic block structure for high turbidity water separation and purification. *RSC Adv.* **2017**, *7* (46), 28918–28930.
- (110) Jha, A.; Agrawal, S.; Mishra, A.; Rai, J. P. Synthesis, characterization and flocculation efficiency of poly(acrylamide-co-acrylic acid) in tannery waste-water. *Iran. Polym. J.* **2001**, *10* (2), 85–90.
- (111) Rahul, R.; Jha, U.; Sen, G.; Mishra, S. Carboxymethyl inulin: A novel flocculant for wastewater treatment. *Int. J. Biol. Macromol.* **2014**, *63*, 1–7.
- (112) Mittal, H.; Jindal, R.; Kaith, B. S.; Maity, A.; Ray, S. S. Synthesis and flocculation properties of gum ghatti and poly(acrylamide-co-acrylonitrile) based biodegradable hydrogels. *Carbohydr. Polym.* **2014**, *114*, 321–329.
- (113) Ghimici, L.; Suflet, D. M. Phosphorylated polysaccharide derivatives as efficient separation agents for zinc and ferric oxides particles from water. *Sep. Purif. Technol.* **2015**, *144*, 31–36.
- (114) Mishra, S.; Usha Rani, G.; Sen, G. Microwave initiated synthesis and application of polyacrylic acid grafted carboxymethyl cellulose. *Carbohydr. Polym.* **2012**, *87* (3), 2255–2262.
- (115) Bratskaya, S.; Avramenko, V.; Schwarz, S.; Philippova, I. Enhanced flocculation of oil-in-water emulsions by hydrophobically modified chitosan derivatives. *Colloids Surfaces A Physicochem. Eng. Asp.* **2006**, *275* (1), 168–176.
- (116) Candau, F.; Selb, J. Hydrophobically-modified polyacrylamides prepared by micellar polymerization. *Adv. Colloid Interface Sci.* **1999**, *79*, 149–172.
- (117) Ren, H.; Chen, W.; Zheng, Y.; Luan, Z. Effect of hydrophobic group on flocculation

- properties and dewatering efficiency of cationic acrylamide copolymers. *React. Funct. Polym.* **2007**, *67* (7), 601–608.
- (118) Zhao, H.-Z.; Luan, Z.-K.; Gao, B.-Y.; Yue, Q.-Y. Synthesis and flocculation properties of poly(diallyldimethyl ammonium chloride-vinyl trimethoxysilane) and poly(diallyldimethyl ammonium chloride-acrylamide-vinyl trimethoxysilane). *J. Appl. Polym. Sci.* **2002**, *84* (2), 335–342.
- (119) Dragan, S.; Maftuleac, A.; Dranca, I.; Ghimici, L.; Lupascu, T. Flocculation of montmorillonite by some hydrophobically modified polycations containing quaternary ammonium salt groups in the backbone. *J. Appl. Polym. Sci.* **2002**, *84* (4), 871–876.
- (120) Lee, K. E.; Morad, N.; Poh, B. T.; Teng, T. T. Comparative study on the effectiveness of hydrophobically modified cationic polyacrylamide groups in the flocculation of kaolin. *Desalination* **2011**, *270* (1), 206–213.
- (121) Shang, H.; Liu, J.; Zheng, Y.; Wang, L. Synthesis, characterization, and flocculation properties of poly(acrylamide-methacryloxyethyltrimethyl ammonium chloride-methacryloxypropyltrimethoxy silane). *J. Appl. Polym. Sci.* **2009**, *111* (3), 1594–1599.
- (122) Yang, Z. L.; Gao, B. Y.; Li, C. X.; Yue, Q. Y.; Liu, B. Synthesis and characterization of hydrophobically associating cationic polyacrylamide. *Chem. Eng. J.* **2010**, *161* (1), 27–33.
- (123) Shang, H.; Zheng, Y.; Liu, J. Synthesis in inverse emulsion and decolorization properties of hydrophobically modified cationic polyelectrolyte. *J. Appl. Polym. Sci.* **2011**, *119* (3), 1602–1609.
- (124) Zheng, H.; Sun, Y.; Zhu, C.; Guo, J.; Zhao, C.; Liao, Y.; Guan, Q. UV-initiated polymerization of hydrophobically associating cationic flocculants: Synthesis, characterization, and dewatering properties. *Chem. Eng. J.* **2013**, *234*, 318–326.
- (125) Zheng, H.; Sun, Y.; Guo, J.; Li, F.; Fan, W.; Liao, Y.; Guan, Q. Characterization and evaluation of dewatering properties of PADB, a highly efficient cationic flocculant. *Ind. Eng. Chem. Res.* **2014**, *53* (7), 2572–2582.
- (126) Lü, T.; Qi, D.; Zhao, H.; Cheng, Y. Synthesis of hydrophobically modified flocculant by aqueous dispersion polymerization and its application in oily wastewater treatment. *Polym. Eng. Sci.* **2015**, *55* (1), 1–7.
- (127) Hami, M. L.; Al-Hashimi, M. A.; Al-Doori, M. M. Effect of activated carbon on BOD

- and COD removal in a dissolved air flotation unit treating refinery wastewater. *Desalination* **2007**, *216*, 116–122.
- (128) Benito, J. M.; Cambiella, A.; Lobo, A.; Gutiérrez, G.; Coca, J.; Pazos, C. Formulation, characterization and treatment of metalworking oil-in-water emulsions. *Clean Technol. Environ. Policy* **2010**, *12* (1), 31–41.
- (129) MacAdam, J.; Ozgencil, H.; Autin, O.; Pidou, M.; Temple, C.; Parsons, S.; Jefferson, B. Incorporating biodegradation and advanced oxidation processes in the treatment of spent metalworking fluids. *Environ. Technol.* **2012**, *33* (24), 2741–2750.
- (130) Ahmad, A. L.; Sumathi, S.; Hameed, B. H. Adsorption of residue oil from palm oil mill effluent using powder and flake chitosan: Equilibrium and kinetic studies. *Water Res.* **2005**, *39*, 2483–2494.
- (131) Michael, I.; Panagi, A.; Ioannou, L. A.; Frontistis, Z.; Fatta-Kassinos, D. Utilizing solar energy for the purification of olive mill wastewater using a pilot-scale photocatalytic reactor after coagulation-flocculation. *Water Res.* **2014**, *60*, 28–40.
- (132) Fitó, M.; Covas, M. I.; Lamuela-Raventós, R. M.; Vila, J.; Torrents, J.; de la Torre, C.; Marrugat, J. Protective effect of olive oil and its phenolic compounds against low density lipoprotein oxidation. *Lipids* **2000**, *35* (6), 633–638.
- (133) Paraskeva, C. A.; Papadakis, V. G.; Tsarouchi, E.; Kanellopoulou, D. G.; Koutsoukos, P. G. Membrane processing for olive mill wastewater fractionation. *Desalination* **2007**, *213* (1–3), 218–229.
- (134) Kestioğlu, K.; Yonar, T.; Azbar, N. Feasibility of physico-chemical treatment and Advanced Oxidation Processes (AOPs) as a means of pretreatment of olive mill effluent (OME). *Process Biochem.* **2005**, *40* (7), 2409–2416.
- (135) Celano, G.; Smejkalova, D.; Spaccini, R.; Piccolo, A. Reduced toxicity of olive mill waste waters by oxidative coupling with biomimetic catalysis. *Environ. Sci. Technol.* **2008**, *42* (13), 4896–4901.
- (136) Salam, D. A.; Naik, N.; Suidan, M. T.; Venosa, A. D. Assessment of aquatic toxicity and oxygen depletion during aerobic biodegradation of vegetable oil: Effect of oil loading and mixing regime. *Environ. Sci. Technol.* **2012**, *46* (4), 2352–2359.
- (137) Benitez, J.; Beltran-Heredia, J.; Torregrosa, J.; Acero, J. L.; Cercas, V. Aerobic

- degradation of olive mill wastewaters. *Appl. Microbiol. Biotechnol.* **1997**, *47* (2), 185–188.
- (138) Stamatelatou, K.; Kopsahelis, A.; Blika, P. S.; Paraskeva, C. A.; Lyberatos, G. Anaerobic digestion of olive mill wastewater in a periodic anaerobic baffled reactor (PABR) followed by further effluent purification via membrane separation technologies. *J. Chem. Technol. Biotechnol.* **2009**, *84* (6), 909–917.
- (139) Rivas, F. J.; Beltrá, F. J.; Gimeno, O.; Frades, J. Treatment of olive oil mill wastewater by Fenton's reagent. *J. Agric. Food Chem.* **2001**, *49* (4), 1873–1880.
- (140) Kiril Mert, B.; Yonar, T.; Yalili Kiliç, M.; Kestioglu, K. Pre-treatment studies on olive oil mill effluent using physicochemical, Fenton and Fenton-like oxidations processes. *J. Hazard. Mater.* **2010**, *174* (1), 122–128.
- (141) El-Abbassi, A.; Khayet, M.; Hafidi, A. Micellar enhanced ultrafiltration process for the treatment of olive mill wastewater. *Water Res.* **2011**, *45* (15), 4522–4530.
- (142) Ginos, A.; Manios, T.; Mantzavinos, D. Treatment of olive mill effluents by coagulation–flocculation–hydrogen peroxide oxidation and effect on phytotoxicity. *J. Hazard. Mater.* **2006**, *133* (1), 135–142.
- (143) Tezcan Ün, Ü.; Uğur, S.; Koparal, A. S.; Bakır Öğütveren, Ü. Electrocoagulation of olive mill wastewaters. *Sep. Purif. Technol.* **2006**, *52* (1), 136–141.
- (144) Fiorentino, A.; Gentili, A.; Isidori, M.; Lavorgna, M.; Parrella, A.; Temussi, F. Olive oil mill wastewater treatment using a chemical and biological approach. *J. Agric. Food Chem.* **2004**, *52* (16), 5151–5154.
- (145) Bressan, M.; Liberatore, L.; D'alejandro, N.; Tonucci, L.; Belli, C.; Ranalli, G. Improved combined chemical and biological treatments of olive oil mill wastewaters. *J. Agric. Food Chem.* **2004**, *52* (5), 1228–1233.
- (146) Ochando-Pulido, J. M.; Stoller, M.; Di Palma, L.; Martínez-Ferez, A. On the optimization of a flocculation process as fouling inhibiting pretreatment on an ultrafiltration membrane during olive mill effluents treatment. *Desalination* **2016**, *393*, 151–158.
- (147) Hodaifa, G.; Páez, J.; Agabo, C.; Ramos, E.; Gutiérrez, J.; Rosal, A. Flocculation on the treatment of olive oil mill wastewater: Pretreatment. *World Acad. Sci. Eng. Technol. Int. J. Chem. Mol. Nucl. Mater. Metall. Eng.* **2015**, *9* (5), 645–650.

- (148) Pelendridou, K.; Michailides, M. K.; Zagklis, D. P.; Tekerlekopoulou, A. G.; Paraskeva, C. A.; Vayenas, D. V. Treatment of olive mill wastewater using a coagulation-flocculation process either as a single step or as post-treatment after aerobic biological treatment. *J. Chem. Technol. Biotechnol.* **2014**, *89* (12), 1866–1874.
- (149) Rizzo, L.; Lofrano, G.; Belgiorno, V. Olive mill and winery wastewaters pre-treatment by coagulation with chitosan. *Sep. Sci. Technol.* **2010**, *45* (16), 2447–2452.
- (150) Iakovides, I. C.; Pantziaros, A. G.; Zagklis, D. P.; Paraskeva, C. A. Effect of electrolytes/polyelectrolytes on the removal of solids and organics from olive mill wastewater. *J. Chem. Technol. Biotechnol.* **2014**, *91* (1), 204–211.
- (151) Amuda, O.; Amoo, I. Coagulation/flocculation process and sludge conditioning in beverage industrial wastewater treatment. *J. Hazard. Mater.* **2007**, *141* (3), 778–783.
- (152) Kestioglu, K.; Yonar, T.; Azbar, N. Feasibility of physico-chemical treatment and Advanced Oxidation Processes (AOPs) as a means of pretreatment of olive mill effluent (OME). *Process Biochem.* **2005**, *40* (7), 2409–2416.
- (153) Rizzo, L.; Lofrano, G.; Grassi, M.; Belgiorno, V. Pre-treatment of olive mill wastewater by chitosan coagulation and advanced oxidation processes. *Sep. Purif. Technol.* **2008**, *63* (3), 648–653.
- (154) Meyssami, B.; Kasaeian, A. B. Use of coagulants in treatment of olive oil wastewater model solutions by induced air flotation. *Bioresour. Technol.* **2005**, *96* (3), 303–307.
- (155) Sarika, R.; Kalogerakis, N.; Mantzavinos, D. Treatment of olive mill effluents: Part II. Complete removal of solids by direct flocculation with poly-electrolytes. *Environ. Int.* **2005**, *31* (2), 297–304.
- (156) Azbar, N.; Keskin, T.; Catalkaya, E. C. Improvement in anaerobic degradation of olive mill effluent (OME) by chemical pretreatment using batch systems. *Biochem. Eng. J.* **2008**, *38* (3), 379–383.
- (157) Yazdanbakhsh, A.; Mehdipour, F.; Eslami, A.; Maleksari, H. S.; Ghanbari, F. The combination of coagulation, acid cracking and Fenton-like processes for olive oil mill wastewater treatment: phytotoxicity reduction and biodegradability augmentation. *Water Sci. Technol.* **2015**, *71* (7), 1097–1105.
- (158) Raghunath, B. V.; Punthagairasi, A.; Rajarajan, G.; Irshad, A.; Elango, A.; Mahesh

- kumar, G. Impact of dairy effluent on environment—a review. In *Integrated Waste Management in India. Environmental Science and Engineering*; Springer, Cham, 2016; pp 239–249.
- (159) Särkkä, H.; Vepsäläinen, M.; Sillanpää, M. Natural organic matter (NOM) removal by electrochemical methods — A review. *J. Electroanal. Chem.* **2015**, *755*, 100–108.
- (160) Vidal, G.; Carvalho, A.; Méndez, R.; Lema, J. M. Influence of the content in fats and proteins on the anaerobic biodegradability of dairy wastewaters. *Bioresour. Technol.* **2000**, *74* (3), 231–239.
- (161) Kushwaha, J. P.; Srivastava, V. C.; Mall, I. D. An overview of various technologies for the treatment of dairy wastewaters. *Crit. Rev. Food Sci. Nutr.* **2011**, *51* (5), 442–452.
- (162) Carta, F.; Alvarez, P.; Romero, F.; Pereda, J. Aerobic purification of dairy wastewater in continuous regime; reactor with support. *Process Biochem.* **1999**, *34* (6), 613–619.
- (163) Omil, F.; Garrido, J. M.; Arrojo, B.; Méndez, R. Anaerobic filter reactor performance for the treatment of complex dairy wastewater at industrial scale. *Water Res.* **2003**, *37* (17), 4099–4108.
- (164) Koster, I. W. Abatement of long-chain fatty acid inhibition of methanogenesis by calcium addition. *Biol. Wastes* **1987**, *22* (4), 295–301.
- (165) Kushwaha, J. P.; Chandra Srivastava, V.; Mall, I. D. Treatment of dairy wastewater by inorganic coagulants: Parametric and disposal studies. *Water Res.* **2010**, *44* (20), 5867–5874.
- (166) Melchioris, M. S.; Piovesan, M.; Becegato, V. R.; Becegato, V. A.; Tambourgi, E. B.; Paulino, A. T. Treatment of wastewater from the dairy industry using electroflocculation and solid whey recovery. *J. Environ. Manage.* **2016**, *182*, 574–580.
- (167) Luo, J.; Ding, L.; Qi, B.; Jaffrin, M. Y.; Wan, Y. A two-stage ultrafiltration and nanofiltration process for recycling dairy wastewater. *Bioresour. Technol.* **2011**, *102* (16), 7437–7442.
- (168) Chollangi, A.; Hossain, M. M. Separation of proteins and lactose from dairy wastewater. *Chem. Eng. Process. Process Intensif.* **2007**, *46* (5), 398–404.
- (169) Aghili, F.; Ghoreyshi, A. A.; Rahimpour, A.; Rahimnejad, M. Enhanced treatment of pretreated sour whey by PAC adsorption/membrane process. *Chem. Eng. Process. Process*



- Intensif.* **2016**, *99*, 80–85.
- (170) Madaeni, S. S.; Mansourpanah, Y. Chemical cleaning of reverse osmosis membranes fouled by whey. *Desalination* **2004**, *161* (1), 13–24.
- (171) Teh, C. Y.; Budiman, P. M.; Shak, K. P. Y.; Wu, T. Y. Recent advancement of coagulation–flocculation and its application in wastewater treatment. *Ind. Eng. Chem. Res.* **2016**, *55* (16), 4363–4389.
- (172) Chen, W.; Liu, J. The possibility and applicability of coagulation-MBR hybrid system in reclamation of dairy wastewater. *Desalination* **2012**, *285*, 226–231.
- (173) Ji, J.; Qiu, J.; Wai, N.; Wong, F.-S.; Li, Y. Influence of organic and inorganic flocculants on physical–chemical properties of biomass and membrane-fouling rate. *Water Res.* **2010**, *44* (5), 1627–1635.
- (174) Formentini-Schmitt, D. M.; Alves, Á. C. D.; Veit, M. T.; Bergamasco, R.; Vieira, A. M. S.; Fagundes-Klen, M. R. Ultrafiltration combined with coagulation/ flocculation/ sedimentation using *Moringa oleifera* as coagulant to treat dairy industry wastewater. *Water, Air, Soil Pollut.* **2013**, *224* (9), 1682.
- (175) Rusten, B.; Lundar, A.; Eide, O.; Ødegaard, H. Chemical pretreatment of dairy wastewater. *Water Sci. Technol.* **1993**, *28* (2), 67–76.
- (176) Selmer-Olsen, E.; Ratanweera, H. C.; Pehrson, R. A novel treatment process for dairy wastewater with chitosan produced from shrimp-shell waste. *Water Sci. Technol.* **1996**, *34* (11), 33–40.
- (177) Hamdani, A.; Chennaoui, M.; Assobhei, O. Dairy effluent characterizat on and treatment by coagulation decantation. *Lait* **2004**, *84* (3), 317–328.
- (178) Sarkar, B.; Chakrabarti, P. P.; Vijaykumar, A.; Kale, V. Wastewater treatment in dairy industries — possibility of reuse. *Desalination* **2006**, *195* (1–3), 141–152.
- (179) Tchamango, S.; Nanseu-Njiki, C. P.; Ngameni, E.; Hadjiev, D.; Darchen, A. Treatment of dairy effluents by electrocoagulation using aluminium electrodes. *Sci. Total Environ.* **2010**, *408* (4), 947–952.
- (180) Rivas, J.; Prazeres, A. R.; Carvalho, F. Treatment of cheese whey wastewater: combined coagulation-flocculation and aerobic biodegradation. *J. Agric. Food Chem* **2010**, *58*, 7871–7877.

- (181) Prakash, N.; Garg, A. Comparative performance evaluation of physicochemical treatment processes for simulated dairy wastewater. *Int. J. Environ. Sci. Technol.* **2016**, *13* (11), 2675–2688.
- (182) Loloie, M.; Nekonom, G.; Alidadi, H.; Kor, Y. Study of the coagulation process in wastewater treatment of dairy industries. *Int. J. Environ. Health Eng.* **2014**, *3* (1), 17–21.
- (183) Husein, M. M.; Al-As'ad, A. Effect of coagulant and flocculant addition scheme on the treatment of dairy farm wastewater. *J. Water Reuse Desalin.* **2015**, *5* (3), 271–281.
- (184) Hadjivassilis, I.; Gajdos, S.; Vanco, D.; Nicolaou, M. Treatment of wastewater from the potato chips and snacks manufacturing industry. *Water Sci. Technol.* **1997**, *36* (2–3), 329–335.
- (185) Sajjad Haydar, Ghulam Hussain, Obaidullah Nadeem, Husnain Haider, A.J. Bari, A. H. Performance evaluation of anaerobic-aerobic treatment for the wastewater of potato processing industry: A case study of a local chips factory. *Pakistan J. Eng. Appl. Sci.* **2014**, *14*, 27–37.
- (186) Kobya, M.; Hiz, H.; Senturk, E.; Aydiner, C.; Demirbas, E. Treatment of potato chips manufacturing wastewater by electrocoagulation. *Desalination* **2006**, *190* (1–3), 201–211.
- (187) Krzemińska, D.; Neczaj, E.; Borowski, G. Advanced oxidation processes for food industrial wastewater decontamination. *J. Ecol. Eng.* **2015**, *16* (2), 61–71.
- (188) Wu, D.; Yang, Z.; Wang, W.; Tian, G.; Xu, S.; Sims, A. Ozonation as an advanced oxidant in treatment of bamboo industry wastewater. *Chemosphere* **2012**, *88* (9), 1108–1113.
- (189) Asghar, A.; Abdul Raman, A. A.; Wan Daud, W. M. A. Advanced oxidation processes for in-situ production of hydrogen peroxide/hydroxyl radical for textile wastewater treatment: a review. *J. Clean. Prod.* **2015**, *87*, 826–838.
- (190) Lin, K. C. Aeration of anaerobically treated potato-processing wastewater. *Agric. Wastes* **1985**, *12* (1), 1–11.
- (191) Malladi, B.; Ingham, S. C. Thermophilic aerobic treatment of potato-processing wastewater. *World J. Microbiol. Biotechnol.* **1993**, *9* (1), 45–49.
- (192) Kalyuzhnyi, S.; de los Santos, L. E.; Martinez, J. R. Anaerobic treatment of raw and preclarified potato-maize wastewaters in a USAB reactor. *Bioresour. Technol.* **1998**, *66* (3),

- 195–199.
- (193) El-Gohary, F. A.; Nasr, F. A.; Aly, H. I. Cost-effective pre-treatment of food-processing industrial wastewater. *Water Sci. Technol.* **1999**, *40* (7), 17–24.
- (194) Sayed, S. K. I.; El-Ezaby, K. H.; Groendijk, L. Treatment of potato processing wastewater using a membrane bioreactor. *Ninth Int. Water Technol. Conf.* **2005**, 53–68.
- (195) Ma, J.; Van Wambeke, M.; Carballa, M.; Verstraete, W. Improvement of the anaerobic treatment of potato processing wastewater in a UASB reactor by co-digestion with glycerol. *Biotechnol. Lett.* **2008**, *30* (5), 861–867.
- (196) Kupusović, T.; Milanolo, S.; Selmanagić, D. Two-stage aerobic treatment of wastewater: a case study from potato chips industry. *Polish J. Environ. Stud.* **2009**, *18* (6), 1045–1050.
- (197) Haydar, S.; Hussain, G.; Nadeem, O.; Haider, H.; Bari, A. J.; Hayee, A. Performance evaluation of anaerobic-aerobic treatment for the wastewater of potato processing industry: a case study of a local chips factory. *Pakistan J. Eng. Appl. Sci.* **2014**, *14*, 27–37.
- (198) Manhokwe, S.; Parawira, W.; Zvidzai, C. Aerobic mesophilic treatment of potato industry wastewater. *Int. J. Water Resour. Environ. Eng.* **2015**, *7* (7), 92–100.
- (199) Arslan, A.; Topkaya, E.; Özbay, B.; Özbay, I.; Veli, S. Application of O<sub>3</sub>/UV/H<sub>2</sub>O<sub>2</sub> oxidation and process optimization for treatment of potato chips manufacturing wastewater. *Water Environ. J.* **2017**, *31* (1), 64–71.
- (200) Hernandez-Barajas, J.; Wandrey, C.; Hunkeler, D. Polymer flocculants with improved dewatering characteristics. U.S. Pat. 6,667,374 B2, 2003.
- (201) Rasteiro, M. G.; Garcia, F. A. P.; Ferreira, P. J.; Antunes, E.; Hunkeler, D.; Wandrey, C. Flocculation by cationic polyelectrolytes: Relating efficiency with polyelectrolyte characteristics. *J. Appl. Polym. Sci.* **2010**, *116*, 3603–3612.
- (202) Crespy, D.; Landfester, K. Synthesis of polyvinylpyrrolidone/silver nanoparticles hybrid latex in non-aqueous miniemulsion at high temperature. *Polymer (Guildf)*. **2009**, *50* (7), 1616–1620.
- (203) Chen, S.-C.; Liao, C.-M. Health risk assessment on human exposed to environmental polycyclic aromatic hydrocarbons pollution sources. *Sci. Total Environ.* **2006**, *366* (1), 112–123.

- (204) Abramson, S.; Safraou, W.; Malezieux, B.; Dupuis, V.; Borensztajn, S.; Briot, E.; Bée, A. An eco-friendly route to magnetic silica microspheres and nanospheres. *J. Colloid Interface Sci.* **2011**, *364* (2), 324–332.
- (205) Lu, Y.; Larock, R. C. New hybrid latexes from a soybean oil-based waterborne polyurethane and acrylics via emulsion polymerization. *Biomacromolecules* **2007**, *8* (10), 3108–3114.
- (206) Xia, Y.; Larock, R. C. Vegetable oil-based polymeric materials: synthesis, properties, and applications. *Green Chem.* **2010**, *12* (11), 1893–1909.
- (207) Carmichael, K. M.; Limer, A. J.; Colver, P. J.; Chahal, S. P. Inverse emulsions comprising an alkoxyated ester oil. U.S. Patent No. 9,044,622.
- (208) Villarroja, S.; Thurecht, K. J.; Howdle, S. M. HRP-mediated inverse emulsion polymerisation of acrylamide in supercritical carbon dioxide. *Green Chem.* **2008**, *10* (8), 863–867.
- (209) Chang, K. T.; Wells, K. E.; Mello, J. V. Environmentally friendly dispersion system used in the preparation of inverse emulsion polymers. U.S. Patent No. 9,193,898., 2015.
- (210) Quinn, J.; Clausen, C.; Coon, C.; Berger, C. M.; Canaveral, C.; Gulakowski, P. E.; Kugel, A. E. J. Removal of PCB and other halogenated organic contaminants found in ex situ structures. U.S. Patent No. 7,271,199, 2007.
- (211) Pérez-Mosqueda, L. M.; Ramírez, P.; Trujillo-Cayado, L. A.; Santos, J.; Muñoz, J. Development of eco-friendly submicron emulsions stabilized by a bio-derived gum. *Colloids Surfaces B Biointerfaces* **2014**, *123*, 797–802.
- (212) Rawlings, A. V.; Lombard, K. J. A review on the extensive skin benefits of mineral oil. *Int. J. Cosmet. Sci.* **2012**, *34* (6), 511–518.
- (213) Kim, E.; Nam, G. W.; Kim, S.; Lee, H.; Moon, S.; Chang, I. Influence of polyol and oil concentration in cosmetic products on skin moisturization and skin surface roughness. *Skin Res. Technol.* **2007**, *13* (4), 417–424.
- (214) Nash, J. F.; Gettings, S. D.; Diembeck, W.; Chudowski, M.; Kraus, A. L. A toxicological review of topical exposure to white mineral oils. *Food Chem. Toxicol.* **1996**, *34* (2), 213–225.
- (215) Kam, S.; Gregory, J. Charge determination of synthetic cationic polyelectrolytes by

- colloid titration. *Colloids Surfaces A Physicochem. Eng. Asp.* **1999**, *159* (1), 165–179.
- (216) Bourdillon, L.; Hunkeler, D.; Wandrey, C. The analytical ultracentrifuge for the characterization of polydisperse polyelectrolytes. *Anal. Ultracentrifugation VIII* **2006**, *131*, 141–149.
- (217) Malvern Instruments, “Zetasizer Nano Series User Manual.”
- (218) Murugan, R.; Mohan, S.; Bigotto, A. FTIR and polarised Raman spectra of acrylamide and polyacrylamide. *J. Korean Phys. Soc.* **1998**, *32* (4), 505–512.
- (219) Larkin, P. *Infrared and Raman spectroscopy; principles and spectral interpretation*; Elsevier, 2011.
- (220) Trichard, L.; Fattal, E.; Le Bas, G.; Duchêne, D.; Grossiord, J.-L.; Bochot, A. Formulation and characterisation of beads prepared from natural cyclodextrins and vegetable, mineral or synthetic oils. *Int. J. Pharm.* **2008**, *354* (1–2), 88–94.
- (221) Armanet, L.; Hunkeler, D. Phase inversion of polyacrylamide based inverse-emulsions: Effect of the surfactant and monomer on postinversion equilibrium properties. *J. Appl. Polym. Sci.* **2007**, *106* (4), 2328–2341.
- (222) Jarvis, P.; Parsons, S. A.; Henderson, R.; Nixon, N.; Jefferson, B. The practical application of fractal dimension in water treatment practice—the impact of polymer dosing. *Sep. Sci. Technol.* **2008**, *43* (7), 1785–1797.
- (223) Matralis, A.; Sotiropoulou, M.; Bokias, G.; Staikos, G. Water-soluble stoichiometric polyelectrolyte complexes based on cationic comb-type copolymers. *Macromol. Chem. Phys.* **2006**, *207* (12), 1018–1025.
- (224) Li, X.; Zheng, H.; Gao, B.; Zhao, C.; Sun, Y. UV-initiated polymerization of acid- and alkali-resistant cationic flocculant P(AM-MAPTAC): Synthesis, characterization, and application in sludge dewatering. *Sep. Purif. Technol.* **2017**, *187*, 244–254.
- (225) Oberlerchner, J.; Rosenau, T.; Potthast, A. Overview of methods for the direct molar mass determination of cellulose. *Molecules* **2015**, *20* (6), 10313–10341.
- (226) Lounis, F. M.; Chamieh, J.; Gonzalez, P.; Cottet, H.; Leclercq, L. Prediction of polyelectrolyte complex stoichiometry for highly hydrophilic polyelectrolytes. *Macromolecules* **2016**, *49* (10), 3881–3888.
- (227) Dai, F.; Sun, P.; Liu, Y.; Liu, W. Redox-cleavable star cationic PDMAEMA by arm-first approach of ATRP as a nonviral vector for gene delivery. *Biomaterials* **2010**, *31* (3), 559–

- 569.
- (228) Beija, M.; Afonso, C. A. M.; Farinha, J. P. S.; Charreyre, M.-T.; Martinho, J. M. G. Novel malachite green- and rhodamine B-labeled cationic chain transfer agents for RAFT polymerization. *Polymer (Guildf)*. **2011**, *52* (26), 5933–5946.
- (229) Qi, G.; Li, H.; Zhu, R.; Zhang, Z.; Zhou, L.; Kuang, J. Synthesis, characterization, and solution behavior of a long-chain hydrophobic association anionic acrylamide/2-acrylamido-2-methylpropanesulfonic acid/n-octyl acrylate terpolymers. *Arab. J. Sci. Eng.* **2017**, *42* (6), 2425–2432.
- (230) Sharma, B. R.; Dhuldhoya, N. C.; Merchant, U. C. Flocculants—an ecofriendly approach. *J. Polym. Environ.* **2006**, *14* (2), 195–202.
- (231) Liang, L.; Peng, Y.; Tan, J.; Xie, G. A review of the modern characterization techniques for flocs in mineral processing. *Miner. Eng.* **2015**, *84*, 130–144.
- (232) Rasteiro, M. G.; Garcia, F. A. P.; del Mar Pérez, M. Applying LDS to monitor flocculation in papermaking. *Part. Sci. Technol.* **2007**, *25* (3), 303–308.
- (233) Rasteiro, M. G.; Garcia, F. A. P.; Ferreira, P.; Blanco, A.; Negro, C.; Antunes, E. The use of LDS as a tool to evaluate flocculation mechanisms. *Chem. Eng. Process. Process Intensif.* **2008**, *47* (8), 1323–1332.
- (234) Rasteiro, M. G.; Pinheiro, I.; Ferreira, P. J.; Garcia, F. A.; Wandrey, C.; Ahmadloo, H.; Hunkeler, D. Correlating aggregates structure with PEL characteristics using an experimental design methodology. *Procedia Eng.* **2015**, *102*, 1697–1706.
- (235) Chakraborti, R. K.; Gardner, K. H.; Atkinson, J. F.; Van Benschoten, J. E. Changes in fractal dimension during aggregation. *Water Res.* **2003**, *37* (4), 873–883.
- (236) Antunes, E.; Garcia, F. A. P.; Blanco, A.; Negro, C.; Rasteiro, M. G. Evaluation of the flocculation and reflocculation performance of a system with calcium carbonate, cationic acrylamide co-polymers, and bentonite microparticles. *Ind. Eng. Chem. Res.* **2015**, *54* (1), 198–206.
- (237) Chakraborti, R. K.; Atkinson, J. F.; Benschoten, J. E. Van. Characterization of alum floc by image analysis. **2000**, *34* (18), 3969–3976.
- (238) Wågberg, L.; Eriksson, J. New equipment for detection of polymer induced flocculation of cellulosic fibres by using image analysis — application to microparticle

- systems. *Chem. Eng. J.* **2000**, *80* (1), 51–63.
- (239) Schmid, M.; Thill, A.; Purkhold, U.; Walcher, M.; Bottero, J. Y.; Ginestet, P.; Nielsen, P. H.; Wuertz, S.; Wagner, M. Characterization of activated sludge flocs by confocal laser scanning microscopy and image analysis. *Water Res.* **2003**, *37* (9), 2043–2052.
- (240) Teh, C. Y.; Wu, T. Y.; Juan, J. C. Potential use of rice starch in coagulation–flocculation process of agro-industrial wastewater: Treatment performance and flocs characterization. *Ecol. Eng.* **2014**, *71*, 509–519.
- (241) Daims, H.; Wagner, M. Quantification of uncultured microorganisms by fluorescence microscopy and digital image analysis. *Appl. Microbiol. Biotechnol.* **2007**, *75* (2), 237–248.
- (242) Costa, J. C.; Mesquita, D. P.; Amaral, A. L.; Alves, M. M.; Ferreira, E. C. Quantitative image analysis for the characterization of microbial aggregates in biological wastewater treatment: a review. *Environ. Sci. Pollut. Res.* **2013**, *20* (9), 5887–5912.
- (243) Bushell, G. C.; Yan, Y. D.; Woodfield, D.; Raper, J.; Amal, R. On techniques for the measurement of the mass fractal dimension of aggregates. *Adv. Colloid Interface Sci.* **2002**, *95* (1), 1–50.
- (244) De Clercq, B.; Lant, P. A.; Vanrolleghem, P. A. Focused beam reflectance technique for in situ particle sizing in wastewater treatment settling tanks. *J. Chem. Technol. Biotechnol.* **2004**, *79* (6), 610–618.
- (245) Thapa, K. B.; Qi, Y.; Hoadley, A. F. Using FBRM to investigate the sewage sludge flocculation efficiency of cationic polyelectrolytes. *Water Sci. Technol.* **2009**, *59* (3), 583–593.
- (246) Senaputra, A.; Jones, F.; Fawell, P. D.; Smith, P. G. Focused beam reflectance measurement for monitoring the extent and efficiency of flocculation in mineral systems. *AIChE J.* **2014**, *60* (1), 251–265.
- (247) Heath, A. R.; Fawell, P. D.; Bahri, P. A.; Swift, J. D. Estimating average particle size by focused beam reflectance measurement (FBRM). *Part. Part. Syst. Charact.* **2002**, *19* (2), 84–95.
- (248) Hamilton, J. *Time series analysis (Vol.2)*; Princeton university press: Princeton, New Jersey, 1994.
- (249) Wold, S.; Sjöström, M.; Eriksson, L. PLS-regression: a basic tool of chemometrics.

- Chemom. Intell. Lab. Syst.* **2001**, *58* (2), 109–130.
- (250) Warne, M. A.; Lenz, E. M.; Osborn, D.; Weeks, J. M.; Nicholson, J. K. Comparative biochemistry and short-term starvation effects on the earthworms *Eisenia veneta* and *Lumbricus terrestris* studied by <sup>1</sup>H NMR spectroscopy and pattern recognition. *Soil Biol. Biochem.* **2001**, *33* (9), 1171–1180.





---

# APPENDIX



## Appendix A

### Supporting information for Chapter 3: Health-friendly synthesis formulations

#### $^{13}\text{C}$ NMR SPECTRA

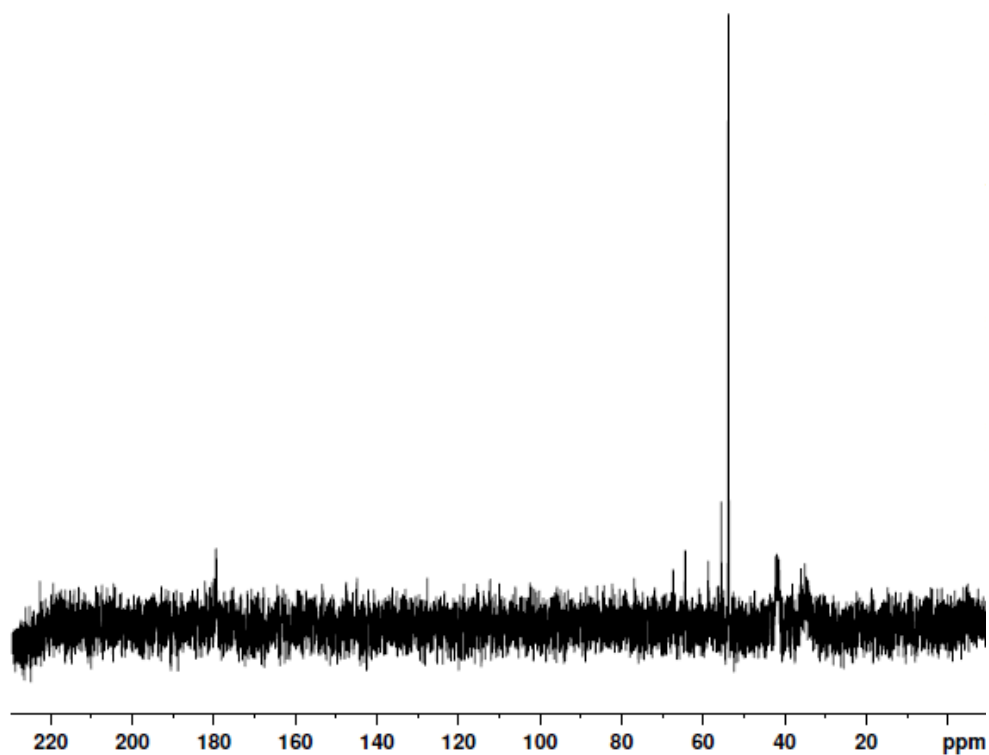


Figure A.1  $^{13}\text{C}$  NMR spectra for the Poly(AAm-AETAC) copolymer 40\_Carnation.

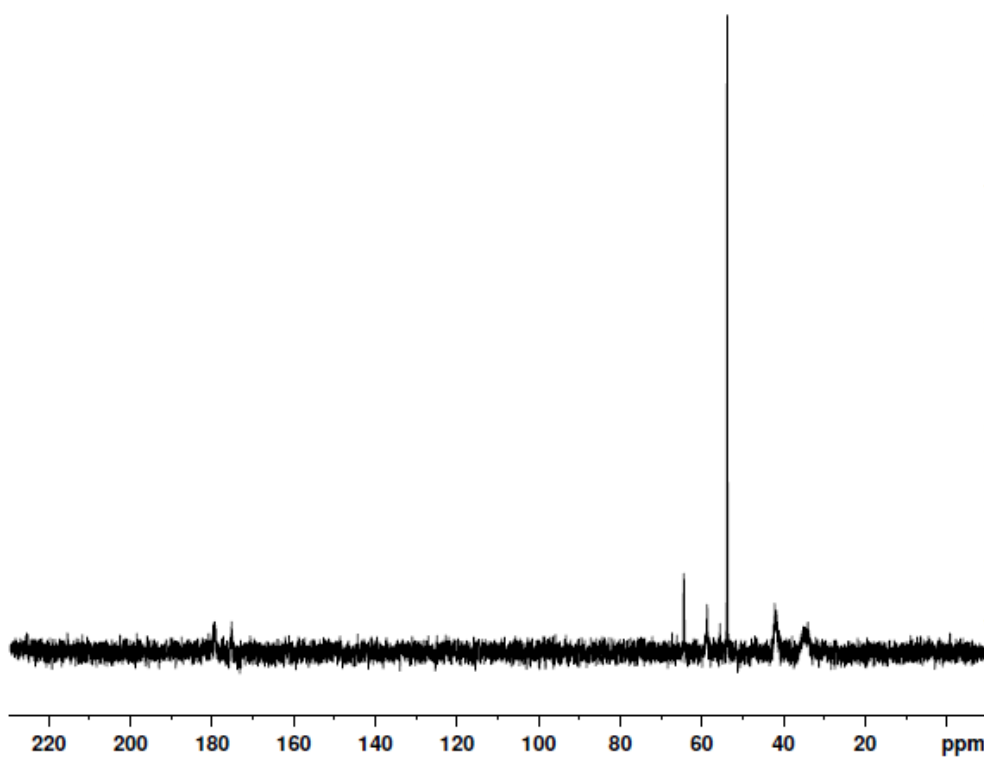


Figure A.2  $^{13}\text{C}$  NMR spectra for the Poly(AAm-AETAC) copolymer 60\_Carnation.

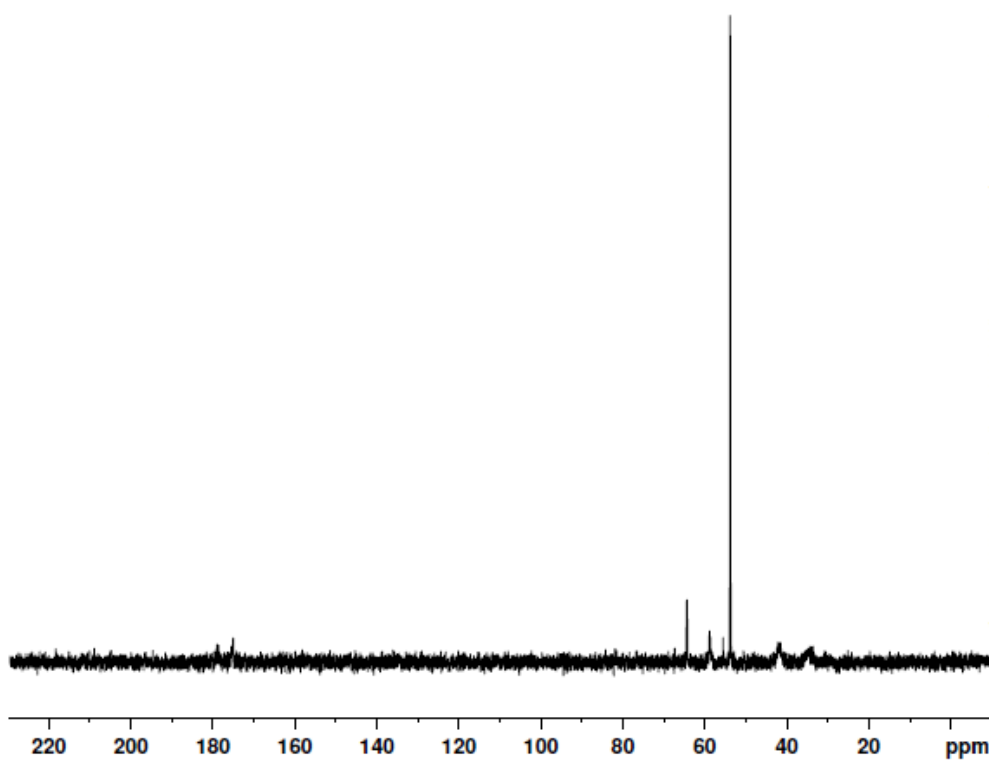


Figure A.3  $^{13}\text{C}$  NMR spectra for the Poly(AAm-AETAC) copolymer 80\_Puresyn4.

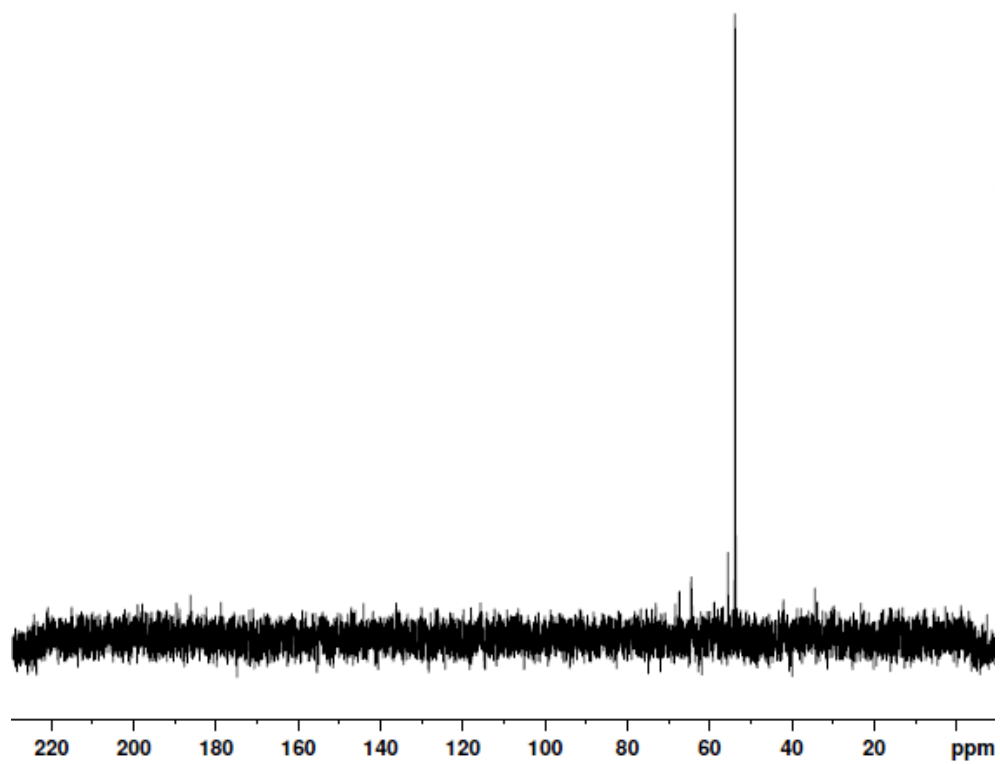
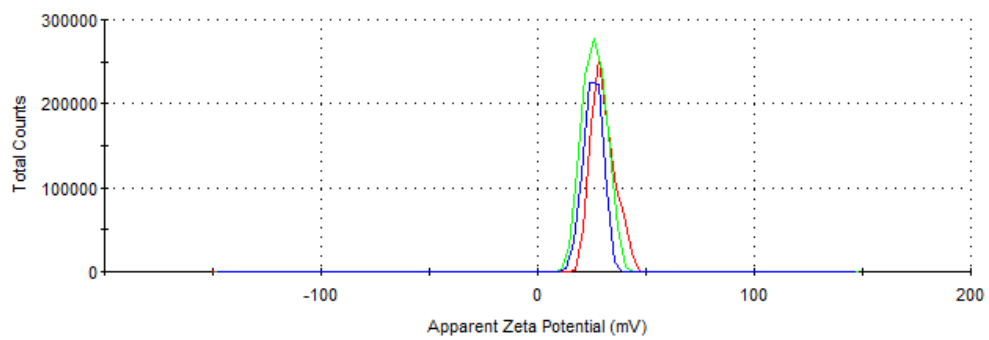
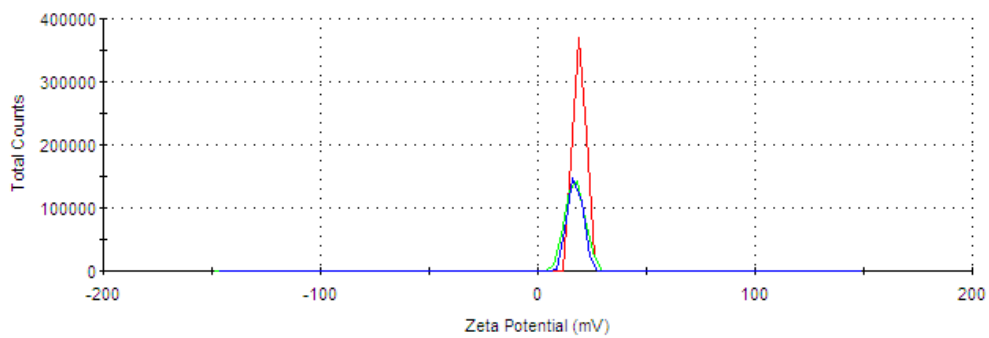


Figure A.4  $^{13}\text{C}$  NMR spectra for the Poly(AAm-AETAC) copolymer 80\_Carnation.

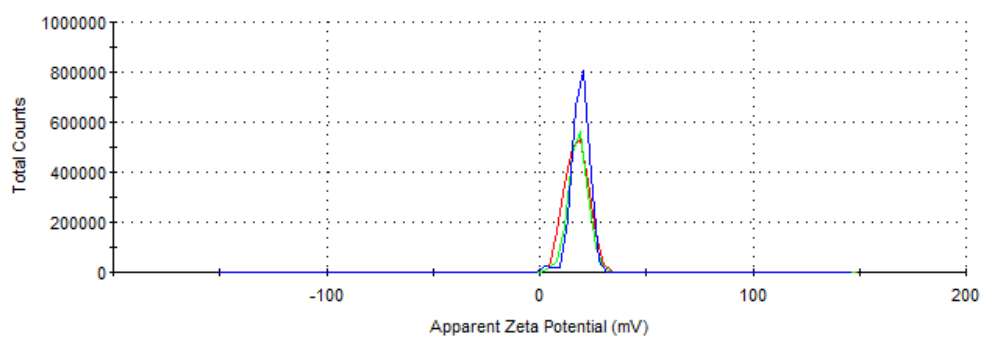
## ZETA POTENTIAL DISTRIBUTIONS



(a)

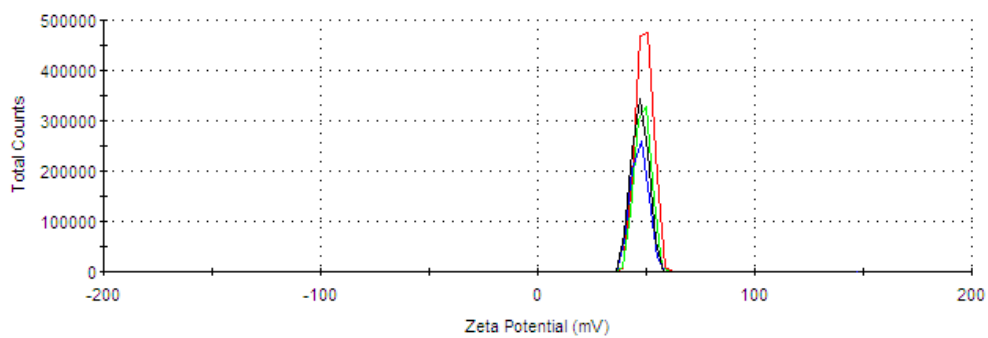


(b)

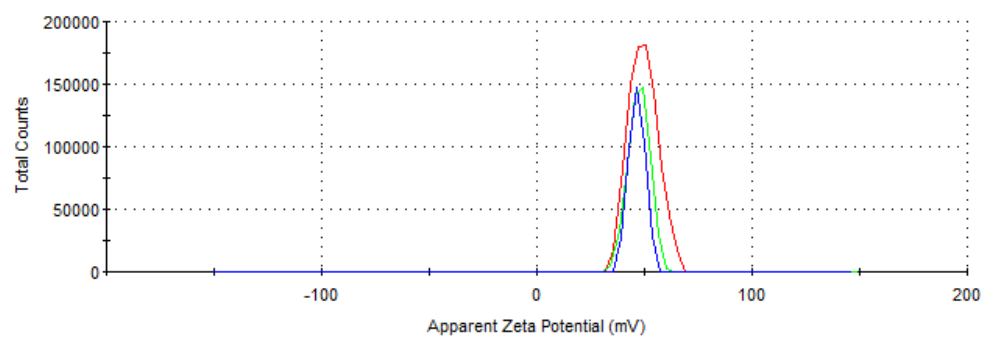


(c)

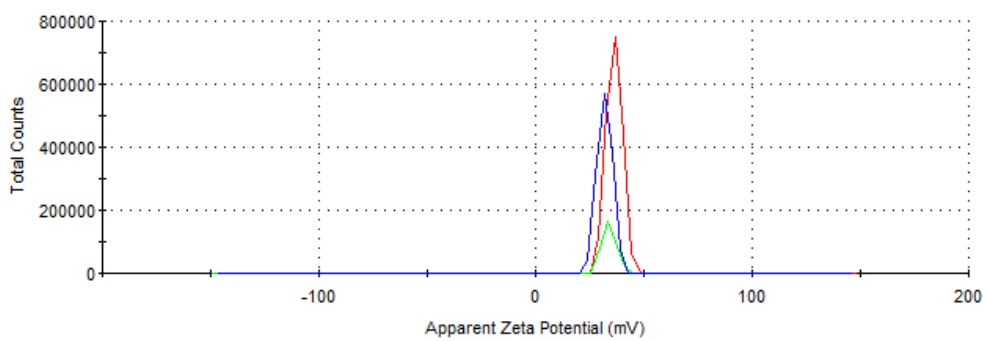
Figure A.5 Zeta potential distributions for 40 series polymers: (a) 40\_Puresyn4; (b) 40\_Carnation; (c) 40\_Marcol82.



(a)



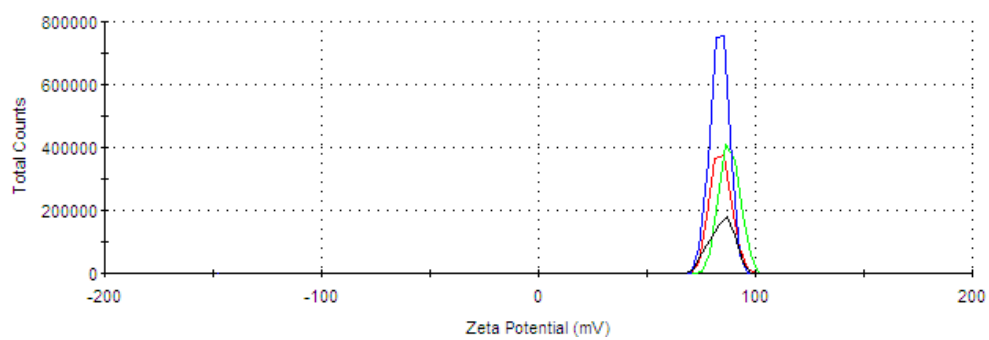
(b)



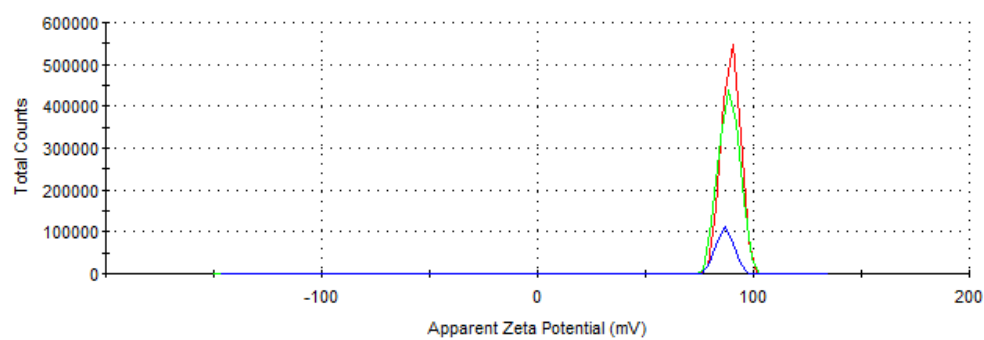
(c)

Figure A.6 Zeta potential distributions for 60 series polymers: (a) 60\_Puresyn4; (b) 60\_Carnation; (c) 60\_Marcol82.

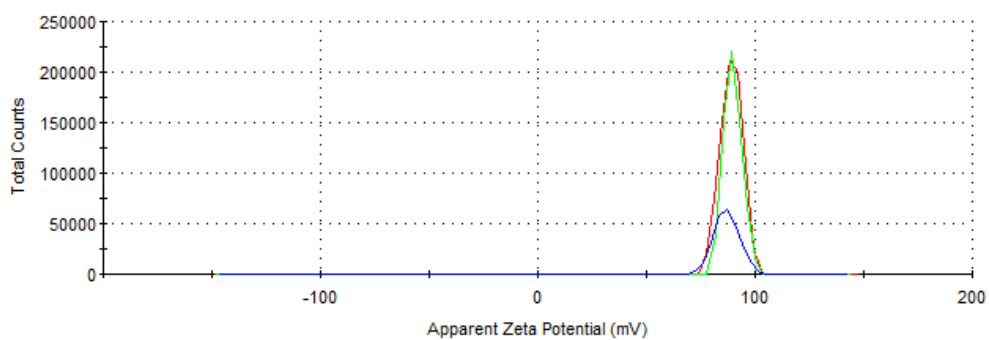




(a)



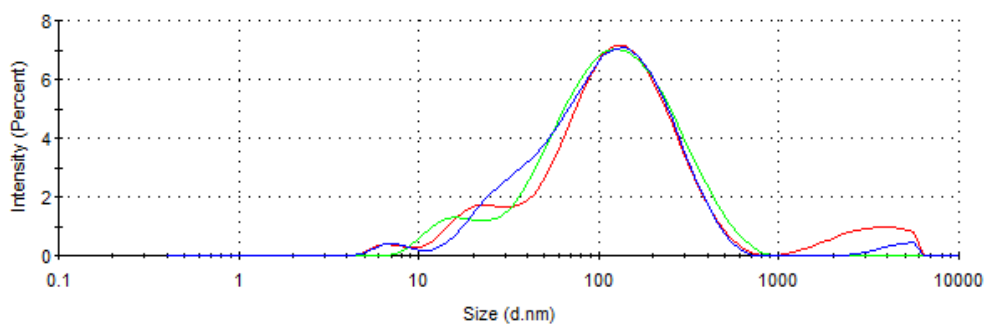
(b)



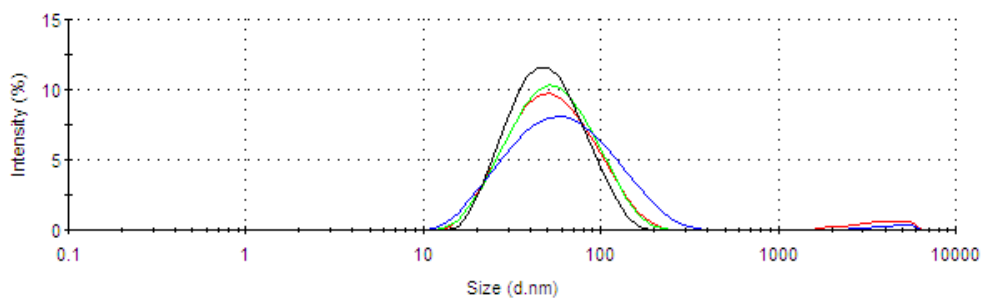
(c)

Figure A.7 Zeta potential distributions for 80 series polymers: (a) 80\_Puresyn4; (b) 80\_Carnation; (c) 80\_Marcol82.

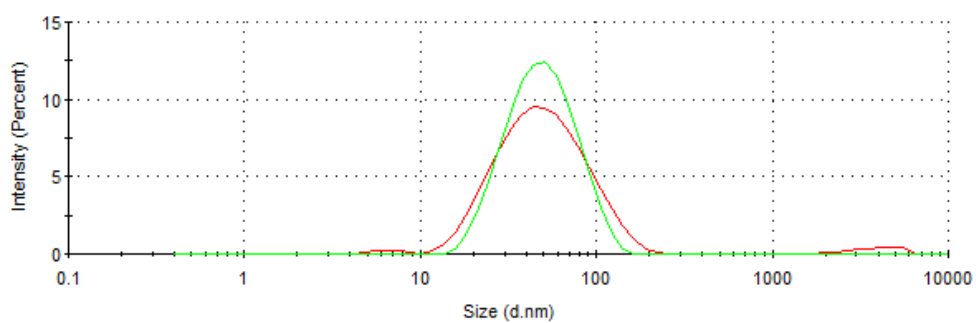
## HYDRODYNAMIC DIAMETER DISTRIBUTIONS



(a)

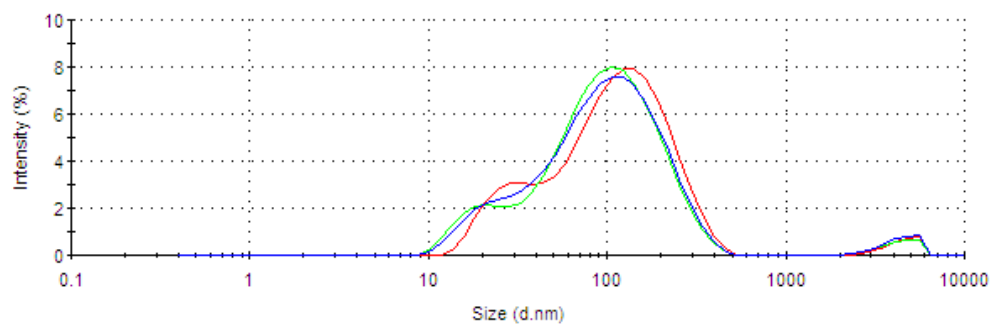


(b)

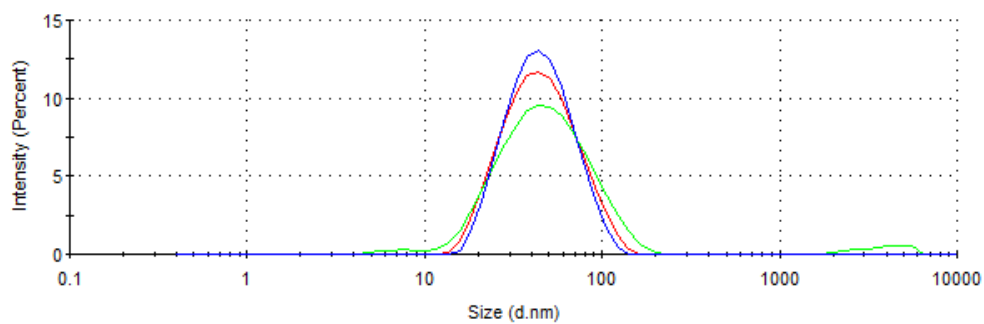


(c)

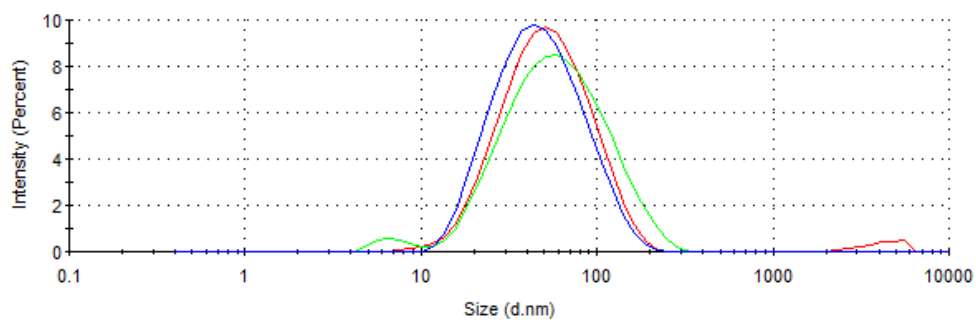
Figure A.8 Hydrodynamic diameter distributions for 40 series polymers: (a) 40\_Puresyn4; (b) 40\_Carnation; (c) 40\_Marcol82.



(a)

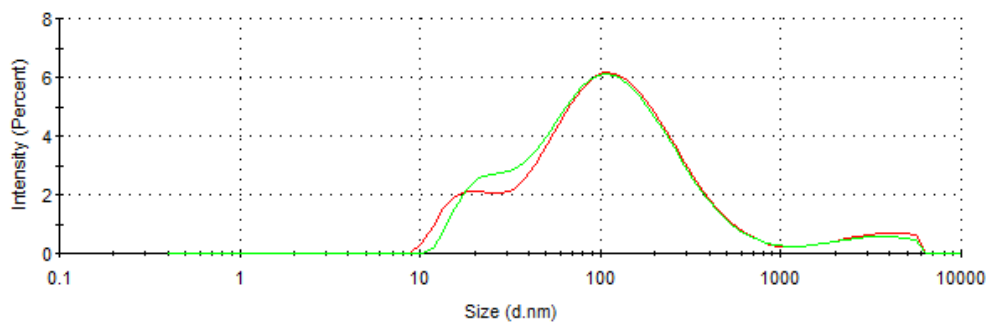


(b)

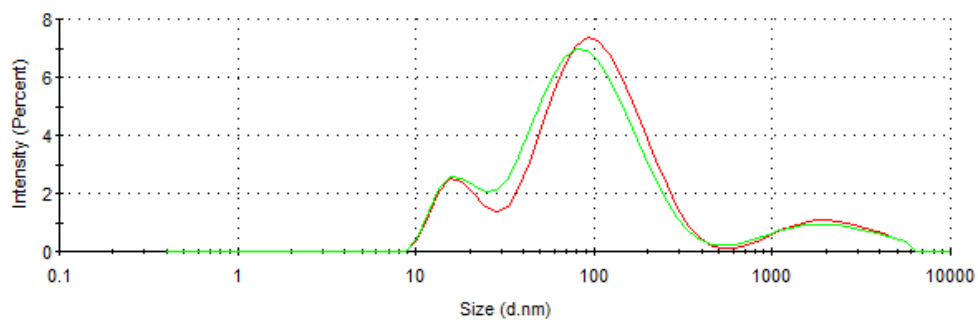


(c)

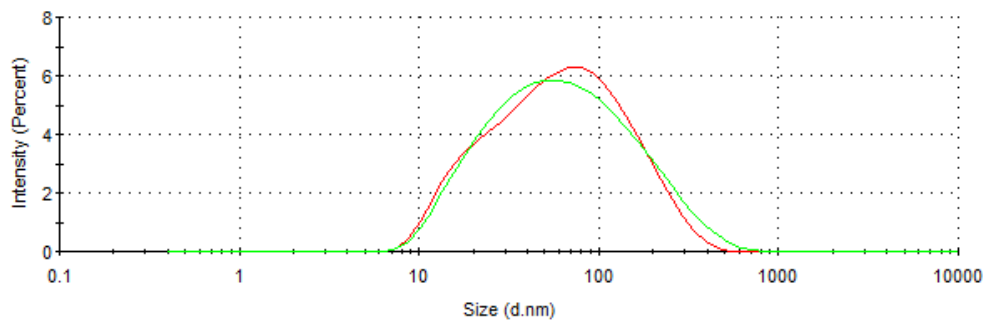
Figure A.9 Hydrodynamic diameter distributions for 60 series polymers: (a) 60\_Puresyn4; (b) 60\_Carnation; (c) 60\_Marcol82.



(a)



(b)

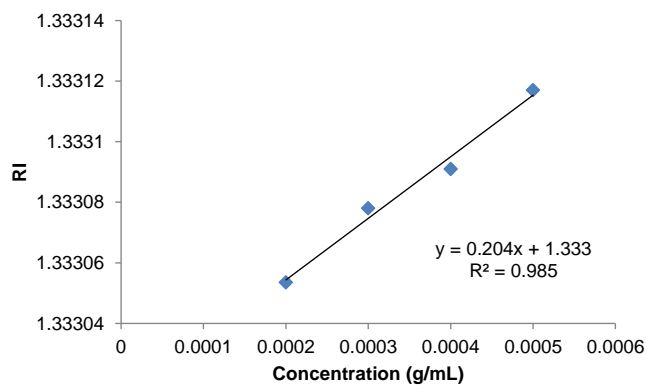


(c)

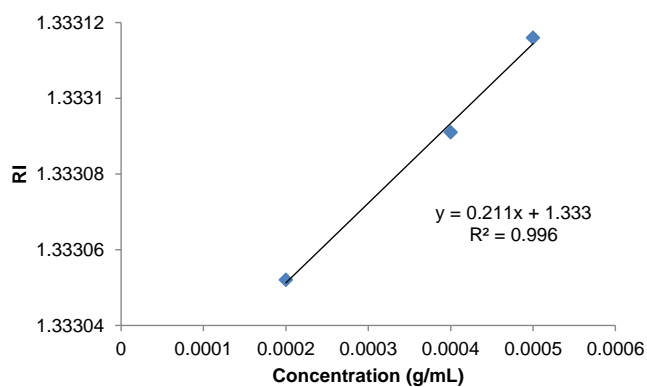
Figure A.10 Hydrodynamic diameter distributions for 80 series polymers: (a) 80\_Puresyn4; (b) 80\_Carnation; (c) 80\_Marcol82.

## MOLECULAR WEIGHT DETERMINATION BY SLS

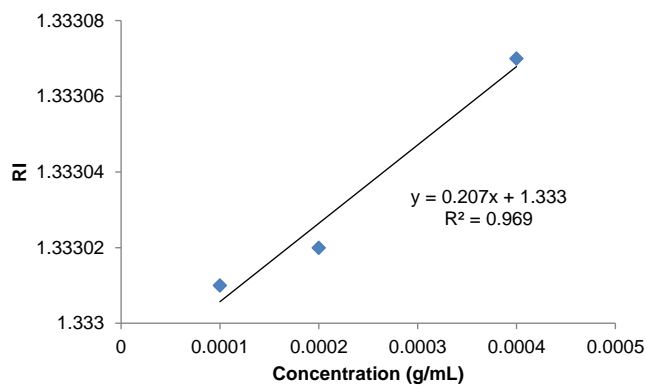
- Determination of  $dn/dc$



(a)

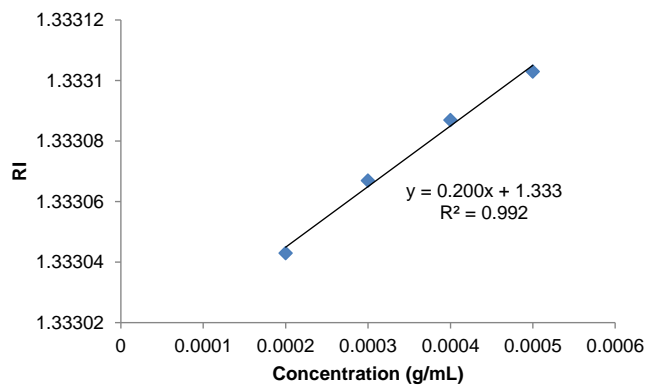


(b)

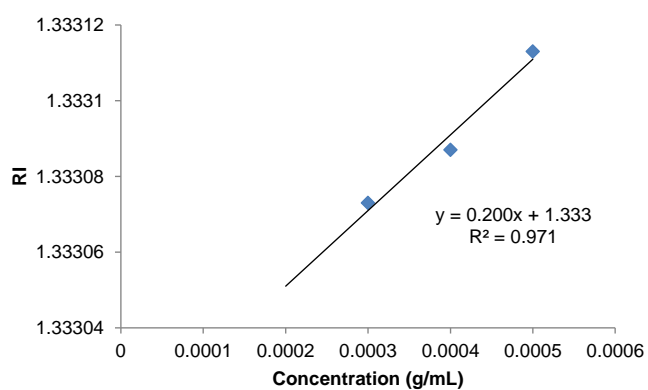


(c)

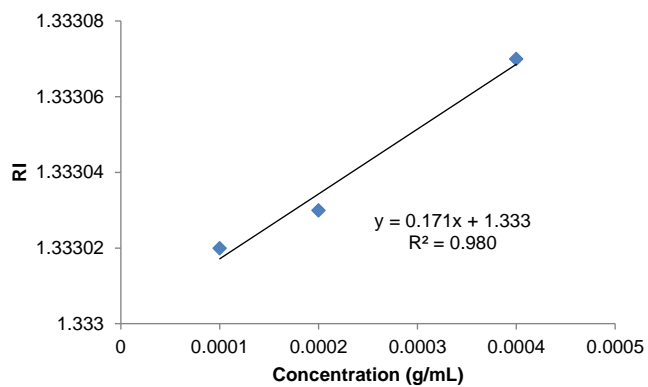
Figure A.11 Determination of the  $dn/dc$  value for 40 series polymers: (a) 40\_Puresyn4; (b) 40\_Carnation; (c) 40\_Marcol82.



(a)

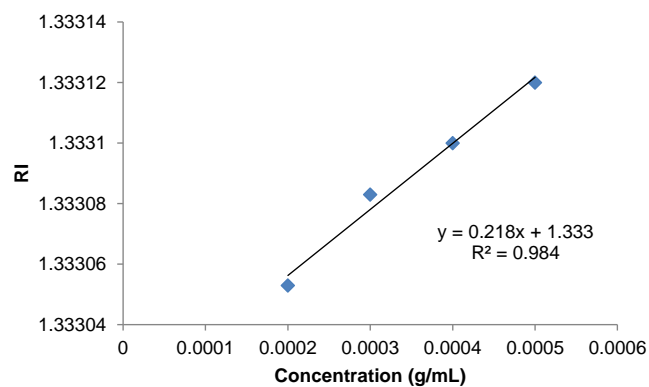


(b)

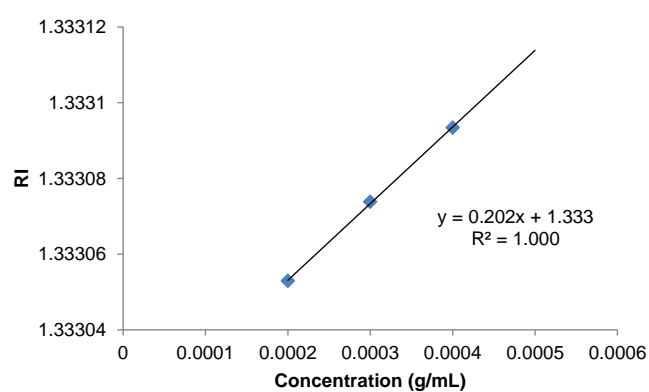


(c)

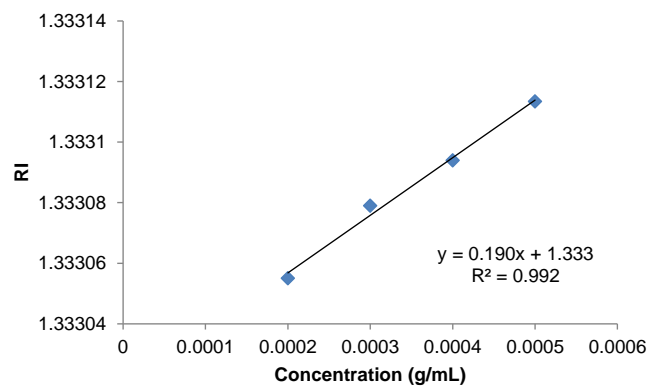
Figure A.12 Determination of the  $dn/dc$  value for 60 series polymers: (a) 60\_Puresyn4; (b) 60\_Carnation; (c) 60\_Marcol82.



(a)



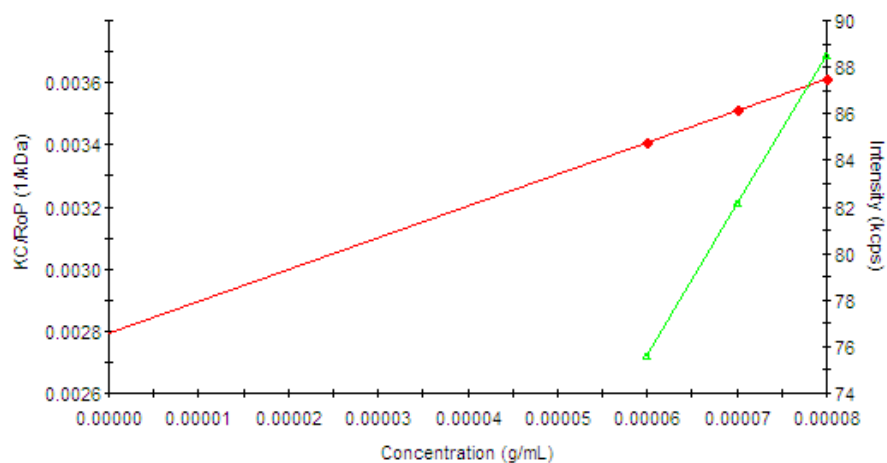
(b)



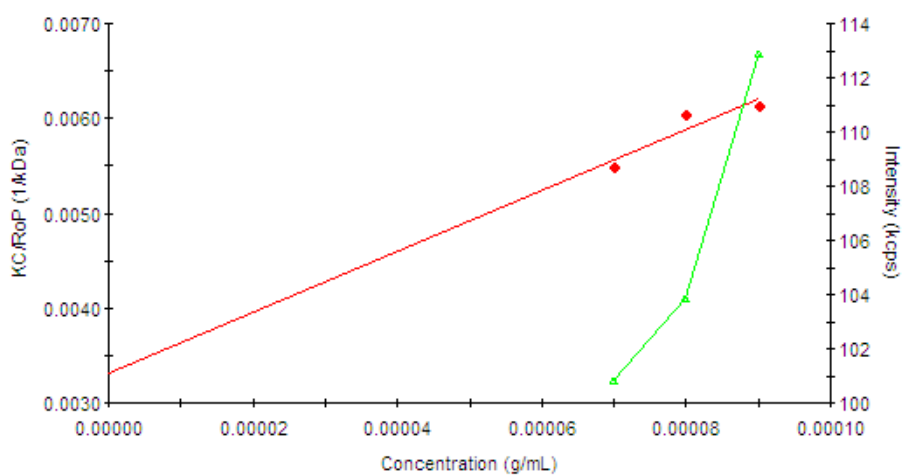
(c)

Figure A.13 Determination of the  $dn/dc$  value for 80 series polymers: (a) 80\_Puresyn4; (b) 80\_Carnation; (c) 80\_Marcol82.

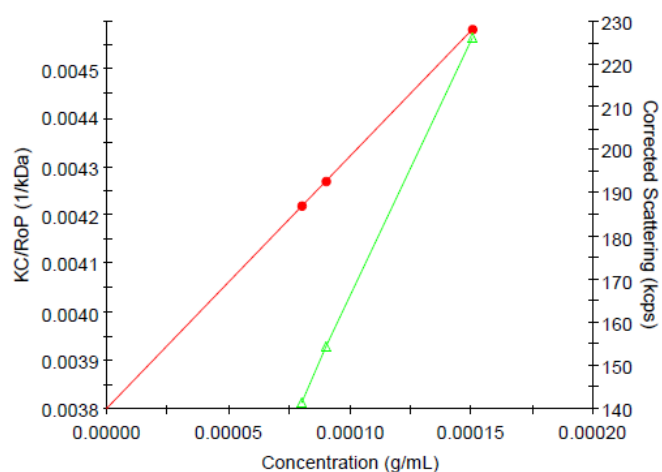
## - Determination of molecular weight



(a)



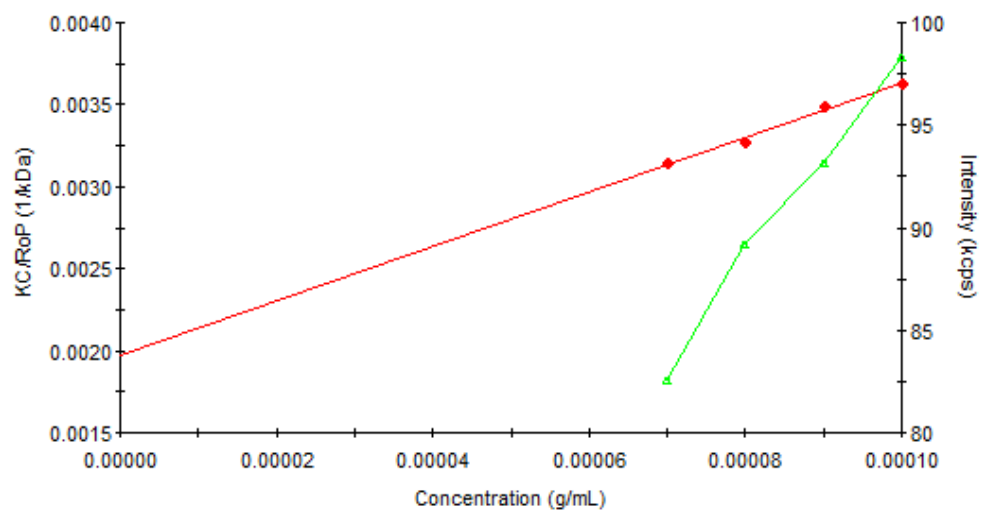
(b)



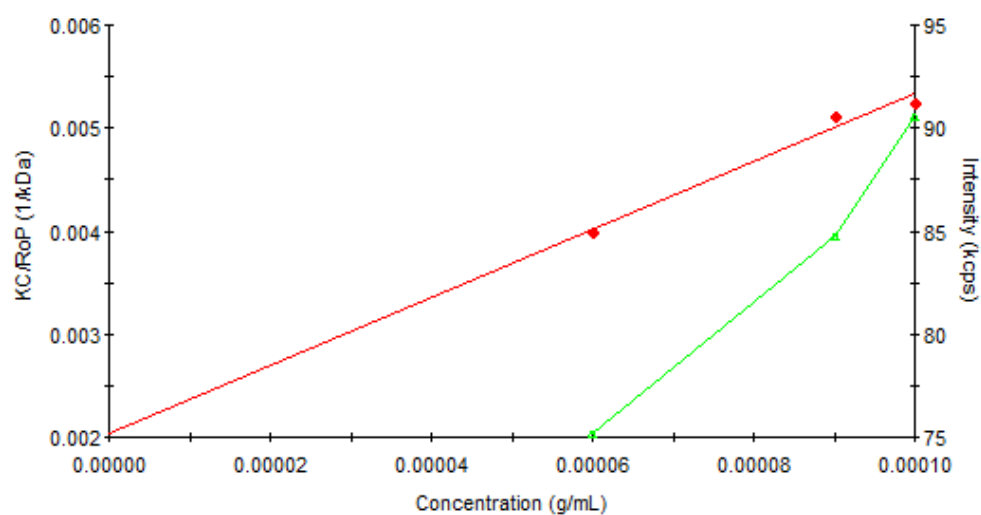
(c)

Figure A.14 Debye plot for weight-average molecular weight determination of 40 series polymers: (a) 40\_Puresyn4; (b) 40\_Carnation; (c) 40\_Marcol82.

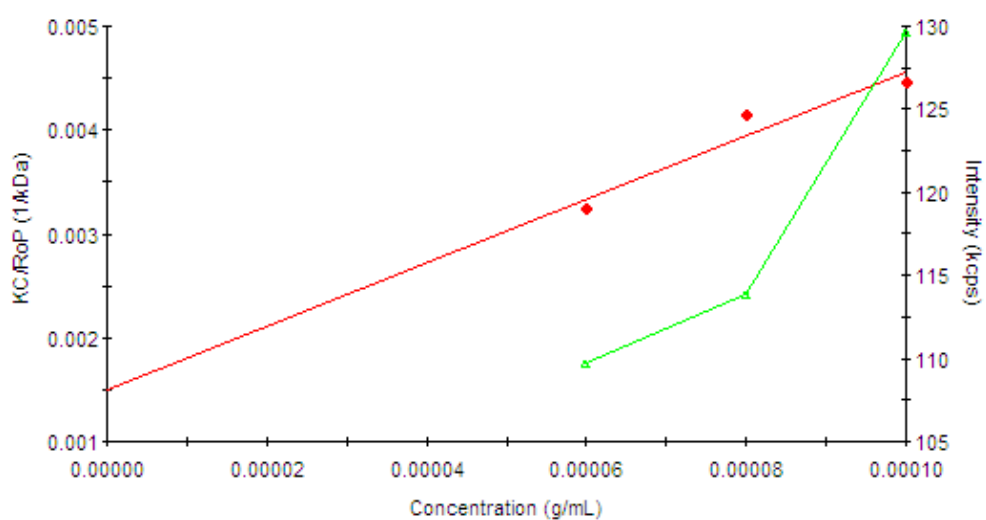




(a)

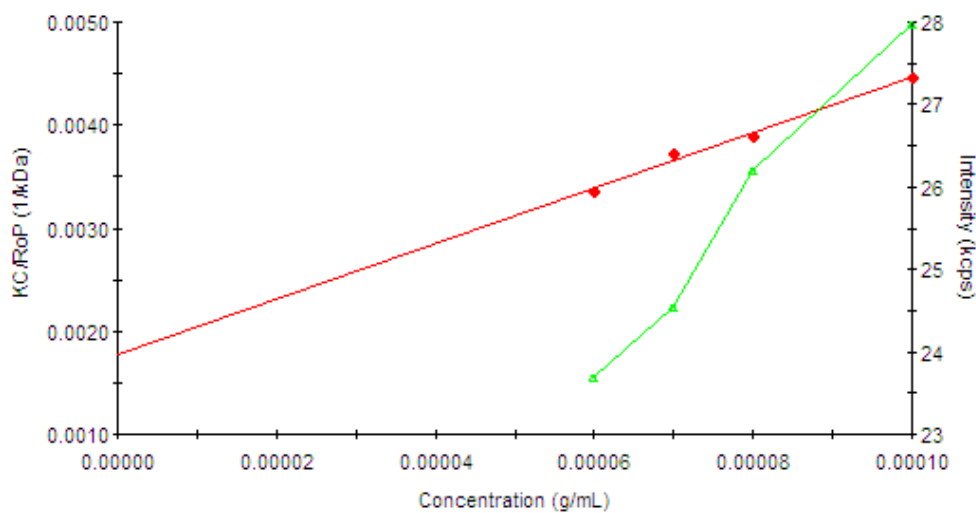


(b)

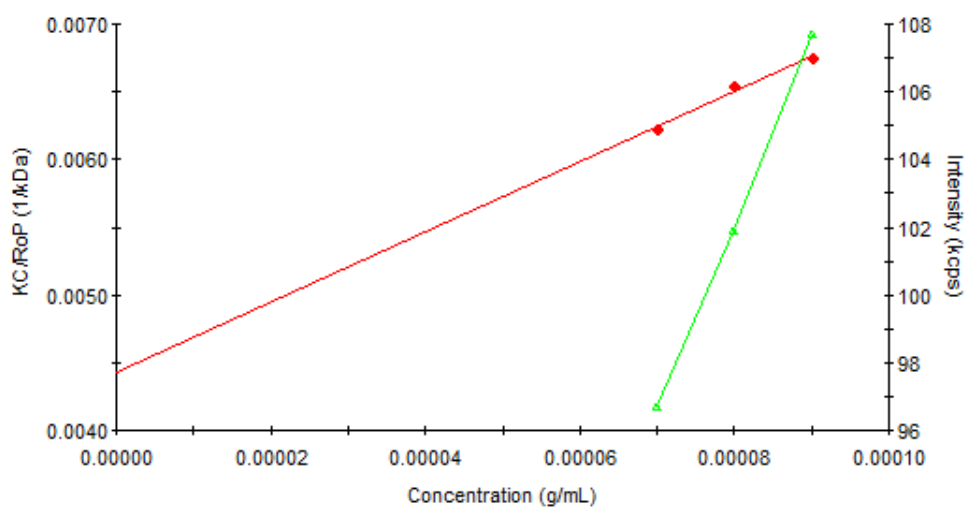


(c)

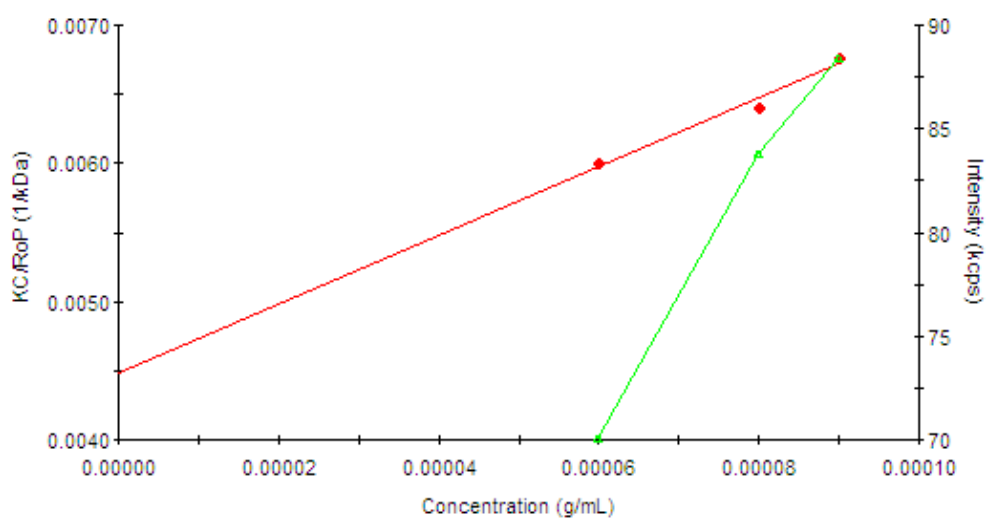
Figure A.15 Debye plot for weight-average molecular weight determination of 60 series polymers: (a) 60\_Puresyn4; (b) 60\_Carnation; (c) 60\_Marcol82.



(a)



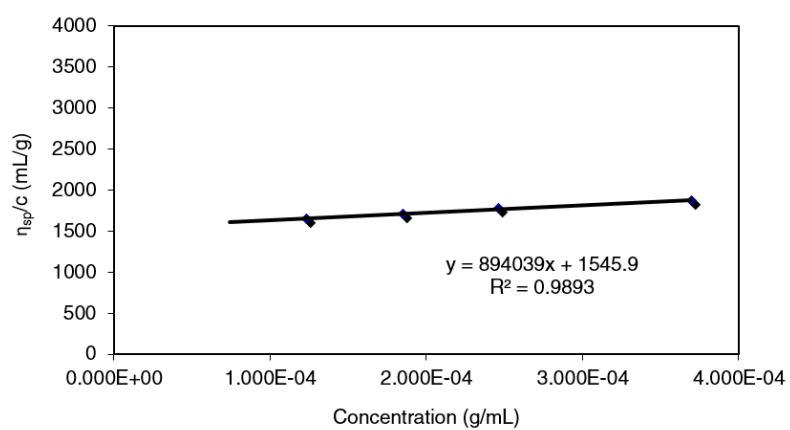
(b)



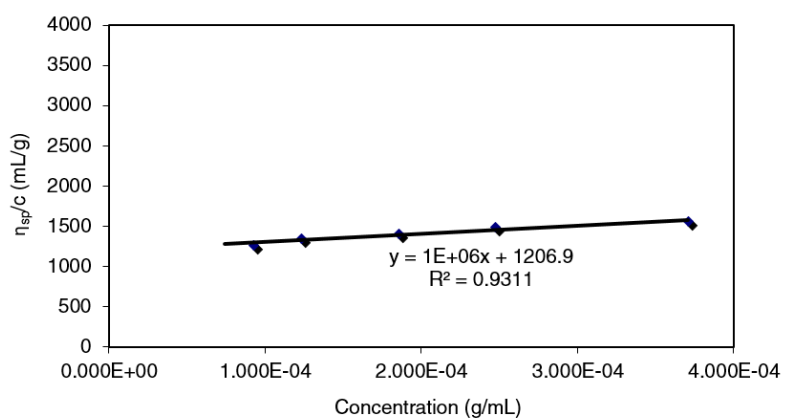
(c)

Figure A.16 Debye plot for weight-average molecular weight determination of 80 series polymers: (a) 80\_Puresyn4; (b) 80\_Carnation; (c) 80\_Marcol82.

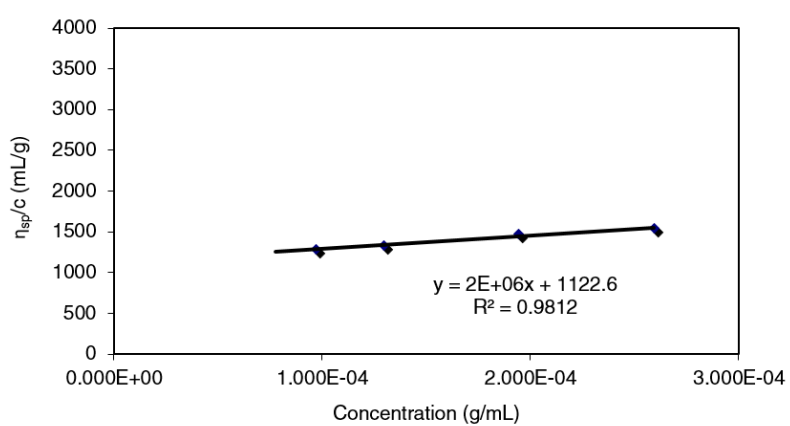
## INTRINSIC VISCOSITY DETERMINATION



(a)

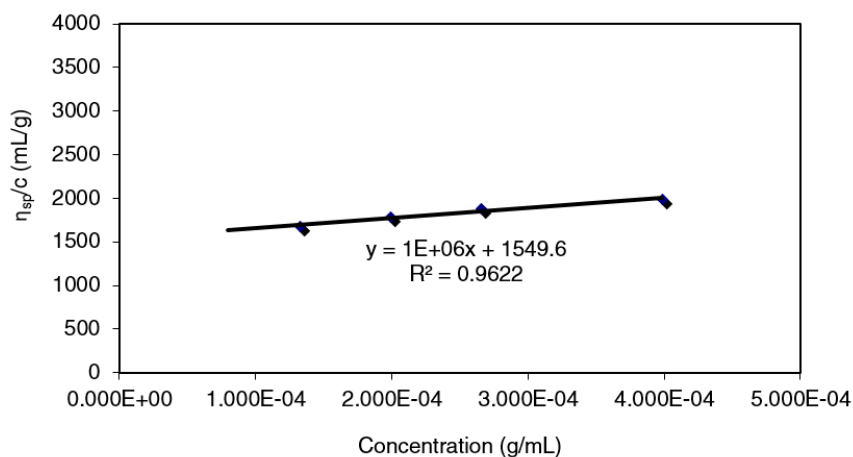


(b)

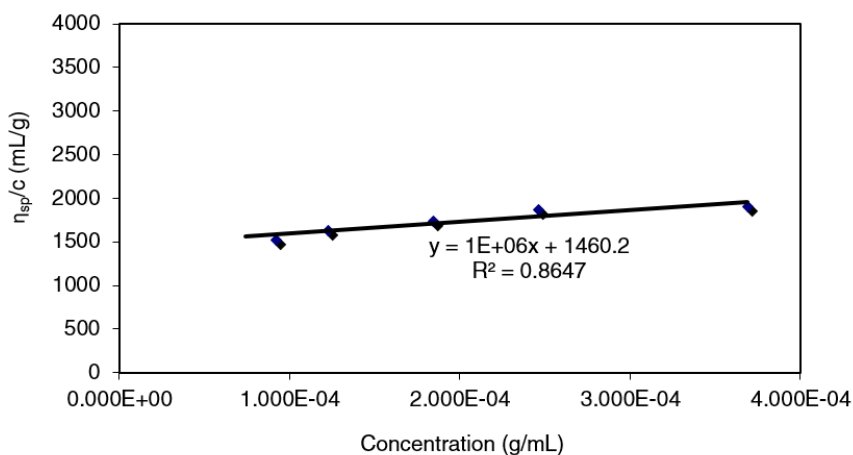


(c)

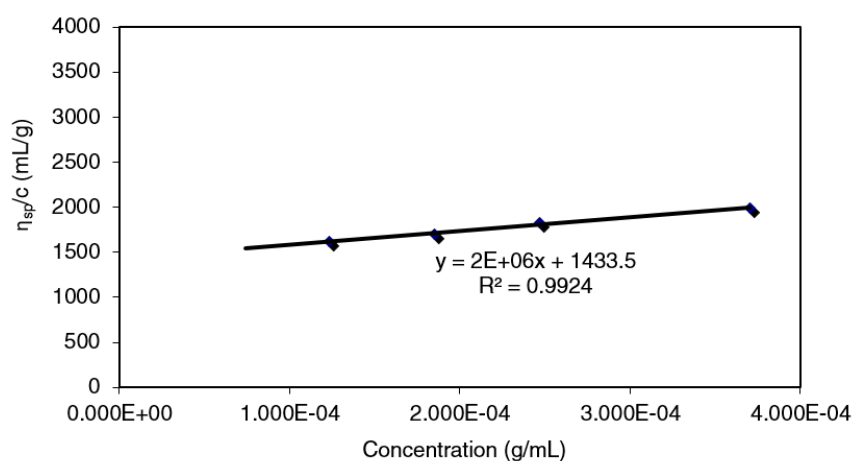
Figure A.17 Intrinsic viscosity extrapolation for 40 series polymers: (a) 40\_Puresyn4; (b) 40\_Carnation; (c) 40\_Marcol82.



(a)

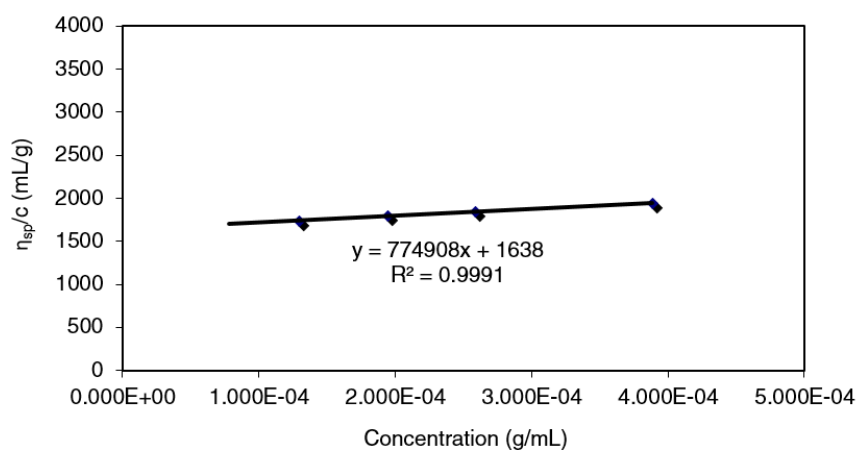


(b)

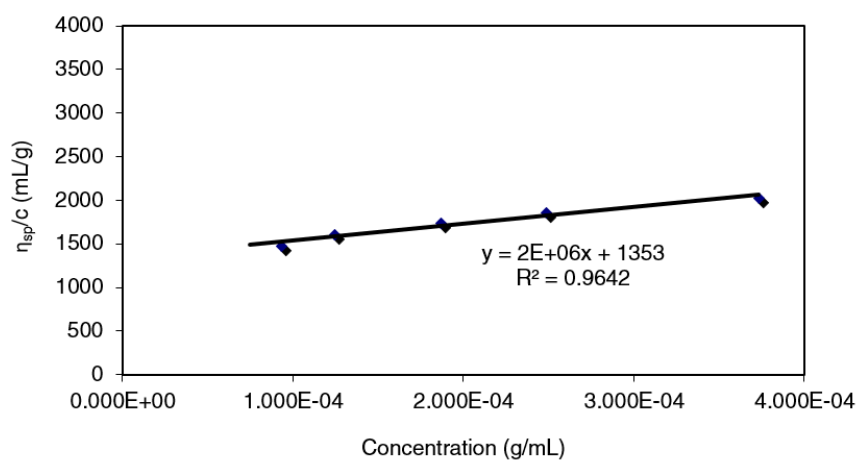


(c)

Figure A.18 Intrinsic viscosity extrapolation for 60 series polymers: (a) 60\_Puresyn4; (b) 60\_Carnation; (c) 60\_Marcol82.



(a)



(b)

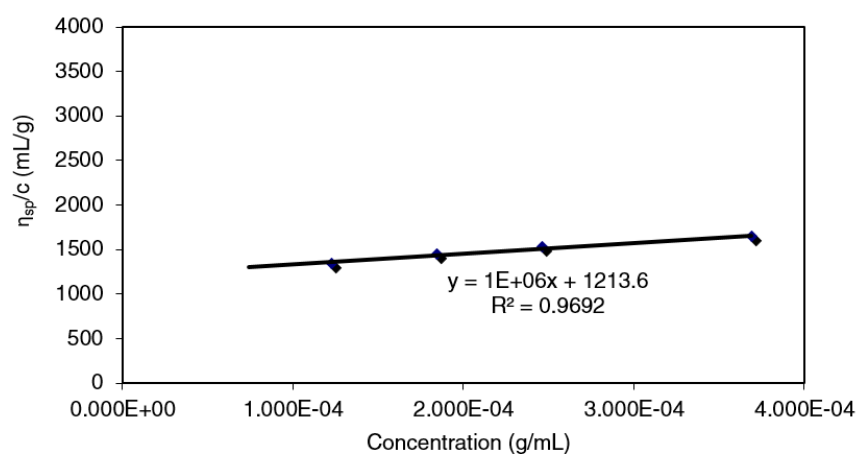
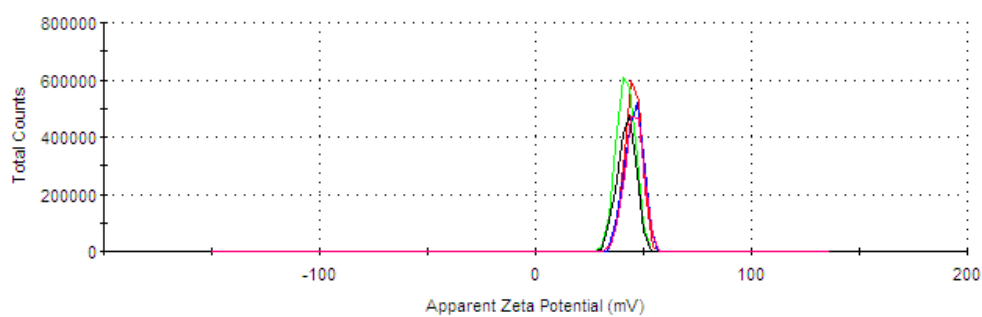


Figure A.19 Intrinsic viscosity extrapolation for 80 series polymers: (a) 80\_Puresyn4; (b) 80\_Carnation; (c) 80\_Marcol82.

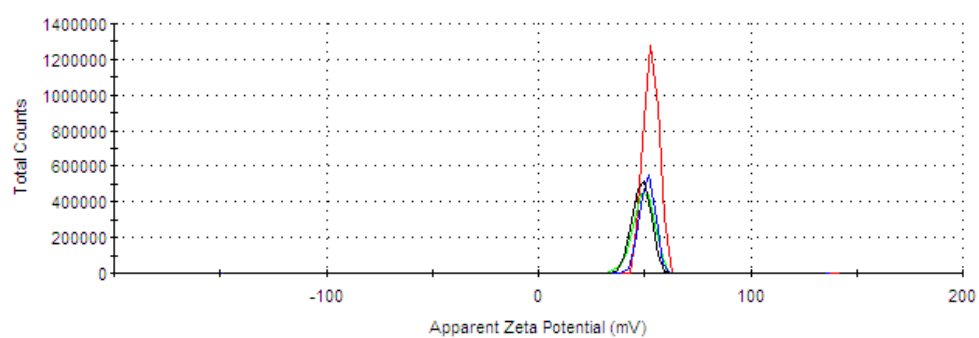
## Appendix B

### Supporting information for Chapter 4: Synthesis of new polyelectrolytes

#### ZETA POTENTIAL DISTRIBUTIONS FOR CATIONIC POLYELECTROLYTES

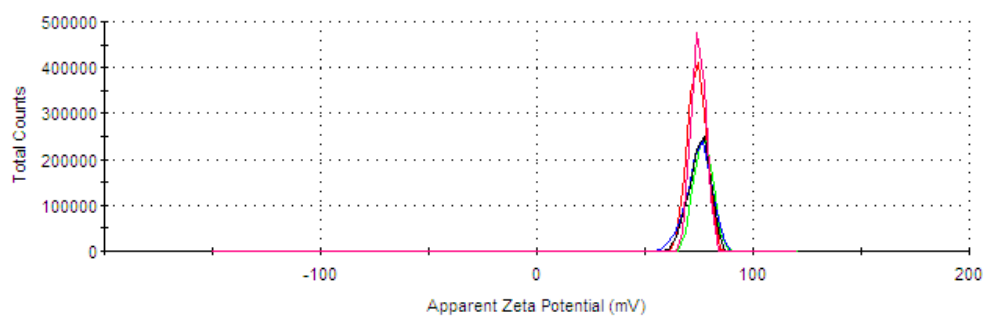


(a)

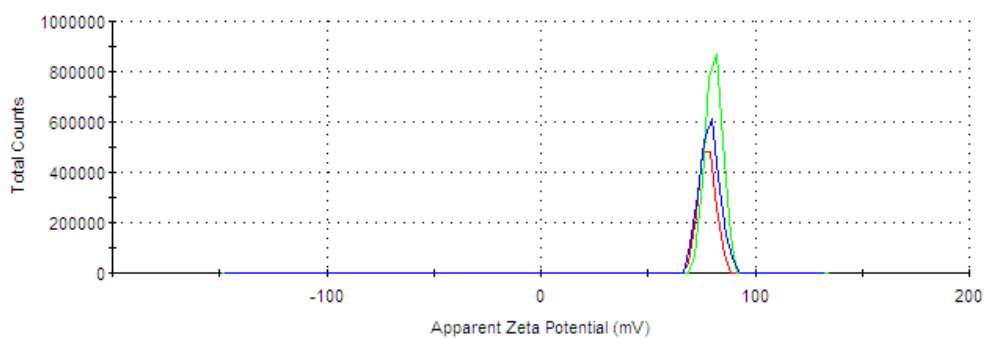


(b)

Figure B.1 Zeta potential distributions for cationic copolymers of 25 series: (a) 25MC; (b) 25MP.

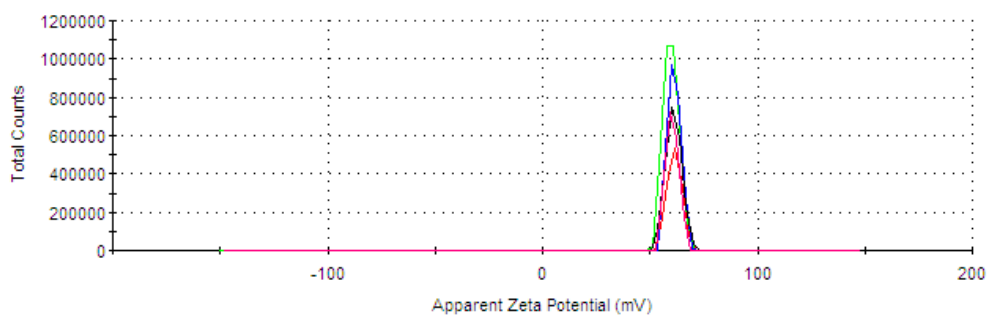


(a)

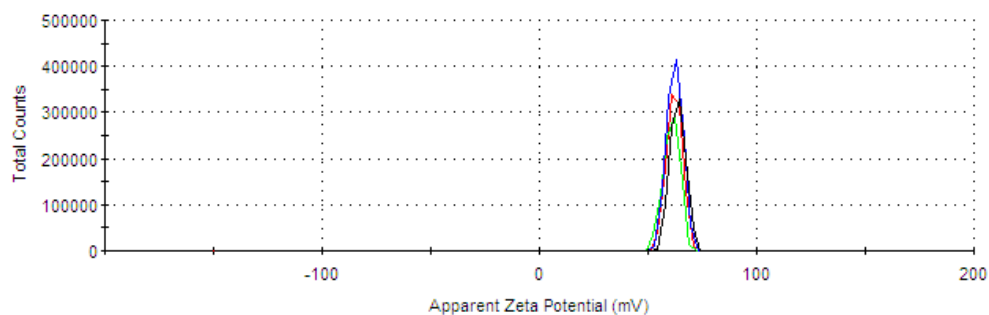


(b)

Figure B.2 Zeta potential distributions for cationic copolymers of 60 series: (a) 60MC; (b) 60MP.

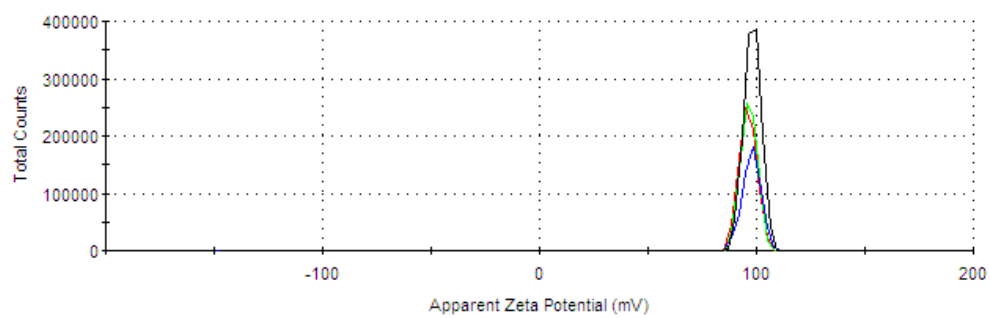


(a)

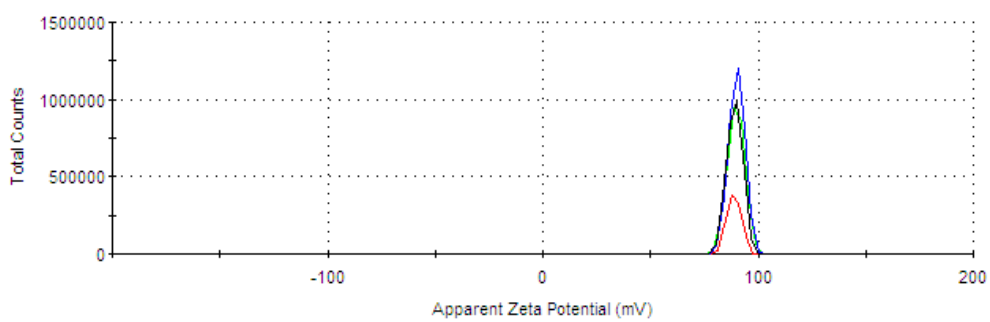


(b)

Figure B.3 Zeta potential distributions for cationic terpolymers of 25 series: (a) 25M1SC; (b) 25M2SC.



(a)

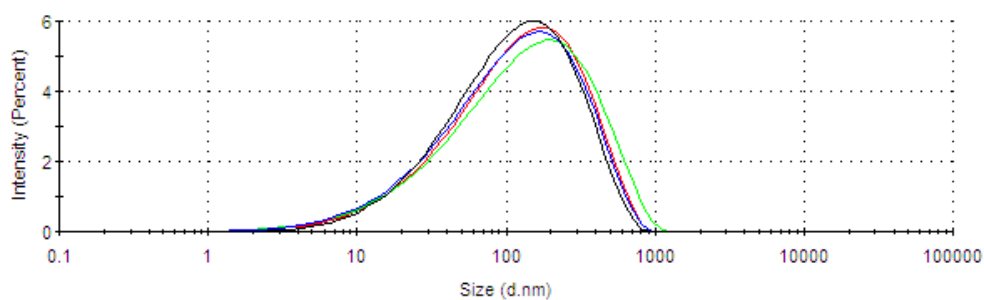


(b)

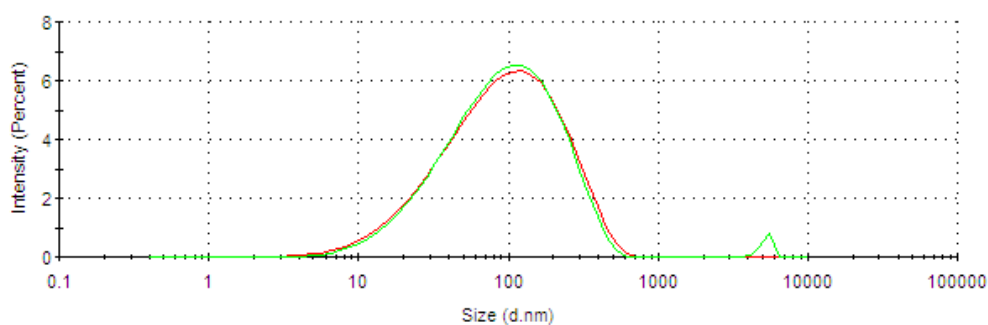
Figure B.4 Zeta potential distributions for cationic terpolymers of 60 series: (a) 60M1SC; (b) 60M2SC.



## HYDRODYNAMIC DIAMETER DISTRIBUTIONS FOR CATIONIC POLYELECTROLYTES

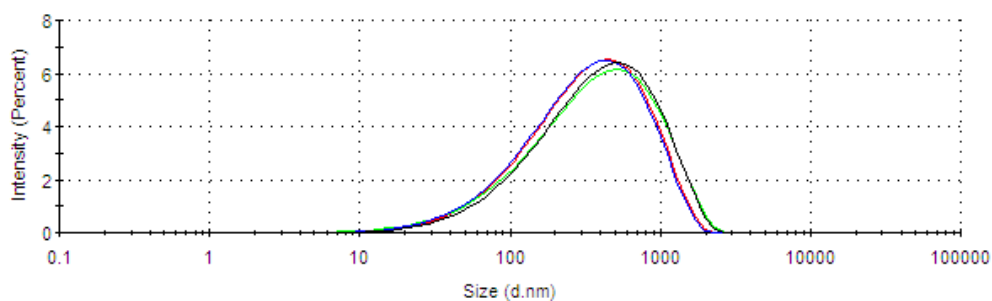


(a)

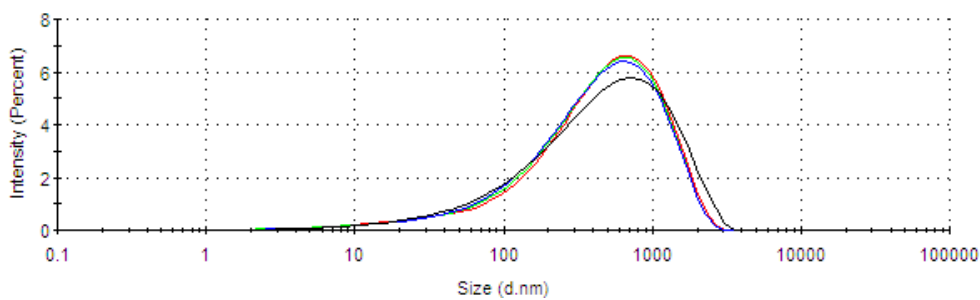


(b)

Figure B.5 Hydrodynamic diameter distributions for cationic copolymers of 25 series: (a) 25MC; (b) 25MP.

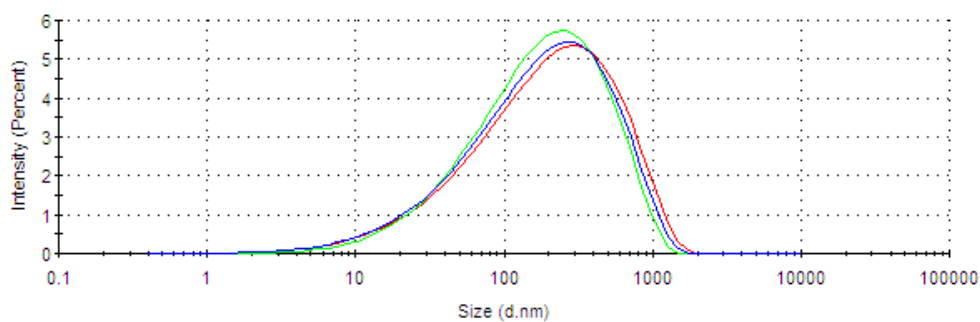


(a)

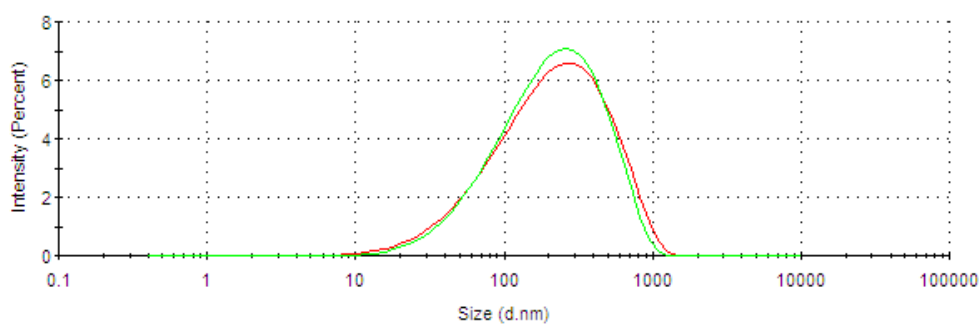


(b)

Figure B.6 Hydrodynamic diameter distributions for cationic copolymers of 60 series: (a) 60MC; (b) 60MP.

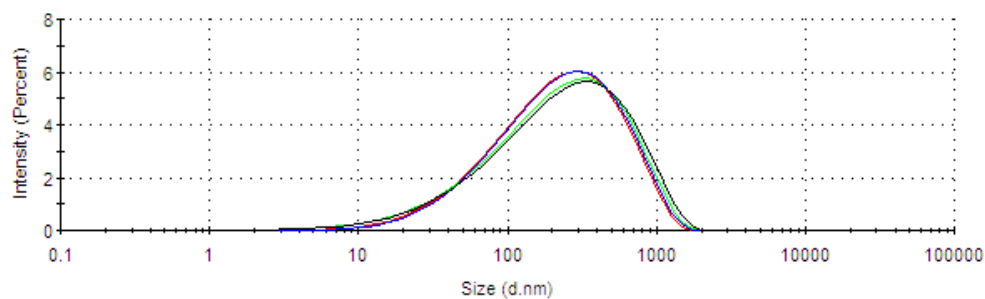


(a)

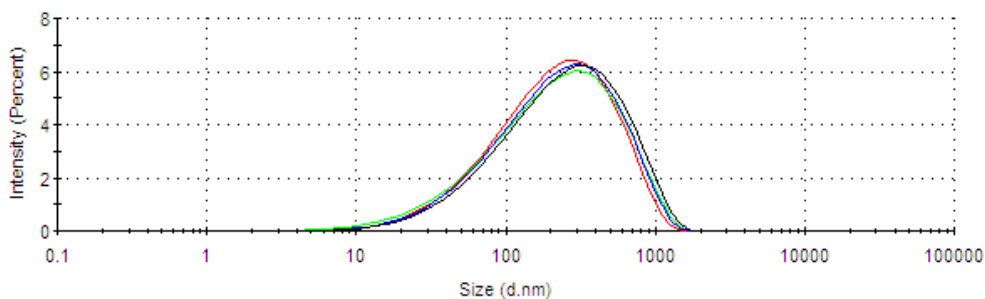


(b)

Figure B.7 Hydrodynamic diameter distributions for cationic terpolymers of 25 series: (a) 25M1SC; (b) 25M2SC.



(a)

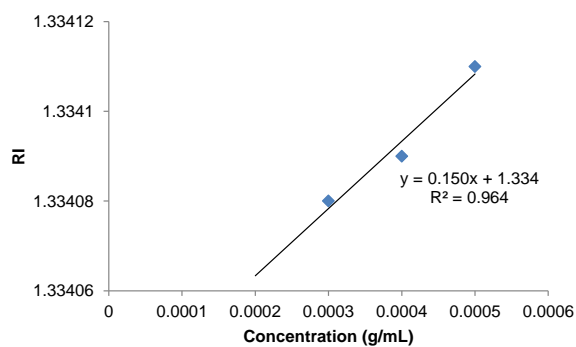


(b)

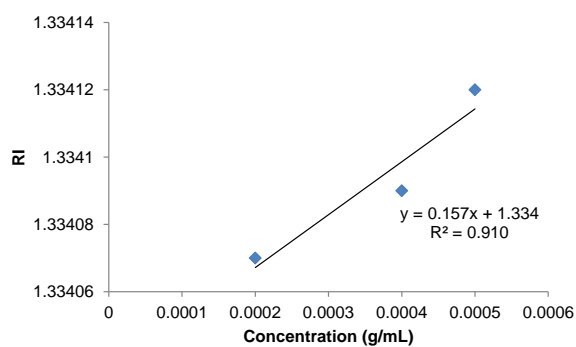
Figure B.8 Hydrodynamic diameter distributions for cationic terpolymers of 60 series: (a) 60M1SC; (b) 60M2SC.

## MOLECULAR WEIGHT DETERMINATION FOR CATIONIC POLYELECTROLYTES BY SLS

- Determination of  $dn/dc$

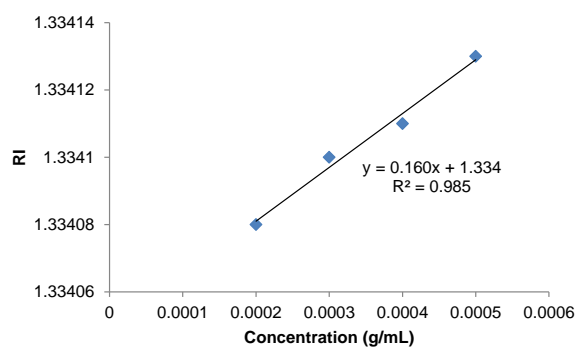


(a)

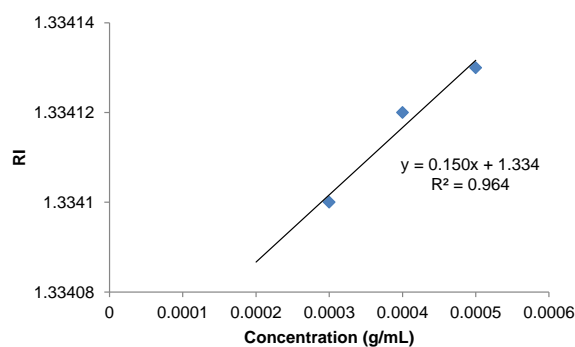


(b)

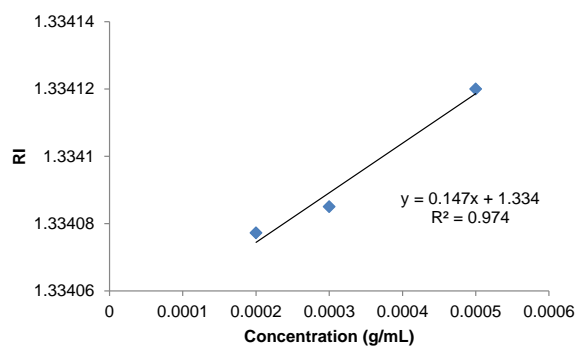
Figure B.9 Determination of the  $dn/dc$  value for cationic copolymers of 25 series: (a) 25MC; (b) 25MP.



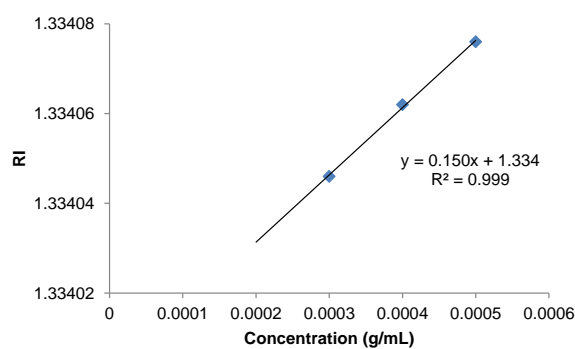
(a)



(b)

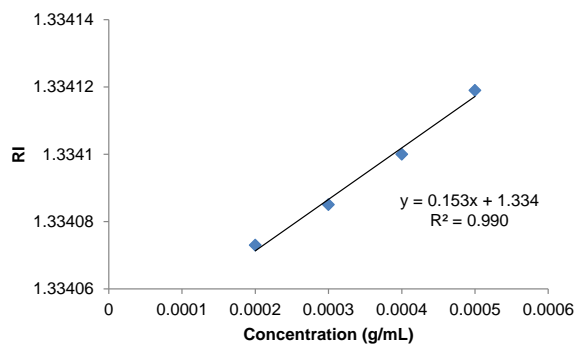
Figure B.10 Determination of the  $dn/dc$  value for cationic copolymers of 60 series: (a) 60MC; (b) 60MP.

(a)

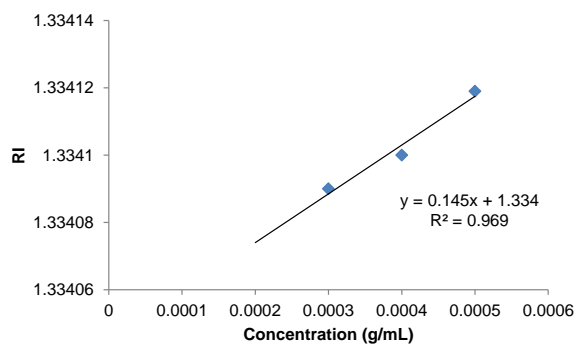


(b)

Figure B.11 Determination of the  $dn/dc$  value for cationic terpolymers of 25 series: (a) 25M1SC; (b) 25M2SC.



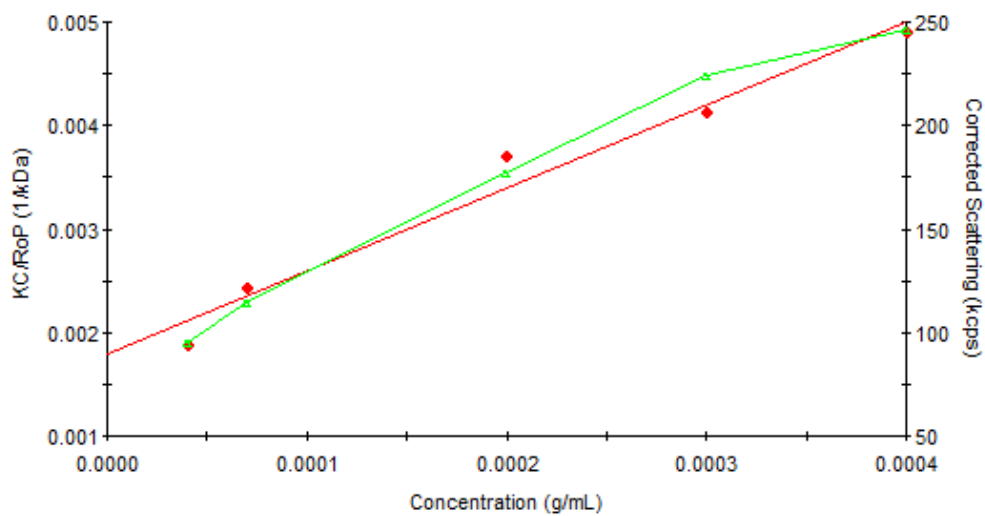
(a)



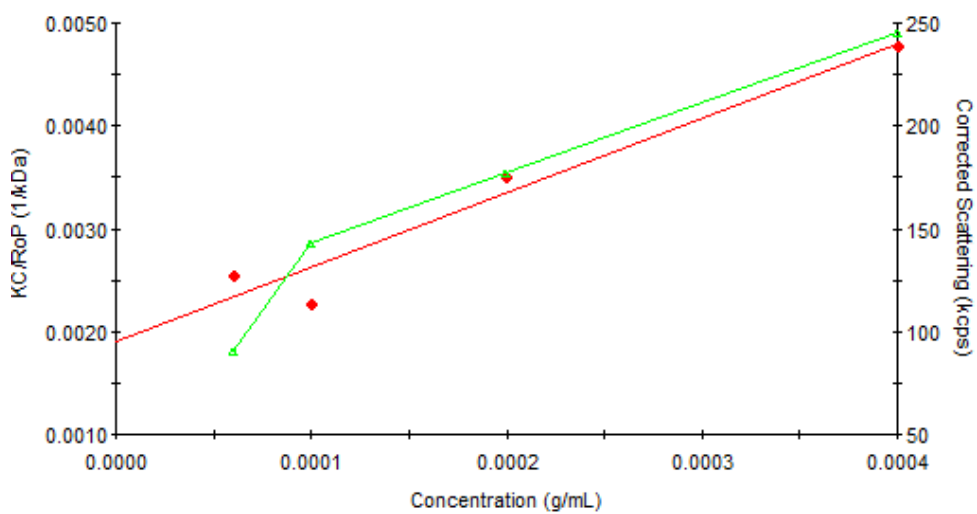
(b)

Figure B.12 Determination of the  $dn/dc$  value for cationic terpolymers of 60 series: (a) 60M1SC; (b) 60M2SC.

## - Determination of molecular weight

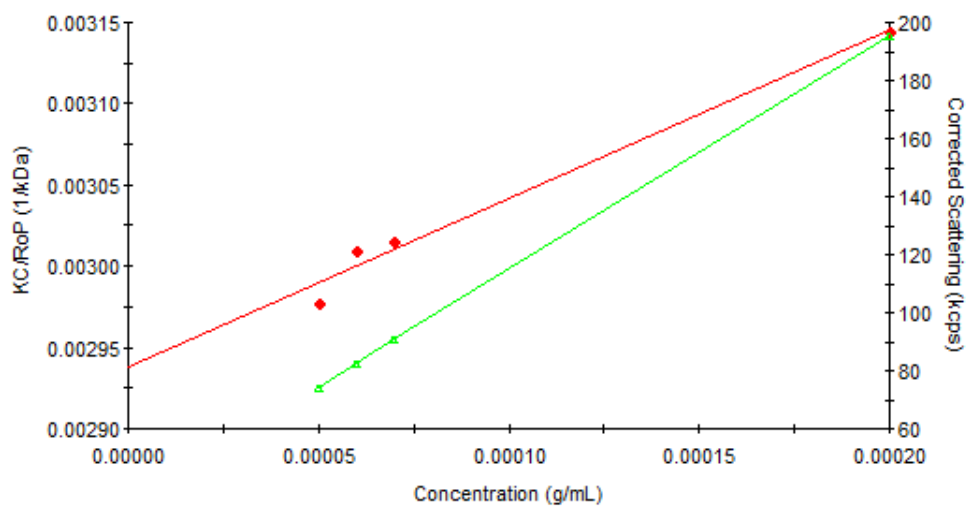


(a)

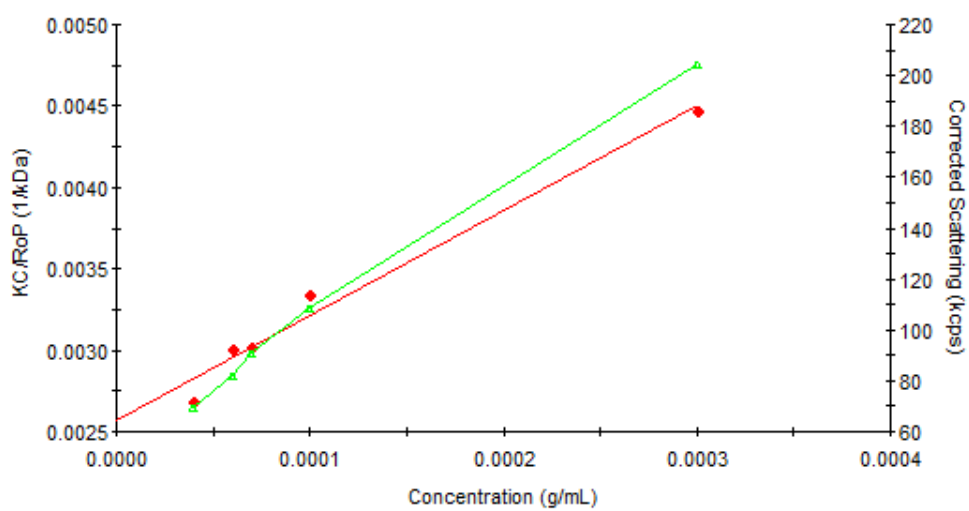


(b)

Figure B.13 Debye plot for weight-average molecular weight determination of cationic copolymer 25MC: (a) first measurement; (b) second measurement.

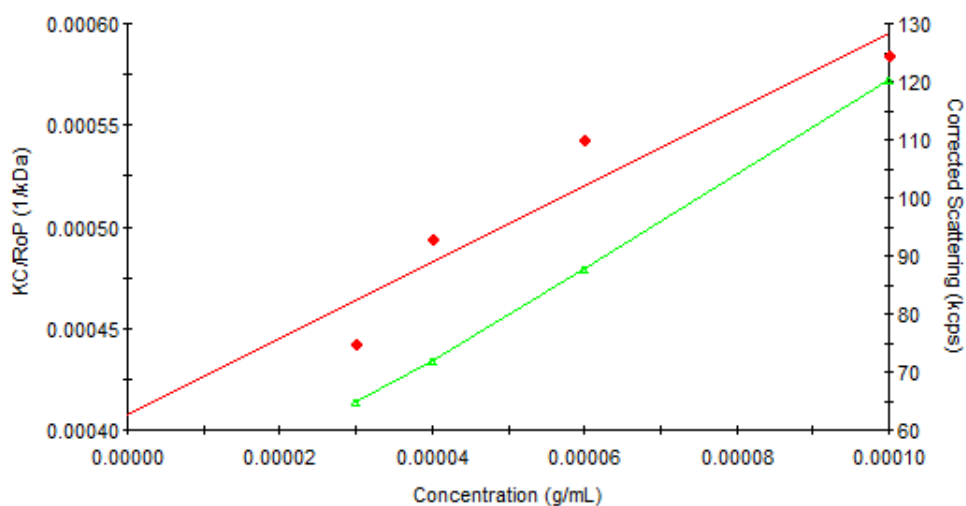


(a)

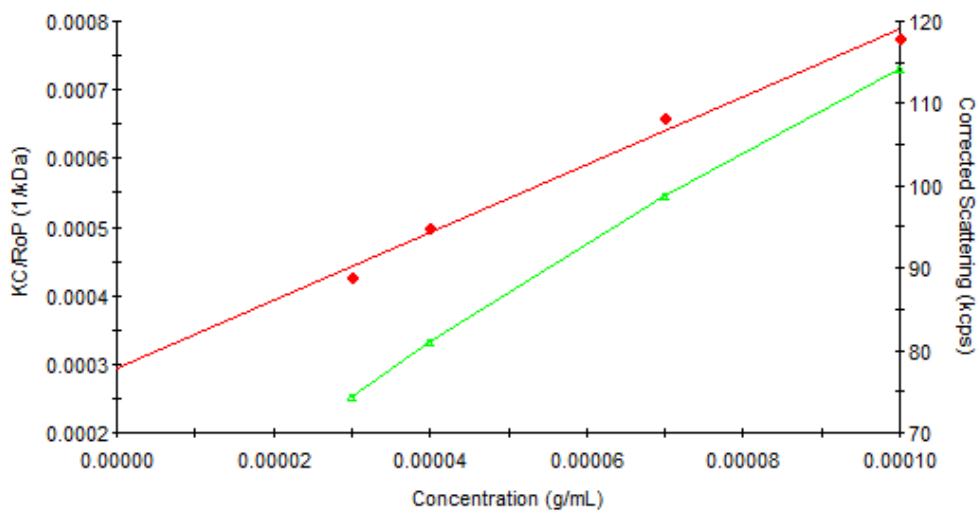


(b)

Figure B.14 Debye plot for weight-average molecular weight determination of cationic copolymer 25MP: (a) first measurement; (b) second measurement.



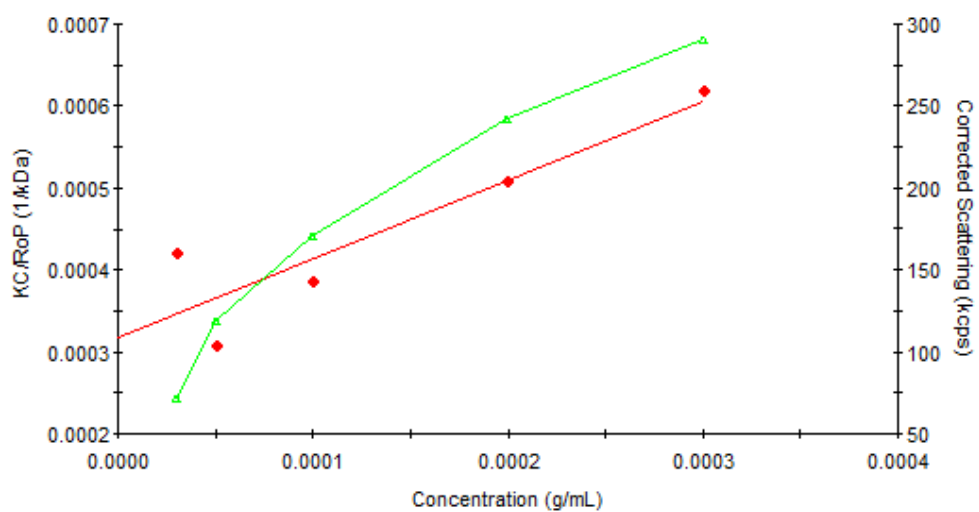
(a)



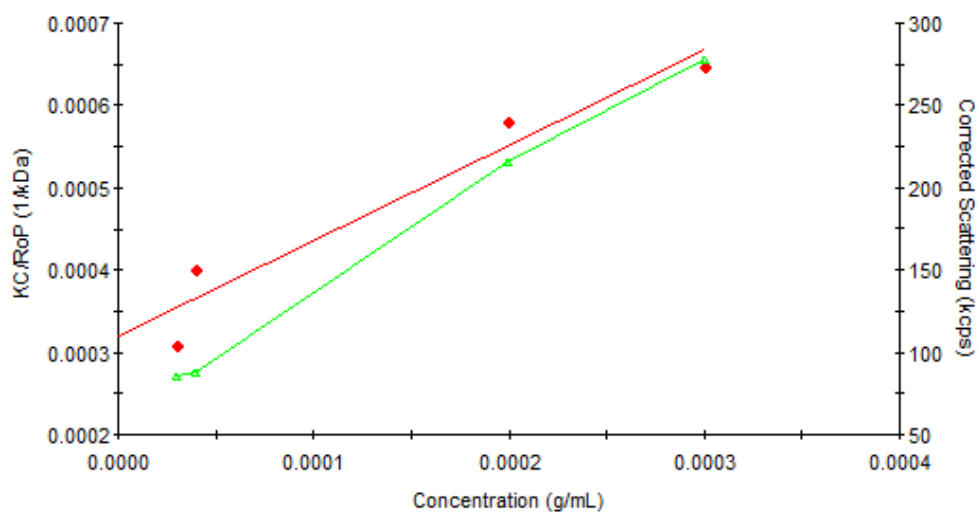
(b)

Figure B.15 Debye plot for weight-average molecular weight determination of cationic copolymer 60MC: (a) first measurement; (b) second measurement.



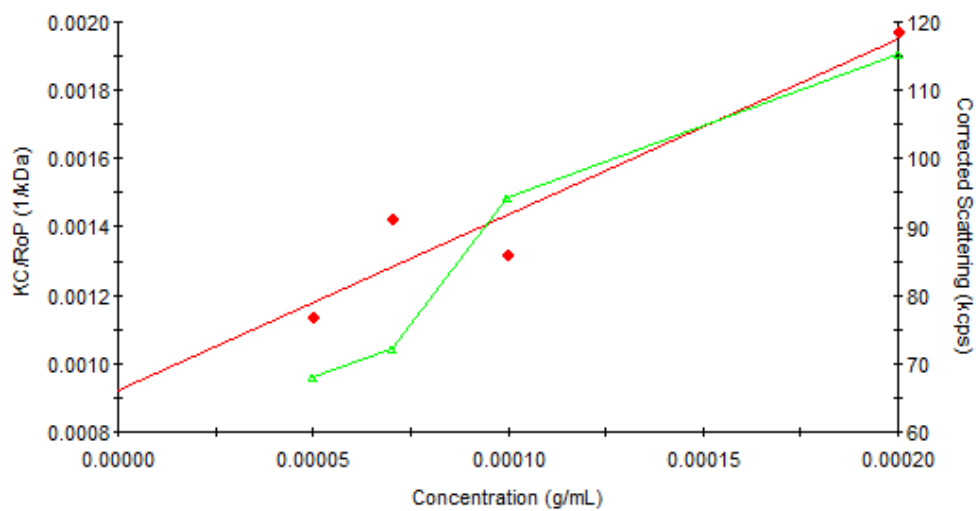


(a)

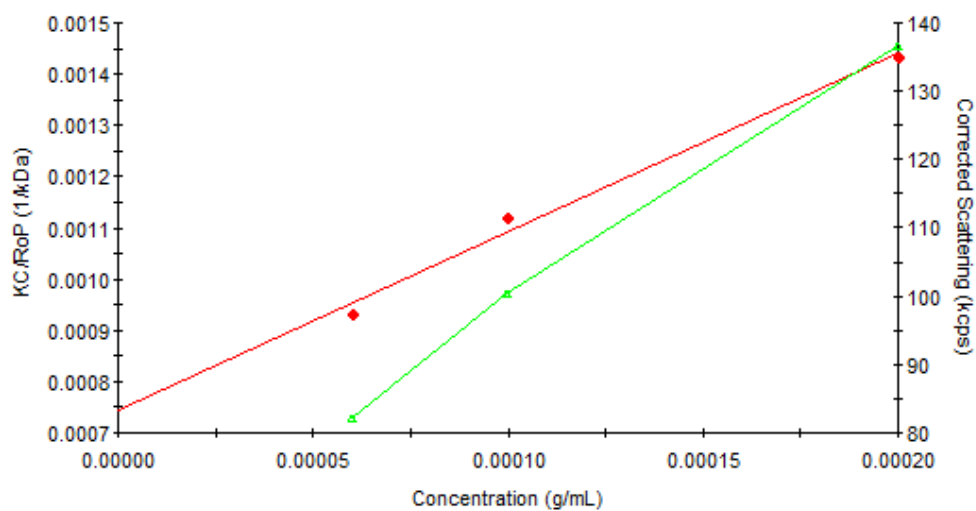


(b)

Figure B.16 Debye plot for weight-average molecular weight determination of cationic copolymer 60MP: (a) first measurement; (b) second measurement.

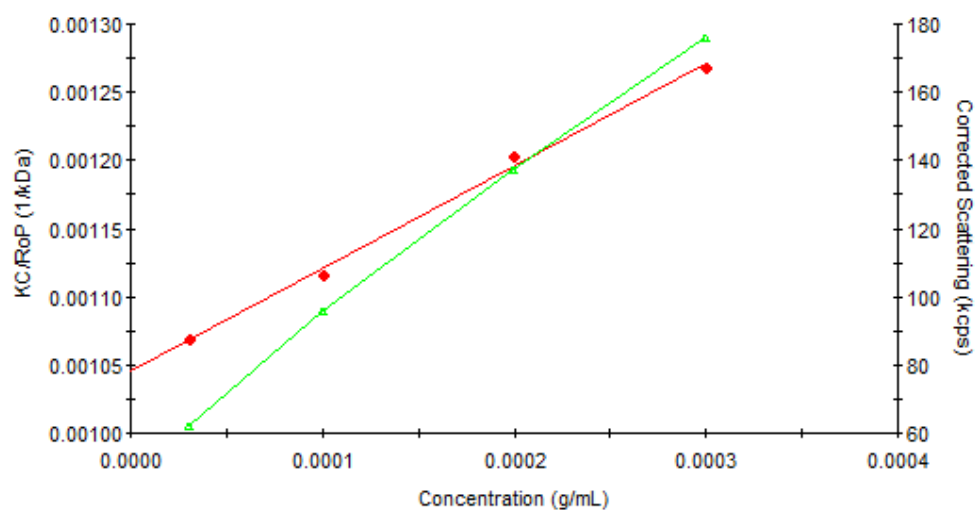


(a)

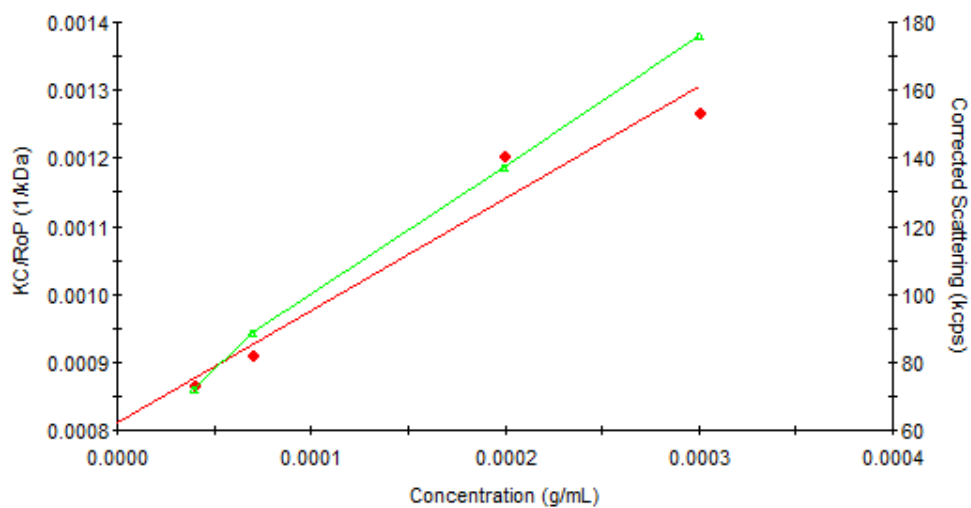


(b)

Figure B.17 Debye plot for weight-average molecular weight determination of cationic copolymer 25M1SC: (a) first measurement; (b) second measurement.

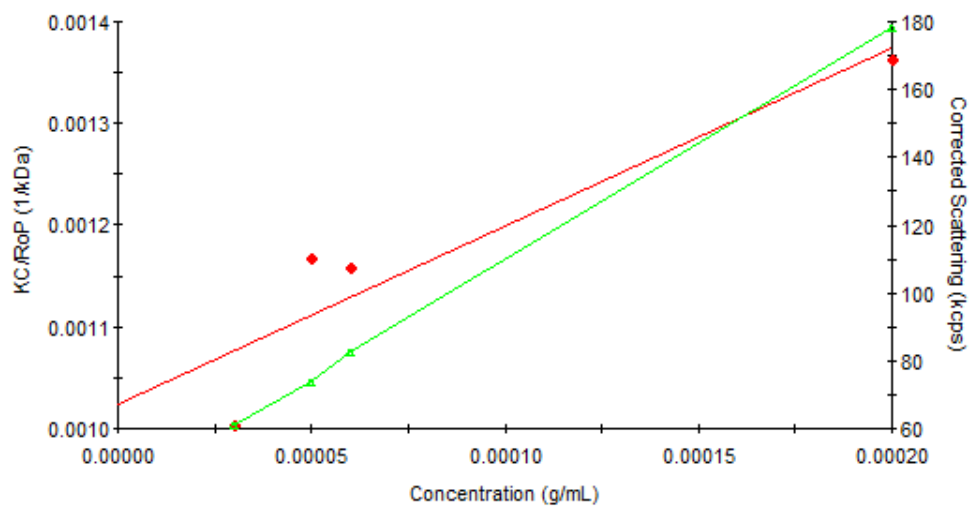


(a)

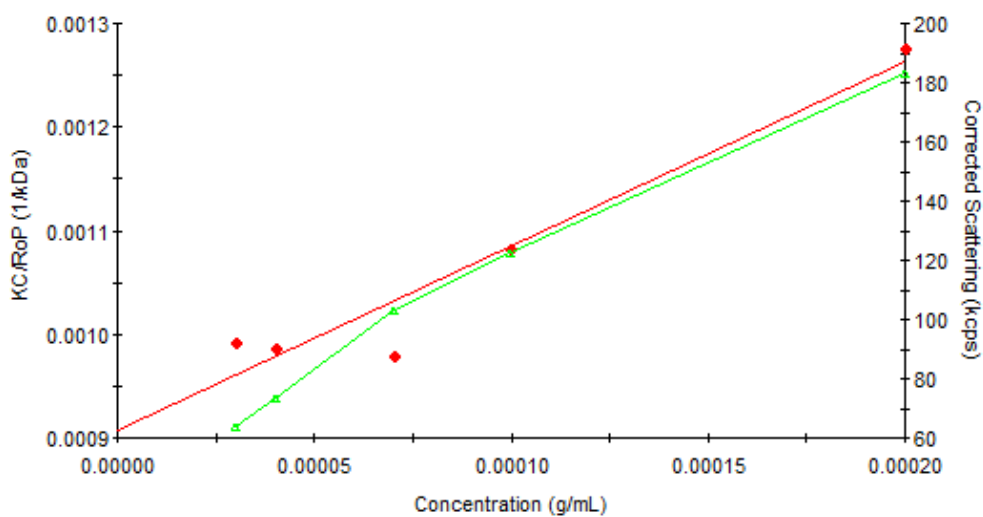


(b)

Figure B.18 Debye plot for weight-average molecular weight determination of cationic copolymer 25M2SC: (a) first measurement; (b) second measurement.

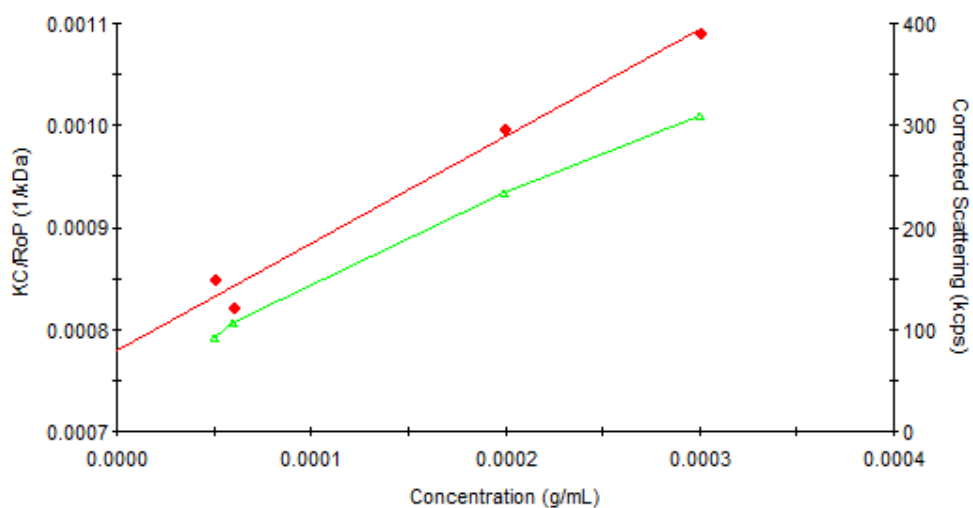


(a)

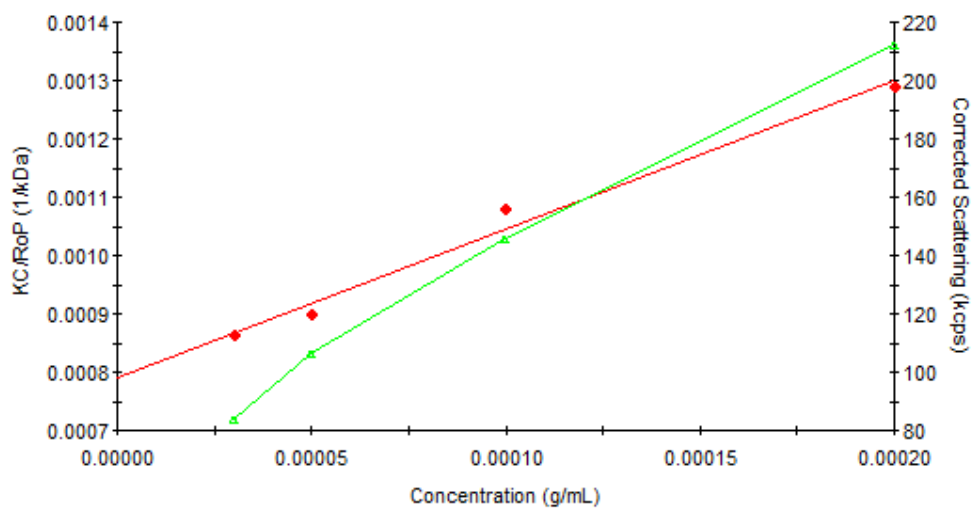


(b)

Figure B.19 Debye plot for weight-average molecular weight determination of cationic copolymer 60M1SC: (a) first measurement; (b) second measurement.



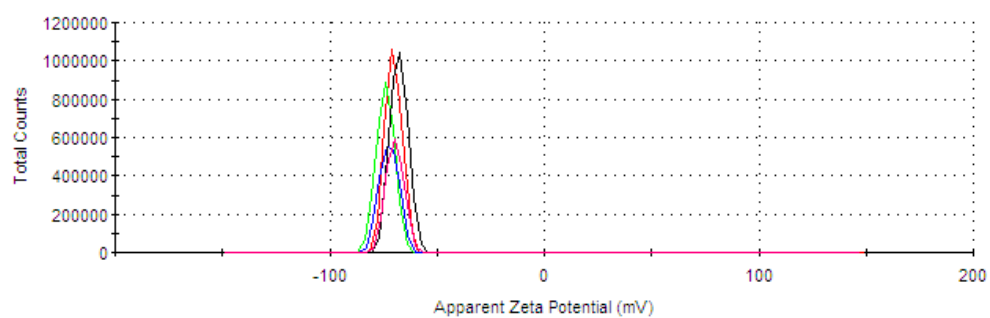
(a)



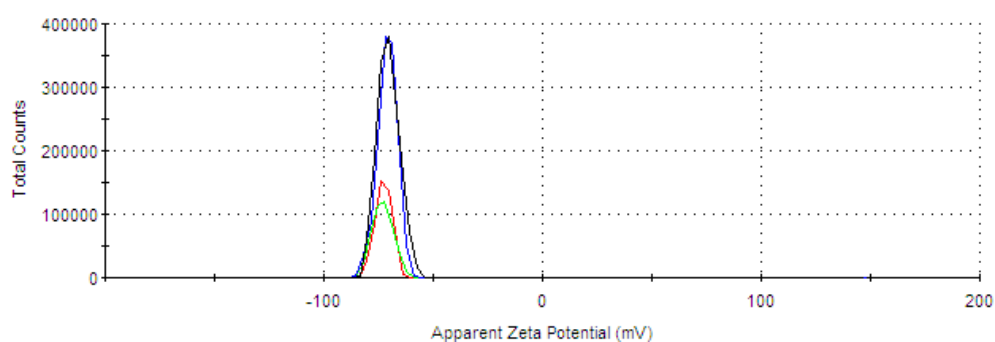
(b)

Figure B.20 Debye plot for weight-average molecular weight determination of cationic copolymer 60M2SC: (a) first measurement; (b) second measurement.

## ZETA POTENTIAL DISTRIBUTIONS FOR ANIONIC POLYELECTROLYTES

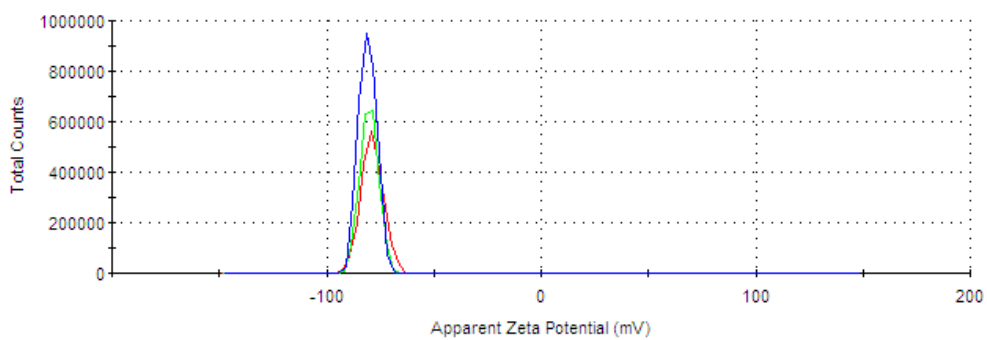


(a)

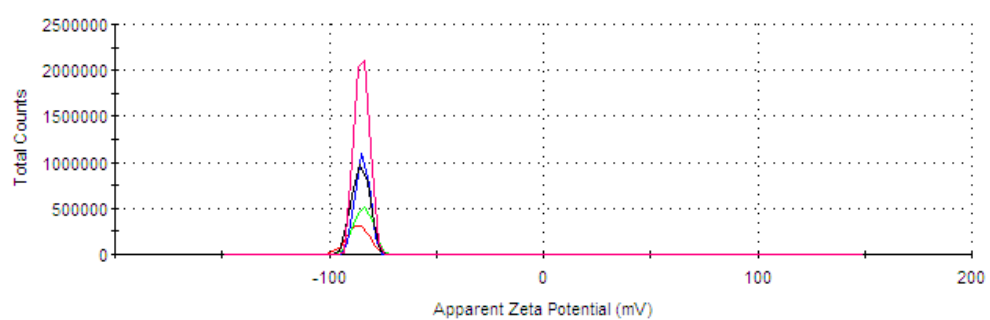


(b)

Figure B.21 Zeta potential distributions for anionic copolymers of 50 series: (a) 50AC; (b) 50AP.

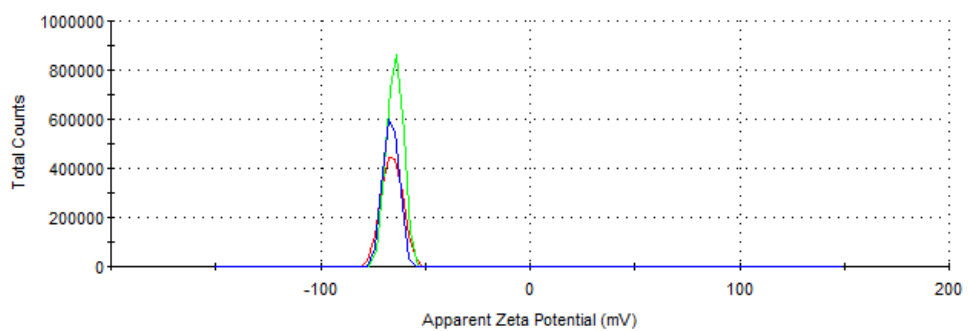


(a)

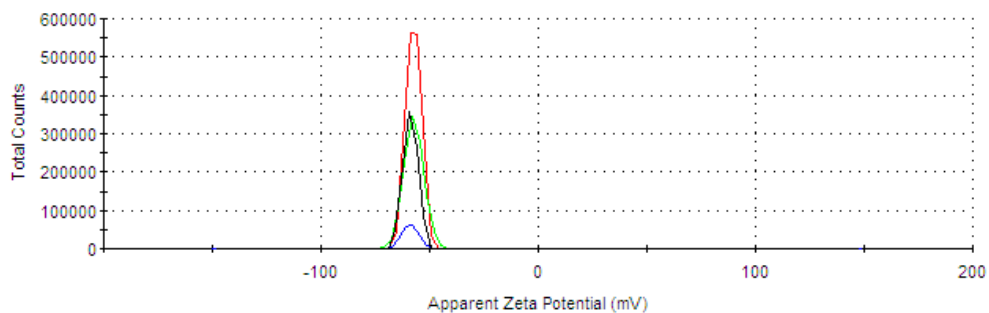


(b)

Figure B.22 Zeta potential distributions for anionic copolymers of 80 series: (a) 80AC; (b) 80AP.

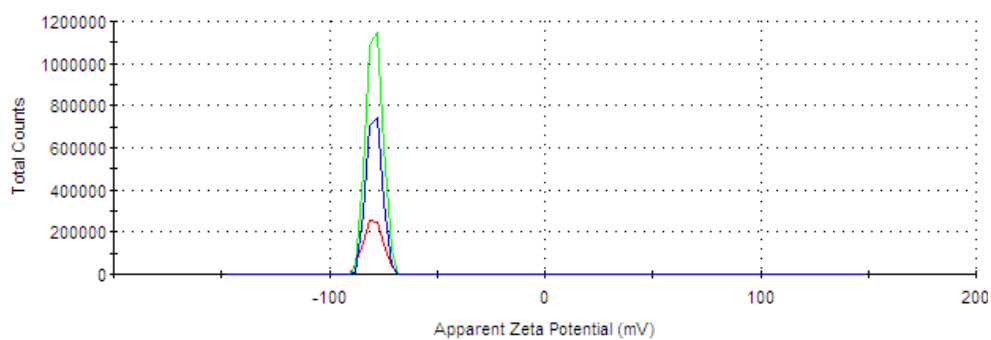


(a)

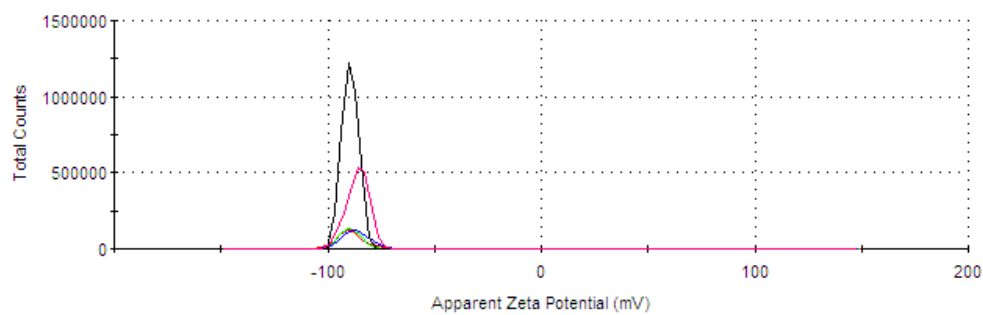


(b)

Figure B.23 Zeta potential distributions for anionic terpolymers of 50 series: (a) 50A1EC; (b) 50A3EC.

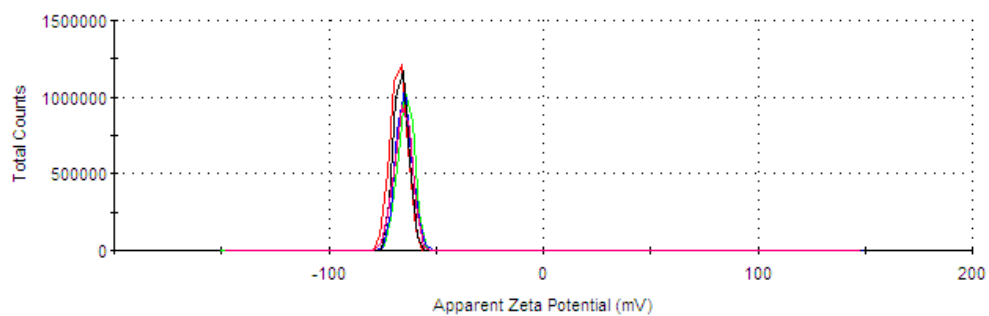


(a)

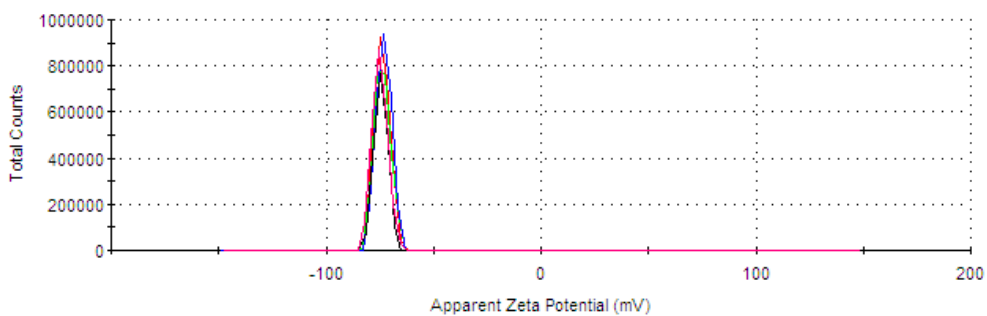


(b)

Figure B.24 Zeta potential distributions for anionic terpolymers of 80 series: (a) 80A1EC; (b) 80A3EC.

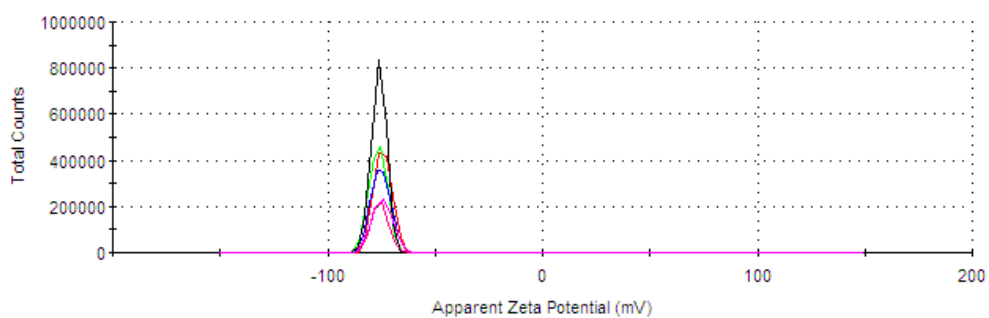


(a)

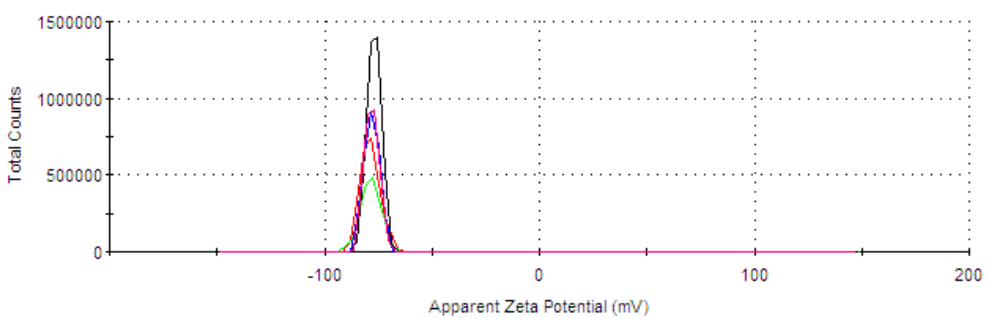


(b)

Figure B.25 Zeta potential distributions for anionic terpolymers of 50 series: (a) 50A1LC; (b) 50A3LC.



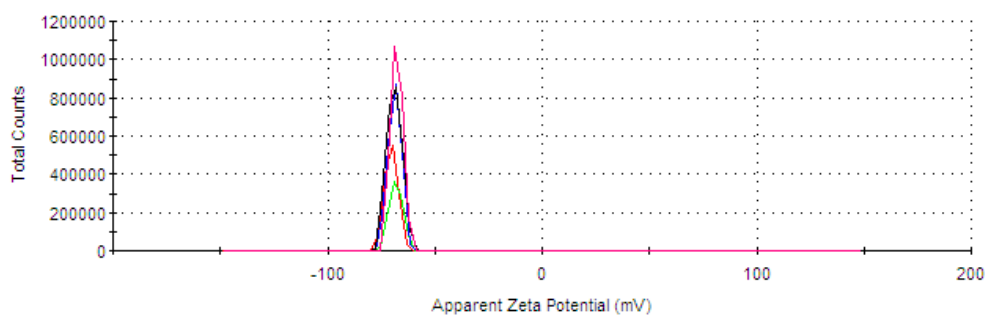
(a)



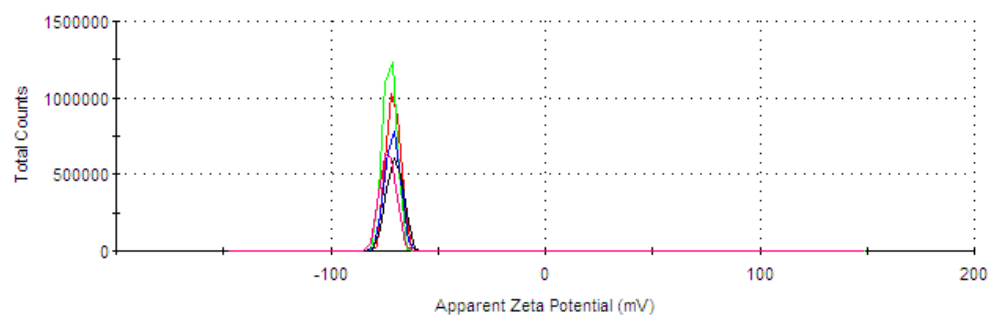
(b)

Figure B.26 Zeta potential distributions for anionic terpolymers of 80 series: (a) 80A1LC; (b) 80A3LC.



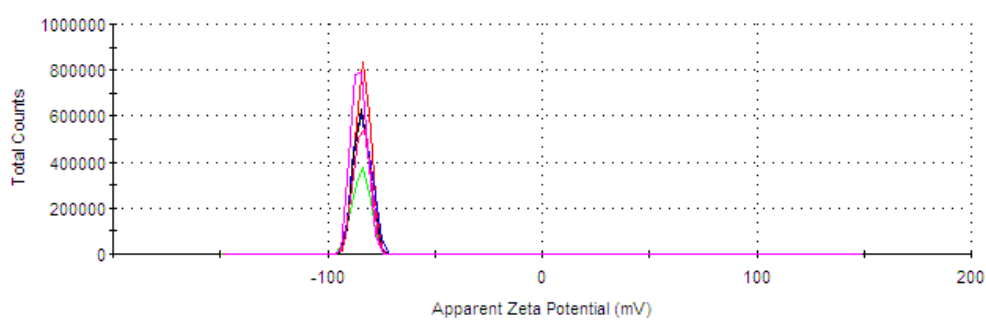


(a)

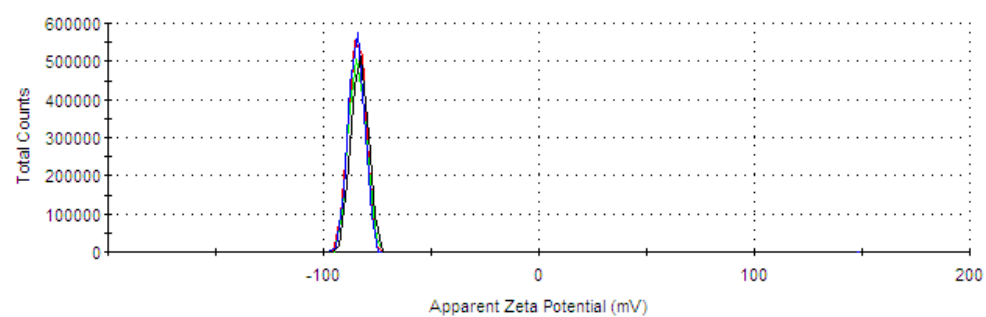


(b)

Figure B.27 Zeta potential distributions for anionic terpolymers of 50 series: (a) 50A1SC; (b) 50A3SC.



(a)



(b)

Figure B.28 Zeta potential distributions for anionic terpolymers of 80 series: (a) 80A1SC; (b) 80A3SC.

## HYDRODYNAMIC DIAMETER DISTRIBUTIONS FOR ANIONIC POLYELECTROLYTES

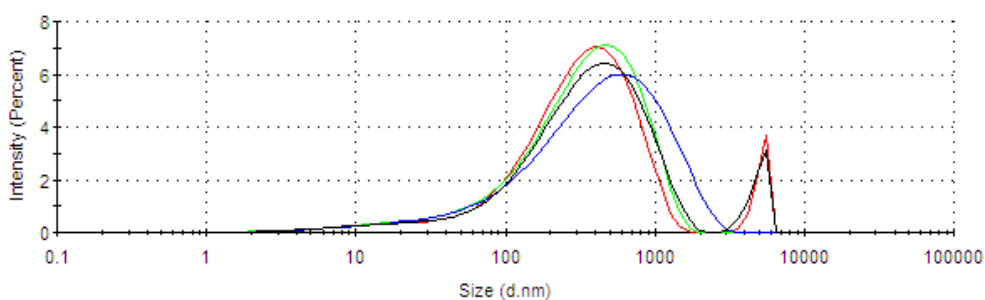
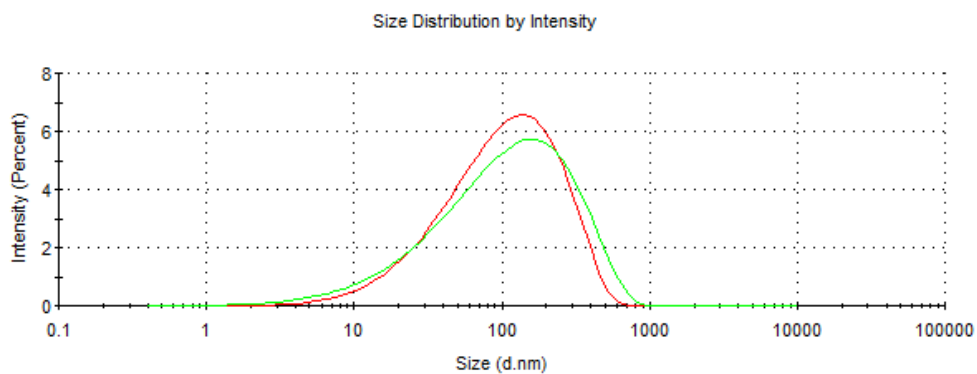


Figure B.29 Hydrodynamic diameter distributions for anionic copolymers of 50 series: (a) 50AC; (b) 50AP.

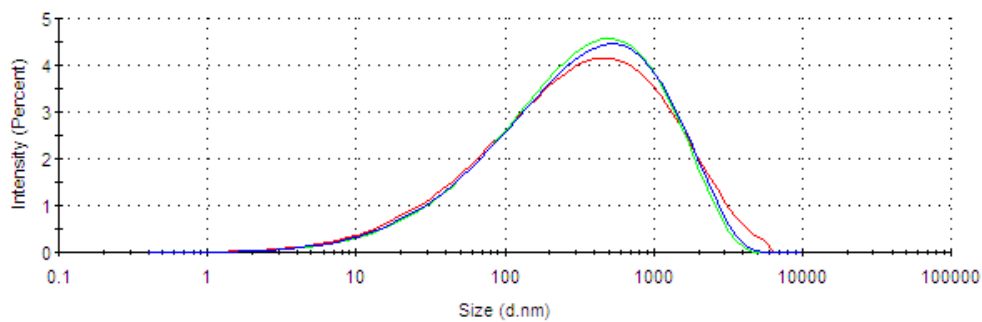
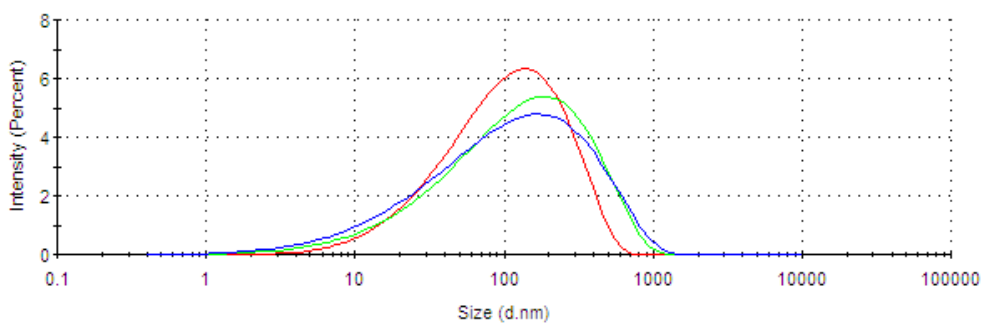
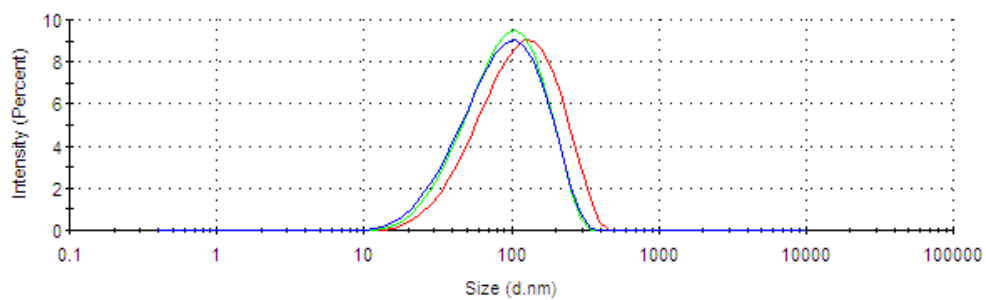
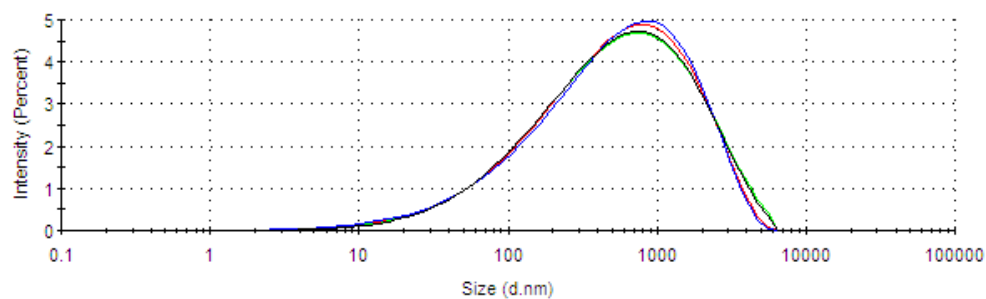


Figure B.30 Hydrodynamic diameter distributions for anionic copolymers of 80 series: (a) 80AC; (b) 80AP.

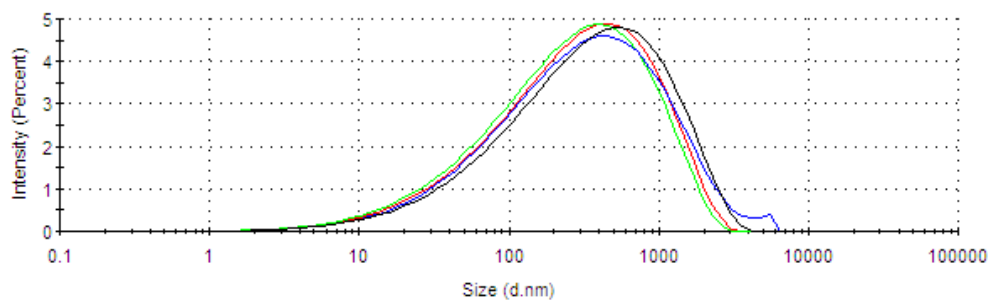


(a)

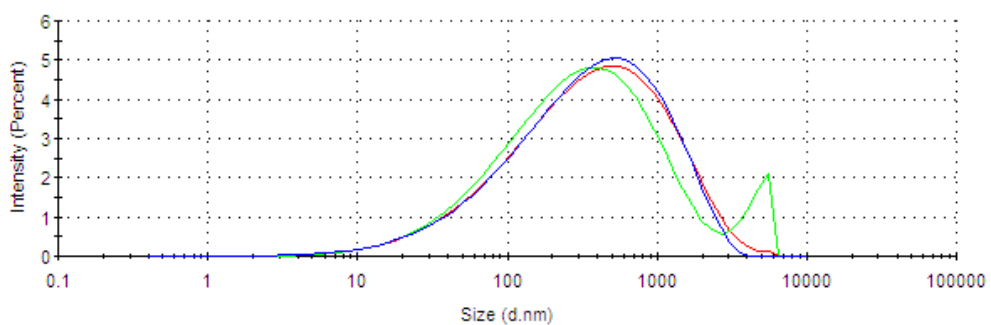


(b)

Figure B.31 Hydrodynamic diameter distributions for anionic terpolymers of 50 series: (a) 50A1EC; (b) 50A3EC.

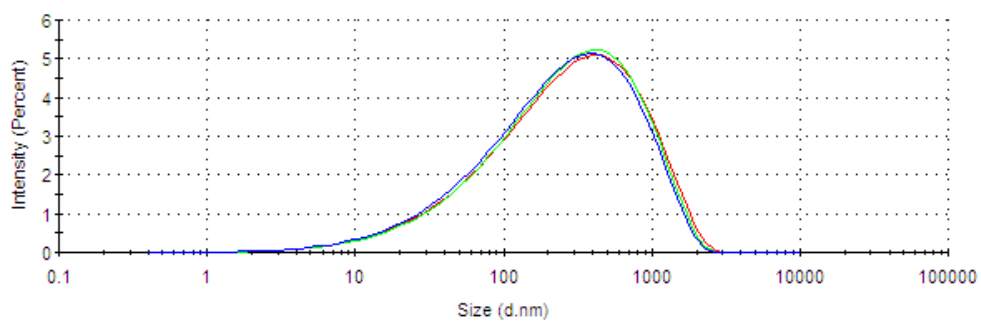


(a)

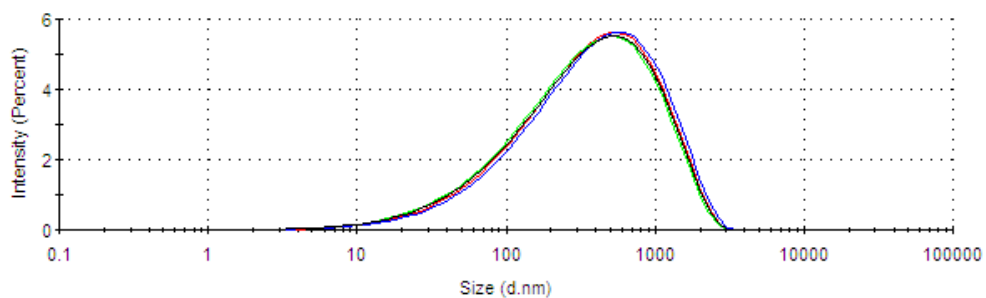


(b)

Figure B.32 Hydrodynamic diameter distributions for anionic terpolymers of 80 series: (a) 80A1EC; (b) 80A3EC.

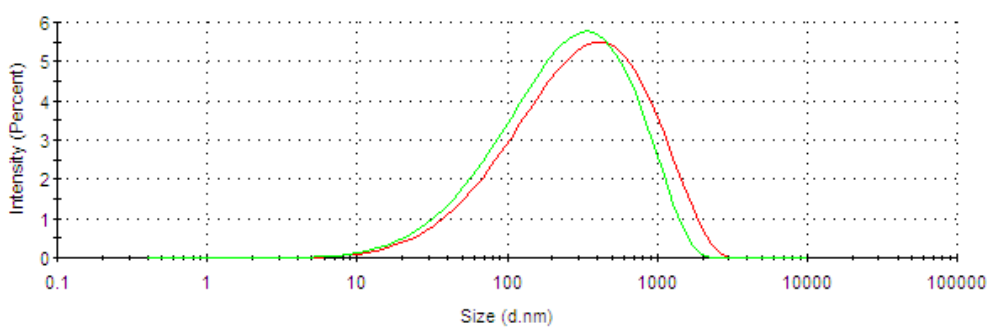


(a)

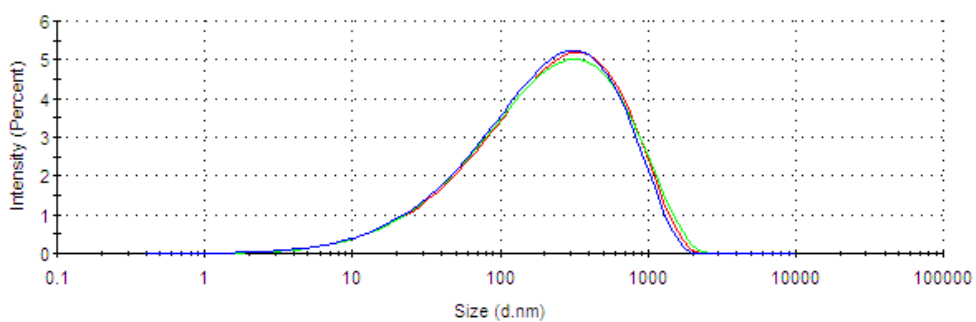


(b)

Figure B.33 Hydrodynamic diameter distributions for anionic terpolymers of 50 series: (a) 50A1LC; (b) 50A3LC.

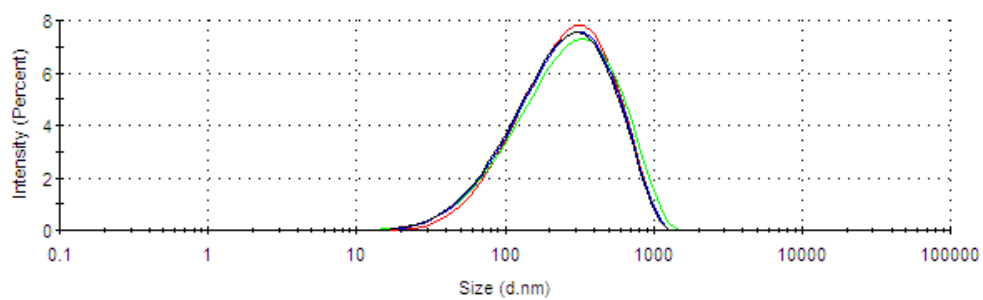


(a)

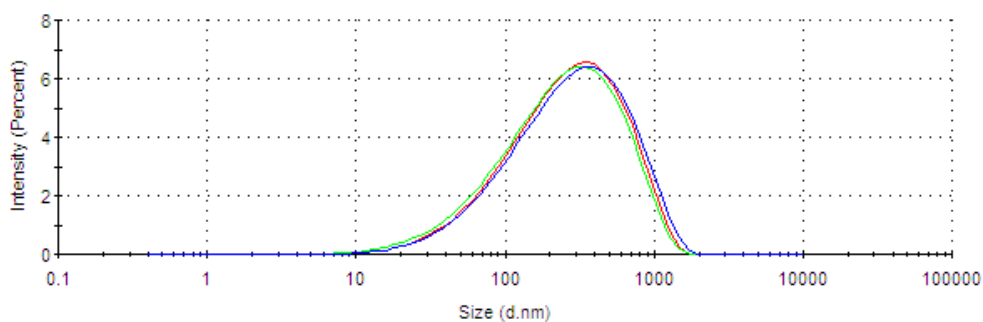


(b)

Figure B.34 Hydrodynamic diameter distributions for anionic terpolymers of 80 series: (a) 80A1LC; (b) 80A3LC.

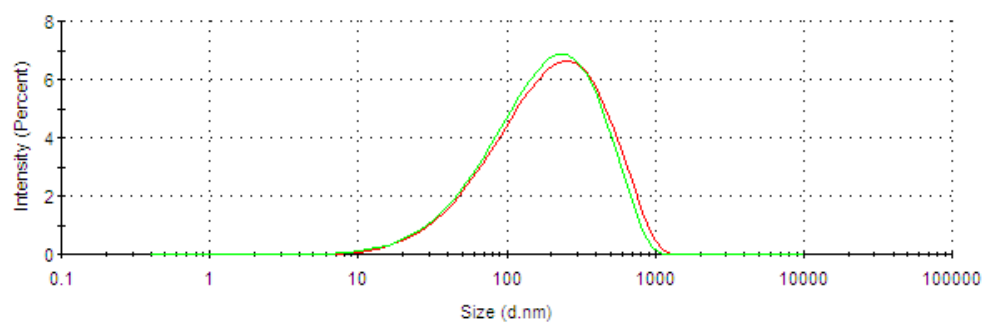


(a)

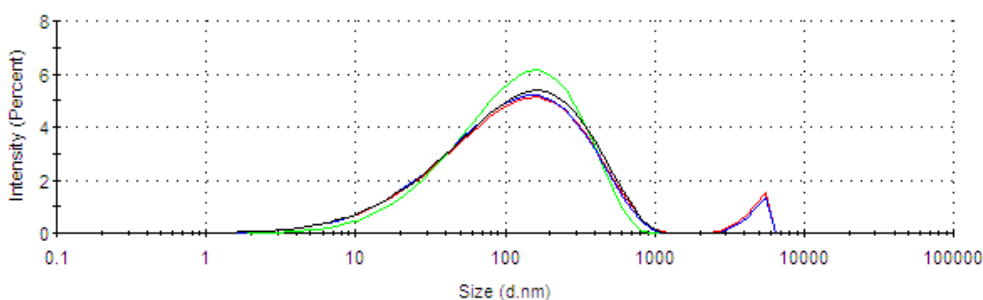


(b)

Figure B.35 Hydrodynamic diameter distributions for anionic terpolymers of 50 series: (a) 50A1SC; (b) 50A3SC.



(a)

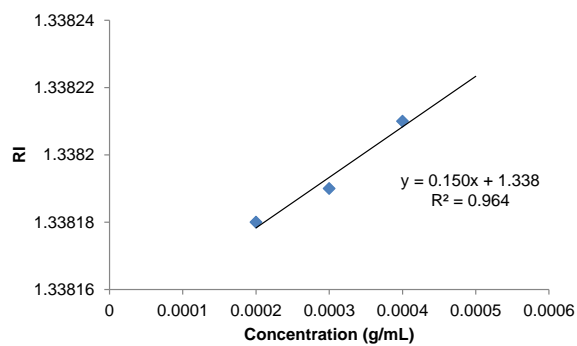


(b)

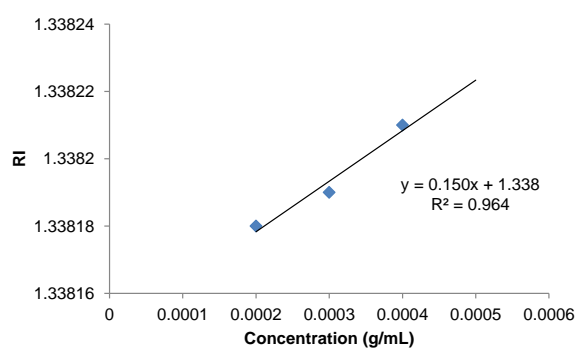
Figure B.36 Hydrodynamic diameter distributions for anionic terpolymers of 80 series: (a) 80A1SC; (b) 80A3SC.

## MOLECULAR WEIGHT DETERMINATION FOR ANIONIC POLYELECTROLYTES BY SLS

- Determination of  $dn/dc$

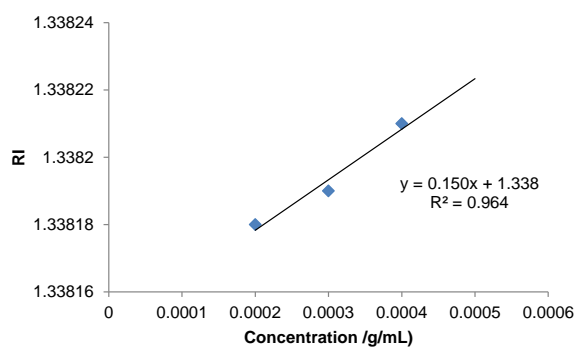


(a)

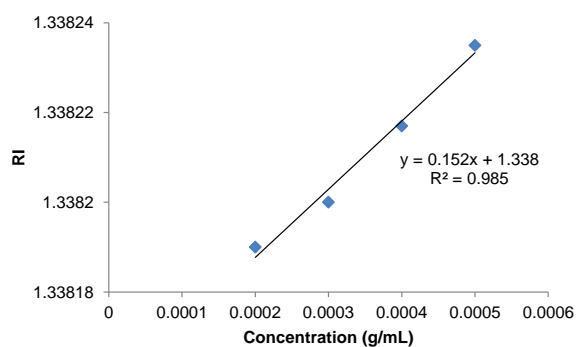


(b)

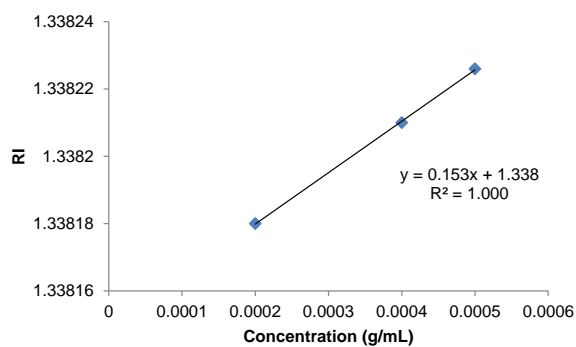
Figure B.37 Determination of the  $dn/dc$  value for anionic copolymers of 50 series: (a) 50AC; (b) 50AP.



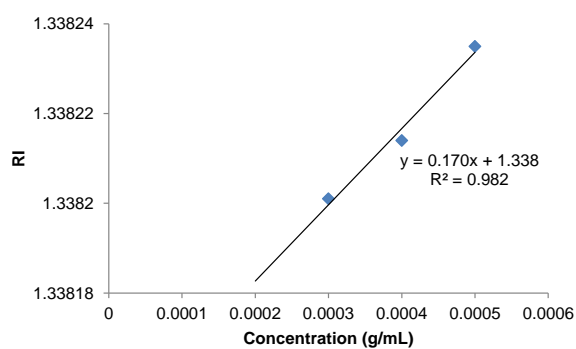
(a)



(b)

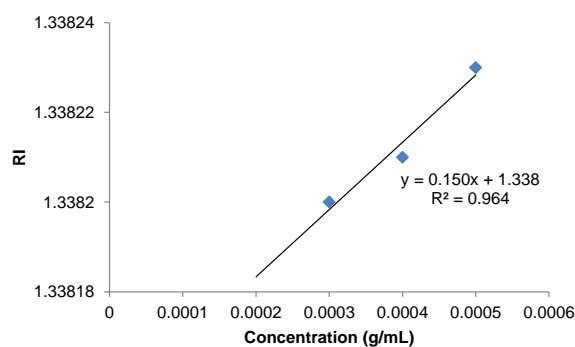
Figure B.38 Determination of the  $dn/dc$  value for anionic copolymers of 80 series: (a) 80AC; (b) 80AP.

(a)

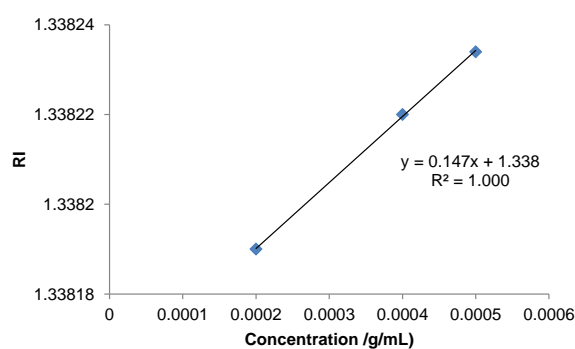


(b)

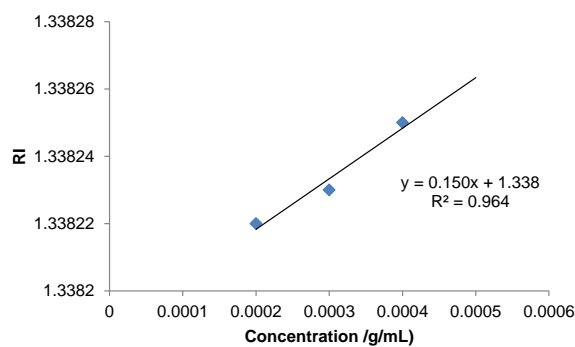
Figure B.39 Determination of the  $dn/dc$  value for anionic terpolymers of 50 series: (a) 50A1EC; (b) 50A3EC.



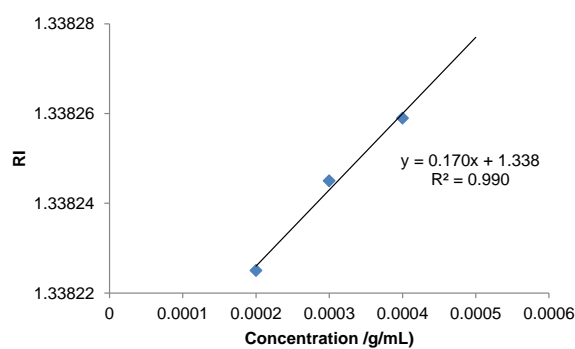
(a)



(b)

Figure B.40 Determination of the  $dn/dc$  value for anionic terpolymers of 80 series: (a) 80A1EC; (b) 80A3EC.

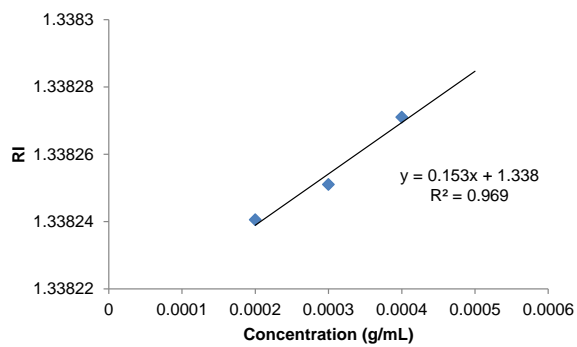
(a)



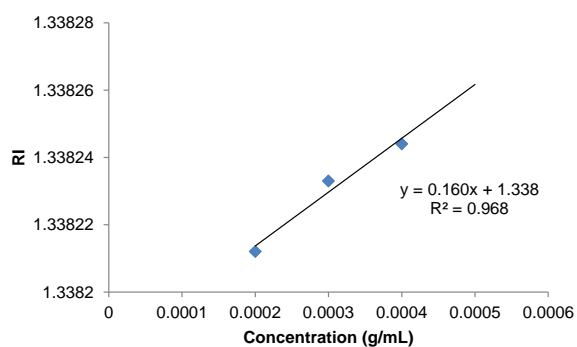
(b)

Figure B.41 Determination of the  $dn/dc$  value for anionic terpolymers of 50 series: (a) 50A1LC; (b) 50A3LC.

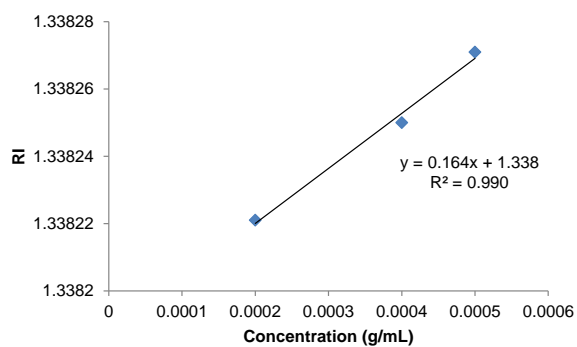




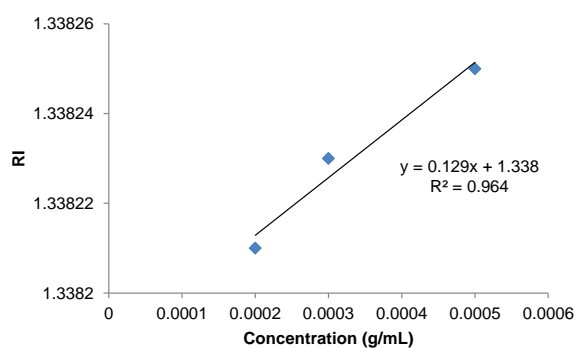
(a)



(b)

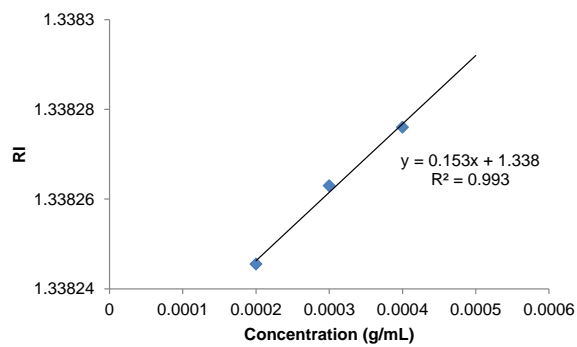
Figure B.42 Determination of the  $dn/dc$  value for anionic terpolymers of 80 series: (a) 80A1LC; (b) 80A3LC.

(a)

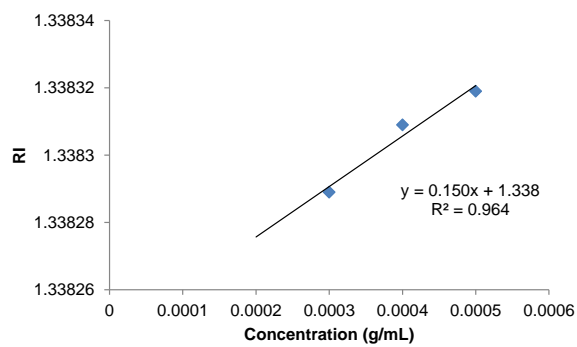


(b)

Figure B.43 Determination of the  $dn/dc$  value for anionic terpolymers of 50 series: (a) 50A1SC; (b) 50A3SC.



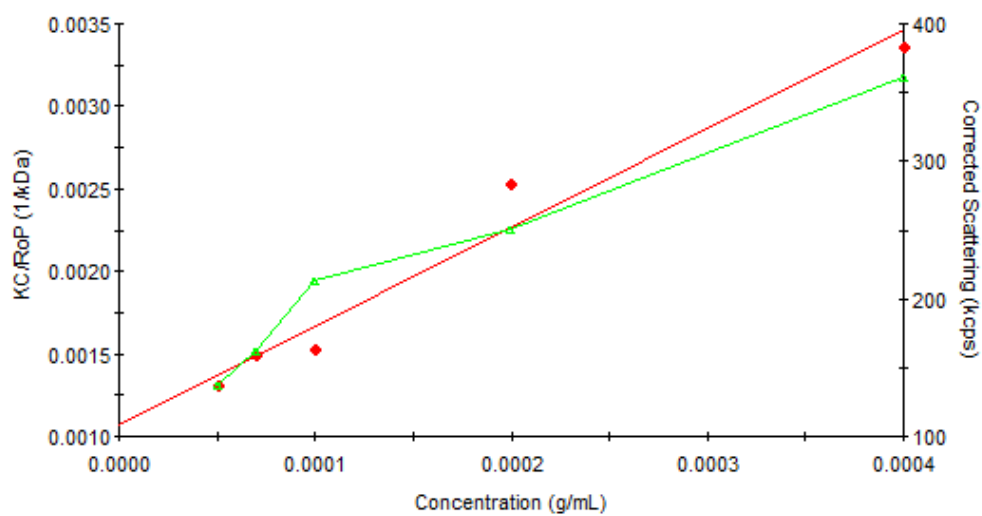
(a)



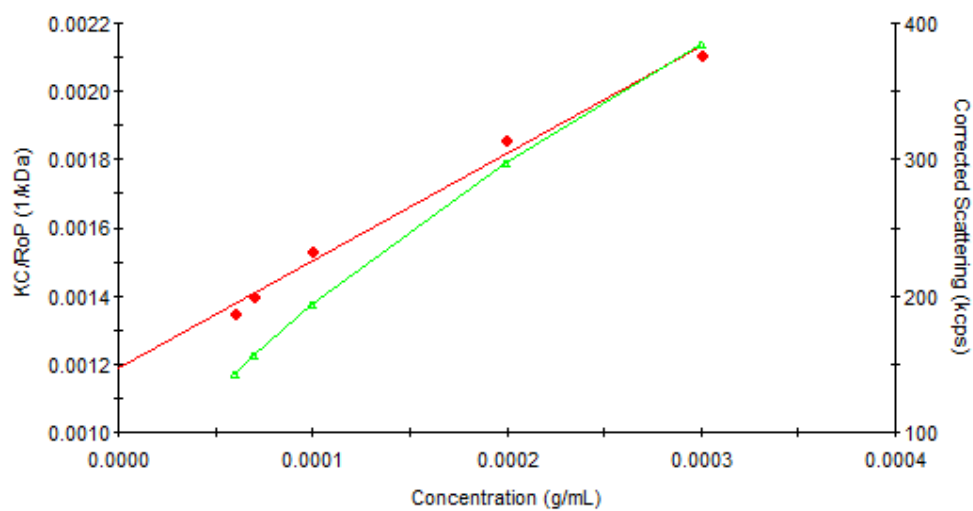
(b)

Figure B.44 Determination of the  $dn/dc$  value for anionic terpolymers of 80 series: (a) 80A1SC; (b) 80A3SC.

## - Determination of molecular weight

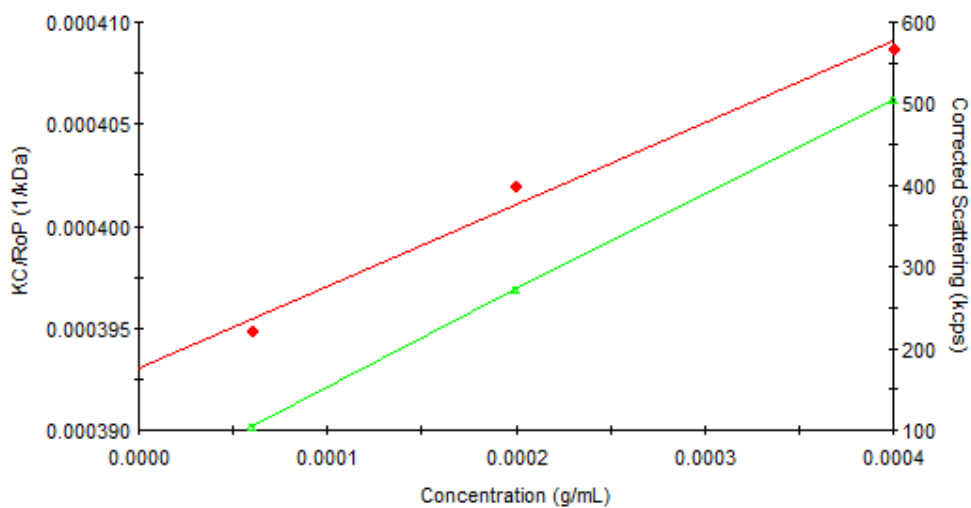


(a)

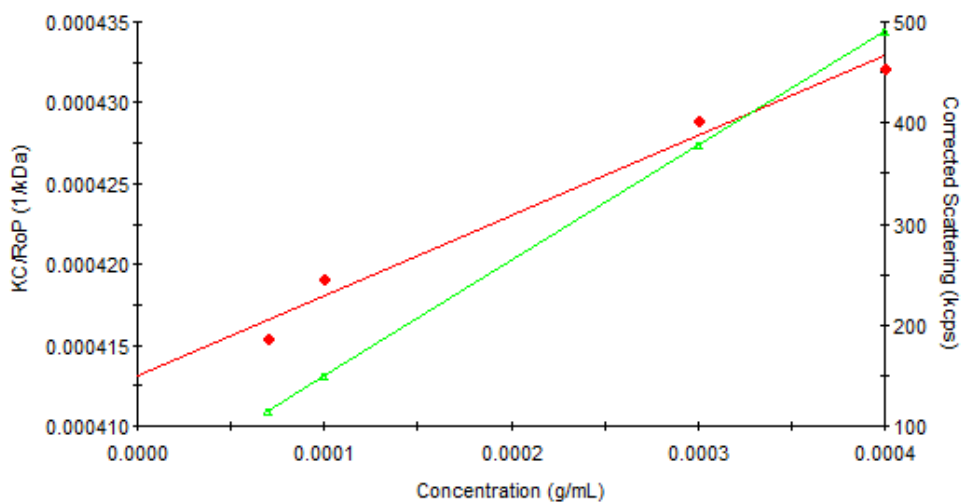


(b)

Figure B.45 Debye plot for weight-average molecular weight determination of cationic copolymer 50AC: (a) first measurement; (b) second measurement.

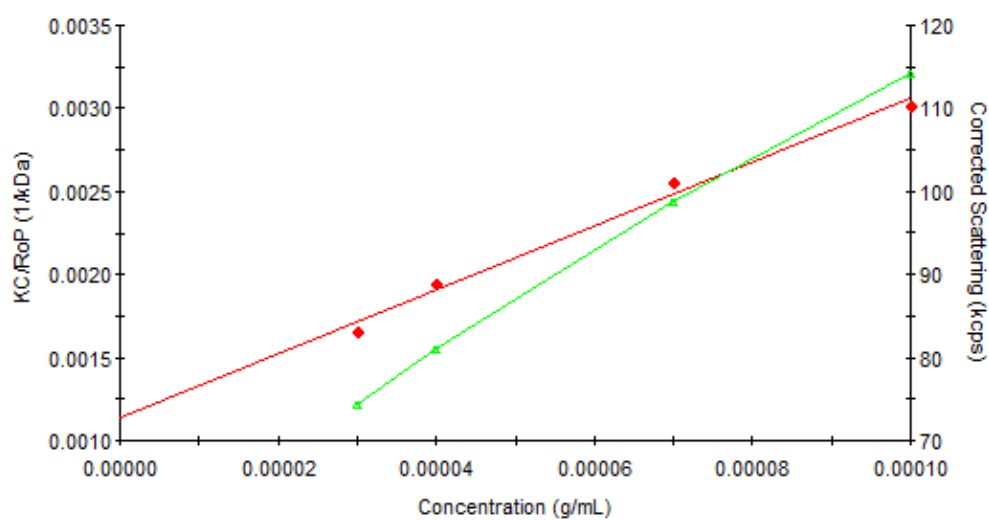


(a)

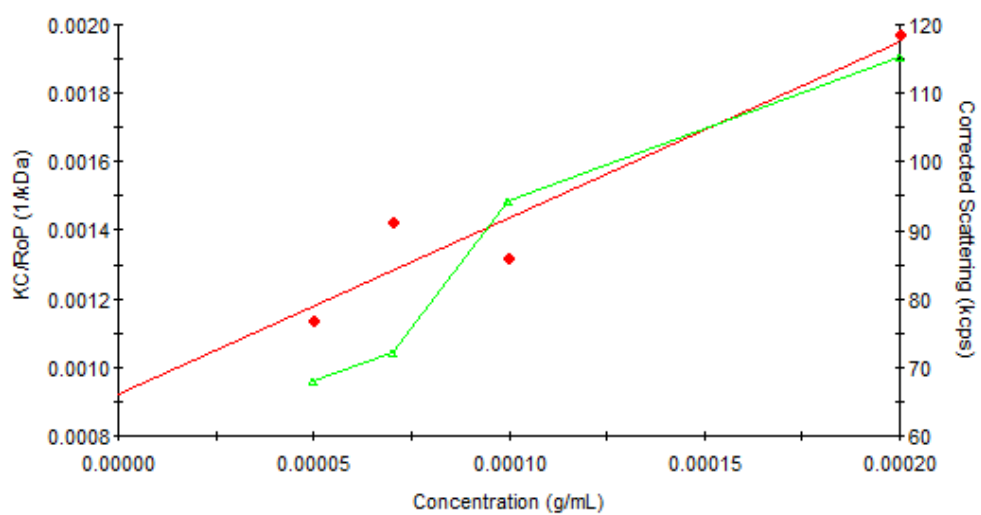


(b)

Figure B.46 Debye plot for weight-average molecular weight determination of cationic copolymer 50AP: (a) first measurement; (b) second measurement.

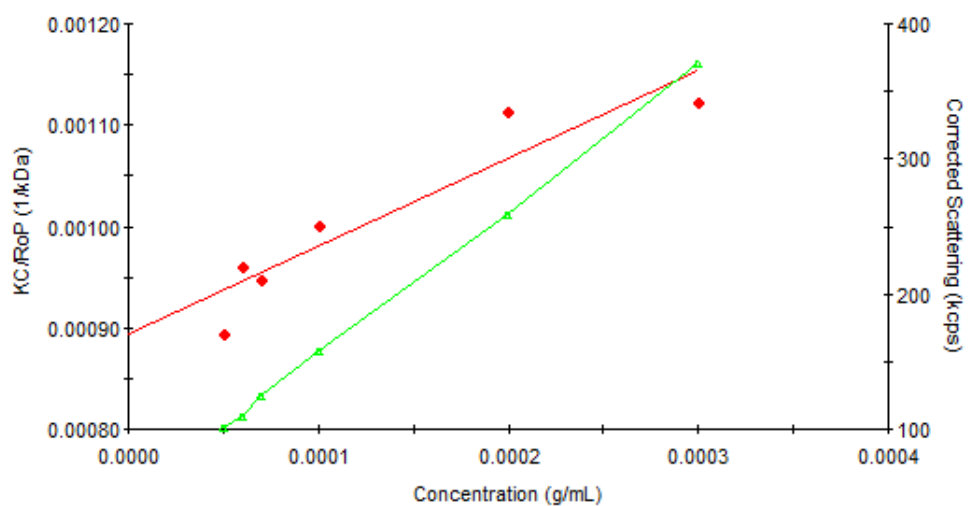


(a)

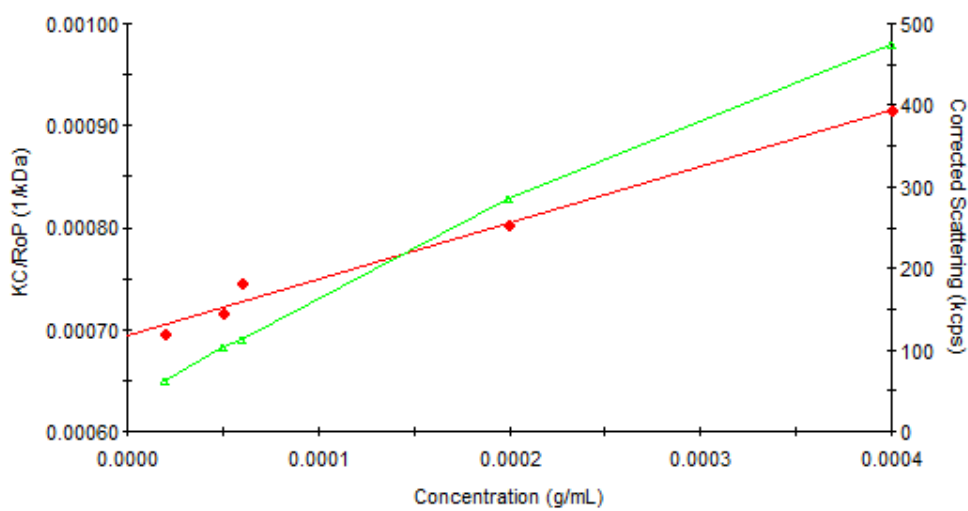


(b)

Figure B.47 Debye plot for weight-average molecular weight determination of cationic copolymer 80AC: (a) first measurement; (b) second measurement.

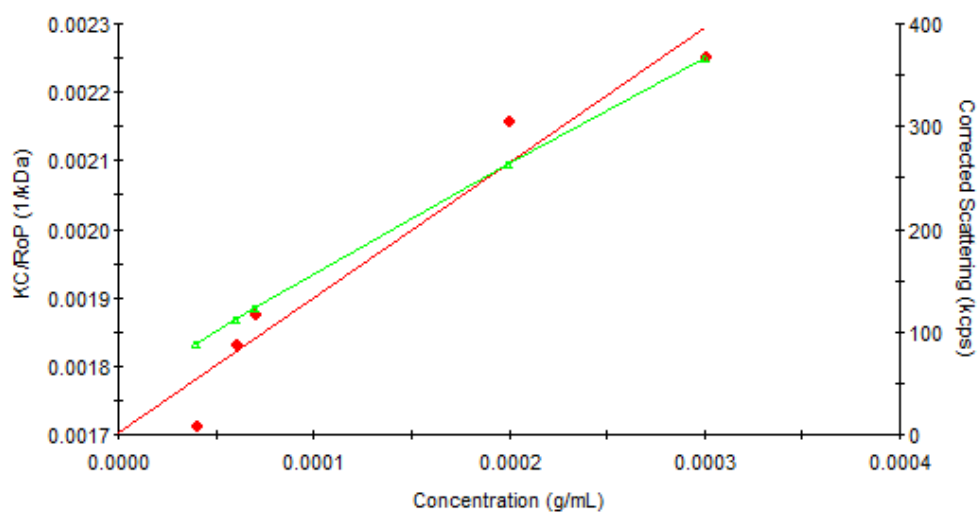


(a)

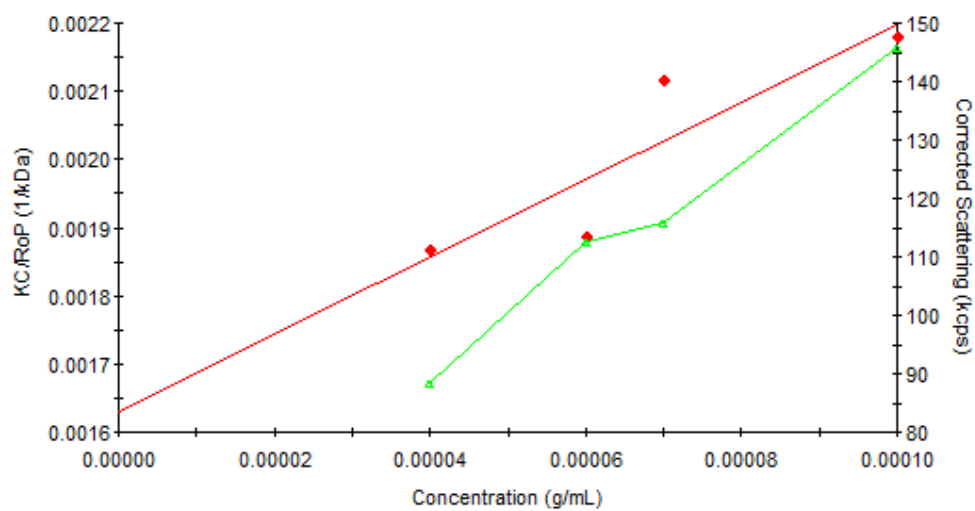


(b)

Figure B.48 Debye plot for weight-average molecular weight determination of cationic copolymer 80AP: (a) first measurement; (b) second measurement.

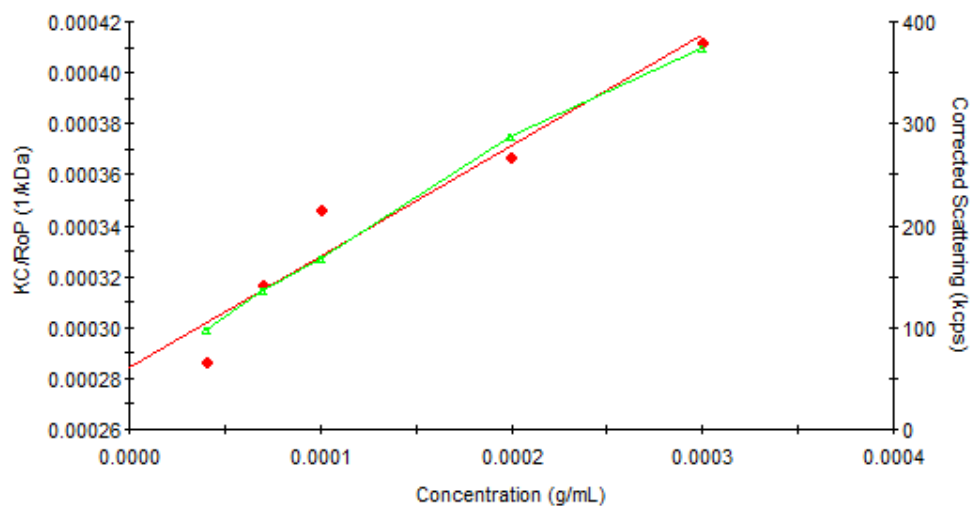


(a)

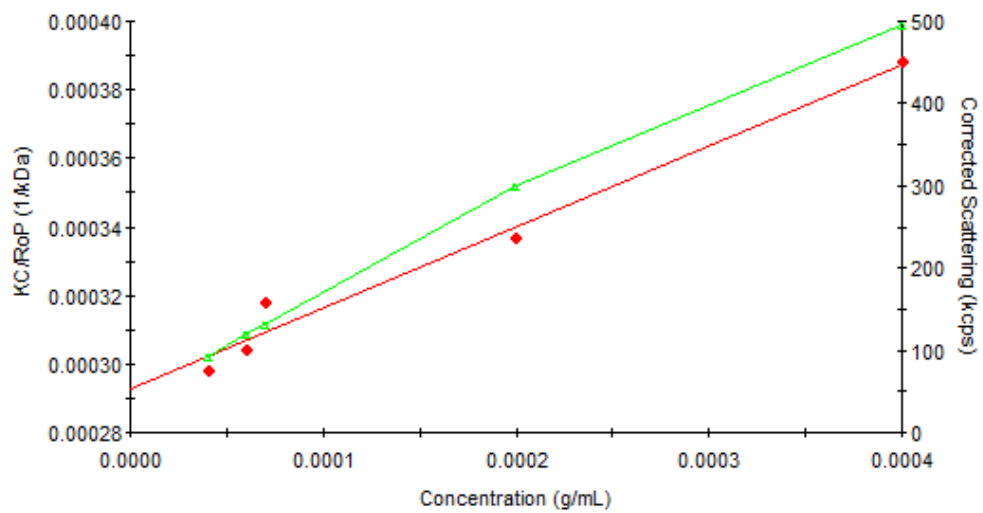


(b)

Figure B.49 Debye plot for weight-average molecular weight determination of cationic copolymer 50A1EC: (a) first measurement; (b) second measurement.



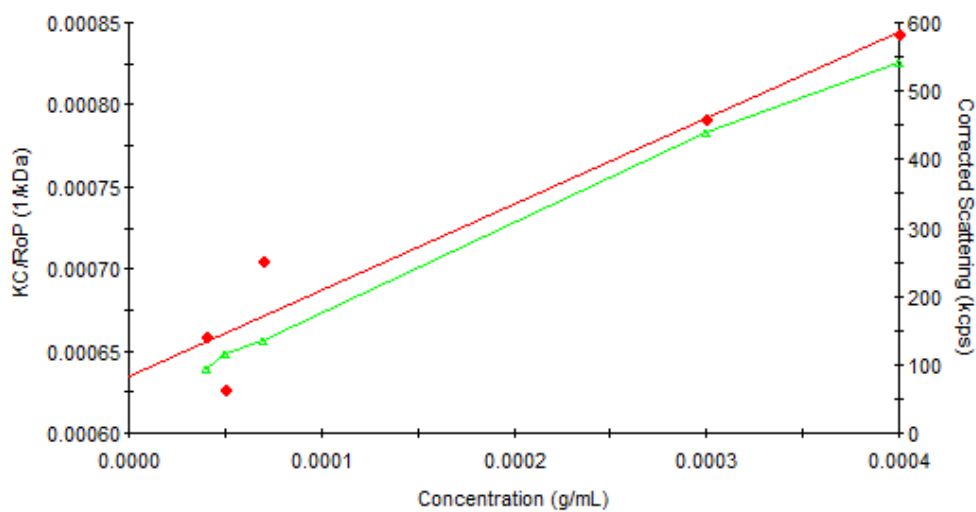
(a)



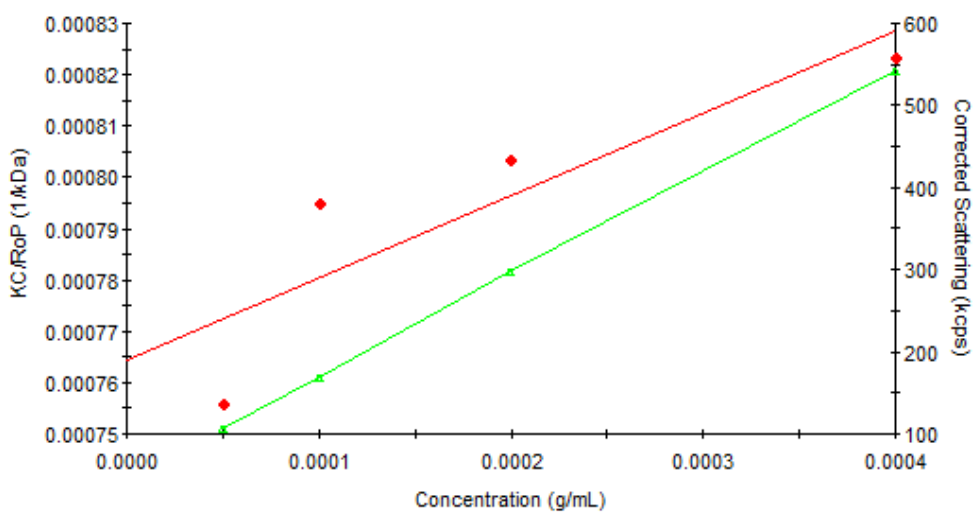
(b)

Figure B.50 Debye plot for weight-average molecular weight determination of cationic copolymer 50A3EC: (a) first measurement; (b) second measurement.



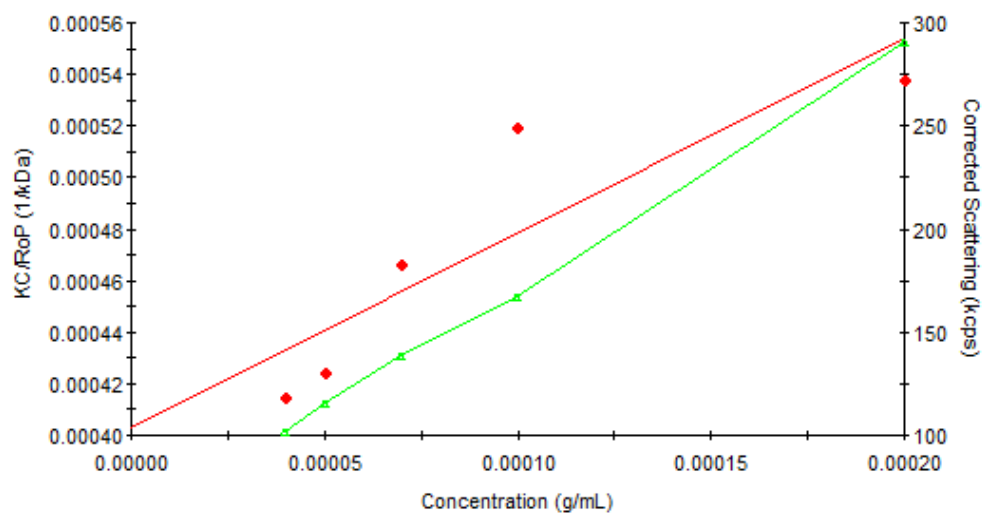


(a)

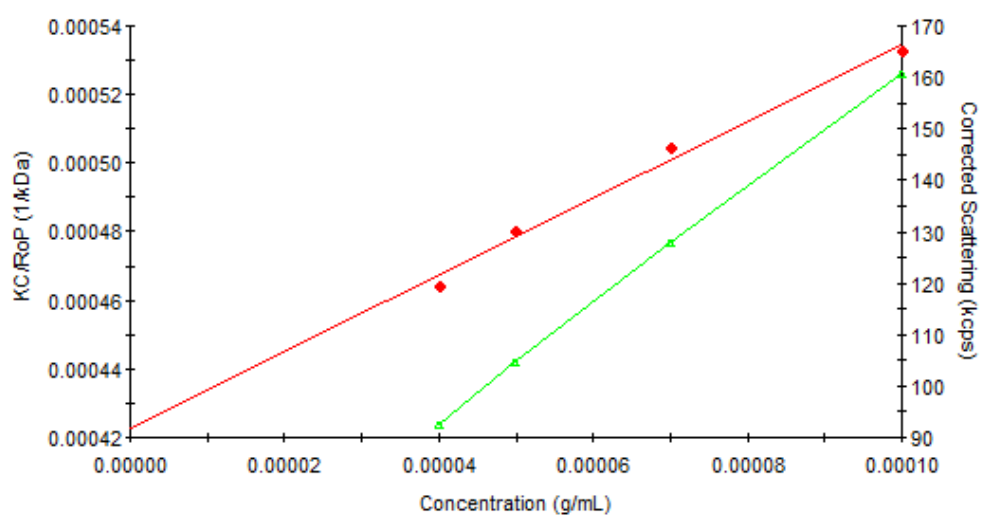


(b)

Figure B.51 Debye plot for weight-average molecular weight determination of cationic copolymer 80A1EC: (a) first measurement; (b) second measurement.

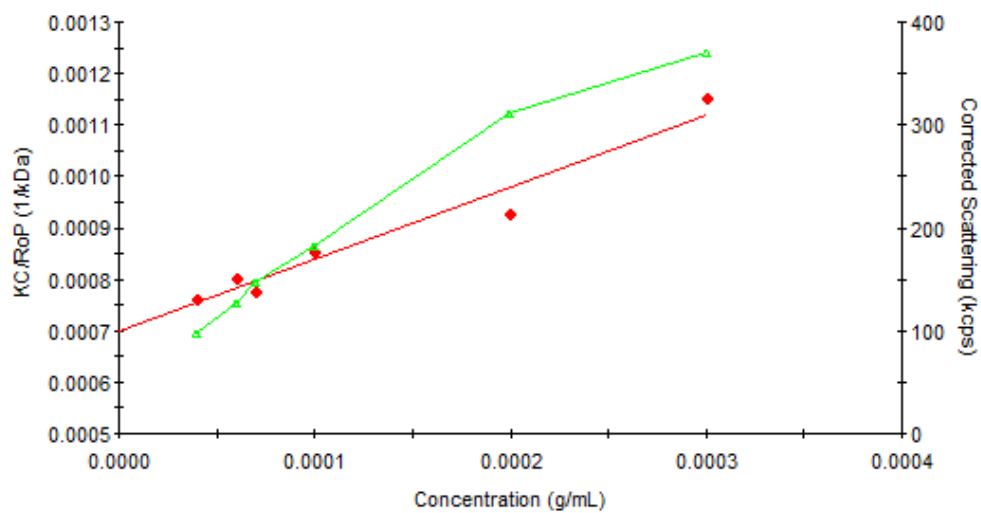


(a)

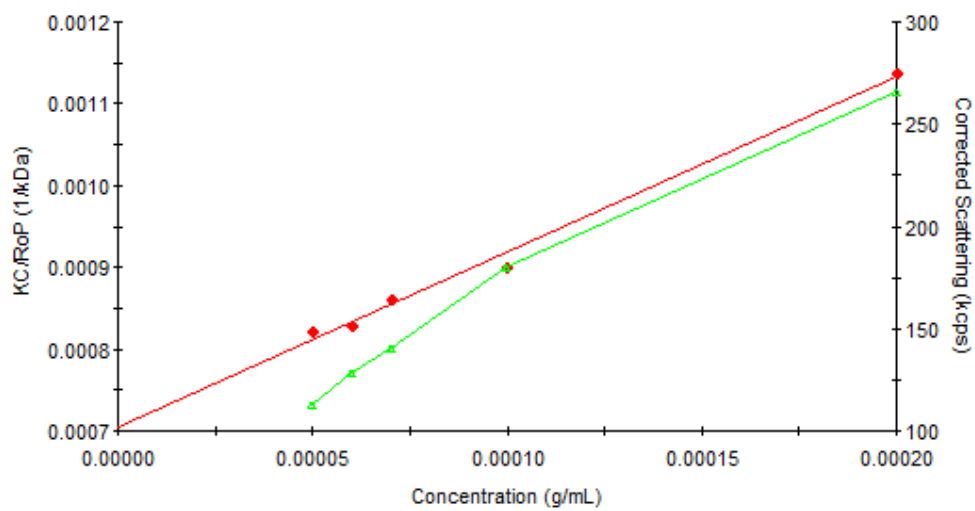


(b)

Figure B.52 Debye plot for weight-average molecular weight determination of cationic copolymer 80A3EC: (a) first measurement; (b) second measurement.

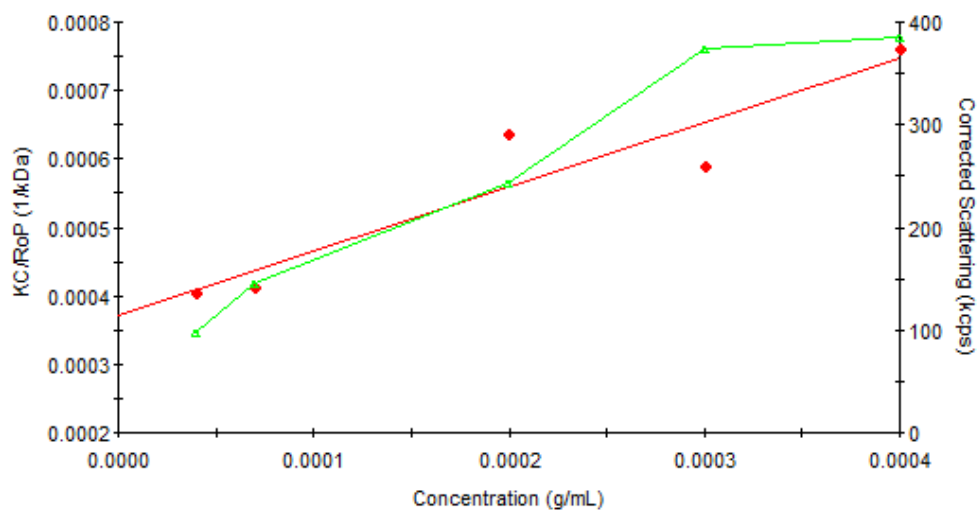


(a)

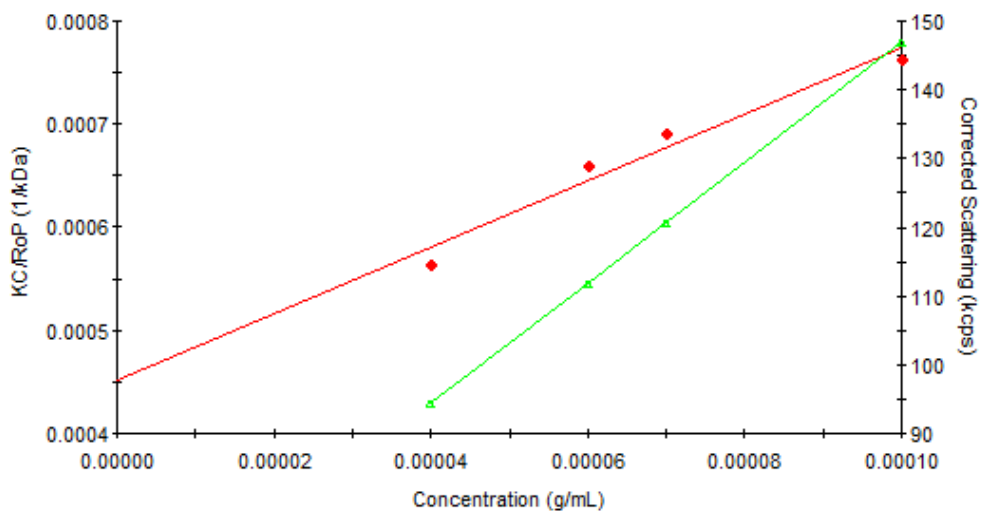


(b)

Figure B.53 Debye plot for weight-average molecular weight determination of cationic copolymer 50A1LC: (a) first measurement; (b) second measurement.

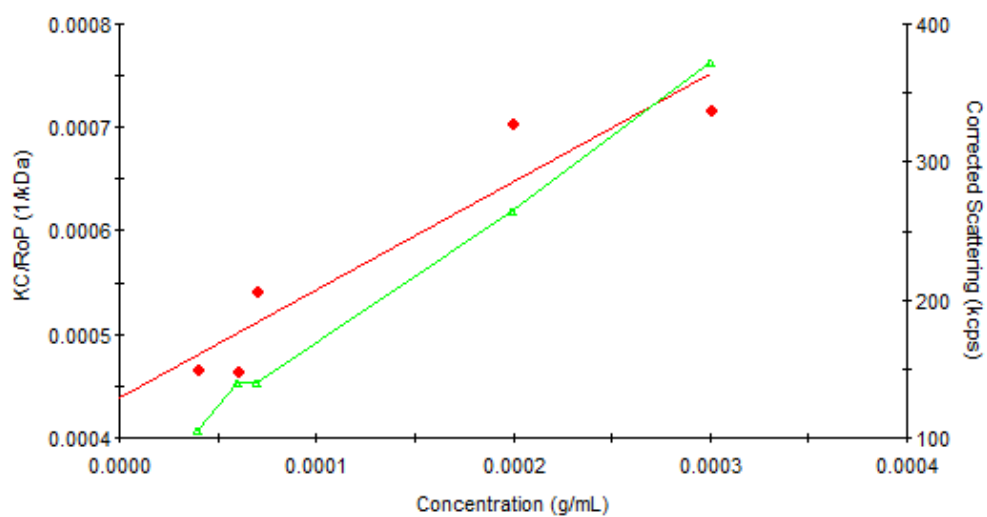


(a)

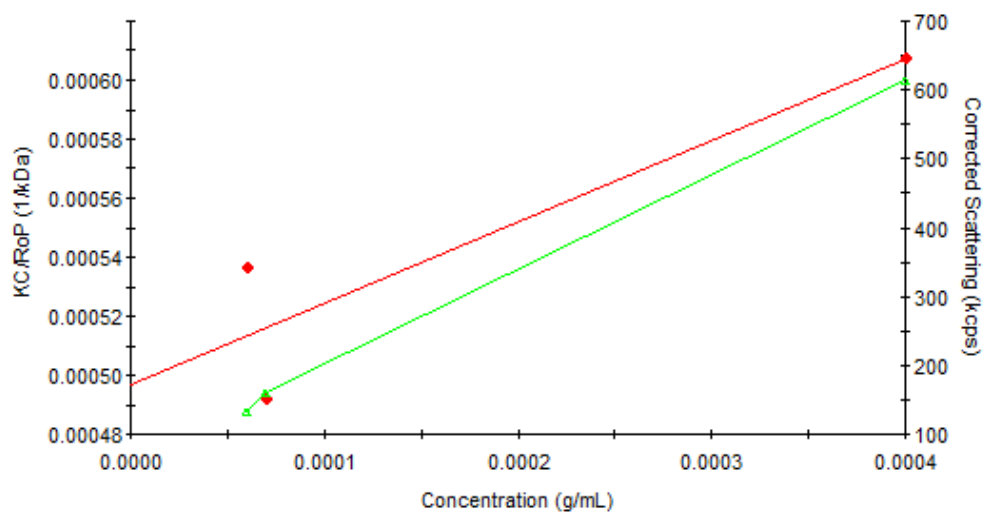


(b)

Figure B.54 Debye plot for weight-average molecular weight determination of cationic copolymer 50A3LC: (a) first measurement; (b) second measurement.

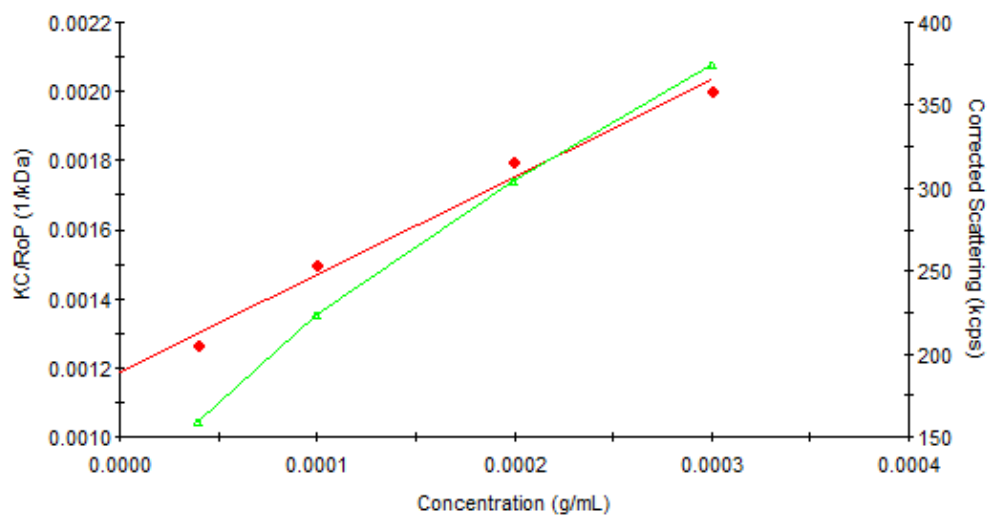


(a)

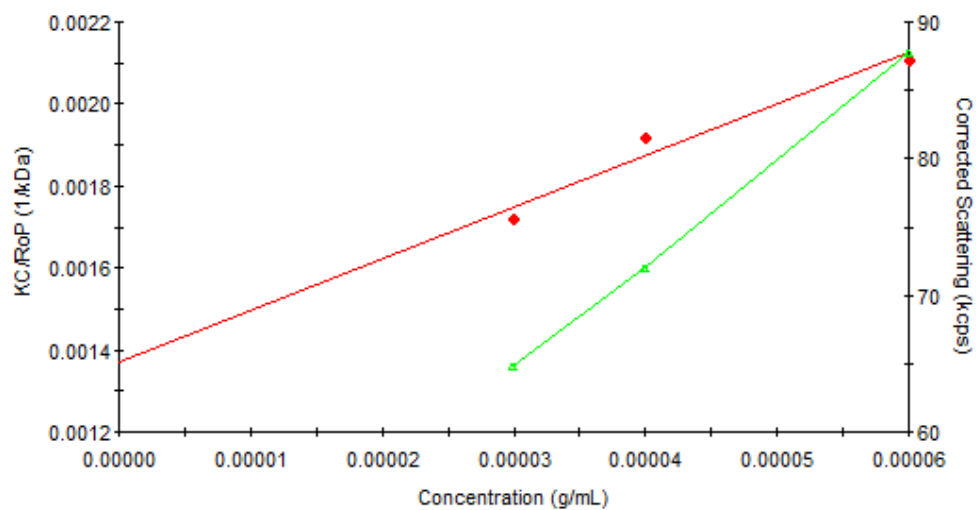


(b)

Figure B.55 Debye plot for weight-average molecular weight determination of cationic copolymer 80A1LC: (a) first measurement; (b) second measurement.

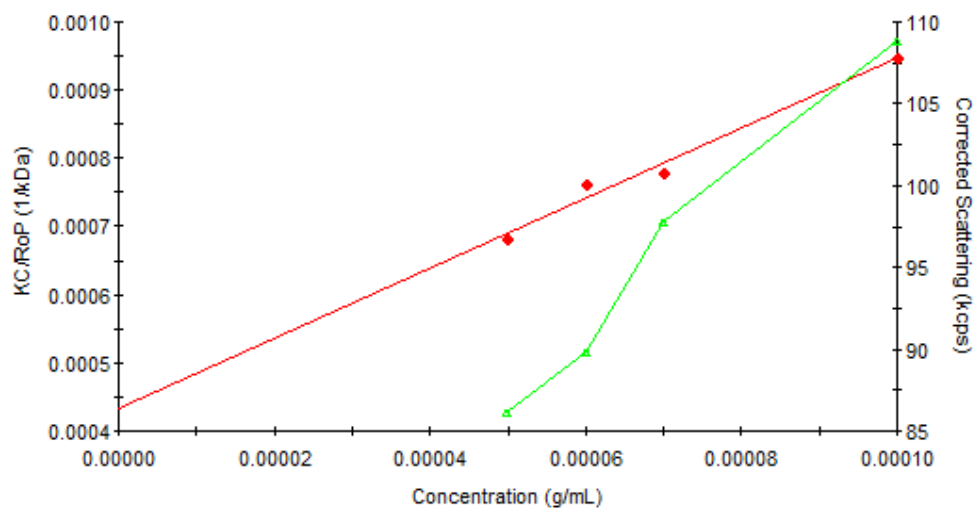


(a)

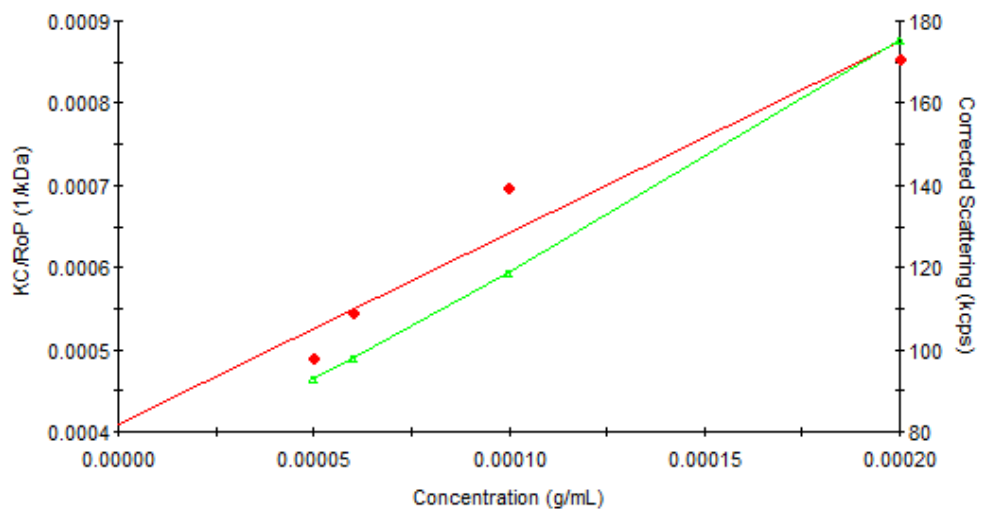


(b)

Figure B.56 Debye plot for weight-average molecular weight determination of cationic copolymer 80A3LC: (a) first measurement; (b) second measurement.

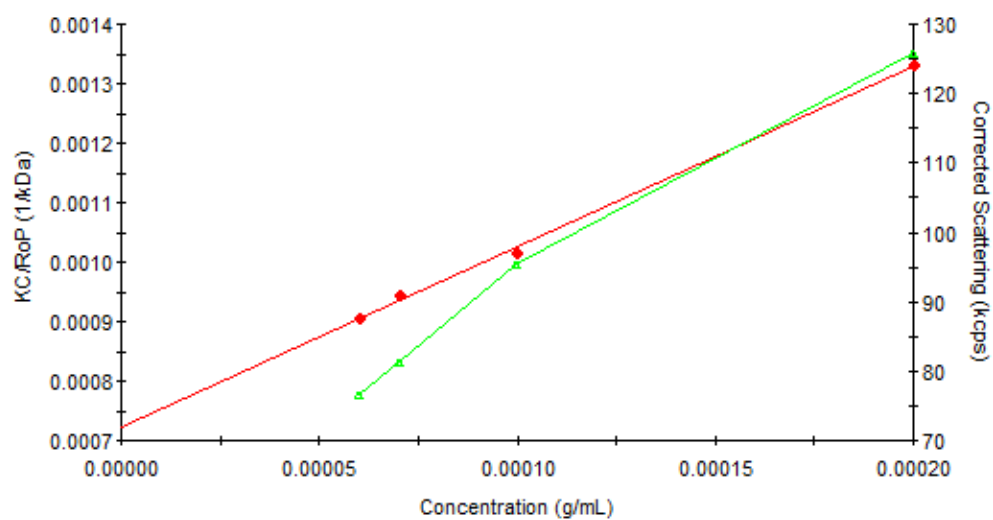


(a)

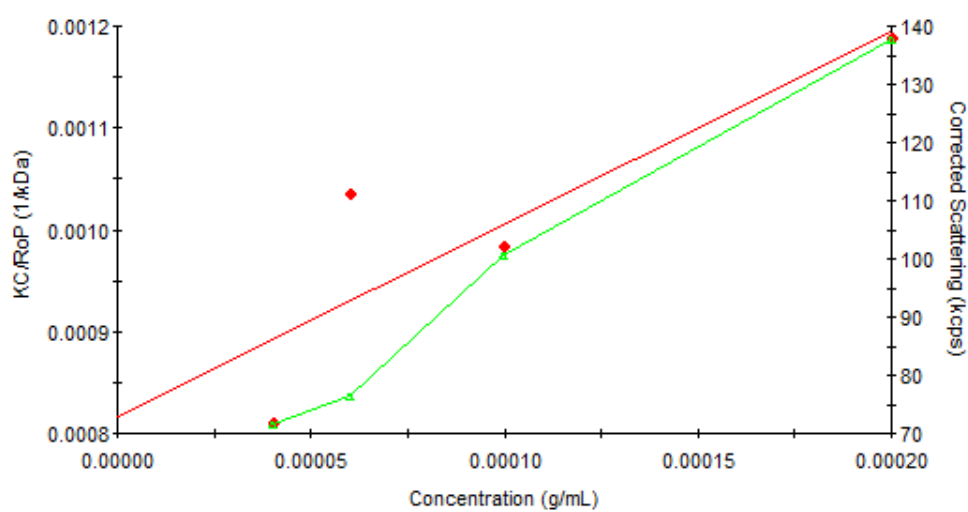


(b)

Figure B.57 Debye plot for weight-average molecular weight determination of cationic copolymer 50A1SC: (a) first measurement; (b) second measurement.



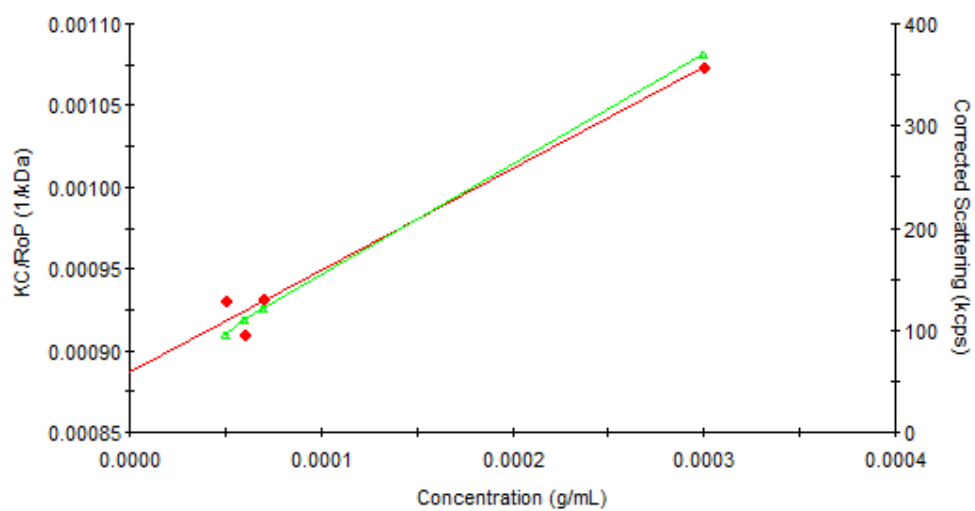
(a)



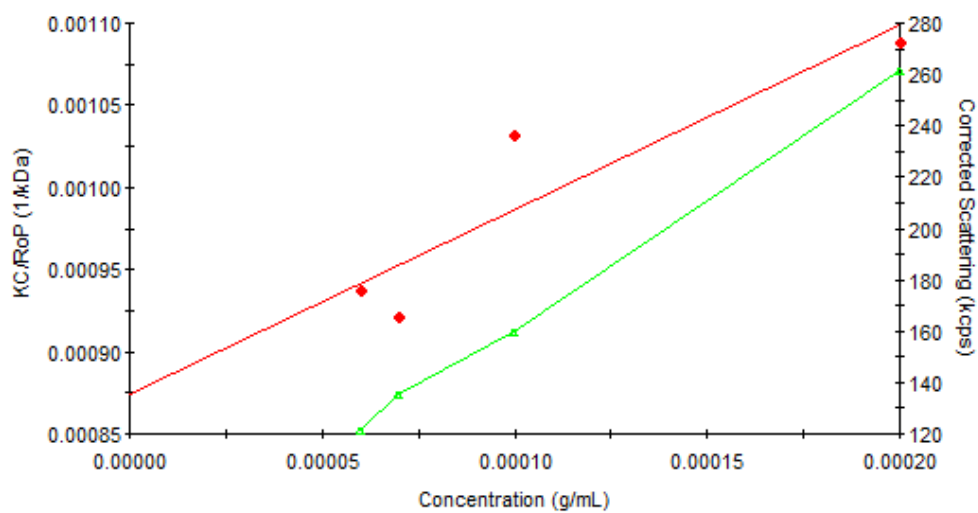
(b)

Figure B.58 Debye plot for weight-average molecular weight determination of cationic copolymer 50A3SC: (a) first measurement; (b) second measurement.



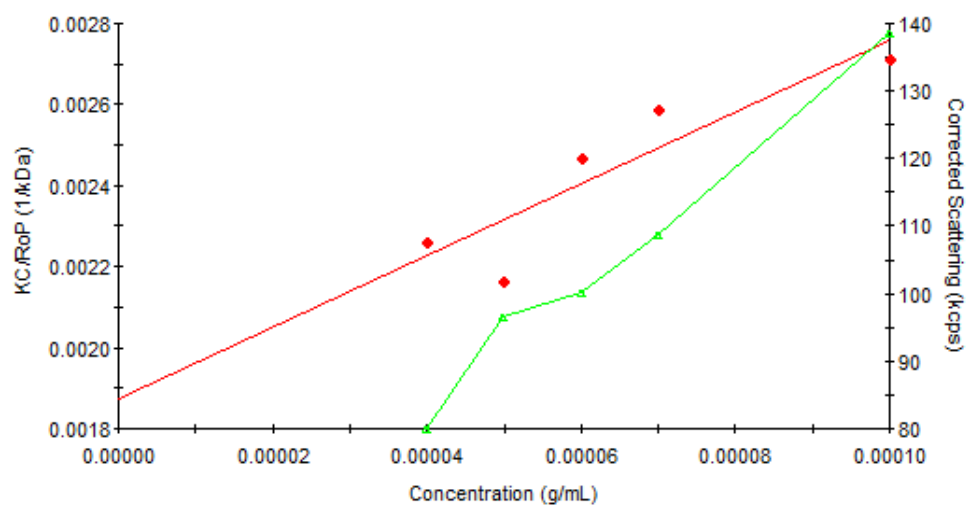


(a)

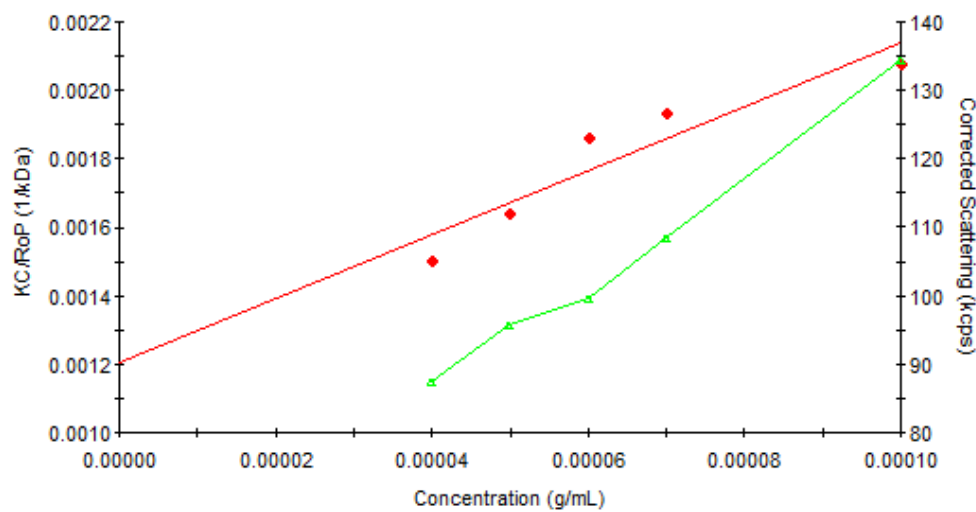


(b)

Figure B.59 Debye plot for weight-average molecular weight determination of cationic copolymer 80A1SC: (a) first measurement; (b) second measurement.



(a)



(b)

Figure B.60 Debye plot for weight-average molecular weight determination of cationic copolymer 80A3SC: (a) first measurement; (b) second measurement.

## MOLECULAR WEIGHT DETERMINATION BY SEC

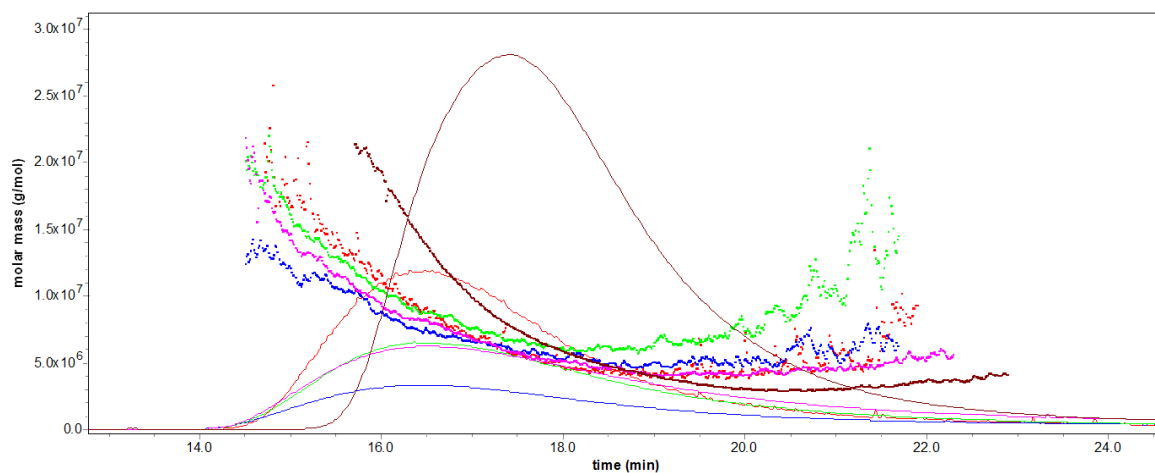


Figure B.61 Molecular weight distributions obtained by size exclusion chromatography for cationic copolymer 50AC, for five replicates.

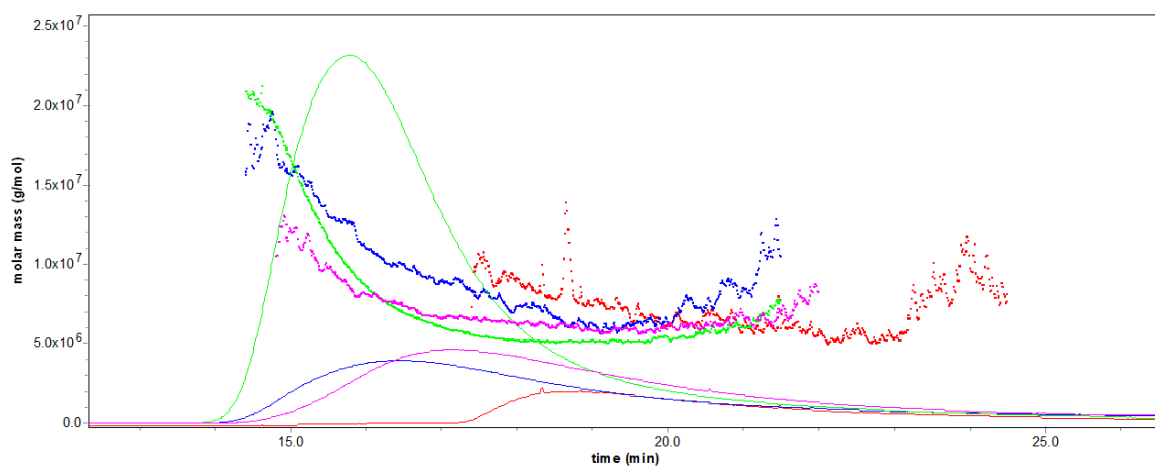


Figure B.62 Molecular weight distributions obtained by size exclusion chromatography for cationic copolymer 80AC, for four replicates.

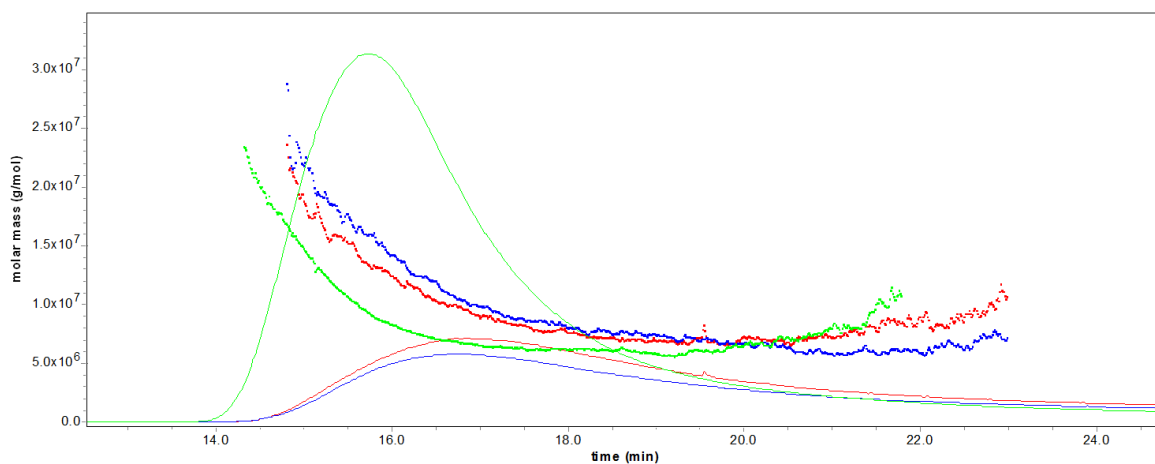
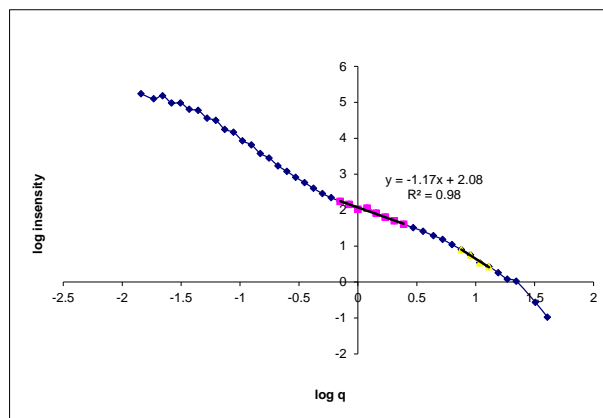


Figure B.63 Molecular weight distributions obtained by size exclusion chromatography for cationic copolymer 80AP, for three replicates.

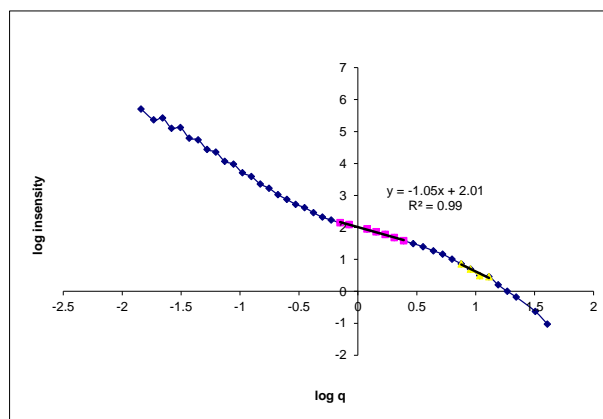
## Appendix C

## Supporting information for Chapter 6: Flocculation process analysis

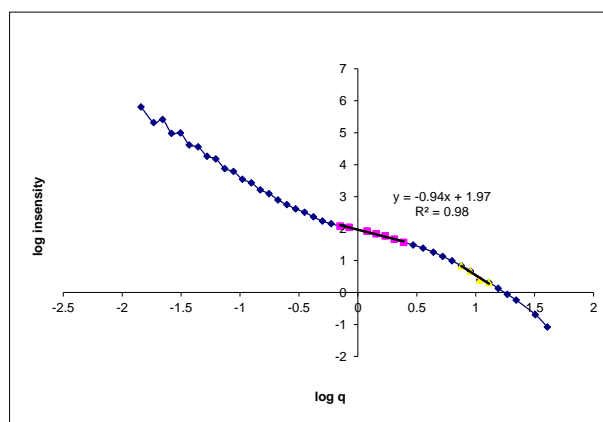
## SCATTERING EXPONENT DETERMINATION



(a)

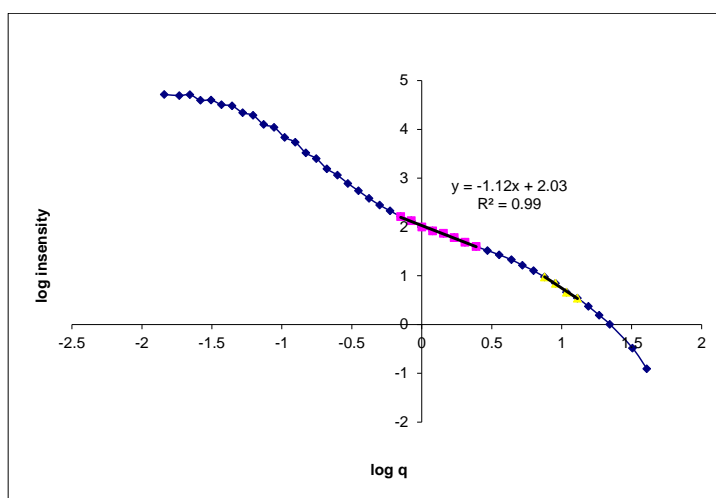


(b)

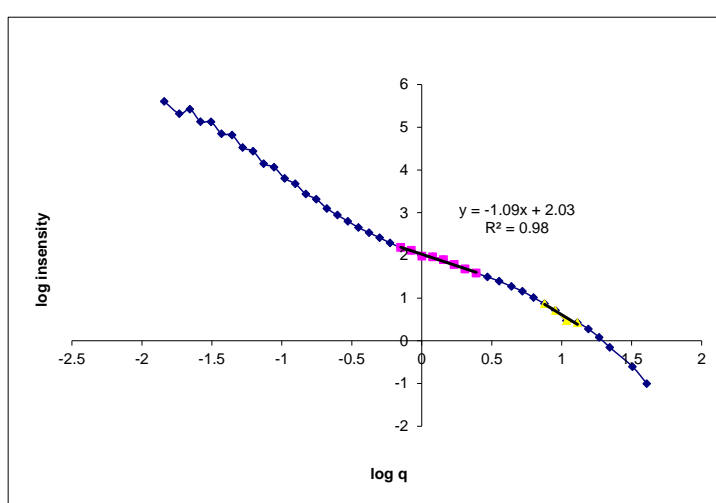


(c)

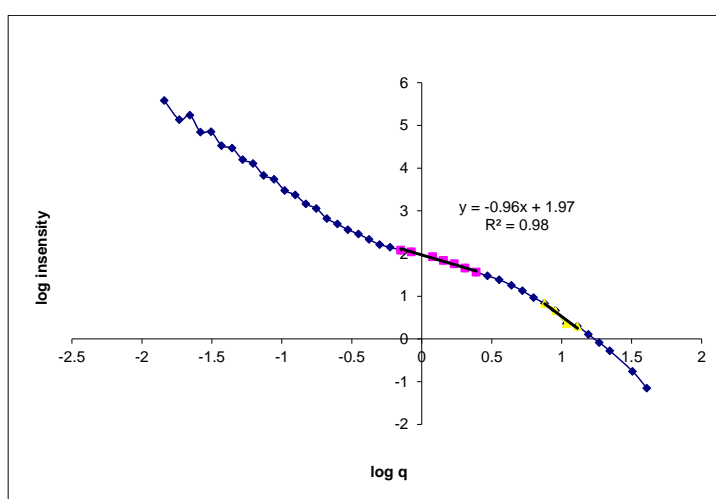
Figure C.1 Determination of SE (plot of scattering intensity versus  $q$ ) for cationic copolymer 60MC at 6 min: (a) 3.3 mg/L; (b) 6.5 mg/L; (c) 13 mg/L.



(a)

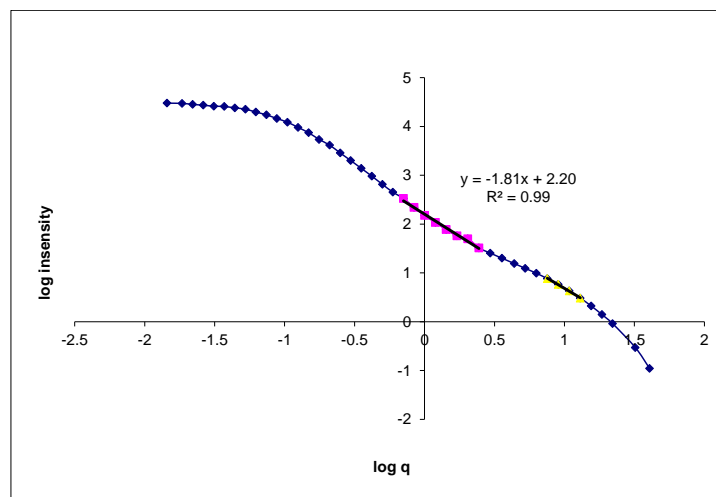


(b)

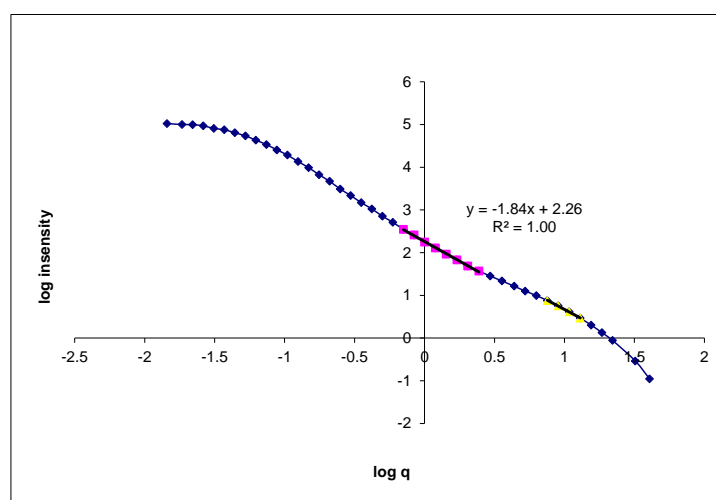


(c)

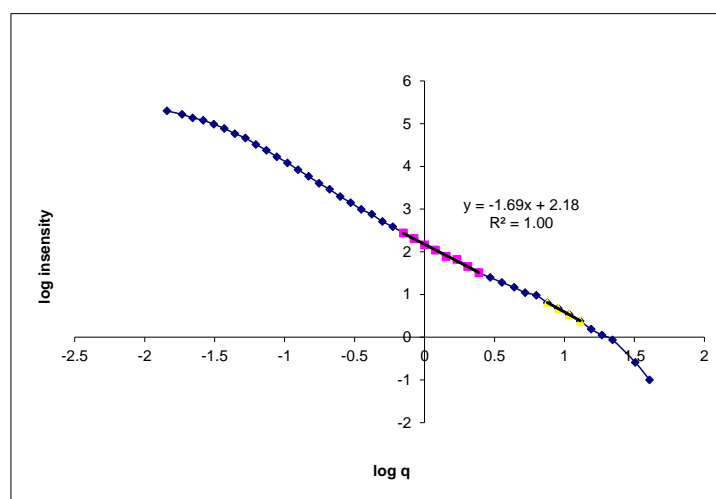
Figure C.2 Determination of SE (plot of scattering intensity versus  $q$ ) for cationic copolymer 60MP at 6 min: (a) 3.3 mg/L; (b) 6.5 mg/L; (c) 13 mg/L.



(a)

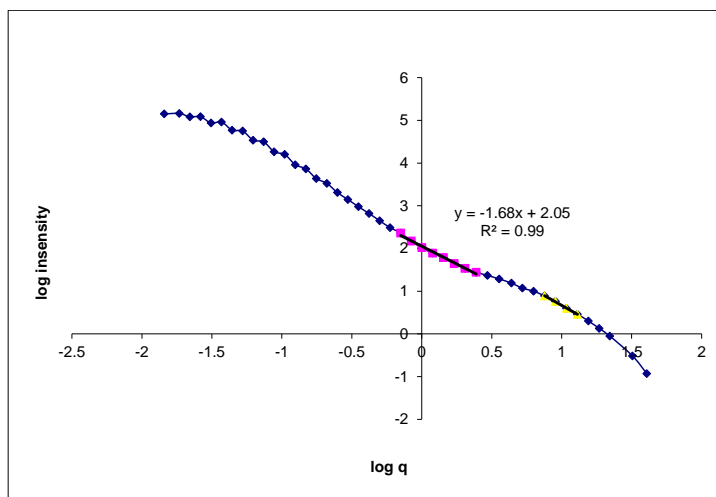


(b)

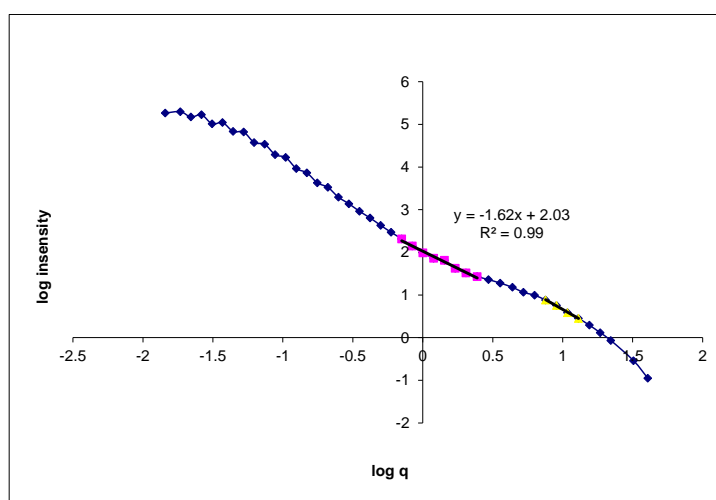


(c)

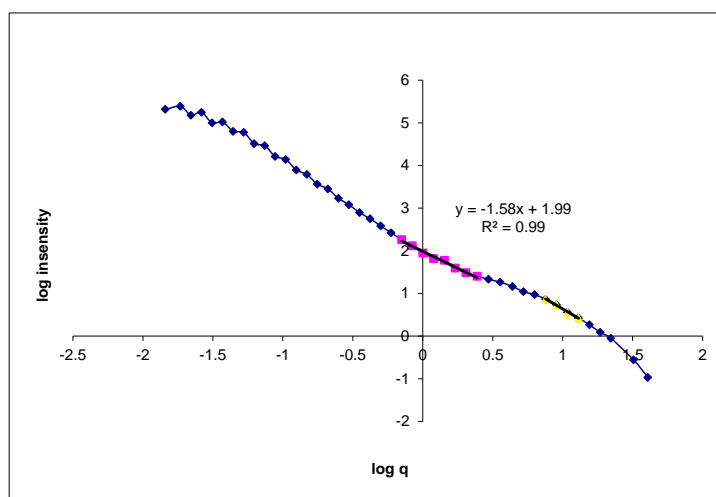
Figure C.3 Determination of SE (plot of scattering intensity versus  $q$ ) for cationic copolymer 50AC at 6 min: (a) 3.3 mg/L; (b) 6.5 mg/L; (c) 13 mg/L.



(a)

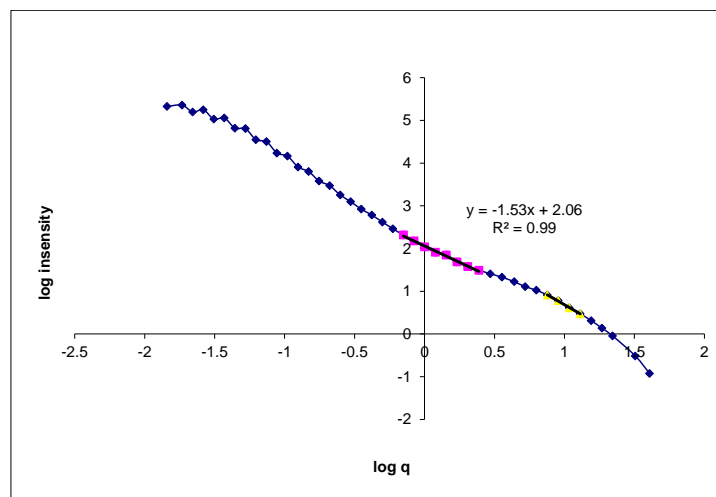


(b)

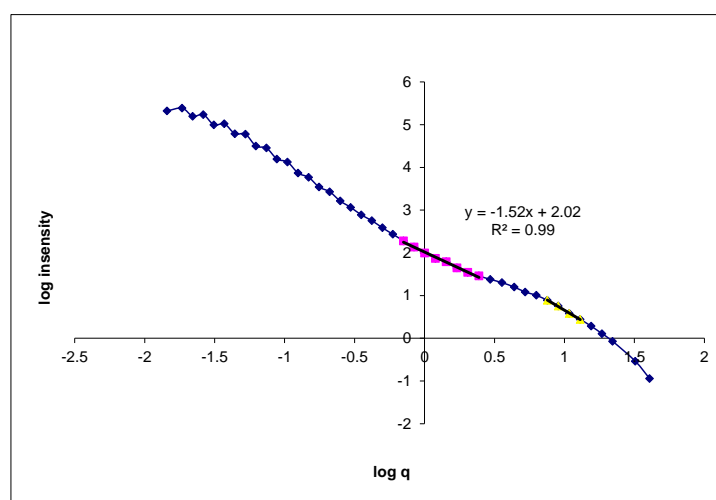


(c)

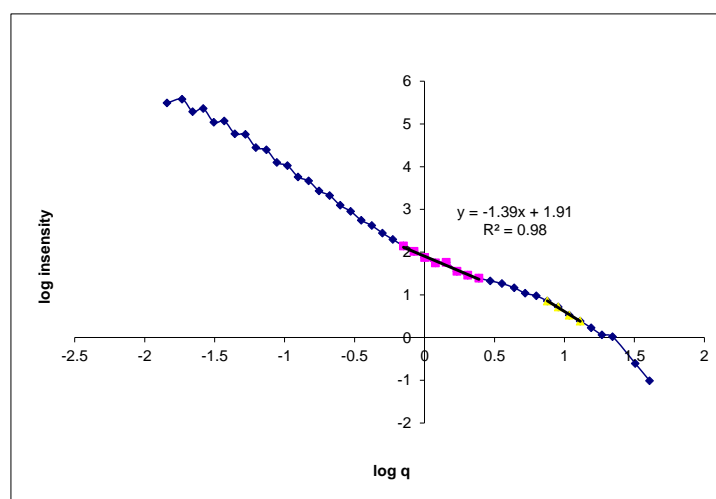
Figure C.4 Determination of SE (plot of scattering intensity versus  $q$ ) for cationic copolymer 80AC at 6 min: (a) 3.3 mg/L; (b) 6.5 mg/L; (c) 13 mg/L.



(a)



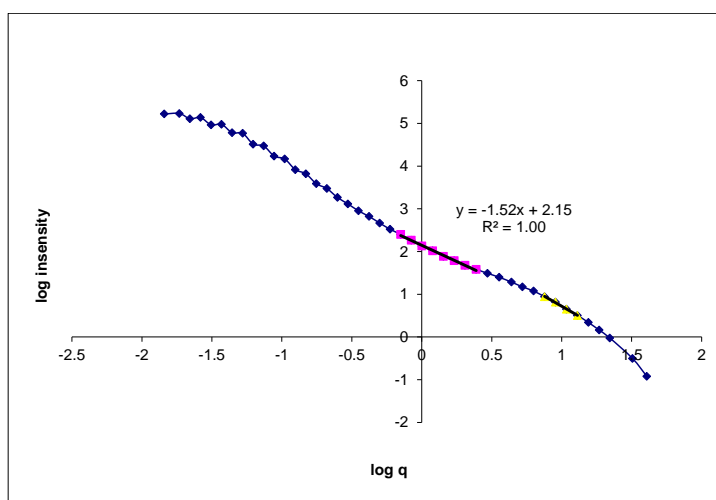
(b)



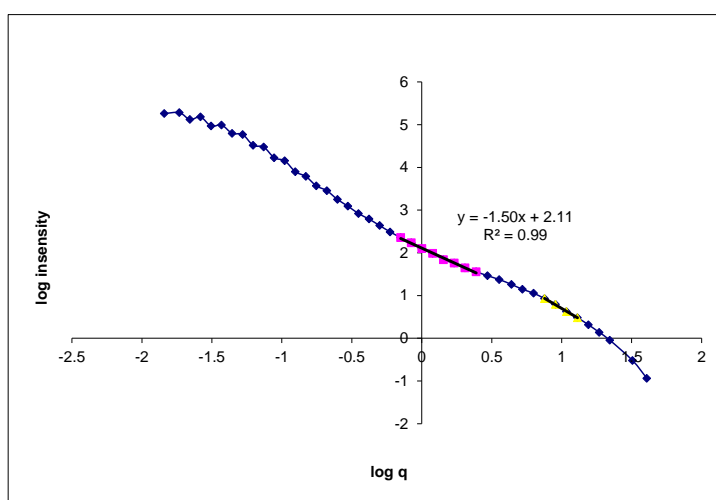
(c)

Figure C.5 Determination of SE (plot of scattering intensity versus  $q$ ) for cationic copolymer 50AP at 6 min: (a) 3.3 mg/L; (b) 6.5 mg/L; (c) 13 mg/L.

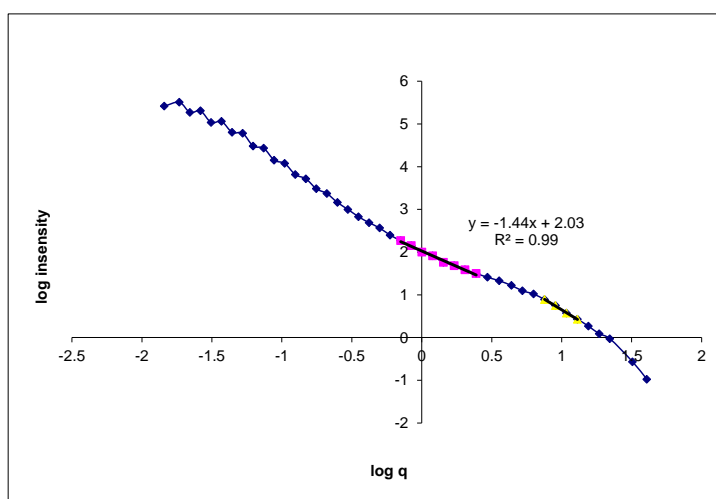




(a)

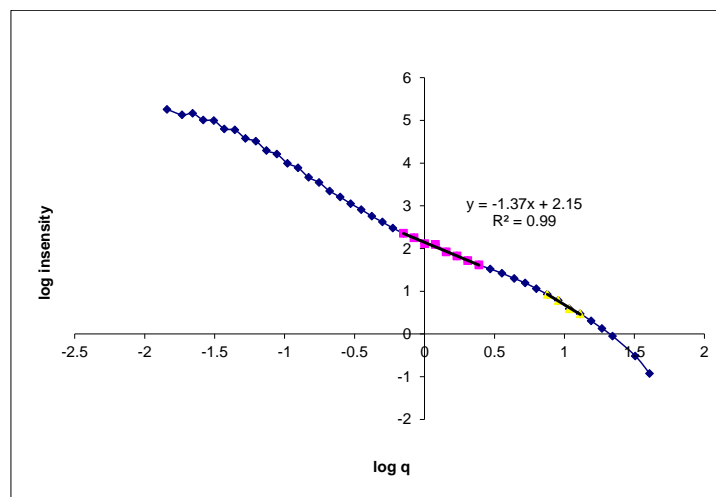


(b)

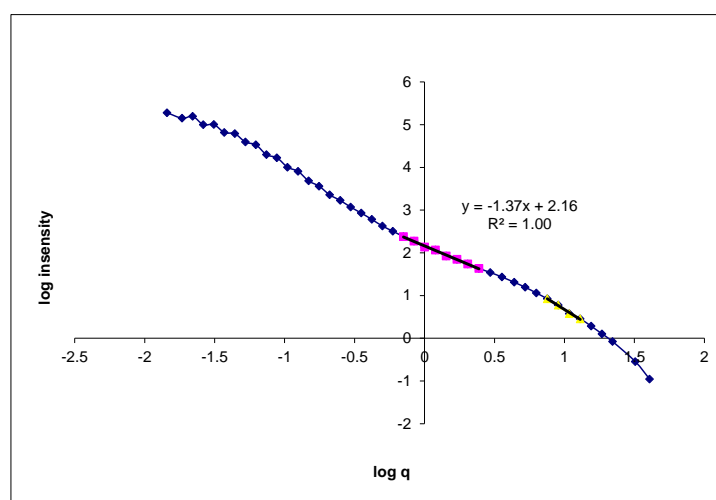


(c)

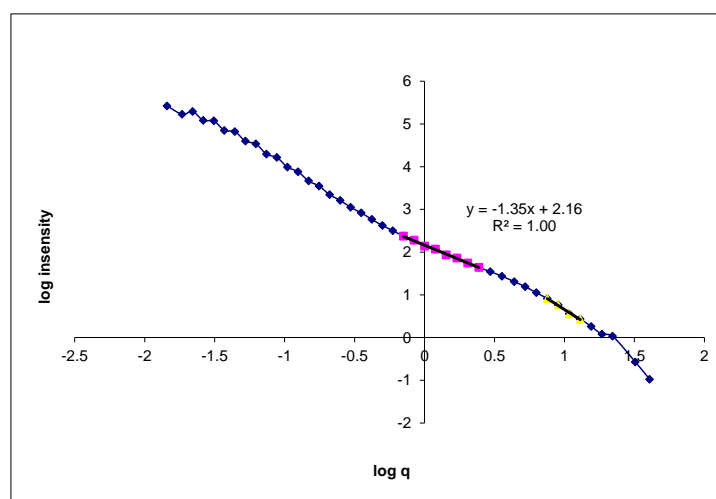
Figure C.6 Determination of SE (plot of scattering intensity versus  $q$ ) for cationic copolymer 80AP at 6 min: (a) 3.3 mg/L; (b) 6.5 mg/L; (c) 13 mg/L.



(a)

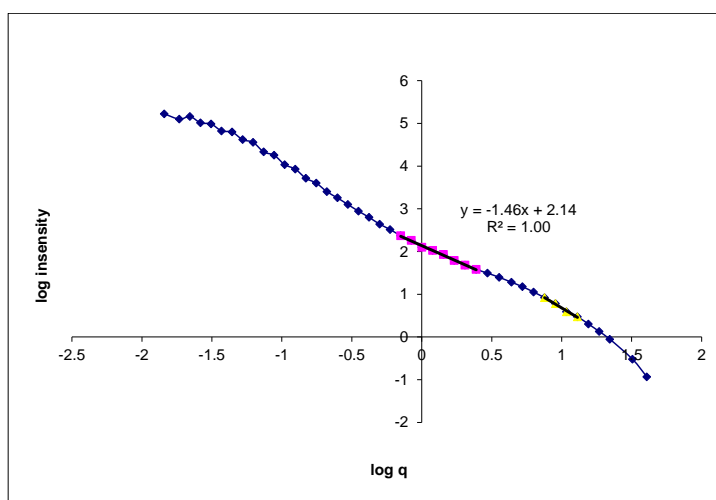


(b)

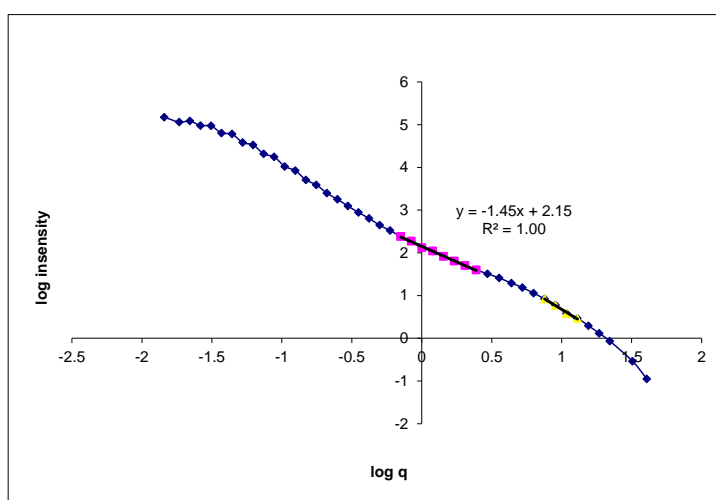


(c)

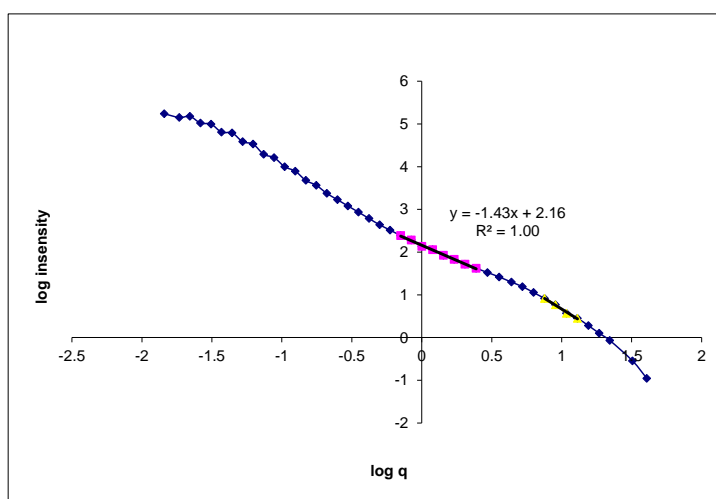
Figure C.7 Determination of SE (plot of scattering intensity versus  $q$ ) for cationic copolymer 50A1EC at 6 min: (a) 3.3 mg/L; (b) 6.5 mg/L; (c) 13 mg/L.



(a)

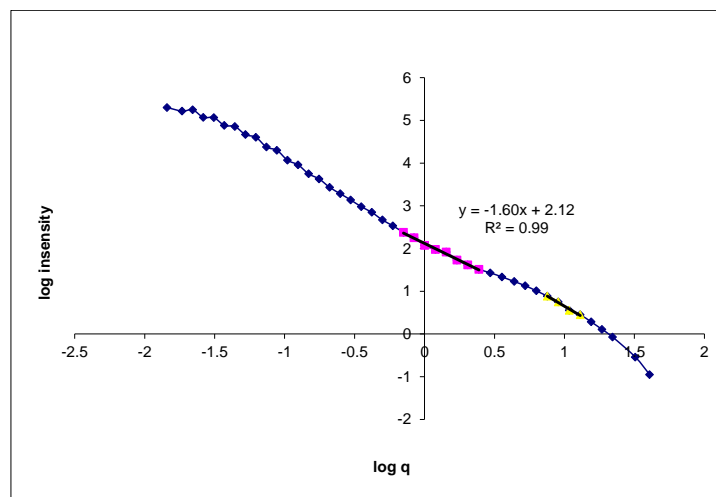


(b)

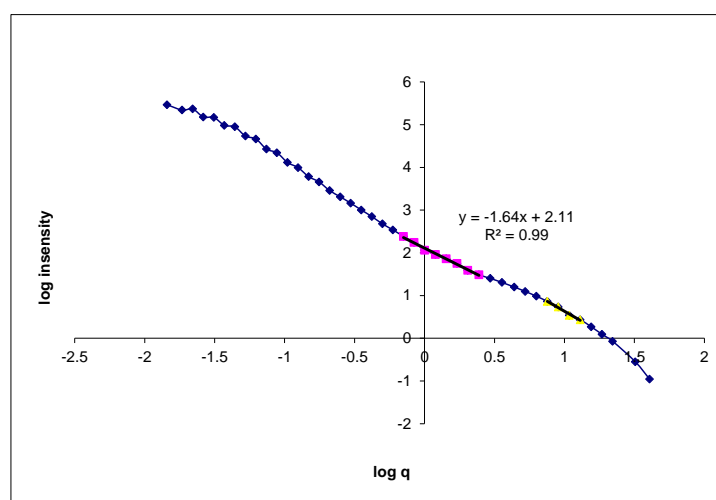


(c)

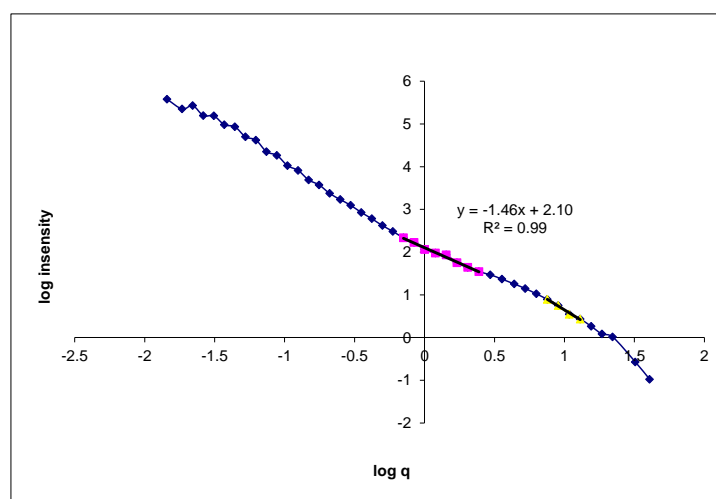
Figure C.8 Determination of SE (plot of scattering intensity versus  $q$ ) for cationic copolymer 50A3EC at 6 min: (a) 3.3 mg/L; (b) 6.5 mg/L; (c) 13 mg/L.



(a)

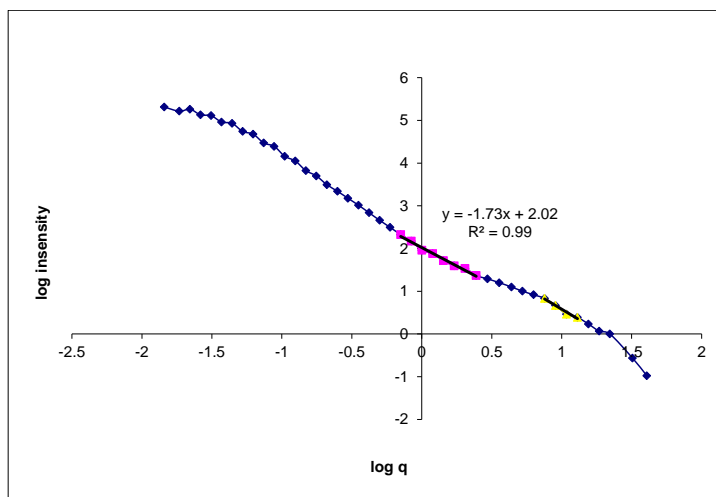


(b)

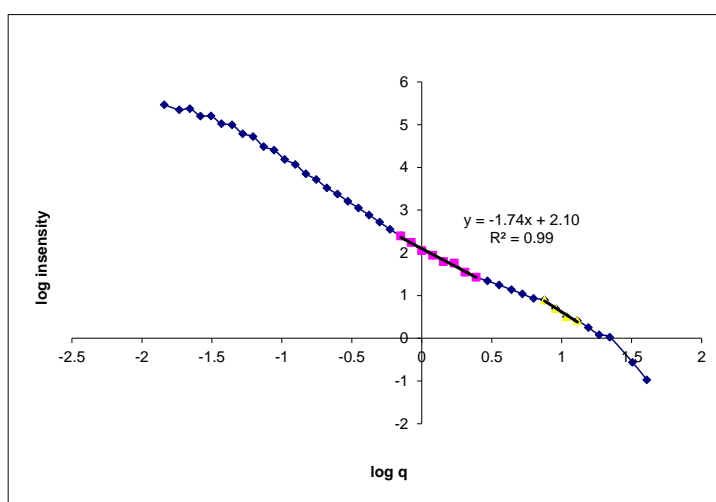


(c)

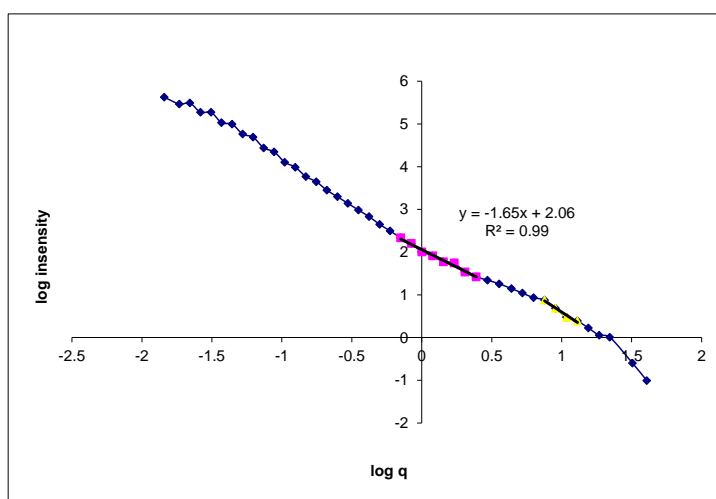
Figure C.9 Determination of SE (plot of scattering intensity versus  $q$ ) for cationic copolymer 80A1EC at 6 min: (a) 3.3 mg/L; (b) 6.5 mg/L; (c) 13 mg/L.



(a)

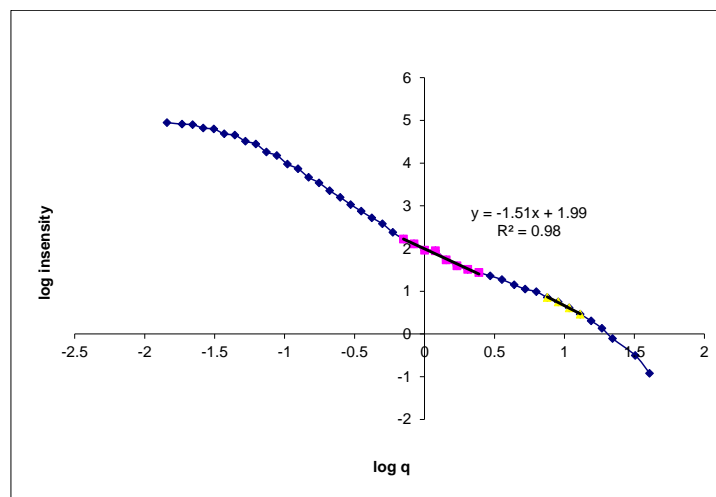


(b)

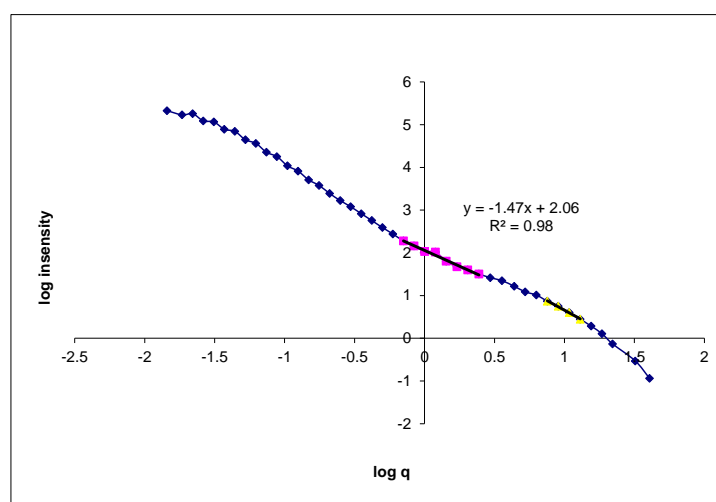


(c)

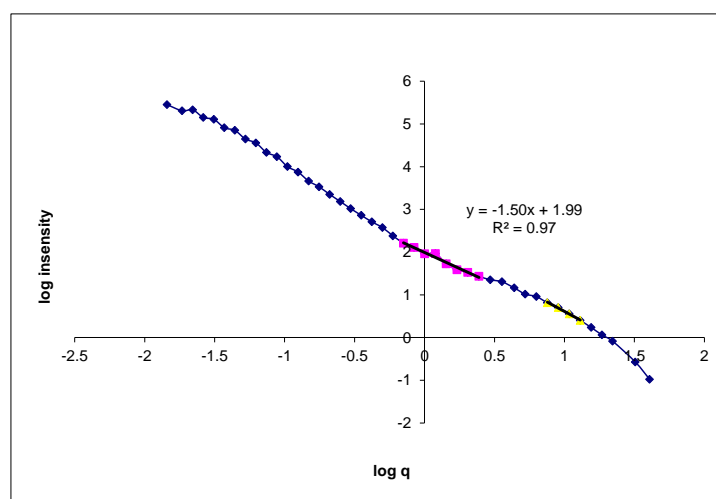
Figure C.10 Determination of SE (plot of scattering intensity versus  $q$ ) for cationic copolymer 80A3EC at 6 min: (a) 3.3 mg/L; (b) 6.5 mg/L; (c) 13 mg/L.



(a)

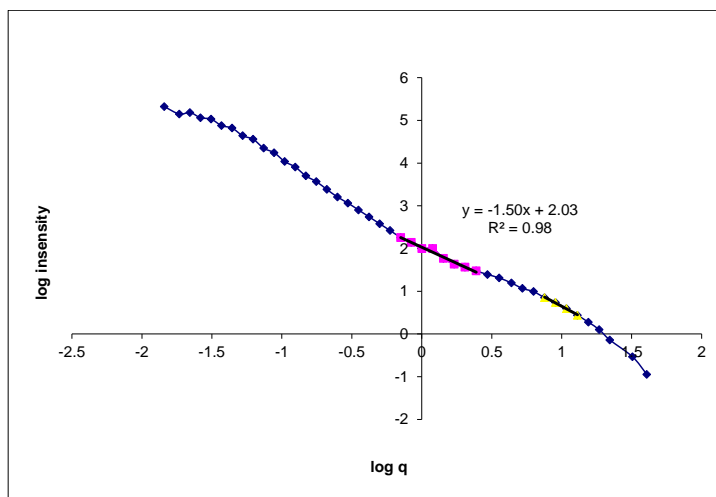


(b)

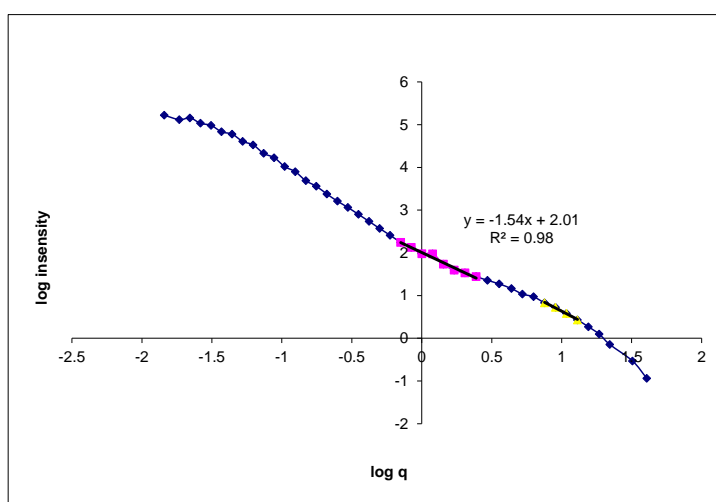


(c)

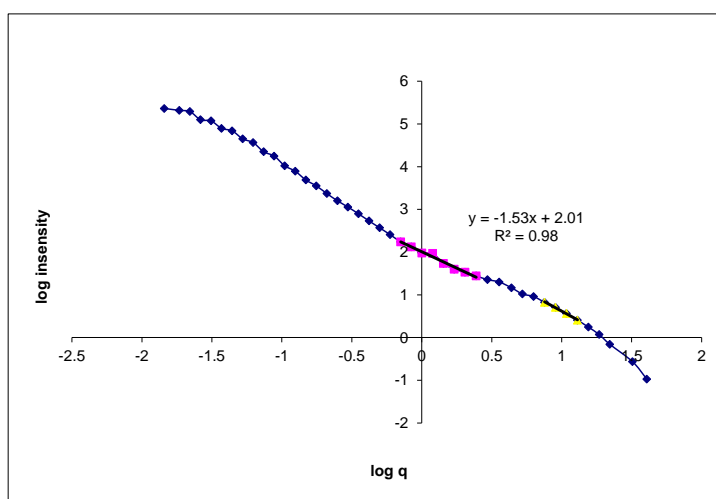
Figure C.11 Determination of SE (plot of scattering intensity versus  $q$ ) for cationic copolymer 50A1LC at 6 min: (a) 3.3 mg/L; (b) 6.5 mg/L; (c) 13 mg/L.



(a)

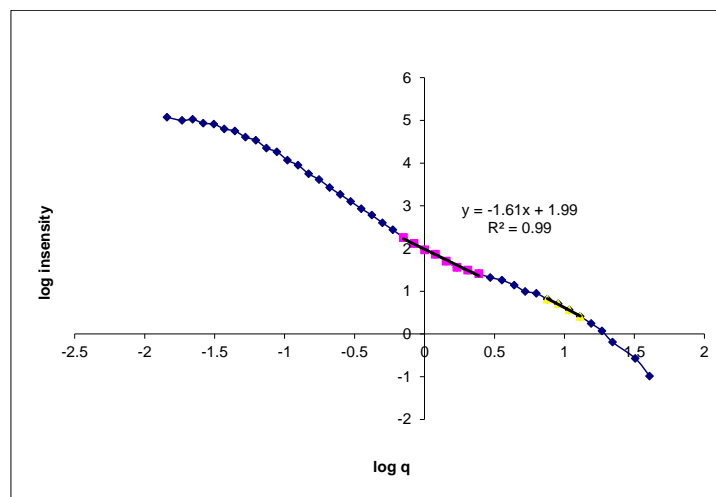


(b)

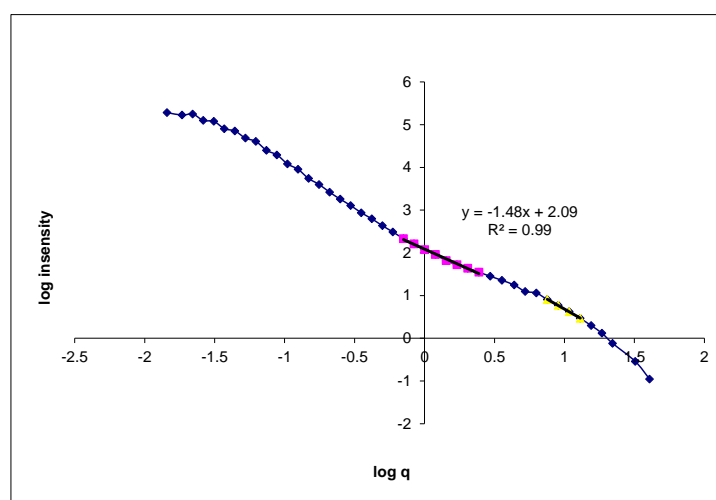


(c)

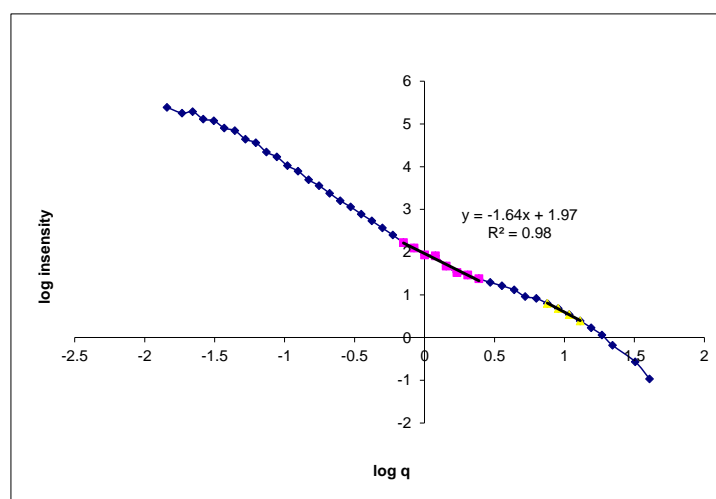
Figure C.12 Determination of SE (plot of scattering intensity versus  $q$ ) for cationic copolymer 50A3LC at 6 min: (a) 3.3 mg/L; (b) 6.5 mg/L; (c) 13 mg/L.



(a)



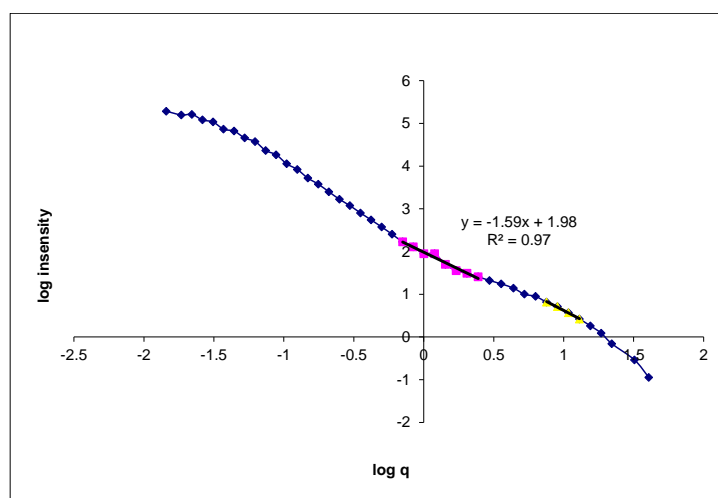
(b)



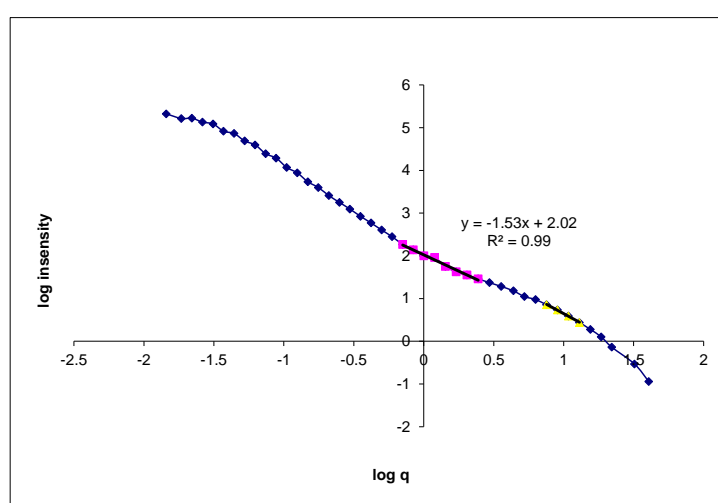
(c)

Figure C.13 Determination of SE (plot of scattering intensity versus  $q$ ) for cationic copolymer 80A1LC at 6 min: (a) 3.3 mg/L; (b) 6.5 mg/L; (c) 13 mg/L.

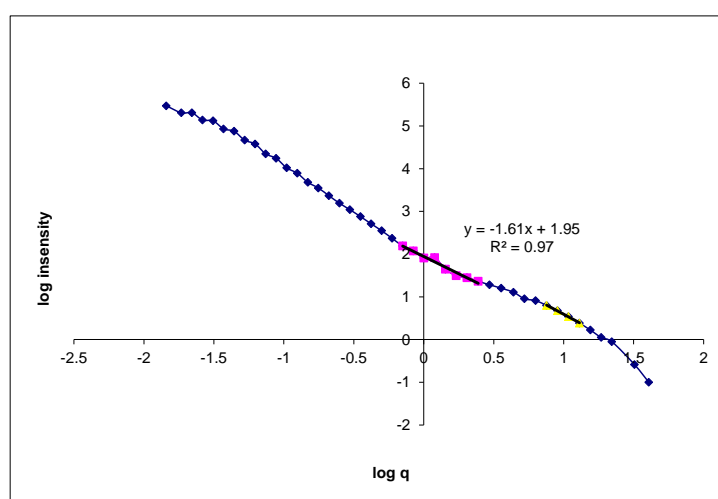




(a)



(b)



(c)

Figure C.14 Determination of SE (plot of scattering intensity versus  $q$ ) for cationic copolymer 80A3LC at 6 min: (a) 3.3 mg/L; (b) 6.5 mg/L; (c) 13 mg/L.

## CORRELATION BETWEEN POLYELECTROLYTES PROPERTIES

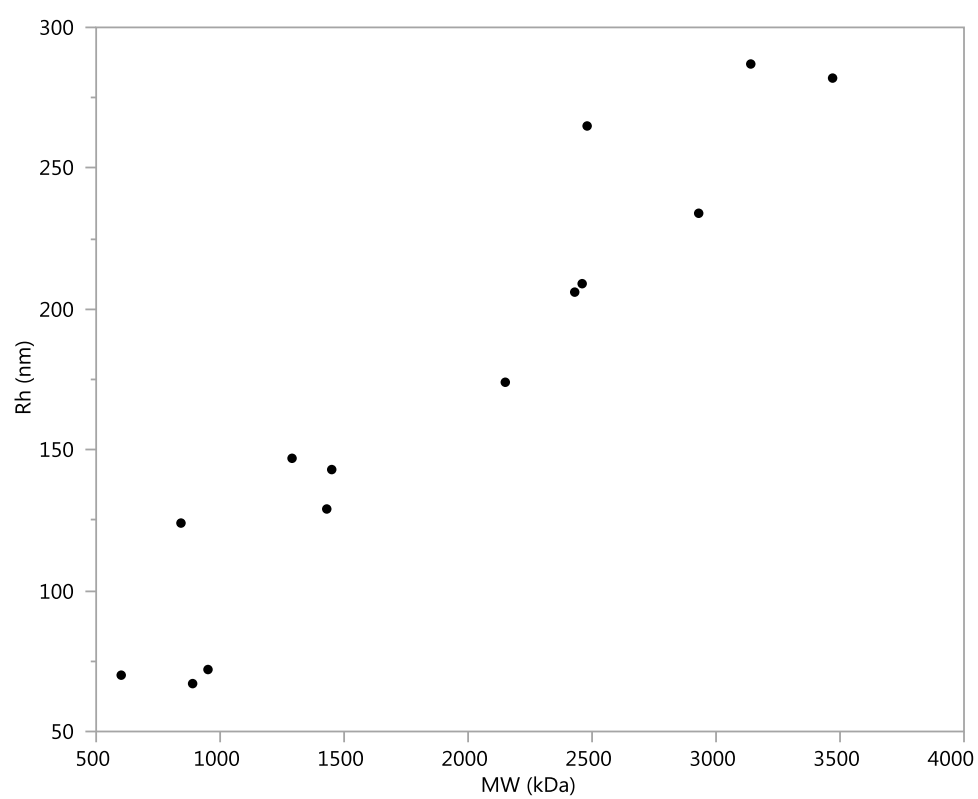


Figure C.15 Correlation between weight-average molecular weight and hydrodynamic diameter for the polyelectrolytes used in the statistical analysis.



# Appendix D

## List of publications resulting from this work

### PAPER 1

Colloid Polym Sci  
DOI 10.1007/s00396-017-4184-8



ORIGINAL CONTRIBUTION

## A more eco-friendly synthesis of flocculants to treat wastewaters using health-friendly solvents

Anita Lourenço<sup>1,2</sup> · Julien Arnold<sup>2</sup> · José A. F. Gamelas<sup>1</sup> · Maria G. Rasteiro<sup>1</sup>

Received: 2 November 2016 / Revised: 29 June 2017 / Accepted: 21 August 2017  
© Springer-Verlag GmbH Germany 2017

**Abstract** The main objective of this work was to investigate the possibility of producing new polyelectrolytes (flocculants) synthesized using health-friendly ingredients. A well-known copolymer used in water treatment, poly(acrylamide-co-2-(acryloyloxy)ethyltrimethyl ammonium chloride), was prepared by inverse-emulsion polymerization using new alternative organic phases. Specifically, three different purified oils of liquid saturated hydrocarbons with high boiling point and high purity were tested as synthesis media in the development of copolymers with different charge densities. In all of these oils, the toxic polycyclic aromatics and the heavy metals were not present. The polyelectrolytes were characterized in terms of shear viscosity, hydrodynamic diameter, molecular weight, zeta potential, intrinsic viscosity, and chemical composition (<sup>13</sup>C NMR and FTIR). Final results revealed the success of the application of the new health-friendly formulation in the polymerization to produce polyelectrolytes and, additionally, the polymers produced had good flocculation efficiency in two different real industrial effluents.

**Keywords** Polyelectrolytes · Inverse-emulsion polymerization · Health-friendly oils · Wastewater treatment · Flocculation

### Introduction

Oily wastewaters present one of the main challenges not only in petroleum, petrochemical, and steel industries, but also in food, cosmetics, and pharmaceutical production [1–4]. Oil-contaminated effluents have been documented as one of the most worrying pollution sources [5, 6]. It is considered as hazardous industrial wastewater due to the presence of toxic substances such as phenols, petroleum hydrocarbons, and polyaromatic hydrocarbons, which are inhibitory to plant and animal growth and also are carcinogenic and mutagenic to humans [7].

Flocculation is an essential method for separation of oily waters due to its capability of destabilization and aggregation of colloidal particles, which usually carry charges on the surface. Charge neutralization, polymer bridging, and electrostatic patches are the main mechanisms used to describe the removal of dissolved and particulate contaminants using polyelectrolytes [8, 9]. These mechanisms are strongly related with the adsorption of polymer on particle surfaces, collision of particles containing an adsorbed flocculant, and adsorption of the flocculant onto other particles to form flocs by consecutive collision and adsorption, which will occur only if there is some affinity between the polymer and the particle surface.

Organic polyelectrolytes are extensively used currently as flocculants due to their ability to flocculate efficiently at low dosage [10]. These polymers can be obtained using different processes; however, the use of inverse-emulsion polymerization permits high molecular weights, one of the critical characteristics in the performance of flocculants. This process involves the dispersion of an aqueous monomer(s) solution in an aliphatic continuous oil phase.

The aforementioned synthesis process has been conventionally employing aliphatic mineral oils as continuous phase. Examples of hydrocarbon fluids applied for many years in this

✉ Maria G. Rasteiro  
mgr@eq.uc.pt

<sup>1</sup> Chemical Engineering Department, CIEPQPF, University of Coimbra, Pólo II, Rua Sílvio Lima, 3030-790 Coimbra, Portugal

<sup>2</sup> Aqua+Tech Specialities SA, Chemin du Chalet-du-Bac 4, Geneva 1237 Avully, Switzerland

type of synthesis include mixtures of normal paraffins, iso-paraffins, cyclo-paraffins, and aromatics [11–13]. These oils allow high chemical and oxidative stability, as well as inertness to provide high performance capabilities during the inverse polymerization processes [11, 14]. They also have a similar molar volume to typical fatty acid ester surfactants, enabling the formation of a relatively condensed interface and stable droplets. However, the presence of aromatic components, even at levels as low as 0.01 wt%, does not meet health or environmental regulations, exhibiting human and aquatic toxicity levels, thus potentiating their classification under the symbol GSH08 “health hazard” as irritants in contact with skin [15].

Vegetable or plant oils represent a promising renewable route to develop sustainable products. Their ready availability, inherent biodegradability, low toxicity, and the relatively low cost make plant oils an industrially attractive material. Unfortunately, to perform an emulsion polymerization using as continuous phase vegetable oil has not, so far, proved to be successful. The main constituents of plant oils are triglycerides, products of the esterification of glycerol with fatty acids. The double bonds and ester groups present in these triglycerides are reactive sites and may act as radical scavengers or increase the tendency for the oil to polymerize itself [16, 17].

Alternatively, the oil phase used in inverse-emulsion polymerization should have low content in highly unsaturated components and it is desirable that there are no free hydroxyl groups. The high density is also an important parameter of the oil, reducing the driving force that promotes sedimentation of the emulsion. Alternative continuous phases include white mineral oils or hydrogenated polyalphaolefins. White mineral oils are highly refined mineral oils, products of distillation and processing by several methods of crude petroleum oils. The various fractions produced from crude oil distillation result in products with different molecular weight, viscosity, and boiling range. These fractions can suffer further refinement by solvent extraction in order to remove the toxic polycyclic aromatics and the heavy metals.

These alternative oils are listed in the International Nomenclature for Cosmetics Ingredients (I.N.C.I.) under the designation “Paraffinum Liquidum” and comply with many pharmacopeia and FDA regulations [18]. They are non-irritating, with high boiling point, high stability and high purity, free of harmful ingredients, color, odor, and taste. These oils differ by their chemical composition and viscosity and they are of high interest in industry, due to their physical properties and the level of purity which are required for use in personal care, food, and pharmaceuticals [19, 20].

In the present study, a well-known copolymer used in water treatment, poly(acrylamide-co-2-(acryloyloxy)ethyltrimethyl ammonium chloride) (AAm-co-AETAC) with high molecular weight, was synthesized by inverse-emulsion polymerization using three different health-friendly oils as organic phase, an

iso-paraffin (Carnation), a hydrogenated polydecene (Puresyn 4), and a mixture of liquid paraffinic hydrocarbons (Marcol 82). Different monomers ratios were tested in order to evaluate if it is possible the control of charge density in the synthesized polymers using this new process. To evaluate the performance of the flocculants developed with a novel health-friendly formulation, they were applied for treatment of oily wastewaters from two different industries.

## Materials and methods

### Materials

Acrylamide solution (AAM), at 50 wt%, was purchased from Kemira (Botlek, Netherlands). The monomer 2-(acryloyloxy)ethyltrimethyl ammonium chloride, at 80 wt% (AETAC), was purchased from BASF (Bradford, UK) and used as received. Tert-butyl hydroperoxide (TBHP) was purchased from Acros Organics (Geel, Belgium). Sodium meta bisulfite (MBS) was purchased from Brenntag (Esseco, Italy). Diethylenetriamine-pentaacetic acid pentasodium salt solution (Pentasodium DTPA) was purchased from Keininghaus Chemie (Essen, Germany). Adipic acid was purchased from Merck (Hohenbrunn, Germany). The surfactants Sorbitan isostearate (Crill 6) and Synperonic LF/30 were purchased from Croda (Goole, England). PEG-7 Hydrogenated Castor Oil (Cremophor WO7) was purchased from BASF (Ludwigshafen, Germany). The oils Puresyn 4 and Marcol 82 were purchased from ExxonMobil (Switzerland). Carnation was purchased from Sonneborn (Amsterdam, Netherlands).

Oily wastewaters tested include effluent obtained from dairy industry (Lactogal, Portugal) and effluent from fried snacks industry (SIA, Portugal).

Table 1 compares the characteristics of an example of a traditional oil, Exxsol D100, with the health-friendly oils used, Carnation, Puresyn 4, and Marcol 82.

### Inverse-emulsion polymerization

Inverse-emulsion polymerization was carried out in a 500-mL glass reactor. Prior to reaction, the aqueous phase was prepared with deionized water, acrylamide (AAM), 2-(acryloyloxy)ethyltrimethyl ammonium chloride (AETAC), and 0.625 wt% of adipic acid for hydrolytic stability of the polymers. The copper was chelated with 334 ppm of Pentasodium DTPA and the viscosity was controlled by adding lactic acid in the suitable amount. The total monomer level of the initial emulsion was 40.0 wt%. Sorbitan isostearate and PEG-7 Hydrogenated Castor Oil were the surfactants blended to obtain a hydrophilic-lipophilic balance

**Table 1** Comparison between traditional and alternative health-friendly oils

	Aromatic content (wt%)	Density (g/mL)	Viscosity (mm <sup>2</sup> /s at 40 °C)	Flash point (°C)
Exxsol D100	< 0.5	0.819	3.12	103
Carnation	0	0.829–0.859	18.3	186
Puresyn 4	0	0.820	18	221
Marcol 82	0	0.842–0.855	14.5–17.5	182

(HLB) between 4.5 and 5.5 according with the organic phase. Carnation, Puresyn 4, and Marcol 82 were used as organic phases. The aqueous phase was added to the organic phase under mechanical stirring for 30 min and the viscosity was measured. The monomers emulsion was then degassed with nitrogen for 60 min under mechanical stirring (700 rpm). Polymerizations were initiated by injecting 100 ppm of tert-butyl hydroperoxide (TBHP) aqueous solution to the reactor and then a solution of MBS 1.0 wt%. TBHP and MBS were used as the initiator redox couple. The peak temperature was between 60 and 65 °C, being the exact maximum of the exotherm, monomers composition dependent. Additional quantities of TBHP and MBS were added to scavenge residual monomer. After the batch had cooled down to 32 °C, 2.20 wt% of wetting agent (Synperonic LF/30) was added to allow a rapid inversion of the polymer when added to water.

For each organic phase, three different monomers ratios were used (see Table 2).

#### Inversion of the inverse-emulsion

In a large plastic beaker (1 L capacity), 500 g of deionized water was stirred at 500 rpm using an impeller (diameter 7.5 cm). A pre-calculated amount of emulsion (containing the inverting surfactant) was added to yield 0.5 wt% of active polymer in solution, within a short time, directly to the center of the vortex. The polymer was allowed to mix during 45 min and the viscosity of the final solution was determined with a RVDVII  $\beta$  model viscometer (Brookfield, spindle 3, Stoughton, MA, USA) at 30 rpm and 24–26 °C temperature.

The temperature of the solution was maintained using a recirculating bath.

#### Isolation of polymers

All polymers were isolated by dilution of 3 g of emulsion in 9 mL of hexane and following addition to a mixture of 240 mL of acetone and 18 mL of isopropanol under stirring. After 15 min, the precipitate was filtered off under vacuum, washed with fresh acetone, and dried in an oven at 60 °C overnight. The samples were stored in a desiccator.

#### Polyelectrolytes characterization

The FTIR spectra were recorded on a Bruker Tensor 27 spectrometer, equipped with an attenuated total reflection (ATR) MKII Golden Gate accessory with a diamond crystal 45° top plate. The spectra were collected in the 500–4000 cm<sup>-1</sup> range with a resolution of 4 cm<sup>-1</sup> and a number of scans of 128. For the measurements, polymers in the powder state were used.

The <sup>13</sup>C NMR spectra were recorded on a Bruker Avance III 400-MHz NMR spectrometer. Samples were dissolved at room temperature in deuterium oxide at about 5% (w/v) concentration and put inside 5-mm NMR tubes. <sup>13</sup>C NMR spectra were acquired at 25 °C using spectral width 220 ppm, relaxation delay 2 s, acquisition time 1.37 s, 90° pulse, and 20,000 scans. Signals were referenced to sodium 3-(trimethylsilyl)propionate-d<sub>4</sub>. Based on the intensity (area) of the carbon resonance signals at 175 ppm (I1) from the cationic unit (AETAC) of the copolymer chain and at

**Table 2** Monomers ratios and organic phases used for the copolymers production

Copolymer designation	Monomer 1	Ratio (wt%)	Ratio (mol%)	Monomer 2	Ratio (wt%)	Ratio (mol%)	Organic phase
40_Puresyn4	AAm	60	80	AETAC	40	20	Puresyn 4
40_Carnation	AAm	60	80	AETAC	40	20	Carnation
40_Marcol82	AAm	60	80	AETAC	40	20	Marcol 82
60_Puresyn4	AAm	40	65	AETAC	60	35	Puresyn 4
60_Carnation	AAm	40	65	AETAC	60	35	Carnation
60_Marcol82	AAm	40	65	AETAC	60	35	Marcol 82
80_Puresyn4	AAm	20	41	AETAC	80	59	Puresyn 4
80_Carnation	AAm	20	41	AETAC	80	59	Carnation
80_Marcol82	AAm	20	41	AETAC	80	59	Marcol 82

179 ppm (I2) from the AAm unit [21], the content of charged groups in the copolymer (in mol%) was estimated as  $[I1 / (I1 + I2)] \times 100$ .

The intrinsic viscosity (IV) of the isolated and redissolved copolymers was determined in 0.05 M NaCl aqueous solution at  $20 \pm 0.1$  °C by dilution viscometry, using an automatic capillary viscometer Viscologic T11 (Sematech, France), with a capillary of 0.58 mm. At least two measurements were conducted for each test. The extrapolation to zero concentration was performed according to Huggins equation [22].

Hydrodynamic diameter, molecular weight, and zeta potential of isolated and redissolved polymers were determined by dynamic light scattering, static light scattering, and electrophoretic light scattering, respectively, in a Malvern Zetasizer Nano ZS, model number ZEN3600 (Malvern Instruments Ltd., UK). For hydrodynamic diameter, stock solutions (0.1 g/L) of each polymer were prepared in Milli-Q water and stirred overnight. All samples were sonicated during 2 min and passed through 1- $\mu$ m syringe filters prior to analysis. The measurement temperature was set to 25 °C and backscatter detection was used (173° angle), with at least three measurements for each sample performed. Molecular weight measurements of polymers were performed using stock solutions (0.1 g/L) of each polymer prepared in NaCl 0.05 M and stirred overnight. The samples for analysis were then obtained by diluting the stock solutions at concentrations of 0.09, 0.08, 0.07, and 0.06 g/L. All samples were sonicated during 2 min and passed through 0.45- $\mu$ m syringe filters prior to analysis. For zeta potential measurements, 1 mL of each stock solution (0.2 g/L) in Milli-Q water was carefully injected with a syringe into a folded capillary cell, closed by cell stoppers. At least three measurements were conducted for each sample.

### Performance evaluation

A 200-mL stock solution of 0.1 wt% (solids base) concentration was prepared for each polymer by adding 0.8 g of emulsion to 199.2 g of distilled water under magnetic stirring and keeping the mixing for 60 min. Polymer solution samples of 1 mL were added to 200-mL samples of pre-agitated wastewater with a successive increase of concentration from 27 ppm until a maximum of 108 ppm. In each addition, the suspension-polymer mixture was manually agitated for 10 s. For the dairy industry effluent, the tests were conducted at pH 5 and with addition of 5 drops of ferric chloride 1.0% solution before the flocculant addition, which proved to help in the flocculation process. For the fried snacks industry effluent, the tests were performed at pH 11.6 without the addition of any acid, since different coagulants were tested and no improvement in the flocs formation was observed. The size of the flocculated particles was visually assessed and the

absorbance of the treated supernatant water was measured for the polymer concentration that showed better results, after 30 min of settling, using a UV/Vis spectrophotometer (Beckman, DU 650).

## Results and discussion

In this section, the results of the polymerization of AAm-AETAC in health-friendly oils will be presented, including the characterization of the new polymers and the results of the performance tests.

### Inverse-emulsion polymerization

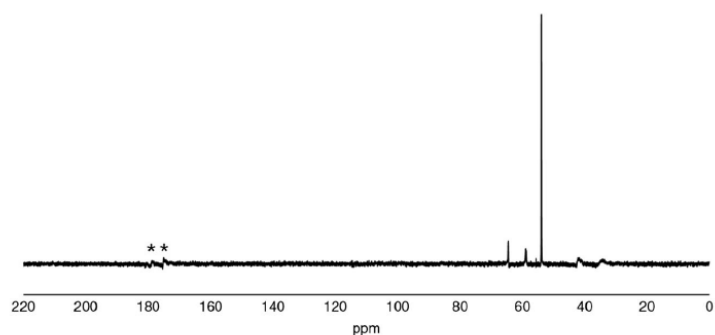
In the synthesis of this well-known copolymer using health-friendly organic phases, the main goals were to achieve polymers with high molecular weight, controllable charge density, and good copolymerization performance. The new formulations have been found very successful to prepare polymers with suitable solution viscosities. A target viscosity above 1000 cPs (25 °C, Brookfield RV) in a 0.5% solids solution was set as the initial goal for the final application and it could always be reached independently of the organic phase used (Table 3).

### Polyelectrolytes characterization

Based on previous literature referring to AAm-co-AETAC copolymer [11], series of this copolymer with various charge densities were developed using health-friendly new oils as organic phase in the inverse-emulsion polymerization. After a complete purification of the copolymers, they were characterized for their chemical compositions.  $^{13}\text{C}$  NMR spectroscopy (Fig. 1) evidenced the presence of the two different

**Table 3** Shear viscosity measured for in a 0.5% solids solution for each polymer

Copolymer	Charge density (wt%)	Health-friendly oil used	(mPa.s)
40_Puresyn4	40	Puresyn 4	1093
40_Carnation	40	Carnation	1130
40_Marcol82	40	Marcol 82	1003
60_Puresyn4	60	Puresyn 4	1200
60_Carnation	60	Carnation	1210
60_Marcol82	60	Marcol 82	1313
80_Puresyn4	80	Puresyn 4	1333
80_Carnation	80	Carnation	1103
80_Marcol82	80	Marcol 82	1030

**Fig. 1**  $^{13}\text{C}$  NMR spectra for 80\_Marcol82

monomers: the  $^{13}\text{C}$  NMR spectra were dominated by a very intense signal at 54 ppm due to the resonance of the three methyl carbons of the AETAC unit; signals due to the carbons from the amide functions of AAm and ester functions of AETAC, were also observed (marked with asterisk in Fig. 1), which, as explained above in the experimental section, allowed the estimation of the content of cationic groups in the copolymers (Table 4). The contents of charged groups of a set of copolymers were found to be very close to the monomers feed ratios used in the synthesis (Table 4), demonstrating that the three monomers levels used in the copolymerization were adequate. The results also confirmed that the increase of the proportion of AETAC monomer increases the fraction of cationic groups in the final product, as desired.

ATR-FTIR spectroscopy provided a good insight into the main structural features of the copolymers obtained using the health-friendly formulations. Bands due to both constituents of the copolymer were clearly distinguished in the spectra. The spectra (Fig. 2) showed the characteristic bands of AAm monomers at ca.  $3345$  and  $3185\text{ cm}^{-1}$ , due to the asymmetric and symmetric  $\text{NH}_2$  stretching [23], being the latter reduced in relative intensity when a lower proportion of AAm was used in the synthesis. A band at  $1655\text{ cm}^{-1}$  due to the  $\text{C}=\text{O}$  stretching (amide I) in AAm was also observed, which was accompanied by the amide II band at  $1615\text{ cm}^{-1}$ . Besides, AETAC characteristic bands [24] were also observed:  $1730\text{ cm}^{-1}$  from the  $\text{C}=\text{O}$  stretching in ester bond,  $1478\text{ cm}^{-1}$  (asymmetric bending of  $\text{CH}_3$  groups),  $1163\text{ cm}^{-1}$  ( $\text{C}-\text{O}$  stretching in ester bond), and  $952\text{ cm}^{-1}$  (asymmetric

stretching of  $\text{C}-\text{N}$  bonds). The relative intensity of the bands from AETAC increased with the increase of the proportion of AETAC (vs. AAm) used in the synthesis (Fig. 2). Interestingly, for the same monomers' ratio, similar infrared spectra were obtained regardless of the oil used in the copolymerization reaction (Fig. 3), which indicates that the composition of the final products did not differ much if the reaction conditions were kept similar.

Zeta potential revealed consistent results, considering the charge density of the polymers calculated from the mass balance, which is the key parameter affecting this value. The polymers with lower charge density have lower values of zeta potential while the polymers with higher charge density have higher values of zeta potential. The values are also similar between polymers with the same charge density produced in different oils. Table 5 summarizes the results of the characterization of the final emulsions and the isolated solids thereof (shear viscosity, zeta potential, and hydrodynamic diameter).

The particle size of the copolymers was determined by dynamic light scattering and the results are also presented in Table 5. In aqueous solution, the smaller particles have a mean diameter 44 nm and the larger particles 77 nm. Table 6 shows all values of the intrinsic viscosity and molecular weight obtained for the different polymers. All the values of molecular weight and intrinsic viscosity (IV) are in similar order of magnitude, meaning that the different oils used in the synthesis process do not have a considerable influence in the final size of the polymer chain. Additionally, IV is also dependent on the charge density of the polymer, higher charge density leading

**Table 4** Contents of cationic groups in the copolymers calculated from the initial mass balance and estimated from the  $^{13}\text{C}$  NMR

Copolymer	Cationic content from the initial mass balance <sup>a</sup>	Cationic content estimated from the $^{13}\text{C}$ NMR spectra <sup>a</sup>
60_Carnation	35%	39%
80_Puresyn4	59%	61%
80_Marcol82	59%	56%

<sup>a</sup> Content in mol%



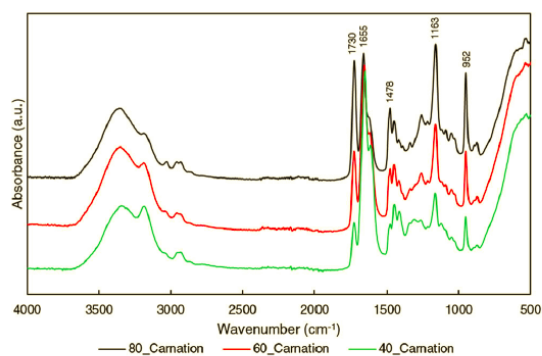


**Fig. 2** ATR-FTIR spectra for copolymers of AAm and AETAC developed in the same oil (Carnation)

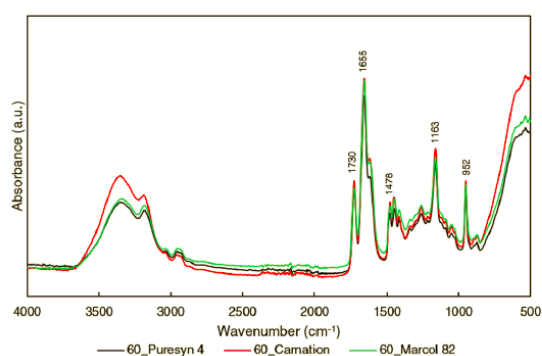


**Fig. 3** ATR-FTIR spectra of copolymers of AAm and AETAC obtained with the same charge density, but employing different oils

to higher IV for the same molecular weight. The values for IV are slightly lower than those reported in literature for similar copolymers analyzed in similar conditions [11, 25, 26]. However, the IV values still represent polymers of high molecular weight, which is the main objective, as is possible to observe in Table 6.

**Table 5** Shear viscosity of the final emulsions, zeta potential measured by electrophoretic light scattering, and hydrodynamic diameter measured by dynamic light scattering of the isolated solids

Copolymer	Viscosity of emulsion (cPs)	Zeta Potential (mV)	Hydrodynamic diameter (nm)
40_Puresyn4	2540	26 ± 4	77 ± 5
40_Carnation	3593	17 ± 3	45 ± 3
40_Marcol82	2073	19 ± 4	44 ± 1
60_Puresyn4	3060	47 ± 4	70 ± 2
60_Carnation	3440	47 ± 4	41 ± 2
60_Marcol82	2160	32 ± 3	40 ± 4
80_Puresyn4	2970	84 ± 5	75 ± 3
80_Carnation	3060	87 ± 4	63 ± 5
80_Marcol82	2153	87 ± 6	44 ± 1

**Table 6** Intrinsic viscosity in 0.05 M NaCl calculated according to Huggins equation and molecular weight measured by static light scattering

Copolymer	Intrinsic viscosity (mL/g)	Molecular weight (kDa)
40_Puresyn4	1546	358 ± 1.7
40_Carnation	1207	301 ± 74.3
40_Marcol82	1123	267 ± 1.5
60_Puresyn4	1550	507 ± 27.4
60_Carnation	1460	562 ± 79.9
60_Marcol82	1434	637 ± 105
80_Puresyn4	1638	564 ± 45.0
80_Carnation	1353	218 ± 36.7
80_Marcol82	1214	223 ± 13.8

In Palomino et al. [25], a polymer similar to 80\_Puresyn4, 80\_Carnation, and 80\_Marcol82, though produced in a traditional medium, was characterized (AF BHMW). Values of zeta potential for the polymers here developed using health-friendly formulations are slightly higher while values for hydrodynamic diameter are lower. In theory, higher values of zeta potential should conduce to higher hydrodynamic diameter; however, the corresponding molecular weight is also lower, which corroborate the lower hydrodynamic diameter.

Looking at Fig. 4, it is possible to see an increase of intrinsic viscosity with the increase of hydrodynamic diameter even if there are some fluctuations. Looking deeper into the values of both properties, polymers obtained with Marcol 82 present always the lowest values of IV and hydrodynamic diameter (see Fig. 5), when compared with polymers with the same charge density produced in the other two oils. On the opposite, the polymers developed in Puresyn 4 present the highest values.

#### Performance evaluation

Two oily wastewaters from industry were used to evaluate the flocculants performance. Table 7 summarizes the results

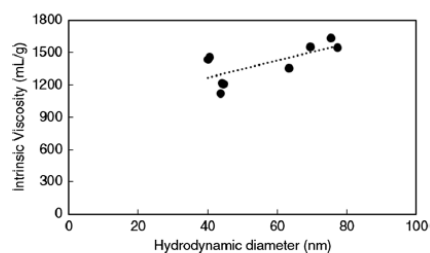


Fig. 4 Intrinsic viscosity versus hydrodynamic diameter of polymers

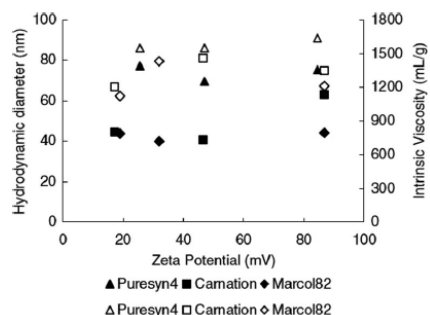


Fig. 5 Hydrodynamic diameter (filled symbols) and intrinsic viscosity (hollow symbols) versus zeta potential of polymers

obtained for the best conditions (pH and presence or not of aid) and with the optimized concentrations of flocculant, from which no more absorbance reduction was observed. The flocculation performance is described by the absorbance reduction of the supernatant waters. Considering the effluent from dairy industry, the cationic flocculant with 80 wt% of charged groups produced using Carnation as organic phase provided the best results, at the mentioned conditions, giving the higher absorbance reduction. This is the polymer which combines a

higher zeta potential with a higher hydrodynamic diameter. Using other cationic charges with Carnation as organic phase, 60 wt% and 40 wt%, the reduction of absorbance was not significant and the floc formation was not visible. The same happened when the synthesis was conducted in Puresyn 4 or Marcol 82. With the cationic flocculant with 80% of charge produced using Puresyn 4 or Marcol 82 as organic phase, the absorbance was also reduced; however, the result was not as good of that produced using the Carnation oil (higher zeta potential and higher hydrodynamic diameter of this last polymer, when compared with the aforementioned other two polymers with the same charge density as calculated through the mass balance).

Regarding the effluent from fried snacks industry, the cationic flocculant with 80% of charge and produced using Carnation as organic phase provided the best results, giving an absorbance reduction of 76%, even if the flocculants produced in the other oils and having the same charge density showed comparable results. Using polymers with the other charge densities, 40 and 60%, the reduction of the water turbidity was lower, even if the polymers with 60% charge density did also show reasonable results. Apparently, for this effluent the synthesis medium does not seem to have a strong effect on the flocculant performance.

The influence of zeta potential in the flocculation performance is represented in Fig. 6. The higher reduction of absorbance is achieved for polymers with higher zeta potential value. The main factor having influence in the zeta potential is the charge density of the polymer. The low values of zeta potential for flocculants of 40 and 60% charged fraction can be the reason for their relatively lower performance, since there is not enough positive charges in the molecules to build up big flocs.

This effect is more notorious in the case of the fried snacks effluent where there seems to be an almost linear relation between the reduction in absorbance and zeta potential. For

Table 7 Absorbance reduction for effluents from dairy and fried snacks industries

Copolymer	Dairy industry (pH 5 and addition of 5 drops of ferric chloride)		Fried snacks industry (pH 11.6 and no coagulant)	
	Absorbance reduction (%)	Dosage (ppm)	Absorbance reduction (%)	Dosage (ppm)
40_Puresyn4	8.9	80	67.3	108
40_Carnation	7.6	80	72.2	108
40_Marcol82	20.8	80	70.2	108
60_Puresyn4	28.0	80	74.9	108
60_Carnation	6.7	80	74.2	108
60_Marcol82	17.4	80	73.3	108
80_Puresyn4	60.6	80	73.8	108
80_Carnation	73.7	80	76.0	108
80_Marcol82	36.7	80	74.9	108

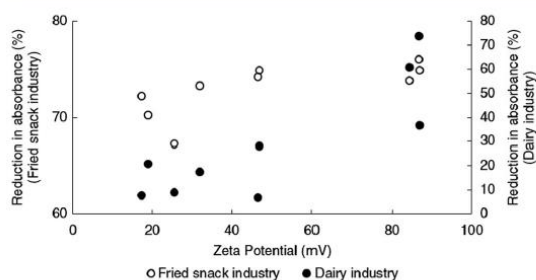


Fig. 6 Absorbance reduction in each effluent versus zeta potential of the polymer used

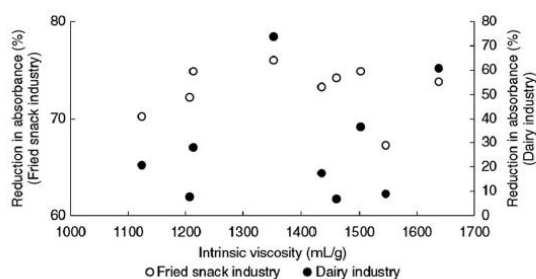


Fig. 7 Absorbance reduction in each effluent versus intrinsic viscosity of the polymer used

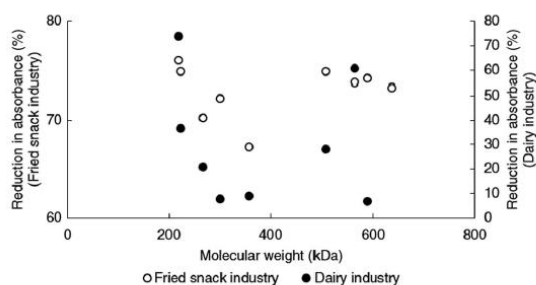


Fig. 8 Absorbance reduction in each effluent versus molecular weight of the polymer used

the dairy industry effluent, there are two distinct zones: a region of higher absorbance reduction corresponding to the polymers with 80% charge density, and a region of low absorbance reduction corresponding to the polymers with 60 or 40% charge density.

No clear trend could be deduced concerning the influence of molecular weight or intrinsic viscosity in the performance of the tested polymers (Figs. 7 and 8). In this case, it can be assumed that charge density is the main factor affecting the flocculation efficacy and, then, electrostatic patching must be the predominant flocculation mechanism. The high charge density of the more charged polymers allows the polymer chain to adsorb onto the particles surface, and this then leads to localized areas with contrary charge on each particle that will interact with the bare areas of the other particles, and form flocs. These flocs are quite visible in Fig. 9. Moreover, the range of molecular weights achieved is relatively narrow.

## Conclusions

Tested health-friendly oils showed to be able to be used as organic phase in inverse-emulsion polymerization of well-known cationic polyelectrolytes applied in industrial wastewater treatment. Characterization of the polymers revealed suitable characteristics for the developed polymers, which include good copolymerization performance, adequate molecular weight, and tunable charge density, though slightly distinct when comparing with similar polymers developed in traditional medium. These characteristics were confirmed by several characterization techniques. Despite some differences in the characteristics of the polymers developed with the new formulations when compared with the traditional ones, evaluation of performance using the developed polymers suggests an effective flocculation ability in two oily wastewaters from different industries. The best results were accomplished with polymers with the highest charge density and using Carnation oil as organic phase.

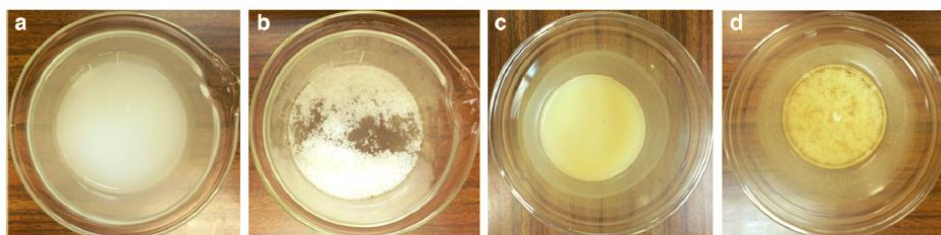


Fig. 9 Visual representation of best results for each effluent. Initial effluent from dairy industry (a) and after addition of 80 ppm of flocculant 80\_Carnation (b). Initial fried snack industry effluent (c) and after addition of 108 ppm of flocculant 80\_Carnation (d)

Finally, in this way it was possible to successfully develop a more eco-friendly formulation to produce flocculants that can be applied in effluent treatment.

**Acknowledgments** The authors would like to thank the financial support from the Marie Curie Initial Training Networks (ITN)—European Industrial Doctorate (EID), through Grant agreement FP7-PEOPLE-2013-ITN- 604825 and Pest/C/EQB/UI0102/2013, financed by FCT/MCTES (PIDDAC) and co-financed by the European Regional Development Fund (ERDF) through the program COMPETE (POFC).

#### Compliance with ethical standards

**Conflict of interest** The authors declare that they have no conflict of interest.

#### References

- Alrawi RA, Ab Rahman NNN, Ahmad A et al (2013) Characterization of oily and non-oily natural sediments in palm oil mill effluent. *J Chem* 2013:1-11. <https://doi.org/10.1155/2013/298958>
- Imran H (2005) Wastewater monitoring of pharmaceutical industry: treatment and reuse options. *Electron J Environ Agric Food Chem* 4:994-1004
- Gomec CY, Erdim E, Turan I et al (2007) Advanced oxidation treatment of physico-chemically pre-treated olive mill industry effluent. *J Environ Sci Health B* 42:741-747. <https://doi.org/10.1080/03601230701466021>
- Zhong J, Sun X, Wang C (2003) Treatment of oily wastewater produced from refinery processes using flocculation and ceramic membrane filtration. *Sep Purif Technol* 32:93-98. [https://doi.org/10.1016/S1383-5866\(03\)00067-4](https://doi.org/10.1016/S1383-5866(03)00067-4)
- Raghunath B V, Punnagaiarasi A, Rajarajan G et al (2016) Impact of dairy effluent on environment—a review. In: *Integrated Waste Management in India*. Springer, Berlin, pp 239-249. [https://doi.org/10.1007/978-3-319-27228-3\\_22](https://doi.org/10.1007/978-3-319-27228-3_22)
- Jamaly S, Giwa A, Hasan SW (2015) Recent improvements in oily wastewater treatment: progress, challenges, and future opportunities. *J Environ Sci* 37:15-30. <https://doi.org/10.1016/j.jes.2015.04.011>
- Mater L, Sperb RM, Madureira LAS, et al. (2006) Proposal of a sequential treatment methodology for the safe reuse of oil sludge-contaminated soil. *J Hazard Mater* 136:967-971. <https://doi.org/10.1016/j.jhazmat.2006.01.041>
- Bolto B, Gregory J (2007) Organic polyelectrolytes in water treatment. *Water Res* 41:2301-2324. <https://doi.org/10.1016/j.watres.2007.03.012>
- Renault F, Sancey B, Badot P-M, Crini G (2009) Chitosan for coagulation/flocculation processes—an eco-friendly approach. *Eur Polym J* 45:1337-1348. <https://doi.org/10.1016/j.eurpolymj.2008.12.027>
- Radoiu M (2004) Preparation of polyelectrolytes for wastewater treatment. *J Hazard Mater* 106:27-37. <https://doi.org/10.1016/j.jhazmat.2003.08.014>
- Hernandez-Barajas J, Wandrey C, Hunkeler D (2003) Polymer flocculants with improved dewatering characteristics, U.S. Patent No. 6,617,402
- Rasteiro MG, Garcia FAP, Ferreira PJ, et al. (2010) Flocculation by cationic polyelectrolytes: relating efficiency with polyelectrolyte characteristics. *J Appl Polym Sci* 116:3603-3612. <https://doi.org/10.1002/app.31903>
- Hernandez-Barajas J, Wandrey C, Hunkeler D (2003) Polymer flocculants with improved dewatering characteristics. U.S. Patent No. 6,294,622
- Crespy D, Landfester K (2009) Synthesis of polyvinylpyrrolidone/silver nanoparticles hybrid latex in non-aqueous miniemulsion at high temperature. *Polymer* 50:1616-1620. <https://doi.org/10.1016/j.polymer.2009.02.003>
- Chen S-C, Liao C-M (2006) Health risk assessment on human exposed to environmental polycyclic aromatic hydrocarbons pollution sources. *Sci Total Environ* 366:112-123. <https://doi.org/10.1016/j.scitotenv.2005.08.047>
- Lu Y, Larock RC (2007) New hybrid latexes from a soybean oil-based waterborne polyurethane and acrylics via emulsion polymerization. *Biomacromolecules* 8:3108-3114. <https://doi.org/10.1021/bm700522z>
- Xia Y, Larock RC (2010) Vegetable oil-based polymeric materials: synthesis, properties, and applications. *Green Chem* 12:1893-1909. <https://doi.org/10.1039/c0gc00264j>
- Rawlings AV, Lombard KJ (2012) A review on the extensive skin benefits of mineral oil. *Int J Cosmet Sci* 34:511-518. <https://doi.org/10.1111/j.1468-2494.2012.00752.x>
- Kim E, Nam GW, Kim S, et al. (2007) Influence of polyol and oil concentration in cosmetic products on skin moisturization and skin surface roughness. *Skin Res Technol* 13:417-424. <https://doi.org/10.1111/j.1600-0846.2007.00246.x>
- Nash JF, Gettings SD, Diembeck W, et al. (1996) A toxicological review of topical exposure to white mineral oils. *Food Chem Toxicol* 34:213-225. [https://doi.org/10.1016/0278-6915\(95\)00106-9](https://doi.org/10.1016/0278-6915(95)00106-9)
- Lafuma F, Durand G (1989) <sup>13</sup>C NMR spectroscopy of cationic copolymers of acrylamide. *Polym Bull* 21:315-318. <https://doi.org/10.1007/BF00955924>
- Bourdillon L, Hunkeler D, Wandrey C (2006) The analytical ultracentrifuge for the characterization of polydisperse polyelectrolytes. *Anal Ultracentrifugation VIII* 131:141-149. [https://doi.org/10.1007/2882\\_018](https://doi.org/10.1007/2882_018)
- Murugan R, Mohan S, Bigotto A (1998) FTIR and polarised Raman spectra of acrylamide and polyacrylamide. *J Korean Phys Soc* 32:505-512
- Larkin P (2011) *Infrared and Raman spectroscopy; principles and spectral interpretation*. Elsevier, USA
- Palomino D, Hunkeler D, Stoll S (2011) Comparison of two cationic polymeric flocculant architectures on the destabilization of negatively charged latex suspensions. *Polymer* 52:1019-1026. <https://doi.org/10.1016/j.polymer.2010.12.033>
- Armanet L, Hunkeler D (2007) Phase inversion of polyacrylamide based inverse-emulsions: effect of the surfactant and monomer on postinversion equilibrium properties. *J Appl Polym Sci* 106:2328-2341. <https://doi.org/10.1002/app.25309>



Contents lists available at ScienceDirect

Journal of Environmental Chemical Engineering

journal homepage: [www.elsevier.com/locate/jece](http://www.elsevier.com/locate/jece)

Research Paper

## Pre-treatment of industrial olive oil mill effluent using low dosage health-friendly cationic polyelectrolytes

Anita Lourenço<sup>a,b</sup>, Julien Arnold<sup>b</sup>, José A.F. Gamelas<sup>a</sup>, Olivier J. Cayre<sup>c</sup>, Maria G. Rasteiro<sup>a,\*</sup><sup>a</sup> Chemical Engineering Department, CIEPQPF, University of Coimbra, Pólo II, Rua Sílvio Lima, 3030-790 Coimbra, Portugal<sup>b</sup> Aqua+Tech Specialities SA, Chemin du Chalet-du-Bac 4, 1237 Avully, Geneva, Switzerland<sup>c</sup> School of Chemical and Process Engineering, University of Leeds, Woodhouse Lane, Leeds LS2 9JT, UK

## ARTICLE INFO

## Keywords:

Flocculation  
Olive oil mill effluent  
Wastewater treatment  
Polyelectrolytes

## ABSTRACT

Olive oil production involves a significant annual release of industrial olive oil mill effluent to the environment. These discharges bring serious environmental problems since they are extremely hazardous for the aquatic environment due to their organic matter and high turbidity levels. The present study comprises the development of new, hydrophobically modified, cationic flocculants directed to oily effluents application. A health-friendly formulation was used in their synthesis process performed by inverse-emulsion. In particular, Poly(AAm-MAPTAC) was synthesized in two different polymer compositions and, as well, with the presence of a hydrophobic monomer (Poly(AAm-MAPTAC-SMA)) at several compositions up to 8 wt%. The obtained polyelectrolytes were characterized in terms of final composition, hydrodynamic diameter, zeta potential and molecular weight. Their flocculation performance was evaluated in an industrial oily effluent from an olive oil mill. Results revealed that the hydrophobic modification improves noticeably the flocculation performance of cationic polyelectrolytes in the treatment of olive oil mill effluents. In the best conditions, it was possible to achieve 90% turbidity reduction, 47% COD removal and 34% total solids removal with only 53 mg/L of flocculant. Moreover, 79% of turbidity was reduced after addition of 13 mg/L.

## 1. Introduction

Olive oil mill effluents (OME) have increased significantly in the last years as a result of the quick increasing demand for olive oil, and the existing oil extraction techniques that involve high amounts of water [1].

The composition of the produced wastewater change with climate, cultivation conditions and milling processes [2]. Typically, OME possess the following characteristics: a high concentration of solids resulting from washing actions, an intense dark color, an acidic pH and a strong odor. These effluents, when disposed off in the environment, lead to acute problems including coloration and pollution of waters, changes in soil quality and phytotoxicity, plants growth inhibition and odor nuisance [3]. Moreover, direct discharge on fields decreases the amount of dissolved oxygen, harming aquatic fauna [4].

Therefore, OME must be treated before disposal and several treatment technologies and integrated processes have been offered to shape a suitable and effective method to deal with the produced wastewater [5]. Open evaporation ponds, or lagooning, lead to insect reproduction and increase the risk of surface and groundwater contamination [6].

Biological methods include microbiological treatment, co-digestion, aerobic and anaerobic digestion. However the OME has high concentration of fats, lipids and phenols that can compromise the growth of microorganisms and, consequently, the OME degradability [7].

Co-digestion consists in the co-treatment of one wastewater with other wastewater, which has the advantage of providing the necessary pH or nutrients level for further treatment [8,9]. The aerobic treatment stage is able to reduce the toxicity through the reduction of phenols. Several species can be used for this purpose. Hamdi et al. [10] and Cereti et al. [11] used *Aspergillus niger* and reduced chemical oxygen demand (COD) in about 52.5% and 35–64%, respectively. *Aspergillus terreus*, *Azotobacter chroococcum* and *Geotrichum candidum* were also used in different studies [12–14], and were able to reduce COD in 63.3, 74.3 and 70% and phenols in 65.6, 90 and 94.3%, respectively. Anaerobic digestion is performed by anaerobic microorganisms, generally bacteria, in the absence of molecular oxygen. This process has low energy requirements and produces low amount of sludge. Recent studies using anaerobic sludge bed reactors reported COD removals of 70–80% [15,16]. Procedure using an anaerobic sequencing batch reactor reached COD removals up to 80% [17].

\* Corresponding author.

E-mail address: [mgr@eq.uc.pt](mailto:mgr@eq.uc.pt) (M.G. Rasteiro).<https://doi.org/10.1016/j.jece.2017.11.029>

Received 1 August 2017; Received in revised form 16 October 2017; Accepted 9 November 2017

Available online 10 November 2017

2213-3437/ © 2017 Elsevier Ltd. All rights reserved.

Advanced oxidation processes, consisting in Fenton and Fenton-like oxidation and ozonation, can also be applied [18–20]. Physico-chemical treatment methods such as ultrafiltration, reverse osmosis, sedimentation, centrifugation, coagulation-flocculation and electro-coagulation are actually the most used methods [21–24]. Nevertheless, most of these treatment processes, on their own, are not cost effective and reported results present significant drawbacks, indicating that combined technologies are needed in order to reduce the organic load, and thus reducing the operating costs. These hybrid systems can include ozonation and aerobic biological treatment, coagulation-flocculation combined with anaerobic biological process, electro-Fenton and anaerobic digestion or chemical oxidative procedure in combination with aerobic biological treatment, among others [25,26].

In particular, coagulation-flocculation processes have proved to be very useful has a pre-treatment stage in the OME processing procedures [27,28], involving low CO<sub>2</sub> emissions [29]. The addition of organic and inorganic compounds stimulates the destabilization of colloidal materials and promotes the agglomeration of small particles in large flocs that are able to quickly settle. Coagulants, such as alum, ferric, starch, chitosan and lime, and cationic or anionic flocculants, like poly(diallyldimethylammonium chloride) (PDADMAC), [poly(allylamine) (PAA) or poly(allylamine) hydrochloride (PAH), have been tested [23,30,31]. Experiments showed considerable reduction of solids, color and COD. However, usually a combination of both (inorganic and organic additives) is required or, when in single use, a very high concentration of polymer is used, which generates large amount of sludge [32]. Minimization of sludge production is important considering the costs related with consequent sludge treatment and disposal [33].

Synthesis of the aforementioned treatment products commonly comprises the presence of aromatic compounds, even at very low concentrations, that exhibit human and aquatic toxicity levels [34]. Health-friendly formulations for production of polyelectrolytes by inverse-emulsion polymerization [35] were tested and presented in a previous work [36]. The polymers are synthesized using alternative oils that are listed in the International Nomenclature for Cosmetics Ingredients (I.N.C.I.) under the designation “Paraffinum Liquidum” and comply with many pharmacopoeia and FDA regulations. The main characteristics include non-irritating, high boiling point, high stability and high purity, free of harmful ingredients, color, odor and taste. These oils have high interest in industry, due to their physical properties and level of purity, which is required for use in personal care, food and pharmaceutical products [37].

In this work, cationic polyelectrolytes were synthesized using two different health-friendly formulations and applied as low dosage flocculation agents in the pre-treatment step for olive oil mill wastewater, and their performance was studied. The main objective of this paper was to examine the feasibility of using low dosage of high molecular weight polymers, specially designed for this type of effluents, in order to reduce the cost of the treatment. Moreover, the influence of hydrophobic content in the polymers, as well as the concentration of polyelectrolyte for different pH values was assessed. Turbidity reduction, chemical oxygen demand and total solids content were the selected criteria to screen the effectiveness of the process.

## 2. Materials and methods

### 2.1. Materials

Acrylamide (AAM) solution, at 50 wt%, was purchased from Kemira (Botlek, Netherlands). The monomer [3-(Methacryloylamino) propyl] trimethyl ammonium chloride (MAPTAC) was purchased from Qingdao Finechem Chemical Co. (Qingdao, China) and used as received. Stearyl methacrylate (SMA) was purchased from BASF (Ludwigshafen, Germany). *Tert*-butyl hydroperoxide (TBHP) was purchased from Acros Organics (Geel, Belgium). Sodium meta bisulfite (MBS) was purchased from Brenntag (Esseco, Italy). Diethylenetriaminepentaacetic acid

pentasodium salt solution (Pentasodium DTPA) was purchased from Keininghaus Chemie (Essen, Germany). Adipic acid was purchased from Merck (Hohenbrunn, Germany). The surfactants Sorbitan isostearate (Grill 6) and Synperonic LF/30 were purchased from Croda (Goole, England). PEG-7 Hydrogenated Castor Oil (Cremophor WO7) was purchased from BASF (Ludwigshafen, Germany). The oil Puresyn 4, a hydrogenated polydecene, was purchased from ExxonMobil (Switzerland). Carnation, an *iso*-paraffin, was purchased from Sonneborn (Amsterdam, Netherlands). Oily wastewaters tested include effluent obtained from olive oil mill (provided by Adventech Group, Portugal).

### 2.2. Inverse-emulsion polymerization

Inverse-emulsion polymerization was carried out in a 500 mL glass reactor. Prior to reaction, the aqueous phase was prepared with deionized water, acrylamide (AAM), [3-(Methacryloylamino) propyl] trimethyl ammonium chloride (MAPTAC) and 0.625 wt% of adipic acid for hydrolytic stability of the polymers. The copper was chelated with 334 ppm of Pentasodium DTPA. The total monomer level of the initial emulsion was 34.0 wt%. Sorbitan isostearate and PEG-7 Hydrogenated Castor Oil were the surfactants blended to obtain a hydrophilic-lipophilic balance (HLB) between 5.0 and 5.3 according with the monomers composition. Carnation and Puresyn 4 were used as organic phases. The aqueous phase was added to the organic phase under mechanical stirring for 30 min. In the case of the hydrophobically-modified polymers (Poly(AAM-MAPTAC-SMA)), the desired amount of hydrophobic monomer, stearyl methacrylate (SMA), was added at this point to the emulsion. The monomers emulsion was then degassed with nitrogen for 60 min under mechanical stirring (700 rpm), at room temperature. Polymerizations were initiated by injecting 100 ppm of *tert*-butyl hydroperoxide (TBHP) aqueous solution to the reactor and then a solution of MBS 1.0 wt%. TBHP and sodium MBS were used as the initiator redox couple. The peak temperature was between 45 and 52 °C, being the exact maximum temperature of the exotherm dependent on comonomer composition. Additional quantities of TBHP and MBS were added to scavenge residual monomer. After the batch had cooled down to 32 °C, 2.20 wt% of wetting agent (Synperonic LF/30) was added to allow a rapid inversion of the flocculant when added to water. A schematic representation of the synthesis reaction of the hydrophobically-modified cationic polyelectrolytes is shown in Scheme 1.

### 2.3. Isolation of polymers

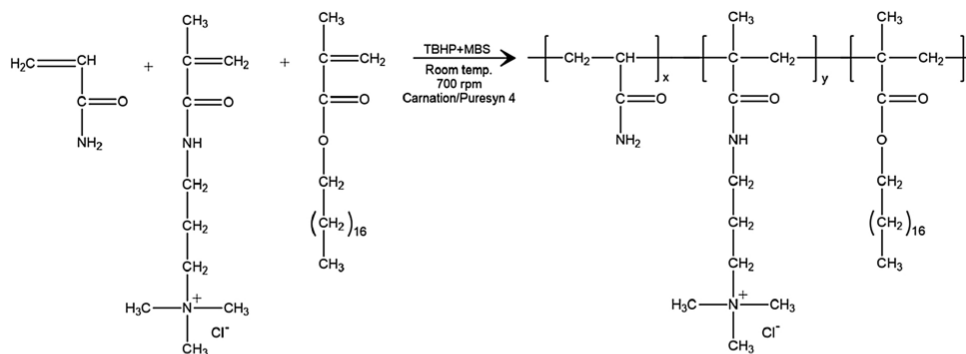
All polymers were isolated by dilution of 3 g of emulsion in 9 mL of hexane and following addition to a mixture of 240 mL of acetone and 18 mL of isopropanol under stirring. After 15 min, the precipitate was filtered under vacuum, washed with fresh acetone and dried in an oven at 60 °C overnight. The samples were stored in a desiccator.

### 2.4. Polyelectrolytes characterization

FTIR spectra were recorded on a Bruker Tensor 27 spectrometer, equipped with an attenuated total reflection (ATR) MKII Golden Gate accessory with a diamond crystal 45° top plate. The spectra were collected in the 500–4000 cm<sup>-1</sup> range with a resolution of 4 cm<sup>-1</sup> and a number of scans of 128. For the measurements, polymers in the powder state were used.

Charge density was determined by the colloid titration method with potassium polyvinyl sulphate (PPVS) using methylene blue as indicator, as described in the literature previously [38]. At least three measurements for each sample were performed.

Hydrodynamic diameter, molecular weight and zeta potential of isolated and redissolved polymers were determined by dynamic light scattering, static light scattering and electrophoretic light scattering, respectively, in a Malvern Zetasizer Nano ZS, model ZEN3600 (Malvern



Scheme 1. Representation of the synthesis reaction for Poly(AAm-MAPTAC-SMA), using monomers of acrylamide, MAPTAC and stearyl methacrylate.

Instruments Ltd, UK). For the hydrodynamic diameter, stock solutions of 0.1 g/L for non-hydrophobically-modified polymers and 0.05 g/L for hydrophobically-modified polymers were prepared in Milli-Q water and stirred overnight. All samples were sonicated during 2 min and passed through 0.45- $\mu\text{m}$  syringe filters prior to analysis. The measurement temperature was set to 25 °C and backscatter detection was used (173° angle), with at least three measurements for each sample performed. Molecular weight measurements of polymers were performed using stock solutions (0.5 g/L) of each polymer prepared in NaCl 0.1 M and stirred overnight. The samples for analysis were then obtained by diluting the stock solutions at several concentrations from 0.02–0.5 g/L. All samples were sonicated during 2 min and passed through 0.45- $\mu\text{m}$  syringe filters prior to analysis. For zeta potential measurements, 1 mL of each stock solution (0.1 g/L) in Milli-Q water was carefully injected with a syringe into a folded capillary cell, closed by cell stoppers. At least three measurements were conducted for each sample.

Table 1 summarizes the initial composition of the developed polyelectrolytes.

### 2.5. Flocculation tests

A 200-mL polymer stock solution at a 0.4 wt% concentration was prepared with distilled water using magnetic stirring for sixty minutes. 75-mL samples of pre-agitated wastewater (industrial effluent) were adjusted to three different pHs using HCl or NaOH aqueous solutions, specifically 3 mL of HCl 1 mol/L were added for pH 3, and 0.2 mL and 5.5 mL of NaOH 1 mol/L were added for pH 5 and 10, respectively. Polymer solution samples with different volumes were added to the wastewater sample, with a successive increase of flocculant concentration from 13 mg/L until a maximum of 180 mg/L. In each addition, the suspension-polymer mixture was manually agitated for 10 s, allowed to settle for 2 min and the turbidity of the supernatant assessed with at least three repetitions, using a Photometer MD600 (Lovibond, UK). The variance in the measurements of turbidity was always below

1.0%. Total solids content and COD of the treated supernatant water were measured for the polymers that showed better results in turbidity reduction. A commercially available polymer flocculant provided by Aqua + Tech Specialities SA (Geneva, Switzerland) was also tested in the same conditions as a reference – this was the polymer under the commercial name AlpineFloc DHMW, a high molecular weight cationic polyacrylamide with 60 wt% charged fraction.

## 3. Results and discussion

### 3.1. Polyelectrolytes characterization

The feasibility of carrying out polymerizations in health-friendly formulations has already been studied in a previous work [36]. The choice of Carnation and Puresyn 4 as organic phases in the inverse-emulsion polymerization of these polyelectrolytes was mainly related with economic issues. Since Carnation and Puresyn 4 led to very similar copolymer characteristics, subsequent hydrophobic modification was conducted only using the oil Carnation.

After purification of the polymers their compositions were assessed (Table 2). The amount of charged groups, and the corresponding actual charge density of all synthesized polymers, was evaluated by titration. For non-hydrophobic polyelectrolytes, it was observed that the amount of charged groups was slightly lower in the final polymer than the initial monomer ratios of the formulation, which can be due to both a difference in monomers reactivity ratios and a non-complete polymerization of the feed monomers. In the case of the hydrophobically-modified polyelectrolytes, it is clear that charged fraction is increased as compared to the corresponding polyelectrolytes that do not contain any hydrophobic monomers.

ATR-FTIR spectroscopy was used to characterize the copolymers for their main structural features. The spectra of the copolymers (Fig. 1) showed bands at ca. 3330  $\text{cm}^{-1}$  and 3190  $\text{cm}^{-1}$ , attributed to the N–H stretching vibrations in the monomers. The characteristic amide I band

Table 1  
Summary of the polyelectrolytes initial composition at the beginning of the polymerization. Poly(AAm-MAPTAC): 25MC, 25MP, 60MC and 60MP. Poly(AAm-MAPTAC-SMA): 25M1SC, 25M2SC, 60M1SC and 60M2SC.

Copolymer designation	Monomer 1	Ratio (wt%)	Ratio (mol%)	Monomer 2	Ratio (wt%)	Ratio (mol%)	Monomer 3	Ratio (wt%)	Ratio (mol%)	Organic phase
25MC	AAm	75	90	MAPTAC	25	10				Carnation
60MC	AAm	40	67	MAPTAC	60	33				Carnation
25MP	AAm	75	90	MAPTAC	25	10				Puresyn 4
60MP	AAm	40	67	MAPTAC	60	33				Puresyn 4
25M1SC	AAm	73	90	MAPTAC	23	9	SMA	4	1	Carnation
25M2SC	AAm	71	89	MAPTAC	21	9	SMA	8	2	Carnation
60M1SC	AAm	38.5	67	MAPTAC	58.5	32	SMA	3	1	Carnation
60M2SC	AAm	37	66	MAPTAC	57	32	SMA	6	2	Carnation

Table 2

Charged fractions calculated from the initial mass balance and estimated by titration. Poly(AAm-MAPTAC): 25MC, 25MP, 60MC and 60MP. Poly(AAm-MAPTAC-SMA): 25M1SC, 25M2SC, 60M1SC and 60M2SC.

Copolymer	Charged fraction from the initial mass balance (wt%)	Charged fraction estimated by titration method (wt%)
25MC	25	22.7 ± 0.8
60MC	60	41.5 ± 2.2
25MP	25	23.4 ± 0.7
60MP	60	42.9 ± 0.2
25M1SC	23	29.3 ± 0.1
25M2SC	21	28.2 ± 0.1
60M1SC	58.5	46.7 ± 0.2
60M2SC	57	45.6 ± 0.2

(C=O stretching in the amide groups) of the monomers appeared as a very strong band with maximum at 1651–1660  $\text{cm}^{-1}$ . The frequency of this absorption maximum changed slightly between copolymer samples depending on the relative content of each monomer, i.e., acrylamide (primary amide) and MAPTAC (secondary amide) in the sample, whose amide functions absorb at a slightly different frequency. Bands showing clearly the presence of MAPTAC were observed at 1532  $\text{cm}^{-1}$  (amide II of secondary amide), 1479  $\text{cm}^{-1}$  (asymmetric bending of  $\text{CH}_3$  groups), 967  $\text{cm}^{-1}$  and 915  $\text{cm}^{-1}$  (asymmetric stretching of  $\text{C}_4\text{-N}$  bonds), with an increased intensity for the samples with a higher content of MAPTAC (60MC, 60MP, 60M1SC and 60M2SC).

It is noteworthy that FTIR spectroscopy confirmed the aforementioned results of the monomer composition in the copolymers determined by colloidal titration (Table 2), as demonstrated by the similar spectra obtained for samples 25MC and 25MP or 60MC and 60MP (of comparable monomer composition) and samples 25M1SC and 25M2SC, and samples 60M1SC and 60M2SC. Results also confirmed the reduced influence of the oil used as medium in the copolymerization reactions (similar FTIR spectra were obtained for the 25MC and 25MP samples or between the 60MC and 60MP samples, produced with different oils: MC series in Carnation and MP series in Puresyn 4).

The presence of the hydrophobic monomer used in the preparation of Poly(AAm-MAPTAC-SMA) samples was revealed by the appearance of two sharp bands in the region of the C–H stretching bands, at 2922 and 2852  $\text{cm}^{-1}$ , which were better resolved in the spectra of 60M1SC and 60M2SC samples. These bands are due to the asymmetric and

Table 3

Polyelectrolytes characterization: zeta potential, hydrodynamic diameter and molecular weight. Poly(AAm-MAPTAC): 25MC, 25MP, 60MC and 60MP. Poly(AAm-MAPTAC-SMA): 25M1SC, 25M2SC, 60M1SC and 60M2SC.

Copolymer	Zeta Potential (mV)	Hydrodynamic diameter (nm)	Molecular weight ( $10^6$ Da)
25MC	44 ± 2	70 ± 2	0.5 ± 0.02
60MC	75 ± 1	234 ± 9	2.9 ± 0.7
25MP	66 ± 1	51 ± 2	0.4 ± 0.04
60MP	79 ± 2	287 ± 13	3.1 ± 0.03
25M1SC	61 ± 1	101 ± 5	1.1 ± 0.03
25M2SC	62 ± 1	138 ± 1	1.1 ± 0.2
60M1SC	97 ± 1	138 ± 9	1.0 ± 0.09
60M2SC	89 ± 1	159 ± 7	1.3 ± 0.01

Table 4

Characteristics of the industrial olive oil mill effluent.

Parameter	Values
pH	4.7
COD ( $\text{gO}_2/\text{L}$ )	11.8
Total solids ( $\text{g/L}$ )	5.99
Turbidity (NTU)	3440
Colour	Dark brown

symmetric stretching of the  $\text{CH}_2$  groups of the hydrophobic chain, respectively. Additionally, for the 60M1SC and 60M2SC samples, a band of small intensity at 1729  $\text{cm}^{-1}$  was visible in the FTIR spectra, due to the C=O stretching in the ester bonds of the hydrophobic monomer.

A summary of the polyelectrolytes characterization, including zeta potential, hydrodynamic diameter and molecular weight is given in Table 3. The zeta potential values for the different polymers are consistent with the charge density of the polyelectrolytes evaluated by titration (Table 2). Charged groups are the crucial parameter affecting this value. Comparing the co-polymers produced in the two different formulations, it is possible to observe that polyelectrolytes synthesized using Puresyn 4 oil present higher zeta potential values, and also higher charged fraction (Table 2), when compared with polyelectrolytes synthesized using Carnation oil. Furthermore, comparing polyelectrolytes developed using the same oil in formulation (Carnation), when hydrophobic content is present the zeta potential increases, as well as the

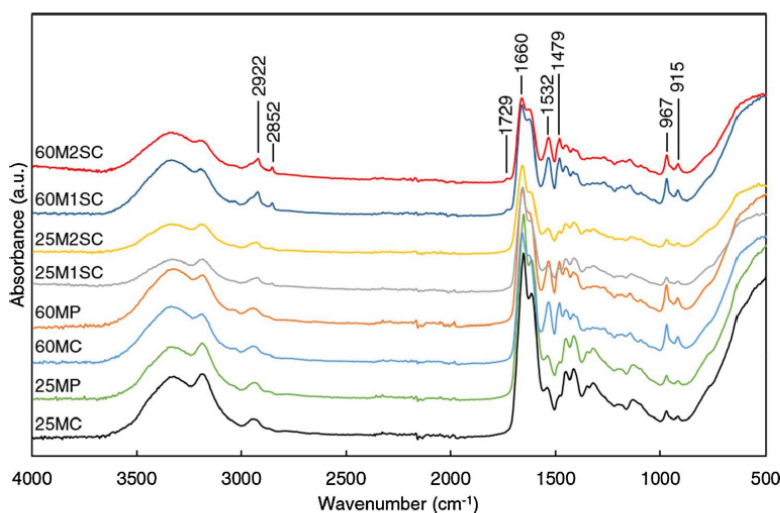


Fig. 1. ATR-FTIR spectra for the polyelectrolytes prepared. Poly(AAm-MAPTAC): 25MC, 25MP, 60MC and 60MP. Poly(AAm-MAPTAC-SMA): 25M1SC, 25M2SC, 60M1SC and 60M2SC.



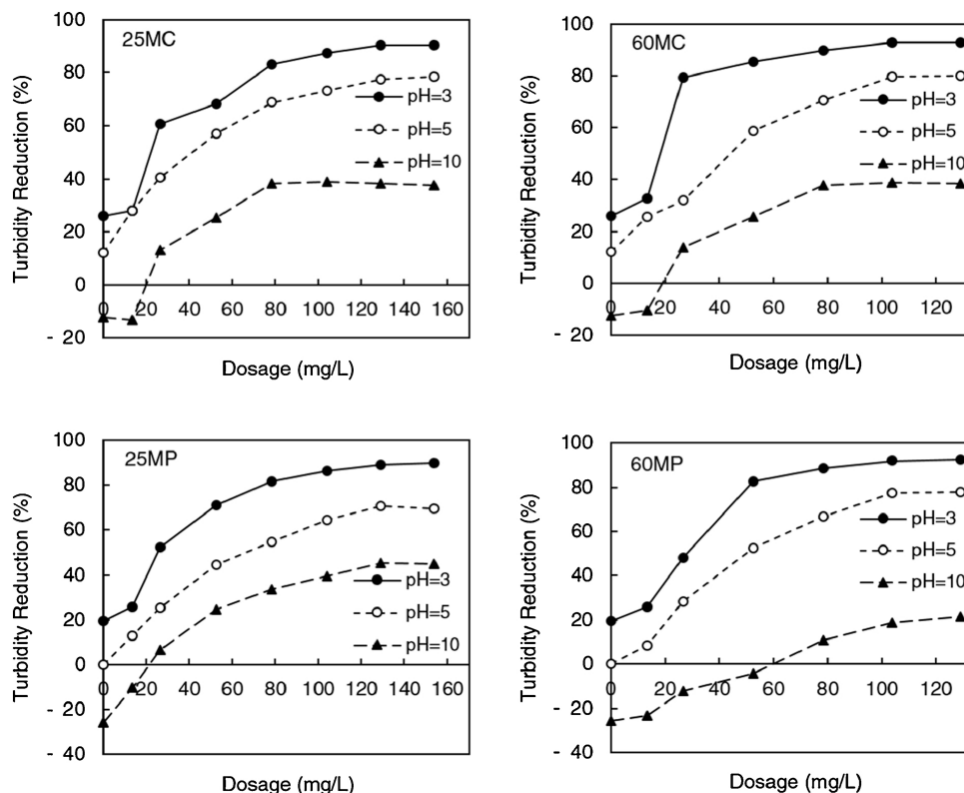


Fig. 2. Turbidity reduction curves for the industrial olive oil mill effluent treated by polyelectrolytes Poly(AAm-MAPTAC): 25MC, 25MP, 60MC and 60MP, at three different pHs.

charged fraction in the final polymer is also higher (compare 25MC with 25M1SC and 25M2SC, and 60MC with 60M1SC and 60M2SC). The hydrodynamic diameter supplies information about the polymer conformation in solution. There is a good correlation between hydrodynamic diameter and polymer molecular weight for polymers with identical charge density. Also, when charge density increases for similar molecular weight, the hydrodynamic diameter increases, as expected (compare 25M2SC and 60M2SC). Since the hydrodynamic diameters were measured in water solutions, the hydrophobicity present in the polyelectrolytes can affect their conformation in water, leading to similar diameters even when charge density increases (compare 25M2SC and 60M1SC). The molecular weight values of polymers produced are in accordance with the molecular weight range presented in the literature for polymers used in the same application [28,31].

### 3.2. Flocculation efficiency in an industrial effluent

The characteristics of the olive oil effluent sample used in the flocculation tests are summarized in Table 4.

Cationic flocculants have inherent positively charged groups, which are active in neutralization of negative charges on suspended colloidal particles and oil droplets during the flocculation process of oily wastewater [39]. Average-zeta potential of the suspended particles and droplets in the effluent sample was  $-12.6$  mV, with a distribution from  $-25.4$  to  $0.9$  mV, indicative of a heterogeneous effluent, confirming nonetheless the adequacy in the use of cationic flocculants. Also, long polymer chains with medium charge density can promote the bridging

effect between the particles, due to the polymer adsorption on the particle surface in a way that is extended and can interact with other particles [40–42].

The influence of pH and dosage of each flocculant was evaluated. Herein, the supernatant water turbidity was used to evaluate the oil removal efficiency. Figs. 2 and 3 show the effect of pH on polyelectrolytes performance in OME treatment at different concentrations from 0 to 180 mg/L, until the turbidity reduction reaches a stable value, for the different polyelectrolytes produced. As can be seen, with increasing dosage, gradual increase was observed in the reduction of turbidity. Acidic conditions always appear to lead to higher removal efficiencies, and the addition of flocculant did not change the effluent pH. Furthermore, adjustment of the effluent to pH 3 decreased, by itself, the turbidity in about 20%. At pH 3, turbidity reduction was at the highest level for all the polymers tested, and was almost complete for dosages above 80 mg/L for all polyelectrolytes with the highest charge density (60 series). When these four flocculants were used for different pHs, the wastewater needed much higher concentrations of polymer to reduce turbidity. Moreover, adjusting pH to basic conditions increased the turbidity of the initial wastewater by itself, severely reducing the flocculant efficiency.

When the charge density is lower, the concentration of polymer required to achieve the same turbidity reduction is higher. This may be attributed to the fact that lower cationic charge density is less effective in neutralizing the negative charge on the oil droplets. Besides the charge density, these polymers present a higher hydrodynamic diameter, favoring, also, the bridging mechanism.

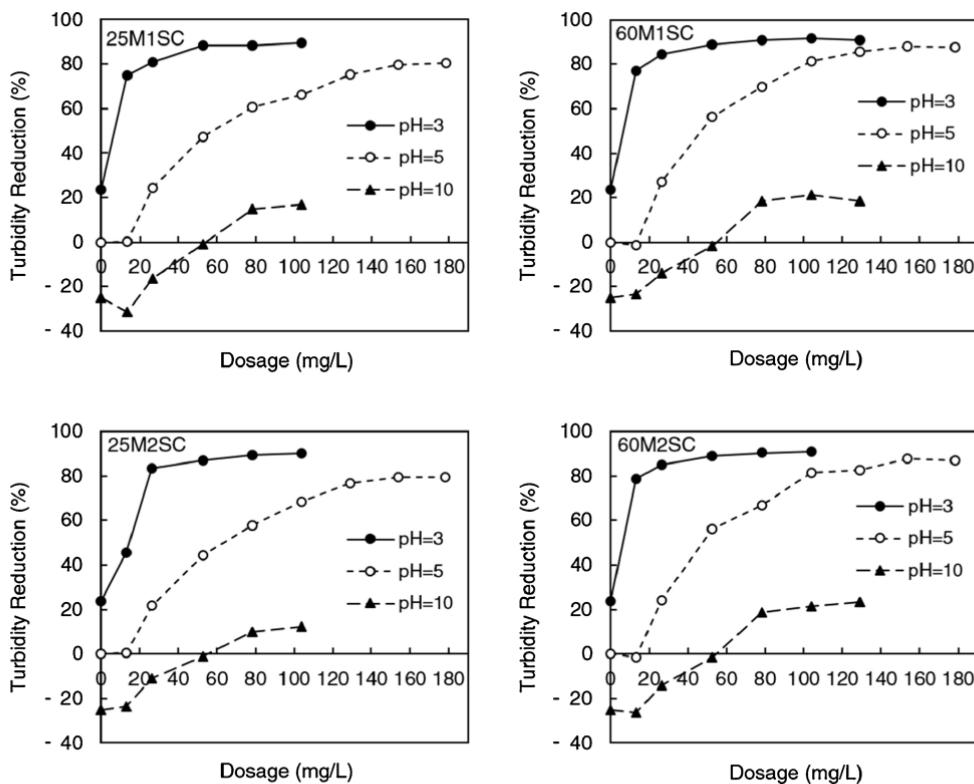


Fig. 3. Turbidity reduction curves for the industrial olive oil mill effluent treated by polyelectrolytes Poly(AAm-MAPTAC-SMA): 25M1SC, 25M2SC, 60M1SC and 60M2SC, at three different pHs.

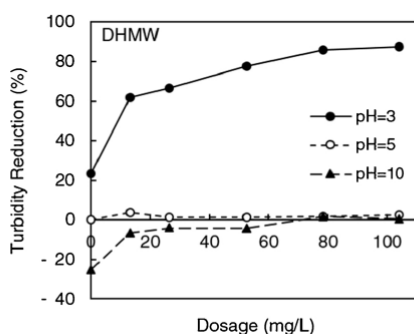


Fig. 4. Turbidity reduction curves for the industrial olive oil mill effluent treated by reference polymer, AlpineFloc DHMW, at various pHs.

When the hydrophobic monomer is introduced in the polymer chain, higher levels of oil removal were achieved with lower polymer dosages. In addition, better performance is obtained for the higher charge densities. When the amount of the hydrophobic monomer increased, the performance of the polymer improved slightly, a lower dosage of flocculant being required for the same removal efficiency, particularly in the case of the higher charge density polymers.

The use of either Carnation, *iso*-paraffin, or Puresyn 4, hydrogenated polydecene, in the synthesis process did not affect the

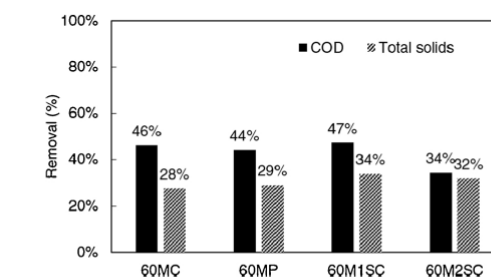


Fig. 5. COD and total solids removal after the treatment of the industrial olive oil mill effluent with 60MC, 60MP, 60M1SC and 60M2SC flocculants, in optimized conditions of pH and concentration.

performance of the polyelectrolytes (compare the graphs for the MC and MP series of polymers), which is consistent with the similarity of the characterization parameters (zeta potential, hydrodynamic diameter and molecular weight) for these two types of polyelectrolytes for similar amounts of the cationic monomer (see Table 2). A more structural analysis regarding the influence of the organic phases used has already been presented in a previous study [36].

Considering that molecular weight of the higher charge density hydrophobically-modified polymers is lower, improvement of performance must be justified by the affinity between the hydrophobic part of the polymer and the oil droplets in the effluent. Previously Lü et al. [43]

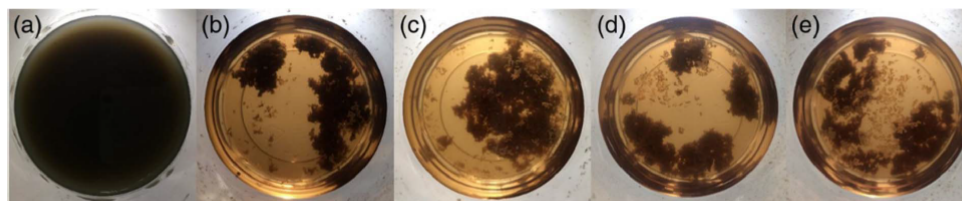


Fig. 6. Initial effluent (a) and effluent after treatment with flocculants 60MC (b), 60MP (c), 60M1SC (d), and 60M2SC (e), in optimized conditions of pH and concentration.

and Bratskaya et al. [44] demonstrated that oil removal efficiency was significantly enhanced using hydrophobically-modified cationic flocculants.

The performance of the new polyelectrolytes developed in this study was compared with the reference polymer (Fig. 4) commercially available from Aqua + Tech. AlpineFloc DHMW, which has a similar charge density to the 60 series in this work. Looking at the results for pH 3, which provided the highest oil removal efficiency, the reference polymer showed a similar behavior as the newly developed copolymers with analogous charge density. Nevertheless, 60MC and 60MP achieved higher turbidity reduction values than DHMW when comparing the same dosages. When comparing the performance of the hydrophobically-modified polyelectrolytes developed (25M1SC, 25M2SC, 60M1SC and 60M2SC) with this reference commercial polymer, the former show much higher removal efficiency. This evidence proves once again that addition of a hydrophobic monomer to the copolymers highly improves the flocculation performance of cationic polyelectrolytes in the treatment of industrial olive oil mill effluents.

Additionally, it must also be stressed the new polymers developed present always better performance than the reference commercial polymer when testing at all other pHs, particularly for pH 5. In fact, the commercial flocculant shows almost zero removal for these pH values.

The total solids and COD removal efficiencies were measured (Fig. 5) for the polymers that presented higher turbidity reduction and in the optimized conditions of pH and concentration, in order to confirm that pre-treatment was also efficient regarding these two parameters. For both parameters, the removal for the different polymers tested was very similar with a slightly better performance of the polyelectrolyte 60M1SC. Comparing these results with previous publications for coagulation/flocculation of olive oil mill effluents, the removal range is similar, however much lower dosage was needed to reach a similar effect. In Sarika et al. [45], four cationic and two anionic polyelectrolytes were tested in direct flocculation and shown to be capable to remove nearly completely total suspended solids (TSS) and reduce considerably COD (55%) with a minimum dosage of about 2500–3000 mg/L, in the best cases. Michael et al. [46] studied coagulation/flocculation as pre-treatment in the application of a solar-driven advanced oxidation process (solar Fenton), using ferrous sulfate ( $\text{FeSO}_4$ ) (6670 mg/L) as the coagulant, and an anionic polyelectrolyte (287 mg/L) as flocculant, leading to approximately 44% of COD removal and TSS was removed by 94%, in line with the results obtained in the present work, for COD removal. Rizzo et al. [30] investigated the coagulation of olive mill wastewater by natural organic coagulants, as possible alternative to conventional metal based coagulants. Chitosan was chosen and provided high performances in terms of turbidity (94%) and TSS (81%) removals under an optimized dosage of 400 mg/L.

The digital micrographs displayed in Fig. 6 show the flocs structure after addition of the suitable dosage of 60MC (b), 60MP (c), 60M1SC (d) and 60M2SC (e) to the initial effluent sample (a), at pH 3. Flocs resulting from the flocculation with the new developed polyelectrolytes had very fast growing and settling performance, presenting a high resistance to breaking actions and strong and compact structure after formation, suggesting a low water content in the flocculated fraction.

#### 4. Conclusions

Direct-flocculation is a simple and easily applicable method for treatment of wastewaters. The health-friendly formulations used in the development of the flocculation agents, presented in this work, led to polyelectrolytes with suitable characteristics for the final application. The characterization of the polyelectrolytes produced proved the success of the hydrophobic content integration, without affecting the factors that have the main influence in the flocculation process, like zeta potential or molecular weight.

The cationic polyelectrolytes produced revealed to be very promising as pre-treatment agents for treatment of olive oil mill effluents. Moreover, the hydrophobic modification of the polymers improves the treatment efficiency, reducing, simultaneously, the associated treatment cost, since lower dosages are needed to reach the same treatment effectiveness.

The application of hydrophobically-modified polyelectrolytes, with 46–47 wt% of charged fraction, in dosages around 53 mg/L, were the most effective in the flocculation process. Turbidity removal of 90%, COD removal of 47% and total solids removal of 34% were achieved. Furthermore, encouraging results were obtained after addition of only 13 mg/L of flocculant, with reduction of turbidity around 79%.

In summary, the polyelectrolytes developed for direct flocculation proved to be an effective pre-treatment solution for the harsh effluent targeted (olive oil mill effluent), considering the different parameters usually analyzed, and also a more economic method when compared with alternative/standard coagulation-flocculation procedures which use larger amounts of flocculant and generate high volumes of sludge, expensive to treat.

#### Acknowledgments

This work was supported by Marie Curie Initial Training Networks (ITN) – European Industrial Doctorate (EID), through Grant agreement FP7-PEOPLE-2013-ITN-604825, and Portuguese Science and Technology Foundation (Pest/C/EQB/UI0102/2013). The authors would like to thank to Adventech Group (Portugal) for supplying the effluent.

#### References

- 1) M. Fitó, M.I. Covas, R.M. Lamuela-Raventós, J. Vila, J. Torrents, C. de la Torre, J. Marrugat, Protective effect of olive oil and its phenolic compounds against low density lipoprotein oxidation, *Lipids* 35 (2000) 633–638, <http://dx.doi.org/10.1007/s11745-000-0567-1>.
- 2) C.A. Paraskeva, V.G. Papadakis, E. Tsarouchi, D.G. Kanelloupolou, P.G. Koutsoukos, Membrane processing for olive mill wastewater fractionation, *Desalination* 213 (2007) 218–229, <http://dx.doi.org/10.1016/j.desal.2006.04.087>.
- 3) A.C. Barbera, C. Maucieri, V. Cavallaro, A. Ioppolo, G. Spagna, Effects of spreading olive mill wastewater on soil properties and crops, a review, *Agric. Water Manag.* 119 (2013) 43–53, <http://dx.doi.org/10.1016/j.agwat.2012.12.009>.
- 4) D.A. Salam, N. Naik, M.T. Suidan, A.D. Venosa, Assessment of aquatic toxicity and oxygen depletion during aerobic biodegradation of vegetable oil: effect of oil loading and mixing regime, *Environ. Sci. Technol.* 46 (2012) 2352–2359, <http://dx.doi.org/10.1021/es2037993>.
- 5) G. Celano, D. Smejkalova, R. Spaccini, A. Piccolo, Reduced toxicity of olive mill waste waters by oxidative coupling with biomimetic catalysis, *Environ. Sci. Technol.* 42 (2008) 4896–4901, <http://dx.doi.org/10.1021/es8000745>.

- [6] J. Benitez, J. Beltran-Heredia, J. Torregrosa, J.L. Acero, V. Cercas, Aerobic degradation of olive mill wastewaters, *Appl. Microbiol. Biotechnol.* 47 (1997) 185–188, <http://dx.doi.org/10.1007/s002530050910>.
- [7] K. Stamatelidou, A. Kopsellis, P.S. Blika, C.A. Paraskeva, G. Lyberatos, Anaerobic digestion of olive mill wastewater in a periodic anaerobic baffled reactor (PABR) followed by further effluent purification via membrane separation technologies, *J. Chem. Technol. Biotechnol.* 84 (2009) 909–917, <http://dx.doi.org/10.1002/jctb.2170>.
- [8] I.P. Marques, Anaerobic digestion treatment of olive mill wastewater for effluent reuse in irrigation, *Desalination* 137 (2001) 233–239, [http://dx.doi.org/10.1016/S0011-9164\(01\)00224-7](http://dx.doi.org/10.1016/S0011-9164(01)00224-7).
- [9] I.P. Marques, A. Teixeira, L. Rodrigues, S.M. Dias, J.M. Novais, Anaerobic treatment of olive mill wastewater with digested piggy effluent, *Water Environ. Res.* 70 (1998) 1056–1061, <http://dx.doi.org/10.2175/106143098X123390>.
- [10] M. Hamdi, R. Ellouz, Use of *Aspergillus niger* to improve filtration of olive mill wastewater, *J. Chem. Technol. Biotechnol.* 53 (1992) 195–200, <http://dx.doi.org/10.1002/jctb.280530215>.
- [11] C.F. Ceretti, F. Rossini, F. Federici, D. Quarantino, N. Vassilev, M. Fenice, Reuse of microbially treated olive mill wastewater as fertiliser for wheat (*Triticum durum* Desf.), *Bioresour. Technol.* 91 (2004) 135–140, [http://dx.doi.org/10.1016/S0960-8524\(03\)00181-0](http://dx.doi.org/10.1016/S0960-8524(03)00181-0).
- [12] R. Borja, J. Alba, S.E. Garrido, L. Martinez, M.P. Garcia, C. Incerti, A. Ramos-Correnzana, Comparative study of anaerobic digestion of olive mill wastewater (OMW) and OMW previously fermented with *Aspergillus terreus*, *Bioprocess. Eng.* 13 (1995) 317–322, <http://dx.doi.org/10.1007/BF00369564>.
- [13] R. Borja, A. Martin, V. Alonso, I. Garcia, C.J. Banks, Influence of different aerobic pretreatments on the kinetics of anaerobic digestion of olive mill wastewater, *Water Res.* 29 (1995) 489–495, [http://dx.doi.org/10.1016/0043-1354\(94\)00180-F](http://dx.doi.org/10.1016/0043-1354(94)00180-F).
- [14] R. Borja, J. Alba, A. Mancha, A. Martín, V. Alonso, E. Sánchez, Comparative effect of different aerobic pretreatments on the kinetics and macroenergetic parameters of anaerobic digestion of olive mill wastewater in continuous mode, *Bioprocess. Eng.* 18 (1998) 127–134, <http://dx.doi.org/10.1007/s004490050422>.
- [15] G. Ubay, I. Öztürk, Anaerobic treatment of olive mill effluents, *Water Sci. Technol.* 36 (1997) 287–294.
- [16] F. Raposo, R. Borja, E. Sanchez, M.A. Martín, A. Martín, Performance and kinetic evaluation of the anaerobic digestion of two-phase olive mill effluents in reactors with suspended and immobilized biomass, *Water Res.* 38 (2004) 2017–2026, <http://dx.doi.org/10.1016/j.watres.2004.01.007>.
- [17] B.Y. Ammary, Treatment of olive mill wastewater using an anaerobic sequencing batch reactor, *Desalination* 177 (2005) 157–165, <http://dx.doi.org/10.1016/j.desal.2004.12.006>.
- [18] B. Kiril Mert, T. Yonar, M. Yalili Kiliç, K. Kestiöglu, Pre-treatment studies on olive oil mill effluent using physicochemical, Fenton and Fenton-like oxidations processes, *J. Hazard. Mater.* 174 (2010) 122–128, <http://dx.doi.org/10.1016/j.jhazmat.2009.09.025>.
- [19] F.J. Rivas, F.J. Beltrá, O. Gimeno, J. Frades, Treatment of olive oil mill wastewater by Fenton's reagent, *J. Agric. Food Chem.* 49 (2001) 1873–1880, <http://dx.doi.org/10.1021/jf001223b>.
- [20] N. Wang, T. Zheng, G. Zhang, P. Wang, A review on Fenton-like processes for organic wastewater treatment, *J. Environ. Chem. Eng.* 4 (2016) 762–787, <http://dx.doi.org/10.1016/j.jece.2015.12.016>.
- [21] R. Elkacmi, N. Kamil, M. Bennajah, Separation and purification of high purity products from three different olive mill wastewater samples, *J. Environ. Chem. Eng.* 5 (2017) 829–837, <http://dx.doi.org/10.1016/j.jece.2017.01.005>.
- [22] A. El-Abbassi, M. Khayet, A. Hafidi, Micellar enhanced ultrafiltration process for the treatment of olive mill wastewater, *Water Res.* 45 (2011) 4522–4530, <http://dx.doi.org/10.1016/j.watres.2011.05.044>.
- [23] A. Ginos, T. Manios, D. Mantzavinos, Treatment of olive mill effluents by coagulation-flocculation-hydrogen peroxide oxidation and effect on phytotoxicity, *J. Hazard. Mater.* 133 (2006) 135–142, <http://dx.doi.org/10.1016/j.jhazmat.2005.10.024>.
- [24] Ü. Tezcan, S. Uğur, A.S. Kopalal, Ü. Bakır Ögütveren, Electrocoagulation of olive mill wastewaters, *Sep. Purif. Technol.* 52 (2006) 136–141, <http://dx.doi.org/10.1016/j.seppur.2006.03.029>.
- [25] A. Fiorentino, A. Gentili, M. Isidori, M. Lavorgna, A. Parrella, F. Temussi, Olive oil mill wastewater treatment using a chemical and biological approach, *J. Agric. Food Chem.* 52 (2004) 5151–5154, <http://dx.doi.org/10.1021/jf049799e>.
- [26] M. Bressan, L. Liberatore, N. d'Alessandro, L. Tonucci, C. Belli, G. Ranalli, Improved combined chemical and biological treatments of olive oil mill wastewaters, *J. Agric. Food Chem.* 52 (2004) 1228–1233, <http://dx.doi.org/10.1021/jf035128p>.
- [27] J.M. Ochando-Pulido, M. Stoller, L. Di Palma, A. Martínez-Ferez, On the optimization of a flocculation process as fouling inhibiting pretreatment on an ultrafiltration membrane during olive mill effluents treatment, *Desalination* 393 (2016) 151–158, <http://dx.doi.org/10.1016/j.desal.2015.12.021>.
- [28] G. Hodafa, J.A. Pérez, C. Agabo, E. Ramos, J.C. Gutiérrez, A. Rosal, Flocculation on the treatment of olive oil mill wastewater: pretreatment, *Int. Sch. Sci. Res. Innov.* 9 (2015) 645–650.
- [29] K. Pelendridou, M.K. Michailides, D.P. Zagklis, A.G. Tekerlekopoulou, C.A. Paraskeva, D.V. Vayenas, Treatment of olive mill wastewater using a coagulation-flocculation process either as a single step or as post-treatment after aerobic biological treatment, *J. Chem. Technol. Biotechnol.* 89 (2014) 1866–1874, <http://dx.doi.org/10.1002/jctb.4269>.
- [30] L. Rizzo, G. Lofrano, V. Belgiorno, Olive mill and winery wastewaters pre-treatment by coagulation with chitosan, *Sep. Sci. Technol.* 45 (2010) 2447–2452, <http://dx.doi.org/10.1080/01496395.2010.487845>.
- [31] I.C. Iakovides, A.G. Pantziaros, D.P. Zagklis, C.A. Paraskeva, Effect of electrolytes/polyelectrolytes on the removal of solids and organics from olive mill wastewater, *J. Chem. Technol. Biotechnol.* 91 (2014) 204–211, <http://dx.doi.org/10.1002/jctb.4563>.
- [32] O. Amuda, I. Amoo, Coagulation/flocculation process and sludge conditioning in beverage industrial wastewater treatment, *J. Hazard. Mater.* 141 (2007) 778–783, <http://dx.doi.org/10.1016/j.jhazmat.2006.07.044>.
- [33] K. Kestiöglu, T. Yonar, N. Azbar, Feasibility of physico-chemical treatment and Advanced Oxidation Processes (AOPs) as a means of pretreatment of olive mill effluent (OME), *Process Biochem.* 40 (2005) 2409–2416, <http://dx.doi.org/10.1016/j.procbio.2004.09.015>.
- [34] S.-C. Chen, C.-M. Liao, Health risk assessment on human exposed to environmental polycyclic aromatic hydrocarbons pollution sources, *Sci. Total Environ.* 366 (2006) 112–123, <http://dx.doi.org/10.1016/j.scitotenv.2005.08.047>.
- [35] L. Armanet, D. Hunkeler, Phase inversion of polyacrylamide based inverse-emulsions: effect of the surfactant and monomer on postinversion equilibrium properties, *J. Appl. Polym. Sci.* 106 (2007) 2328–2341, <http://dx.doi.org/10.1002/app.25309>.
- [36] A. Lourenço, J. Arnold, J.A.F. Gamelas, M.G. Rasteiro, A more eco-friendly synthesis of flocculants to treat wastewaters using health-friendly solvents, *Colloids Polym. Sci.* 295 (2017) 2123–2131.
- [37] E. Kim, G.W. Nam, S. Kim, H. Lee, S. Moon, I. Chang, Influence of polyol and oil concentration in cosmetic products on skin moisturization and skin surface roughness, *Ski. Res. Technol.* 13 (2007) 417–424, <http://dx.doi.org/10.1111/j.1600-0846.2007.00246.x>.
- [38] S. Kam, J. Gregory, Charge determination of synthetic cationic polyelectrolytes by colloid titration, *Colloids Surf. A Physicochem. Eng. Asp.* 159 (1999) 165–179, [http://dx.doi.org/10.1016/S0927-7757\(99\)00172-7](http://dx.doi.org/10.1016/S0927-7757(99)00172-7).
- [39] D. Palomino, D. Hunkeler, S. Stoll, Comparison of two cationic polymeric flocculant architectures on the destabilization of negatively charged latex suspensions, *Polymer (Guildf.)* 52 (2011) 1019–1026, <http://dx.doi.org/10.1016/j.polymer.2010.12.033>.
- [40] S. Biggs, M. Habgood, G.J. Jameson, Y. Yan, Aggregate structures formed via a bridging flocculation mechanism, *Chem. Eng. J.* 80 (2000) 13–22, [http://dx.doi.org/10.1016/S1383-5866\(00\)00072-1](http://dx.doi.org/10.1016/S1383-5866(00)00072-1).
- [41] I. Pinheiro, P.J. Ferreira, F.A. Garcia, M.S. Reis, A.C. Pereira, C. Wandrey, H. Ahmadloo, J.L. Amaral, D. Hunkeler, M.G. Rasteiro, An experimental design methodology to evaluate the importance of different parameters on flocculation by polyelectrolytes, *Powder Technol.* 238 (2013) 2–13, <http://dx.doi.org/10.1016/j.powtec.2012.08.004>.
- [42] C.S. Lee, J. Robinson, M.F. Chong, A review on application of flocculants in wastewater treatment, *Process Saf. Environ. Prot.* 92 (2014) 489–508, <http://dx.doi.org/10.1016/j.psep.2014.04.010>.
- [43] T. Lü, D. Qi, H. Zhao, Y. Cheng, Synthesis of hydrophobically modified flocculant by aqueous dispersion polymerization and its application in oily wastewater treatment, *Polym. Eng. Sci.* 55 (2015) 1–7, <http://dx.doi.org/10.1002/pen.23856>.
- [44] S. Bratskaya, V. Avramenko, S. Schwarz, I. Philippova, Enhanced flocculation of oil-in-water emulsions by hydrophobically modified chitosan derivatives, *Colloids Surf. A Physicochem. Eng. Asp.* 275 (2006) 168–176, <http://dx.doi.org/10.1016/j.colsurfa.2005.09.036>.
- [45] R. Sarika, N. Kalogerakis, D. Mantzavinos, Treatment of olive mill effluents: part II. Complete removal of solids by direct flocculation with poly-electrolytes, *Environ. Int.* 31 (2005) 297–304, <http://dx.doi.org/10.1016/j.envint.2004.10.006>.
- [46] I. Michael, A. Panagi, L.A. Ioannou, Z. Frontistis, D. Fatta-Kassinos, Utilizing solar energy for the purification of olive mill wastewater using a pilot-scale photocatalytic reactor after coagulation-flocculation, *Water Res.* 60 (2014) 28–40, <http://dx.doi.org/10.1016/j.watres.2014.04.032>.

PAPER 3 (*reply to reviewers submitted*)

## **Flocculation treatment of an industrial effluent: performance assessment by Laser Diffraction Spectroscopy**

*Anita Lourenço<sup>1,2</sup>, Julien Arnold<sup>2</sup>, Olivier J. Cayre<sup>3</sup> and Maria G. Rasteiro<sup>1\*</sup>*

<sup>1</sup> Chemical Engineering Department, CIEQPFF, University of Coimbra Pólo II, Rua Sílvio Lima,  
3030-790 Coimbra, Portugal

<sup>2</sup> Aqua+Tech Specialities SA, Chemin du Chalet-du-Bac 4, 1237 Avully, Geneva, Switzerland

<sup>3</sup> School of Chemical and Process Engineering, University of Leeds, Woodhouse Lane, Leeds LS2  
9JT, UK

\*mgr@eq.uc.pt

### ABSTRACT

Flocculation processes are extensively used as separation method to remove suspended and dissolved solids, colloids and organic substances in effluents. As flocculation performance affects the economy of many industrial processes, it is important to understand the underlying mechanisms, as well as the predominant flocculant properties influencing the final results. In the present study, a strategy based on the use of laser diffraction spectroscopy (LDS) was developed to screen different flocculants performance in an industrial potato crisps manufacturing effluent, using anionic polyelectrolytes as flocculants. The flocculation process was monitored over time and information on floc average size and structure was obtained. The effect of flocculants properties, including their hydrophobic content, and concentration on the flocculation process and on flocs density was investigated. With this methodology for continuous monitoring of the flocculation process in real effluents, it is possible to obtain simultaneously information about the kinetics of floc size evolution, and also about the evolution of floc structure with time. This is an important proof of concept, since it will allow, in the future, to perform pre-screening of polymers to be used in the flocculation treatment of a specific effluent, minimizing, in this way, pilot trials

The highest polyelectrolyte concentration studied leads to the largest flocs obtained, which were, however, very sensitive to the turbulent environment. This agrees with the low scattering exponent

values obtained for all the flocs, which indicate an open and porous floc structure. Characteristics of the polymers used proved to have an important role in the floc size. Higher zeta potential, hydrodynamic diameter and molecular weight of the flocculant resulted in larger flocs. The presence of hydrophobicity in the polyelectrolyte also showed to influence the floc properties, although an optimum content could be identified, above which flocculation was hindered.

## KEYWORDS

Polyelectrolytes, wastewater treatment, flocculation, laser diffraction spectroscopy, scattering exponent.

## INTRODUCTION

Wastewater from industrial processes usually contains dissolved solids, very fine suspended solids, organic and inorganic particles, metals and other insoluble impurities with very small size and some surface charge. Due to this, self-aggregation of these particles in a way that it is possible to have a reasonable separation and obtain dense flocs for settling and filtration is a challenge <sup>1,2</sup>.

Flocculation is the most extensively used separation process to remove suspended and dissolved solids, colloids and organic substances in industrial wastewater <sup>3</sup>. Generally, floc formation involves several steps occurring sequentially including dispersion of the flocculant in the solution, diffusion near and to the solid-liquid interface, adsorption of the flocculant onto the surface of the particles, collision of particles containing adsorbed polymer with other particles and adsorption of the flocculant on the free surface of those particles. These standard steps typically lead to the formation of aggregates and enable growth of initial microflocs to larger and stronger flocs by consecutive polymer adsorption and particle collisions and aggregation or, alternatively, establishment of bonds between flocculant chains adsorbed onto different particles <sup>4-6</sup>.

Destabilization of particle suspensions by polymers can be associated to different flocculation mechanisms such as charge neutralization <sup>6,7</sup>, polymer bridging <sup>8,9</sup> and electrostatic patches interactions <sup>9,10</sup>. These mechanisms are strongly related with the way adsorption of flocculants on particle surfaces occurs, which depends on the chemical affinity between the polymer and the particle surface <sup>3</sup>.

To optimize the flocculation performance there are several parameters that need to be controlled during the process. The optimised flocculant concentration depends on the content of suspended solids and colloids in the wastewater, including dissolved organic content, and the treatment success usually increases with the increase of flocculant input, until a certain optimum level from which there is no further improvement of performance. The treatment efficiency often achieves a maximum and decreases if the polymer dosage is too high <sup>11</sup>. An important mechanical factor in the flocculation process is the mixing, which enhances contact between the flocculant and the

suspended solids in the system, thus accelerating the formation of flocs. There are two stages in the mixing process in a typical flocculation process and they are associated with rapid and slow stirring. The rapid stirring is used to achieve a good dispersion of the flocculant after addition, while slow stirring is used to promote the flocs growth and limit the breakup of aggregates<sup>12</sup>.

Synthetic polyelectrolytes have been commonly used as flocculants to enhance the flocculation process efficiency, with promising results<sup>13</sup>. Polymer characteristics such as molecular weight, structure (linear or branched), charge density, charge type and composition have a strong influence on the flocculation process<sup>14</sup>.

In order to investigate the floc behavior during the formation process, as well as the flocculation kinetics, the floc characteristics can be monitored in-situ using a laser diffraction particle size analyzer system (LDS)<sup>15</sup>. It is well reported in the literature that LDS is useful to follow flocculation processes, even if most studies refer to model systems<sup>15</sup>. Rasteiro *et al.*<sup>15,16</sup> presented the application of LDS to monitor flocculation in papermaking and to evaluate the flocculation mechanisms in flocculation studies of precipitated calcium carbonate. Using LDS it is possible to perform an evaluation of the flocculants performance, providing information on floc size distribution, average size and aggregate structure described by the fractal dimension ( $d_F$ ) and scattering exponent (SE), in a continuous approach<sup>17</sup>. The fractal dimension provides information about the primary particles that fill the space in the nominal volume of an aggregate, being a useful parameter to characterize the density of the flocs<sup>18</sup>. However, for secondary aggregates resulting from the aggregation of primary aggregates, the fractal theory can no longer be applied and the scattering exponent is used to obtain information regarding the flocs structure, providing information for the larger length scales of larger flocs<sup>17,19</sup>. Moreover, flocculation can be conducted in controlled hydrodynamic conditions that can easily be reproduced in industrial flocculation processes<sup>20</sup>.

In LDS measurement, the scattering angle, the angle between the incident and scattered lights, is inversely correlated with the particles size. Thus, by collecting the intensity of the scattered light for different angles it is possible to extract information about the number of particles in each size class. The information collected regarding the different scattering angles, results in the scattering matrix, from which the particle size distribution can be obtained using the adequate model<sup>21</sup>.

In this study, flocculation was followed continuously, using LDS, for a real industrial effluent from potato crisps manufacturing industry, treated with high molecular weight anionic polyelectrolytes with two different polymer compositions (co-polymers). The effect of the incorporation of a hydrophobic monomer at different ratios (ter-polymers) within the polymer flocculant structure, onto the efficiency of the flocculation process was also studied. Recently, hydrophobic modification of polymers has been extensively investigated for application in solid-liquid separation, due to their capacity of enhancing polymer performance<sup>22</sup>. Hydrophobically-modified polymers can be obtained by chemical grafting or copolymerization procedures, through

the introduction of a relatively low amount of hydrophobic monomer into the polymer structure<sup>23</sup>. The synergetic effects between the charge functionality and the hydrophobic group have shown a remarkable improve of performance in wastewater treatment<sup>22,24</sup>.

In this study the applied polymers were synthesized by inverse-emulsion polymerization using three different health-friendly formulations, which have replaced the organic phase and surfactants of traditional formulations<sup>25</sup>. Two health-friendly oils, according to the international nomenclature of cosmetic ingredients INCI, were used as organic phase in the synthesis process: an iso-paraffin (Carnation) and a hydrogenated polydecene (Puresyn4). These health-friendly formulations, which have been explained in a previous reference from the authors<sup>26</sup>, have already proved to be suitable to synthesize standard commercial polymers for application as flocculants in water treatment. Results regarding size, structure and strength of the flocs, as well as flocculation kinetics were obtained and analyzed. Correlation between polyelectrolyte characteristics and flocs size and structure is presented here and the prevailing flocculation mechanisms discussed. The main objective of this work is the development of a new screening methodology, based on LDS, to pre-select the best flocculant for a specific application. This will allow the detailed analysis of the obtained aggregates, depending on the flocculation products used and operating conditions, and allow correlating polyelectrolyte characteristics with specific floc properties, thus facilitating the choice of the best polyelectrolyte for a certain application, minimizing the need for pilot trials.

## EXPERIMENTAL SECTION

### Materials

Acrylamide (AAm) solution, at 50 wt %, was purchased from Kemira (Botlek, Netherlands). The monomer Acrylamido-2-methyl-1-propanesulfonic acid sodium salt solution (Na-AMPS), at 50 wt%, was purchased from Lubrizol (Bradford, UK) and used as received. Ethyl acrylate (EA) was purchased from Evonik (Darmstadt, Germany). Tert-butyl hydroperoxide (TBHP) was purchased from Acros Organics (Geel, Belgium). Sodium metabisulfite (MBS) was purchased from Brenntag (Esseco, Italy). Adipic acid was purchased from Merck (Hohenbrunn, Germany). The surfactants Sorbitan isostearate (Crill 6) and Synperonic LF/30 were purchased from Croda (Goole, England). PEG-7 hydrogenated castor oil (Cremophor WO7) was purchased from BASF (Ludwigshafen, Germany). The oil Puresyn4, a hydrogenated polydecene, was purchased from ExxonMobil (Switzerland). Carnation, an iso-paraffin, was purchased from Sonneborn (Amsterdam, Netherlands). PPVS and methylene blue were supplied by Sigma-Aldrich (St. Louis, USA). Sodium Chloride (NaCl) was purchased from VWR (Leuven, Belgium).

The flocculation tests were carried out on an industrial oily effluent from potato crisps manufacturing industry, which was supplied by Adventech Group (Portugal). The initial effluent sample presented a pH of 12.8, COD of 21.6 gO<sub>2</sub>/L, total solids of 9.7 g/L and a turbidity of 3050



NTU. The zeta potential of the effluent was measured in a Zetasizer Nano-ZS (Malvern Instruments) and the average value obtained was  $-17$  mV at the initial pH (12.8) and  $-5$  mV at pH 6, even if a wide distribution of zeta potential was obtained, indicative of particles with different charges. Considering that a few particles in the effluent were over  $100\ \mu\text{m}$  (being the maximum particle size recommended for this equipment  $100\ \mu\text{m}$ ) and also the low zeta potential of the effluent particles, the number of runs for each measurement was increased, as well as the acquisition time, according to recommendations in the equipment manual. The software quality report did always confirm good quality of the measurements.

### Polyelectrolytes synthesis

Anionic polyelectrolytes, co- and ter-polymers of acrylamide, Na-AMPS and ethyl acrylate, were synthesized by inverse-emulsion polymerization using health-friendly formulations. The polymerization was carried out in a 500 mL glass reactor. Prior to reaction, the aqueous phase was prepared with deionized water, acrylamide, Na-AMPS and with 0.625 wt % of adipic acid. Sorbitan isostearate and PEG-7 hydrogenated castor oil were, as well, the surfactants blend to obtain a hydrophilic–lipophilic balance (HLB) between 4.75 and 5.75, adapted to the monomers composition and organic phase used. Carnation and Puresyn4 were used as organic phases. The aqueous phase was added to the organic phase under mechanical stirring and in the case of the combination with the hydrophobic monomer, the desired amount of EA was added at this point to the emulsion. TBHP and sodium MBS were used as the initiator redox couple. After the batch had cooled down to  $32\ ^\circ\text{C}$ , 2.20 wt% of a wetting agent (Synperonic LF/30) was added.

Table 1 presents a summary of the flocculants produced. Lower anionic fraction is represented as the 50 series, while higher anionic fraction is represented as the 80 series. MC and MP series in the list correspond to the use of Carnation and Puresyn4, respectively, as the health-friendly synthesis organic phase. For the ter-polymers, only Carnation was used as organic phase. A, refers to the use of Na-AMPS monomer, while E refers to the introduction in the polymer of the hydrophobic monomer EA.

Polyelectrolytes solutions were prepared with distilled water at 0.4% (w/w). In order to guarantee the effectiveness of the flocculants, the diluted solutions must be prepared every day.

**Table 1** Summary of the polyelectrolytes composition. Co-polymers: 50AC, 80AC, 50AP and 80AP. Ter-polymers: 50A1EC, 50A3EC, 80A1EC, 80A3EC.

Polymer designation	AAm ratio		Na-AMPS ratio		EA ratio		Synthesis organic phase
	(wt%)	(mol%)	(wt%)	(mol%)	(wt%)	(mol%)	
50AC	50.0	74.0	50.0	26.0	-	-	Carnation

80AC	20.0	42.0	80.0	58.0	-	-	Carnation
50AP	50.0	74.0	50.0	26.0	-	-	Puresyn4
80AP	20.0	42.0	80.0	58.0	-	-	Puresyn4
50A1EC	49.4	74.0	49.4	25.0	1.2	1.0	Carnation
50A3EC	48.5	72.0	48.5	25.0	3.0	3.0	Carnation
80A1EC	19.7	42.0	79.7	57.0	0.6	1.0	Carnation
80A3EC	19.0	40.0	79.0	57.0	2.0	3.0	Carnation

### Polyelectrolytes characterization

All polymers were isolated using hexane, acetone and isopropanol, and the characterization experiments performed in samples in the dry powder state.

Charge density was determined by elemental analysis using an element analyser EA 1108 CHNS-O (Fisons) and 2,5-Bis(5-tert-butyl-benzoxazol-2-yl) thiophene as standard. C, H and N elemental analyses were performed and the N element was used in the calculation of the charged fraction. At least three measurements for each sample were performed.

Hydrodynamic diameter, molecular weight and zeta potential of isolated and redissolved polymers were determined by dynamic light scattering (DLS), static light scattering (SLS) and electrophoretic light scattering (ELS), respectively, in a Malvern Zetasizer Nano ZS, model ZEN3600 (Malvern Instruments Ltd, UK).

For the hydrodynamic diameter, stock solutions of 0.05 g/L for copolymers and 0.03 g/L for terpolymers were prepared in Milli-Q water and stirred overnight. All samples were sonicated during 2 min and passed through 0.45  $\mu\text{m}$  syringe filters prior to analysis. The measurement temperature was set to 25  $^{\circ}\text{C}$ , backscatter detection (173 $^{\circ}$  angle) was used and the CONTIN model was used to treat the signal, with at least three measurements for each sample performed.

Weight-average molecular weight measurements of polymers were performed using stock solutions (0.5 g/L) of each polymer prepared in NaCl 0.5 M and stirred overnight. The samples for analysis were then obtained by diluting the stock solutions at several concentrations from 0.5-0.02g/L. All samples were sonicated during 2 min and passed through 0.45  $\mu\text{m}$  syringe filters prior to analysis. Toluene was used as standard. Previously, the refractive index of each solution was determined, in the refractometer Atago RX-5000D. By plotting refractive index versus concentration we could obtain  $dn/dc$  (variation of refractive index with concentration) which was supplied to the SLS software. The molecular weight value was extracted from the interception point on the X axis of the Debye plot, which represents the intensity of the scattered light versus the concentration of the sample used <sup>27</sup>.

For zeta potential measurements, 1 mL of each stock solution (0.1 g/L) in Milli-Q water was carefully injected with a syringe into a folded capillary cell (ref. DTS1070), closed by cell stoppers.

At least three measurements were conducted for each sample. Table 2 summarizes the flocculants characteristics.

**Table 2** Summary of flocculants characteristics. Co-polymers: 50AC, 80AC, 50AP and 80AP. Ter-polymers: 50A1EC, 50A3EC, 80A1EC, 80A3EC.

Polymer designation	Charged fraction estimated from elemental analysis (wt%)	Zeta Potential (mV)	Hydrodynamic diameter (nm)	Weight-average molecular weight ( $10^6$ Da)
50AC	$41.5 \pm 0.2$	$-71 \pm 2$	$67 \pm 2$	$0.9 \pm 0.07$
80AC	$62.9 \pm 0.5$	$-80 \pm 1$	$72 \pm 1$	$1.0 \pm 0.08$
50AP	$41.9 \pm 2.3$	$-72 \pm 1$	$265 \pm 37$	$2.5 \pm 0.09$
80AP	$68.1 \pm 2.1$	$-85 \pm 1$	$147 \pm 4$	$1.3 \pm 0.2$
50A1EC	$39.5 \pm 0.4$	$-65 \pm 2$	$70 \pm 1$	$0.6 \pm 0.02$
50A3EC	$39.7 \pm 1.2$	$-58 \pm 1$	$282 \pm 32$	$3.5 \pm 0.07$
80A1EC	$62.2 \pm 1.7$	$-79 \pm 1$	$143 \pm 10$	$1.5 \pm 0.2$
80A3EC	$61.6 \pm 1.5$	$-79 \pm 2$	$206 \pm 22$	$2.4 \pm 0.08$

### Flocculation jar tests

For each polymer developed, a 200-mL stock solution at a 0.4 wt% concentration was prepared with distilled water using magnetic stirring for sixty minutes. 75-mL samples of pre-agitated wastewater (industrial effluent) were adjusted to three different pHs using hydrochloric acid or sodium hydroxide aqueous solutions, using a pH meter SCAN3BW (Scansci). The pH values were chosen after a first pre-screening over all pH range. Polymer solution samples with different volumes were added to the wastewater sample, increasing successively the flocculant concentration from 13 mg/L until a maximum of 180 mg/L. In each addition, the suspension-polymer mixture was manually agitated for 10 seconds, allowed to settle for 2 min and the turbidity of the supernatant assessed, with at least three repetitions, using a Photometer MD600 (Lovibond, UK). The variance in the measurements of turbidity was always below 1.0 %.

### Flocculation process monitoring

A 200-mL polymer stock solution at 0.4 wt% concentration was prepared with distilled water using magnetic stirring for sixty minutes.

LDS was used to monitor the flocculation process in slight turbulent conditions and supplies information about the flocculation kinetics and, simultaneously, on the alteration with time of the

floc structure according to previous studies<sup>15,20</sup>. The tests were conducted in a Malvern Masterziser 2000 (Malvern Instruments). 200 mL of effluent sample were added to 600 mL of distilled water in the equipment beaker, and the pH was maintained at a value of 6 using hydrochloric acid, according to the turbidity reduction tests. Dilution was required to ensure an acceptable level of obscuration, which was initially below 80%, to guarantee that during the flocculation process, the end obscuration value was always above 5%, as suggested by Rasteiro *et al.*<sup>15</sup>. The measurements of the initial effluent, before any treatment, were carried out at a stirring speed of 2000 rpm. The flocculant was added after the first particle size acquisition of initial effluent at pH 6, as to obtain overall concentrations of the flocculant in the system of 3.3, 6.5 and 13 mg/L, according with the turbidity tests presented previously. Considering that, in the turbidity tests performed, the lowest concentration used (13 mg/L) conducted to very high turbidity reductions, sometimes to maximum reduction, thus, only this concentration and concentrations lower than this one were selected for the LDS monitoring experiments, in order to be able to observe considerable differences in floc sizes, and try to understand the presence of different and eventually complementary flocculation mechanisms. Moreover, economic considerations led also to the selection of a concentration of 13 mg/L as the basis concentration for the LDS tests. The predetermined amount of flocculant solution was added at once to the effluent. During the entire process, the flocculation vessel was stirred mechanically using the sample unit of the Malvern Mastersizer 2000 at a stirring speed of 300 rpm to avoid floc breakage but still ensuring that floc sedimentation was not occurring. Different stirring speeds were tested, from 200 to 900 rpm, however 300 rpm was found to be the optimized speed allowing the largest floc size while ensuring that flocs were successfully circulating in the system. The size of the flocs was measured every 36 sec for a period of 6.6 min. The reported values of the median particle size ( $d(0.5)$ ) represent an average of at least three measurements.

Moreover, the scattering exponent of the flocs was calculated at the end of the flocculation process, from the scattering matrix obtained by LDS. This scattering exponent provides information about floc structure and is determined from the scattering pattern, corresponding to scattering at large length scales, considering that we are dealing with large and quite open aggregates<sup>14</sup>. From the scattering matrix obtained by the LDS, it is possible to plot, in logarithmic scale, the scattering intensity versus  $q$ , and the slope of the first region of the plot is related to the SE<sup>17,19</sup>. The  $q$  value is defined by the following equation (1):

$$q = \frac{4\pi n_0}{\lambda_0} \sin(\theta/2) \quad (\text{Eq. 1})$$

where  $n_0$  is the refractive index of the dispersion medium,  $\theta$  is the scattering angle and  $\lambda_0$  is the incident light wavelength. The scattering matrix is exported through the Malvern software to an

excel spreadsheet and the data is then processed, offline, for each acquisition, in order to obtain the scattering exponents.

## RESULTS AND DISCUSSION

### **Flocculation jar tests**

Results for turbidity removal with developed anionic flocculants at pH 3, 6 and 10 are presented in Figures 1 and 2. For this effluent, anionic co- and ter-polymers show very high turbidity reductions, with values above 97% at concentrations below 60 mg/L for the optimum pH (pH 6) and for polymers with lower anionic fraction (50 series). Since the removal results obtained for the co-polymers are already very high, the hydrophobically-modified terpolymers did not lead to further improvements. In the case of the 50 series polyelectrolytes, the presence of the hydrophobic monomer seems not to affect much their performance, suggesting that this modification is not required for the achievement of good turbidity reductions, even if the kinetics of turbidity removal seems to be slightly faster in the case of the hydrophobically modified polymers (compare Figure 1 (a) with Figures 2 (a) and (c)). Looking at performances with the 80 series, there is a reduction of efficacy for the flocculant with a higher amount of the hydrophobic monomer, which leads to less turbidity reduction, indicating that a high amount of hydrophobicity is not beneficial for this specific case. This has already been observed by other authors previously<sup>28</sup>.

The best performances were achieved with flocculants 50AC (97% turbidity reduction), 50AP (97% reduction), 50A1EC (97% reduction) and 50A3EC (97% reduction), in general, polymers with a higher molecular weight and medium charge density, which favors the bridging mechanism. Flocculation using polyelectrolytes with high molecular weight and medium charge density promotes the bridging effect, since the polymer chain adsorbs on the effluent particles surface and extends enough to interact with several particles. At pH 3 there is also significant turbidity removals for most of the polymers studied, however not as efficient as at pH 6 due to the initial destabilization of the particles observed at this specific pH, which leads to a very low absolute value of zeta potential. On the other hand, at pH 10 substantial reductions are only observed with the 80 series flocculants. Furthermore, for the co-polymers, a similar behavior was observed for polyelectrolytes developed with Carnation or Puresyn4 as organic phases, suggesting that the oil used in the synthesis formulation does not affect the flocculation performance.

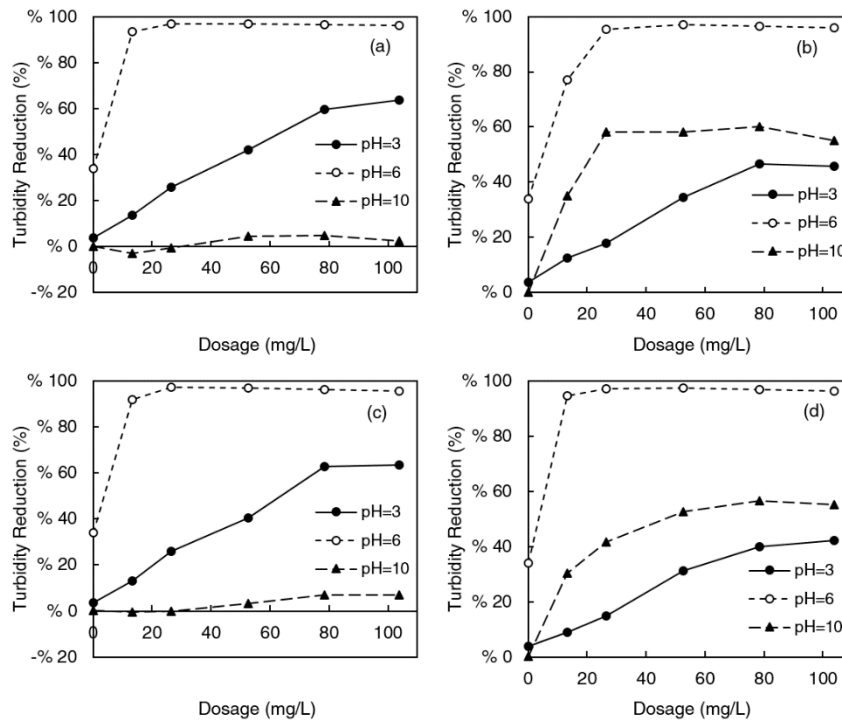


**Figure 1** Turbidity removal curves for potato crisps manufacturing industry effluent treated by the anionic copolymers 50AC (a), 80AC (b), 50AP (c) and 80AP (d), at various pH.

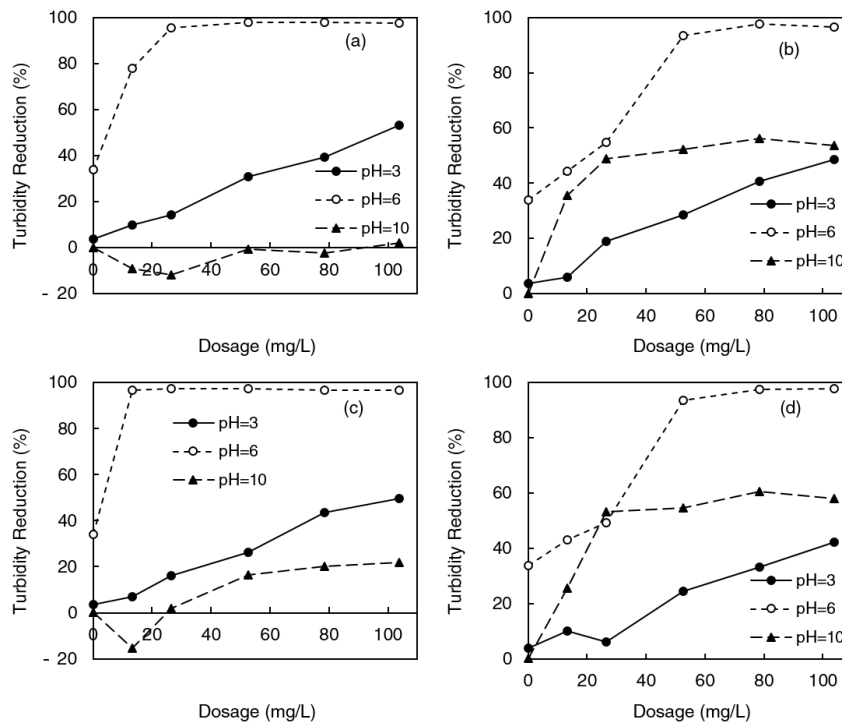


**Figure 2** Turbidity removal curves for potato crisps manufacturing industry effluent treated by the anionic terpolymers 50A1EC (a), 50A3EC (b), 80A1EC (c) and 80A3EC (d), at various pH.

### **Flocculation process monitoring**

Tables 1 and 2 present the composition and the results of the polyelectrolyte characterization. The composition measurements confirmed the targeted differences between polymers. This initial characterization subsequently allowed the separate study of each parameter influence (charge density and presence/absence of hydrophobic content) for polyelectrolytes with similar composition and architecture.

Zeta potential for initial effluent as collected (pH 12.8) and for effluent after adjustment to pH 6 (optimum pH for treatment, according with previous results) were measured and a decrease of the absolute value was observed (to -5mV) with the decrease of pH. Considering that this is an average value and the distribution curve goes between -20 mV and 15 mV, typical of a heterogeneous system as is the case of this real effluent, this means a large number of particles in the effluent have a positively charged surface, which justifies the success of anionic polyelectrolytes application. Anionic polyelectrolytes will attach to the positively charged particles of the effluent and the flocculation process must start from there, in a first stage, extending to the other particles through bridging and sweeping flocculation.

An example of the particle size distribution of the initial effluent, the pH 6 adjusted effluent and the effluent at the end of the flocculation process are shown in Figure 3, for treatment with terpolymer 80A3EC. The particle size distribution evolves from a bimodal to monomodal distribution, being displaced towards higher particle sizes at the end of flocculation, as expected. The median size of the particles in the initial effluent, measured by LDS, was 39  $\mu\text{m}$ , while after the pH adjustment it was 22  $\mu\text{m}$ . This decrease of particle size is mainly due to the constant strong stirring speed applied during the measurement, until the polymer addition, which may cause breakage of existent small aggregates. Addition of flocculant increased drastically the median size of the particles. Specifically, adding the optimal dosage of 80A3EC (13mg/L) increased the median particle size to a value of 514  $\mu\text{m}$ .

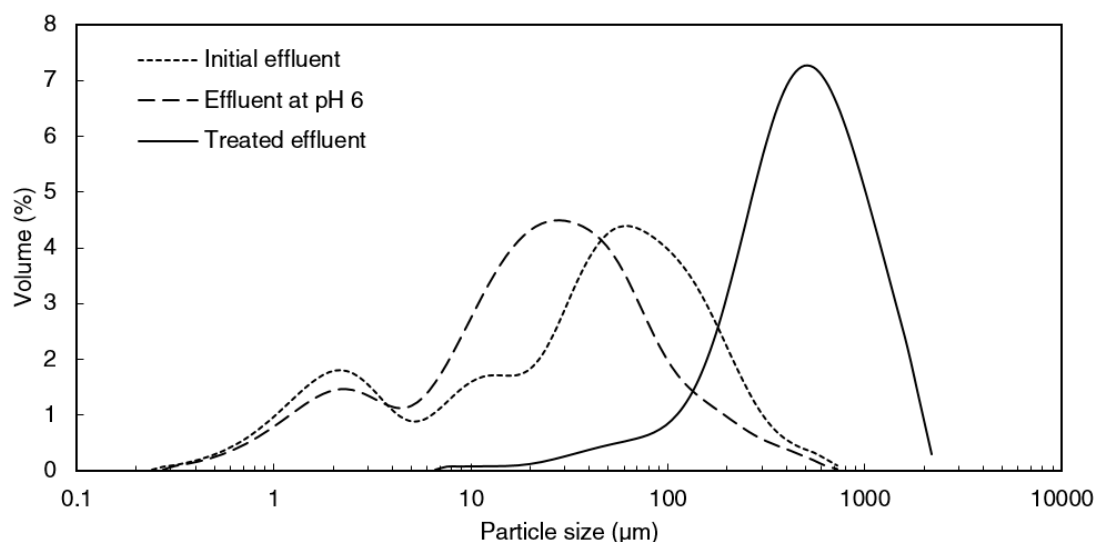


**Figure 3** Particle size distribution of the initial effluent, pH 6 adjusted effluent and floc size distribution at the end of the flocculation with ter-polymer 80A3EC, for a polymer concentration of 13 mg/L.

Industrial effluent flocculation was monitored by measuring the aggregate size over time using the LDS technique. Figures 4 and 5 provide representation of flocculation kinetic curves obtained by LDS for the polymers tested (50AC, 80AC, 50AP, 80AP, 50A1EC, 50A3EC, 80A1EC and 80A3EC), for three different polymer concentrations (3.3, 6.5 and 13 mg/L). The trend in the kinetic curves is, in general, similar for all the cases tested. The average floc sizes reach their maximum within 2 min after polymer addition and then stabilize, without any apparent aggregate reformation<sup>17</sup>. Analyzing the kinetic curves, and considering the instability of the flocs size over the time of flocculation, it is possible to conclude that flocs are considerably large and sensitive to the turbulent environment. The flocculant dosage for the polymers tested that led to larger flocs was always 13 mg/L, the highest concentration used in this study. Using lower concentration leads to a faster reach of the equilibrium point in some cases, but always resulting in smaller floc sizes.

Looking closer into the kinetic plots for the 13 mg/L concentration for the different polymers (Figure 4 and 5), it can be observed a floc size decrease after reaching a maximum size. This can be a result of the breakage of flocs by the hydrodynamic forces resulting from stirring, since the particles do appear to re-flocculate following breakage without visible restructuring, which, if present, would be noticeable through a steep decrease of flocs size, after reaching a maximum, in the median diameter curve versus time<sup>20</sup>. However, for lower concentrations of polymer, this behavior is less pronounced and the floc sizes are much more stable over time, confirming, as expected, that larger flocs are more sensitive to hydrodynamic forces resulting from mixing.



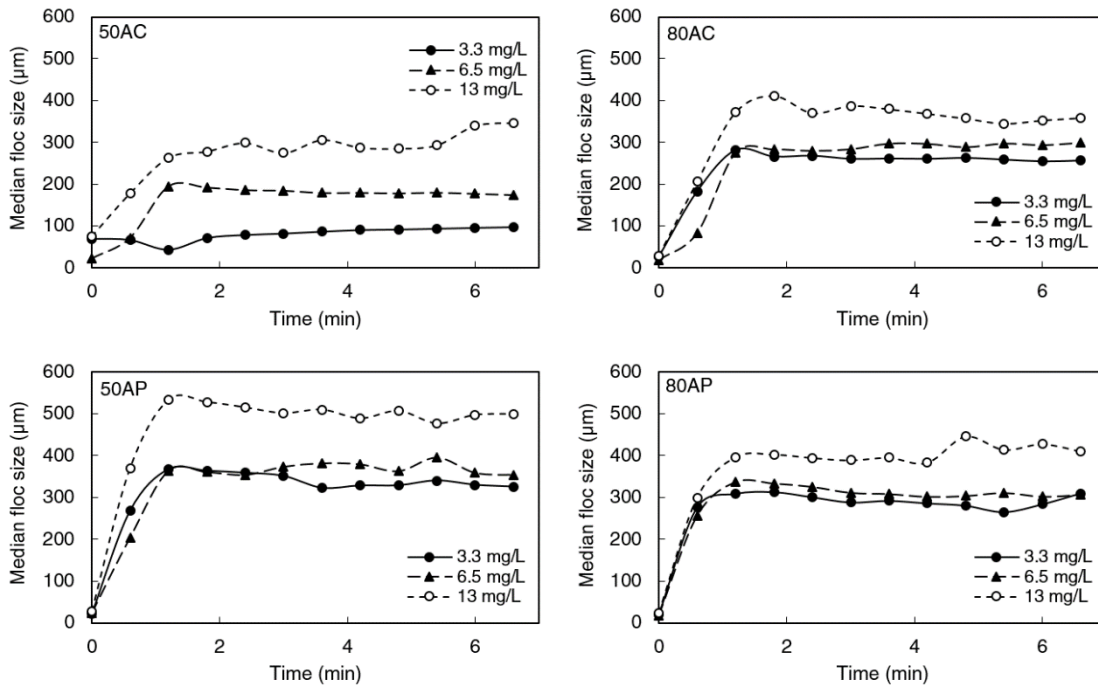


**Figure 4** Evolution of average particle size over time obtained via LDS for three different flocculant dosages for copolymers 50AC, 80AC, 50AP and 80AP.

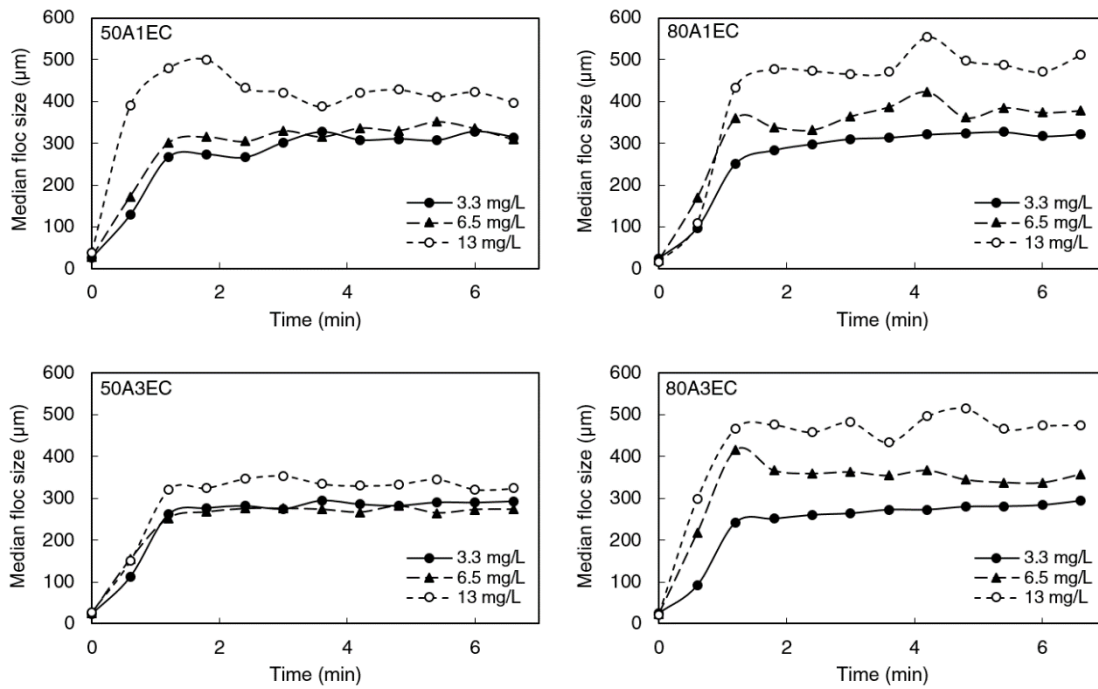


**Figure 5** Evolution of average particle size over time obtained via LDS for three different flocculant dosages for terpolymers 50A1EC, 50A3EC, 80A1EC and 80A3EC.

The SE profiles, calculated from the scattering matrix obtained by LDS, were plotted and the SE value after 6 min of flocculation, for each concentration and polymer, was extracted. These values are summarized in Table 3, alongside with particle sizes recorded 6 min after addition of the

corresponding flocculant. Since the SE profiles for the different polymers follow all the same pattern, Figure 6 gives two examples of how SE evolves with time during the flocculation process, for two of the polyelectrolytes studied (80AC and 80A3EC), both with similar structure and charge, but differing by the ratio of hydrophobic monomer EA, used in the polymer synthesis. For all the cases, the scattering exponent increases rapidly at the beginning of the flocculation process, when a rapid growth of the floc size occurs. As the flocs grow, more particles are integrated within the flocs and the SE value increases correspondingly, until it eventually stabilizes within a few minutes. Higher SE values mean more compact flocs. Although it was not possible to obtain a value of SE for the initial effluent, due to the heterogeneity of the small size particles, a continuous increase of SE is still verified, revealing an increase of flocs compactness during flocculation, also due to the hydrodynamic forces. In general, and comparing with literature <sup>20,29</sup>, where systems of calcium carbonate were used, values of SE for this specific effluent are lower, corresponding to more porous flocs. These results regarding floc structure suggest that the aggregation process takes place mainly by the bridging mechanism, supported by the fast flocculation rate and by the open floc structure. For these two polymers, a higher polymer concentration leads to more porous flocs. Additionally, the presence of the hydrophobic monomer within the polymer flocculant results in slightly more compact flocs.

The flocculation kinetics are largely dependent on the flocculant characteristics and on the flocculation mechanism involved <sup>15</sup>. Bridging is likely the main flocculation mechanism, since the polymers charge density varies between 25 and 58 mol% and, for lower charges, more extended conformation of the polymer chain is obtained on the effluent particles surface, due to the lower number of sites available for adsorption, leading to large and more open flocs. This is more evident by the analysis of the 50 series polyelectrolytes. The lowest values of SE (very open flocs), correspond to the larger flocs, and the opposite is also verified (Table 3). In general, introducing hydrophobic content in the polymer lead to larger and more porous flocs, suggesting an additional interaction promoted by the affinity between the oily effluent and the hydrophobic part of the polyelectrolytes. Comparing specifically 50A3EC and 80A3EC, which have similar hydrophobic content and different anionic fraction, it is possible to see higher SE values for 80A3EC, which means more compact flocs, compatible with the higher number of negative charges in the polymer chain. Additionally, flocs obtained with P series polymers (50AP and 80AP) are larger and more porous, in agreement with the higher molecular weight of these polymers.

Concerning the median floc size values (after 6 min) in Table 3, it is possible to see, for each polymer tested, an increase with the increase of the flocculant concentration, which was expected since more polymer in solution allows to create larger flocs by aggregating more particles. Also, comparing polyelectrolytes with the same characteristics of hydrophobicity, it is visible a tendency where larger flocs are obtained using flocculants with higher charge density (e.g. compare 50AC

with 80AC or 50A1EC and 80A1EC). The exception is when comparing 50AP and 80AP, possible due to the much higher molecular weight of 50AP.

**Table 3** Summary of the experimental value of SE after 6 minutes of flocculation for each polyelectrolyte and maximum floc size for each concentration tested.

Polymer	Concentration (mg/L)	SE after 6 min	Floc size after 6 min ( $\mu\text{m}$ )
50AC	3.3	1.81	95
	6.5	1.84	177
	13	1.69	340
80AC	3.3	1.68	254
	6.5	1.62	294
	13	1.58	352
50AP	3.3	1.53	330
	6.5	1.52	359
	13	1.39	497
80AP	3.3	1.52	283
	6.5	1.50	302
	13	1.44	428
50A1EC	3.3	1.37	328
	6.5	1.37	335
	13	1.35	423
50A3EC	3.3	1.46	290
	6.5	1.45	273
	13	1.43	322
80A1EC	3.3	1.60	317
	6.5	1.64	374
	13	1.46	471
80A3EC	3.3	1.73	284
	6.5	1.74	337
	13	1.65	474

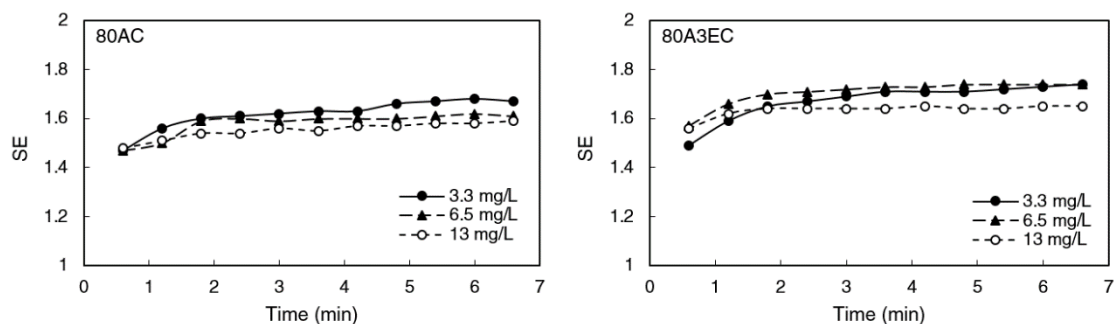


**Figure 6** Evolution of floc structure (SE) for 80AC and 80A3EC, at different concentrations.

### Correlating polymer characteristics with performance in flocculation

Figure 7 shows the influence on the floc size (Table 3) of charged fraction (a), zeta potential (b), hydrodynamic diameter (c) and molecular weight (d) of the polyelectrolytes, for the higher polyelectrolyte concentration used (13 mg/L). The results plotted refer to the flocs average size, in the average size over time curves, after 6 min of flocculation. In general, higher charged fraction and zeta potential, in absolute value, lead to larger flocs, since there is more charged moieties on the polymer, resulting in increased number of attachment events to particle surface per polymer chain, thus increasing the statistical possibility of one chain adsorbing to two or more particles, conducting to aggregates with a larger number of particles. This tendency is not completely linear, but for both co- and ter-polymers it can be verified in most of the cases, with only the exception of co-polymer 50AP (identified in the graph), which presents a molecular weight value much higher than the other co-polymers, introducing, thus, another parameter that can mask the trend. When considering the polymer hydrodynamic diameter, it is evident that the floc size increases when the hydrodynamic diameter increases, with the exception for the ter-polymer 50A3EC (identified in the graph), which appears as an outlier, for which a molecular weight value higher than for the other ter-polymers was also measured. However, the size distribution of this ter-polymer indicates the existence of some aggregation which may be masking the molecular weight measurement and even the hydrodynamic diameter measurement. Moreover, previous studies in the literature <sup>28</sup>, have already referred to the possibility of an optimum amount of hydrophobic monomer incorporation in the polymer chain, above which flocculation is no longer improved, as will also be discussed here later. Since hydrodynamic diameter is very well correlated with molecular weight values, the tendency observed regarding the influence of hydrodynamic diameter is similar to the one observed in Figure 5 (d) for the influence of molecular weight. Longer polymer chains result in larger flocs, as one polymer chain can adsorb to the surface of a larger number of particles in the same floc, which, consequently, are usually also more porous. Moreover, the inclusion of the hydrophobic monomer usually leads to larger flocs as the result of two phenomena: higher affinity to the particles and higher molecular weight and hydrodynamic diameter (see Table 2).

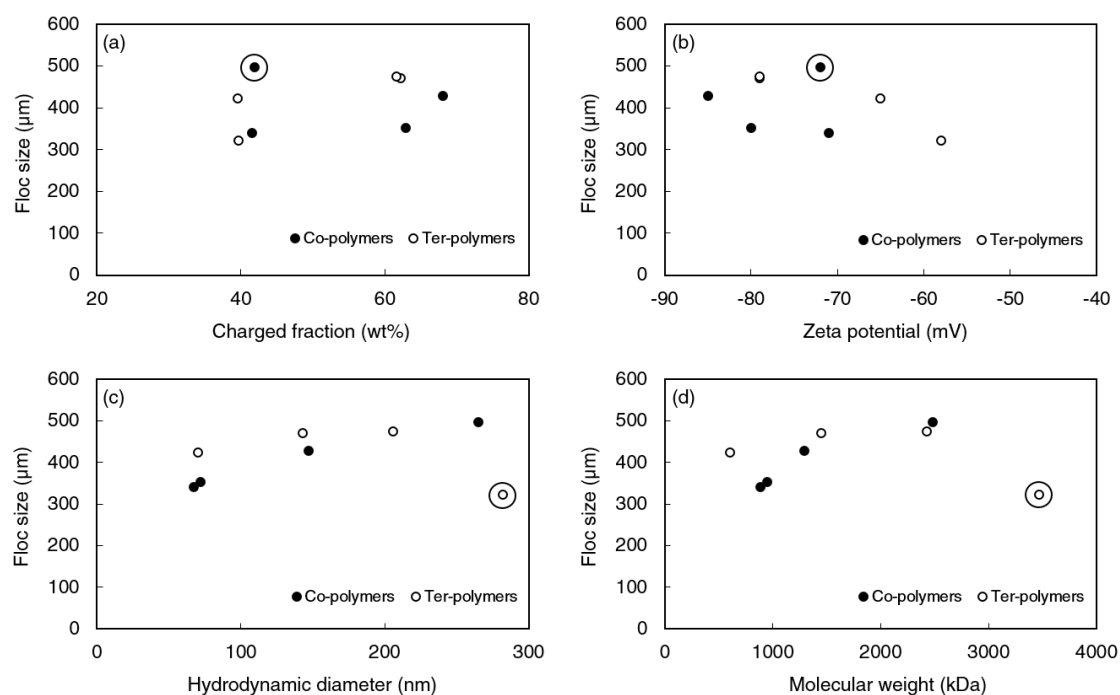


**Figure 7** Floc size after 6 min as function of charged fraction (a), zeta potential (b), hydrodynamic diameter (c) and molecular weight (d) for the highest polyelectrolyte concentration tested (13 mg/L).

The influence of zeta potential (a) and hydrodynamic diameter (b) of the polyelectrolytes on scattering exponent (Table 3), for the higher polyelectrolyte concentration used (13 mg/L), is presented in Figure 8.

Polyelectrolytes with higher absolute values of zeta potential, corresponding to a higher charge density in the chain, are expected to form more compact flocs (higher SE values), since there are more regions in the polymer chain able to adsorb to the effluent particles. However, this is only observed in the case of the ter-polymers with a strong effect of charge density on the flocs structure. Co-polymers show almost no influence of charge density on the floc structure, perhaps due to the overall lower molecular weight of these polymers.

Regarding influence of hydrodynamic diameter, it is expected that higher hydrodynamic diameter will lead to more open flocs (lower SE values), since the polymer chains are longer, allowing more free space between bridged particles. This hypothesis appears to only hold surely in the case of co-polymers. For ter-polymers no general trend can be observed. This suggests that hydrophobic interactions between the oil in the effluent and the polymer chain affect the flocs structure, and the shorter the flocculant molecule the more evident is this effect.

Similar trend of zeta potential and hydrodynamic diameter effects on SE (Figure 8) was verified when looking at charge density and molecular weight effects, respectively, as was previously

shown for the influences on floc size (Figure 7). Thus, only plots for the influence of zeta potential and hydrodynamic diameter on SE are presented here.

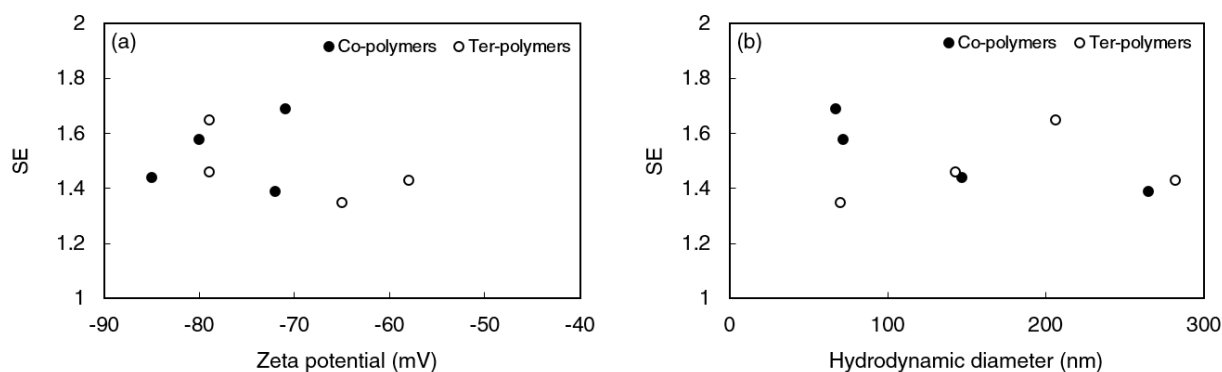


**Figure 8** SE after 6 min as function of zeta potential (a) and hydrodynamic diameter (b) for the highest polyelectrolyte concentration tested (13 mg/L).

In Figure 9, floc size is plotted as a function of hydrophobic content of the polymer flocculant (for polyelectrolytes synthesized using the same organic phase (Carnation)), which is indicated by the molar ratio of monomer 3 in the polyelectrolyte composition. Each polymer series contains a different ratio of charged monomer within the polymer composition (0%, 1% and 3% as indicated in Table 1). For each polymer series, there is an increase of the maximum floc size with the addition of a small amount of hydrophobic content (1 mol%) to the initially fully hydrophilic composition, which then stabilizes or decreases when the hydrophobic content is increased to higher concentrations (3 mol%). This suggests that the presence of hydrophobicity is favorable for the flocculation process, though there is an optimum content that improves the floc size and above that value the presence of higher degree of hydrophobicity can be detrimental, in spite of the higher molecular weights obtained. This can be attributed, for instance, to a more difficult dissolution of the polymer. The improvement of flocculation performance in the presence of hydrophobically-modified polyelectrolytes was already discussed in the literature for other formulations<sup>22,30</sup>. The affinity between the hydrophobic part of the polymer and the oil droplets in the effluent appears to significantly enhance the treatment efficiency, as observed in the present study.

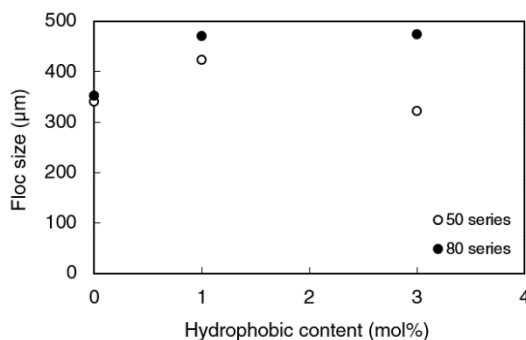


**Figure 9** Floc size after 6 min, for the higher concentration tested (13 mg/L), as function of hydrophobic content quantified by the ratio (mol%) of monomer 3 in the polyelectrolyte composition.

## CONCLUSIONS

The results obtained in this study suggest the viability of using the LDS technique to access and understand the flocculation progression in a real industrial oily effluent, and to determine some important floc characteristics under mild turbulent environment.

Anionic polyelectrolytes, varying in charge density, molar mass and hydrophobicity were tested in terms of performance in flocculation, encouraging the execution of further pilot scale testing under industrial conditions in order to confirm the suitability for the final application. The experimental technique used, which was tested for the first time in a real industrial effluent, allowed extracting information on the influence of the polyelectrolytes characteristics on the flocculation process. This can be extremely important in the future, when dealing with the selection/optimization of the right flocculant to treat a specific effluent, as well as the tuning of the operational conditions. As expected, results show that high molecular weight polyelectrolytes with medium to high charge density induce flocculation by bridging mechanism. Results also demonstrate the influence of increasing flocculant concentration: floc size increases and more porous aggregates are obtained. Polyelectrolytes characteristics proved to be critical in the floc size obtained. Higher zeta potential, hydrodynamic diameter and molecular weight lead to larger flocs. The effect of the hydrophobic content suggests that the presence of hydrophobicity is favorable for the flocculation process, however there is an optimum hydrophobic content that improves the floc size and above that value the effect is no longer beneficial.



## AUTHOR INFORMATION

### **Corresponding Author**

Maria G. Rasteiro (E-mail: mgr@eq.uc.pt)

### **Author Contributions**

The manuscript was written through contributions of all authors. All authors have given approval to the final version of the manuscript.

## ACKNOWLEDGMENTS

The authors would like to thank financial support from Marie Curie Initial Training Networks (ITN) – European Industrial Doctorate (EID), through Grant agreement FP7-PEOPLE-2013-ITN-604825 and from the Portuguese Science and Technology Foundation (Pest/C/EQB/UI0102/2013). Also, acknowledgements to Adventech Group (Portugal) are due for supplying the effluent.

## REFERENCES

- (1) Sonune, A.; Ghate, R. Developments in Wastewater Treatment Methods. *Desalination* **2004**, *167*, 55.
- (2) Iselau, F.; Phan Xuan, T.; Trefalt, G.; Matic, A.; Holmberg, K.; Bordes, R. Formation and Relaxation Kinetics of Starch–particle Complexes. *Soft Matter* **2016**, *12*, 9509.
- (3) Lee, C. S.; Robinson, J.; Chong, M. F. A Review on Application of Flocculants in Wastewater Treatment. *Process Saf. Environ. Prot.* **2014**, *92*, 489.
- (4) Pavlovic, M.; Adok-Sipiczki, M.; Nardin, C.; Pearson, S.; Bourgeat-Lami, E.; Prevot, V.; Szilagy, I. Effect of MacroRAFT Copolymer Adsorption on the Colloidal Stability of Layered Double Hydroxide Nanoparticles. *Langmuir* **2015**, *31*, 12609.
- (5) Hierrezuelo, J.; Szilagy, I.; Vaccaro, A.; Borkovec, M. Probing Nanometer-Thick Polyelectrolyte Layers Adsorbed on Oppositely Charged Particles by Dynamic Light Scattering. *Macromolecules* **2010**, *43*, 9108.
- (6) Kleimann, J.; Gehin-Delval, C.; Auweter, H.; Borkovec, M. Super-Stoichiometric Charge Neutralization in Particle-Polyelectrolyte Systems. *Langmuir* **2005**, *21*, 3688.
- (7) Ahmad, A.; Wong, S.; Teng, T.; Zuhairi, A. Improvement of Alum and PACl Coagulation by Polyacrylamides (PAMs) for the Treatment of Pulp and Paper Mill Wastewater. *Chem. Eng. J.* **2008**, *137*, 510.
- (8) Caskey, J. A.; Primus, R. J. The Effect of Anionic Polyacrylamide Molecular Conformation and Configuration on Flocculation Effectiveness. *Environ. Prog.* **1986**, *5*, 98.
- (9) Blanco, A.; Fuente, E.; Negro, C.; Tijero, J. Flocculation Monitoring: Focused Beam Reflectance Measurement as a Measurement Tool. *Can. J. Chem. Eng.* **2008**, *80*, 1.
- (10) Eriksson, L.; Alm, B.; Stenius, P. Formation and Structure of Polystyrene Latex Aggregates Obtained by Flocculation with Cationic Polyelectrolytes. *Colloids Surfaces A Physicochem. Eng. Asp.* **1993**, *70*, 47.
- (11) Biggs, S.; Habgood, M.; Jameson, G. J.; Yan, Y. Aggregate Structures Formed via a Bridging Flocculation Mechanism. *Chem. Eng. J.* **2000**, *80*, 13.
- (12) Thomas, D. N.; Judd, S. J.; Fawcett, N. Flocculation Modelling: A Review. *Water Res.* **1999**, *33*, 1579.
- (13) Dao, V. H.; Cameron, N. R.; Saito, K. Synthesis, Properties and Performance of Organic Polymers Employed in Flocculation Applications. *Polym. Chem.* **2016**, *7*, 11.
- (14) Pinheiro, I.; Ferreira, P. J.; Garcia, F. A.; Reis, M. S.; Pereira, A. C.; Wandrey, C.; Ahmadloo, H.; Amaral, J. L.; Hunkeler, D.; Rasteiro, M. G. An Experimental Design Methodology to Evaluate the Importance of Different Parameters on Flocculation by Polyelectrolytes. *Powder Technol.* **2013**, *238*, 2.
- (15) Rasteiro, M. G.; Garcia, F. A. P.; Ferreira, P.; Blanco, A.; Negro, C.; Antunes, E. The Use

- of LDS as a Tool to Evaluate Flocculation Mechanisms. *Chem. Eng. Process. Process Intensif.* **2008**, *47*, 1323.
- (16) Rasteiro, M. G.; Garcia, F. A. P.; del Mar Pérez, M. Applying LDS to Monitor Flocculation in Papermaking. *Part. Sci. Technol.* **2007**, *25*, 303.
- (17) Rasteiro, M. G.; Pinheiro, I.; Ferreira, P. J.; Garcia, F. A.; Wandrey, C.; Ahmadloo, H.; Hunkeler, D. Correlating Aggregates Structure with PEL Characteristics Using an Experimental Design Methodology. *Procedia Eng.* **2015**, *102*, 1697.
- (18) Chakraborti, R. K.; Gardner, K. H.; Atkinson, J. F.; Van Benschoten, J. E. Changes in Fractal Dimension during Aggregation. *Water Res.* **2003**, *37*, 873.
- (19) Liao, J. Y. H.; Selomulya, C.; Bushell, G.; Bickert, G.; Amal, R. On Different Approaches to Estimate the Mass Fractal Dimension of Coal Aggregates. *Part. Part. Syst. Charact.* **2005**, *22*, 299.
- (20) Antunes, E.; Garcia, F. A. P.; Blanco, A.; Negro, C.; Rasteiro, M. G. Evaluation of the Flocculation and Reflocculation Performance of a System with Calcium Carbonate, Cationic Acrylamide Co-Polymers, and Bentonite Microparticles. *Ind. Eng. Chem. Res.* **2015**, *54*, 198.
- (21) Liang, L.; Peng, Y.; Tan, J.; Xie, G. A Review of the Modern Characterization Techniques for Floccs in Mineral Processing. *Miner. Eng.* **2015**, *84*, 130.
- (22) Bratskaya, S.; Avramenko, V.; Schwarz, S.; Philippova, I. Enhanced Flocculation of Oil-in-Water Emulsions by Hydrophobically Modified Chitosan Derivatives. *Colloids Surfaces A Physicochem. Eng. Asp.* **2006**, *275*, 168.
- (23) Candau, F.; Selb, J. Hydrophobically-Modified Polyacrylamides Prepared by Micellar Polymerization. *Adv. Colloid Interface Sci.* **1999**, *79*, 149.
- (24) Ren, H.; Chen, W.; Zheng, Y.; Luan, Z. Effect of Hydrophobic Group on Flocculation Properties and Dewatering Efficiency of Cationic Acrylamide Copolymers. *React. Funct. Polym.* **2007**, *67*, 601.
- (25) Palomino, D.; Hunkeler, D.; Stoll, S. Comparison of Two Cationic Polymeric Flocculant Architectures on the Destabilization of Negatively Charged Latex Suspensions. *Polymer (Guildf)*. **2011**, *52*, 1019.
- (26) Lourenço, A.; Arnold, J.; Gamelas, J. A. F.; Rasteiro, M. G. A More Eco-Friendly Synthesis of Flocculants to Treat Wastewaters Using Health-Friendly Solvents. *Colloids Polym. Sci.* **2017**, *295*, 2123.
- (27) Malvern Instruments, “Zetasizer Nano Series User Manual.”
- (28) Lee, K. E.; Morad, N.; Poh, B. T.; Teng, T. T. Comparative Study on the Effectiveness of Hydrophobically Modified Cationic Polyacrylamide Groups in the Flocculation of Kaolin. *Desalination* **2011**, *270*, 206.
- (29) Rasteiro, M. G.; Garcia, F. A. P.; Ferreira, P. J.; Antunes, E.; Hunkeler, D.; Wandrey, C.

- Flocculation by Cationic Polyelectrolytes: Relating Efficiency with Polyelectrolyte Characteristics. *J. Appl. Polym. Sci.* **2010**, *116*, 3603.
- (30) Lü, T.; Qi, D.; Zhao, H.; Cheng, Y. Synthesis of Hydrophobically Modified Flocculant by Aqueous Dispersion Polymerization and Its Application in Oily Wastewater Treatment. *Polym. Eng. Sci.* **2015**, *55*, 1.